frontiers | Research Topics

Biomarkers in neurology, volume II

Edited by
Wael M. Y. Mohamed, Firas H. Kobeissy
and Stefania Mondello

Published in
Frontiers in Neurology

ISSN 1664-8714
ISBN 978-2-8325-3105-1
DOI 10.3389/978-2-8325-3105-1

About Frontiers

Frontiers is more than just an open access publisher of scholarly articles: it is a pioneering approach to the world of academia, radically improving the way scholarly research is managed. The grand vision of Frontiers is a world where all people have an equal opportunity to seek, share and generate knowledge. Frontiers provides immediate and permanent online open access to all its publications, but this alone is not enough to realize our grand goals.

Frontiers journal series

The Frontiers journal series is a multi-tier and interdisciplinary set of open-access, online journals, promising a paradigm shift from the current review, selection and dissemination processes in academic publishing. All Frontiers journals are driven by researchers for researchers; therefore, they constitute a service to the scholarly community. At the same time, the *Frontiers journal series* operates on a revolutionary invention, the tiered publishing system, initially addressing specific communities of scholars, and gradually climbing up to broader public understanding, thus serving the interests of the lay society, too.

Dedication to quality

Each Frontiers article is a landmark of the highest quality, thanks to genuinely collaborative interactions between authors and review editors, who include some of the world's best academicians. Research must be certified by peers before entering a stream of knowledge that may eventually reach the public - and shape society; therefore, Frontiers only applies the most rigorous and unbiased reviews. Frontiers revolutionizes research publishing by freely delivering the most outstanding research, evaluated with no bias from both the academic and social point of view. By applying the most advanced information technologies, Frontiers is catapulting scholarly publishing into a new generation.

What are Frontiers Research Topics?

Frontiers Research Topics are very popular trademarks of the *Frontiers journals series*: they are collections of at least ten articles, all centered on a particular subject. With their unique mix of varied contributions from Original Research to Review Articles, Frontiers Research Topics unify the most influential researchers, the latest key findings and historical advances in a hot research area.

Find out more on how to host your own Frontiers Research Topic or contribute to one as an author by contacting the Frontiers editorial office: frontiersin.org/about/contact

Biomarkers in neurology, volume II

Topic editors

Wael M. Y. Mohamed — International Islamic University Malaysia, Malaysia

Firas H. Kobeissy — Neuroscience Institute, Morehouse School of Medicine, United States

Stefania Mondello — University of Messina, Italy

Citation

Mohamed, W. M. Y., Kobeissy, F. H., Mondello, S., eds. (2023). *Biomarkers in neurology, volume II*. Lausanne: Frontiers Media SA.

doi: 10.3389/978-2-8325-3105-1

Table of contents

05 Editorial: Biomarkers in neurology, volume II
Wael M. Y. Mohamed, Firas Kobeissy and Stefania Mondello

08 Usability of serum annexin A7 as a biochemical marker of poor outcome and early neurological deterioration after acute primary intracerebral hemorrhage: A prospective cohort study
Chuan-Liu Wang, Yan-Wen Xu, Xin-Jiang Yan and Cheng-Liang Zhang

21 HMGB1 in nervous system diseases: A common biomarker and potential therapeutic target
Di Mao, Yuan Zheng, Fenfen Xu, Xiao Han and Hongyang Zhao

36 Utility of serum nuclear factor erythroid 2-related factor 2 as a potential prognostic biomarker of severe traumatic brain injury in adults: A prospective cohort study
Xin-Jiang Yan, Cheng-Peng Zhan, Yao Lv, Dan-Dan Mao, Ri-Cheng Zhou, Yong-Min Xv and Guo-Feng Yu

50 Methylmalonic acid levels in serum, exosomes, and urine and its association with cblC type methylmalonic acidemia-induced cognitive impairment
Shuqi Sun, Hong Jin, Yu Rong, Wenqi Song and Qiliang Li

63 Epileptic high-frequency oscillations occur in neonates with a high risk for seizures
Nicola Kuhnke, Courtney J. Wusthoff, Eroshini Swarnalingam, Mina Yanoussi and Julia Jacobs

72 CSF biomarkers for early-onset Alzheimer's disease in Chinese population from PUMCH dementia cohort
Dan Lei, Chenhui Mao, Jie Li, Xinying Huang, Longze Sha, Caiyan Liu, Liling Dong, Qi Xu and Jing Gao

82 Utility of serum amyloid A as a potential prognostic biomarker of aneurysmal subarachnoid hemorrhage
Zhongbo Sun, Yaqiang Li, Fu Chang and Ke Jiang

93 Correlation between cerebrospinal fluid abnormalities before ventriculoperitoneal shunt and postoperative intracranial infection in adult patients with hydrocephalus: A clinical study
Huan Zhang, Xiaozheng He, Linghai Xie, Hongbo Zhang, Xusheng Hou and Shizhong Zhang

105 Prognostic significance of serum NLRC4 in patients with acute supratentorial intracerebral hemorrhage: A prospective longitudinal cohort study
Wei Li, Xuan Lv, Yijun Ma, Yong Cai and Suijun Zhu

116 A nomogram for predicting the risk of pulmonary embolism in neurology department suspected PE patients: A 10-year retrospective analysis
Qiang Jianling, Jin Lulu, Qiu Liuyi, Feng Lanfang, Ma Xu, Li Wenchen and Wang Maofeng

131 Dysregulation of miR-146a: a causative factor in epilepsy pathogenesis, diagnosis, and prognosis
Shiqi Mao, Jinhan Wu, Jingkai Yan, Weijun Zhang and Feng Zhu

142 Inflammatory cytokines associated with mild traumatic brain injury and clinical outcomes: a systematic review and meta-analysis
Shazia Malik, Omar Alnaji, Mahnoor Malik, Teresa Gambale, Forough Farrokhyar and Michel P. Rathbone

158 The trend of neutrophil-to-lymphocyte ratio and platelet-to-lymphocyte ratio in spontaneous intracerebral hemorrhage and the predictive value of short-term postoperative prognosis in patients
Jian Zhang, Chunlong Liu, Yaofeng Hu, Aoran Yang, Yonghui Zhang and Yang Hong

168 The neutrophil-to-lymphocyte ratio as a prognostic biomarker in Guillain-Barre syndrome: a systematic review with meta-analysis
Miguel Cabanillas-Lazo, Carlos Quispe-Vicuña, Claudia Cruzalegui-Bazán, Milagros Pascual-Guevara, Nicanor Mori-Quispe and Carlos Alva-Diaz

179 Correlation between neutrophil gelatinase phase lipocalin and cerebral small vessel disease
Ying-hao Yang, Shan-shan Li, Yun-chao Wang, Lu-lu Yu, Hang-hang Zhu, Jing-hao Wu, Wen-kai Yu, Lu An, Wen-xin Yuan, Yan Ji, Yu-ming Xu, Yuan Gao and Yu-sheng Li

frontiers | Frontiers in Neurology

TYPE Editorial
PUBLISHED 12 July 2023
DOI 10.3389/fneur.2023.1244536

OPEN ACCESS

EDITED AND REVIEWED BY
Isabella Zanella,
University of Brescia, Italy

*CORRESPONDENCE
Wael M. Y. Mohamed
✉ wmy107@gmail.com

RECEIVED 22 June 2023
ACCEPTED 30 June 2023
PUBLISHED 12 July 2023

CITATION
Mohamed WMY, Kobeissy F and Mondello S (2023) Editorial: Biomarkers in neurology, volume II. *Front. Neurol.* 14:1244536. doi: 10.3389/fneur.2023.1244536

Editorial: Biomarkers in neurology, volume II

Wael M. Y. Mohamed[1]*, Firas Kobeissy[2] and Stefania Mondello[3]

[1]Basic Medical Science Department, Kulliyyah of Medicine, International Islamic University Malaysia, Kuantan, Pahang, Malaysia, [2]Department of Neurobiology, Center for Neurotrauma, Multiomics & Biomarkers (CNMB), Morehouse School of Medicine, Neuroscience Institute, Atlanta, GA, United States, [3]Department of Biomedical and Dental Sciences and Morphofunctional Imaging, University of Messina, Messina, Italy

KEYWORDS

biomarkers, neurological disorders, TBI, mTBI, HMGB1

Editorial on the Research Topic
Biomarkers in neurology, volume II

Early diagnosis of most neurological disorders is considered a mainstay for early and successful management. The difficult accessibility to brain tissue represents a major problem in the diagnosis of brain diseases. Moreover, the evaluation of disease progression and predicting prognosis is hampered by the lack of sensitive and specific diagnostic tools. Biomarkers' definition exceeds the conventional understanding of chemical changes that accompany the disease process. Nowadays, we have radiological biomarkers, genetic biomarkers, and even microbial biomarkers (microbiomarkers). In some cases, early diagnostic clinical tests are considered biomarkers. As such, research in the field of biomarkers development is multidisciplinary, involving biochemists, geneticists, neurologists, radiologists, and more.

The demand for biomarkers, in particular those that may be used to stratify for therapy eligibility and to assess treatment success, is growing as new therapeutic options emerge. The function of a biomarker determines how it should be categorized. In the United States, the Food and Drug Administration (FDA) has established a task force that has identified seven broad classes of biomarkers; (1) first, there are diagnostic biomarkers, which aid in the detection or confirmation of a disease's presence or the identification of individuals with a subtype of the disease; (2) second, there are prognostic biomarkers, which determine the likelihood of a clinical event or disease progression in a patient with the disease; (3) third, there are predictive biomarkers, which determine which patients are more likely to benefit from a given medical product. (4) Fourth, response bio-markers, which show that a biological response has occurred in an individual exposed to medical treatment (for example, pharma-codynamic biomarkers, which measure the biological activity of the medical product, not necessarily concluding clinical outcome), (5) fifth, monitoring biomarkers, which allow for repeated assessment of the status of a disease or the effect of medical treatment, (6) safety bio-markers, which indicate toxicity of medical treatment, and finally, (7) risk biomarkers (1). Although there has been a lot of research on potential biomarkers, there is still a long way to go. The identification of several multimodal potential biomarkers for diagnostic, prognostic, and predictive purposes has not (yet) resulted in the emergence of a single, definitive marker. This is why the purpose of this Research Topic was to initiate a discussion on strategies for creating, validating, and accrediting biomarkers for brain injury. Given the wide variety of possible biomarkers, this concept is accessible to a wide range of researchers. Our project's ultimate goal was to identify a sensitive and specific biomarker for brain illness

that is also simple, accessible, and inexpensive. Also, before a biomarker is used in clinical settings, we'd want to draw your attention to the importance of validating it. Quite simply, a paradigm change in the treatment of brain illness might result from the discovery of a reliable biomarker.

In this Research Topic, Wang et al. conducted a study aimed to assess the clinical utility of serum ANXA7 as a predictor of severity, early neurological deterioration (END), and prognosis after intracerebral hemorrhage (ICH). A total of 126 people with ICH and 126 people without ICH served as controls for this study. The National Institutes of Health Stroke Scale (NIHSS) was used to quantify the severity of stroke-related symptoms. The ABC/2 approach was used to calculate the volume of the ICH lesion. Patients had considerably greater blood ANXA7 levels compared to controls, and these levels were shown to be independently linked with the NIHSS score. Therefore, serum ANXA7 may be a valuable blood-derived biomarker for evaluating ICH severity, END, and prognosis.

Similarly, Yan et al. proposed that the protein Nrf2 (nuclear factor erythroid 2-related factor 2) may have a neuroprotective function in the body naturally. They aimed to determine whether or not serum Nrf2 is a useful prognostic indicator of severe Traumatic Brain Injury (TBI). Serum Nrf2 levels were measured in 105 healthy individuals and 105 people with traumatic brain injury as part of prospective cohort research. Using multivariate analysis, they were able to determine its associations with trauma severity and 180-day overall survival, death, and poor prognosis (extended Glasgow Outcome Scale score 1–4). Patients' serum Nrf2 levels were significantly higher than those of healthy controls. The substantial predictive impact of serum Nrf2 in mTBI (mild Traumatic Brain Injury) is therefore supported by the strong correlation between elevated serum Nrf2 levels and traumatic severity and outcome. In addition to pointing the way for future mTBI investigations, the study by Malik et al. underlines the lack of unanimity in the methodology of studies that assess inflammatory cytokines in the blood after mTBI.

CSF levels of leukocytes, chloride, glucose, aspartate aminotransferase, lactate dehydrogenase, adenosine deaminase, lactic acid, and protein were examined prior to ventriculoperitoneal shunt placement to determine their association with infection. When the cerebrospinal fluid glucose level is 2.8 mmol/L and the lactic acid level is >2.8 mmol/L, it is recommended to perform ventriculoperitoneal shunt after further improvement of cerebrospinal fluid indicators, otherwise, hasty operation will increase the postoperative infection rate in adults with hydrocephalus who do not have clinical manifestations of intracranial infection. Surgery with a ventriculoperitoneal shunt is associated with a high postoperative fever rate and a quick decline in body temperature. After 3 days post-op, the possibility of an intracranial infection should be explored if the patient still has a fever (Zhang J. et al.). Lei et al. looked at 125 people (onset 65) from the PUMCH dementia cohort, who were recruited systematically and divided into Alzheimer's disease (AD), non-AD dementia, and control groups. ELISA INNOTEST (Fujirebio, Ghent, Belgium) was used to determine amyloid- 42 (A42), total tau (t-tau), and phosphorylated tau (p-tau) levels. The differences between the groups are analyzed using either the students' *t*-test or a non-parametric test. To demonstrate the diagnostic efficacy of markers, the area under the receiver operating characteristic (ROC) curve (AUC ROC) was developed. To improve the diagnostic capability of a panel of indicators, a diagnostic model is established using logistic regression. Their findings provide credence to the use of biomarkers and established cutoff values in the diagnosis of AD in its earliest stages. They demonstrated that using ratios of t-tau to A42 and p-tau to A42 is more sensitive than using A42 levels alone and that adding biomarkers may further increase diagnostic accuracy. Similarly, cerebrospinal fluid vessel disease (CSVD) is prevalent in the elderly. Recent research has shown a link between NGAL (neutrophil gelatinase-associated lipocalin) and CVD and CVA (Cerebrovascular Accident). Inflammation brought on by NGAL damages the vascular endothelium and contributes to the development of various illnesses. The researchers aimed to find out whether CSVD patients' blood NGAL levels were a reliable indicator of how severely their illness will progress (Yang et al.).

Multiple genetic and environmental variables have been linked to the development of epilepsy, making it one of the most common neurological illnesses. Recent studies of the human scalp and cerebral EEG have shown novel markers for high-frequency oscillations (HFOs) between 80 and 500 Hz. HFOs may be produced in the brains of newborns. Newborns at risk for developing epilepsy may have a detectable biomarker in HFO. Preliminary findings from Kuhnke et al. imply that HFOs are more common in infants with abnormal background activity. To determine whether HFO incidence is related to seizure production and if this could predict the onset of epilepsy, larger data sets are required. As a new biomarker for epilepsy diagnosis, prognosis, and therapy, the aberrant expression patterns of miR-146a in various kinds and stages of epilepsy and its putative molecular control mechanism are summarized by Mao S. et al.. Similarly, the potential of HMGB1 (High-Mobility Group Box 1) as a biomarker for neurodegenerative illnesses such as Parkinson's disease, stroke, traumatic brain injury, epilepsy, autism, depression, multiple sclerosis, and amyotrophic lateral sclerosis was discussed by Mao D. et al.. The underlying biological pathways and clinical translation need more study in the future. The immune system causes the neuropathy known as Guillain-Barre syndrome (GBS). This suggests that the neutrophil-lymphocyte ratio (NLR) might serve as a diagnostic for its effectiveness. To summarize the evidence for NLR as a possible biomarker for GBS, Cabanillas-Lazo et al., did a systematic review and meta-analysis.

Conclusion

In the current Research Topic, we highlighted the importance of the development of new biomarkers for early diagnosis of many neurological disorders. We are at a pivotal juncture in human history, one that may forever alter our culture's approach to the treatment of neurological illnesses. Developing effective policies for preventing, assessing, and treating many neurological disorders, as well as allocating responsibility when they occur, is hindered by our current inability to use sufficiently objective tests for

diagnosis, prognosis, and monitoring of neurological disorders. While the objective symptoms of certain neurological disorders are being established, the great majority are not yet suitable for use in a clinical context where they may influence diagnosis, prognosis, and therapy. However, despite their potential, most of them are not ready for implementation in established legal or policy frameworks. There is a risk of exploitation of the legal system for unjust gain if blood biomarkers are not adequately standardized for their correct and reliable application in both the therapeutic and legal spheres. In all of this, courts will have the difficult issue of deciding what scientific evidence is admissible. The ultimate goal of biomarker development is to enhance clinical treatment for persons who have suffered from neurological illnesses, to create legislation that is consistent and well-informed concerning certain neurological diseases like TBI, and to provide more accurate and fair outcomes in litigation involving neurological disorders.

Author contributions

All authors listed have made a substantial, direct, and intellectual contribution to the work and approved it for publication.

Acknowledgments

We sincerely acknowledge all the authors for their articles and the reviewers who have contributed to improving and clarifying these diverse contributions due to their valuable comments. Finally, we thank the Specialty Chief Editors and the Frontiers in Neurology of for their continuous support.

Conflict of interest

The authors declare that the research was conducted in the absence of any commercial or financial relationships that could be construed as a potential conflict of interest.

Publisher's note

References

1. FDA-NIH Biomarker Working Group. BEST (Biomarkers, EndpointS, and other Tools) Resource. In: *Food and Drug Administration (US), Silver Spring (MD) Bethesda (MD).* (2016)

frontiers | Frontiers in Neurology

TYPE Original Research
PUBLISHED 08 August 2022
DOI 10.3389/fneur.2022.954631

OPEN ACCESS

EDITED BY
Wael M. Y. Mohamed,
International Islamic University Malaysia, Malaysia

REVIEWED BY
Ilaria Maestrini,
Policlinico Tor Vergata, Italy
Chang Liu,
Second Affiliated Hospital of Chongqing Medical University, China

*CORRESPONDENCE
Cheng-Liang Zhang
chengliang19890721@163.com

SPECIALTY SECTION
This article was submitted to Neurological Biomarkers, a section of the journal Frontiers in Neurology

RECEIVED 27 May 2022
ACCEPTED 18 July 2022
PUBLISHED 08 August 2022

CITATION
Wang C-L, Xu Y-W, Yan X-J and Zhang C-L (2022) Usability of serum annexin A7 as a biochemical marker of poor outcome and early neurological deterioration after acute primary intracerebral hemorrhage: A prospective cohort study. *Front. Neurol.* 13:954631. doi: 10.3389/fneur.2022.954631

Usability of serum annexin A7 as a biochemical marker of poor outcome and early neurological deterioration after acute primary intracerebral hemorrhage: A prospective cohort study

Chuan-Liu Wang[1], Yan-Wen Xu[1], Xin-Jiang Yan[2] and Cheng-Liang Zhang[1]*

[1]Department of Neurology, The Quzhou Affiliated Hospital of Wenzhou Medical University, Quzhou People's Hospital, Quzhou, China, [2]Department of Neurosurgery, The Quzhou Affiliated Hospital of Wenzhou Medical University, Quzhou People's Hospital, Quzhou, China

Objective: Annexin A7 (ANXA7), a calcium-dependent phospholipid-binding protein, may act to aggravate brain injury. This study aimed to assess the clinical utility of serum ANXA7 as a predictor of severity, early neurological deterioration (END), and prognosis after intracerebral hemorrhage (ICH).

Methods: A total of 126 ICH patients and 126 healthy controls were enrolled. Symptomatic severity was evaluated utilizing the National Institutes of Health Stroke Scale (NIHSS) score. The lesion volume of ICH was measured according to the ABC/2 method. END was referred to as an increase of 4 or greater points in the NIHSS score or death at post-stroke 24 h. The unfavorable functional outcome was a combination of death and major disability at post-stroke 90 days.

Results: Serum ANXA7 levels were significantly higher in patients than in controls (median, 46.5 vs. 9.7 ng/ml; $P < 0.001$). Serum ANXA7 levels were independently correlated with NIHSS score [beta: 0.821; 95% confidence interval (CI): 0.106–1.514; variance inflation factor: 5.180; $t = 2.573$; $P = 0.014$] and hematoma volume (beta: 0.794; 95% CI: 0.418–1.173; variance inflation factor: 5.281; $t = 2.781$; $P = 0.007$). Serum ANXA7 levels were significantly elevated with increase in modified Rankin scale scores ($P < 0.001$). Also, serum ANXA7, which was identified as a categorical variable, independently predicted END and an unfavorable outcome with odds ratio values of 3.958 (95% CI: 1.290–12.143; $P = 0.016$) and 2.755 (95% CI: 1.051–7.220; $P = 0.039$), respectively. Moreover, serum ANXA7 levels efficiently differentiated END (area under the curve: 0.781; 95% CI: 0.698–0.849) and an unfavorable outcome (area under the curve: 0.776; 95% CI: 0.693–0.846).

Conclusion: Serum ANXA7 may represent a useful blood-derived biomarker for assessing the severity, END, and prognosis of ICH.

KEYWORDS

biomarkers, intracerebral hemorrhage, severity, functional outcome, early neurological deterioration, annexin A7

Introduction

Intracerebral hemorrhage (ICH), one of the most severe forms of stroke, accounts for 15–20% of all strokes and is characterized by high morbidity and mortality (1). After ICH, blood rapidly accumulates within the surrounding brain, thereby resulting in primary brain injury (2). Afterward, secondary brain injury is induced, which involves inflammatory response, neuronal apoptosis, disrupted blood-brain barrier, and brain edema, finally resulting in neurological dysfunction (2). In general, the National Institutes of Health Stroke Scale (NIHSS) score, Glasgow Coma Scale (GCS) score, ICH score, and bleeding size are the four most common prognostic determinants of ICH (3–5). Early neurological deterioration (END) is an adverse event often encountered during the early period of ICH, and its occurrence markedly increases the risk of poor outcome (6). In recent decades, a growing body of study has focused on exploring blood-derived biochemical markers to facilitate the development of END and outcome predictions after ICH (7, 8).

Annexins are well-known as calcium-dependent phospholipid-binding proteins and are implicated in multiple cellular functions, including membrane trafficking, Ca^{2+} homeostasis, and exocytosis (9). Annexin A7 (ANXA7), also named synexin, is the first isolated annexin (10). In the central nervous system, ANXA7 was found mainly in human and animal neurons (11–15). Moreover, its expression was significantly upregulated in brain tissues of rats with traumatic brain injury (11), ICH (12), subarachnoid hemorrhage (13), or acquired epilepsy (14), and even in those of refractory epilepsy patients (15). Experimental data showed that ANXA7 may function to aggravate brain damage *via* affecting glutamate release, inducing neuronal apoptosis, disrupting the blood–brain barrier, and increasing brain edema, thereby worsening neurological function after traumatic brain injury (11), ICH (12), and subarachnoid hemorrhage (13). Hence, it is postulated that ANXA7 may be a biomarker of acute brain injury. However, to the best of our knowledge, ANXA7 has not been measured in human peripheral blood after acute brain injury. This study was designed to assess whether serum ANXA7 levels are associated with illness severity, END, and neurological functional outcome after ICH.

Abbreviations: AUC, area under the curve; CI, confidence interval; CT, computerized tomography; ICH, intracerebral hemorrhage; NIHSS, National Institutes of Health Stroke Scale; OR, odds ratio; ROC, receiver operating characteristic; 95% CI, 95% confidence interval; ANXA7, annexin A7.

Materials and methods

Study design and participant selection

In this prospective, cohort study performed at our hospital between May 2018 and May 2021, patients with non-traumatic first-ever ICH were consecutively enrolled. Next, we excluded those patients with age of <18 years, hospital admission of >24 h after stroke onset, a surgical evacuation of hematoma, primary intraventricular hemorrhage, bleedings resulting from other causes (e.g., intracranial tumor, cerebral arteriovenous malformation, hemorrhagic transformation of cerebral infarction, moyamoya disease, and intracranial aneurysm), history of neurological diseases (for instance, ischemic or hemorrhagic stroke, severe traumatic brain injury, and multiple sclerosis), or other specific diseases or conditions (such as autoimmune diseases, malignancies, pregnancies, uremia, liver cirrhosis, and chronic heart or lung disease). In addition, a group of healthy volunteers was recruited as controls.

This study was carried out in compliance with the tenets of the Declaration of Helsinki and the protocol confirmed with the ethical standards of our hospital on human subjects. The study protocol was approved by the Human Investigations Committee at our hospital. We acquired written informed consent to participate in this study from legal representatives of patients or controls themselves.

Clinical assessment and biochemical investigations

Upon arrival at the emergency center, we collected some data including demographics (age and gender), vascular risk factors (hypertension, diabetes mellitus, and hyperlipidemia), lifestyle risk factors (cigarette smoking and alcohol drinking), medication history (use of statins, anticoagulation drugs, and antiplatelet drugs), anthropometric measurements (systolic blood pressure, diastolic blood pressure, and body mass index), and time from stroke onset to hospital admission. The stroke symptomatic severity was assessed using the NIHSS (16). The severity of the stroke consciousness was evaluated using GCS (17). Hematoma volume was estimated in accordance with the ABC/2 method (18). Hematoma locations were divided into infratentorial and lobar hemorrhages. Extension of hematoma into the intraventricular cavity or subarachnoidal space was also recorded. ICH score was estimated based on age, hematoma volume, GCS score, infratentorial hemorrhage, and extension of hematoma into the intraventricular cavity (3). END was referred to as an increase of ≥4 points in the NIHSS score or death at 24 h from symptoms onset (19). ICH patients were followed up until death or completion of 90 days after ICH.

An unfavorable outcome was defined as a combination of death and major disability [modified Rankin Scale score (mRS) of 3 or greater] (20).

Venous blood samples were obtained from ICH patients at emergency center and from controls at entry into the study. We performed some routine blood tests, including white blood cell count, serum C-reactive protein levels, and blood glucose levels. In order to determine ANXA7 levels, serum was stored at −80°C until assayed. The same technician, who was blinded to study data, employed a commercial enzyme-linked immunosorbent assay kit (Shanghai Beinuo Biotechnology Co., Ltd, China) to gauge serum ANXA7 levels in all participants based on the manufacturer's instructions. Samples were measured in duplicate, and the mean value of two measurements was utilized for further statistical analysis.

Statistical analysis

The statistical software used in this study were the Statistical Package for the Social Sciences version 19.0 (SPSS Inc., Chicago, IL, United States) and MedCalc 9.6.4.0 (MedCalc Software,

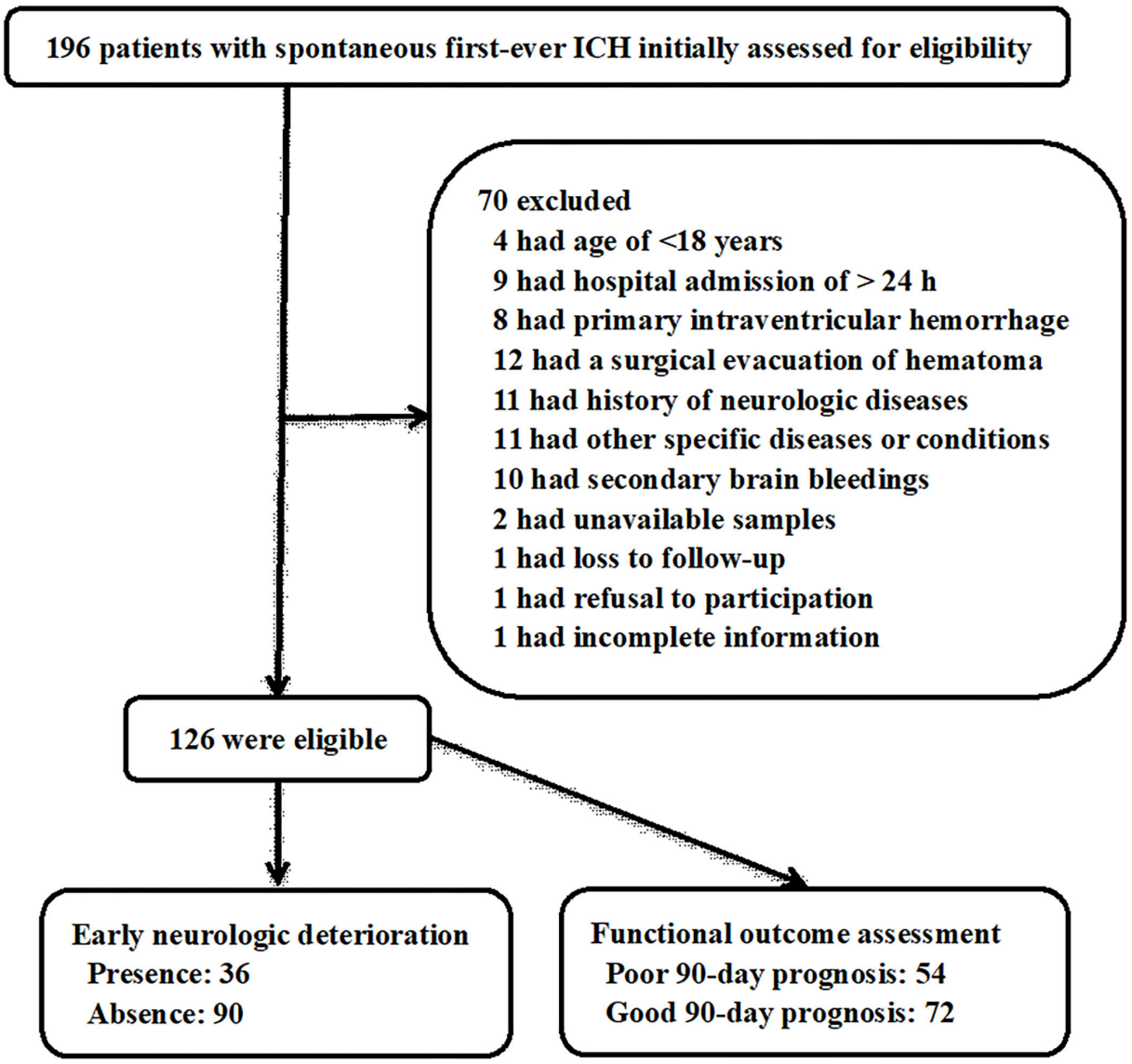

FIGURE 1
Flowchart for selecting eligible patients with spontaneous intracerebral hemorrhage. A total of 196 intracerebral hemorrhage patients were first screened and then 70 of them were excluded from this study. Finally, a total of 126 patients were eligible for further analysis, among whom, there were 36 patients with early neurological deterioration and 54 with poor prognosis at 90 days after stroke. ICH, intracerebral hemorrhage.

Mariakerke, Belgium), and graphs were plotted using the GraphPad Prism 5.0 software (GraphPad Software, La Jolla, CA, United States). Qualitative variables were shown as counts (percentages). After the Kolmogorov–Smirnov test, normally and non-normally distributed quantitative data were presented as means ± standard deviations and medians (lower-upper quartiles), respectively. The differences in baseline demographic, clinical, radiological, and biochemical data between the two groups were determined using the chi-square test, Fisher's exact test, independent *t*-test, or Mann–Whitney *U* test where appropriate. Serum ANXA7 levels were compared among multiple groups using Kruskal–Wallis *H* test. Spearman correlation analysis was carried out to assess the bivariate correlations between serum ANXA7 levels and other variables, and ρ values were reported for showing correlations. The multivariate linear regression model, which included other significantly pertinent variables ($P < 0.05$) in univariate correlation analysis, was built to determine factors, which were independently correlated with serum ANXA7 levels. The influence of serum ANXA7 levels on the occurrence of END or the development of an unfavorable outcome was investigated using multivariate logistic regression analysis, which allowed adjustment for some conventional confounding factors (e.g., age, NIHSS scores, hematoma volume, GCS scores, and intraventricular hemorrhage), which were also significant ($P < 0.05$) on univariate analysis. The results were reported as odds ratio (OR) and 95% confidence interval (CI) to show associations. However, as the ICH score was composed of 5 subcomponents, namely, age, hematoma volume, GCS score, infratentorial hemorrhage, and extension of hematoma into the intraventricular cavity, the ICH score was not incorporated into the multivariate model. Area under the receiver operating characteristic (ROC) curve (AUC) and the corresponding 95% CI were calculated to reflect the predictive ability. Using the Youden method, an optimal value of serum ANXA7 levels was selected, which generated the corresponding sensitivity and specificity values. A *P*-value of <0.05 indicated significance.

Results

Participant characteristics

In this study, we first enrolled a total of 196 patients with non-traumatic first-ever ICH and thereafter excluded

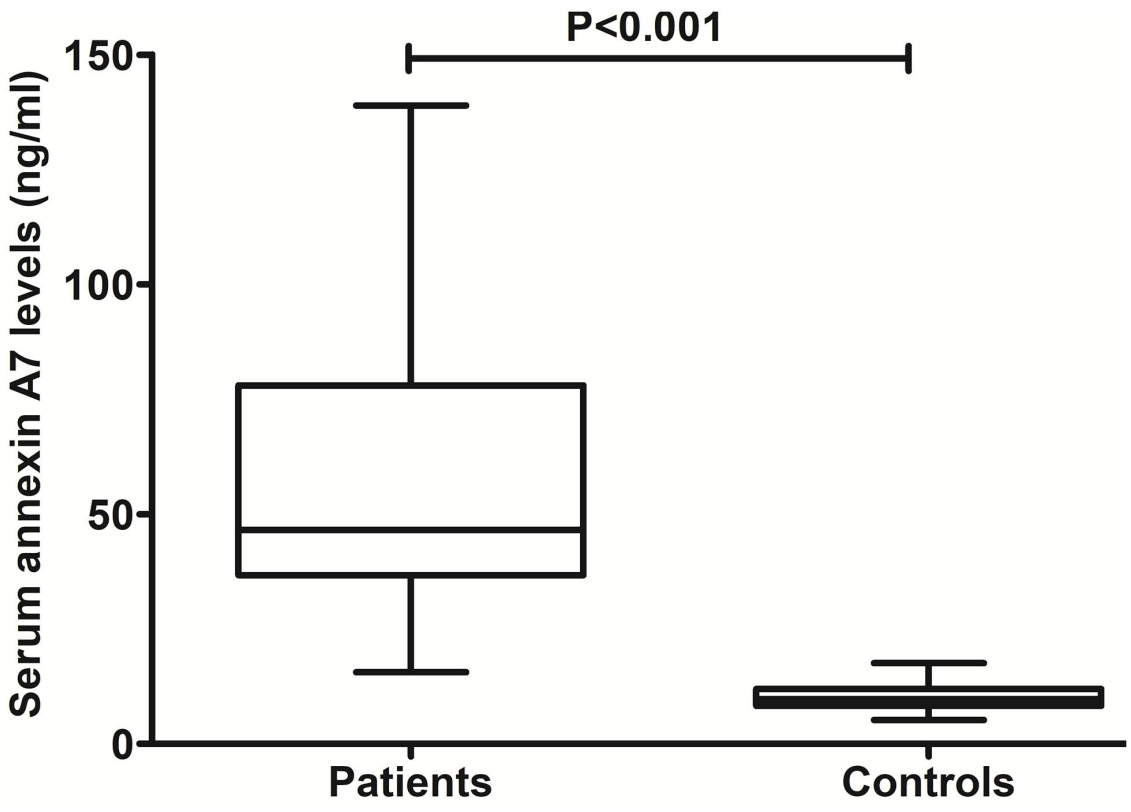

FIGURE 2
Change of serum annexin A7 levels after spontaneous intracerebral hemorrhage. There was a substantial enhancement in serum annexin A7 levels of patients with intracerebral hemorrhage relative to healthy controls using the Mann–Whitney *U* test ($P < 0.001$).

70 patients due to reasons that are outlined in Figure 1. Ultimately, a total of 126 eligible ICH patients were included in the study analysis. In addition, 126 healthy controls were enrolled, who were aged from 24 to 88 years (mean, 58.1 years; standard deviation, 14.3 years) and included 68 males and 58 females. Age and gender did not differ significantly between 126 ICH patients and 126 healthy controls (both $P > 0.05$).

The stroke patients, 70 being males and 56 being females, were aged from 40 to 82 years (mean, 59.6 years; standard deviation, 10.9 years). Body mass index ranged from 19.7 to 30.3 kg/m^2 (mean, 25.0 kg/m^2; standard deviation, 1.9 kg/m^2). Vascular risk factors included hypertension (78 patients, 61.9%), diabetes mellitus (20 patients, 15.9%), and hyperlipidemia (36 patients, 28.6%). Adverse lift habits comprised cigarette smoking (40 patients, 31.8%) and alcohol drinking (42 patients, 33.3%). Previous specific oral medications included statins (28 patients, 22.2%), anticoagulation drugs (8 patients, 6.4%), and antiplatelet drugs (17 patients, 13.5%). The median time was 12.0 h (range, 0.5–24.0 h; lower-upper quartiles, 7.5–18.8 h)

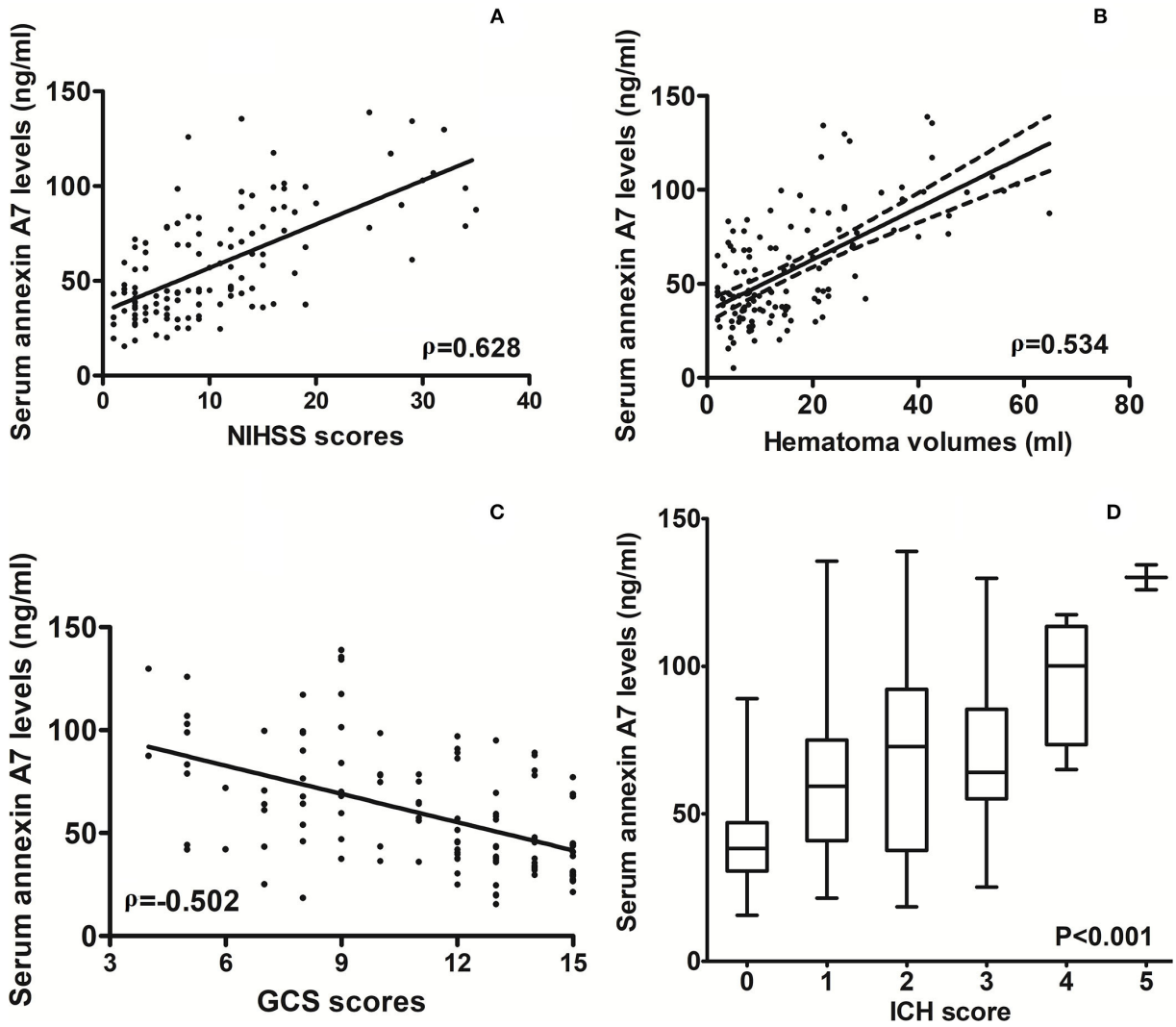

FIGURE 3
Relationship between serum annexin A7 levels and illness severity after spontaneous intracerebral hemorrhage. **(A)** Correlation of serum annexin A7 levels with National Institutes of Health Stroke Scale scores following acute intracerebral hemorrhage. **(B)** Relationship between serum annexin A7 levels and hematoma volume after acute intracerebral hemorrhage. **(C)** Relation of serum annexin A7 levels to Glasgow Coma Scale scores after acute intracerebral hemorrhage. **(D)** Differences in serum annexin A7 levels across intracerebral hemorrhage scores. Bivariate correlations were analyzed using the Spearman's correlation coefficient, and associations were reported as *r* values. Comparison of data was done among multiple groups using the Kruskal–Wallis *H* test. Graphs show that serum annexin A7 levels were significantly associated with stroke severity (all $P < 0.001$). NIHSS, National Institutes of Health Stroke Scale; GCS, Glasgow Coma Scale; ICH, intracerebral hemorrhage.

from stroke onset to hospital admission, and the median time was 14.0 h (range, 1.0–29.0 h; lower-upper quartiles, 9.0–20.5 h) from stroke onset to blood acquirement. Mean values of systolic arterial pressure, diastolic arterial pressure, and mean arterial pressure were 162.2 ± 24.3 mmHg, 90.0 ± 17.0 mmHg, and 114.1 ± 17.9 mmHg, respectively. Lobar and infratentorial hemorrhages were found in 26 (20.6%) and 19 patients (15.1%), respectively. Extensions of hematomas into the intraventricular cavity and subarachnoidal space were revealed in 22 (17.5%) and 9 patients (7.1%), respectively. Median values of NIHSS score, GCS score, and ICH score were 9 (lower-upper quartiles, 4–14), 12 (lower-upper quartiles, 9–14), and 1 (lower-upper quartiles, 0–2), respectively. Median hematoma volume was 12 ml (lower-upper quartiles, 7–22 ml). In aggregate, 36 patients (28.6%) experienced END, and 54 patients (42.9%) had an unfavorable outcome at post-stroke 90 days.

TABLE 1 Correlated factors of serum annexin A7 levels after acute intracerebral hemorrhage.

Variables	ρ	*P*-value
Age (years)	0.151	0.091
Gender (male/female)	0.134	0.136
Body mass index (kg/m^2)	0.143	0.109
Hypertension	0.017	0.851
Diabetes mellitus	0.195	0.028
Hyperlipidemia	0.093	0.298
Current smoking	0.063	0.483
Alcohol consumption	0.122	0.174
Previous use of statins	0.081	0.367
Previous use of anticoagulation drugs	−0.167	0.062
Previous use of antiplatelet drugs	0.011	0.901
Time from onset to inclusion (h)	0.108	0.228
Time from onset to blood-collection (h)	0.123	0.172
Systolic arterial pressure (mmHg)	0.163	0.067
Diastolic arterial pressure (mmHg)	0.102	0.254
Mean arterial pressure (mmHg)	0.119	0.183
Lobar hemorrhage	0.115	0.201
Infratentorial hemorrhage	0.159	0.076
Intraventricular hemorrhage	0.427	<0.001
Subarachnoidal hemorrhage	0.274	0.002
NIHSS score	0.628	<0.001
Hematoma volume (ml)	0.534	<0.001
ICH score	0.491	<0.001
Glasgow coma scale score	−0.502	<0.001
Blood leucocyte count (×10^9/l)	0.152	0.088
Serum glucose levels (mmol/l)	0.419	<0.001
Serum C-reactive protein levels (mg/l)	0.371	<0.001

Statistical analysis was done using the Spearman's correlation coefficient. NIHSS, National Institutes of Health Stroke Scale; ICH, intracerebral hemorrhage.

Serum ANXA7 levels and hemorrhagic severity

As compared to healthy controls, there was a significant elevation of serum ANXA7 levels in ICH patients (Figure 2, $P < 0.001$). In this study, NIHSS scores, GCS scores, hematoma volume, and ICH scores were estimated as the severity indicators of ICH. Serum ANXA7 levels were strongly correlated with NIHSS scores (Figure 3A, $P < 0.001$), hematoma volume (Figure 3B, $P < 0.001$), and GCS scores (Figure 3C, $P < 0.001$); serum ANXA7 levels were significantly raised with increasing ICH scores (Figure 3D, $P < 0.001$).

Table 1 shows that serum ANXA7 levels were closely correlated with diabetes mellitus, extension of hematoma into the intraventricular cavity, extension of hematoma into subarachnoidal space, NIHSS scores, hematoma volume, GCS scores, ICH scores, serum glucose levels, and serum C-reactive protein levels (all $P < 0.05$). When the aforementioned variables, except ICH scores, were forced into the multivariate linear regression model, we found that serum ANXA7 levels were independently correlated with NIHSS scores (beta: 0.821; 95% CI: 0.106–1.514; variance inflation factor: 5.180; $t = 2.573$; $P = 0.014$) and hematoma volume (beta: 0.794; 95% CI: 0.418–1.173; variance inflation factor: 5.281; $t = 2.781$; $P = 0.007$).

Serum ANXA7 levels and END

In Figure 4A, serum ANXA7 levels were substantially higher in patients with development of END than in those not suffering from END ($P < 0.001$). Serum ANXA7 levels had significantly efficient discriminatory ability for patients at risk of END with an AUC of 0.781 (95% CI: 0.698–0.849). Using the maximum Youden index (namely, 0.489), 57.4 ng/ml was selected as an optimal cutoff value of serum ANXA7 levels, which differentiated patients who experienced END with medium-high sensitivity and specificity (Figure 4B).

Table 2 shows that, as compared to patients not experiencing END, those at risk of END had significantly raised possibility of serum annexin A7 levels >57.4 ng/ml and extension of hematoma into intraventricular cavity, tended to display substantially increased NIHSS scores, hematoma volume, ICH scores, blood leucocyte count, blood glucose levels, and serum C-reactive protein levels, as well as exhibited markedly decreased GCS scores (all $P < 0.05$). Using multivariate analysis, serum annexin A7 levels >57.4 ng/ml independently predicted END after adjustment for intraventricular hemorrhage, NIHSS scores, hematoma volume, and GCS scores (Table 3).

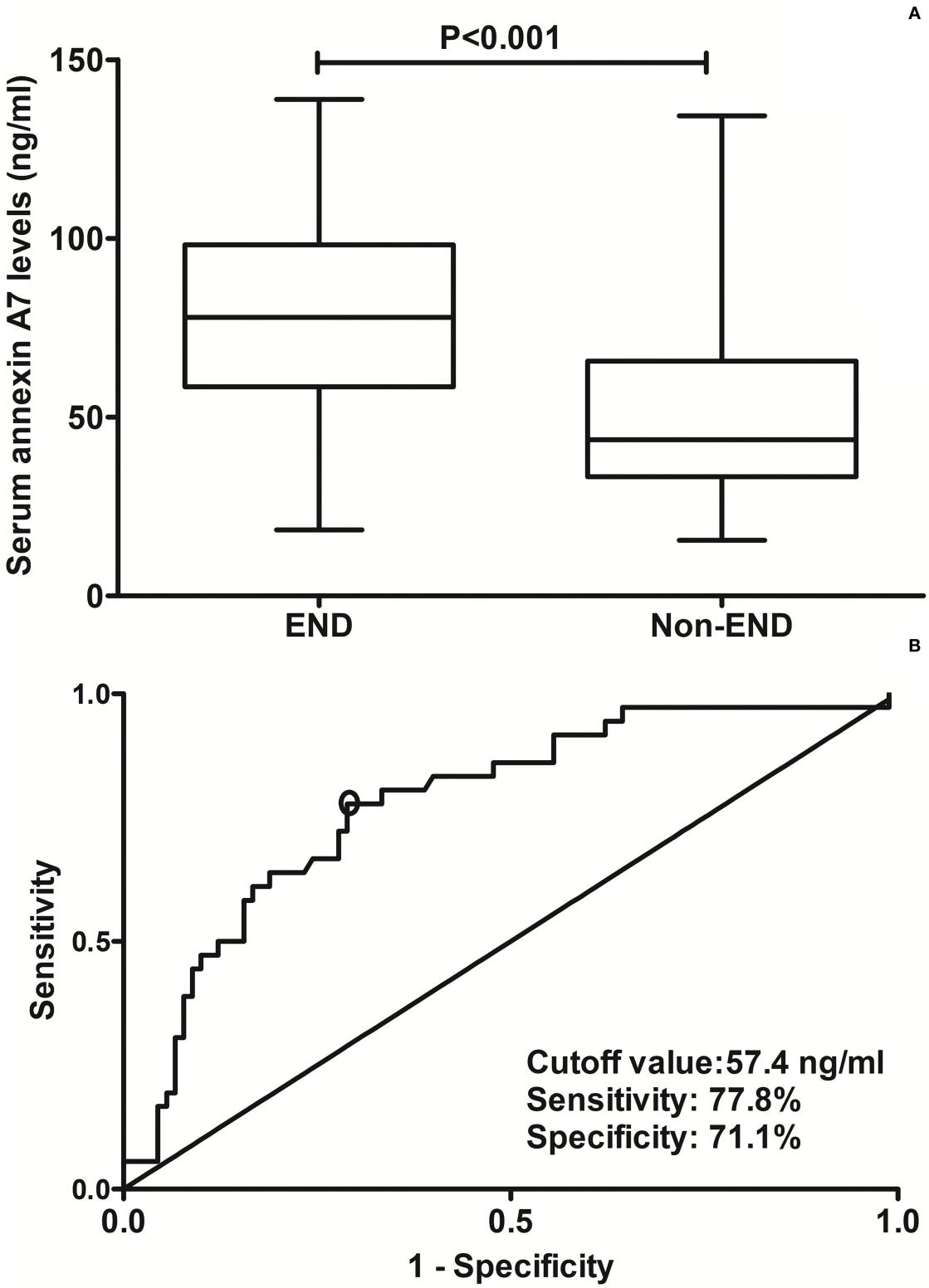

FIGURE 4
Analysis regarding the predictive value of serum annexin A7 levels for early neurological deterioration after acute intracerebral hemorrhage. **(A)** Comparison of serum annexin A7 levels between patients with development of early neurological deterioration and those not presenting with early neurological deterioration. **(B)** Assessment of the discriminatory ability of serum annexin A7 levels for early neurological deterioration

(Continued)

FIGURE 4
under the receiver operating characteristic curve. Serum annexin A7 levels were dramatically higher in patients suffering from early neurological deterioration than in those who did not using Mann–Whitney *U* test ($P < 0.001$). Serum annexin A7 levels significantly discriminate risk of early neurological deterioration with an area under the curve at 0.781 (95% confidence interval: 0.698–0.849). Using maximum Youden index, serum annexin A7 levels above 57.4 ng/ml differentiated development of END with medium-high sensitivity and specificity. END, early neurological deterioration.

TABLE 2 Related factors of early neurological deterioration in acute intracerebral hemorrhage.

Variables	Early neurologic deterioration		P Value
	Presence ($n = 36$)	Absence ($n = 90$)	
Age (years)	62.1 ± 10.4	58.7 ± 10.9	0.107
Gender (male/female)	21/15	49/41	0.691
Body mass index (kg/m^2)	25.4 ± 1.7	24.8 ± 1.9	0.110
Hypertension	26 (72.2%)	52 (57.8%)	0.131
Diabetes mellitus	8 (22.2%)	12 (13.3%)	0.217
Hyperlipidemia	12 (33.3%)	24 (26.7%)	0.454
Current smoking	8 (22.2%)	32 (35.6%)	0.146
Alcohol consumption	13 (36.1%)	29 (32.2%)	0.676
Previous use of statins	9 (25.0%)	19 (21.1%)	0.635
Previous use of anticoagulation drugs	1 (2.8%)	7 (7.8%)	0.438
Previous use of antiplatelet drugs	8 (22.2%)	9 (10.0%)	0.086
Time from onset to inclusion (h)	12.0 (6.0–17.5)	12.0 (8.0–20.0)	0.422
Time from onset to blood-collection (h)	13.0 (8.0–20.0)	14.0 (9.0–22.0)	0.276
Systolic arterial pressure (mmHg)	165.4 ± 27.6	160.8 ± 22.8	0.337
Diastolic arterial pressure (mmHg)	92.8 ± 23.3	88.9 ± 13.6	0.350
Mean arterial pressure (mmHg)	117.0 ± 23.5	112.9 ± 15.1	0.242
Lobar hemorrhage	5 (13.9%)	21 (23.3%)	0.237
Infratentorial hemorrhage	4 (11.1%)	15 (16.7%)	0.431
Intraventricular hemorrhage	19 (25.0%)	3 (3.3%)	<0.001
Subarachnoidal hemorrhage	3 (8.3%)	6 (6.7%)	0.714
NIHSS score	15 (12–18)	7 (3–12)	< 0.001
Hematoma volume (ml)	27.8 (15.4–42.1)	8.7 (6.2–15.0)	< 0.001
ICH score	2 (1–3)	0 (0–1)	< 0.001
Glasgow coma scale score	8 (7–12)	13 (10–14)	< 0.001
Blood leucocyte count ($\times 10^9$/l)	9.2 (6.8–13.0)	7.9 (6.4–9.9)	0.041
Serum glucose levels (mmol/l)	11.1 (9.0–12.3)	8.7 (7.5–12.0)	0.032
Serum C-reactive protein levels (mg/l)	16.1 (14.5–21.1)	13.9 (12.0–17.2)	0.015
Serum annexin A7 levels > 57.4 ng/ml	28 (77.8%)	26 (28.9%)	< 0.001

Variables were presented as count (percentage), median (upper-lower quartiles), or mean ± standard deviation as appropriate. Statistical methods included the chi-square test, Fisher's exact test, unpaired Student's t-test, and Mann–Whitney U test. NIHSS, National Institutes of Health Stroke Scale; ICH, intracerebral hemorrhage.

Serum ANXA7 levels and 90-day unfavorable outcome

In Figure 5A, serum ANXA7 levels were substantially elevated after ICH, with increasing mRS scores at post-stroke 90 days. In addition, patients with mRS scores of 3–6 had significantly higher serum ANXA7 levels than those with mRS scores of 0–2 (Figure 5B, $P < 0.001$). Moreover, serum ANXA7 levels significantly discriminated against patients who experienced 90-day unfavorable outcome, with AUC at 0.776 (95% CI: 0.693–0.846), and serum ANXA7 levels above 57.0 ng/ml predicted patients with an unfavorable outcome with medium-high sensitivity and specificity (Figure 5C).

Just as listed in Table 4, there were substantial differences in terms of age, NIHSS scores, hematoma volume, ICH scores, GCS scores, serum glucose levels, and serum C-reactive protein levels, as well as percentages of serum ANXA7 levels above 57.0 ng/ml and extension of hematoma into the intraventricular cavity (all *P*

TABLE 3 Relation of serum annexin A7 levels to early neurological deterioration using multivariate analysis.

	B	S.E.	Wals	Odds ratio (95% CI)	*P*
Model 1	2.154	0.463	21.591	8.615 (3.474–21.369)	<0.001
Model 2	1.376	0.572	5.785	3.958 (1.290–12.143)	0.016

In model 1, results were reported using univariate binary logistic regression analysis. In model 2, results were shown using multivariate binary logistic regression analysis, with adjustment for intraventricular hemorrhage, National Institutes of Health Stroke Scale scores, hematoma volume, and Glasgow Coma Scale score. 95% CI indicates 95% confidence interval.

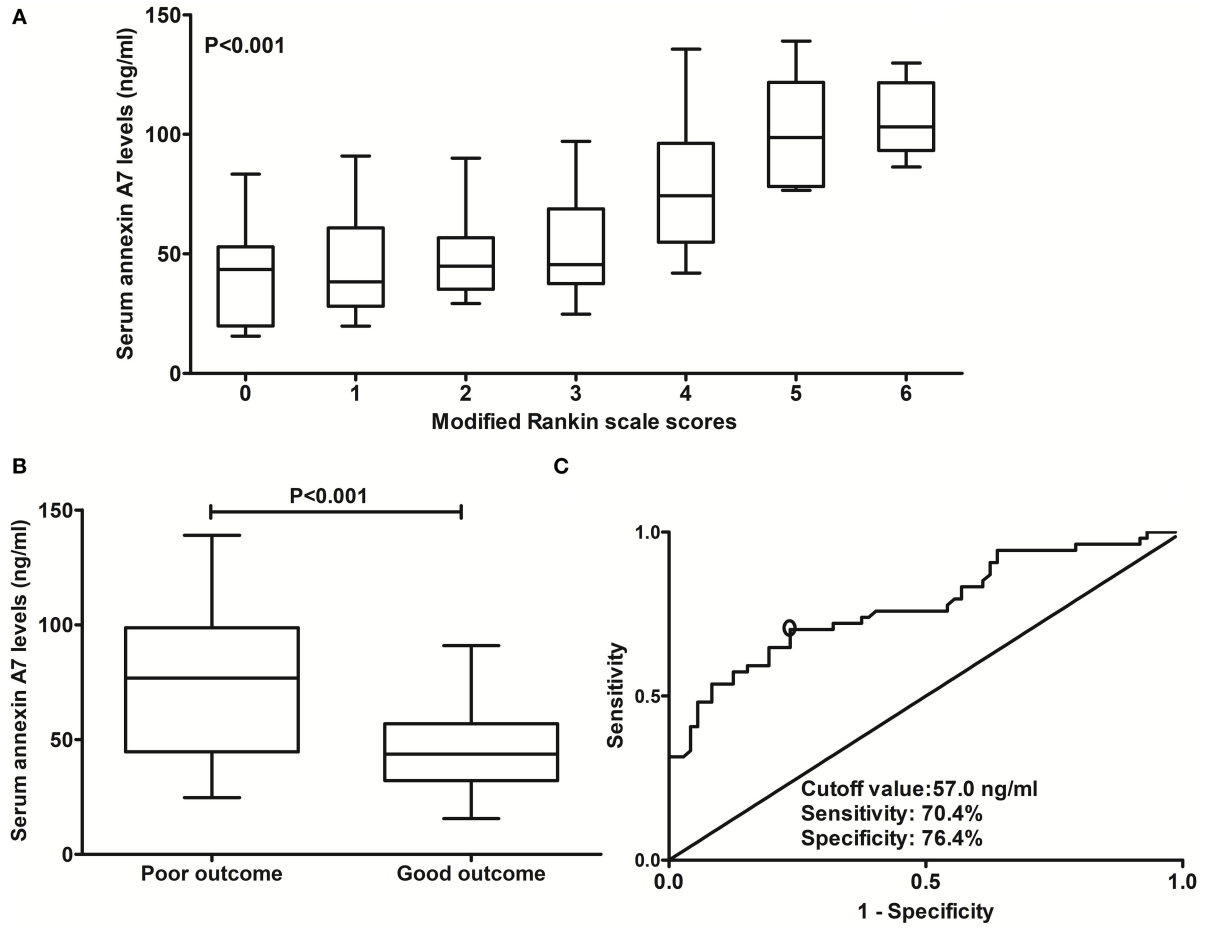

FIGURE 5
Relationship between serum annexin A7 levels and prognosis at 90 days after intracerebral hemorrhage. **(A)** Relationship between serum annexin A7 levels and modified Rankin Scale score among patients with acute intracerebral hemorrhage. **(B)** Comparison of serum annexin A7 levels between patients with poor outcome and those with a good outcome. **(C)** Analysis with respect to the predictive value of serum annexin A7 levels for 90-day poor outcome after acute intracerebral hemorrhage. Comparison of data was done among multiple groups using the Kruskal–Wallis *H* test. There was a significant elevation of serum annexin A7 levels after hemorrhagic stroke by modified Rankin Scale scores ($P < 0.001$). Serum annexin A7 levels were dramatically higher in patients with poor outcome than in those with good outcome using Mann–Whitney *U* test ($P < 0.001$). Serum annexin A7 levels significantly predicted 90-day poor outcome, with area under the curve at 0.776 (95% confidence interval: 0.693–0.846); and serum annexin A7 levels above 57.0 ng/ml predicted a poor outcome with medium-high sensitivity and specificity under the receiver operating characteristic curve. A poor outcome was referred to as a modified Rankin scale score above 2.

< 0.05). Using multivariate analysis, serum ANXA7 levels above 57.0 ng/ml were retained as the independent predictor of post-injury 90-day unfavorable outcome after adjustment for age, intraventricular hemorrhage, NIHSS scores, hematoma volume, and GCS scores (Table 5).

Discussion

To the best of our knowledge, this is the first series investigating the relationship between serum ANXA7 levels and severity plus prognosis after acute brain injury as well as

TABLE 4 Pertinent factors of 90-day poor outcome after acute intracerebral hemorrhage.

Variables	90-day poor outcome		*P*-value
	Presence ($n = 54$)	Absence ($n = 72$)	
Age (years)	62.5 ± 11.4	57.5 ± 10.0	0.011
Gender (male/female)	29/25	41/31	0.717
Body mass index (kg/m^2)	25.3 ± 2.1	24.7 ± 1.6	0.059
Hypertension	34 (63.0%)	44 (61.1%)	0.832
Diabetes mellitus	11 (20.4%)	9 (12.5%)	0.232
Hyperlipidemia	15 (27.8%)	21 (29.2%)	0.864
Current smoking	17 (31.5%)	23 (31.9%)	0.956
Alcohol consumption	19 (35.2%)	23 (31.9%)	0.703
Previous use of statins	13 (24.1%)	15 (20.8%)	0.665
Previous use of anticoagulation drugs	2 (3.7%)	6 (8.3%)	0.465
Previous use of antiplatelet drugs	7 (13.0%)	10 (13.9%)	0.880
Time from onset to inclusion (h)	12.0 (7.0–18.5)	11.5 (8.0–19.5)	0.875
Time from onset to blood-collection (h)	14.0 (8.0–20.0)	13.5 (9.0–21.5)	0.910
Systolic arterial pressure (mmHg)	163.5 ± 24.6	161.2 ± 24.2	0.601
Diastolic arterial pressure (mmHg)	92.8 ± 20.7	88.0 ± 13.3	0.112
Mean arterial pressure (mmHg)	116.4 ± 20.5	112.4 ± 15.6	0.216
Lobar hemorrhage	7 (13.0%)	19 (26.4%)	0.065
Infratentorial hemorrhage	8 (14.8%)	11 (15.3%)	0.943
Intraventricular hemorrhage	17 (31.5%)	5 (6.9%)	<0.001
Subarachnoidal hemorrhage	6 (11.1%)	3 (4.2%)	0.134
NIHSS score	13 (11–17)	6 (3–9)	<0.001
Hematoma volume (ml)	21.1 (14.0–36.9)	7.9 (5.0–12.9)	<0.001
ICH score	2 (1–2)	0 (0–1)	<0.001
Glasgow coma scale score	10 (8–12)	14 (10–15)	<0.001
Blood leucocyte count ($\times 10^9$/l)	8.8 (6.8–11.8)	7.9 (6.3–9.7)	0.068
Serum glucose levels (mmol/l)	10.2 (8.1–13.2)	8.6 (7.4–11.4)	0.029
Serum C-reactive protein levels (mg/l)	15.9 (13.1–21.0)	14.1 (11.8–16.2)	0.017
Serum annexin A7 levels >57.0 ng/ml	38 (70.4%)	17 (23.6%)	<0.001

Variables were presented as count (percentage), median (upper-lower quartiles), or mean ± standard deviation as appropriate. Statistical methods included the chi-square test, Fisher's exact test, unpaired Student's t-test, and Mann–Whitney U test. NIHSS, National Institutes of Health Stroke Scale; ICH, intracerebral hemorrhage.

TABLE 5 Relation of serum annexin A7 levels to 90-day poor outcome using multivariate analysis.

	B	S.E.	Wals	Odds ratio (95% CI)	*P*
Model 1	2.039	0.407	25.075	7.684 (3.459–17.069)	<0.001
Model 2	1.013	0.492	4.248	2.755 (1.051–7.220)	0.039

In model 1, results were reported using univariate binary logistic regression analysis. In model 2, results were shown using multivariate binary logistic regression analysis, with adjustment for age, intraventricular hemorrhage, National Institutes of Health Stroke Scale scores, hematoma volume, and Glasgow Coma Scale scores. 95% CI indicates 95% confidence interval.

subsequently showing the interesting results. The main findings of our study were that (1) there was a marked enhancement in serum ANXA7 levels after ICH, as compared to healthy controls; (2) serum ANXA7 levels were substantially correlated with NIHSS scores, bleeding size, GCS scores, and ICH scores following ICH; (3) serum ANXA7, which was identified as a categorical variable, remained as an independent predictor for END and 90-day unfavorable outcome after ICH; and (4) serum ANXA7 levels efficiently differentiated patients with END or 90-day unfavorable outcome among ICH patients. Overall, serum ANXA7 may be a promising biochemical variable for assessing stroke severity and predicting clinical outcome.

ANXA7 was predominantly located in neurons of normal human or animal cerebral cortices (11–15). Moreover, its

expression was greatly upregulated not only in brain tissues of rats with traumatic brain injury (11), ICH (12), subarachnoid hemorrhage (13), or acquired epilepsy (14) but also in those of refractory epilepsy patients (15). Specifically, ANXA7 protein expression was increased significantly in brain tissues of rats with acquired epilepsy at 6, 24, and 48 h after the onset of seizure (14). In neurons of rats with ICH, mRNA levels of ANXA7 were raised substantially from 6 h after ICH, reached the highest point at 24 h, and then declined gradually (12). After traumatic brain injury, expression levels of rat cortical ANXA7 increased during the 6-h period immediately, peaked in 24 h, plateaued at 48 h, decreased gradually thereafter, and was substantially higher than those in sham-operational rats during the 72-h period (11). Also, ANXA7 protein expression was enhanced markedly at 24 h following experimental subarachnoid hemorrhage (13). There was the median time of 14.0 h from stroke onset to blood acquirement in this study. We found a significant elevation of ANXA7 levels in the peripheral blood of humans with ICH. Taken together, ANXA7 expression is presumed to increase significantly in the acute period after acute brain injury. Because blood–brain barrier permeability is obviously enhanced after ICH (21), ANXA7 may be increasingly released from the central nervous system. Collectively, increased ANXA7 levels in the peripheral blood may be at least partially attributed to its release from brain tissues after ICH.

ANXA7 mainly functions in accordance with the Ca^{2+} concentration (22). And, *via* binding to the cell membrane, it can change the permeability of the cell membrane, thereby facilitating the release of neurotransmitters and vesicle transport (23). In rats with traumatic brain injury, the inhibition of ANXA7 using small interfering RNA significantly decreased the expression of A7 in the injured brain tissue, as well as also depressed brain edema, lessened blood–brain barrier permeability, attenuated cell death, and reduced neuronal apoptosis, as compared to the sham rats (11). In rats with subarachnoid hemorrhage, ANXA7 knockdown markedly reduced early brain injury *via* alleviating disruption of blood–brain barrier, ameliorating brain edema, and depressing neuronal apoptosis (13). Glutamate, *via* binding to N-methyl-D-aspartate (NMDA) receptors, induces excitotoxicity (24). ANXA7 knockdown dramatically decreased glutamate release from injured brain tissues in rats with subarachnoid hemorrhage (13). Synaptosome associated protein 25 (SNAP25) and SNAP23 are involved in presynaptic glutamate release and post-synaptic glutamate receptor (NMDA receptor) trafficking, respectively (25, 26). ANXA7 interacted with SNAP25 at presynaptic axon terminals and SNAP23 at post-synaptic axon terminals, subsequently mediating glutamate toxicity after ICH (12). Taken together, ANXA7 may aggravate secondary brain injury at least partially *via* promoting excitatory neurotoxicity; and ANXA7-targeting therapy may be a promising approach to attenuate secondary brain injury.

High expression of ANXA7 was intimately related to the poor neurological status of subarachnoid hemorrhage rats (13). However, it remains unclear whether circulating ANXA7 levels are associated with hemorrhagic severity and clinical outcome after acute brain injury. Generally, the rates of END and unfavorable outcome were ∼ 30 and 45%, respectively (7, 8, 27, 28). In our study, 36 patients (28.6%) experienced END, and 54 patients (42.9%) had an unfavorable outcome at post-stroke 90 days. Hence, our data about rates of END and unfavorable outcome after ICH were in line with previous reports (7, 8, 27, 28). In addition, 54 patients who developed a poor prognosis at 90 days included 36 patients with END at 24 h and 24 patients were in overlap between the two groups. Using multivariate analysis, our study found some interesting results that serum ANXA7 levels were independently associated with illness severity, END, and 90-day prognosis after ICH. Moreover, under ROC curve, serum ANXA7 levels possessed efficient prognostic predictive ability for END and 90-day poor prognosis, which was defined as mRS scores of 3–6. Such data may be supportive of the notion that serum ANXA7 may be a potential prognostic biomarker of acute brain injury.

There are several limitations to this study. First, when we investigated the relationship between serum ANXA7 levels and prognosis of ICH, we excluded those patients who underwent a surgical evacuation of hematoma in order to decrease the clinical heterogeneity. Although only a very small portion of patients (namely, 12 patients) were excluded from the final analysis, those excluded patients are likely to have developed END and, therefore, their exclusion may represent a selection bias. Second, we used multivariate analysis to demonstrate the relationship serum ANXA7 levels and severity, END, and prognosis after ICH. Compelling data have shown that END is related to poor prognosis (29, 30). It is significant to study the association of serum ANXA7 levels with a poor prognosis of ICH. Alternatively, univariate analysis has 20 variables. However, infection complications, malnutrition, and ischemic or hemorrhagic relapses may be confounding factors, which were not investigated in this study. Hence, a further study that includes such confounding factors is warranted.

Conclusion

This is the first series to ascertain whether serum ANXA7 levels are associated with stroke severity and clinical outcome of ICH. Using multivariate analysis, it is revealed that rising serum ANXA7 levels are dramatically related to NIHSS scores and hematoma volume, as well as END and 90-day unfavorable outcome after ICH. Hence, it is possible that serum ANAX7 levels can be used to reflect severity and clinical outcome after ICH.

Data availability statement

The raw data supporting the conclusions of this article will be made available by the authors, without undue reservation.

Ethics statement

The studies involving human participants were reviewed and approved by the Human Investigations Committee of the Quzhou Affiliated Hospital of Wenzhou Medical University. The patients/participants provided their written informed consent to participate in this study.

Author contributions

All authors listed have made a substantial, direct, and intellectual contribution to the work and approved it for publication.

Conflict of interest

The authors declare that the research was conducted in the absence of any commercial or financial relationships that could be construed as a potential conflict of interest.

Publisher's note

All claims expressed in this article are solely those of the authors and do not necessarily represent those of their affiliated organizations, or those of the publisher, the editors and the reviewers. Any product that may be evaluated in this article, or claim that may be made by its manufacturer, is not guaranteed or endorsed by the publisher.

References

1. Chan S, Hemphill JC III. Critical care management of intracerebral hemorrhage. *Crit Care Clin*. (2014) 30:699–17. doi: 10.1016/j.ccc.2014.06.003

2. Zheng H, Chen C, Zhang J, Hu Z. Mechanism and therapy of brain edema after intracerebral hemorrhage. *Cerebrovasc Dis*. (2016) 42:155–69. doi: 10.1159/000445170

3. Hemphill JC III, Bonovich DC, Besmertis L, Manley GT, Johnston SC. The ICH score: a simple, reliable grading scale for intracerebral hemorrhage. *Stroke*. (2001) 32:891–7. doi: 10.1161/01.STR.32.4.891

4. Cho DY, Chen CC, Lee HC, Lee WY, Lin HL. Glasgow Coma Scale and hematoma volume as criteria for treatment of putaminal and thalamic intracerebral hemorrhage. *Surg Neurol*. (2008) 70:628–33. doi: 10.1016/j.surneu.2007.08.006

5. Mantero V, Scaccabarozzi C, Aliprandi A, Sangalli D, Rifino N, Filizzolo M, et al. NIHSS as predictor of clinical outcome at 6 months in patients with intracerebral hemorrhage. *Neurol Sci*. (2020) 41:717–9. doi: 10.1007/s10072-019-04070-4

6. Leira R, Dávalos A, Silva Y, Gil-Peralta A, Tejada J, Garcia M, et al. Early neurologic deterioration in intracerebral hemorrhage: predictors and associated factors. *Neurology*. (2004) 63:461–7. doi: 10.1212/01.WNL.0000133204.81153.AC

7. Cai Y, Zhuang YK, Wu XY, Dong XQ, Du Q, Yu WH, et al. Serum hypoxia-inducible factor 1alpha levels correlate with outcomes after intracerebral hemorrhage. *Ther Clin Risk Manag*. (2021) 17:717–26. doi: 10.2147/TCRM.S313433

8. Wu XY, Zhuang YK, Cai Y, Dong XQ, Wang KY, Du Q, et al. Serum glucose and potassium ratio as a predictive factor for prognosis of acute intracerebral hemorrhage. *J Int Med Res*. (2021) 49:3000605211009689. doi: 10.1177/03000605211009689

9. Gerke V, Moss SE. Annexins: from structure to function. *Physiol Rev*. (2002) 82:331–71. doi: 10.1152/physrev.00030.2001

10. Laohavisit A, Davies JM. Annexins. *New Phytol*. (2011) 189:40–53. doi: 10.1111/j.1469-8137.2010.03533.x

11. Gao F, Li D, Rui Q, Ni H, Liu H, Jiang F, et al. Annexin A7 levels increase in rats with traumatic brain injury and promote secondary brain injury. *Front Neurosci*. (2018) 12:357. doi: 10.3389/fnins.2018.00357

12. Li H, Liu S, Sun X, Yang J, Yang Z, Shen H, et al. Critical role for annexin A7 in secondary brain injury mediated by its phosphorylation after experimental intracerebral hemorrhage in rats. *Neurobiol Dis*. (2018) 110:82–92. doi: 10.1016/j.nbd.2017.11.012

13. Lin QS, Wang WX, Lin YX, Lin ZY, Yu LH, Kang Y, et al. Annexin A7 induction of neuronal apoptosis via effect on glutamate release in a rat model of subarachnoid hemorrhage. *J Neurosurg*. (2019) 132:777–87. doi: 10.3171/2018.9.JNS182003

14. Zhou SN, Li CS, Liu LQ, Shen L, Li Y. Expression and localization of annexin A7 in the rat lithium-pilocarpine model of acquired epilepsy. *Chin Med J*. (2010) 123:2410–5. doi: 10.3760/cma.j.issn.0366-6999.2010.17.023

15. Zhou SN, Li CS, Liu LQ, Li Y, Wang XF, Shen L. Increased expression of annexin A7 in temporal lobe tissue of patients with refractory epilepsy. *Histol Histopathol*. (2011) 26:571–9. doi: 10.14670/HH-26.571

16. Kwah LK, Diong J. National Institutes of Health Stroke Scale (NIHSS). *J Physiother*. (2014) 60:61. doi: 10.1016/j.jphys.2013.12.012

17. Reith FC, Van den Brande R, Synnot A, Gruen R, Maas AI. The reliability of the Glasgow Coma Scale: a systematic review. *Intensive Care Med*. (2016) 42:3–15. doi: 10.1007/s00134-015-4124-3

18. Kothari RU, Brott T, Broderick JP, Barsan WG, Sauerbeck LR, Zuccarello M, et al. et al. The ABCs of measuring intracerebral hemorrhage volumes. *Stroke*. (1996) 27:1304–95. doi: 10.1161/01.STR.27.8.1304

19. Godoy DA, Boccio A. Early neurologic deterioration in intracerebral hemorrhage: predictors and associated factors. *Neurology*. (2005) 64:931–2. doi: 10.1212/WNL.64.5.931-a

20. Dong XQ, Yu WH, Zhu Q, Cheng ZY, Chen YH, Lin XF, et al. Changes in plasma thrombospondin-1 concentrations following acute intracerebral hemorrhage. *Clin Chim Acta*. (2015) 450:349–55. doi: 10.1016/j.cca.2015.09.013

21. Ballabh P, Braun A, Nedergaard M. The blood-brain barrier: an overview: structure, regulation, and clinical implications. *Neurobiol Dis*. (2004) 16:1–13. doi: 10.1016/j.nbd.2003.12.016

22. Li YZ, Wang YY, Huang L, Zhao YY, Chen LH, Zhang C. Annexin A protein family in atherosclerosis. *Clin Chim Acta*. (2022) 531:406–17. doi: 10.1016/j.cca.2022.05.009

23. Moss SE, Morgan RO. The annexins. *Genome Biol*. (2004) 5:219. doi: 10.1186/gb-2004-5-4-219

24. Chou TH, Tajima N, Romero-Hernandez A, Furukawa H. Structural basis of functional transitions in mammalian NMDA receptors. *Cell*. (2020) 182:357–71.e13. doi: 10.1016/j.cell.2020.05.052

25. Suh YH, Terashima A, Petralia RS, Wenthold RJ, Isaac JT, Roche KW, et al. A neuronal role for SNAP-23 in postsynaptic glutamate receptor trafficking. *Nat Neurosci*. (2010) 13:338–43. doi: 10.1038/nn.2488

26. Sørensen JB, Nagy G, Varoqueaux F, Nehring RB, Brose N, Wilson MC, et al. Differential control of the releasable vesicle pools by SNAP-25 splice variants and SNAP-23. *Cell*. (2003) 114:75–86. doi: 10.1016/S0092-8674(03)00477-X

27. Gu Y, Deng X, Liang C, Chen Y, Lei H, Zhang Q. Soluble triggering receptor expressed on myeloid cells-1 as a serum biomarker of early neurologic deterioration and prognosis in acute supratentorial intracerebral hemorrhage. *Clin Chim Acta*. (2021) 523:290–6. doi: 10.1016/j.cca.2021.10.010

28. Yan XJ, Li YB, Liu W, Dai WM, Wang CL. Predictive value of serum visinin-like protein-1 for early neurologic deterioration and three-month clinical outcome in acute primary basal ganglia hemorrhage: a prospective and observational study. *Clin Chim Acta*. (2022) 531:62–7. doi: 10.1016/j.cca.2022.03.008

29. Law ZK, Dineen R, England TJ, Cala L, Mistri AK, Appleton JP, et al. Predictors and outcomes of neurological deterioration in intracerebral hemorrhage: results from the TICH-2 Randomized Controlled Trial. *Transl Stroke Res*. (2021) 12:275–83. doi: 10.1007/s12975-020-00845-6

30. Specogna AV, Turin TC, Patten SB, Hill MD. Factors associated with early deterioration after spontaneous intracerebral hemorrhage: a systematic review and meta-analysis. *PLoS ONE*. (2014) 9:e96743. doi: 10.1371/journal.pone.0096743

frontiers | Frontiers in Neurology

TYPE Review
PUBLISHED 31 October 2022
DOI 10.3389/fneur.2022.1029891

OPEN ACCESS

EDITED BY
Wael M. Y. Mohamed,
International Islamic University Malaysia, Malaysia

REVIEWED BY
Alain Ndayisaba,
Brigham and Women's Hospital and Harvard Medical School, United States
Jessika Suescun,
University of Texas Health Science Center at Houston, United States

*CORRESPONDENCE
Hongyang Zhao
drzhaohongyang@163.com

SPECIALTY SECTION
This article was submitted to Neurological Biomarkers, a section of the journal Frontiers in Neurology

RECEIVED 28 August 2022
ACCEPTED 10 October 2022
PUBLISHED 31 October 2022

CITATION
Mao D, Zheng Y, Xu F, Han X and Zhao H (2022) HMGB1 in nervous system diseases: A common biomarker and potential therapeutic target. *Front. Neurol.* 13:1029891. doi: 10.3389/fneur.2022.1029891

HMGB1 in nervous system diseases: A common biomarker and potential therapeutic target

Di Mao[1], Yuan Zheng[2], Fenfen Xu[2], Xiao Han[2] and Hongyang Zhao[2]*

[1]Department of Pediatrics, Jinan Central Hospital, Shandong University, Jinan, China, [2]Department of Pediatrics, Central Hospital Affiliated to Shandong First Medical University, Jinan, China

High-mobility group box-1 (HMGB1) is a nuclear protein associated with early inflammatory changes upon extracellular secretion expressed in various cells, including neurons and microglia. With the progress of research, neuroinflammation is believed to be involved in the pathogenesis of neurological diseases such as Parkinson's, epilepsy, and autism. As a key promoter of neuroinflammation, HMGB1 is thought to be involved in the pathogenesis of Parkinson's disease, stroke, traumatic brain injury, epilepsy, autism, depression, multiple sclerosis, and amyotrophic lateral sclerosis. However, in the clinic, HMGB1 has not been described as a biomarker for the above-mentioned diseases. However, the current preclinical research results show that HMGB1 antagonists have positive significance in the treatment of Parkinson's disease, stroke, traumatic brain injury, epilepsy, and other diseases. This review discusses the possible mechanisms by which HMGB1 mediates Parkinson's disease, stroke, traumatic brain injury, epilepsy, autism, depression, multiple sclerosis, amyotrophic lateral sclerosis, and the potential of HMGB1 as a biomarker for these diseases. Future research needs to further explore the underlying molecular mechanisms and clinical translation.

KEYWORDS

HMGB1, biomarker, nervous system diseases, neuroinflammation, therapeutic target

Introduction

High-mobility group protein (HMG) was first discovered in bovine thymus in 1973 (1). Subsequent studies found that inhibition of high-mobility group-1 (HMG-1) protein could reduce the mortality of patients with sepsis, thus confirming the role of HMG-1 as an inflammatory factor (2). In 2000, Bustin (3) systematically classified the HMG family and divided them into three categories: high-mobility group-A (HMGA), high-mobility group box (HMGB), and high-mobility group-N (HMGN) according to their functions. Among them, HMGB was further divided into HMGB1, HMGB2, and HMGB3. HMGB1 is composed of three domains, including two DNA-binding domains (A box and B box) and an acidic tail (Figure 1) (4). Both A box and B box are composed of three α-helix structures, which can interact with deoxyribonucleic acid (DNA) nonspecifically (5). HMGB1 has two nuclear localization sequences (NLSs) located between the A box (aa 28–44) and the B box and C-terminal tail

(aa 179–185) (6). When immune cells respond to endogenous or exogenous stimuli such as endotoxin, interleukin, and hypoxia, HMGB1 can be actively released (7). Meanwhile, necrotic or damaged cells can passively release HMGB1 (8). In addition, phagocytosis of apoptotic cells by macrophages can lead to the further release of HMGB1 (9). HMGB1 utilizes various membrane receptors during its signaling cascade. Among the numerous HMGB1 extracellular receptors, the receptor for advanced glycation end products (RAGE) and toll-like receptor 4 (TLR4) are the widely studied and reported receptors. Binding to RAGE occurs at residues 150–183 of the molecule, while TLR4 binding occurs at residues 89–108 of the HMGB1 B box (6). HMGB1 binds to receptors such as TLR4 and RAGE and leads to the upregulation of cytokines by pro-inflammatory cells by activating nuclear factor kappa-light-chain-enhancer of activated B cells (NF-κB) and mitogen-activated protein (MAP) kinase signaling pathways (Figure 2).

Interestingly, overexpression of extracellular HMGB1 has been observed in clinical and preclinical studies on Parkinson's disease (10), stroke (11), traumatic brain injury (12), epilepsy (13), autism (14), depression (15), multiple sclerosis (16), and amyotrophic lateral sclerosis (17). Although relevant clinical studies are lacking, positive structures have been achieved in animal models based on HMGB1 antagonists (anti-HMGB1 monoclonal antibody, ethyl pyruvate, and glycyrrhizin) targeting extracellular HMGB1 therapy. However, there are different isoforms of HMGB1, fully reduced (frHMGB1) and disulfide HMGB1 (dsHMGB1), which are thought to bind to the receptor and can play a pro-inflammatory role, and fully oxidized HMGB1(oxHMGB1) is inert (5). The fact that a mixture of different HMGB1 isoforms is present in the extracellular matrix challenges determining the exact role of individual antagonists. The preclinical and clinical evidence discussed here reinforces HMGB1 as a promising candidate as a common biomarker and therapeutic target for neurological disorders in which neuroinflammatory pathways play a central role.

Parkinson's disease

Parkinson's disease is the second most common neurodegenerative disorder in the elderly, mainly manifested by resting tremor, bradykinesia, rigidity, and postural reflex abnormalities. Parkinson's disease (PD) is pathologically characterized with loss of dopamine (DA) neurons in the midbrain substantia nigra pars compacta (SNpc) (18) and α-synuclein (α-syn) containing Lewy bodies (LBs) formation (19). The pathogenesis of PD is currently unclear. Recent studies have found that elevated levels of HMGB1 protein were detected in postmortem midbrain tissue as well as cerebrospinal fluid (CSF) and serum of PD patients. At the same time, it was found that HMGB1 protein is mainly located in the cytoplasm of PD patients and in the nucleus of control patients, which may indicate that HMGB1 translocation is involved in the pathogenesis of PD (20). In Parkinson's disease, HMGB1 specifically binds to α-syn aggregated in LBs isolated from rat brain, suggesting a promoting role of HMGB1 in neurodegenerative processes in the chronic phase of the disease (21). Extracellular α-syn aggregates can activate astrocytes or microglia, leading to persistent inflammation and subsequent neurodegeneration (22). In primary cultures of mouse neurons and glial cells, HMGB1 was found to bind to the microglial membrane receptor macrophage antigen complex 1 (Mac1) and activate the NF-κB pathway and nicotinamide adenine dinucleotide phosphate (NADPH) oxidase expression, thereby inducing pro-inflammatory factor expression and neurotoxicity. Furthermore, the HMGB1-Mac1 interaction reduces dopamine uptake and the number of dopaminergic neurons (23). On the contrary, the translocation of HMGB1 from the nucleus to the cytoplasm leads to the binding of HMGB1 to Beclin1 to dissociate Beclin1-B-cell lymphoma (Bcl-2) and induce autophagy (24), promoting the self-clearance of α-syn (24, 25), thereby delaying disease progression. Experiments on the PC12 cell line confirmed that inhibition of HMGB1 translocation inhibits autophagy, resulting in the accumulation of α-syn that exacerbates neuronal damage (26). In a 1-methyl-4-phenyl-1,2,3,6-tetrahydropyridine (MPTP)-induced mouse model of acute Parkinson's disease, HMGB1 can promote the expression of tyrosine hydroxylase (TH) in the striatum, thereby maintaining dopaminergic neuron function (27).

In view of the above, HMGB1-targeted or HMGB1/TLR4 pathway inhibition can serve as a rational approach for PD therapy and may serve as a potential biological target (Tables 1, 2). Intravenous administration of HMGB1 antibody attenuated MPTP-induced dopaminergic cell death (20) and reduced PD behavioral symptoms (28). Injection of ethyl pyruvate (EP) into a mouse subacute Parkinson's model can effectively reduce the activation of microglia and inhibit the neuroinflammation mediated by microglia (29). These results are consistent with another study showing that intravenous injection of anti-HMGB1 monoclonal antibodies (mAbs) in a rat PD model significantly inhibited microglial activation and reduced the loss of dopaminergic neurons in SNpc (33). Furthermore, the anti-HMGB1 treatment group inhibited the disruption of the blood–brain barrier (BBB) and the increase in vascular permeability caused by 6-hydroxydopmaine (6-OHDA) neurotoxicity (28). At present, the conventional methods for the clinical treatment of PD are limited, and the targeted

Abbreviations: OMT, oxymatrine; ROT, rotenone; ALO, alogliptin; MACO, middle cerebral artery occlusion; SSA, Saikosaponin A; Hp, haptoglobin; AG, Arctigenin; CCI, controlled cortical impact; PSNL, partial sciatic nerve ligation; BA, Baicalin; LPS, lipopolysaccharide; SSRI, selective serotonin reuptake inhibitor; PBO, placebo; MOG, myelin oligodendrocyte glycoprotein; AQ, autism spectrum quotient; SQ, systemizing quotient; GI score, gastrointestinal dysfunction scores; ADI-R, Autism Diagnostic Interview-Revised.

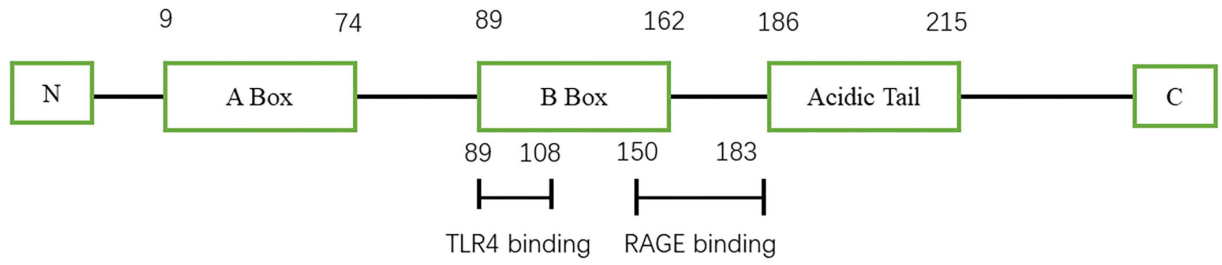

FIGURE 1
Schematic view of HMGB1 structure.

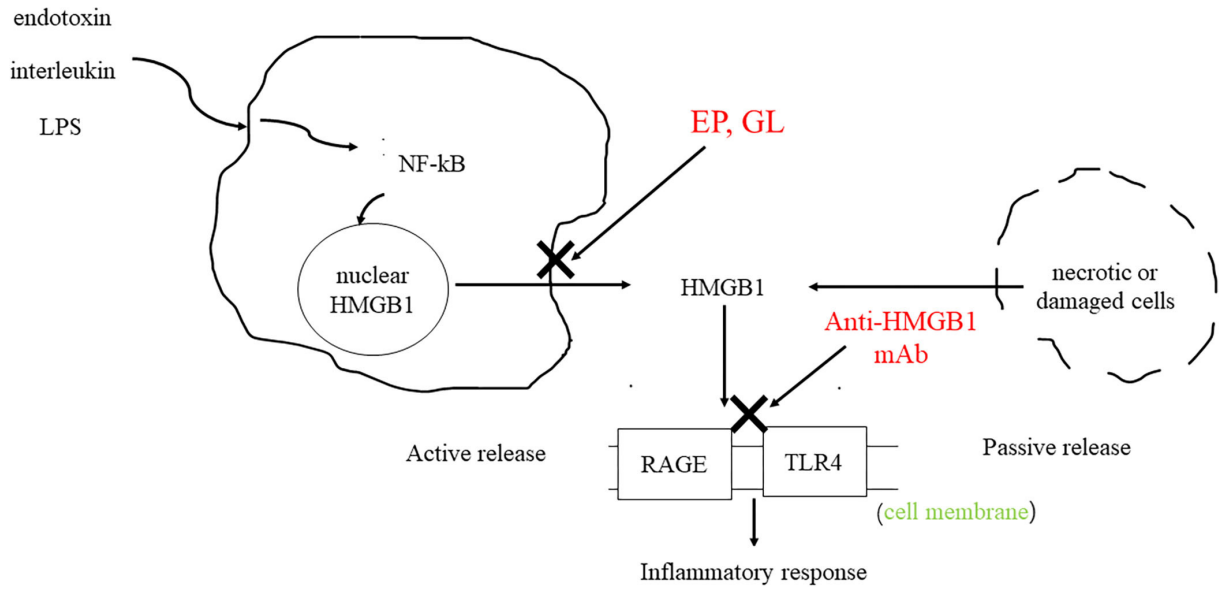

FIGURE 2
HMGB1 can be actively secreted by immune cells or passively secreted by necrotic or damaged cells. HMGB1 binds to RAGE and TLR4 to activate downstream signaling pathways, resulting in the upregulation of cytokines by pro-inflammatory cells. As HMGB1 antagonists, GL and EP can inhibit the release of HMGB1. The anti-HMGB1 mAb neutralizes HMGB1.

therapy of HMGB1 provides a possible idea. However, long-term efficacy and safety in humans have not been studied. At the same time, the related side effects of HMGB1-targeted therapy should also be alerted. However, glycyrrhizin (GL) may lead to complications, such as hypertension and hypokalemia (34). EP is a non-specific HMGB1 inhibitor that inhibits the release of HMGB1 only in live cells, but not in dead cells (35). Long-term use of antibodies may also lead to autoimmune and hematological diseases (28).

Stroke

Stroke is one of the leading causes of disability and death, and its pathophysiology is complex. Neuroinflammation, oxidative stress, and apoptosis are thought to be involved in the occurrence and development of stroke (36). Neuronal HMGB1 release is increased in stroke models. Zhang et al. (37) found elevated levels of HMGB1 in the CSF of an animal model of cerebral ischemia. During ischemic stroke (IS), HMGB1 may signal through its possible receptors, such as RAGE, toll-like receptors (TLRs), and matrix metalloproteinases (MMPs) (38). Studies have found that HMGB1 translocation is very sensitive to hypoxia, and it is released from the nucleus early in stroke to function as a pro-inflammatory factor (39, 40). Animal studies have found that HMGB1 is translocated from the nucleus to the cytoplasm of the peri-infarct cortical region 2 h after ischemia–reperfusion (41). Another study yielded the same results that HMGB1 was released from the nucleus into the cytoplasm of the ipsilateral brain 1 h after intracerebral hemorrhage (ICH) induction, possibly as an early pro-inflammatory mediator promoting neuroinflammation within the neurovascular unit

TABLE 1 Studies targeting HMGB1 in PD.

S.N.	Study model	Treatment	Mode of inhibition	Observations	References
1	MPTP-induced PD mouse model	Anti-HMGB1 mAb	Neutralization	Inhibits dopaminergic cell death and reduces RAGE and TNF-α levels	(20)
2	6-OHDA-induced PD mouse model	Anti-HMGB1 mAb	Neutralization	inhibits the activation of microglia, the destruction of the BBB and the expression of IL-1β and IL-6 Reduced PD behavioral symptoms	(28)
3	MPTP-induced PD mouse model	EP	Release inhibition	Restoration of dopaminergic neuron numbers in substantia nigra and striatum	(29)
4	MPTP-induced PD zebrafish larvae model	GL	Release inhibition	Increases the length of DA neurons in the zebrafish brain and reduces the number of apoptotic cells in the zebrafish brain	(30)

(42). In addition, HMGB1 can increase the level of glutamate leading to excitotoxicity (43). PC12 cells exposed to oxygen-glucose deprivation (OGD) increased HMGB1 secretion and induced cell death in a dose-dependent manner (44, 45). Furthermore, there was a correlation between extracellular HMGB1 levels and stroke severity in the rat middle cerebral artery occlusion (MCAO) model. Higher levels of extracellular HMGB1 in serum and cerebrospinal fluid were associated with larger infarct volume (46) and more severe disease (11).

Anti-HMGB1 antibody can significantly reduce the size of cerebral infarction in rats and improve the symptoms of neurological deficit (47). In addition, studies have found that anti-HMGB1 antibodies can protect the BBB, reduce circulating HMGB1, and at the same time reduce brain edema (48). Anti-HMGB1 mAbs treatment inhibited neuronal translocation and release of HMGB1 itself, suggesting the existence of a positive feedback loop between HMGB1 mobilization and brain inflammatory responses (49). Short hairpin RNA-mediated HMGB1 (ShHMGB1) can reduce the infarct size in the rat MCAO model, which may be caused by shHMGB1 reducing HMGB1 expression in the acute phase (39). GL, a natural inhibitor of HMGB1, potently inhibits MMP-9 activity, protects tight junction claudin-5 and extracellular matrix collagen IV, and preserves BBB integrity in the brain of delayed tissue plasminogen activator (t-PA)-treated ischemia–reperfusion rats. In addition, in the setting of delayed t-PA treatment, GL reduces mortality, neurological deficit scores, and brain edema in MCAO brains (48). In contrast, in a rodent ICH model, HMGB1-RAGE signaling appears to upregulate vascular endothelial growth factor (VEGF) expression and promote angiogenesis in the late post-ICH period (50). In conclusion, HMGB1 may be involved in the pathophysiology of stroke, but animal experiments have shown that HMGB1 has a biphasic effect in stroke patients, and it is unclear to what extent it promotes the development of the disease. However, elevated levels of HMGB1 within the first 24 h after ischemic stroke are considered to be a good predictor of stroke severity and clinical outcome (51), thus serving as a potential therapeutic target (Table 3). However, how to inhibit the harmful form of HMGB1 while retaining its vascular remodeling function presents new challenges for future research.

Traumatic brain injury

Traumatic brain injury (TBI) is a global public health problem, and severe TBI is characterized with high mortality (56). Neuroinflammation plays an important role in the pathological process of TBI. One study found that plasma HMGB1 levels in TBI patients were significantly higher than those in healthy controls, and HMGB1 could be used as a predictor of TBI 1-year survival (57). Animal studies found that 30 min after TBI, HMGB1 staining disappeared from the core of the contused area and was transferred to the cytoplasm at the edge of the contused area (58). Another study validated this finding by detecting HMGB1 in the cytoplasm of glial cells 4 h after TBI (59). The translocation indicated the functional activity of HMGB1 as an inflammatory mediator. However, the release of HMGB1 was age-dependent, with increases in extracellular HMGB1 in both the lesion and the perilesional neocortex in both young (3 weeks) and adult mice (8–10 weeks). However, the elevation of HMGB1 was only statistically significant in the perilesional neocortex of adult mice (60). However, enzyme-linked immunosorbent assay (ELISA) cannot distinguish between actively and passively released HMGB1, so the detected levels of HMGB1 may be actively released by immune cells, or passively released by necrotic cells, or a combination of the two (61). TBI induces an inflammatory response in brain tissue characterized by nucleocytoplasmic translocation of HMGB1, upregulation of HMGB1/HMGB1

TABLE 2 Studies targeting HMGB1/TLR4 pathway in PD.

S.N.	Study model	Treatment	Mechanism	Observations	References
1	MPTP-induced PD mouse model	OMT	Inhibition of HMGB1/TLR4/NF-κB pathway	Inhibits HMGB1/TLR4/NF-κB signaling pathway Attenuates microglia-mediated neuroinflammatory responses Dose-dependently attenuates MPTP-induced dyskinesia	(31)
2	ROT-induced PD mouse model	ALO	Inhibition of HMGB1/TLR4/NLRP3 pathway	Inhibits striatal microglial activation	(32)

TABLE 3 Studies targeting HMGB1 in stroke.

S.N.	Study model	Treatment	Mode of inhibition	Observations	References
1	MACO-induced stroke mouse model	GL	Release inhibition	Reduces the mortality of t-PA delayed treatment of ischemic stroke model rats, reduce hemorrhagic transformation, brain swelling, BBB damage, neuronal apoptosis, and improve neurological function Inhibits ONOO-/HMGB1/TLR2 signaling pathway	(48)
2	MACO-induced stroke mouse model	Berberine	Release inhibition	Dose-dependently inhibits nuclear-cytoplasmic translocation of HMGB1 protein Inhibits HMGB1/TLR4/NF-κB signaling pathway	(52)
3	MACO-induced stroke mouse model	SSA	Release inhibition	Inhibits the release of HMGB1 in the nucleus	(53)
4	MACO-induced stroke mouse model	HP	Neutralization	Binds HMGB1 Inhibits activation of macrophages/microglia	(54)
5	MACO-induced stroke mouse model	Anti-HMGB1 antibody	Neutralization	–	(55)

receptors (TLR4 and RAGE), enhanced NF-κB activation, and promotion of inflammatory factors interleukin (IL)-1β, tumor necrosis factor-α (TNF-α), and IL-6 and other inflammatory cytokines (62). The HMGB1 protein contributes to brain edema by causing a decrease in occludin, claudin-5, and zonula occludens-1 (ZO-1). HMGB1 protein was also found to increase apoptosis by increasing caspase-3 levels and decreasing bcl-2 levels and to increase oxidative damage by increasing total oxidative status (63). High HMGB1 levels may impair synaptic plasticity late in TBI (64).

Currently, the treatment of TBI patients is limited and the prognosis is poor, so it is imperative to deeply study the pathophysiology of TBI and find new therapeutic targets. The prognostic value of HMGB1 is similar to the Glasgow coma score (GCS); elevated levels of HMGB1 in the ventricular CSF are associated with poorer prognosis after TBI in children (65). This suggests that HMGB1 has potential as a TBI biomarker. Primary examples of therapeutics targeting HMGB1 include GL, EP, and anti-HMGB1 mAbs (Table 4). Animal studies have found that GL can reduce inflammation by inhibiting HMGB1 translocation, inhibiting NF-κB DNA binding activity, and reducing the expression of inflammatory cytokines (62). In addition, GL can reduce brain edema, reduce apoptosis, and improve motor function recovery after TBI. GL attenuated TBI by inhibiting HMGB1, thereby inhibiting microglia/macrophages (M1) phenotype activation and promoting microglia/macrophages (M2) phenotype activation in microglia/macrophages (66). HMGB1 A-box significantly reduces brain edema, improves cellular degeneration, reduces the expression of pro-inflammatory cytokines in post-traumatic brain injury, and improves behavioral performance in TBI mice by protecting the integrity of the BBB (67) (Table 4). The expression of HMGB1 decreased after the application of EP in TBI rats, while improving cerebral edema and reducing

TABLE 4 Studies targeting HMGB1 in TBI.

S.N.	Study model	Treatment	Mode of inhibition	Observations	References
1	CCI-induced TBI mouse model	GL	Release inhibition	Improves short-term spatial memory and motor learning impairments	(12)
2	CCI-induced TBI mouse model	EP	Release inhibition	Inhibits the expression of HMGB1 and TLR4, IL-1β, TNF-α and IL-6 Improves walking ability, cerebral edema	(63)
3	CCI-induced TBI mouse model	GL	Release inhibition	Improves neurological recovery after traumatic brain injury Reduces injury volume Inhibits the release of HMGB1	(66)
4	CCI-induced TBI mouse model	HMGB1 A-box	Neutralization	The HMGB1 A-box fragment is an antagonist that competes with full-length HMGB1 receptor binding Protects the integrity of the BBB, reduces cerebral edema, reduces the expression of pro-inflammatory cytokines after brain trauma, and reverses brain damage in mice with brain trauma	(67)
5	CCI-induced TBI mouse model	ω-3 PUFA	Release inhibition	Inhibits HMGB1 nucleocytoplasmic translocation/extracellular secretion is suppressed	(68)
6	Fluid percussion -induced TBI mouse model	Anti-HMGB1 mAb	Neutralization	Inhibits the activation of microglia and the death of hippocampal neurons in the ipsilateral hemisphere rat after traumatic brain injury	(69)

TABLE 5 Studies targeting HMGB1 in epilepsy.

S.N.	Study model	Treatment	Mode of inhibition	Observations	References
1	Pilocarpine-induced SE mouse model	GL	Release inhibition	Decreases levels of malondialdehyde and glutathione in brain regions	(82)
2	Pilocarpine-induced epilepsy mouse model	anti-HMGB1 mAb	Neutralization	Attenuates damage such as increased intracellular space in the hippocampus caused by seizures in epileptic mice	(83)
3	Pentylenetetrazol-induced epilepsy zebrafish model	GL	Release inhibition	Anticonvulsant Inhibits HMGB1/TLR4/NF-κB signaling pathway	(84)
4	Lithium-pilocarpine induced epilepsy mouse model	GL	Release inhibition	Inhibits the translocation of HMGB1 from the nucleus to the cytoplasm Improves the neuronal damage in the CA1 and CA3 regions of the hippocampus after SE Protects BBB	(85)

oxidative damage (63). As an immunonutrient, Omega-3 polyunsaturated fatty acid (omega-3 PUFA) can inhibit HMGB1 nuclear translocation and HMGB1-mediated activation of TLR4/NF-κB signaling pathway, inhibit the induced microglial activation and subsequent inflammatory response, and thus exert neuroprotective effects (70) (Table 4). However, studies have found that the serum HMGB1 concentration in adults remained relatively stable in TBI, and the serum HMGB1

TABLE 6 Overview of the original research studies investigating the role of HMGB1 in autism spectrum disorder.

Authors	Study population		HMGB1 in ASD patients		Symptoms
	Patients	Controls	Serums	Fecal	
Makris G (14)	42	38	↑	–	AQ attention to detail subscale SQ total score
Babinská K (89)	31	16	↑	–	GI sign severity
Emanuele E (90)	22	28	↑	–	ADI-R Social Scores
Russo AJ (91)	38	40	↑	–	–
Carissimi C (92)	30	14	–	↑	GI sign severity

TABLE 7 Studies targeting HMGB1 in depression.

S.N.	Study model	Treatment	Mode of inhibition	Observations	References
1	CUMS-induced depression mouse model	GL	Release inhibition	Improves chronic stress-induced depression	(106)
2	CUMS-induced depression mouse model	EP	Release inhibition	Depressed behavioral tendency	(108)
3	LPS-induced depression mouse model	GL	Release inhibition	Eliminates LPS-induced cognitive dysfunction, anxiety and depression-like behaviors	(113)
4	PSNL-induced depression mouse model	Anti-HMGB1 mAb	Neutralization	Reduces microglia activation and anxiety-depression-like behavior	(114)

concentration in children increased (60). Therefore, children may benefit more in targeting HMGB1 inhibition for the treatment of TBI-induced neuroinflammation. In conclusion, animal experiments show that HMGB1-targeted therapy is an effective treatment for TBI, which can protect the integrity of the BBB, reduce brain edema, and inhibit neuroinflammation to exert neuroprotective effects. However, current animal experiments have not proved that HMGB1-targeted therapy can improve cognitive ability, and its long-term effect still needs further research. In addition, current research suggests that disulfide bond-HMGB1 plays a major role in the process of inflammation (71). How to target and inhibit the harmful subtype of HMGB1 presents a new challenge for future clinical translation.

Epilepsy

Epilepsy is considered to be one of the most common neurological disorders worldwide (72). Epilepsy and the mechanism of seizures are not well understood, but inflammation is thought to be an important contributor to seizures (72). In studies on animal models of epilepsy, HMGB1 has attracted attention. Animals with active epilepsy have elevated blood levels of HMGB1 compared to healthy or well-controlled individuals (73). At the same time, a clinical study found that HMGB1 levels were proportional to the severity of epilepsy, and high levels of HMGB1 may represent an increased possibility of antiepileptic drug resistance (74). Serum HMGB1 concentration can predict seizure frequency (75). In conclusion, HMGB1 can be used as a potential biomarker to predict epilepsy recurrence and prognosis. Animal studies have found that translocation and release of HMGB1 occur in pathological foci of different types of epilepsy (76, 77). Glial activation plays an important role in the development of epilepsy, and HMGB1 may mediate microglial activation during epileptic seizures through the TLR4/NF-κB signaling pathway (78). HMGB1 activates the IL-1R/TLR signaling pathway in neurons and plays a key role in seizures and relapse by catalyzing the phosphorylation of the NR2B subunit of the *N*-methyl-D-aspartate (NMDA-NR2B) receptor *via* rapid sarcoma family kinases (79). HMGB1 affects neuronal excitability by inhibiting astrocyte glutamate transporter to increase extracellular glutamate concentration (80). It has been reported that phosphorylation of the NMDA-NR2B receptor upon activation by HMGB1/RAGE/TLR4 signaling results in Ca^{2+} influx, which increases neuronal cell excitability, which in turn induces epileptogenesis (59). Increased RAGE expression may also lead to neuronal hyperexcitability associated with amyloid-β synthesis (81). Among neurotransmitter receptors, TNF-α induces a rapid increase in neuronal synaptic expression of the amino-3-hydroxy-5-methyl-4-isoxazole propionic acid

TABLE 8 Studies targeting HMGB1/TLR4 pathway in depression.

S.N.	Study model	Treatment	Mechanism	Observations	References
1	CUMS-induced depression mouse model	BA	Inhibition of HMGB1/TLR4/NF-κB pathway	Inhibits HMGB1/TLR4/NF-κB pathway	(100)
2	CUMS-induced depression mouse model	AG	Inhibition of HMGB1/TLR4/NF-κB pathway	Inhibits HMGB1/TLR4/NF-κB pathway	(111)
3	LPS-induced depression mouse model	polydatin	Inhibition of HMGB1/NF-κB pathway	Inhibits Sirt1/HMGB1/NF-κB pathway	(115)

TABLE 9 Clinical studies targeting HMGB1 in depression.

S.N.	Type of study	Treatment		Observations	limitation	References
		Experimental	Control			
1	Randomized, double-blind, placebo-controlled clinical trial	SSRI + GL	SSRI + PBO	The SSRI + GL group had more relief of depressive symptoms than the SSRI+PBO group	The sample size of this study was not large enough and the follow-up time was relatively short	(116)

receptor (AMPAR) and acts on AMPAR to promote neuronal excitability (82). Seizures lead to brain cell damage, leading to passive release of HMGB1, creating a vicious cycle.

There are currently limited data on HMGB1 inhibitors in animal models of epilepsy. GL was neuroprotective against lithium/pilocarpine-induced status epilepticus (SE) in rats and ameliorated pilocarpine-induced oxidative damage and inflammatory responses by inhibiting gliosis and downregulating pro-inflammatory factors, but showed no antiepileptic activity (82) (Table 5). Anti-HMGB1 mAb may exert an antiepileptic effect by inhibiting the HMGB1-TLR4 regulatory axis, reducing seizure frequency (83) (Table 5). RAGE may play a dual role in epilepsy: Constitutively expressed neuronal RAGE contributes to hippocampal cornu ammonis (CA)1 cell survival early in SE and is detrimental in subsequent stages of epileptogenesis (before spontaneous seizures or after the first seizure), leading to increased neuronal excitability (77). Current studies have shown that HMGB1 inhibitors (GL and anti-HMGB1 mAb) can reduce the frequency of different types of seizures, but data are limited (86). In addition, short-term seizure remission does not predict its long-term prognosis.

Autism

Autism is a type of neurodevelopmental disorder starting in early childhood, with characteristic symptoms of social interaction and communication disorder, and repetitive patterns of behavior. The pathogenesis of autism is currently unclear (87). From fetal development to adulthood, the immune system and the central nervous system interact with each other, and the activation of maternal immunity during fetal development can be a risk factor for autism. Patients with autism have altered immune responses, ranging from alterations in peripheral immune markers to increased activation of microglia in the central nervous system (CNS), all of which contribute to a chronic state of low-grade inflammation in the CNS (88). Clinical studies have found that plasma HMGB1 levels are elevated in ASD patients (89) (Table 6). Animal experiments have demonstrated that HMGB1 is associated with alterations in intestinal barrier function (93). At the same time, the serum HMGB1 level is positively correlated with the severity of autism, and the higher the HMGB1 level, the worse the social interaction ability (90). HMGB1 acts *via* HMGB1/RAGE/TLR4 axis, and activation of TLR4 signaling leads to the upregulation of NADPH oxidase 2 (NOX-2)-dependent reactive oxygen species (ROS) production by immune cells (94), increased vascular permeability, and leukocyte infiltration into nerve cells, resulting in persistent neuroinflammation (95). The neuropeptide oxytocin (OXT) can affect mood and social functioning and is therefore considered to be closely related to the pathophysiology of autism (96, 97). It was found that HMGB1 binds to endogenous secretory RAGE (esRAGE), resulting in a decrease in plasma RAGE levels, which in turn affects the transport of OXT from the periphery to the brain (14). Therefore, HMGB1 may be involved in the molecular pathway of immune dysfunction in individuals with ASD. Epidermal growth factor receptor (EGFR) is involved in

TABLE 10 Studies targeting HMGB1 in MS.

S.N.	Study model	Treatment	Mode of inhibition	Observations	References
1	MOG-induced EAE mouse model	anti-HMGB1 mAb	Neutralization	Improves clinical and pathological severity of EAE	(127)
2	MOG-induced EAE mouse model	GL	Release inhibition	Decreases HMGB1 release	(128)

TABLE 11 Studies targeting HMGB1/TLR4 pathway in MS.

S.N.	Study model	Treatment	Mechanism	Observations	References
1	MOG-induced EAE mouse model	MAT	Inhibition of HMGB1/TLR4/NF-κB pathway	Relief of inflammatory demyelination and activation of astrocytes and microglia/macrophages in the central nervous system of EAE rats	(131)

TABLE 12 Studies targeting HMGB1 in ALS.

S.N.	Study model	Treatment	Mode of inhibition	Observations	References
1	Transgenic SOD1G93A mice	Anti-HMGB1 mAb	Neutralization	Briefly improves hindlimb grip strength in mice early in the disease, but not prolonged survival Reduces spinal cord TNF-α and complement C5a receptor 1 gene expression, but did not affect overall glial activation	(134)

the growth and differentiation of cells in the central nervous system, and studies have found that plasma EGFR levels are correlated with HMGB1. In addition, the study found that EGFR levels correlated with symptom severity in children with autism (98). However, there are few clinical and preclinical studies on autism at present, and more research is needed to clarify the role of HMGB1 in the pathophysiology of autism and to clarify the specific molecular mechanism by which HMGB1 is involved in autism.

Depression

Depression manifests as a long-term physical and psychological downturn that affects ∼300 million people worldwide (99). Stress is an indirect cause of depression, which induces depression-like behaviors through the HMGB1/TLR4/NF-κB signaling pathway in the hippocampus (100). Persistent expression of HMGB1/RAGE in microglia increases susceptibility to depression (101). The ventral medial prefrontal cortex (vmPFC) is one of the key brain regions involved in the pathogenesis of depression, and it plays a key role in the affective deficits of depression. Animal studies have found increased expression of inflammatory cytokines and decreased astrocytes in rats exposed to chronic unpredictable mild stress (CUMS) in vmPFC (102). The reduction of astrocytes in the prefrontal cortex (PFC) is considered to be one of the pathophysiological changes in depression (103). Chronic unpredictable mild stress (CUMS) induces nucleocytoplasmic translocation of HMGB1 in microglia and neurons (104). HMGB1 may lead to microglial activation and neuroinflammation through TLR4/NF-κB and TNF-α/TNFR1/NF-κB signaling pathways. This neuroinflammation-induced behavioral change is thought to be related to the activation of indoleamine-pyrrole 2,3-dioxygenase (IDO) in the kynurenine pathway and changes in neurotransmitter metabolism (5-hydroxytryptamine, 5-HT) (5). HMGB1 can activate the tryptophan degradation (canine purine) pathway and increase the activity of the rate-limiting enzyme IDO (105, 106). On the one hand, IDO catalyzes the conversion of tryptophan into neurotoxicity. Metabolites, such as quinolinic acid (QUIN), selectively bind to NMDAR, resulting in glutamate signaling and neuronal Ca influx, ultimately leading to excitotoxicity. At the same time, it also activates the secretion of glutamate in neurons (107). Both high concentrations of glutamate and QUIN enhance glutamatergic

neurotransmission, leading to the development of depression (108); on the other hand, 5-HT biosynthesis is reduced and leads to depressive mood (109). Another possible mechanism of HMGB1-mediated depression involves damage to dopaminergic neurons. After exposure to stress, microglia secrete reactive oxygen species (ROS) and nitrogen (NOS), which may rapidly reduce the availability of neopterin and tetrahydrobiopterin (BH4), which in turn leads to the DA synthesis rate-limiting enzyme amphetamine amino acid hydroxylase (PAH) and tyrosine hydroxylase (TH) are inactivated and DA synthesis is blocked (110).

The HMGB1 inhibitors GL and EP can improve depression-like behaviors (104, 108). Arctigenin exhibits significant antidepressant effects in rodent models of depression, attenuates microglial activation and neuroinflammation through HMGB1/TLR4/NF-κB and TNF-α/TNFR1/NF-κB signaling pathways, and inhibits IDO increase and decrease in 5-HT (111). Minocycline can inhibit CUMS-induced HMGB1 nucleocytoplasmic translocation in microglia and neurons and improve behavioral and cognitive deficits in CUMS-depressed mice (104). In addition, inhibition of phosphodiesterase-4 (PDE4) can exert antidepressant effects by inhibiting the HMGB1/RAGE signaling pathway (112). TAK-242 (TLR4 inhibitor) can significantly inhibit dsHMGB1, downregulation of hippocampal myelin basic protein and upregulation of hippocampal TNF-α protein, and improve depressive behavior in rodents (15). The glutamate receptor antagonist ketamine and the IDO inhibitor 1-methyltryptophan can also improve depressive symptoms in rodents (110). In conclusion, inhibition of HMGB1 release or inhibition of HMGB1/TLR4/RAGE signaling pathway by HMGB1 inhibitors is beneficial for the treatment of depression (Tables 7–9). However, most of the study results are based on animal experiments and lack the verification of clinical research results.

Multiple sclerosis

Multiple sclerosis (MS) is an immune-mediated chronic inflammatory demyelinating disease of the central nervous system, often involving the brain, spinal cord, and optic nerves. At the same time, clinical studies have found that the concentration of HMGB1 in the serum and cerebrospinal fluid of MS patients is significantly increased (117). Experimental autoimmune encephalomyelitis (EAE) provides the most widely used MS experimental model (118). EAE model studies have found that HMGB1 may be released by activated macrophages and microglia during MS and induce neuroinflammation (119). Acetylated HMGB1 may be released during chronic inflammation in the clinically stable phase of MS, whereas HMGB1 may be in an unacetylated form during clinically relapsing acute inflammation (120). Serum HMGB1 levels can serve as a potential marker of MS activity and correlate with clinical relapse rates and disease duration (121). HMGB1 may be involved in the pathogenesis of MS by promoting autophagy. HMGB1 can further promote the binding of autophagy factor Beclin1 to type III phosphoinositide 3 kinase (PI3K Class III), thereby promoting the nucleation process of *ex vivo* membranes, thereby initiating autophagy (117). HMGB1 elevates inducible nitric oxide synthase (iNOS) and superoxide, leading to peroxynitrite ($ONOO^-$) formation and increased pro-inflammatory factors (122). ONOO induces ceramide production in astrocytes, which in turn leads to demyelination, inhibition of remyelination, and increased BBB permeability. On the contrary, high levels of ceramides can promote cell death (122). In microglia, ceramides promote the assembly of NOD-like receptor pyrin domain containing 3 (NLRP3) inflammasome activation, thereby increasing the release of the IL-1β and IL-18, which further contributes to neuroinflammation (123). Furthermore, iNOS-mediated cytokine-induced nitric oxide excess can cause tissue damage in the central nervous system of EAE (124). Cellular senescence is a cellular feature of MS progenitor cells, and senescent neural progenitor cells can secrete HMGB1 oligodendrocyte progenitors (OPCs) to mature into myelinating oligodendrocytes (OLs), promoting chronic demyelination (125, 126).

HMGB1 monoclonal antibody has been shown to improve the progression of EAE (127) (Table 10). Meanwhile, HMGB1 promotes the release of Sonic hedgehog (Shh) through the HMGB1-RAGE signaling pathway, which can repair the BBB and reduce BBB permeability to promote axonal growth in spinal cord injury (129). Genetic inhibition of acid sphingomyelinase (aSMase)/ceramide prevents classic MS-like pathophysiology, including BBB disruption, leukocyte extravasation, and demyelination, in a model of EAE (130). Matrine (MAT) and GL alleviate inflammatory demyelination and activation of astrocytes and microglia/macrophages in the central nervous system of EAE rats by inhibiting HMGB1 (131, 132) (Tables 10, 11). The cumulative effect of HMGB1 will determine the outcome of the local inflammatory response of HMGB1 in terms of tissue damage. Blocking the HMGB1-RAGE interaction in damaged nerves reduces neurite outgrowth. On the contrary, inhibition of HMGB1 at inappropriate times may prevent tissue repair due to its role in neurite outgrowth and stem cell chemotaxis. Therefore, the role of HMGB1 in MS still needs further study.

Amyotrophic lateral sclerosis

Amyotrophic lateral sclerosis (ALS) is a neurodegenerative disease that selectively damages motor neurons, resulting in rapid muscle wasting and weakness after onset (133). The pathogenesis of ALS is still unclear, but current studies have found that immune and inflammatory factors

may be involved in the pathophysiology of ALS. HMGB1 induces neuroinflammation through the HMGB1/RAGE or HMGB1/TLR4 signaling pathway leading to increased release of tumor necrosis factor-α and interleukin (134). Serum levels of HMGB1 autoantibodies were upregulated in ALS patients compared with age-matched healthy controls (135). At the same time, the nucleocytoplasmic translocation of HMGB1 in reactive astrocytes and microglia was observed in ALS patients and mouse models (134). Therefore, HMGB1 may serve as a biomarker for ALS diagnosis and clinical assessment. In SOD1G93A mice exhibiting overt disease symptoms, HMGB1-immunopositive motor neurons progressively decreased, possibly due to passive release from damaged cells, whereas the subcellular distribution of HMGB1 in glial cells did not change, which helps stability and regulation of transcriptional activity during maintenance of its responsive response to motor neuron degeneration (136). The binding of HMGB1 to RAGE and TLR4 leads to the activation of NF-κB and inflammatory cytokines, the latter of which have been implicated in the pathogenesis of ALS. Animal studies have found that TLR4 signaling may lead to motor nerve death and, ultimately, ALS disease progression. Loss of TLR4 and RAGE can prolong survival and improve hindlimb grip strength (137, 138).

HMGB1 antibody improved early symptoms in SOD1G93A transgenic mice, but did not prolong survival or improve exercise performance (134) (Table 12). HMGB1 blockade therapy has limited efficacy in the SOD1G93A mouse model, possibly due to the presence of other endogenous ligands that activate TLR2, TLR4, and RAGE (134). On the contrary, astrocyte HMGB1 signaling in ALS can protect nerves by releasing neurotrophic factors, such as brain-derived neurotrophic factor and glial cell-derived neurotrophic factor (139).

Conclusion

Neuroinflammation is thought to be involved in the pathogenesis of Parkinson's disease, stroke, traumatic brain injury, epilepsy, autism, depression, multiple sclerosis, and amyotrophic lateral sclerosis, and HMGB1 plays an important role as a neuroinflammatory mediator in the above diseases. Meanwhile, HMGB1 has the potential as a common biomarker for the aforementioned neurological diseases and may be an important therapeutic target for these neurological diseases. Anti-HMGB1 monoclonal antibodies and HMGB1 inhibitors have been shown to improve neurological symptoms in animal models of the above diseases within a specific therapeutic time window, providing a new therapeutic idea. Antagonists such as anti-HMGB1 monoclonal antibodies, ethyl pyruvate, inhibit HMGB1 by interfering with its cytoplasmic export, while other antagonists such as glycyrrhizin directly bind to HMGB1 and render its receptors unavailable. However, the current research still has certain limitations. Although clinical and preclinical studies have shown elevated levels of HMGB1 in the blood and cerebrospinal fluid of patients with Parkinson's disease, stroke, traumatic brain injury, epilepsy, autism, depression, multiple sclerosis, and amyotrophic lateral sclerosis, it is unclear to what extent HMGB1 contributes to the disease phenotype. In addition, most clinical or preclinical studies detect serum or cerebrospinal fluid HMGB1 content by ELISA, which cannot distinguish between active release of HMGB1 from immune cells or passive release from necrotic cells and cannot distinguish HMGB1 subtypes. Different isoforms of HMGB1 play different roles in the process of inflammation, and the currently studied HMGB1 inhibitors cannot target the harmful HMGB1 isoforms. Meanwhile, the duration of HMGB1 neutralization/inhibition by HMGB1 antagonists still needs further study. Although HMGB1 antagonists have yielded positive results in animal studies, clinical findings are limited. Finally, HMGB1 is thought to promote post-injury inflammation in vertebrates, but its benefit in neuroregeneration cannot be ruled out. Therefore, the role of HMGB1 in the nervous system injury response, the release mechanism of HMGB1, and the structure–function interaction with inflammatory receptors and downstream signaling pathways need to be further studied, and the clinical translation of HMGB1 antagonists still needs a lot of clinical research.

Author contributions

DM, YZ, FX, and XH participated in writing the manuscript. HZ was responsible for critical reading of the manuscript. All authors read and approved the final version of manuscript.

Conflict of interest

The authors declare that the research was conducted in the absence of any commercial or financial relationships that could be construed as a potential conflict of interest.

Publisher's note

References

1. Goodwin GH, Sanders C, Johns EW. A new group of chromatin-associated proteins with a high content of acidic and basic amino acids. *Eur J Biochem*. (1973) 38:14–9. doi: 10.1111/j.1432-1033.1973.tb03026.x

2. Wang H, Bloom O, Zhang M, Vishnubhakat JM, Ombrellino M, Che J, et al. HMG-1 as a late mediator of endotoxin lethality in mice. *Science*. (1999) 285:248–51. doi: 10.1126/science.285.5425.248

3. Bustin M. Revised nomenclature for high mobility group (HMG) chromosomal proteins. *Trends Biochem Sci*. (2001) 26:152–3. doi: 10.1016/S0968-0004(00)01777-1

4. Souery D, Papakostas GI, Trivedi MH. Treatment-resistant depression. *J Clin Psychiatry*. (2006) 67(Suppl 6):16—22.

5. Rana T, Behl T, Mehta V, Uddin MS, Bungau S. Molecular insights into the therapeutic promise of targeting HMGB1 in depression. *Pharmacol Rep*. (2021) 73:31–42. doi: 10.1007/s43440-020-00163-6

6. Xue J, Suarez JS, Minaai M, Li S, Gaudino G, Pass HI, et al. HMGB1 as a therapeutic target in disease. *J Cell Physiol*. (2021) 236:3406–19. doi: 10.1002/jcp.30125

7. Frank MG, Weber MD, Watkins LR, Maier SF. Stress sounds the alarmin: the role of the danger-associated molecular pattern HMGB1 in stress-induced neuroinflammatory priming. *Brain Behav Immun*. (2015) 48:1–7. doi: 10.1016/j.bbi.2015.03.010

8. Singh V, Roth S, Veltkamp R, Liesz A. HMGB1 as a key mediator of immune mechanisms in ischemic stroke. *Antioxid Redox Signal*. (2016) 24:635–51. doi: 10.1089/ars.2015.6397

9. Qu Y, Zhan Y, Yang S, Ren S, Qiu X, Rehamn ZU, et al. Newcastle disease virus infection triggers HMGB1 release to promote the inflammatory response. *Virology*. (2018) 525:19–31. doi: 10.1016/j.virol.2018.09.001

10. Baran A, Bulut M, Kaya MC, Demirpençe Ö, Sevim B, Akil E, et al. High-sensitivity C-reactive protein and high mobility group box-1 levels in Parkinson's disease. *Neurol Sci*. (2019) 40:167–73. doi: 10.1007/s10072-018-3611-z

11. Le K, Mo S, Lu X, Idriss Ali A, Yu D, Guo Y. Association of circulating blood HMGB1 levels with ischemic stroke: a systematic review and meta-analysis. *Neurol Res*. (2018) 40:907–16. doi: 10.1080/01616412.2018.1497254

12. Webster KM, Shultz SR, Ozturk E, Dill LK, Sun M, Casillas-Espinosa P, et al. Targeting high-mobility group box protein 1 (HMGB1) in pediatric traumatic brain injury: chronic neuroinflammatory, behavioral, and epileptogenic consequences. *Exp Neurol*. (2019) 320:112979. doi: 10.1016/j.expneurol.2019.112979

13. Huang Q, Liu J, Shi Z, Zhu X. Correlation of MMP-9 and HMGB1 expression with the cognitive function in patients with epilepsy and factors affecting the prognosis. *Cell Mol Biol*. (2020) 66:39–47. doi: 10.14715/cmb/2020.66.3.6

14. Makris G, Chouliaras G, Apostolakou F, Papageorgiou C, Chrousos GP, Papassotiriou I, et al. Increased serum concentrations of high mobility group box 1 (HMGB1) protein in children with autism spectrum disorder. *Children*. (2021) 8:478. doi: 10.3390/children8060478

15. Lian YJ, Gong H, Wu TY, Su WJ, Zhang Y, Yang YY, et al. Ds-HMGB1 and fr-HMGB induce depressive behavior through neuroinflammation in contrast to nonoxid-HMGB1. *Brain Behav Immun*. (2017) 59:322–32. doi: 10.1016/j.bbi.2016.09.017

16. Bucova M, Majernikova B, Durmanova V, Cudrakova D, Gmitterova K, Lisa I, et al. HMGB1 as a potential new marker of disease activity in patients with multiple sclerosis. *Neurol Sci*. (2020) 41:599–604. doi: 10.1007/s10072-019-04136-3

17. Hwang CS, Liu GT, Chang MD, Liao IL, Chang HT. Elevated serum autoantibody against high mobility group box 1 as a potent surrogate biomarker for amyotrophic lateral sclerosis. *Neurobiol Dis*. (2013) 58:13–8. doi: 10.1016/j.nbd.2013.04.013

18. Chatterjee M, van Steenoven I, Huisman E, Oosterveld L, Berendse H, van der Flier WM, et al. Contactin-1 is reduced in cerebrospinal fluid of Parkinson's disease patients and is present within lewy bodies. *Biomolecules*. (2020) 10:1177. doi: 10.3390/biom10081177

19. Novellino F, Saccà V, Donato A, Zaffino P, Spadea MF, Vismara M, et al. Innate immunity: a common denominator between neurodegenerative and neuropsychiatric diseases. *Int J Mol Sci*. (2020) 21:1115. doi: 10.3390/ijms21031115

20. Santoro M, Maetzler W, Stathakos P, Martin HL, Hobert MA, Rattay TW, et al. *In-vivo* evidence that high mobility group box 1 exerts deleterious effects in the 1-methyl-4-phenyl-1,2,3,6-tetrahydropyridine model and Parkinson's disease which can be attenuated by glycyrrhizin. *Neurobiol Dis*. (2016) 91:59–68. doi: 10.1016/j.nbd.2016.02.018

21. Lindersson EK, Højrup P, Gai WP, Locker D, Martin D, Jensen PH. alpha-Synuclein filaments bind the transcriptional regulator HMGB-1. *Neuroreport*. (2004) 15:2735—9.

22. Harms AS, Thome AD, Yan Z, Schonhoff AM, Williams GP, Li X, et al. Peripheral monocyte entry is required for alpha-Synuclein induced inflammation and neurodegeneration in a model of Parkinson disease. *Exp Neurol*. (2018) 300:179–87. doi: 10.1016/j.expneurol.2017.11.010

23. Gao HM, Zhou H, Zhang F, Wilson BC, Kam W, Hong JS. HMGB1 acts on microglia Mac1 to mediate chronic neuroinflammation that drives progressive neurodegeneration. *J Neurosci*. (2011) 31:1081–92. doi: 10.1523/JNEUROSCI.3732-10.2011

24. Tang D, Kang R, Livesey KM, Cheh CW, Farkas A, Loughran P, et al. Endogenous HMGB1 regulates autophagy. *J Cell Biol*. (2010) 190:881–92. doi: 10.1083/jcb.200911078

25. Karim MR, Liao EE, Kim J, Meints J, Martinez HM, Pletnikova O, et al. α-Synucleinopathy associated c-Abl activation causes p53-dependent autophagy impairment. *Mol Neurodegener*. (2020) 15:27. doi: 10.1186/s13024-020-00364-w

26. Wang K, Huang J, Xie W, Huang L, Zhong C, Chen Z. Beclin1 and HMGB1 ameliorate the α-synuclein-mediated autophagy inhibition in PC12 cells. *Diagn Pathol*. (2016) 11:15. doi: 10.1186/s13000-016-0459-5

27. Kim SJ, Ryu MJ, Han J, Jang Y, Lee MJ, Ju X, et al. Non-cell autonomous modulation of tyrosine hydroxylase by HMGB1 released from astrocytes in an acute MPTP-induced Parkinsonian mouse model. *Lab Invest*. (2019) 99:1389–99. doi: 10.1038/s41374-019-0254-5

28. Sasaki T, Liu K, Agari T, Yasuhara T, Morimoto J, Okazaki M, et al. Anti-high mobility group box 1 antibody exerts neuroprotection in a rat model of Parkinson's disease. *Exp Neurol*. (2016) 275(Pt 1):220–31. doi: 10.1016/j.expneurol.2015.11.003

29. Tian Y, Cao Y, Chen R, Jing Y, Xia L, Zhang S, et al. HMGB1 A box protects neurons by potently inhibiting both microglia and T cell-mediated inflammation in a mouse Parkinson's disease model. *Clin Sci*. (2020) 134:2075–90. doi: 10.1042/CS20200553

30. Ren Q, Jiang X, Paudel YN, Gao X, Gao D, Zhang P, et al. Co-treatment with natural HMGB1 inhibitor Glycyrrhizin exerts neuroprotection and reverses Parkinson's disease like pathology in Zebrafish. *J Ethnopharmacol*. (2022) 292:115234. doi: 10.1016/j.jep.2022.115234

31. Gan P, Ding L, Hang G, Xia Q, Huang Z, Ye X, et al. Oxymatrine attenuates dopaminergic neuronal damage and microglia-mediated neuroinflammation through cathepsin D-dependent HMGB1/TLR4/NF-κB pathway in Parkinson's disease. *Front Pharmacol*. (2020) 11:776. doi: 10.3389/fphar.2020.00776

32. Safar MM, Abdelkader NF, Ramadan E, Kortam MA, Mohamed AF. Novel mechanistic insights towards the repositioning of alogliptin in Parkinson's disease. *Life Sci*. (2021) 287:120132. doi: 10.1016/j.lfs.2021.120132

33. Zhang K, Tu M, Gao W, Cai X, Song F, Chen Z, et al. Hollow Prussian blue nanozymes drive neuroprotection against ischemic stroke *via* attenuating oxidative stress, counteracting inflammation, and suppressing cell apoptosis. *Nano Lett*. (2019) 19:2812–23. doi: 10.1021/acs.nanolett.8b04729

34. Nazari S, Rameshrad M, Hosseinzadeh H. Toxicological effects of *Glycyrrhiza glabra* (Licorice): a review. *Phytother Res*. (2017) 31:1635–50. doi: 10.1002/ptr.5893

35. Seo MS, Kim HJ, Kim H, Park SW. Ethyl pyruvate directly attenuates active secretion of HMGB1 in proximal tubular cells *via* induction of heme oxygenase-1. *J Clin Med*. (2019) 8:629. doi: 10.3390/jcm8050629

36. Woodruff TM, Thundyil J, Tang SC, Sobey CG, Taylor SM, Arumugam TV. Pathophysiology, treatment, and animal and cellular models of human ischemic stroke. *Mol Neurodegener*. (2011) 6:11. doi: 10.1186/1750-1326-6-11

37. Zhang J, Takahashi HK, Liu K, Wake H, Liu R, Maruo T, et al. Anti-high mobility group box-1 monoclonal antibody protects the blood-brain barrier from ischemia-induced disruption in rats. *Stroke*. (2011) 42:1420–8. doi: 10.1161/STROKEAHA.110.598334

38. Richard SA, Sackey M, Su Z, Xu H. Pivotal neuroinflammatory and therapeutic role of high mobility group box 1 in ischemic stroke. *Biosci Rep*. (2017) 37:BSR20171104. doi: 10.1042/BSR20171104

39. Kim JB, Sig Choi J, Yu YM, Nam K, Piao CS, Kim S, et al. HMGB1, a novel cytokine-like mediator linking acute neuronal death and delayed neuroinflammation in the postischemic brain. *J Neurosci*. (2006) 26:6413–21. doi: 10.1523/JNEUROSCI.3815-05.2006

40. Nishibori M, Wang D, Ousaka D, Wake H. High mobility group box-1 and blood-brain barrier disruption. *Cells*. (2020) 9:2650. doi: 10.3390/cells9122650

41. Qiu J, Nishimura M, Wang Y, Sims JR, Qiu S, Savitz SI, et al. Early release of HMGB-1 from neurons after the onset of brain ischemia. *J Cereb Blood Flow Metab*. (2008) 28:927–38. doi: 10.1038/sj.jcbfm.9600582

42. Lei C, Lin S, Zhang C, Tao W, Dong W, Hao Z, et al. High-mobility group box1 protein promotes neuroinflammation after intracerebral hemorrhage in rats. *Neuroscience*. (2013) 228:190–9. doi: 10.1016/j.neuroscience.2012.10.023

43. Pedrazzi M, Raiteri L, Bonanno G, Patrone M, Ledda S, Passalacqua M, et al. Stimulation of excitatory amino acid release from adult mouse brain glia subcellular particles by high mobility group box 1 protein. *J Neurochem*. (2006) 99:827–38. doi: 10.1111/j.1471-4159.2006.04120.x

44. Kikuchi K, Kawahara K, Biswas KK, Ito T, Tancharoen S, Morimoto Y, et al. Minocycline attenuates both OGD-induced HMGB1 release and HMGB1-induced cell death in ischemic neuronal injury in PC12 cells. *Biochem Biophys Res Commun*. (2009) 385:132–6. doi: 10.1016/j.bbrc.2009.04.041

45. Kikuchi K, Kawahara K, Tancharoen S, Matsuda F, Morimoto Y, Ito T, et al. The free radical scavenger edaravone rescues rats from cerebral infarction by attenuating the release of high-mobility group box-1 in neuronal cells. *J Pharmacol Exp Ther*. (2009) 329:865–74. doi: 10.1124/jpet.108.149484

46. Kim ID, Lee H, Kim SW, Lee HK, Choi J, Han PL, et al. Alarmin HMGB1 induces systemic and brain inflammatory exacerbation in post-stroke infection rat model. *Cell Death Dis*. (2018) 9:426. doi: 10.1038/s41419-018-0438-8

47. Liu K, Mori S, Takahashi HK, Tomono Y, Wake H, Kanke T, et al. Anti-high mobility group box 1 monoclonal antibody ameliorates brain infarction induced by transient ischemia in rats. *FASEB J*. (2007) 21:3904–16. doi: 10.1096/fj.07-8770com

48. Chen H, Guan B, Wang B, Pu H, Bai X, Chen X, et al. Glycyrrhizin prevents hemorrhagic transformation and improves neurological outcome in ischemic stroke with delayed thrombolysis through targeting peroxynitrite-mediated HMGB1 signaling. *Transl Stroke Res*. (2020) 11:967–82. doi: 10.1007/s12975-019-00772-1

49. Nishibori M, Mori S, Takahashi HK. Anti-HMGB1 monoclonal antibody therapy for a wide range of CNS and PNS diseases. *J Pharmacol Sci*. (2019) 140:94–101. doi: 10.1016/j.jphs.2019.04.006

50. Lei C, Zhang S, Cao T, Tao W, Liu M, Wu B. Corrigendum to "HMGB1 may act *via* RAGE to promote angiogenesis in the later phase after intracerebral hemorrhage" [Neuroscience 295 (2015) 39-47]. *Neuroscience*. (2022) 481:238–9. doi: 10.1016/j.neuroscience.2021.11.041

51. Tian X, Liu C, Shu Z, Chen G. Review: therapeutic targeting of HMGB1 in stroke. *Curr Drug Deliv*. (2017) 14:785–90. doi: 10.2174/1567201813666160808111933

52. Zhu JR, Lu HD, Guo C, Fang WR, Zhao HD, Zhou JS, et al. Berberine attenuates ischemia-reperfusion injury through inhibiting HMGB1 release and NF-κB nuclear translocation. *Acta Pharmacol Sin*. (2018) 39:1706–15. doi: 10.1038/s41401-018-0160-1

53. Wang X, Yang G. Saikosaponin A attenuates neural injury caused by ischemia/reperfusion. *Transl Neurosci*. (2020) 11:227–35. doi: 10.1515/tnsci-2020-0129

54. Morimoto M, Nakano T, Egashira S, Irie K, Matsuyama K, Wada M, et al. Haptoglobin regulates macrophage/microglia-induced inflammation and prevents ischemic brain damage *via* binding to HMGB1. *J Am Heart Assoc*. (2022) 11:e024424. doi: 10.1161/JAHA.121.024424

55. Halder SK, Ueda H. Amlexanox inhibits cerebral ischemia-induced delayed astrocytic high-mobility group box 1 release and subsequent brain damage. *J Pharmacol Exp Ther*. (2018) 365:27–36. doi: 10.1124/jpet.117.245340

56. Maas A, Menon DK, Adelson PD, Andelic N, Bell MJ, Belli A, et al. Traumatic brain injury: integrated approaches to improve prevention, clinical care, and research. *Lancet Neurol*. (2017) 16:987–1048. doi: 10.1016/S1474-4422(17)30371-X

57. Wang KY, Yu GF, Zhang ZY, Huang Q, Dong XQ. Plasma high-mobility group box 1 levels and prediction of outcome in patients with traumatic brain injury. *Clin Chim Acta*. (2012) 413:1737–41. doi: 10.1016/j.cca.2012.07.002

58. Gao TL, Yuan XT, Yang D, Dai HL, Wang WJ, Peng X, et al. Expression of HMGB1 and RAGE in rat and human brains after traumatic brain injury. *J Trauma Acute Care Surg*. (2012) 72:643–9. doi: 10.1097/TA.0b013e31823c54a6

59. Manivannan S, Harari B, Muzaffar M, Elalfy O, Hettipathirannahelage S, James Z, et al. Glycyrrhizin blocks the detrimental effects of HMGB1 on cortical neurogenesis after traumatic neuronal injury. *Brain Sci*. (2020) 10:760. doi: 10.3390/brainsci10100760

60. Webster KM, Sun M, Crack PJ, O'Brien TJ, Shultz SR, Semple BD. Age-dependent release of high-mobility group box protein-1 and cellular neuroinflammation after traumatic brain injury in mice. *J Comp Neurol*. (2019) 527:1102–17. doi: 10.1002/cne.24589

61. Au AK, Aneja RK, Bell MJ, Bayir H, Feldman K, Adelson PD, et al. Cerebrospinal fluid levels of high-mobility group box 1 and cytochrome C predict outcome after pediatric traumatic brain injury. *J Neurotrauma*. (2012) 29:2013–21. doi: 10.1089/neu.2011.2171

62. Pang H, Huang T, Song J, Li D, Zhao Y, Ma X. Inhibiting HMGB1 with glycyrrhizic acid protects brain injury after DAI *via* its anti-inflammatory effect. *Mediators Inflamm*. (2016) 2016:4569521. doi: 10.1155/2016/4569521

63. Su X, Wang H, Zhao J, Pan H, Mao L. Beneficial effects of ethyl pyruvate through inhibiting high-mobility group box 1 expression and TLR4/NF-κB pathway after traumatic brain injury in the rat. *Mediators Inflamm*. (2011) 2011:807142. doi: 10.1155/2011/807142

64. Tan SW, Zhao Y, Li P, Ning YL, Huang ZZ, Yang N, et al. HMGB1 mediates cognitive impairment caused by the NLRP3 inflammasome in the late stage of traumatic brain injury. *J Neuroinflammation*. (2021) 18:241. doi: 10.1186/s12974-021-02274-0

65. Paudel YN, Angelopoulou E, Piperi C, Othman I, Shaikh MF. HMGB1-mediated neuroinflammatory responses in brain injuries: potential mechanisms and therapeutic opportunities. *Int J Mol Sci*. (2020) 21:4609. doi: 10.3390/ijms21134609

66. Gao T, Chen Z, Chen H, Yuan H, Wang Y, Peng X, et al. Inhibition of HMGB1 mediates neuroprotection of traumatic brain injury by modulating the microglia/macrophage polarization. *Biochem Biophys Res Commun*. (2018) 497:430–6. doi: 10.1016/j.bbrc.2018.02.102

67. Yang L, Wang F, Yang L, Yuan Y, Chen Y, Zhang G, et al. HMGB1 a-box reverses brain edema and deterioration of neurological function in a traumatic brain injury mouse model. *Cell Physiol Biochem*. (2018) 46:2532–42. doi: 10.1159/000489659

68. Chen X, Chen C, Fan S, Wu S, Yang F, Fang Z, et al. Omega-3 polyunsaturated fatty acid attenuates the inflammatory response by modulating microglia polarization through SIRT1-mediated deacetylation of the HMGB1/NF-κB pathway following experimental traumatic brain injury. *J Neuroinflammation*. (2018) 15:116. doi: 10.1186/s12974-018-1151-3

69. Okuma Y, Wake H, Teshigawara K, Takahashi Y, Hishikawa T, Yasuhara T, et al. Anti-high mobility group box 1 antibody therapy may prevent cognitive dysfunction after traumatic brain injury. *World Neurosurg*. (2019) 122:e864–71. doi: 10.1016/j.wneu.2018.10.164

70. Chen X, Wu S, Chen C, Xie B, Fang Z, Hu W, et al. Omega-3 polyunsaturated fatty acid supplementation attenuates microglial-induced inflammation by inhibiting the HMGB1/TLR4/NF-κB pathway following experimental traumatic brain injury. *J Neuroinflammation*. (2017) 14:143. doi: 10.1186/s12974-017-0917-3

71. Andersson U, Yang H, Harris H. High-mobility group box 1 protein (HMGB1) operates as an alarmin outside as well as inside cells. *Semin Immunol*. (2018) 38:40–8. doi: 10.1016/j.smim.2018.02.011

72. Riazi K, Galic MA, Pittman QJ. Contributions of peripheral inflammation to seizure susceptibility: cytokines and brain excitability. *Epilepsy Res*. (2010) 89:34–42. doi: 10.1016/j.eplepsyres.2009.09.004

73. Pauletti A, Terrone G, Shekh-Ahmad T, Salamone A, Ravizza T, Rizzi M, et al. Targeting oxidative stress improves disease outcomes in a rat model of acquired epilepsy. *Brain*. (2019) 142:e39. doi: 10.1093/brain/awz130

74. Kan M, Song L, Zhang X, Zhang J, Fang P. Circulating high mobility group box-1 and toll-like receptor 4 expressions increase the risk and severity of epilepsy. *Braz J Med Biol Res*. (2019) 52:e7374. doi: 10.1590/1414-431x20197374

75. Zhu M, Chen J, Guo H, Ding L, Zhang Y, Xu Y. High mobility group protein B1 (HMGB1) and interleukin-1β as prognostic biomarkers of epilepsy in children. *J Child Neurol*. (2018) 33:909–17. doi: 10.1177/0883073818801654

76. Maroso M, Balosso S, Ravizza T, Liu J, Aronica E, Iyer AM, et al. Toll-like receptor 4 and high-mobility group box-1 are involved in ictogenesis and can be targeted to reduce seizures. *Nat Med*. (2010) 16:413–9. doi: 10.1038/nm.2127

77. Iori V, Maroso M, Rizzi M, Iyer AM, Vertemara R, Carli M, et al. Receptor for advanced glycation endproducts is upregulated in temporal lobe epilepsy and contributes to experimental seizures. *Neurobiol Dis*. (2013) 58:102–14. doi: 10.1016/j.nbd.2013.03.006

78. Shi Y, Zhang L, Teng J, Miao W. HMGB1 mediates microglia activation *via* the TLR4/NF-κB pathway in coriaria lactone induced epilepsy. *Mol Med Rep*. (2018) 17:5125–31. doi: 10.3892/mmr.2018.8485

79. Paudel YN, Shaikh MF, Chakraborti A, Kumari Y, Aledo-Serrano Á, Aleksovska K, et al. HMGB1: a common biomarker and potential target for TBI, neuroinflammation, epilepsy, and cognitive dysfunction. *Front Neurosci*. (2018) 12:628. doi: 10.3389/fnins.2018.00628

80. Terrone G, Balosso S, Pauletti A, Ravizza T, Vezzani A. Inflammation and reactive oxygen species as disease modifiers in epilepsy. *Neuropharmacology*. (2020) 167:107742. doi: 10.1016/j.neuropharm.2019.107742

81. Scharfman HE. "Untangling" Alzheimer's disease and epilepsy. *Epilepsy Curr.* (2012) 12:178–83. doi: 10.5698/1535-7511-12.5.178

82. González-Reyes S, Santillán-Cigales JJ, Jiménez-Osorio AS, Pedraza-Chaverri J, Guevara-Guzmán R. Glycyrrhizin ameliorates oxidative stress and inflammation in hippocampus and olfactory bulb in lithium/pilocarpine-induced status epilepticus in rats. *Epilepsy Res.* (2016) 126:126–33. doi: 10.1016/j.eplepsyres.2016.07.007

83. Ying C, Ying L, Yanxia L, Le W, Lili C. High mobility group box 1 antibody represses autophagy and alleviates hippocampus damage in pilocarpine-induced mouse epilepsy model. *Acta Histochem.* (2020) 122:151485. doi: 10.1016/j.acthis.2019.151485

84. Paudel YN, Khan SU, Othman I, Shaikh MF. Naturally occurring HMGB1 inhibitor, glycyrrhizin, modulates chronic seizures-induced memory dysfunction in zebrafish model. *ACS Chem Neurosci.* (2021) 12:3288–302. doi: 10.1021/acschemneuro.0c00825

85. Li YJ, Wang L, Zhang B, Gao F, Yang CM. Glycyrrhizin, an HMGB1 inhibitor, exhibits neuroprotective effects in rats after lithium-pilocarpine-induced status epilepticus. *J Pharm Pharmacol.* (2019) 71:390–9. doi: 10.1111/jphp.13040

86. Ravizza T, Vezzani A. Pharmacological targeting of brain inflammation in epilepsy: therapeutic perspectives from experimental and clinical studies. *Epilepsia Open.* (2018) 3:133–42. doi: 10.1002/epi4.12242

87. Dipasquale V, Cutrupi MC, Colavita L, Manti S, Cuppari C, Salpietro C. Neuroinflammation in autism spectrum disorders: role of high mobility group box 1 protein. *Int J Mol Cell Med.* (2017) 6:148–55. doi: 10.22088/acadpub.BUMS.6.3.148

88. Barbosa IG, Rodrigues DH, Rocha NP, Sousa LF, Vieira EL, Simões-E-Silva AC, et al. Plasma levels of alarmin IL-33 are unchanged in autism spectrum disorder: a preliminary study. *J Neuroimmunol.* (2015) 278:69–72. doi: 10.1016/j.jneuroim.2014.11.021

89. Babinská K, Bucová M, Durmanová V, Lakatošová S, Jánošíková D, Bakoš J, et al. Increased plasma levels of the high mobility group box 1 protein (HMGB1) are associated with a higher score of gastrointestinal dysfunction in individuals with autism. *Physiol Res.* (2014) 63:S613–8. doi: 10.33549/physiolres.932932

90. Emanuele E, Boso M, Brondino N, Pietra S, Barale F, Ucelli di Nemi S, et al. Increased serum levels of high mobility group box 1 protein in patients with autistic disorder. *Prog Neuropsychopharmacol Biol Psychiatry.* (2010) 34:681–3. doi: 10.1016/j.pnpbp.2010.03.020

91. Russo AJ. Decreased epidermal growth factor (EGF) associated with HMGB1 and increased hyperactivity in children with autism. *Biomarker Insights.* (2013) 8:35–41. doi: 10.4137/BMI.S11270

92. Carissimi C, Laudadio I, Palone F, Fulci V, Cesi V, Cardona F, et al. Functional analysis of gut microbiota and immunoinflammation in children with autism spectrum disorders. *Dig Liver Dis.* (2019) 51:1366–74. doi: 10.1016/j.dld.2019.06.006

93. Sappington PL, Yang R, Yang H, Tracey KJ, Delude RL, Fink MP. HMGB1 B box increases the permeability of Caco-2 enterocytic monolayers and impairs intestinal barrier function in mice. *Gastroenterology.* (2002) 123:790–802. doi: 10.1053/gast.2002.35391

94. Nadeem A, Ahmad SF, Bakheet SA, Al-Harbi NO, Al-Ayadhi LY, Attia SM, et al. Toll-like receptor 4 signaling is associated with upregulated NADPH oxidase expression in peripheral T cells of children with autism. *Brain Behav Immun.* (2017) 61:146–54. doi: 10.1016/j.bbi.2016.12.024

95. Nadeem A, Siddiqui N, Alharbi NO, Alharbi MM. Airway and systemic oxidant-antioxidant dysregulation in asthma: a possible scenario of oxidants spill over from lung into blood. *Pulm Pharmacol Ther.* (2014) 29:31–40. doi: 10.1016/j.pupt.2014.06.001

96. Huang Y, Huang X, Ebstein RP, Yu R. Intranasal oxytocin in the treatment of autism spectrum disorders: a multilevel meta-analysis. *Neurosci Biobehav Rev.* (2021) 122:18–27. doi: 10.1016/j.neubiorev.2020.12.028

97. Husarova VM, Lakatosova S, Pivovarciova A, Babinska K, Bakos J, Durdiakova J, et al. Plasma oxytocin in children with autism and its correlations with behavioral parameters in children and parents. *Psychiatry Investig.* (2016) 13:174–83. doi: 10.4306/pi.2016.13.2.174

98. Russo AJ. Increased epidermal growth factor receptor (EGFR) associated with hepatocyte growth factor (HGF) and symptom severity in children with autism spectrum disorders (ASDs). *J Cent Nerv Syst Dis.* (2014) 6:79–83. doi: 10.4137/JCNSD.S13767

99. Yang F, Zhu W, Cai X, Zhang W, Yu Z, Li X, et al. Minocycline alleviates NLRP3 inflammasome-dependent pyroptosis in monosodium glutamate-induced depressive rats. *Biochem Biophys Res Commun.* (2020) 526:553–9. doi: 10.1016/j.bbrc.2020.02.149

100. Liu L, Dong Y, Shan X, Li L, Xia B, Wang H. Anti-depressive effectiveness of Baicalin *in vitro* and *in vivo*. *Molecules.* (2019) 24:326. doi: 10.3390/molecules24020326

101. Franklin TC, Wohleb ES, Zhang Y, Fogaça M, Hare B, Duman RS. Persistent increase in microglial RAGE contributes to chronic stress-induced priming of depressive-like behavior. *Biol Psychiatry.* (2018) 83:50–60. doi: 10.1016/j.biopsych.2017.06.034

102. Fan C, Song Q, Wang P, Li Y, Yang M, Yu SY. Neuroprotective EFFECTS of ginsenoside-Rg1 against depression-like behaviors *via* suppressing glial activation, synaptic deficits, and neuronal apoptosis in rats. *Front Immunol.* (2018) 9:2889. doi: 10.3389/fimmu.2018.02889

103. Banasr M, Duman RS. Glial loss in the prefrontal cortex is sufficient to induce depressive-like behaviors. *Biol Psychiatry.* (2008) 64:863–70. doi: 10.1016/j.biopsych.2008.06.008

104. Wang B, Huang X, Pan X, Zhang T, Hou C, Su WJ, et al. Minocycline prevents the depressive-like behavior through inhibiting the release of HMGB1 from microglia and neurons. *Brain Behav Immun.* (2020) 88:132–43. doi: 10.1016/j.bbi.2020.06.019

105. Wang B, Lian YJ, Su WJ, Liu LL, Li JM, Jiang CL, et al. Fr-HMGB1 and ds-HMGB1 activate the kynurenine pathway *via* different mechanisms in association with depressive-like behavior. *Mol Med Rep.* (2019) 20:359–67. doi: 10.3892/mmr.2019.10225

106. Wang B, Lian YJ, Dong X, Peng W, Liu LL, Su WJ, et al. Glycyrrhizic acid ameliorates the kynurenine pathway in association with its antidepressant effect. *Behav Brain Res.* (2018) 353:250–7. doi: 10.1016/j.bbr.2018.01.024

107. Maddison DC, Giorgini F. The kynurenine pathway and neurodegenerative disease. *Semin Cell Dev Biol.* (2015) 40:134–41. doi: 10.1016/j.semcdb.2015.03.002

108. Wang B, Lian YJ, Su WJ, Peng W, Dong X, Liu LL, et al. HMGB1 mediates depressive behavior induced by chronic stress through activating the kynurenine pathway. *Brain Behav Immun.* (2018) 72:51–60. doi: 10.1016/j.bbi.2017.11.017

109. Myint AM, Kim YK. Network beyond IDO in psychiatric disorders: revisiting neurodegeneration hypothesis. *Prog Neuropsychopharmacol Biol Psychiatry.* (2014) 48:304–13. doi: 10.1016/j.pnpbp.2013.08.008

110. Zhang H, Ding L, Shen T, Peng D. HMGB1 involved in stress-induced depression and its neuroinflammatory priming role: a systematic review. *Gen Psychiatry.* (2019) 32:e100084. doi: 10.1136/gpsych-2019-100084

111. Xu X, Piao HN, Aosai F, Zeng XY, Cheng JH, Cui YX, et al. Arctigenin protects against depression by inhibiting microglial activation and neuroinflammation *via* HMGB1/TLR4/NF-κB and TNF-α/TNFR1/NF-κB pathways. *Br J Pharmacol.* (2020) 177:5224–45. doi: 10.1111/bph.15261

112. Xie J, Bi B, Qin Y, Dong W, Zhong J, Li M, et al. Inhibition of phosphodiesterase-4 suppresses HMGB1/RAGE signaling pathway and NLRP3 inflammasome activation in mice exposed to chronic unpredictable mild stress. *Brain Behav Immun.* (2021) 92:67–77. doi: 10.1016/j.bbi.2020.11.029

113. Ghosh D, Singh A, Kumar A, Sinha N. High mobility group box 1 (HMGB1) inhibition attenuates lipopolysaccharide-induced cognitive dysfunction and sickness-like behavior in mice. *Immunol Res.* (2022). doi: 10.1007/s12026-022-09295-8

114. Hisaoka-Nakashima K, Tomimura Y, Yoshii T, Ohata K, Takada N, Zhang FF, et al. High-mobility group box 1-mediated microglial activation induces anxiodepressive-like behaviors in mice with neuropathic pain. *Prog Neuropsychopharmacol Biol Psychiatry.* (2019) 92:347–62. doi: 10.1016/j.pnpbp.2019.02.005

115. Bian H, Xiao L, Liang L, Xie Y, Wang H, Slevin M, et al. (2022). Polydatin prevents neuroinflammation and relieves depression *via* regulating Sirt1/HMGB1/NF-κB signaling in mice. *Neurotox Res*, 40, 1393–404. doi: 10.1007/s12640-022-00553-z

116. Cao ZY, Liu YZ, Li JM, Ruan YM, Yan WJ, Zhong SY, et al. Glycyrrhizic acid as an adjunctive treatment for depression through anti-inflammation: a randomized placebo-controlled clinical trial. *J Affect Disord.* (2020) 265:247–54. doi: 10.1016/j.jad.2020.01.048

117. Zhen C, Wang Y, Li D, Zhang W, Zhang H, Yu X, et al. Relationship of High-mobility group box 1 levels and multiple sclerosis: a systematic review and meta-analysis. *Mult Scler Relat Disord.* (2019) 31:87–92. doi: 10.1016/j.msard.2019.03.030

118. Constantinescu CS, Farooqi N, O'Brien K, Gran B. Experimental autoimmune encephalomyelitis (EAE) as a model for multiple sclerosis (MS). *Br J Pharmacol.* (2011) 164:1079–106. doi: 10.1111/j.1476-5381.2011.01302.x

119. Andersson A, Covacu R, Sunnemark D, Danilov AI, Dal Bianco A, Khademi M, et al. Pivotal advance: HMGB1 expression in active lesions of

human and experimental multiple sclerosis. *J Leukoc Biol.* (2008) 84:1248–55. doi: 10.1189/jlb.1207844

120. Sternberg Z, Sternberg D, Chichelli T, Drake A, Patel N, Kolb C, et al. High-mobility group box 1 in multiple sclerosis. *Immunol Res.* (2016) 64:385–91. doi: 10.1007/s12026-015-8673-x

121. Malhotra S, Fissolo N, Tintoré M, Wing AC, Castilló J, Vidal-Jordana A, et al. Role of high mobility group box protein 1 (HMGB1) in peripheral blood from patients with multiple sclerosis. *J Neuroinflammation.* (2015) 12:48. doi: 10.1186/s12974-015-0269-9

122. Anderson G, Rodriguez M, Reiter RJ. Multiple sclerosis: melatonin, orexin, and ceramide interact with platelet activation coagulation factors and gut-microbiome-derived butyrate in the circadian dysregulation of mitochondria in glia and immune cells. *Int J Mol Sci.* (2019) 20:5500. doi: 10.3390/ijms20215500

123. Scheiblich H, Schlütter A, Golenbock DT, Latz E, Martinez-Martinez P, Heneka MT. Activation of the NLRP3 inflammasome in microglia: the role of ceramide. *J Neurochem.* (2017) 143:534–50. doi: 10.1111/jnc.14225

124. Okuda Y, Nakatsuji Y, Fujimura H, Esumi H, Ogura T, Yanagihara T, et al. Expression of the inducible isoform of nitric oxide synthase in the central nervous system of mice correlates with the severity of actively induced experimental allergic encephalomyelitis. *J Neuroimmunol.* (1995) 62:103–12. doi: 10.1016/0165-5728(95)00114-H

125. Nicaise AM, Wagstaff LJ, Willis CM, Paisie C, Chandok H, Robson P, et al. Cellular senescence in progenitor cells contributes to diminished remyelination potential in progressive multiple sclerosis. *Proc Natl Acad Sci U S A.* (2019) 116:9030–9. doi: 10.1073/pnas.1818348116

126. Rouillard ME, Hu J, Sutter PA, Kim HW, Huang JK, Crocker SJ. The cellular senescence factor extracellular HMGB1 directly inhibits oligodendrocyte progenitor cell differentiation and impairs CNS remyelination. *Front Cell Neurosci.* (2022) 16:833186. doi: 10.3389/fncel.2022.833186

127. Uzawa A, Mori M, Taniguchi J, Masuda S, Muto M, Kuwabara S. Anti-high mobility group box 1 monoclonal antibody ameliorates experimental autoimmune encephalomyelitis. *Clin Exp Immunol.* (2013) 172:37–43. doi: 10.1111/cei.12036

128. Sun Y, Chen H, Dai J, Wan Z, Xiong P, Xu Y, et al. Glycyrrhizin protects mice against experimental autoimmune encephalomyelitis by inhibiting high-mobility group box 1 (HMGB1) expression and neuronal HMGB1 release. *Front Immunol.* (2018) 9:1518. doi: 10.3389/fimmu.2018.01518

129. Xiao Y, Sun Y, Liu W, Zeng F, Shi J, Li J, et al. HMGB1 promotes the release of sonic hedgehog from astrocytes. *Front Immunol.* (2021) 12:584097. doi: 10.3389/fimmu.2021.584097

130. Becker KA, Halmer R, Davies L, Henry BD, Ziobro-Henry R, Decker Y, et al. Blockade of experimental multiple sclerosis by inhibition of the acid sphingomyelinase/ceramide system. *Neurosignals.* (2017) 25:88–97. doi: 10.1159/000484621

131. Chu Y, Jing Y, Zhao X, Wang M, Zhang M, Ma R, et al. Modulation of the HMGB1/TLR4/NF-κB signaling pathway in the CNS by matrine in experimental autoimmune encephalomyelitis. *J Neuroimmunol.* (2021) 352:577480. doi: 10.1016/j.jneuroim.2021.577480

132. Paudel YN, Angelopoulou E, Semple B, Piperi C, Othman I, Shaikh MF. Potential neuroprotective effect of the HMGB1 inhibitor glycyrrhizin in neurological disorders. *ACS Chem Neurosci.* (2020) 11:485–500. doi: 10.1021/acschemneuro.9b00640

133. Grad LI, Rouleau GA, Ravits J, Cashman NR. Clinical spectrum of amyotrophic lateral sclerosis (ALS). *Cold Spring Harb Perspect Med.* (2017) 7:a024117. doi: 10.1101/cshperspect.a024117

134. Lee JD, Liu N, Levin SC, Ottosson L, Andersson U, Harris HE, et al. Therapeutic blockade of HMGB1 reduces early motor deficits, but not survival in the SOD1G93A mouse model of amyotrophic lateral sclerosis. *J Neuroinflammation.* (2019) 16:45. doi: 10.1186/s12974-019-1435-2

135. Paudel YN, Angelopoulou E, Piperi C, Othman I, Shaikh MF. Implication of HMGB1 signaling pathways in amyotrophic lateral sclerosis (ALS): from molecular mechanisms to pre-clinical results. *Pharmacol Res.* (2020) 156:104792. doi: 10.1016/j.phrs.2020.104792

136. Lo Coco D, Veglianese P, Allievi E, Bendotti C. Distribution and cellular localization of high mobility group box protein 1 (HMGB1) in the spinal cord of a transgenic mouse model of ALS. *Neurosci Lett.* (2007) 412:73–7. doi: 10.1016/j.neulet.2006.10.063

137. Lee JD, McDonald TS, Fung J, Woodruff TM. Absence of receptor for advanced glycation end product (RAGE) reduces inflammation and extends survival in the hSOD1G93A mouse model of amyotrophic lateral sclerosis. *Mol Neurobiol.* (2020) 57:4143–55. doi: 10.1007/s12035-020-02019-9

138. Lee JY, Lee JD, Phipps S, Noakes PG, Woodruff TM. Absence of toll-like receptor 4 (TLR4) extends survival in the hSOD1 G93A mouse model of amyotrophic lateral sclerosis. *J Neuroinflammation.* (2015) 12:90. doi: 10.1186/s12974-015-0310-z

139. Brambilla L, Martorana F, Guidotti G, Rossi D. Dysregulation of astrocytic HMGB1 signaling in amyotrophic lateral sclerosis. *Front Neurosci.* (2018) 12:622. doi: 10.3389/fnins.2018.00622

frontiers | Frontiers in Neurology

TYPE Original Research
PUBLISHED 01 November 2022
DOI 10.3389/fneur.2022.1013062

OPEN ACCESS

EDITED BY
Wael M. Y. Mohamed,
International Islamic University Malaysia, Malaysia

REVIEWED BY
Theodoros Kyprianou,
King's College Hospital NHS Foundation Trust, United Kingdom
Malgorzata Anna Mikaszewska-Sokolewicz,
Medical University of Warsaw, Poland

*CORRESPONDENCE
Guo-Feng Yu
quzhouguofengyu@163.com

SPECIALTY SECTION
This article was submitted to Neurological Biomarkers, a section of the journal Frontiers in Neurology

RECEIVED 06 August 2022
ACCEPTED 10 October 2022
PUBLISHED 01 November 2022

CITATION
Yan X-J, Zhan C-P, Lv Y, Mao D-D, Zhou R-C, Xv Y-M and Yu G-F (2022) Utility of serum nuclear factor erythroid 2-related factor 2 as a potential prognostic biomarker of severe traumatic brain injury in adults: A prospective cohort study. *Front. Neurol.* 13:1013062. doi: 10.3389/fneur.2022.1013062

Utility of serum nuclear factor erythroid 2-related factor 2 as a potential prognostic biomarker of severe traumatic brain injury in adults: A prospective cohort study

Xin-Jiang Yan, Cheng-Peng Zhan, Yao Lv, Dan-Dan Mao, Ri-Cheng Zhou, Yong-Min Xv and Guo-Feng Yu*

Department of Neurosurgery, The Quzhou Affiliated Hospital of Wenzhou Medical University, Quzhou People's Hospital, Quzhou, China

Objective: Nuclear factor erythroid 2-related factor 2 (Nrf2) may harbor endogenous neuroprotective role. We strived to ascertain the prognostic significance of serum Nrf2 in severe traumatic brain injury (sTBI).

Methods: This prospective cohort study included 105 controls and 105 sTBI patients, whose serum Nrf2 levels were quantified. Its relations to traumatic severity and 180-day overall survival, mortality, and poor prognosis (extended Glasgow Outcome Scale score 1–4) were discerned using multivariate analysis.

Results: There was a substantial enhancement of serum Nrf1 levels of patients (median, 10.9 vs. 3.3 ng/ml; $P < 0.001$), as compared to controls. Serum Nrf2 levels were independently correlative to Rotterdam computed tomography (CT) scores ($\rho = 0.549$, $P < 0.001$; t = 2.671, $P = 0.009$) and Glasgow Coma Scale (GCS) scores ($\rho = -0.625$, $P < 0.001$; t = −3.821, $P < 0.001$). Serum Nrf2 levels were significantly higher in non-survivors than in survivors (median, 12.9 vs. 10.3 ng/ml; $P < 0.001$) and in poor prognosis patients than in good prognosis patients (median, 12.5 vs. 9.4 ng/ml; $P < 0.001$). Patients with serum Nrf2 levels > median value (10.9 ng/ml) had markedly shorter 180-day overall survival time than the other remainders (mean, 129.3 vs. 161.3 days; $P = 0.002$). Serum Nrf2 levels were independently predictive of 180-day mortality (odds ratio, 1.361; $P = 0.024$), overall survival (hazard ratio, 1.214; $P = 0.013$), and poor prognosis (odds ratio, 1.329; $P = 0.023$). Serum Nrf2 levels distinguished the risks of 180-day mortality and poor prognosis with areas under receiver operating characteristic curve (AUCs) at 0.768 and 0.793, respectively. Serum Nrf2 levels > 10.3 ng/ml and 10.8 ng/ml discriminated patients at risk of 180-day mortality and poor prognosis with the maximum Youden indices of 0.404 and 0.455, respectively. Serum Nrf2 levels combined with GCS scores and Rotterdam CT scores for death prediction (AUC, 0.897; 95% CI, 0.837–0.957) had significantly higher AUC than GCS scores ($P = 0.028$), Rotterdam CT scores ($P = 0.007$), or serum Nrf2 levels ($P = 0.006$) alone, and the combination for poor outcome prediction (AUC, 0.889; 95% CI, 0.831–0.948) displayed

significantly higher AUC than GCS scores ($P = 0.035$), Rotterdam CT scores ($P = 0.006$), or serum Nrf2 levels ($P = 0.008$) alone.

Conclusion: Increased serum Nrf2 levels are tightly associated with traumatic severity and prognosis, supporting the considerable prognostic role of serum Nrf2 in sTBI.

KEYWORDS

biomarkers, nuclear factor erythroid 2-related factor 2, severity, prognosis, traumatic brain injury

Introduction

Severe traumatic brain injury (sTBI), one of the most severe traumas, is characterized by high morbidity and mortality (1). Its pathological mechanisms involve primary brain injury and secondary brain injury (2). Its molecular processes are very complex and include inflammation, oxidative stress, and apoptosis (3). Clinically, the Glasgow Coma Scale (GCS) and Rotterdam computed tomography (CT) scale are the two frequently used severity indicators, which are strongly associated with prognosis of TBI (4, 5). Recently, researchers have paid extensive attention to biomarkers with respect to severity assessment and prognosis prediction of TBI (6–8).

Nuclear factor erythroid 2-related factor 2 (Nrf2) is a kind of recently discovered nuclear factor for antioxidant response element (ARE)-regulated genes, which is also a key regulator of endogenous inducible defense systems in the body (9). Acute oxidative stress or inflammation can greatly upregulate expressions of Nrf2 in neurons of animals or humans under some pathological conditions, such as TBI, intracerebral hemorrhage, and ischemic stroke (10–14). Accumulating experimental data have shown that Nrf2 may confer brain-protective effects *via* regulating the expression of genes coding antioxidant, anti-inflammatory, and detoxifying proteins (10–13). Thus, it is postulated that circulating Nrf2 may serve as a promising biochemical maker of acute brain injury. Our study aimed to explore the prognostic value of serum Nrf2 in a group of sTBI patients.

Abbreviations: CT, computerized tomography; GCS, Glasgow Coma Scale; ROC, receiver operating characteristic; sTBI, severe traumatic brain injury; ROC, receiver operating characteristic; AUC, area under curve; OR, odds ratio; HR, hazard ratio; ROS, reactive oxygen species; Nrf2, nuclear factor erythroid 2-related factor 2; ARE, antioxidant response element; GOSE, extended Glasgow Outcome Scale.

Materials and methods

Study design and participant selection

Patients diagnosed with sTBI (GCS scores < 9) were enrolled into this prospective observational study, which was performed at our hospital from February 2017 to May 2021. The inclusion criteria were as follows: (1) age $\geq$ 18 years, (2) injury severity score < 9 in non-cranial aspects, (3) blunt trauma, and (4) hospital admission within 12 h after trauma. The exclusion criteria were as follows: (1) previous neurological diseases, such as stroke, intracranial tumors, cerebral aneurysms, vascular malformations, and severe head trauma, and (2) other specific conditions or diseases, e.g., severe infections within recent a month, autoimmune diseases, pregnancies, severe hepatic, renal or cardiac diseases, and malignancies. In addition, controls were a group of healthy non-patient volunteers recruited from May 2020 to May 2021 at our hospital, who were free of some chronic diseases, such as hypertension, diabetes mellitus, and coronary heart disease, and were normal in routine tests, e.g., blood leucocyte count, blood hemoglobin levels, and blood platelet count. This study followed the ethical guidelines of the Declaration of Helsinki, and the approval for the protocol of this study was acquired from the institutional review committee at our hospital. All the relatives of patients and controls themselves gave informed written consent prior to inclusion in the study.

Demographic, clinical, and radiological information

We gathered demographic information, past medical history, cigarette smoking history, and alcohol drinking history. Baseline GCS scores were recorded to reflect clinical severity of head trauma. The radiological parameters were determined by research personnel blinded to clinical data using the first available head CT scan. Positive radiological appearances included abnormal cisterns, midline shift, epidural hematoma, subdural hematoma, subarachnoid hemorrhage, intraventricular hemorrhage, intracerebral hematoma, brain

contusion, and pneumocephalus. Rotterdam CT scores were calculated to assess radiological severity of head trauma. A functional outcome was evaluated using eight-grade extended Glasgow Outcome Scale (GOSE) at 180 days following trauma. GOSE was dichotomized into poor outcome (1–4 points) and good outcome (4–6 points) (15).

Measurement of serum Nrf2 levels

Blood samples were collected from all study participants, including patients and controls. The blood was centrifuged, and then, serum samples were immediately preserved at −80°C until required for further analysis. The same technician, who was blinded to clinical data, performed measurement of serum Nrf2 levels using a commercially available DNA-binding enzyme-linked immunosorbent assay (ELISA) (TransAM Nrf2, Active Motif, Carlsbad, CA, USA) as per the manufacturer's protocol. In brief, the samples were incubated for 1 h in a pre-coated 96-well-plate, followed by primary antibody incubation for 1 h. After incubation, all the wells were washed and incubated with horseradish peroxidase-conjugated antibody for 1 h, followed by trimethylbenzene substrate for 15 min in the dark. The reaction was stopped by the addition of stop solution, and the plate was read at 450 nm on a microplate reader (Multiskan GO; Thermo Fisher Scientific, Waltham, MA, USA). Each sample was in duplicate determined, and the results were averaged for further analysis.

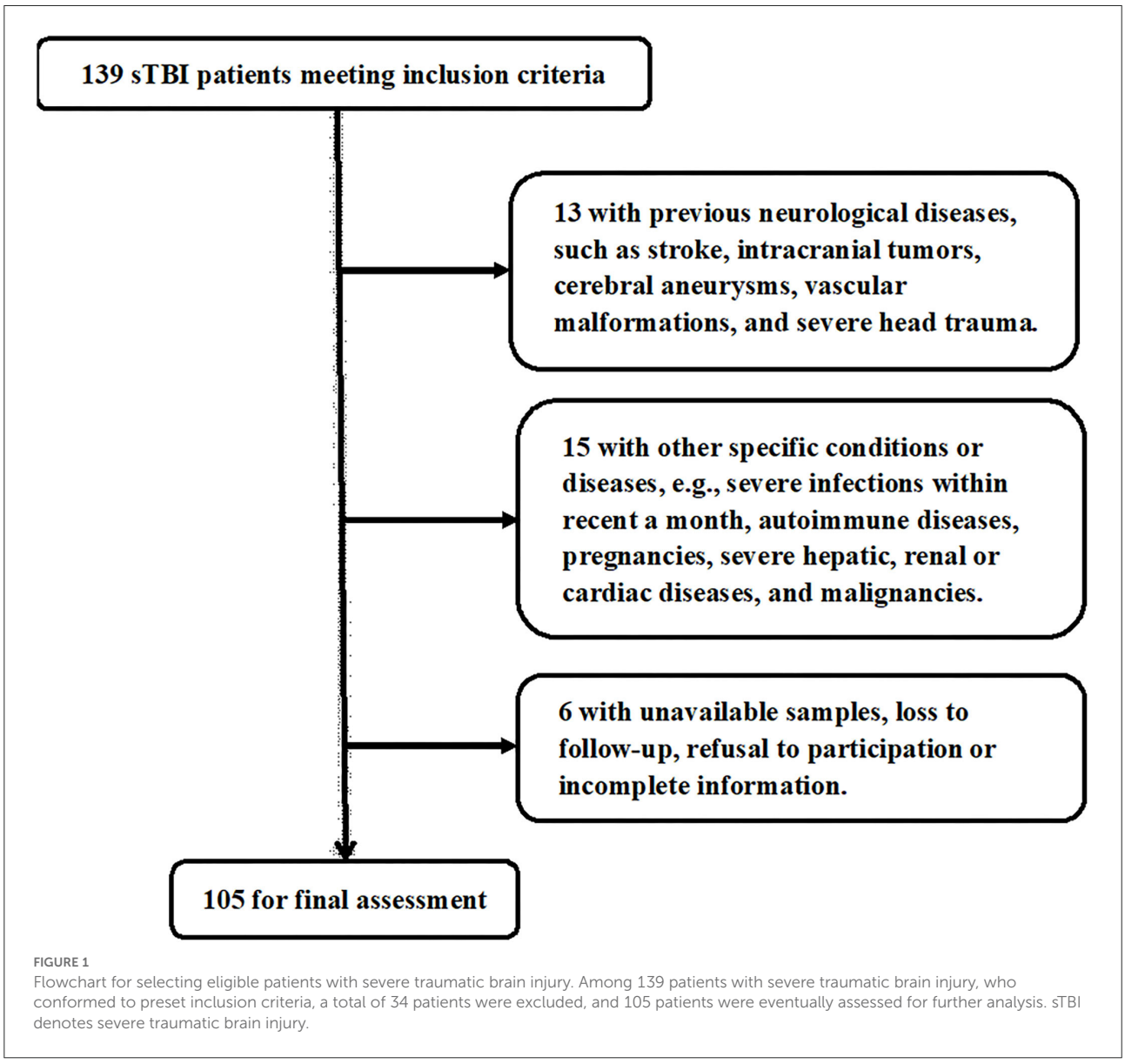

FIGURE 1
Flowchart for selecting eligible patients with severe traumatic brain injury. Among 139 patients with severe traumatic brain injury, who conformed to preset inclusion criteria, a total of 34 patients were excluded, and 105 patients were eventually assessed for further analysis. sTBI denotes severe traumatic brain injury.

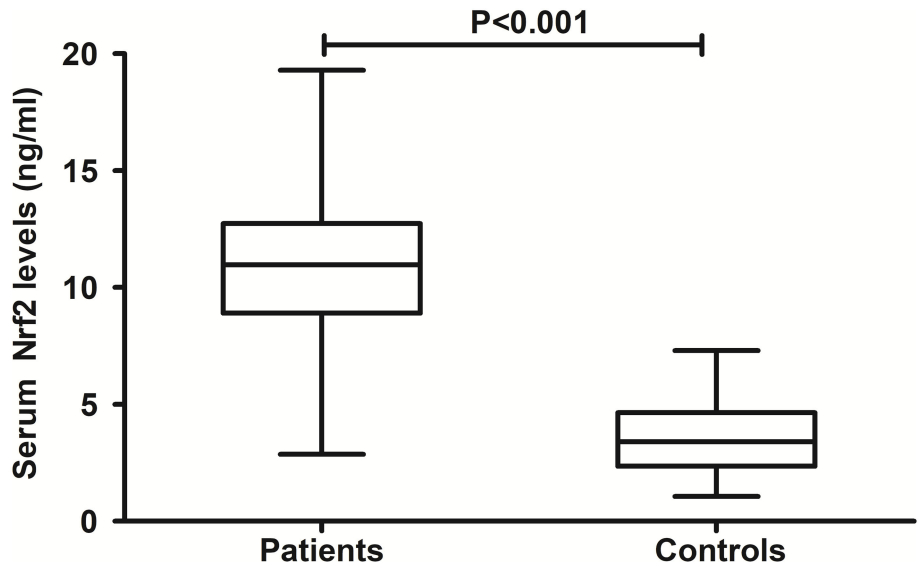

FIGURE 2
Comparison of serum nuclear factor erythroid 2-related factor 2 levels between controls and patients with severe traumatic brain injury. Patients with severe traumatic brain injury had significantly higher serum nuclear factor erythroid 2-related factor 2 levels than healthy controls ($P < 0.001$). Nrf2 means nuclear factor erythroid 2-related factor 2.

TABLE 1 Factors correlated with serum nuclear factor erythroid 2-related factor 2 levels after severe traumatic brain injury.

	ρ	*P*-value
Gender (male/female)	0.093	0.344
Age (y)	0.214	0.028
Current cigarette smoking	0.139	0.158
Alcohol abuse	0.091	0.354
Hypertension	0.046	0.638
Diabetes mellitus	0.211	0.030
Hyperlipidemia	0.050	0.610
Hospital admission time (h)	−0.098	0.319
Blood-sampling time (h)	−0.100	0.308
Traumatic causes	−0.157	0.110
GCS scores	−0.625	<0.001
Rotterdam CT scores	0.549	<0.001
Systolic arterial pressure (mmHg)	−0.164	0.095
Diastolic arterial pressure (mmHg)	−0.075	0.448
Blood glucose levels (mmol/l)	0.171	0.082
Blood leucocyte count ($\times 10^9$/l)	0.137	0.165

Correlations were analyzed using Spearman's test. CT, computerized tomography; GCS, Glasgow Coma Scale.

Statistical analysis

Receiver operating characteristic (ROC) curve analysis was carried out using MedCalc statistical software version 17.4 (MedCalc Software, Mariakerke, Belgium), and other data analyses were performed utilizing the SPSS 20.0 statistical package (SPSS Inc., Chicago, Illinois, USA). Qualitative variables were shown as frequencies (proportions). Categorical data were compared between two groups using Pearson's Chi-square test or Fisher's exact test as appropriate. Quantitative data, which were tested for normal distribution, were presented as means (standard deviations, SDs) if normally distributed or medians (percentages 25th−75th) if non-normally distributed. Statistical methods of intergroup comparisons of quantitative data included the independent *t*-test for normally distributed data and the Mann–Whitney test for non-normally distributed data. Using the Kruskal–Wallis H test, serum Nrf2 levels were compared among multiple groups divided by GCS scores and Rotterdam CT scores. Serum Nrf2 levels were dichotomized based on its median value, and 180-day overall survival time was compared using the log-rank test. Under ROC curve, the prognostic predictive capability was assessed, and area under ROC curve (AUC) and the corresponding 95% confidence interval (CI) were yielded. 180-day death and poor prognosis were regarded as two dependent variables. The two multivariate binary logistic regression models were established, and significant variables in univariate analysis were forced to identify independent predictors of 180-death and poor prognosis. Associations were reported as odds ratio (ORs) and 95% CIs. Univariate Cox's proportional hazard analysis was performed to screen variables, which were substantially related to 180-day overall survival, and afterward, multivariate Cox's proportional hazard analysis was performed to discern

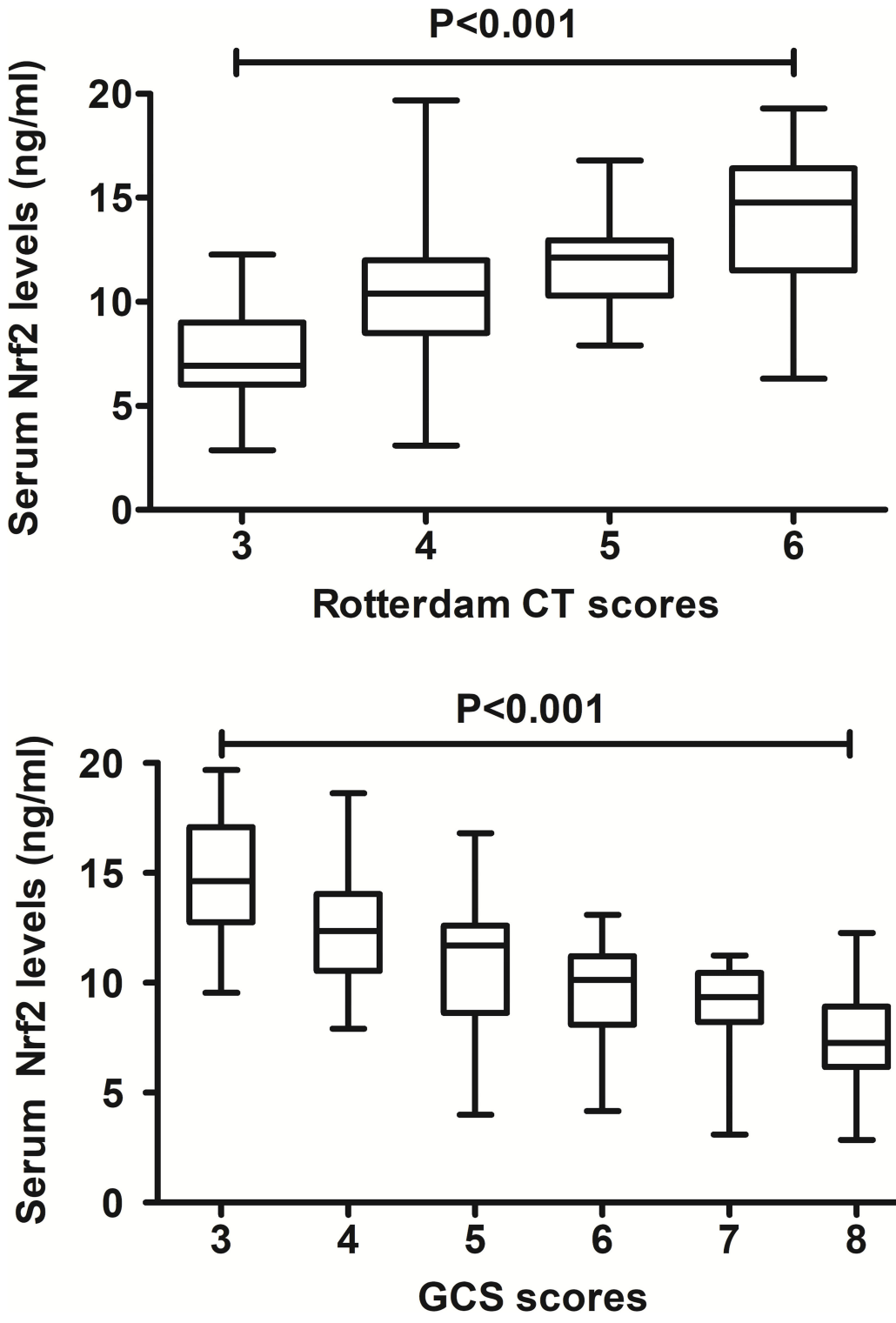

FIGURE 3
Relationship between serum nuclear factor erythroid 2-related factor 2 levels and traumatic severity in patients with severe traumatic brain injury. There were substantial differences in terms of serum nuclear factor erythroid 2-related factor 2 levels among subgroups divided by Rotterdam computed tomography scores and Glasgow Coma Scale scores in patients with severe traumatic brain injury (both $P < 0.001$). Nrf2 indicates nuclear factor erythroid 2-related factor 2; CT, computed tomography; GCS, Glasgow Coma Scale.

independent predictors. Hazard ratio (HRs) and 95% CIs were reported for showing associations. Bivariate correlations were analyzed using the Spearman test, and thereafter, multivariate linear regression model was configured to ascertain variables, which were independently correlated with serum Nrf2 levels. For all tests, the two-sided $P < 0.05$ were considered statistically significant.

Results

Patient selection and participant characteristics

In Figure 1, a total of 139 sTBI patients fitted the inclusion criteria, 34 patients were thereafter removed from this study based on the exclusion criteria, and eventually 105 patients were analyzed for epidemiological investigation. In addition, a group of controls, including 105 healthy individuals, were enrolled. Patients were composed of 60 males and 45 females and were aged from 18 to 78 years (mean, 42.3 years; SD, 14.2 years). And controls were comprised of 54 males and 51 females and were aged from 18 to 77 years (mean, 43.8 years; SD, 13.8 years). Age and gender percentage were not significantly different between controls and patients (both $P > 0.05$).

Among this cohort of patients, 32 were cigarette smokers, 33 consumed alcohol, 17 suffered from hypertension, 12 presented with diabetes mellitus, and 17 were inflicted with hyperlipidemia. Hospital admission time ranged from 0.5 to 12.0 h after trauma (median, 4.8 h; percentiles 25–75th, 3.5–6.3 h). Blood-sampling time ranged from 1.0 to 14.5 h (median, 6.3 h; percentiles 25–75th, 4.5–8.1 h) following trauma. Traumas of 52 cases were caused by automobile/motorcycle; those of 44 cases, by fall/jump; and those of 9 cases, by others. GCS score ranged from 3 to 8 (median, 5; upper-lower quartiles, 4–6). Rotterdam CT score ranged from 3 to 6 (median, 4; upper-lower quartiles, 4–5). The mean systolic and diastolic arterial pressures were 125.7 mmHg (SD, 29.6 mmHg; range, 75–182 mmHg) and 74.7 mmHg (SD, 17.1 mmHg; range, 45–109 mmHg), respectively. Blood glucose levels ranged from 5.2 to 20.7 mmol/l (median, 8.8 mmol/l; lower–upper quartiles, 7.2–11.4 mmol/l). Blood leucocyte count ranged from 3.2 to 16.1 $\times 10^9$/l (median, 7.5 $\times 10^9$/l; lower–upper quartiles, 6.0–10.0 $\times 10^9$/l).

TABLE 2 Factors associated with 180-day mortality after severe traumatic brain injury.

	The dead	The alive	*P*-value
Gender (male/female)	16/10	44/35	0.602
Age (y)	47.6 ± 16.2	40.5 ± 13.1	0.026
Current cigarette smoking	11 (42.3%)	21 (26.6%)	0.131
Alcohol abuse	11 (42.3%)	22 (27.9%)	0.168
Hypertension	7 (26.9%)	10 (12.7%)	0.123
Diabetes mellitus	5 (19.2%)	7 (8.9%)	0.166
Hyperlipidemia	5 (19.2%)	12 (15.2%)	0.759
Hospital admission time (h)	4.5 (2.9–5.5)	5.1 (3.9–6.5)	0.117
Blood-sampling time (h)	5.2 (3.6–7.5)	6.8 (4.9–8.4)	0.100
Traumatic causes			0.391
Automobile/motorcycle	15	37	
Fall/jump	8	36	
Others	3	6	
GCS scores	4 (3–4)	5 (5–7)	<0.001
Rotterdam CT scores	6 (5–6)	4 (4–5)	<0.001
Systolic arterial pressure (mmHg)	126.2 ± 29.2	125.6 ± 29.8	0.925
Diastolic arterial pressure (mmHg)	76.0 ± 17.4	73.6 ± 17.1	0.532
Blood glucose levels (mmol/l)	10.4 (8.6–12.6)	8.4 (6.8–10.9)	0.003
Blood leucocyte count ($\times 10^9$/l)	8.5 (6.2–10.8)	7.3 (5.8–9.6)	0.478
Serum Nrf2 levels (ng/ml)	12.9 (11.0–15.2)	10.3 (8.3–12.4)	<0.001

Data were shown as mean ± standard deviation, median (25–75th percentiles), or count (percentage) where appropriate. Statistical methods for intergroup comparison included the t-test, Mann–Whitney U test, Pearson Chi-square test, or Fisher's exact test as appropriate. CT, computerized tomography; GCS, Glasgow Coma Scale; Nrf2, nuclear factor erythroid 2-related factor 2.

Change of serum Nrf2 levels and its relation to trauma severity

In Figure 2, there was a substantial elevation of serum Nrf2 levels in patients, as compared to controls ($P < 0.001$). Just as listed in Table 1, variables, which were intimately correlated with serum Nrf2 levels of patients using Spearman's test, were age, diabetes mellitus, GCS scores, and Rotterdam CT scores. Using multivariate logistic linear analysis, variables, which retained independently correlated with serum Nrf2 levels, were GCS scores ($t = -3.821$, $P < 0.001$) and Rotterdam CT scores ($t = 2.671$, $P = 0.009$). Alternatively, 14, 25, 29, 15, 10, and 12 patients had GCS scores 3, 4, 5, 6, 7, and 8, respectively. Moreover, 11, 50, 25, and 19 patients had Rotterdam CT scores 3, 4, 5, and 6, respectively. In Figure 3, serum Nrf2 levels were significantly lowest in patients with Rotterdam CT score 3, followed by Rotterdam CT scores 4 and 5, and were substantially highest in those with Rotterdam CT score 6 ($P < 0.001$). Similarly, there were markedly highest serum Nrf2 levels in patients with GCS score 3, followed by GCS scores 4, 5, 6, and 7, and

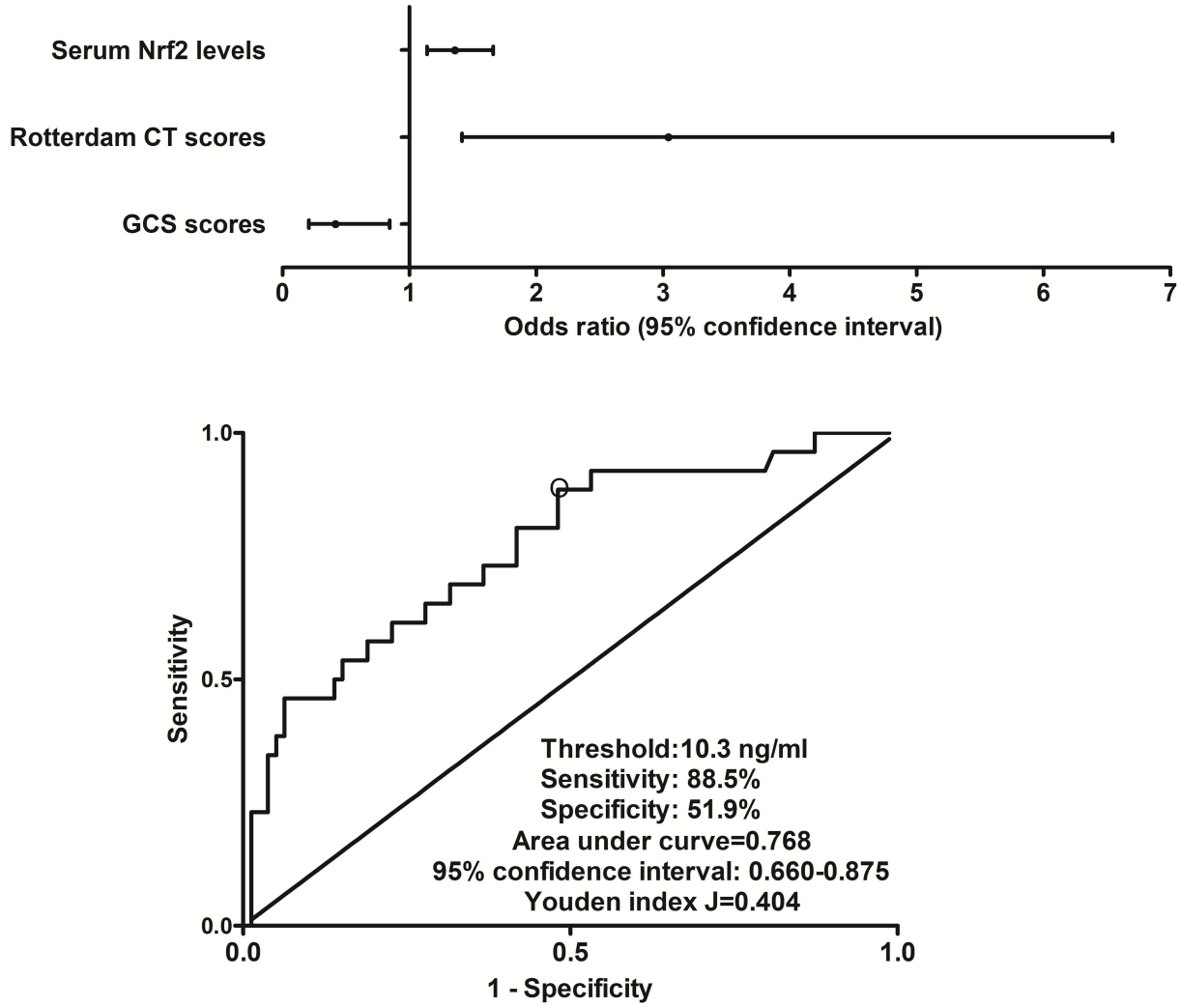

FIGURE 4
Relationship between serum nuclear factor erythroid 2-related factor 2 levels and 180-day death after severe traumatic brain injury. Serum nuclear factor erythroid 2-related factor 2 levels, Rotterdam computed tomography scores, and Glasgow Coma Scale scores were the three independent predictors of 180-day death after severe traumatic brain injury (all $P < 0.05$). Serum nuclear factor erythroid 2-related factor 2 levels were significantly predictive of 180-day death under receiver operating characteristic curve ($P < 0.001$), and using Youden's method, an optimal value of nuclear factor erythroid 2-related factor 2 levels was chosen, which produced medium–high sensitivity and specificity values for death prediction. Nrf2 indicates nuclear factor erythroid 2-related factor 2; CT, computed tomography; GCS, Glasgow Coma Scale.

pronouncedly lowest in those with GCS score 8 ($P < 0.001$, Figure 3).

Relationship between serum Nrf2 levels and death within post-traumatic 180 days

In this group of sTBI patients, 180-day mortality was 24.8% (26/105). Non-survivors were significantly older than survivors, GCS scores were substantially lower, and Rotterdam CT scores were markedly higher in the dead than in the alive, and serum Nrf2 levels and blood glucose levels were profoundly raised in non-surviving patients, as compared to surviving ones (all $P < 0.05$, Table 2). The preceding variables were forced into the binary logistic regression model, and as a subsequence, GCS scores, Rotterdam CT scores, and serum Nrf2 levels emerged as the three independent factors of 180-day death (all $P < 0.05$, Figure 4). Also, serum Nrf2 levels significantly distinguished the risk of 180-day death, and using Youden's method, an optimal value of serum Nrf2 levels was selected, which generated medium–high sensitivity and

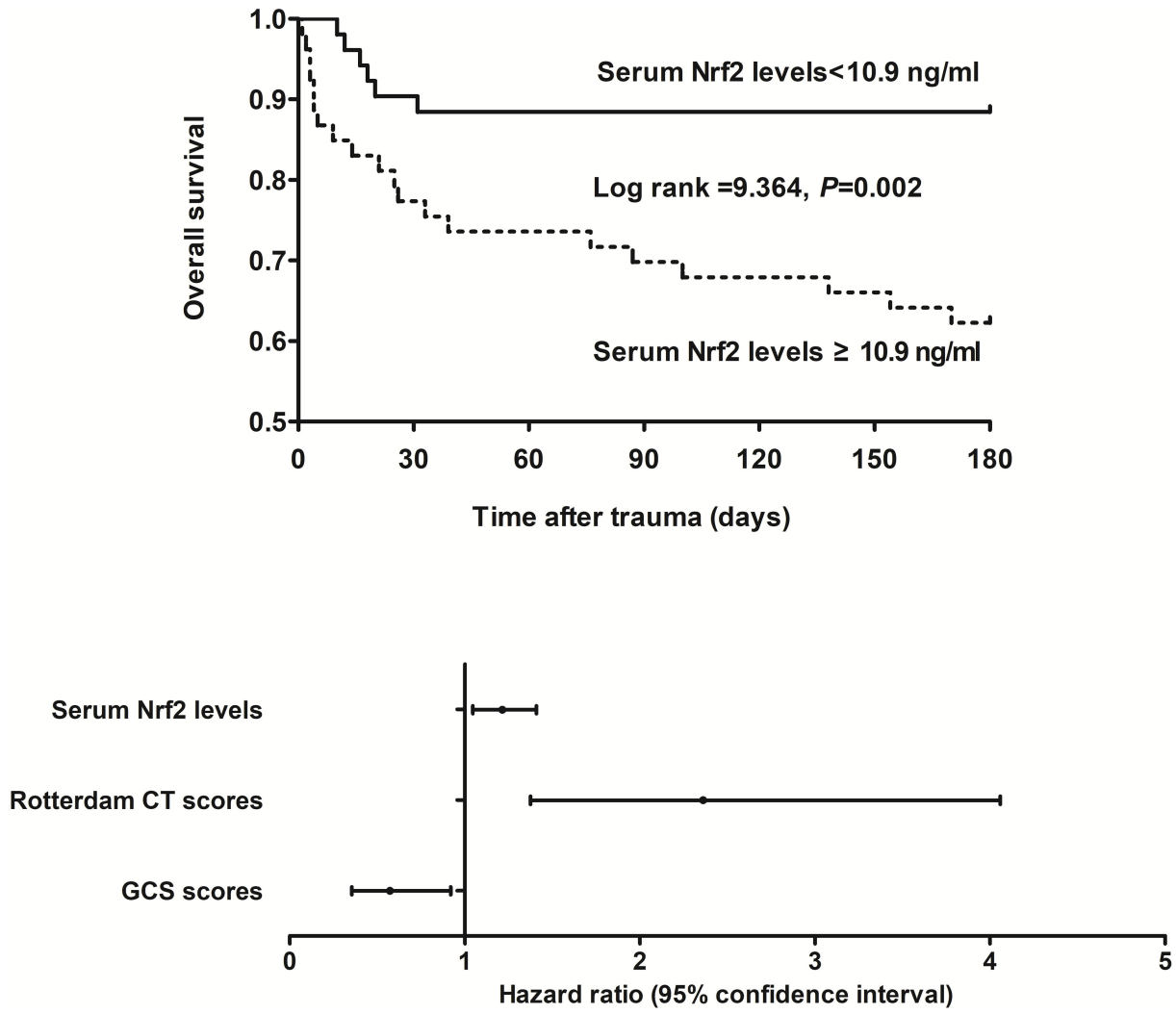

FIGURE 5
Relationship between serum nuclear factor erythroid 2-related factor 2 levels and 180-day overall survival after severe traumatic brain injury. Serum nuclear factor erythroid 2-related factor 2 levels, Rotterdam computed tomography scores, and Glasgow Coma Scale scores were independently associated with 180-day overall survival after severe traumatic brain injury (all $P < 0.05$). Patients with serum nuclear factor erythroid 2-related factor 2 levels $\geq$ 10.9 ng/ml (median value) displayed substantially shorter 180-day overall survival time than the other remainders ($P < 0.01$). Nrf2 indicates nuclear factor erythroid 2-related factor 2; CT, computed tomography; GCS, Glasgow Coma Scale.

specificity values for death prediction (Figure 4). In addition, its death predictive ability was equivalent to those of GCS scores (AUC, 0.836; 95% CI, 0.762-0.909; $P = 0.177$) and Rotterdam CT scores (AUC, 0.824; 95% CI, 0.735–0.914; $P = 0.325$). Serum Nrf2 levels combined with GCS scores and Rotterdam CT scores (AUC, 0.897; 95% CI, 0.837–0.957) had significantly higher AUC than GCS scores ($P = 0.028$), Rotterdam CT scores ($P = 0.007$), or serum Nrf2 levels ($P = 0.006$) alone.

Relationship between serum Nrf2 levels and 180-day overall survival after trauma

This cohort of sTBI patients had the mean overall survival time of 145.2 days (95% CI, 132.6–157.7 days) during 180-day follow-up after head trauma. In accordance with the median value of serum Nrf2 levels (namely, 10.9 ng/ml), all patients were dichotomized. In Figure 5, patients with serum Nrf2 levels $\geq$ 10.9 ng/ml exhibited profoundly shorter 180-day

TABLE 3 Factors associated with 180-day overall survival after severe traumatic brain injury.

	Hazard ratio	95% CI	*P*-value
Gender (male/female)	1.218	0.553–2.685	0.624
Age (y)	1.031	1.003–1.059	0.028
Current cigarette smoking	1.688	0.775–3.675	0.187
Alcohol abuse	1.678	0.770–3.653	0.193
Hypertension	2.089	0.878–4.972	0.096
Diabetes mellitus	2.116	0.798–5.612	0.132
Hyperlipidemia	1.267	0.478–3.359	0.635
Hospital admission time (h)	0.904	0.772–1.057	0.207
Blood-sampling time (h)	0.899	0.783–1.034	0.136
Traumatic causes			
Automobile/motorcycle	Reference		
Fall/jump	0.798	0.231–2.757	0.724
Others	0.506	0.134–1.907	0.314
GCS scores	0.374	0.249–0.561	<0.001
Rotterdam CT scores	3.783	2.315–6.182	<0.001
Systolic arterial pressure (mmHg)	1.001	0.988–1.014	0.921
Diastolic arterial pressure (mmHg)	1.008	0.985–1.032	0.484
Blood glucose levels (mmol/l)	1.120	1.025–1.225	0.013
Blood leucocyte count ($\times 10^9$/l)	1.059	0.929–1.206	0.394
Serum Nrf2 levels (ng/ml)	1.324	1.179–1.488	<0.001

Associations were reported as hazard ratios using univariate Cox's proportional hazard regression analysis. CT, computerized tomography; GCS, Glasgow Coma Scale; Nrf2, nuclear factor erythroid 2-related factor 2; 95% CI, 95% confidence interval.

overall survival time, as compared to those with serum Nrf2 levels < 10.9 ng/ml ($P < 0.01$). Just as displayed in Table 3, the factors, which were significantly related to 180-day overall survival following trauma, were age, GCS scores, Rotterdam CT scores, blood glucose levels, and serum Nrf2 levels using univariate Cox's proportional hazard model (all $P < 0.05$). Furthermore, the afore-mentioned significant pertinent variables were incorporated in multivariate Cox's proportional hazard model, and sequentially, it was confirmed that GCS score, Rotterdam CT score, and serum Nrf2 levels were independently associated with 180-day overall survival after head trauma (all $P < 0.05$, Figure 5).

Relationship between serum Nrf2 levels and 180-day poor outcome after trauma

At post-injury 180 days, GOSE scores of patients ranged from 1 to 8 (median, 5; lower–upper quartiles, 2–6), and a total of 26, 9, 6, 8, 23, 16, 10, and 7 patients showed GOSE scores 1, 2, 3, 4, 5, 6, 7, and 8, respectively. In Figure 6, serum Nrf2 levels were markedly and inversely correlated with GOSE scores ($P < 0.001$), and patients with GOSE 1 had significantly highest serum Nrf2 levels and those with GOSE 8 displayed substantially lowest serum Nrf2 levels ($P < 0.001$). In aggregate, 49 patients had the development of a poor outcome (46.7%) at 180 days after trauma. In Table 4, as compared to patients with good outcome, poor outcome patients were prone to exhibit markedly increased proportion of diabetes mellitus, tended to show significantly decreased GCS scores, and were likely to exhibit substantially raised Rotterdam CT score, blood glucose levels, and serum Nrf2 levels. Furthermore, using the binary logistic regression model which contained the preceding variables, the factors independently associated with 180-day poor outcome were GCS scores, Rotterdam CT scores, and serum Nrf2 levels (all $P < 0.05$, Figure 7). Also, serum Nrf2 levels substantially discriminated patients at risk of 180-day poor outcome. Utilizing Youden's method, an optimal value of serum Nrf2 levels was chosen, which yielded medium–high sensitivity and specificity values for prediction of a poor outcome at 180 days after head trauma (Figure 7). Alternatively, its predictive capability for poor outcome was similar to those of GCS scores (AUC, 0.837; 95% CI, 0.767–0.907; $P = 0.299$) and Rotterdam CT scores (AUC, 0.822; 95% CI, 0.751–0.893; $P = 0.544$). Serum Nrf2 levels combined with GCS scores and Rotterdam CT scores (AUC, 0.889; 95% CI, 0.831–0.948) had significantly higher AUC than GCS scores ($P = 0.035$), Rotterdam CT scores ($P = 0.006$), or serum Nrf2 levels ($P = 0.008$) alone.

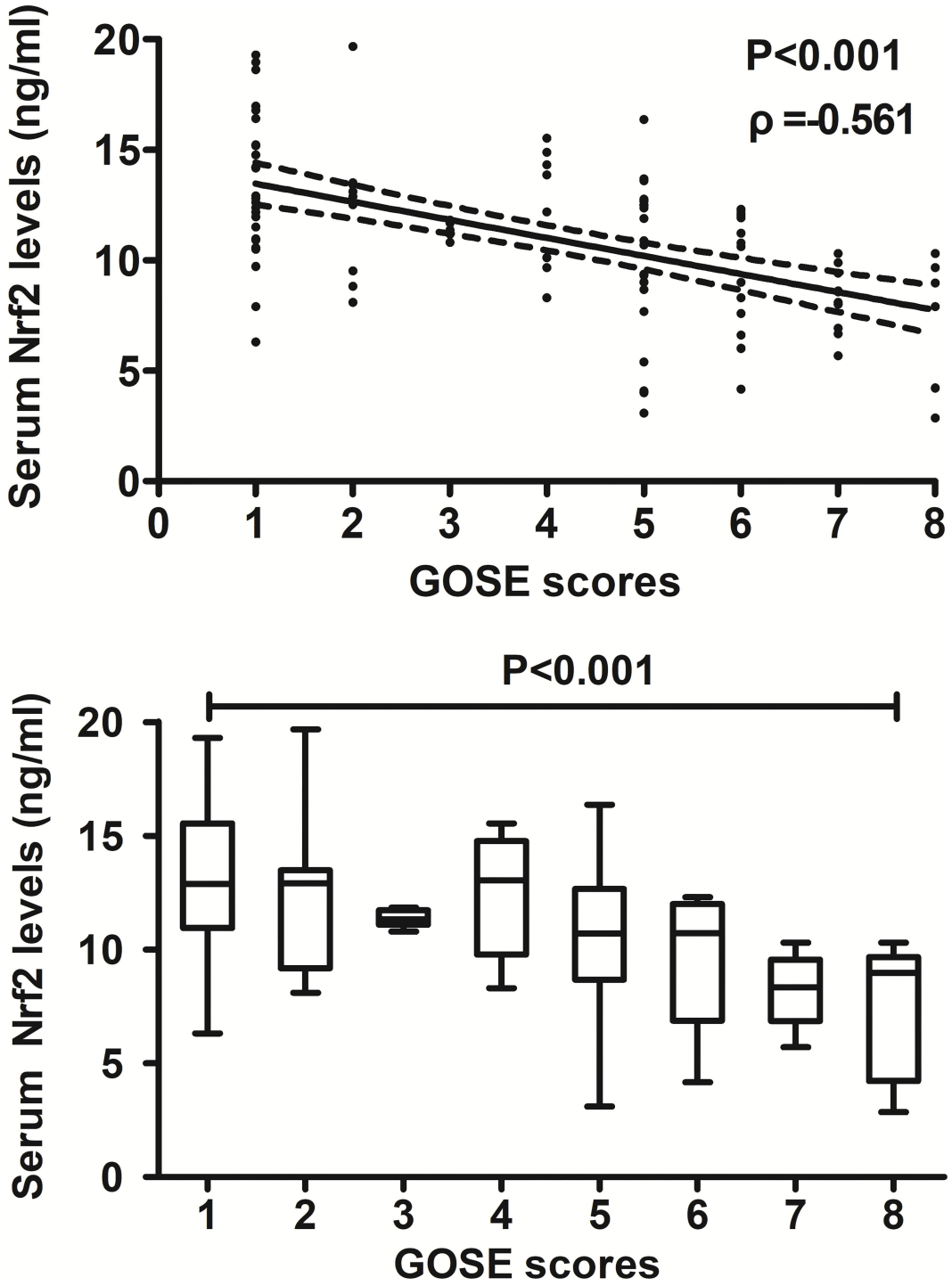

FIGURE 6
Relationship between serum nuclear factor erythroid 2-related factor 2 levels and 180-day extended Glasgow Outcome Scale scores after severe traumatic brain injury. Serum nuclear factor erythroid 2-related factor 2 levels were significantly and inversely correlated with extended Glasgow Outcome Scale scores ($P < 0.001$) and were substantially different among subgroups divided by extended Glasgow Outcome Scale scores ($P < 0.001$). Nrf2 indicates nuclear factor erythroid 2-related factor 2; GOSE, extended Glasgow Outcome Scale.

TABLE 4 Factors associated with 180-day poor outcome after severe traumatic brain injury.

	Poor outcome	Good outcome	*P*-value
Gender (male/female)	28/21	32/24	1.000
Age (y)	45.0 ± 15.1	39.9 ± 13.0	0.070
Current cigarette smoking	19 (38.8%)	13 (23.2%)	0.084
Alcohol abuse	16 (32.7%)	17 (30.4%)	0.800
Hypertension	11 (22.5%)	6 (10.7%)	0.103
Diabetes mellitus	9 (18.4%)	3 (5.4%)	0.037
Hyperlipidemia	9 (18.4%)	8 (14.3%)	0.571
Hospital admission time (h)	4.7 (3.1–6.2)	5.1 (4.0–6.5)	0.182
Blood-sampling time (h)	6.2 (4.0–7.9)	6.8 (5.1–8.3)	0.203
Traumatic causes			0.351
Automobile/motorcycle	25	27	
Fall/jump	18	26	
Others	6	3	
GCS scores	4 (3–5)	5 (5–7)	<0.001
Rotterdam CT scores	5 (4–6)	4 (3–4)	<0.001
Systolic arterial pressure (mmHg)	122.9 ± 31.0	128.2 ± 28.2	0.356
Diastolic arterial pressure (mmHg)	74.8 ± 15.9	73.5 ± 18.6	0.713
Blood glucose levels (mmol/l)	9.8 (8.0–13.3)	8.2 (6.5–10.6)	0.011
Blood leucocyte count ($\times 10^9$/l)	8.5 (6.2–10.9)	7.1 (5.6–9.3)	0.159
Serum Nrf2 levels (ng/ml)	12.5 (10.9–14.8)	9.4 (7.7–12.0)	<0.001

Data were shown as mean ± standard deviation, median (25–75th percentiles), or count (percentage) where appropriate. Statistical methods for intergroup comparison included the t-test, Mann–Whitney U test, Pearson Chi-square test, or Fisher's exact test as appropriate. CT, computerized tomography; GCS, Glasgow Coma Scale; Nrf2, nuclear factor erythroid 2-related factor 2.

Discussion

To the best of our knowledge, this study, for the first time, measured Nrf2 levels in the peripheral blood of patients with acute brain injury and further discerned the relationship between serum Nrf2 levels and illness severity plus functional outcome after sTBI. The main findings of our study are that (1) sTBI patients had significantly higher serum Nrf2 levels than healthy controls; (2) serum Nrf2 levels were in independent correlation with GCS scores and Rotterdam CT scores; (3) serum Nrf2 was an independent predictor of 180-day death, overall survival, and poor outcome; and (4) serum Nrf2 levels were in possession of significant prognostic predictive ability. Assumably, serum Nrf2 levels may be highly correlated with trauma severity and be tightly associated with a long-term functional outcome after sTBI, indicating that serum Nrf2 should represent a potential prognostic biochemical marker of sTBI.

Oxidative stress harbors an important role in some pathophysiologic processes that emerge following acute brain injury, including TBI (16). As a fact, oxidative stress appears when there is a disbalance between antioxidants and oxidants (17). Reactive oxygen species (ROS) belong to oxidants (18). ROS damage permeability of blood–brain barrier, promote vascular and cellular brain edema, and result in occurrence and progression of neuroinflammation after TBI (19). Nrf2 is identified as a new transcription factor which can regulate a set of ARE-dependent gene (20). After exposure to oxidative stress, Nrf2 translocates to the nucleus, activates ARE-dependent gene expression, and thereby leads to upregulation of expressions of various detoxification and antioxidant enzymes, such as superoxide dismutase, glutathione, and thioredoxin (21). In some experimental studies, Nrf2 knockout obviously increased production of ROS, aggravated brain injury, and worsened neurological function of animals with acute brain injury, including TBI (10–13), thus supporting the notion that Nrf2 may confer brain-protective function *via* reducing oxidative damage.

Nuclear factor erythroid 2-related factor 2 was greatly expressed in mouse brain after transient middle cerebral artery occlusion (11) and in brain of rats with intracerebral hemorrhage (22). Also, the expression of Nrf2 was obviously upregulated in brain tissues of patients with cerebral cortex contusion (14). Clearly, Nrf2 is located in glial cells and neuronal cells (11, 14, 22). Our study showed that serum Nrf2 levels were markedly higher in patients with sTBI than in healthy controls. Collectively, Nrf2 in the peripheral blood may be at least partially derived from injured brain tissues after sTBI. Given that Nrf2 may be protective against oxidative damage in

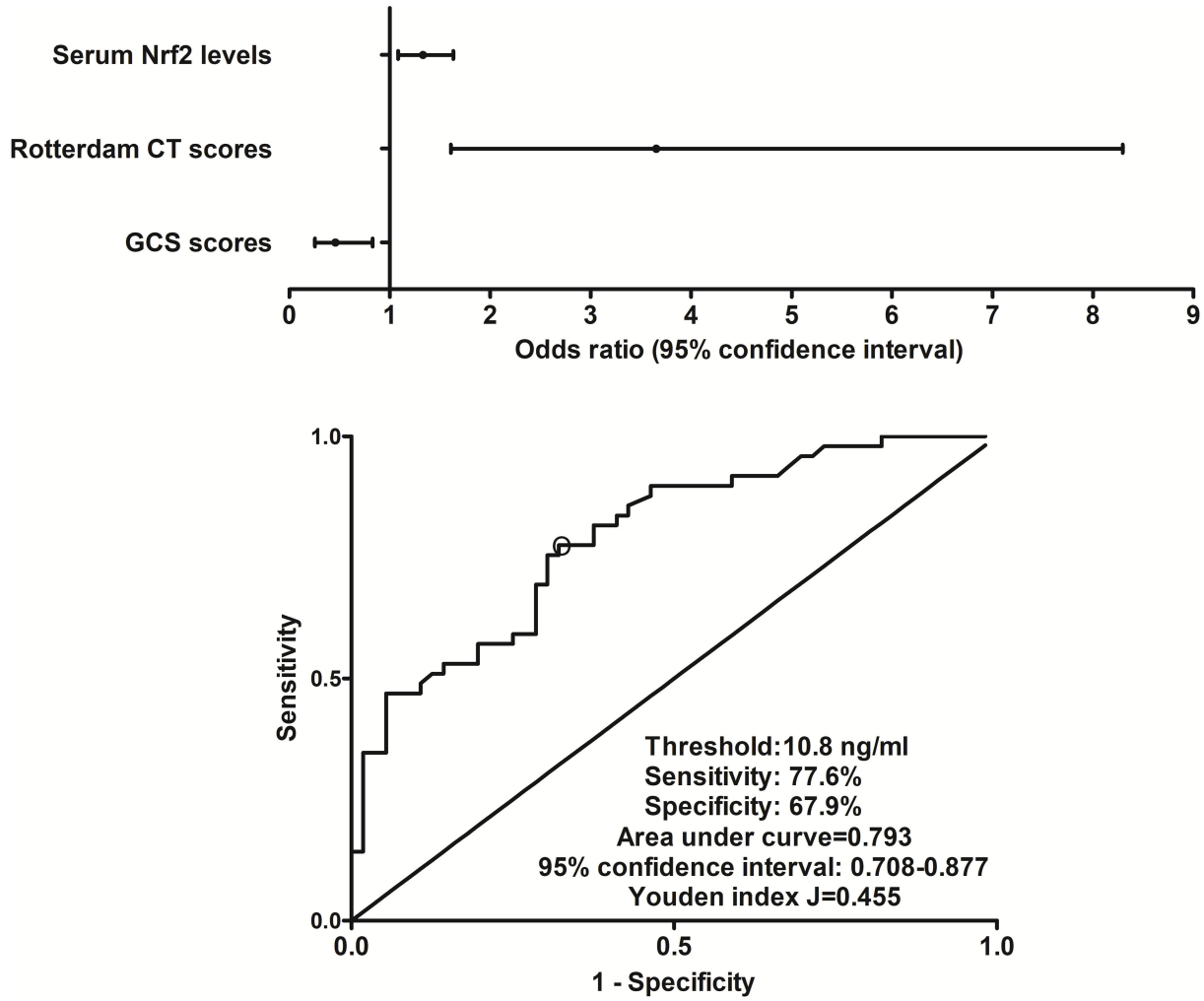

FIGURE 7
Relationship between serum nuclear factor erythroid 2-related factor 2 levels and 180-day poor outcome after severe traumatic brain injury. Serum nuclear factor erythroid 2-related factor 2 levels, Rotterdam computed tomography scores, and Glasgow Coma Scale scores remained as the three independent predictors of 180-day poor outcome (extended Glasgow Outcome Scale scores of 1–4) following severe traumatic brain injury (all $P < 0.05$). Serum nuclear factor erythroid 2-related factor 2 levels markedly discriminated patients at risk of 180-day poor outcome based on receiver operating characteristic curve ($P < 0.001$), and using Youden's method, an optimal criterion of nuclear factor erythroid 2-related factor 2 levels was selected, which yielded medium–high sensitivity and specificity values for poor outcome prediction. Nrf2 indicates nuclear factor erythroid 2-related factor 2; CT, computed tomography; GCS, Glasgow Coma Scale.

animal experiments (10–13), Nrf2 expressions is hypothesized to be upregulated in response to brain oxidative injury after sTBI.

In the current study, in order to assess relationship between serum Nrf2 levels and trauma severity in addition to long-term prognosis, GCS and Rotterdam CT classification were selected as the two indicators of trauma severity, and 180-day GOSE scores and death were regarded as prognostic parameters. As regards statistical methods, multiple multivariate models were configured. Our data showed that serum Nrf2 levels were in independent correlation with trauma severity reflected by GCS scores and Rotterdam CT scores and were independently predictive of death, overall survival, and poor prognosis at 180 days after head trauma. Meanwhile, its prognostic predictive capability was confirmed under ROC curve. Intriguingly, serum Nrf2 levels combined with GCS scores and Rotterdam CT scores for death or poor outcome prediction displayed significantly higher AUC than GCS scores, Rotterdam CT scores, or serum Nrf2 levels alone. In summary, serum Nrf2 may serve as a promising prognostic biomarker.

There are several limitations in this study. First, the blood of sTBI patients was collected at a median value of 6.3 h after trauma. No treatments for glycemic control had been done, and serum Nrf2 levels were not significantly correlated with

blood glucose levels in this study. However, Nrf2 signaling pathways regulation was associated with the hypoglycemic effect of specific agents and hypoglycemia-induced blood–brain barrier endothelial dysfunction *in vitro* (23). Thus, it would be very interesting to study whether glycemic control may affect serum Nrf2 levels after head trauma. Second, some treatments or complications, such as emergency operation, hypoxemia, and shock, may be associated with prognosis of sTBI (1) and therefore are considered as the confounding factors. In this study, the preceding factors are not investigated, and consequently, it will be significant for supplementing such variables in outcome analysis in future. Third, 180-day or 6-month neurological functional status is very commonly used to assess clinical outcome of patients with sTBI (24, 25). Length of ICU stay is sometimes selected as a prognostic parameter in the outcome study of head trauma (26, 27). Hence, it may be of clinical value that length of ICU stay is determined with respect to outcome analysis of human TBI. Last, there is an obvious difference in Nrf2 serum levels published values (28, 29) and values reported in this study. In the current study, we used the DNA-binding ELISA kit, which is in use in another clinical study (30) and is different from that utilized in previous studies (28, 29). So, differences in terms of serum Nrf2 levels between this study and others (28, 29) may be caused by different ELISA kits. However, it is necessary that values of serum Nrf2 levels can be validated using at least two sorts of ELISA kits in future.

Conclusion

To the best of my knowledge, our study, for the first time, showed that increased serum Nrf2 levels of sTBI patients are independently correlated with GCS scores and Rotterdam CT scores and were independently predictive of 180-day death, overall survival, and poor outcome. Moreover, serum Nrf2 levels combined with GCS scores and Rotterdam CT scores for death or poor outcome prediction had significantly higher discriminatory efficiency than any one of them. Thus, it is hypothesized that serum Nrf2 may represent a potential prognostic biomarker of sTBI.

Data availability statement

The raw data supporting the conclusions of this article will be made available by the authors, without undue reservation.

Ethics statement

The studies involving human participants were reviewed and approved by the Quzhou Affiliated Hospital of Wenzhou Medical University. The patients/participants provided their written informed consent to participate in this study.

Author contributions

All authors listed have made a substantial, direct, and intellectual contribution to the work and approved it for publication.

Acknowledgments

The authors thank all participants for providing us with their clinical information and for their willingness to participate in this study.

Conflict of interest

The authors declare that the research was conducted in the absence of any commercial or financial relationships that could be construed as a potential conflict of interest.

Publisher's note

References

1. Stocchetti N, Carbonara M, Citerio G, Ercole A, Skrifvars MB, Smielewski P, et al. Severe traumatic brain injury: targeted management in the intensive care unit. *Lancet Neurol.* (2017) 16:452–64. doi: 10.1016/S1474-4422(17)30118-7

2. Capizzi A, Woo J, Verduzco-Gutierrez M. Traumatic brain injury: an overview of epidemiology, pathophysiology, and medical management. *Med Clin North Am.* (2020) 104:213–38. doi: 10.1016/j.mcna.2019.11.001

3. Dixon KJ. Pathophysiology of traumatic brain injury. *Phys Med Rehabil Clin N Am.* (2017) 28:215–25. doi: 10.1016/j.pmr.2016.12.001

4. Rakhit S, Nordness MF, Lombardo SR, Cook M, Smith L, Patel MB. Management and challenges of severe traumatic brain injury. *Semin Respir Crit Care Med.* (2021) 42:127–44. doi: 10.1055/s-0040-1716493

5. Gao G, Wu X, Feng J, Hui J, Mao Q, Lecky F, et al. Clinical characteristics and outcomes in patients with traumatic brain injury in China: a prospective, multicentre, longitudinal, observational study. *Lancet Neurol.* (2020) 19:670–7. doi: 10.1016/S1474-4422(20)30182-4

6. Dong XQ, Yu WH, Du Q, Wang H, Zhu Q, Yang DB, et al. Serum periostin concentrations and outcomes after severe traumatic brain injury. *Clin Chim Acta.* (2017) 471:298–303. doi: 10.1016/j.cca.2017.06.020

7. Lorente L, Martín MM, Pérez-Cejas A, González-Rivero AF, Abreu-González P, Ramos L, et al. Traumatic brain injury patients mortality and serum total antioxidant capacity. *Brain Sci.* (2020) 10:110. doi: 10.3390/brainsci10020110

8. Ni P, Qiao Y, Tong W, Zhao C, Zheng P. Associations between serum tau, neurological outcome, and cognition following traumatic brain injury. *Neurol India.* (2020) 68:462–7. doi: 10.4103/0028-3886.284380

9. Pi J, Hayes JD, Yamamoto M. New insights into nuclear factor erythroid 2-related factors in toxicology and pharmacology. *Toxicol Appl Pharmacol.* (2019) 367:33–5. doi: 10.1016/j.taap.2019.01.014

10. Zhao X, Sun G, Ting SM, Song S, Zhang J, Edwards NJ, et al. Cleaning up after ICH: the role of Nrf2 in modulating microglia function and hematoma clearance. *J Neurochem.* (2015) 133:144–52. doi: 10.1111/jnc.12974

11. Tanaka N, Ikeda Y, Ohta Y, Deguchi K, Tian F, Shang J, et al. Expression of Keap1-Nrf2 system and antioxidative proteins in mouse brain after transient middle cerebral artery occlusion. *Brain Res.* (2011) 1370:246–53. doi: 10.1016/j.brainres.2010.11.010

12. Bhowmick S, D'Mello V, Caruso D, Abdul-Muneer PM. Traumatic brain injury-induced downregulation of Nrf2 activates inflammatory response and apoptotic cell death. *J Mol Med.* (2019) 97:1627–41. doi: 10.1007/s00109-019-01851-4

13. Zolnourian A, Galea I, Bulters D. Neuroprotective role of the Nrf2 pathway in subarachnoid haemorrhage and its therapeutic potential. *Oxid Med Cell Longev.* (2019) 2019:6218239. doi: 10.1155/2019/6218239

14. Guo XS, Wen SH, Dong WW, Li BX, Chen ZY, Wang LL, et al. Expression of Nrf2 in different cells after human cerebral cortex contusion. *Fa Yi Xue Za Zhi.* (2019) 35:273–9. doi: 10.12116/j.issn.1004-5619.2019.03.002

15. Yeatts SD, Martin RH, Meurer W, Silbergleit R, Rockswold GL, Barsan WG, et al. Sliding scoring of the glasgow outcome scale-extended as primary outcome in traumatic brain injury trials. *J Neurotrauma.* (2020) 37:2674–9. doi: 10.1089/neu.2019.6969

16. Khatri N, Thakur M, Pareek V, Kumar S, Sharma S, Datusalia AK. Oxidative stress: major threat in traumatic brain injury. *CNS Neurol Disord Drug Targets.* (2018) 17:689–95. doi: 10.2174/1871527317666180627120501

17. Cornelius C, Crupi R, Calabrese V, Graziano A, Milone P, Pennisi G, et al. Traumatic brain injury: oxidative stress and neuroprotection. *Antioxid Redox Signal.* (2013) 19:836–53. doi: 10.1089/ars.2012.4981

18. Kumar S, Theis T, Tschang M, Nagaraj V, Berthiaume F. Reactive oxygen species and pressure ulcer formation after traumatic injury to spinal cord and brain. *Antioxidants.* (2021) 10:1013. doi: 10.3390/antiox10071013

19. Li L, Tan J, Miao Y, Lei P, Zhang Q. ROS and autophagy: interactions and molecular regulatory mechanisms. *Cell Mol Neurobiol.* (2015) 35:615–21. doi: 10.1007/s10571-015-0166-x

20. Tonelli C, Chio IIC, Tuveson DA. Transcriptional regulation by Nrf2. *Antioxid Redox Signal.* (2018) 29:1727–45. doi: 10.1089/ars.2017.7342

21. He F, Ru X, Wen T. NRF2, a transcription factor for stress response and beyond. *Int J Mol Sci.* (2020) 21:4777. doi: 10.3390/ijms21134777

22. Shang H, Yang D, Zhang W, Li T, Ren X, Wang X, et al. Time course of Keap1-Nrf2 pathway expression after experimental intracerebral haemorrhage: correlation with brain oedema and neurological deficit. *Free Radic Res.* (2013) 47:368–75. doi: 10.3109/10715762.2013.778403

23. Sajja RK, Green KN, Cucullo L. Altered Nrf2 signaling mediates hypoglycemia-induced blood-brain barrier endothelial dysfunction in vitro. *PLoS ONE.* (2015) 10:e0122358. doi: 10.1371/journal.pone.0122358

24. Roquilly A, Moyer JD, Huet O, Lasocki S, Cohen B, Dahyot-Fizelier C, et al. Effect of continuous infusion of hypertonic saline vs standard care on 6-month neurological outcomes in patients with traumatic brain injury: the COBI randomized clinical trial. *JAMA.* (2021) 325:2056–66. doi: 10.1001/jama.2021.5561

25. Rowell SE, Meier EN, McKnight B, Kannas D, May S, Sheehan K, et al. Effect of out-of-hospital tranexamic acid vs placebo on 6-month functional neurologic outcomes in patients with moderate or severe traumatic brain injury. *JAMA.* (2020) 324:961–74. doi: 10.1001/jama.2020.8958

26. Núñez-Patiño RA, Zorrilla-Vaca A, Godoy DA. Effect of intensive glycaemic control on moderate hypoglycaemia and ICU length of stay in severe traumatic brain injury. *Crit Care.* (2018) 22:134. doi: 10.1186/s13054-018-2046-5

27. Moein H, Khalili HA, Keramatian K. Effect of methylphenidate on ICU and hospital length of stay in patients with severe and moderate traumatic brain injury. *Clin Neurol Neurosurg.* (2006) 108:539–42. doi: 10.1016/j.clineuro.2005.09.003

28. Sireesh D, Dhamodharan U, Ezhilarasi K, Vijay V, Ramkumar KM. Association of NF-E2 related factor 2 (Nrf2) and inflammatory cytokines in recent onset type 2 diabetes mellitus. *Sci Rep.* (2018) 8:5126. doi: 10.1038/s41598-018-22913-6

29. Zhang X, Wu Q, Wang Z, Li H, Dai J. Keap1-Nrf2/ARE signal pathway activated by butylphthalide in the treatment of ischemic stroke. *Am J Transl Res.* (2022) 14:2637–46.

30. Ban WH, Kang HH, Kim IK, Ha JH, Joo H, Lee JM, et al. Clinical significance of nuclear factor erythroid 2-related factor 2 in patients with chronic obstructive pulmonary disease. *Korean J Intern Med.* (2018) 33:745–52. doi: 10.3904/kjim.2017.030

frontiers | Frontiers in Neurology

TYPE Original Research
PUBLISHED 13 December 2022
DOI 10.3389/fneur.2022.1090958

OPEN ACCESS

EDITED BY
Wael M. Y. Mohamed,
International Islamic University Malaysia, Malaysia

REVIEWED BY
Claire J. C. Huguenard,
Cryptobiotix, Belgium
Yang Wenming,
First Affiliated Hospital of Anhui University of Traditional Chinese Medicine, China

*CORRESPONDENCE
Qiliang Li
liqiliang2005@126.com

SPECIALTY SECTION
This article was submitted to Neurological Biomarkers, a section of the journal Frontiers in Neurology

RECEIVED 06 November 2022
ACCEPTED 28 November 2022
PUBLISHED 13 December 2022

CITATION
Sun S, Jin H, Rong Y, Song W and Li Q (2022) Methylmalonic acid levels in serum, exosomes, and urine and its association with cblC type methylmalonic acidemia-induced cognitive impairment. *Front. Neurol.* 13:1090958. doi: 10.3389/fneur.2022.1090958

Methylmalonic acid levels in serum, exosomes, and urine and its association with cblC type methylmalonic acidemia-induced cognitive impairment

Shuqi Sun[1], Hong Jin[2], Yu Rong[3], Wenqi Song[1] and Qiliang Li[1]*

[1]Department of Clinical Laboratory, Beijing Children's Hospital, Capital Medical University, National Center for Children's Health, Beijing, China, [2]Department of Neurology, Beijing Children's Hospital, Capital Medical University, National Center for Children's Health, Beijing, China, [3]Department of Rehabilitation, Beijing Children's Hospital, Capital Medical University, National Center for Children's Health, Beijing, China

Background: The cblC type methylmalonic acidemia is the most common methylmalonic acidemia (MMA) in China. The biochemical characteristics of this disease include elevated methylmalonic acid and homocysteine (HCY), increased propionylcarnitine (C3), decreased free carnitine (C0). In this study, we aimed to clarify the roles of these biomarkers in cblC-MMA induced cognitive impairment and evaluate the capacity of methylmalonic acid in different fluids or exosomes to distinguish cblC-MMA induced cognitive impairment.

Methods: 15 non-inherited hyperhomocysteinemia (HHcy) patients, 42 cblC-MMA patients and 57 age- and sex-matched healthy children were recruited in this study. The levels of HCY were detected by an automatic immune analyzer. The levels of acylcarnitines and methylmalonic acid were detected by tandem mass spectrometer.

Results: The main findings were all biomarkers as HCY, acylcarnitines and methylmalonic acid had capacities for distinguishing patients with cblC-MMA induced cognitive impairment from healthy children. The methylmalonic acid in different fluids or exosomes had good performances for distinguishing patients with cblC-MMA induced cognitive impairment from HHcy patients. The methylmalonic acid in serum exosomes and neuronal-derived exosomes were able to distinguishing cblC-MMA patients with cognitive impairment from patients without cognitive impairment. The methylmalonic acid in neuronal-derived exosomes might be helpful to evaluate the severity of cblC-MMA induced cognitive impairment.

Discussion: Methylmalonic acid levels in serum exosomes, especially in serum neuronal-derived exosomes, serve as potential biomarkers for distinguishing cblC-MMA induced cognitive impairment.

KEYWORDS

methylmalonic acidemia, cblC, cognitive impairment, methylmalonic acid, exosomes

Introduction

Methylmalonic acidemia (MMA) is the most common organic acidemia in children. Normally, amino acid (e.g., Valine, Threonine, Isoleucine, Methionine), odd chain fatty acids and cholesterol *in vivo* are metabolized into methylmalonyl coenzyme A. Methylmalonyl coenzyme A converts to succinyl coenzyme A under the catalysis of methylmalonyl coenzyme A mutase and its coenzyme vitamin B12. MMA is caused by enzyme deficiency of methylmalonyl coenzyme A mutase or vitamin B12, which leads to the interruption from methylmalonyl coenzyme A to succinyl coenzyme A and the accumulation of methylmalonic acid. According to the serum homocysteine (HCY) levels, MMAs are divided into isolated MMA and combined MMA and homocystinuria (1, 2). The cblC type methylmalonic acidemia (cblC-MMA) is the most common MMA in China (3–5). The biochemical characteristics of cblC disease include elevated serum methylmalonic acid and HCY, increased propionylcarnitine (C3), decreased free carnitine (C0). Molecular diagnosis of cblC disease relies on the detection of MMACHC mutations (4, 5).

The cblC-MMA patients have a wide spectrum of clinical manifestations which include feeding difficulties, failure to thrive, hydrocephalus, neurological regression, neuropsychiatric symptoms, progressive encephalopathy, neurological deterioration, hypotonia. Most patients are troubled with abnormality of nervous system and cognitive impairments, which include cognitive difficulties, disabling movement disorder, language, and social development impairment (6–8). Methylmalonic acid and homocysteine are recognized as pathogenic substances of these patients (5, 9, 10). Methylmalonic acid, a major neurotoxin, can induce brain injury and cognitive impairment. Previous studies revealed that methylmalonic acid led to neuronal damage by inhibiting mitochondrial respiratory chain (11, 12), transmitochondrial malate shuttle (13), pyruvate carboxylase (14) and β-hydroxybutyrate (15) and inducing neuron apoptosis by mechanisms of oxidative stress injury (16, 17), neuroinflammation (18, 19) and DNA damage (20). Homocysteine is an intermediate thiol amino acid derived from methionine. Normally, methionine synthase catalyzes homocysteine to methionine within the methionine cycle. VitB12 enzyme deficiency leads to the interruption of methionine cycle and the accumulation of homocysteine (21). Some studies reported that homocysteine aggravated neuron injury through redox imbalance and neuronal autophagy over activation (22, 23). Though elevated homocysteine is related to cognitive impairment in adults, few studies reported whether the elevated homocysteine is associated with cognitive decline in cblC disease children.

In addition, the previous studies reported that the levels of propionylcarnitine (C3) increased, free carnitine (C0) decreased and the ratios of C3/C0 elevated in the cblC-MMA patients. However, it is unclear whether the levels of these acylcarnitines are associated with cognitive impairment in MMA patients.

Exosomes (a diameter of 30–100 nm vesicles) are intercellular communication microparticles secreted by numerous cell types, including neurons (24). Exosomes easily cross the blood-brain barrier and package pathological substances from the central nervous system to the blood due to their nanoscale size and structural similarity (24, 25). Some studies reported that neuronal-derived exosomes in patients with neurodegenerative diseases packaged several proteins as potential biomarkers associated with cognitive decline (26–28). However, the rare studies showed whether the levels of methylmalonic acid in the serum exosomes or neuro-exosomes were used as potential biomarkers of cognitive impairment induced by cblC-MMA.

Therefore, this study aimed to (1) clarify the roles of serum homocysteine, C3, C0, and C3/C0 in cblC-MMA induced cognitive impairment (2) evaluate the capacity of serum methylmalonic acid, urinary methylmalonic acid, serum total exosomes and neuro-exosomal methylmalonic acid to distinguish cblC-MMA induced cognitive impairment.

Materials and methods

The participants and samples

This study was conducted according to the principles expressed in the Declaration of Helsinki and approved by the ethic committee of the Medical Ethics Committee of Beijing Children's Hospital, Capital Medical University (approval ID: 2018-29). All the procedures were performed with the Ethical Standards of Medical Ethics Committee of Beijing Children's Hospital. Informed consents were obtained from the participants or legal guardians.

A total of 114 participants were recruited, including 15 non-inherited hyperhomocysteinemia (HHcy) patients, 42 cblC-MMA patients and 57 age- and sex-matched healthy individuals in the same period as controls. The non-inherited hyperhomocysteinemia patients involved abnormally high levels of homocysteine (>15 μmol/L) in the serum (29) and were not with cystathionine beta-synthase deficiency. The cblC-MMA patients were diagnosed by MMACHC mutations (9). Baseline and clinical characteristics were shown in Table 1. The cognitive assessment tests were conducted in participants by a trained interviewer using the Gesell developmental Scales (children ages <6 years), Wechsler preschool and primary scale of intelligence, or Wechsler intelligence scales for children (between 6 and 18 years old) (30). Intelligence quotient (IQ) scores and development quotient (DQ) scores of patients were recorded. The standardized mean of the DQ or IQ is 100 with a

TABLE 1 Clinical and biochemical data of study participants.

	Control	HHcy	cblC-MMA
Men [*n* (%)]	30(52.6)	9(60)	21(50)
Age (years, median, 95% CI)	10.0(6.7–12.0)	16.0(14.5–17.5)	6.5(3.8–9.7)[&]
Age of onset (years, median, 95% CI)	-	14.0 (12.1–15.0)	3.6 (0.8–5.5) [&]
Family history [*n* (%)]	-	0 (0)	4 (9.5)[&]
Creatinine (μmol/L, median, 95% CI)	44 (37–48)	65.5 (57.5–128.7)*	31.4 (25.8–37.8) [&]
Urea (mmol/L, median, 95% CI)	4 (3.3–4.1)	6.98 (6.62–8.73)*	5.06 (4.14–6.30)*
Proteinuria [*n* (%)]	0 (0)	12 (80)*	10 (23.8)*[&]
Hematuria [*n* (%)]	0 (0)	9(60)*	9 (21.4) *[&]
Normal IQ or DQ [*n* (%)]	57 (100)	15 (100)	10 (23.8)*[&]
Mild cognitive impairment [*n* (%)]	0 (0)	0 (0)	14 (33.3)*[&]
Moderate cognitive impairment [*n* (%)]	0 (0)	0 (0)	12 (28.6)*[&]
Severe cognitive impairment [*n* (%)]	0 (0)	0 (0)	6 (14.3)*[&]

*$p < 0.05$, compared with control group; [&]$p < 0.05$, compare with HHcy group. HHcy, non-inherited hyperhomocysteinemia. Continuous Data were shown as median with 95% CI.

standard deviation of 15 (31, 32). DQ scores or IQ scores <70 is classified as cognitive impairment. DQ are classified as 55-69 as mild cognitive impairment, 40–54 as moderate cognitive impairment, scores <40 as severe delay of cognition. IQ scores are classified as 52–69 as mild cognitive impairment, 36–51 as moderate cognitive impairment, scores <36 as severe delay of cognition.

Before treatment, the blood and urine samples of participants were collected. The venous blood was collected into separate gel coagulation-promoting vacuum tube (BD Vacutainer, Plymouth, UK). The specimens were centrifuged (relative centrifugal force, 2,000 g) for 10 min after quiescence clotting for about 45 min at the room temperature (22–25°C). Then the serum was put into well-sealed freezing containers and stored at −80°C within 2 h after collection. All samples were avoided repeated freeze-thaw cycles during the examination process. The samples collection and subsequent experiments were performed with the blind method.

Serum total exosomes isolation

Serum total exosomes were isolated by exosome isolation kit (Invitrogen, Thermo Scientific, Vilnius Lithuania, cat# 4478360) following manufacturer's instructions. Briefly, 1 ml of serum sample was centrifuged (relative centrifugal force, 2,000 g) for 30 min. The supernatant was transferred into a new tube on ice. 200 μl of total exosome isolation reagent was added into the serum supernatant. The mixture was incubated at 4°C for 30 min. After incubation, the sample was centrifuged (relative centrifugal force, 10,000 g) for 10 min. The supernatant was discarded. The pellet was completely resuspended in 200 μl phosphate-buffered saline (PBS, Jiangsu KeyGen Biotech Co., Ltd, cat# KGB5001). The exosomes were stored at −80°C.

Serum neuronal exosomes isolation

Serum neuronal exosomes were isolated with the method reported by previous studies (26, 28, 33). Briefly, 500 μl of Dulbecco's phosphate buffered saline (DPBS, Thermo Fisher Scientific, cat# 14190144) containing the inhibitor cocktails (Roche, cat# 11873580001) was added into 1 ml serum. The mixture was centrifuged (relative centrifugal force, 4,500 g) for 20 min at 4°C. The supernatant was transferred into a new tube on ice. 200 μl of total exosome isolation reagent (Invitrogen, Thermo Scientific, Vilnius Lithuania) was added into the supernatant. After mixing, the sample was incubated 1 h at 4°C. The mixture was centrifuged (relative centrifugal force, 10,000 g) for 10 min at 4°C. The supernatant was discarded. The pellet was completely resuspended in 200 μl DPBS. Each sample received 100 μl DPBS containing 3% bovine serum albumin (BSA, KeyGen Biotech, cat# KGY00810) and was incubated for 1 h at 4°C each with 2 μg of mouse anti-human NCAM antibody (Santa Cruz Biotechnology, Santa Cruz, CA, cat# SC-106), which had been biotinylated with the EZ-Link sulfo-NHS-biotin system (Thermo Scientific, cat# A39256). The mixture was put on the rotating mixer 2 h at 4°C. Then 25 μl of streptavidin-agarose resin (Thermo Scientific, cat# 20347) was added in the mixture and put on the rotating mixer 1 h at 4°C. After centrifugation at 500 g for 10 min at 4°C and removal of the supernatant, each pellet was suspended in 50 μl of 0.05 M glycine-HCl (pH 3.0) with vortex for 10 s. Then the supernatant pH was adjusted to 7.0 with 1 M Tris-HCl (pH 8.6) and was added 150 μl DPBS. The serum neuronal exosomes were stored at −80°C.

Western blot/ confirmation of exosome collection

Sample lysate was prepared by re-suspending isolated exosomes in RIPA buffer (Beyotime, Cat#P0013B) containing protease inhibitor cocktail and loading buffer (KeyGene, Cat#KGP101X). Then sample was heated at 95°C for 10 min. The samples were resolved on 12% SDS-PAGE gels (Bio-rad) and transferred onto PVDF membranes (Pall, Cat#BSP0161). The membranes were blocked with 5% non-fat milk (Roby,

Cat# RBR501-100) in TBST (Tris-buffered saline with 0.05% Tween 20) for 1.5 h and were incubated with primary antibodies in TBST overnight at 4°C. After washing the membranes 3 times for 10 min each in TBST, the membranes were incubated with secondary antibodies for 1 h. After washing, the membranes were incubated with chemiluminescent-HRP substrate (absin, Cat#abs920) according to the manufacture instructions and exposed using enhanced chemiluminescence detection system (Minichemi 610). Anti-CD63(System Biosciences, Cat# EXOAB-CD63A-1, RRID: AB_2561274), anti-TSG101(ABclonal, Cat# A1692, RRID: AB_2763744) and anti-Calnexin (abcam, Cat# ab22595, RRID: AB_2069006, NCAM (ERIC 1) antibody (Santa Cruz Biotechnology, INC, Cat# sc-106, RRID: AB_627128) were used at a dilution of 1: 1,000. Goat anti-rabbit HRP secondary antibody (Beyotime, cat# A0208, RRID: AB_2892644) was used at a dilution of 1: 20,000 in 5% non-fat milk in TBST.

Biochemical assessment

The blood and urine samples of participants were collected. Creatinine and urea were determined using routine chemical methods by Olympus AU5821 biochemistry analyzer (Beckman coulter, Inc. USA). Homocysteine was detected by i2000 automatic immune analyzer. Propionylcarnitine (C3), free carnitine (C0) and methylmalonic acid were detected by a liquid chromatography tandem mass spectrometer (SHIMADZU LC/MS-8050, Japan).

Determination of methylmalonic acid by tandem mass spectrometry

Sample preparation

50 μl of serum or exosome sample was mixed 20 μl internal standard solution (Cambridge Isotope Laboratories). The sample was put in 200 μl solution of 50:50 (by volume) methanol: acetonitrile and mixed for 2 min. The mixture was centrifuged (relative centrifugal force, 10,000 g) for 10 min. The supernatant was collected. The supernatant was evaporated to dryness in 15 min at 60°C under dry nitrogen. The residue was dissolved in 100 μl of 20:80 (by volume) methanol: deionized water.

LC-MS/MS procedure

Autosampler injections of 10 ul per sample were made into the LC mobile phase flow of 0.25 ml/min. Separation of MMA and MMA-d3 from the bulk of the specimen matrix was achieved by use of chromatographic column (Waters HSS T3, 1.8μm, 2.1 × 100 mm). Gradient elution of the analytes was achieved using a program with mobile phase A (methanol 0.2%formic acid) as follows: 0 to 85% B in 0.01 min, 85% B in 3 min, 85 to 10% B in 0.01 min, 10% B in 1 min, 10 to 85% B in 0.01 min, 85% B in 2 min, then back to 0% B in 0.01 min and re-equilibration for 1 min. A triple-quadrupole mass spectrometer (SHIMADZU LC/MS-8050, Japan) operated in positive ion mode (source voltage, 5500 V). The Turbo Ion Spray ionization probe operating with the turbo gas on (10 L/min, 350°C). In the selected reaction monitoring (SRM) mode, we monitored the precursor ion (m/z, 117.4) to product ion (m/z, 73.05) for MMA and precursor ion (m/z, 120.4) to product ion (m/z, 76.10) for MMA-d3, respectively. Data were acquired and processed using the software (LabSolutions LCMS Ver.5.6).

Statistical analysis

Statistical analysis was performed using IBM SPSS software version 26.0 and GraphPad Prism5. The statistical calculations were performed with the blind method. The tests for data normality and variance homogeneity were performed before data statistical calculations. Non-parametric data were displayed as median with 95% confidence interval (CI). Non-parametric statistical analysis was used for multi-group comparisons. The relationships between methylmalonic acid in different body fluids (serum, urine, serum total exosomes and serum neuro-exosomes) or other metabolites and participants' DQ or IQ scores were performed by Kendall's tau-b correlation. To assess the performances of metabolites in diagnosis of cblC-MMA induced cognitive impairment, we computed the area under the curve (AUC), sensitivity, and specificity as well as 95% CI by the receiver operating characteristic (ROC). Then the optimal cut-off of each parameter was calculated through Youden's method. All tests were two-tailed, and the level of significance was set to $P < 0.05$.

Results

Baseline and biochemistry characteristics of participants

The clinical and biochemical data of participants were shown in Table 1. Our results demonstrated that the most of non-inherited HHcy patients were adolescents (onset median age: 14.0 years). There was no family history and cognitive impairment in non-inherited HHcy patients. Proteinuria and hematuria were the most common clinical manifestations of non-inherited HHcy patients. The median onset age of cblC-MMA patients was 3.6 years old. 9.5% (4/42) cblC-MMA patients had family history. 76% (32/42) cblC-MMA patients were troubled with cognitive impairments. More than 20% cblC-MMA patients suffered proteinuria and hematuria. We analyzed the biomarkers data of participants. Compared to the control

TABLE 2 Metabolite analysis in the participants.

	Control	HHcy	cblC-MMA
methylmalonic acid in urine (mmol/mmol creatinine)	0.00 (0.00–0.00)	0.00 (0.00–0.00)	0.74 (0.58–1.14)*&
HCY in serum (μmol/L)	5.44 (4.65–5.78)	89.70 (69.74–112.49) *	156.68 (150.07–171.08)*&
methylmalonic acid in serum (μmol/L)	0.05 (0.04–0.08)	0.06 (0.04–0.12)	5.73 (4.36–7.20)*&
C3 (μmol/L)	3.85 (3.10–4.34)	4.82 (3.48–7.06) *	7.28 (4.87–9.11)*
C0 (μmol/L)	27.4 (25.3–30.5)	25.3 (21.4–28.3)	17.60 (13.9–23.3)*&
C3/C0	0.14 (0.11–0.15)	0.22 (0.14–0.32) *	0.36 (0.25–0.56)*

*$p < 0.01$ compared with control group; &$p < 0.05$ compared with HHcy group; HHcy, non-inherited hyperhomocysteinemia; MMA, methylmalonic acidemia; HCY, homocysteine; C3, propionylcarnitine; C0, free carnitine; C3/C0, the ratio of C3 and C0. Data were shown as median with 95% CI.

group, the levels of albumin in non-inherited HHcy patients ($Z = -3.107$, $p = 0.002$) and cblC-MMA patients ($Z = -6.826$, $p < 0.001$) were markedly decreased. The levels of creatinine ($Z = -2.933$, $p = 0.003$) and urea ($Z = -2.588$, $p = 0.01$) in non-inherited HHcy patients were markedly higher than control group.

Metabolite analysis of participants

We measured metabolites of participants. The data were presented in Table 2. The levels of propionylcarnitine (C3) in HHcy group and cblC-MMA group were significantly higher than the control group. However, there were no difference between HHcy group and cblC-MMA group. The levels of free carnitine (C0) in cblC-MMA group were markedly lower than the control group ($Z = -3.349$, $p = 0.001$) and HHcy group ($Z = -2.084$, $p = 0.037$). The levels of homocysteine of HHcy patients were significantly higher than the control group ($Z = -5.928$, $p < 0.001$), but lower than cblC-MMA patients ($Z = -3.787$, $p < 0.001$). The urinary methylmalonic acid excretion kept very low levels in control group (<0.001 mmol/mmol creatinine) and HHcy patients (<0.001 mmol/mmol creatinine), however, methylmalonic acid excretion significantly increased in cblC-MMA patients (median level 0.74 mmol/mmol creatinine) ($Zc\text{-}_M = -9.041$, $p < 0.001$; $Z_{H-M} = -5.742$, $p < 0.001$). Compared to the control group and HHcy patients, the levels of methylmalonic acid in the serum of cblC-MMA patients significantly increased ($Zc\text{-}_M = -8.475$, $p < 0.001$; $Z_{H-M} = -5.709$, $p < 0.001$).

The levels of metabolites biomarkers in different cognitive states

In this study, serum total exosomes and neuronal-derived exosomes were collected. The exosomes positive markers of CD63 and TSG101 and exosomes negative markers of Calnexin were confirmed by western blot analysis. The results showed that CD63 and TSG101 were expressed and Calnexin was not expressed in the separated pellets (Supplementary Figure 1). The NCAM content was expressed in immunoprecipitated neuro-exosomes (Supplementary Figure 2). Based on these data, we confirmed that serum total exosomes and neuronal-derived exosomes were successfully collected.

Then, the levels of serum homocysteine, urinary methylmalonic acid, serum methylmalonic acid, methylmalonic acid in serum total exosomes and neuronal-derived exosomes in different cognitive states were analyzed. The participants included healthy children, HHcy patients and cblC-MMA patients. The healthy children and HHcy patients possessed normal cognition. According to cognitive state, cblC- MMA patients were divided into patients with cognitive impairment and patients with normal cognition. The cblC-MMA patients with cognitive impairment were further divided into three subgroups of mild, moderate and severe cognitive impairment. The levels of metabolic biomarkers of control group, HHcy group and cblC-MMA subgroups were displayed in the Figure 1. The levels of serum homocysteine (Figure 1A), urinary and serum methylmalonic acid (Figures 1B,C) in cblC-MMA patients were obviously higher than control group and HHcy group, which showed no significance between cblC-MMA patients with cognitive impairment and with normal cognition, no significance among cblC-MMA subgroups of mild, moderate and severe cognitive impairment. Then we detected the concentrations of methylmalonic acid in serum total exosomes and neuronal-derived exosomes separately. As shown in Figure 1, compare to the control group and HHcy group, the levels of methylmalonic acid in serum total exosomes (Figure 1D) and neuro-exosomes (Figure 1E) of the cblC-MMA patients markedly increased. In addition, compare to cblC-MMA patients with normal cognition, the levels of methylmalonic acid in serum total exosomes (Figure 1D) and neuro-exosomes (Figure 1E) of the cblC-MMA patients with cognitive impairment significantly increased. Especially, compared to cblC-MMA patients with mild cognitive impairment, the levels of methylmalonic acid in serum neuronal-derived exosomes

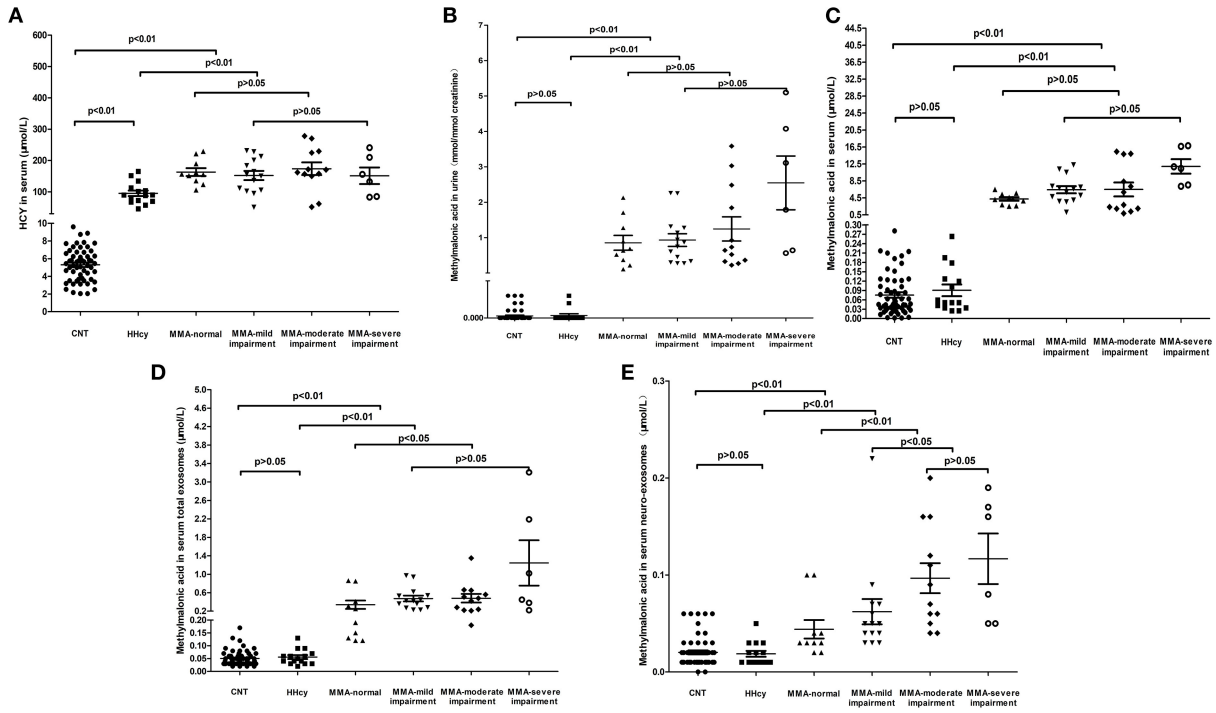

FIGURE 1
The levels of HCY in serum **(A)**, methylmalonic acid in urine **(B)**, methylmalonic acid in serum **(C)**, methylmalonic acid in serum total exosomes **(D)**, and methylmalonic acid in serum neuro-exosomes **(E)** in different groups. HCY, homocysteine; MMA, methylmalonic acidemia; CNT, Control; HHcy, non-inherited hyperhomocysteinemia; neuro-exosomes, neuronal-derived exosomes; MMA-normal, cblC type methylmalonic acidemia patients with normal IQ or DQ; MMA-mild cognitive impairment, cblC type methylmalonic acidemia patients with mild cognitive impairment; MMA-moderate cognitive impairment, cblC type methylmalonic acidemia patients with moderate cognitive impairment; MMA-severe cognitive impairment, cblC type methylmalonic acidemia patients with severe cognitive impairment.

(Figure 1E) markedly increased in the patients with moderate/severe cognitive impairment. But it showed no significance of the methylmalonic acid in serum total exosomes (Figure 1D)among cblC-MMA patients with different degree cognitive impairment.

Correlation between DQ/IQ scores and the metabolites biomarkers

We analyzed the correlation between participants' DQ or IQ scores and metabolite biomarkers in the study for further exploration of the roles of these metabolites in cognitive impairment, the results were presented in Table 3. The results showed that DQ or IQ was negatively correlated with the levels of serum homocysteine, C3, methylmalonic acid in serum, urine, serum total exosomes and neuro-exosomes. The most intense association is between methylmalonic acid in urine and DQ or IQ scores (Kendall's tau-b's correlation coefficient $= -0.609$, $p < 0.001$). Free carnitine was positively correlated with the participants' DQ or IQ scores.

The performance of metabolites biomarkers for cognitive impairment induced by cblC-MMA

To assess the capacities of biomarkers to distinguish cognitive impairment induced by cblC-MMA, ROC with AUC and 95%CI were analyzed. The performances of biomarkers for distinguishing normal children and cognitive impairment induced by cblC-MMA were showed in Table 4. In brief, the homocysteine and methylmalonic acid showed better performance than carnitines for distinguishing normal children and cblC type MMA induced-cognitive impairment.

To distinguish cblC-MMA patients with cognitive impairment from the HHcy patients, the performances of carnitines, homocysteine and methylmalonic acid were evaluated, the data were shown in Figure 2. Carnitine biomarkers had poor performance ($AUC_{c3} = 0.541$, $p = 0.596$; $AUC_{c0} = 0.376$, $p = 0.111$). Area under the ROC curve of serum homocysteine (Figure 2A) for discriminating cognitive impairment induced by cblC-MMA was 0.685, which decreased significantly than the diagnostic power for distinguishing cblC-MMA patients with cognitive impairment from normal

TABLE 3 Correlation between DQ or IQ scores and the metabolites biomarkers.

Parameters	Kendall's tau-b's correlation coefficient	Kendall's tau-b's *P*-value
HCY	−0.455	<0.001
C3	−0.239	<0.001
C0	0.213	0.001
C3/C0	−0.301	<0.001
Methylmalonic acid in urine	−0.609	<0.001
Methylmalonic acid in serum	−0.462	<0.001
Methylmalonic acid in serum total exosomes	−0.475	<0.001
Methylmalonic acid in serum neuro-exosomes	−0.499	<0.001

HCY, homocysteine; C3, propionylcarnitine; C0, free carnitine; neuro-exosomes, neuronal-derived exosomes.

TABLE 4 The performance of biomarkers in distinguish between normal children and cognitive impairment induced by cblC-MMA.

Parameters	AUC (95%CI)	*P*-value
HCY	0.926 (0.875–0.976)	<0.001
C3	0.713 (0.589–0.836)	0.001
C0	0.663 (0.535–0.791)	0.004
C3/C0	0.737 (0.617–0.856)	<0.001
Methylmalonic acid in urine	0.941 (0.897–0.986)	<0.001
Methylmalonic acid in serum	0.955 (0.921–0.990)	<0.001
Methylmalonic acid in serum total exosomes	0.961 (0.924–0.999)	<0.001
Methylmalonic acid in serum neuro-exosomes	0.921 (0.870–0.971)	<0.001

HCY, homocysteine; C3, propionylcarnitine; C0, free carnitine; neuro-exosomes neuronal-derived exosomes.

children. However, the methylmalonic acid (Figures 2B–E) still had good performance.

23.8% (10/42) cblC-MMA patients did not yet suffer cognitive impairment, other patients suffered different degrees of cognitive impairment. In order to identify children with cognitive impairment from cblC-MMA patients, the performances of biomarkers were assessed and the data were showed in Figure 3. The levels of methylmalonic acid in serum total exosomes (Figure 3D) and in serum neuro-exosomes (Figure 3E) showed better performance than serum homocysteine (Figure 3A), methylmalonic acid in the urine (Figure 3B) and in the serum (Figure 3C) for distinguishing cblC-MMA patients with or without cognitive impairment.

14 cblC-MMA patients suffered mild cognitive impairment and 18 cblC-MMA patients suffered moderate or severe cognitive impairment. Our data indicated that the levels of methylmalonic acid in serum neuro-exosomes might be helpful to discriminate cognitive impairment degrees. The AUC of methylmalonic acid in serum neuro-exosomes for distinguishing mild cognitive dysfunction from moderate or severe cognitive impairment was 0.754 (95% CI 0.578–0.930, $p = 0.015$) and the optimum cutoff value was 0.075 μmol/L, corresponding to the sensitivity of 55.6%, specificity of 85.6%, positive predictive value of 83.3% and negative predictive value of 60.0%. The levels of methylmalonic acid in urine (AUC = 0.599, $p = 0.342$), serum (AUC = 0.591, $p = 0.382$), serum total exosomes (AUC = 0.538, $p = 0.718$) had poor performance to distinguish moderate or severe cognitive impairment from mild cognitive impairment induced by cblC-MMA.

The relationship among methylmalonic acid in different body fluids or exosomes

To explore the relationship among methylmalonic acid in different body fluids or exosomes, the correlation analysis was performed. The results were showed in Figure 4. The data showed that methylmalonic acid in urine is positively correlated with methylmalonic acid in serum (Figure 4A, Kendall's tau-b correlation = 0.633, $p < 0.001$). The correlations between methylmalonic acid in exosomes and methylmalonic acid in serum, respectively, were assessed using a similar model. The methylmalonic acid in serum total exosomes was associated with methylmalonic acid in serum (Figure 4B, Kendall's tau-b correlation = 0.539, $p < 0.001$) and methylmalonic acid in serum neuro-exosomes was positive correlation with methylmalonic acid in serum (Figure 4C, Kendall's tau-b correlation = 0.428, $P < 0.001$). The methylmalonic acid in serum neuro-exosomes was positive correlation with in serum total exosomes (Figure 4D, Kendall's tau-b correlation = 0.597, $p < 0.001$).

Discussion

The cblC type MMA is the most common MMA in China. Neurological damage is the most common symptom of this disease. The biochemical metabolic characteristics of the cblC disease include the elevated serum homocysteine, the increased propionylcarnitine and the decreased free carnitine, the elevated ratio of propionylcarnitine and free carnitine and the increased methylmalonic acid levels. Hyperhomocysteinemia should be differentiated from cblC-MMA, which possesses some similar biochemical characteristics with cblC-MMA. Because the incidence of inherited hyperhomocysteinemia (34) is very low (0.02:100,000 individuals in Asians), non-inherited hyperhomocysteinemia patients were included as a comparative group in this study. In this research, 57 healthy children, 15 non-inherited HHcy patients and 42 cblC-MMA patients were

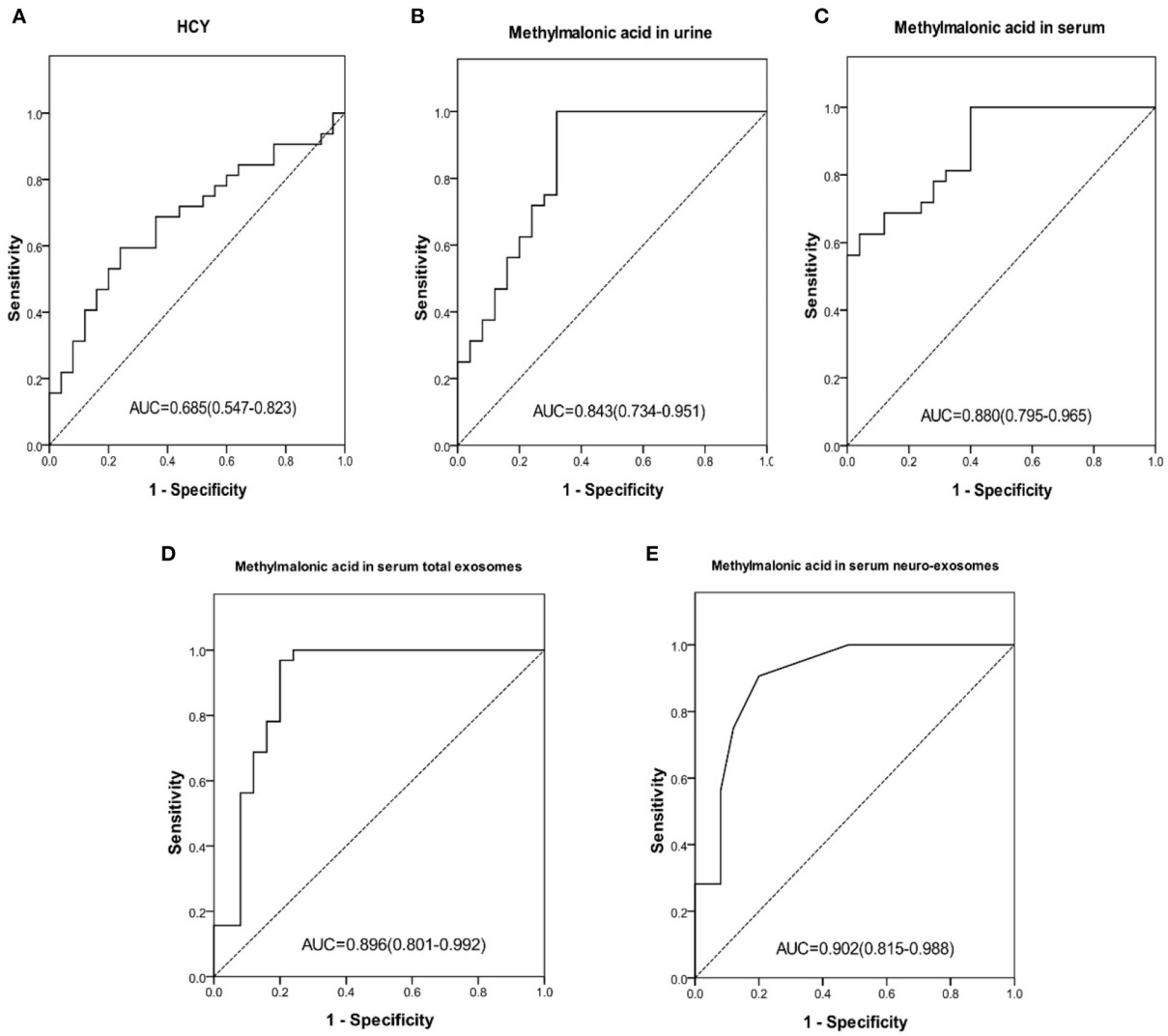

FIGURE 2
ROC curve of HCY in serum **(A)**, methylmalonic acid in urine **(B)**, methylmalonic acid in serum **(C)**, methylmalonic acid in serum total exosomes **(D)**, methylmalonic acid in serum neuro-exosomes **(E)** individually for distinguishing HHcy patients and cblC-MMA patients with cognitive impairment. ROC, receiver operating characteristic; HCY, homocysteine; neuro-exosomes, neuronal-derived exosomes; HHcy, non-inherited hyperhomocysteinemia.

recruited to explore the performances of the biomarkers for diagnosis of cognitive impairment induced by cblC-MMA.

The serum homocysteine, acylcarnitine biomarkers and methylmalonic acid had capacities to distinguish cognitive impairment induced by cblC-MMA from normal children. Then, we found non-inherited HHcy patients were not trouble with cognitive impairment, but the serum homocysteine and acylcarnitine biomarkers of non-inherited HHcy patients had similar elevated trends with cblC-MMA patients. As a result, the patients with cognitive impairment induced by cblC-MMA could not be distinguished from HHcy patients using serum homocysteine and acylcarnitine biomarkers. In addition, serum homocysteine and acylcarnitine biomarkers had a poor performance for distinguishing whether cblC-MMA patients with or without cognitive impairment or indicating the severity of cognitive impairment.

At present, methylmalonic acid is recognized as an important pathogenic substance of MMA (10). Cognitive impairment is the most common symptoms of MMA-induced brain injury. The previous study showed that 60–70% MMA patients were troubled with cognitive impairment (30, 35) and some of them had severe cognitive impairment (35).

In order to determine whether the levels of methylmalonic acid in different body fluids might be biomarkers for the

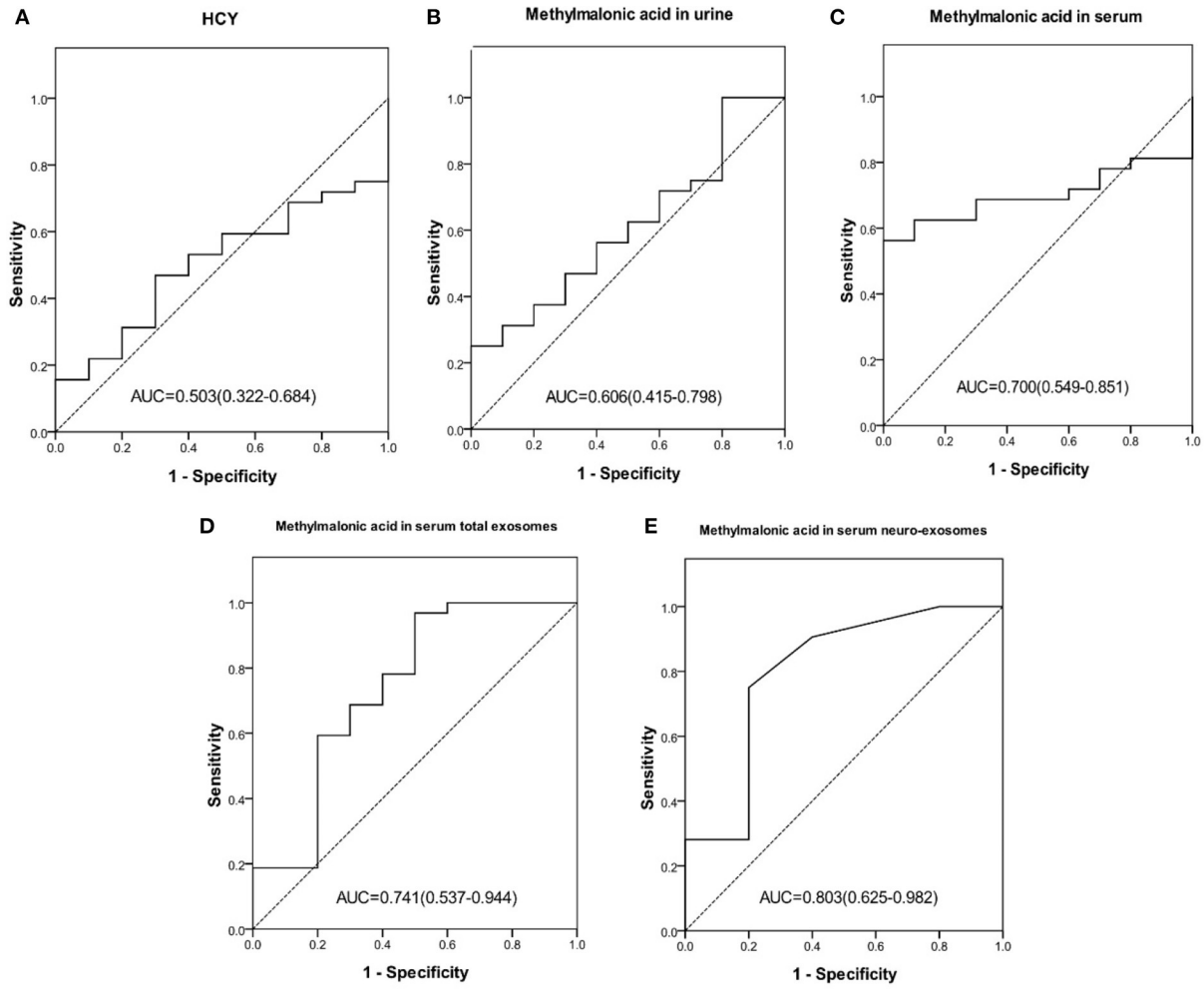

FIGURE 3
ROC curve of HCY in serum **(A)**, methylmalonic acid in urine **(B)**, methylmalonic acid in serum **(C)**, methylmalonic acid in serum total exosomes **(D)**, methylmalonic acid in serum neuro-exosomes **(E)** individually for distinguishing cblC-MMA children with cognitive impairment from without cognitive impairment. ROC, receiver operating characteristic; HCY, homocysteine; neuro-exosomes, neuronal-derived exosomes.

diagnosis of MMA-induced cognitive impairment, the levels of methylmalonic acid in urine, serum, serum total exosomes and serum neuronal-derived exosomes were detected in healthy children, non-inherited HHcy patients and cblC-MMA patients. The results indicated that urinary methylmalonic acid had good performance to distinguish cblC-MMA patients with cognitive impairment from healthy children or non-inherited HHcy patients. However, urinary methylmalonic acid had poor performance to distinguish cblC-MMA patients with cognitive impairment from patients without cognitive impairment. As known, the levels of methylmalonic acid in urine were related to the excretion function of the kidney and the levels of serum methylmalonic acid. The kidney excretion functions of the cblC-MMA patients were affected by high concentrations of methylmalonic acid and homocysteine. The mechanisms of renal injury of cblC-MMA patients included that homocysteine caused vascular coagulation and glomerular vascular injury (36, 37) and methylmalonic acid induced renal tubular acidosis (38, 39). In this study, we found the levels of urea were obviously higher than normal children, which indicated the renal injury in cblC-MMA. Therefore, the urinary methylmalonic acid excretion was a comprehensive reflection of renal function and the levels of toxic metabolites such as serum methylmalonic acid and homocysteine, which was not a specific biomarker for the discrimination of brain injury.

In this study, the levels of the serum methylmalonic acid had good performance for distinguishing cblC-MMA induced cognitive impairment from control children or non-inherited HHcy patients. The levels of serum methylmalonic acid had poor performance to distinguish cblC-MMA patients

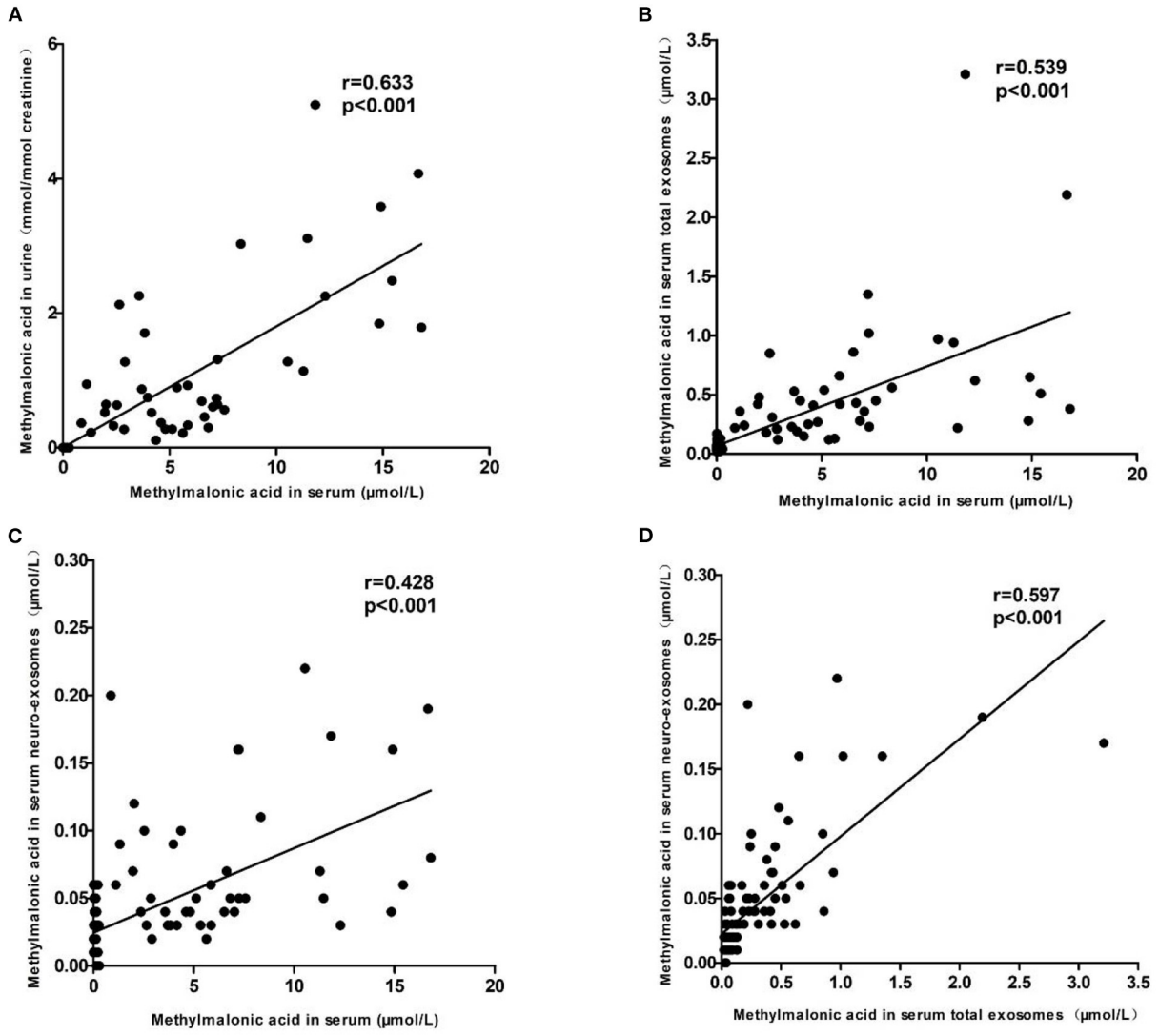

FIGURE 4
The relationship among methylmalonic acid in different body fluids or exosomes. **(A)** Showed the correlation between methylmalonic acid in urine and in serum. **(B)** Showed the correlation between methylmalonic acid in serum total exosomes and methylmalonic acid in serum. **(C)** Showed the correlation between methylmalonic acid in serum neuro-exosomes and methylmalonic acid in serum. **(D)** Showed the correlation between methylmalonic acid in serum neuro-exosomes and methylmalonic acid in serum total exosomes.

with cognitive impairment from patients without cognitive impairment or to determine cblC-MMA patients with moderate and severe cognitive impairment, which was similar with the performance of urinary methylmalonic acid. Therefore, the levels of methylmalonic acid in serum and in urine might not accurately reflect brain injury of cblC-MMA patients. The possible reason was that methylmalonic acid in peripheral circulation could not reflect the injury of the central nervous system due to the existence of blood-brain barrier (BBB). The BBB was blood vessels that prevents the brain from exogenous and circulating toxin. The BBB played the role of a physical barrier and a metabolic barrier. The previous study reported that organic acid transporters 1 (OAT1) and 3 (OAT3) at the BBB with a low capacity for the transport of methylmalonic acid, and there was virtually no transport of methylmalonic acid across the choroid plexus (40). According to the previous study, the transport of methylmalonic acid to the brain should be a long process just relying on OAT1 and OAT3 transporter and MMA induced brain injury should be not easy to happen due to the presence of BBB. However, the brain injury was very common in MMA, which indicated that except OAT1 and OAT3 transporter, other important transport mechanism

played a key role for intracerebral transport of methylmalonic acid. In addition, our previous study showed that subcutaneous continuous injection of methylmalonic acid for 24 days in normal rat cups led to the apoptosis of hippocampal neurons in rats (19), which verified that some important channels or carriers accelerated methylmalonic acid across BBB and induced brain injury.

Exosomes are vesicles that are released from cells into the extracellular space. Exosomes participate in many aspects of nervous system development and function which included regulation of nerve regeneration and synaptic communication (41). Exosomes mediate the transfer of packets of non-secreted proteins, lipids and nucleic acids within a membrane compartment. Exosomes are very important for the enclosing and transport of key proteins during developments as well as neurotoxic misfolded proteins during pathogenesis. In this study, we found the levels of methylmalonic acid in the serum total exosomes reflected the cognitive impairment induced by cblC-MMA more accurately than total methylmalonic acid in the serum. The possible reason was circulating exosomes crossed the BBB in both directions, i.e., from the bloodstream toward the brain, and from the brain to the bloodstream (42, 43), which brought more information about brain injury. In addition, the exosomes released by specific cells could package different molecules or substances from donor cells in the double membrane structure. Specially, when the special exosomes carried specific disease-related cargoes, they possessed potential uses as biomarkers. Therefore, the neuronal-derived exosomes were extracted in the serum by the established method in this study. The levels of methylmalonic acid in serum neuronal-derived exosomes were detected by LC-MS/MS, it accurately reflected existence of the cognitive impairment induced by cblC-MMA and degree of cognitive impairment severity.

In addition, if exosomes were a potential manner of methylmalonic acid transport *in vivo*, the levels of methylmalonic acid in total serum exosomes might reflect the balance of methylmalonic acid from different tissues or organs. Besides currently available cognitive assessment tests, the levels of methylmalonic acid in some special subgroup exosomes in serum derived from different tissues or organs (such as liver, kidney, heart and so on) might be helpful to diagnosis of cblC type MMA-induced injuries of different tissues and organs. It would be our further study in the future.

In summary, this study found that serum homocysteine, acylcarnitine, serum and urinary methylmalonic acid showed promise as biomarkers for distinguishing MMA-induced cognitive impairment from healthy children or non-inherited HHcy patients. More importantly, the methylmalonic acid in serum exosomes had the capacity to differentiate cblC-MMA patients with or without cognitive impairment. Especially, serum neuronal-derived exosomes reflected pathological changes in the brain of cblC-MMA patients, which should serve as a potential biomarker for estimating the severity of MMA-induced cognitive impairment.

The main limitation of the current study was the small sample size, especially we lacked a validation group, the enrollment of the patients was limited by the low prevalence of cblC type MMA (1:46,000 to 1:200,000 in European and American countries and 1:3,220 to 1:21,488 in China) (44–47). These findings warrant further investigation by more patients' enrollment and multiple center studies.

Data availability statement

The raw data supporting the conclusions of this article will be made available by the authors, without undue reservation.

Ethics statement

The studies involving human participants were reviewed and approved by the Medical Ethics Committee of Beijing Children's Hospital, Capital Medical University. Written informed consent to participate in this study was provided by the participants' legal guardian/next of kin.

Author contributions

QL was responsible for the conception and design of the study. SS, HJ, YR, WS, and QL contributed to the data acquisition. SS, HJ, YR, and WS were involved in the analysis and interpretation of data. SS drafted the first version of the article. All authors critically revised the manuscript for important intellectual content and gave final approval of the version to be submitted.

Funding

This study was supported by grants from the National Natural Science Foundation of China (81802061), the Talent Project of Public Health of Beijing (2022-3-024), and Beijing Municipal Administration of Hospitals Incubating Program (PX2018046).

Conflict of interest

The authors declare that the research was conducted in the absence of any commercial or financial relationships that could be construed as a potential conflict of interest.

Publisher's note

All claims expressed in this article are solely those of the authors and do not necessarily represent those

of their affiliated organizations, or those of the publisher, the editors and the reviewers. Any product that may be evaluated in this article, or claim that may be made by its manufacturer, is not guaranteed or endorsed by the publisher.

Supplementary material

The Supplementary Material for this article can be found online at: https://www.frontiersin.org/articles/10.3389/fneur.2022.1090958/full#supplementary-material

References

1. Almási T, Guey LT, Lukacs C, Csetneki K, Vokó Z, Zelei T. Systematic literature review and meta-analysis on the epidemiology of methylmalonic acidemia (MMA) with a focus on MMA caused by methylmalonyl-CoA mutase (mut) deficiency. *Orphanet J Rare Dis.* (2019) 14:84. doi: 10.1186/s13023-019-1063-z

2. Liu J, Peng Y, Zhou N, Liu X, Meng Q, Xu H, et al. Combined methylmalonic acidemia and homocysteinemia presenting predominantly with late-onset diffuse lung disease: a case series of four patients. *Orphanet J Rare Dis.* (2017) 12:58. doi: 10.1186/s13023-017-0610-8

3. Zhou X, Cui Y, Han J. Methylmalonic acidemia: Current status and research priorities. *Intractable Rare Dis Res.* (2018) 7:73–8. doi: 10.5582/irdr.2018.01026

4. Wang C, Li D, Cai F, Zhang X, Xu X, Liu X, et al. Mutation spectrum of MMACHC in Chinese pediatric patients with cobalamin C disease: a case series and literature review. *Eur J Med Genet.* (2019) 62:103713. doi: 10.1016/j.ejmg.2019.103713

5. Wang F, Han L, Yang Y, Gu X, Ye J, Qiu W, et al. Clinical, biochemical, and molecular analysis of combined methylmalonic acidemia and hyperhomocysteinemia (cblC type) in China. *J Inherit Metab Dis.* (2010) 33(Suppl 3):S435–42. doi: 10.1007/s10545-010-9217-0

6. Jiang YZ, Shi Y, Shi Y, Gan LX, Kong YY, Zhu ZJ, et al. Methylmalonic and propionic acidemia among hospitalized pediatric patients: a nationwide report. *Orphanet J Rare Dis.* (2019) 14:292. doi: 10.1186/s13023-019-1268-1

7. Zhang K, Gao M, Wang G, Shi Y, Li X, Lv Y, et al. Hydrocephalus in cblC type methylmalonic acidemia. *Metab Brain Dis.* (2019) 34:451–8. doi: 10.1007/s11011-018-0351-y

8. Yang L, Guo B, Li X, Liu X, Wei X, Guo L. Brain MRI features of methylmalonic acidemia in children: the relationship between neuropsychological scores and MRI findings. *Sci Rep.* (2020) 10:13099. doi: 10.1038/s41598-020-70113-y

9. Carrillo-Carrasco N, Chandler RJ, Venditti CP. Combined methylmalonic acidemia and homocystinuria, cblC type. I Clinical presentations, diagnosis and management. *J Inherit Metab Dis.* (2012) 35:91–102. doi: 10.1007/s10545-011-9364-y

10. Kölker S, Okun JG. Methylmalonic acid–an endogenous toxin? *Cell Mol Life Sci.* (2005) 62:621–4. doi: 10.1007/s00018-005-4463-2

11. Brusque AM, Borba Rosa R, Schuck PF, Dalcin KB, Ribeiro CA, Silva CG, et al. Inhibition of the mitochondrial respiratory chain complex activities in rat cerebral cortex by methylmalonic acid. *Neurochem Int.* (2002) 40:593–601. doi: 10.1016/s0197-0186(01)00130-9

12. Proctor EC, Turton N, Boan EJ, Bennett E, Philips S, Heaton RA, et al. The effect of methylmalonic acid treatment on human neuronal cell coenzyme Q10 status and mitochondrial function. *Int J Mol Sci.* (2020) 21:9137. doi: 10.3390/ijms21239137

13. Halperin ML, Schiller CM, Fritz IB. The inhibition by methylmalonic acid of malate transport by the dicarboxylate carrier in rat liver mitochondria. A possible explantation for hypoglycemia in methylmalonic aciduria. *J Clin Invest.* (1971) 50:2276–82. doi: 10.1172/JCI106725

14. Oberholzer VG, Levin B, Burgess EA, Young WF. Methylmalonic aciduria. An inborn error of metabolism leading to chronic metabolic acidosis. *Arch Dis Child.* (1967) 42:492–504. doi: 10.1136/adc.42.225.492

15. Dutra JC, Dutra-Filho CS, Cardozo SE, Wannmacher CM, Sarkis JJ, Wajner M. Inhibition of succinate dehydrogenase and beta-hydroxybutyrate dehydrogenase activities by methylmalonate in brain and liver of developing rats. *J Inherit Metab Dis.* (1993) 16:147–53. doi: 10.1007/BF00711328

16. Liu Y, Wang S, Zhang X, Cai H, Liu J, Fang S, et al. The Regulation and characterization of mitochondrial-derived methylmalonic acid in mitochondrial dysfunction and oxidative stress: from basic research to clinical practice. *Oxid Med Cell Longev.* (2022) 2022:7043883. doi: 10.1155/2022/7043883

17. Royes LF, Gabbi P, Ribeiro LR, Della-Pace ID, Rodrigues FS, de Oliveira Ferreira AP, et al. A neuronal disruption in redox homeostasis elicited by ammonia alters the glycine/glutamate (GABA) cycle and contributes to MMA-induced excitability. *Amino Acids.* (2016) 48:1373–89. doi: 10.1007/s00726-015-2164-1

18. Gabbi P, Ribeiro LR, Jessié Martins G, Cardoso AS, Haupental F, Rodrigues FS, et al. Methylmalonate induces inflammatory and apoptotic potential: a link to glial activation and neurological dysfunction. *J Neuropathol Exp Neurol.* (2017) 76:160–78. doi: 10.1093/jnen/nlw121

19. Li Q, Song W, Tian Z, Wang P. Aminoguanidine alleviated MMA-induced impairment of cognitive ability in rats by downregulating oxidative stress and inflammatory reaction. *Neurotoxicology.* (2017) 59:121–30. doi: 10.1016/j.neuro.2017.02.005

20. Andrade VM, Dal Pont HS, Leffa DD, Damiani AP, Scaini G, Hainzenreder G, et al. Methylmalonic acid administration induces DNA damage in rat brain and kidney. *Mol Cell Biochem.* (2014) 391:137–45. doi: 10.1007/s11010-014-1996-4

21. Martinelli D, Deodato F, Dionisi-Vici C. Cobalamin C defect: natural history, pathophysiology, and treatment. *J Inherit Metab Dis.* (2011) 34:127–35. doi: 10.1007/s10545-010-9161-z

22. Lehotsky J, Petras M, Kovalska M, Tothova B, Drgova A, Kaplan P. Mechanisms involved in the ischemic tolerance in brain: effect of the homocysteine. *Cell Mol Neurobiol.* (2015) 35:7–15. doi: 10.1007/s10571-014-0112-3

23. Zhao Y, Huang G, Chen S, Gou Y, Dong Z, Zhang X. Homocysteine aggravates cortical neural cell injury through neuronal autophagy overactivation following rat cerebral ischemia-reperfusion. *Int J Mol Sci.* (2016) 17:1196. doi: 10.3390/ijms17081196

24. Budnik V, Ruiz-Cañada C, Wendler F. Extracellular vesicles round off communication in the nervous system. *Nat Rev Neurosci.* (2016) 17:160–72. doi: 10.1038/nrn.2015.29

25. Saint-Pol J, Gosselet F, Duban-Deweer S, Pottiez G, Karamanos Y. Targeting and crossing the blood-brain barrier with extracellular vesicles. *Cells.* (2020) 9:851. doi: 10.3390/cells9040851

26. Jia L, Qiu Q, Zhang H, Chu L, Du Y, Zhang J, et al. Concordance between the assessment of Aβ42, T-tau, and P-T181-tau in peripheral blood neuronal-derived exosomes and cerebrospinal fluid. *Alzheimers Dement.* (2019) 15:1071–80. doi: 10.1016/j.jalz.2019.05.002

27. Jiang C, Hopfner F, Katsikoudi A, Hein R, Catli C, Evetts S, et al. Serum neuronal exosomes predict and differentiate Parkinson's disease from atypical parkinsonism. *J Neurol Neurosurg Psychiatry.* (2020) 91:720–29. doi: 10.1136/jnnp-2019-322588

28. Jia L, Zhu M, Kong C, Pang Y, Zhang H, Qiu Q, et al. Blood neuro-exosomal synaptic proteins predict Alzheimer's disease at the asymptomatic stage. *Alzheimers Dement.* (2021) 17:49–60. doi: 10.1002/alz.12166

29. Kim J, Kim H, Roh H, Kwon Y. Causes of hyperhomocysteinemia and its pathological significance. *Arch Pharm Res.* (2018) 41:372–83. doi: 10.1007/s12272-018-1016-4

30. O'Shea CJ, Sloan JL, Wiggs EA, Pao M, Gropman A, Baker EH, et al. Neurocognitive phenotype of isolated methylmalonic acidemia. *Pediatrics.* (2012) 129:e1541–51. doi: 10.1542/peds.2011-1715

31. Peng Y, Huang B, Biro F, Feng L, Guo Z, Slap G. Outcome of low birthweight in China: a 16-year longitudinal study. *Acta Paediatr.* (2005) 94:843–49. doi: 10.1111/j.1651-2227 2005. Tb 01999.x

32. Lee J, Kalia V, Perera F, Herbstman J, Li T, Nie J, et al. Prenatal airborne polycyclic aromatic hydrocarbon exposure, LINE1 methylation and child development in a Chinese cohort. *Environ Int.* (2017) 99:315–20. doi: 10.1016/j.envint.2016.12.009

33. Mustapic M, Eitan E, Werner JK Jr, Berkowitz ST, Lazaropoulos MP, Tran J, et al. Plasma extracellular vesicles enriched for neuronal origin:

a potential window into brain pathologic processes. *Front Neurosci.* (2017) 11:278. doi: 10.3389/fnins.2017.00278

34. Weber Hoss G R, Sperb-Ludwig F, Schwartz I, Blom H J. Classical homocystinuria: a common inborn error of metabolism? An epidemiological study based on genetic databases. *Mol Gen Genom Med.* (2020) 8:e1214. doi: 10.1002/mgg3.1214

35. de Baulny HO, Benoist JF, Rigal O, Touati G, Rabier D, Saudubray JM. Methylmalonic and propionic acidaemias: management and outcome. *J Inherit Metab Dis.* (2005) 28:415–23. doi: 10.1007/s10545-005-7056-1

36. Chen M, Zhuang J, Yang J, Wang D, Yang Q. Atypical hemolytic uremic syndrome induced by CblC subtype of methylmalonic academia: a case report and literature review. *Medicine.* (2017) 96:e8284. doi: 10.1097/MD.0000000000008284

37. Li QL, Song WQ, Peng XX, Liu XR, He LJ, Fu LB. Clinical characteristics of hemolytic uremic syndrome secondary to cobalamin C disorder in Chinese children. *World J Pediatr.* (2015) 11:276–80. doi: 10.1007/s12519-015-0032-4

38. D'Angio CT, Dillon MJ, Leonard JV. Renal tubular dysfunction in methylmalonic acidaemia. *Eur J Pediatr.* (1991) 150:259–63. doi: 10.1007/BF01955526

39. Morath MA, Hörster F, Sauer SW. Renal dysfunction in methylmalonic acidurias: review for the pediatric nephrologist. *Pediatr Nephrol.* (2013) 28:227–35. doi: 10.1007/s00467-012-2245-2

40. Sauer SW, Opp S, Mahringer A, Kamiński MM, Thiel C, Okun JG, et al. Glutaric aciduria type I and methylmalonic aciduria: simulation of cerebral import and export of accumulatingneurotoxic dicarboxylic acids in *in vitro* models of the blood-brain barrier and the choroid plexus. *Biochim Biophys Acta.* (2010) 1802:552–60. doi: 10.1016/j.bbadis.2010.03.003

41. Yuyama K, Igarashi Y. Physiological and pathological roles of exosomes in the nervous system. *Biomol Concepts.* (2016) 7:53–68. doi: 10.1515/bmc-2015-0033

42. Liu W, Bai X, Zhang A, Huang J, Xu S, Zhang J. Role of exosomes in central nervous system diseases. *Front Mol Neurosci.* (2019) 12:240. doi: 10.3389/fnmol.2019.00240

43. Tian Y, Fu C, Wu Y, Lu Y, Liu X, Zhang Y. Central nervous system cell-derived exosomes in neurodegenerative diseases. *Oxid Med Cell Longev.* (2021) 2021:9965564. doi: 10.1155/2021/9965564

44. Morel CF, Lerner-Ellis JP, Rosenblatt DS. Combined methylmalonic aciduria and homocystinuria (cblC): phenotype-genotype correlations and ethnic-specific observations. *Mol Genet Metab.* (2006) 88:315–21. doi: 10.1016/j.ymgme.2006.04.001

45. Weisfeld-Adams JD, Morrissey MA, Kirmse BM. Newborn screening and early biochemical follow-up in combined methylmalonic aciduria and homocystinuria, cblC type, and utility of methionine as a secondary screening analyte. *Mol Genet Metab.* (2010) 99:116–23. doi: 10.1016/j.ymgme.2009.09.008

46. Zhou W, Li H, Wang C. Newborn Screening for Methylmalonic Acidemia in a Chinese Population: Molecular Genetic Confirmation and Genotype Phenotype Correlations. *Front Genet.* (2019) 9:726. doi: 10.3389/fgene.2018.00726

47. Wang T, Ma J, Zhang Q. Expanded newborn screening for inborn errors of metabolism by tandem mass spectrometry in Suzhou, China: disease spectrum, prevalence, genetic characteristics in a Chinese population. *Front Genet.* (2019) 10:1052. doi: 10.3389/fgene.2019.01052

frontiers | Frontiers in Neurology

TYPE Original Research
PUBLISHED 04 January 2023
DOI 10.3389/fneur.2022.1048629

OPEN ACCESS

EDITED BY
Wael M. Y. Mohamed,
International Islamic University Malaysia, Malaysia

REVIEWED BY
Ganne Chaitanya,
University of Texas Health Science Center at Houston, United States
Bourel-Ponchel Emilie,
University of Picardie Jules Verne, France

*CORRESPONDENCE
Julia Jacobs
julia.jacobs@gmx.de

†These authors share first authorship

SPECIALTY SECTION
This article was submitted to Neurological Biomarkers, a section of the journal Frontiers in Neurology

RECEIVED 19 September 2022
ACCEPTED 30 November 2022
PUBLISHED 04 January 2023

CITATION
Kuhnke N, Wusthoff CJ, Swarnalingam E, Yanoussi M and Jacobs J (2023) Epileptic high-frequency oscillations occur in neonates with a high risk for seizures. *Front. Neurol.* 13:1048629. doi: 10.3389/fneur.2022.1048629

Epileptic high-frequency oscillations occur in neonates with a high risk for seizures

Nicola Kuhnke[1†], Courtney J. Wusthoff[2†], Eroshini Swarnalingam[3], Mina Yanoussi[1] and Julia Jacobs[3*]

[1]Department of Pediatric Neurology and Muscular Disease, University Medical Center, Freiburg, Germany, [2]Stanford University, Palo Alto, CA, United States, [3]Department of Pediatrics, University of Calgary, Alberta Children's Hospital, Calgary, AB, Canada

Introduction: Scalp high-frequency oscillations (HFOs, 80–250 Hz) are increasingly recognized as EEG markers of epileptic brain activity. It is, however, unclear what level of brain maturity is necessary to generate these oscillations. Many studies have reported the occurrence of scalp HFOs in children with a correlation between treatment success of epileptic seizures and the reduction of HFOs. More recent studies describe the reliable detection of HFOs on scalp EEG during the neonatal period.

Methods: In the present study, continuous EEGs of 38 neonates at risk for seizures were analyzed visually for the scalp HFOs using 30 min of quiet sleep EEG. EEGs of 14 patients were of acceptable quality to analyze HFOs.

Results: The average rate of HFOs was 0.34 ± 0.46/min. About 3.2% of HFOs occurred associated with epileptic spikes. HFOs were significantly more frequent in EEGs with abnormal vs. normal background activities ($p = 0.005$).

Discussion: Neonatal brains are capable of generating HFOs. HFO could be a viable biomarker for neonates at risk of developing seizures. Our preliminary data suggest that HFOs mainly occur in those neonates who have altered background activity. Larger data sets are needed to conclude whether HFO occurrence is linked to seizure generation and whether this might predict the development of epilepsy.

KEYWORDS

high-frequency oscillations, Hypoxic Ischemia Encephalopathy (HIE), epilepsy, neonatal, biomarkers

Introduction

High-frequency oscillations (HFOs) between 80 and 500 Hz are new markers identified in the human scalp and intracranial EEG. Physiological HFOs have been described in intracranial recordings and are linked to various cognitive processes, especially memory consolidation (1–3).

A large body of research has shown that the epileptic brain tissue also generates HFOs, which can be used as biomarkers for brain regions generating seizures (4). Many studies using intracranial EEG demonstrate that HFOs mainly occur inside the seizure onset zone, and several studies suggest that the removal of HFO-generating brain tissue correlates with post-surgical seizure outcome in patients with refractory epilepsy (5, 6). In addition, the amount of HFOs captured in an individual's EEG may reflect

seizure propensity (7, 8). Early studies on epileptic HFOs suggested that these have very small generators preventing them from being visible on scalp EEG (9). Nevertheless, several investigators have identified epileptic HFOs on scalp EEG with a clear link to seizure onset areas (10, 11). Treatment response in different pediatric epilepsy syndromes has been linked to a reduction in HFOs (12). Simultaneous intracranial and scalp EEG recordings have proven a link between intracranial and scalp HFOs; simulation studies suggest that scalp HFOs are visible due to the low noise level in the high-frequency spectrum (13). The discovery of epileptic HFOs in scalp EEG substantially broadens the potential of these EEG markers and opens up an opportunity to investigate patients at risk of developing seizures. More recent studies even describe physiological HFOs in scalp recordings (14).

More than in any other age group, neonates are especially susceptible to seizures in the setting of acute brain injury. Among neonates with hypoxic-ischemic encephalopathy or stroke, 40–60% have acute seizures (15, 16) and 10–20% of these patients go on to develop chronic epilepsy with recurrent postneonatal seizures (17). It is unknown whether early treatment and suppression of symptomatic neonatal seizures can improve the overall outcome and reduce the likelihood of epileptogenesis. Multiple observational studies have shown that seizure burden is associated with a negative outcome even independent of other clinical variables, suggesting that the treatment of neonatal seizures may present an opportunity for intervention (15). A reliable biomarker for impending neonatal seizures would be highly valuable for evaluating interventions to prevent or modify these seizures.

The neonatal brain undergoes a rapid developmental change in the first week after birth. Maturation is reflected by changing EEG features during the neonatal period (18). It is now known that the neonatal brain is capable of producing HFOs, which can be detected on scalp EEG (19). The present study aimed to analyze scalp EEG from neonates at risk for seizures to determine whether HFOs are identifiable in this population.

Methods

Patients

All neonates who underwent continuous video EEG between November 2014 and September 2016 either at the Neuro-NICU of Lucile Packard Children's Hospital Stanford or at the NICU of the University Medical Center Freiburg were included. EEG recordings were initiated due to clinical concerns either for suspected seizure or a high-risk condition, such as hypoxic-ischemic encephalopathy. All EEG data were analyzed retrospectively. The study passed the local ethical review board at both University of Freiburg and Stanford. Included subjects had to have a long-term EEG performed due to clinical reasons, with a minimum of 30 min of EEG with low artifacts and a sampling rate $\geq$1,000 Hz. Medical records were used to extract clinical information, such as gestational age, birth weight, APGAR score, complications during pregnancy and birth, the severity of asphyxia or brain damage, hypothermia treatment, age at the time of EEG, and occurrence of seizures.

EEG recording

Each recording was performed using 8–19 gold electrodes placed using adhesive paste. EEG was recorded continuously for at least 12 h in all patients. EEGs in Stanford were recorded using Nihon Kohden (Irvine, USA) with a 2,000 Hz sampling rate; and those in Freiburg with Micromed (Treviso, Italy) with a sampling rate of 2,048 Hz. A 30-min EEG segment was selected manually from a quiet sleep, with at least 2 h time separation from any seizures to sample the interictal period and a period selected to minimize artifacts (20, 21). EEGs were converted to EDF format using ASA software (ANT Neuro HQ, Enschede, the Netherlands).

EEGs were visually analyzed using a bipolar double banana montage. Clinical EEGs were scored according to the classification for Hypoxic Ischemic Encephalopathy (HIE) [Sarnat und (22)] (Normal; Moderately abnormal (Depression of amplitude $<$25 μV, periodic or paroxysmal); Severely abnormal (Periodic or isoelectric). A similar classification could not be made with the other etiologies, as a standardized conceptualization of EEG severity is not currently available for pathologies other than HIE. EEGs with obscuring focal or diffuse artifacts were excluded.

HFO analysis

HFOs were visually identified using Stellate Harmonie Systems (Stellate, Montreal, Canada), as previously described (23). EEG was displayed with a split screen, visualizing the high-pass filtered EEG for HFO analysis, and an EEG with standard filter setup (HFF: 70 Hz, LFF: 1 Hz, and Notch filter: 60 Hz) for spike and artifact identification. For HFO identification, a FIR high-pass filter of 80 Hz was applied and the maximally possible time resolution of 0.6 s/page was selected. All HFO markings were performed visually by two independent reviewers. Only events which were identified by both were taken into the analysis. HFOs were identified as such if the oscillation had a significantly higher amplitude than the background EEG and consisted of at least four oscillations (see Figure 1). In the case of an associated artifact in the unfiltered EEG on the same or a neighboring channel, HFOs occurring simultaneously were excluded (see Figure 2). Rates of spikes and HFOs were calculated for each channel. The rate of HFO occurrence was

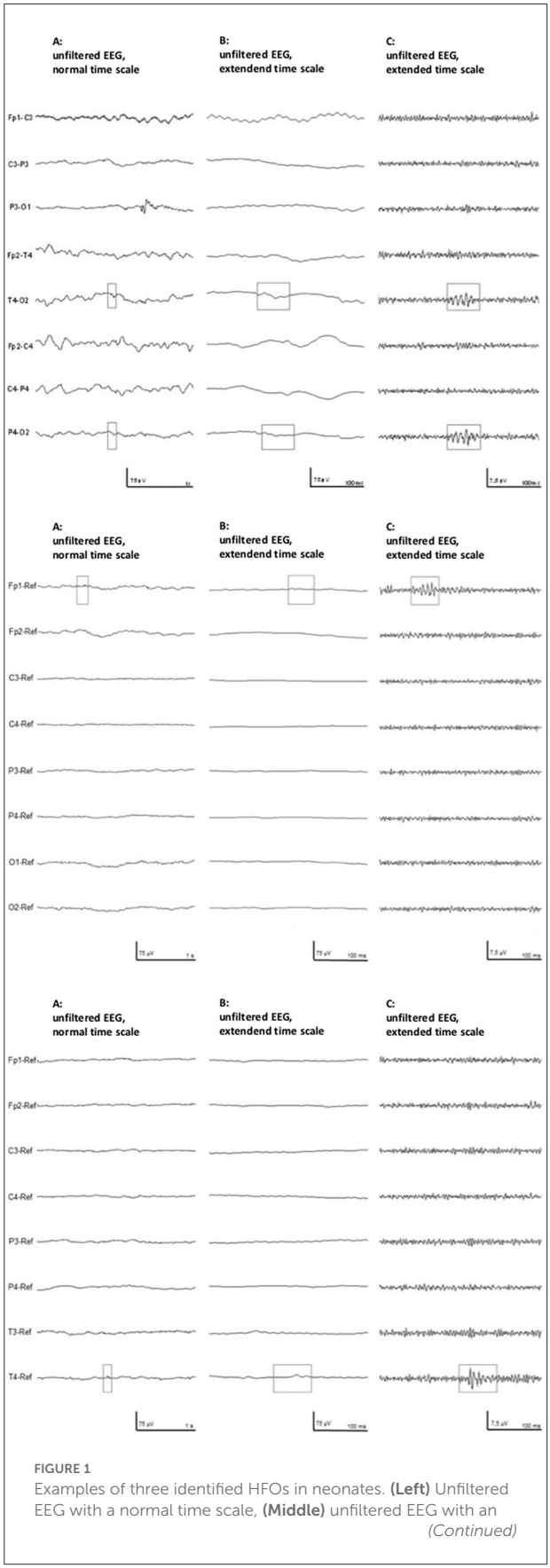

FIGURE 1
Examples of three identified HFOs in neonates. **(Left)** Unfiltered EEG with a normal time scale, **(Middle)** unfiltered EEG with an *(Continued)*

FIGURE 1 (Continued)
extended time scale, and **(Right)** the high-pass filtered EEG with an extended time scale. The top row shows an example from patient #1, the middle row from patient #9, and bottom row shows data from patient #11.

compared between the etiological cohorts of asphyxia vs. non-asphyxia related etiologies.

Statistical analysis

Statistical comparisons of HFO rates between patients with different EEG background patterns as well as between different etiologies were performed through a Mann–Whitney *U*-test. The significance level was defined at $p < 0.05$. All statistics used SPSS software.

Results

Thirty-eight neonates had continuous EEG meeting the inclusion criteria during the study period, but in 24 subjects, high-frequency artifacts were present during the recording. One major cause of these artifacts was electrical interference from the simultaneous use of a stand-alone aEEG machine. Fourteen patients had EEG that could be used for detailed analysis. The average gestational age of our patient population was 38 + 1 weeks with an average birth weight of 3,035.2 g. Of that, 57% were male. The average age of the patients at the time of obtaining the EEG was 9.6 days. Clinical and electrographic seizures were present in 11/14 (78.5%) patients. Asphyxia was the reason to obtain an EEG in 4 out of 14 patients with one patient diagnosed with both perinatal stroke and asphyxia. Neonatal seizures were the reason for EEG acquisition in 4 out of 14 and a vascular event occurred in 3 out of 14. Two patients had a confirmed underlying genetic etiology. The clinical characteristics of these patients are summarized in Table 1.

In seven patients, the EEG background activity was classified as normal; in six patients, moderately abnormal; and in one patient, severely abnormal.

A total of 241 EEG channels could be analyzed. Epileptic spikes were seen in 11 patients. The average rate of spikes was 0.72 ± 0.96/min. HFOs could also be identified in 11 patients (Figure 1). The average rate of HFOs was 0.34 ± 0.46/min. Approximately 3.2% of HFOs occurred at the same time as epileptic spikes. There was no significant difference in HFO rates among patients that showed spikes and those who did not (Figure 3). The three neonates without HFO did not significantly differ from their counterparts either clinically or neurophysiologically.

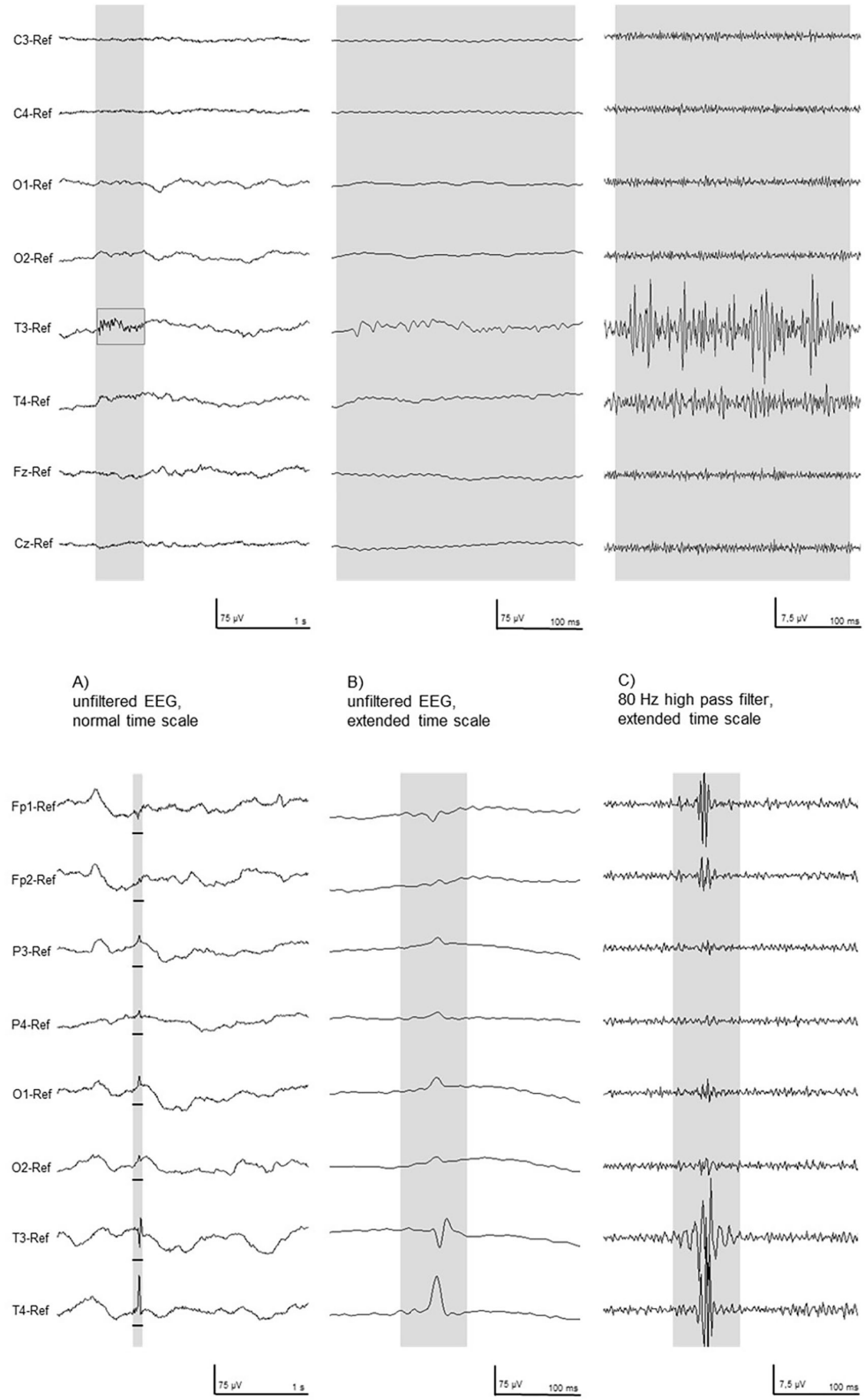

FIGURE 2
Two typical examples of high-frequency activity in the filtered EEG **(Right)** were excluded as artifact, as seen in the unfiltered EEG **(Left)**. These EEG segments were recorded in patient # 10.

TABLE 1 Clinical details of all analyzed patients.

Patient #	M/F	Week of gestation	Birthweight	Age at EEG	APGAR	Reason for EEG/risk	Seizure	Mode of delivery
1	M	38 + 2	2,952 g	2 d	5′8/10′9	Neonatal seizures	Yes	CS
2	F	40 + 0	3,200 g	12 d	5′9/10′9	Neonatal seizures	Yes	VD
3	F	39 + 1	3,400 g	4 d	5′9/10′9	Intracranial hemorrhage	Yes	VD
4	M	39 + 2	3,598 g	20 d	5′5/10′8	Genetic epilepsy/KCNQ2	Yes	CS
5	F	40 + 2	3,349 g	22 d	5′8/10′9	Genetic epilepsy/STXBP1	Yes	VD
6	M	40 + 4	2,740 g	3 d	5′7/10′8	Neonatal seizures	Yes	CS
7	F	40 + 0	3,245 g	1 d	5′4/10′8	Perinatal media infarction	Yes	CS
8	M	40 + 5	3,520 g	1 d	5′8/10′9	Bilateral stroke	Yes	CS
9	M	39 + 0	3,770 g	4 d	5′8/10′9	Neonatal seizures	Yes	CS
10	M	39 + 4	3,620 g	1 d	5′5/10′7	Asphyxia	No	VD
11	M	24 + 0	700 g	2 m	5′4/10′7	Asphyxia	No	CS
12	F	37 + 0	2,200 g	2 d	5′9/10′9	Asphyxia	Yes	CS
13	M	38 + 6	3,400 g	2 d	5′8/10′9	Asphyxia/stroke	Yes	VD
14	F	37 + 6	2,800 g	1 d	5′3/10′5	Ashyxia	No	CS

The term neonatal seizures was used if clinically present seizures were seen without known underlying cause and with normal MRI.
CS, cesarean section; f, female; d, days; m, months; M, male; VD, vaginal delivery.

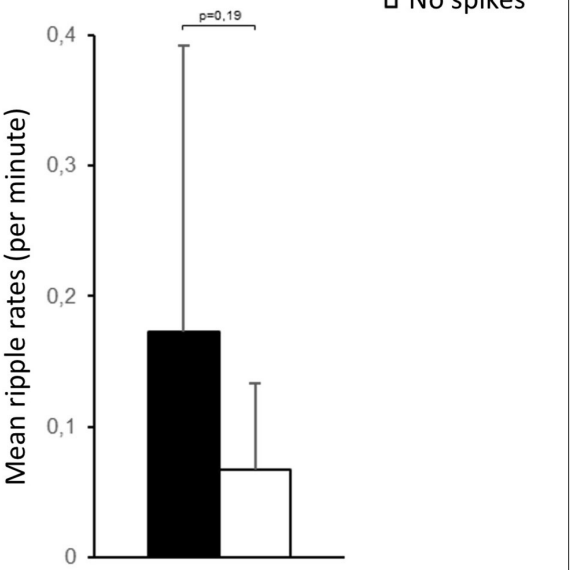

FIGURE 3
No significant difference in HFO rates was seen for channels with and without interictal epileptic spikes.

HFO and spike rates for each patient are presented in Table 2.

For epileptic spikes, no significant differences were found for different background activity, seizure activity, or etiology. HFO rates showed a tendency toward higher HFO rates (0.61 ± 0.57/min) in patients with a moderately abnormal background EEG in comparison to normal background EEG (0.15 ± 0.09/min; Mann–Whitney U-test $p = 0.169$, Figure 4). However, there was a significant difference in HFO rates between patients with normal vs. abnormal EEG backgrounds ($p = 0.005$). There were no significant differences in HFO rates depending on the occurrence of seizures. No differences were found in HFO rates comparing the group of patients with abnormal MRI and the group of neonatal seizures without MRI abnormality.

Discussion

In this study, HFOs were clearly identified on scalp EEG recorded in the neonatal period. All patients under investigation belonged to a high-risk population, and therefore, no conclusion can be drawn in the presence of physiological HFOs in the healthy neonatal brain. The association between abnormal background and higher rates of HFOs suggests that the identified HFOs might be a sign of abnormal function.

Recording EEGs in an ICU environment is often challenging due to the multiple other electronic devices necessary to support and monitor the neonate. In this retrospective data analysis, we had to exclude more than half of the recorded EEGs due to continuous artifacts in the EEG recordings. Some of these artifacts such as ventilation and ECG artifact are obvious and have been described previously (24). In the analysis of high-frequency components in the EEG, more subtle interferences

TABLE 2 Details of EEG results. Rates are given as the length of analyzed EEG was variable due to artifacts.

Patient #	EEG background	# of spikes	Spike rate/min	# of Ripples	Ripple rate/min
1	Normal	80	2.67	4	0.13
2	Normal	8	0.27	8	0.27
3	Moderatly abnormal	8	0.28	47	1.57
4	Normal	30	1	6	0.2
5	Normal	0	0	4	0.13
6	Moderatly abnorm	16	0.53	33	1.1
7	Normal	76	2.53	8	0.27
8	Normal	3	0.1	0	0
9	Moderatly abnormal	17	0.57	17	0.57
10	Moderatly abnormal	0	0	8	0.23
11	Normal	4	0.13	2	0.07
12	Moderatly abnormal	61	2.03	0	0
13	Moderatly abnorm	7	0.23	4	0.13
14	Severly abnormal	0	0	0	0

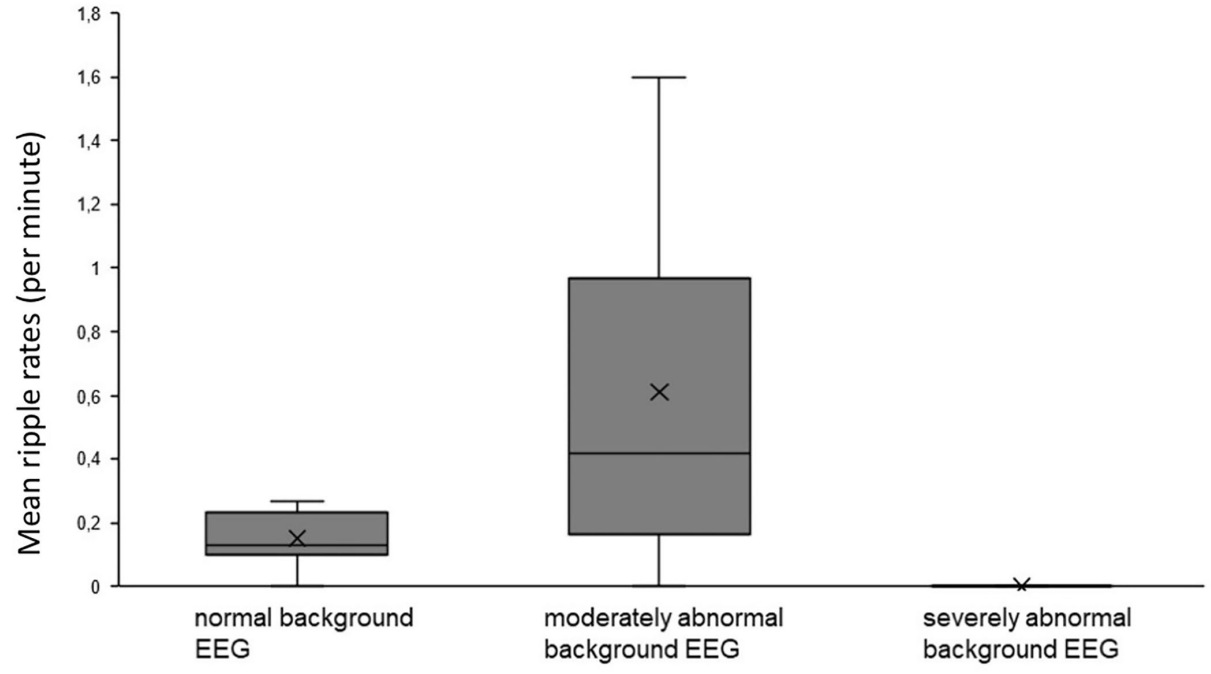

FIGURE 4
No significant difference in HFO rates was seen in patients with abnormal background activity compared to those with normal background activity.

might become visible, which usually do not prevent the clinical analysis of the EEG data. In our case, most prominently continuous high-frequency noise was a result of a separate aEEG machine being concurrently used during EEG recording. Unfortunately, due to the retrospective design of this study, this problem could not be addressed, resulting in a relatively low number of neonates that could be included. Future studies might benefit from the use of combined EEG–aEEG machines as well

as low-noise amplifiers that have been proven to increase the visibility of HFO in intracranial EEG (25).

HFO analysis in scalp EEG cannot be performed automatically, as designed detectors are vulnerable to high noise artifacts and have low specificity (13). For this reason, all HFO markings in this study were performed visually by two reviewers. Only events, which were identified by both, were taken into the analysis. At all times, events that co-occurred with artifacts in the unfiltered EEG were excluded, as suggested by Andrade-Valenca and coauthors (10). This might have led to the exclusion of some real HFO events and explain the lower rate of HFO found in the present study compared with other pediatrics studies (26, 27). Even if the EEG sampling rate would have allowed us to look at frequencies above 250 Hz, we limited our analysis to the ripple frequency range as this has been most often described on scalp EEG (4, 28).

Using a higher density of electrodes has shown to be more sensitive to detecting HFOs (23, 29). However, in the neonatal population, this may come with certain disadvantages, such as the risk of breakage of the fragile neonatal skin. We utilized eight electrodes in two of our patients, while the rest had a set of 18 electrodes for EEG acquisition. However, there was no significant difference in HFO detection between these two groups. Therefore, following the standard of practice, which is to utilize a reduced neonatal montage in scalp EEG acquisition, will likely have no major impact on HFO detection.

In our study, we included all consecutive patients within a 2-year period who underwent continuous EEG monitoring in a NICU setting. The clinical spectrum of disease varied largely, including patients with genetic and structural reasons for developing seizures. No difference in the rate of HFO occurrence was found in different etiological subgroups, mainly between the asphyxia and non-asphyxia groups, which, if replicated in larger studies, may suggest that HFOs are a ubiquitous marker for pathological or epileptic brain activity rather than specific for certain pathology. This is in line with intracranial EEG data recorded from different types of lesions as well as scalp EEG data recorded in epileptic encephalopathies with varying underlying diseases (30–33). A much larger cohort of neonates should be studied to understand under which circumstances HFOs occur in the neonatal brain.

It is also worth mentioning that various central nervous system medications including anti-seizure medications as well as therapeutic hypothermia itself can alter the HFO rates (34). In our patient population, EEG was initiated in all, upon clinical suspicion and before starting anti-seizure medication. However, the potential effect of concomitant sedative medication and therapeutic hypothermia on HFO rates cannot be excluded. It would be useful to further evaluate the impact of concurrent therapies on HFO rates in larger cohorts with etiological heterogeneity.

The main finding of the present study is that the neonatal brain is capable of generating discrete HFOs. The mechanisms of HFO generation are still not completely understood; it has been hypothesized that epileptic HFOs mainly reflect principal cell action potentials in which pathological synchronization of fast-firing interconnected neurons leads to the formation of high-frequency population spikes (35). This mechanism requires a relatively complex neuronal network, which seems to be already in place within the first 4 weeks of life. Simultaneous intracranial and scalp EEG are the strongest proof of the visibility of HFOs on scalp EEG but are ofcourse limited to patients with refractory epilepsy (11, 21). The high skull conductivity of children might increase the visibility of scalp HFOs in the younger population (26). Some prior studies have suggested that HFOs most often are seen in scalp EEG and also show many interictal epileptic spikes (36). In the current study, epileptic spikes were less frequent than have been reported in older pediatric children with seizures (37, 38). In the current study, the observed HFOs were not co-occurring with epileptic spikes as has been described in other age groups. Data in adults suggest that up to 50% of scalp HFOs occur during spikes; the generation of both is not necessarily linked (36). Detailed analyses suggest that HFOs often precede spikes, though not consistently, supporting a hypothesis that there are independent underlying mechanisms for these phenomena (39). This seems to be even more the case in neonates, for whom spikes are not epileptiform (40, 41).

Neonatal brain injury is often associated with acute seizures; seizure burden is associated with long-term outcomes (42, 43). Up to 20% of affected neonates develop chronic epilepsy (15). A reliable non-invasive biomarker for epileptic activity in the neonatal brain would be useful. A previous study has demonstrated that the presence of HFOs can predict the development of epilepsy in older children presenting with their first seizure (44). This study is not able to make a similar inference; however, it shows that HFOs can be identified in neonates and may be associated with pathologic brain activity. Future studies are needed to investigate larger groups of healthy neonates as well as those with different underlying pathologies to further clarify the significance of HFOs in these patients.

Data availability statement

The original contributions presented in the study are included in the article/supplementary material, further inquiries can be directed to the corresponding author.

Author contributions

All authors listed have made a substantial, direct, and intellectual contribution to the work and approved it for publication.

Acknowledgments

The authors wish to thank Ms. Betty Cobb for her assistance in obtaining the digital EEG data.

Conflict of interest

JJ and NK were supported by a grant JAC855/11 of the Forschungskommission, University of Freiburg.

The remaining authors declare that the research was conducted in the absence of any commercial or financial relationships that could be construed as a potential conflict of interest.

Publisher's note

References

1. Chrobak JJ, Lörincz A, Buzsáki G. Physiological patterns in the hippocampo-entorhinal cortex system. *Hippocampus.* (2000) 10:457–65. doi: 10.1002/1098-1063(2000)10:4<457::AID-HIPO12>3.0.CO;2-Z

2. Axmacher N, Elger CE, Fell J. Ripples in the medial temporal lobe are relevant for human memory consolidation. *Brain.* (2008) 131:1806–17. doi: 10.1093/brain/awn103

3. Chrobak JJ, Buzsáki G. High-Frequency oscillations in the output networks of the hippocampal–entorhinal axis of the freely behaving rat. *J Neurosci.* (1996) 16:3056–66. doi: 10.1523/JNEUROSCI.16-09-03056.1996

4. Frauscher B, Bartolomei F, Kobayashi K, Cimbalnik J, van't Klooster MA, Rampp S, et al. High-frequency oscillations: the state of clinical research. *Epilepsia.* (2017) 58:1316–29. doi: 10.1111/epi.13829

5. Akiyama T, McCoy B, Go CY, Ochi A, Elliott IM, Akiyama M, et al. Focal resection of fast ripples on extraoperative intracranial EEG improves seizure outcome in pediatric epilepsy. *Epilepsia.* (2011) 52:1802–11. doi: 10.1111/j.1528-1167.2011.03199.x

6. Jacobs J, Zijlmans M, Zelmann R, Chatillon CÉ, Hall J, Olivier A, et al. High-frequency electroencephalographic oscillations correlate with outcome of epilepsy surgery. *Ann Neurol.* (2010) 67:209–20. doi: 10.1002/ana.21847

7. Zijlmans M, Jacobs J, Zelmann R, Dubeau F, Gotman J. High-frequency oscillations mirror disease activity in patients with epilepsy. *Neurology.* (2009) 72:979–86. doi: 10.1212/01.wnl.0000344402.20334.81

8. Kerber K, LeVan P, Dümpelmann M, Fauser S, Korinthenberg R, Schulze-Bonhage A, et al. High frequency oscillations mirror disease activity in patients with focal cortical dysplasia. *Epilepsia.* (2013) 54:1428–36. doi: 10.1111/epi.12262

9. Bragin A, Mody I, Wilson CL, Engel J. Local generation of fast ripples in epileptic brain. *J Neurosci.* (2002) 22:2012–21. doi: 10.1523/JNEUROSCI.22-05-02012.2002

10. Andrade-Valenca LP, Dubeau F, Mari F, Zelmann R, Gotman J. Interictal scalp fast oscillations as a marker of the seizure onset zone. *Neurology.* (2011) 77:524–31. doi: 10.1212/WNL.0b013e318228bee2

11. Kuhnke N, Klus C, Dümpelmann M, Schulze-Bonhage A, Jacobs J. Simultaneously recorded intracranial and scalp high frequency oscillations help identify patients with poor postsurgical seizure outcome. *Clin Neurophysiol.* (2019) 130:128–37. doi: 10.1016/j.clinph.2018.10.016

12. Kobayashi K, Akiyama T, Oka M, Endoh F, Yoshinaga H. A storm of fast (40-150Hz) oscillations during hypsarrhythmia in west syndrome. *Ann Neurol.* (2015) 77:58–67. doi: 10.1002/ana.24299

13. von Ellenrieder N, Beltrachini L, Perucca P, Gotman J. Size of cortical generators of epileptic interictal events and visibility on scalp EEG. *NeuroImage.* (2014) 94:47–54. doi: 10.1016/j.neuroimage.2014.02.032

14. Mooij AH, Raijmann RCMA, Jansen FE, Braun KPJ, Zijlmans M. Physiological ripples (± 100 Hz) in spike-free scalp EEGs of children with and without epilepsy. *Brain Topogr.* (2017) 30:739–46. doi: 10.1007/s10548-017-0590-y

15. Pisani F, Facini C, Pavlidis E, Spagnoli C, Boylan G. Epilepsy after neonatal seizures: literature review. *Euro J Paediatr Neurol.* (2015) 19:6–14. doi: 10.1016/j.ejpn.2014.10.001

16. Inoue T, Shimizu M, Hamano S, Murakami N, Nagai T, Sakuta R. Epilepsy and west syndrome in neonates with hypoxic-ischemic encephalopathy. *Pediatr Int.* (2014) 56:369–72. doi: 10.1111/ped.12257

17. Vasudevan C, Levene M. Epidemiology and aetiology of neonatal seizures. *Semin Fetal Neonatal Med.* (2013) 18:185–91. doi: 10.1016/j.siny.2013.05.008

18. Ellingson RJ, Peters JF. Development of EEG and daytime sleep patterns in normal full-term infants during the first 3 months of life: longitudinal observations. *Electroencephalogr Clin Neurophysiol.* (1980) 49:112–24. doi: 10.1016/0013-4694(80)90357-0

19. Noorlag L, van't Klooster MA, van Huffelen AC, van Klink NEC, Benders MJNL, de Vries LS, et al. High-frequency oscillations recorded with surface EEG in neonates with seizures. *Clin Neurophysiol.* (2021) 132:1452–61. doi: 10.1016/j.clinph.2021.02.400

20. Mooij AH, Frauscher B, Goemans SAM, Huiskamp GJM, Braun KPJ, Zijlmans M. Ripples in scalp EEGs of children: co-occurrence with sleep-specific transients and occurrence across sleep stages. *Sleep.* (2018) 41:zsy169. doi: 10.1093/sleep/zsy169

21. Zelmann R, Zijlmans M, Jacobs J, Châtillon Claude E, Gotman J. Improving the identification of high frequency oscillations. *Clin Neurophysiol.* (2009) 120:1457–64. doi: 10.1016/j.clinph.2009.05.029

22. Sarnat HB. Neonatal encephalopathy following fetal distress. *Arch Neurol.* (1976) 33:696. doi: 10.1001/archneur.1976.00500100030012

23. Kuhnke N, Schwind J, Dümpelmann M, Mader M, Schulze-Bonhage A, Jacobs J. High frequency oscillations in the ripple band (80–250 Hz) in scalp EEG: higher density of electrodes allows for better localization of the seizure onset zone. *Brain Topogr.* (2018) 31:1059–72. doi: 10.1007/s10548-018-0658-3

24. Shellhaas RA, Chang T, Tsuchida T, Scher MS, Riviello JJ, Abend NS, et al. The american clinical neurophysiology society's guideline on continuous electroencephalography monitoring in neonates. *J Clin Neurophysiol.* (2011) 28:611–7. doi: 10.1097/WNP.0b013e31823e96d7

25. Fedele T, Ramantani G, Burnos S, Hilfiker P, Curio G, Grunwald T, et al. Prediction of seizure outcome improved by fast ripples detected in low-noise intraoperative corticogram. *Clin Neurophysiol.* (2017) 128:1220–6. doi: 10.1016/j.clinph.2017.03.038

26. Wu JY, Koh S, Sankar R, Mathern GW. Paroxysmal fast activity: an interictal scalp EEG marker of epileptogenesis in children. *Epilepsy Res.* (2008) 82:99–106. doi: 10.1016/j.eplepsyres.2008.07.010

27. Kobayashi K, Watanabe Y, Inoue T, Oka M, Yoshinaga H, Ohtsuka Y. Scalp-recorded high-frequency oscillations in childhood sleep-induced electrical status epilepticus. *Epilepsia.* (2010) 51:2190–4. doi: 10.1111/j.1528-1167.2010.02565.x

28. Thomschewski A, Hincapié AS, Frauscher B. Localization of the epileptogenic zone using high frequency oscillations. *Front Neurol.* (2019) 10:94. doi: 10.3389/fneur.2019.00094

29. Zelmann R, Lina JM, Schulze-Bonhage A, Gotman J, Jacobs J. Scalp EEG is not a blur: it can see high frequency oscillations although their generators are small. *Brain Topogr.* (2014) 27:683–704. doi: 10.1007/s10548-013-0321-y

30. Jacobs J, LeVan P, Châtillon CÉ, Olivier A, Dubeau F, Gotman J. High frequency oscillations in intracranial EEGs mark epileptogenicity rather than lesion type. *Brain.* (2009) 132:1022–37. doi: 10.1093/brain/awn351

31. Kobayashi K, Yoshinaga H, Toda Y, Inoue T, Oka M, Ohtsuka Y. High-frequency oscillations in idiopathic partial epilepsy of childhood. *Epilepsia.* (2011) 52:1812–9. doi: 10.1111/j.1528-1167.2011.03169.x

32. Qian P, Li H, Xue J, Yang Z. Scalp-recorded high-frequency oscillations in atypical benign partial epilepsy. *Clin Neurophysiol.* (2016) 127:3306–13. doi: 10.1016/j.clinph.2016.07.013

33. Chaitanya G, Sinha S, Narayanan M, Satishchandra P. Scalp high frequency oscillations (HFOs) in absence epilepsy: an independent component analysis (ICA) based approach. *Epilepsy Res.* (2015) 115:133–40. doi: 10.1016/j.eplepsyres.2015.06.008

34. Jacobs J, Zijlmans M. HFO to measure seizure propensity and improve prognostication in patients with epilepsy. *Epilepsy Curr.* (2020) 20:338–47. doi: 10.1177/1535759720957308

35. Jiruska P, Alvarado-Rojas C, Schevon CA, Staba R, Stacey W, Wendling F, et al. Update on the mechanisms and roles of high-frequency oscillations in seizures and epileptic disorders. *Epilepsia.* (2017) 58:1330–9. doi: 10.1111/epi.13830

36. Melani F, Zelmann R, Dubeau F, Gotman J. Occurrence of scalp-fast oscillations among patients with different spiking rate and their role as epileptogenicity marker. *Epilepsy Res.* (2013) 106:345–56. doi: 10.1016/j.eplepsyres.2013.06.003

37. Alshafai L, Ochi A, Go C, McCoy B, Hawkins C, Otsubo H, et al. Clinical, EEG, MRI, MEG, and surgical outcomes of pediatric epilepsy with astrocytic inclusions versus focal cortical dysplasia. *Epilepsia.* (2014) 55:1568–75. doi: 10.1111/epi.12756

38. van Klink NEC, van't Klooster MA, Leijten FSS, Jacobs J, Braun KPJ, Zijlmans M. Ripples on rolandic spikes: a marker of epilepsy severity. *Epilepsia.* (2016) 57:1179–1189. doi: 10.1111/epi.13423

39. van Klink N, Frauscher B, Zijlmans M, Gotman J. Relationships between interictal epileptic spikes and ripples in surface EEG. *Clin Neurophysiol.* (2016) 127:143–9. doi: 10.1016/j.clinph.2015.04.059

40. Patrizi S, Holmes GL, Orzalesi M, Allemand F. Neonatal seizures: characteristics of EEG ictal activity in preterm and fullterm infants. *Brain Dev.* (2003) 25:427–37. doi: 10.1016/S0387-7604(03)00031-7

41. Ohmori I, Ohtsuka Y, Oka E, Akiyama T, Ohtahara S. Electroclinical study of localization-related epilepsies in early infancy. *Pediatr Neurol.* (1997) 16:131–6. doi: 10.1016/S0887-8994(96)00296-2

42. Glass HC, Glidden D, Jeremy RJ, Barkovich AJ, Ferriero DM, Miller SP. Clinical neonatal seizures are independently associated with outcome in infants at risk for hypoxic-ischemic brain injury. *J Pediatr.* (2009) 155:318–23. doi: 10.1016/j.jpeds.2009.03.040

43. Annegers JF, Hauser WA, Lee JRJ, Rocca WA. Incidence of acute symptomatic seizures in Rochester, Minnesota, 1935-1984. *Epilepsia.* (1995) 36:327–33. doi: 10.1111/j.1528-1157.1995.tb01005.x

44. Klotz KA, Sag Y, Schönberger J, Jacobs J. Scalp ripples can predict development of epilepsy after first unprovoked seizure in childhood. *Ann Neurol.* (2020) 89:134–142. doi: 10.1002/ana.25939

frontiers | Frontiers in Neurology

TYPE Original Research
PUBLISHED 09 January 2023
DOI 10.3389/fneur.2022.1030019

OPEN ACCESS

EDITED BY
Wael M. Y. Mohamed,
International Islamic University Malaysia, Malaysia

REVIEWED BY
Alessandro Martorana,
University of Rome Tor Vergata, Italy
Mona Goli,
Texas Tech University, United States

*CORRESPONDENCE
Jing Gao
✉ gj107@163.com

SPECIALTY SECTION
This article was submitted to Neurological Biomarkers, a section of the journal Frontiers in Neurology

RECEIVED 28 August 2022
ACCEPTED 21 December 2022
PUBLISHED 09 January 2023

CITATION
Lei D, Mao C, Li J, Huang X, Sha L, Liu C, Dong L, Xu Q and Gao J (2023) CSF biomarkers for early-onset Alzheimer's disease in Chinese population from PUMCH dementia cohort. *Front. Neurol.* 13:1030019. doi: 10.3389/fneur.2022.1030019

CSF biomarkers for early-onset Alzheimer's disease in Chinese population from PUMCH dementia cohort

Dan Lei[1], Chenhui Mao[1], Jie Li[1], Xinying Huang[1], Longze Sha[2], Caiyan Liu[1], Liling Dong[1], Qi Xu[2] and Jing Gao[1]*

[1]State Key Laboratory of Complex Severe and Rare Diseases, Department of Neurology, Peking Union Medical College Hospital, Chinese Academy of Medical Science and Peking Union Medical College, Beijing, China, [2]State Key Laboratory of Medical Molecular Biology, Institute of Basic Medical Sciences and Neuroscience Center, Chinese Academy of Medical Sciences and Peking Union Medical College, Beijing, China

Introduction: Alzheimer's disease (AD) is one of the highly concerned degenerative disorders in recent decades. Though vast amount of researches has been done in various aspects, early-onset subtype, however, needs more investigation in diagnosis for its atypical manifestations and progression process. Fundamental CSF biomarkers of early-onset AD are explored in PUMCH dementia cohort to depict its laboratory characteristics.

Materials and methods: A total of 125 individuals (age of onset <65 years old) from PUMCH dementia cohort were recruited consecutively and classified into AD, non-AD dementia, and control groups. Levels of amyloid-β 42 (Aβ42), total tau (t-tau) and phosphorylated tau (p-tau) were measured using ELISA INNOTEST (Fujirebio, Ghent, Belgium). Students' *t*-test or non-parametric test are used to evaluate the differences between groups. Area under curve (AUC) of receiver operating characteristic (ROC) curve was introduced to prove the diagnostic powers of corresponding markers. Logistic regression is used to establish diagnostic model to combine several markers together to promote the diagnostic power.

Results: The average of all three biomarkers and two calculated ratios (t-tau/Aβ42, p-tau/Aβ42) were statistically different in the AD group compared with the other two groups (*Ps* < 0.01). From our data, we were able to provide cutoff values (Aβ42 < 570.9 pg/mL; p-tau > 56.49 pg/mL; t-tau > 241.6 pg/mL; t-tau/Aβ42 > 0.529; p-tau/Aβ42 > 0.0846) with acceptable diagnostic accuracy compared to other studies. Using a combination of biomarkers and logistic regression (area under curve 0.951), we were able to further improve diagnostic efficacy.

Discussion: Our study supports the diagnostic usefulness of biomarkers and defined cutoff values to diagnose early-onset AD. We showed that the ratios of t-tau/Aβ42 and p-tau/Aβ42 are more sensitive than relying on Aβ42 levels alone, and that we can further improve diagnostic accuracy by combining biomarkers.

KEYWORDS

early-onset, Alzheimer's disease, CSF biomarkers, cutoff value, combination

1. Introduction

Early diagnosis of Alzheimer's disease (AD) helps patients receive the treatment and support they need. Screening for amyloid-β 42 (Aβ42), total-tau (t-tau), and phosphorylated-tau (p-tau) in CSF has shown promise in detecting AD (1). Combined with official criteria for diagnosing AD, CSF profiles improve diagnostic accuracy (2–8). However, high variability within and between different populations impedes development of an international standard (9). In particular, China possesses over 1/5 of the world's population, and over 10 million AD patients, but few well-accepted studies have looked at these biomarkers of early-onset AD sub-group. Therefore, we conducted our own study to explore characteristics and estimate cutoff values for these biomarkers specific to patients under the age of 65, the early-onset sub-type of AD.

Early-onset AD differs from late-onset AD in both clinical manifestations and pathological patterns, and its diagnosis is often delayed (10). A substantial percentage of early-onset AD patients have various phenotypes—including logopenic progressive aphasia, frontal lobe variant, cortical basal syndrome, and posterior cortical atrophy (11, 12)—uncharacteristic of typical AD; these patients are frequently misdiagnosed (13). Furthermore, early-onset AD is associated with atrophy in the parietal cortex as opposed to the temporal lobe and hippocampus seen in late-onset AD (14, 15). Nevertheless, both forms of AD show similar CSF profiles: low levels of Aβ42, elevated t-tau and p-tau (16).

As apparently emphasized in the framework of National Institute on Aging and Alzheimer's Association (NIA-AA) in 2018, no universal cut-off value can be applied throughout the world, a reliable cut-off value is urgent for our scientific research and clinical practice. By studying this, we hope to improve early diagnosis for those with atypical symptoms of early-onset AD for our following research and enrich the biomarker database.

2. Materials and methods

2.1. Standard protocol approvals, registrations and patient consents

All patients gave written informed consent and all procedures were undertaken with the approval of the institutional review board of Peking Union Medical College Hospital (No. ZS2009).

2.2. Participants

A total of 201 patients who visited the Neurological Department at Peking Union Medical College Hospital (PUMCH) in Beijing between October 2017 and December 2018 were enrolled in our PUMCH dementia cohort. Of these, 171 patients had presented to the Memory and Leukoencephalopathy Clinic with cognitive or functional impairment, and 30 patients had no cognitive problems but needed diagnostic lumbar puncture from the ward. The inclusion and exclusion criteria are detailed in Figure 1. Since we were interested in studying biomarkers of early-onset AD, we included only those patients who were younger than 65 when their symptoms manifested (n = 139/201; 69.2%). AD (n = 52/139; 37.4%) was diagnosed using the 2011 NIA-AA AD criteria (3). Other categories of dementia (n = 53; 38.1%) were defined using the Diagnostic and Statistical Manual of Mental Disorders, 5th Edition (DSM-V) (17) (for more details see Table 1). The non-dementia control group (n = 20; 14.4%) included patients with Mini-Mental State Examination (MMSE) scores above 26 who showed no cerebral anomaly based on imaging or objective cognitive disturbance on neuropsychological examination. Patients with prion diseases (n = 7), cancer metastasis (n = 4), or rapidly progressive dementia (n = 3) were excluded from this analysis, leaving a sample size of 125 participants.

2.3. Neuropsychological assessment and CSF sampling

All participants were systematically evaluated by two or more well-trained neurologists for diagnosis and follow-up. Enrolled patients were assessed using the MMSE, Montreal Cognitive Assessment (MoCA), Activities of Daily Living (ADL), Hospital Anxiety and Depression scale (HADs), and systemic cognitive assessments covering at least four functional domains, including but not limited to memory, visuospatial, language, and executive abilities (18). Brain MRI (T1, T2 FLAIR, DWI, ADC, and T2*) was routinely assessed. Patients underwent lumbar puncture (LP) within 1 month of their cognitive and MRI assessments (19), with full informed consent. All CSF samples were collected in low protein binding tubes (Eppendorf Protein LoBind Tube, 1.5 mL; Hamburg, Germany) and centrifuged at 1,800 g for 10 min at 4°C. The supernatant was transferred to a new tube and stored at −80°C (20). Commercially-available ELISA kits were used to measure CSF t-tau, p-tau, and Aβ42 [INNOTEST hTAU Ag, PHOSPHO-TAU and β-AMYLOID (1–42); Fujirebio, Ghent, Belgium] in batch within 2 weeks of sampling. All diagnoses were made without any knowledge of CSF protein levels. All individuals were followed-up every 3–6 months until the end of the study.

2.4. Internal quality control

Since measurement procedures or different batches of ELISA kits may introduce bias, we routinely ran quality control on our

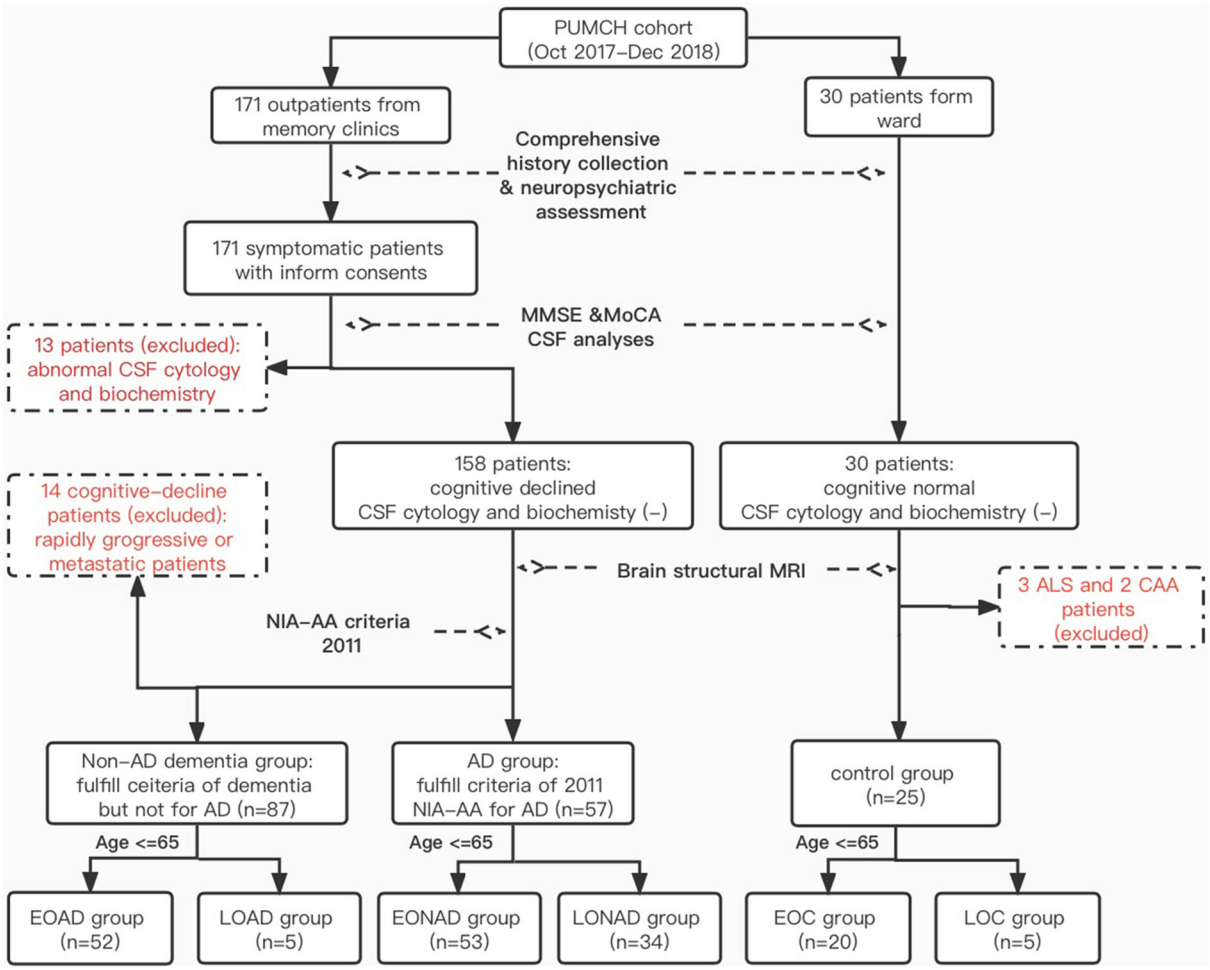

FIGURE 1
Inclusion and exclusion criteria. *PUMCH, Peking Union Medical Collage Hospital; NIA-AA, National Institute on Aging and Alzheimer's Association; MMSE, Mini-Mental State Examination; MoCA, Montreal Cognitive Assessment; EO(LO)AD, early-onset (late-onset) Alzheimer's disease; EO(LO)NAD, early-onset (later-onset) non-Alzheimer dementia; EO(LO)C, early-onset (late-onset) control; ALS, amyotrophic lateral sclerosis; CAA, cerebral amyloid angiopathy.

CSF samples. Five randomly chosen samples from our previous work were remeasured using new kits and reagents, directly from the stored low protein binding tubes every 6 months. We also recently remeasured all samples to check for internal bias. No statistically significant differences were found between the new and old biomarker levels (paired t-test, $P > 0.05$). Of note, at the beginning of our study, we were using normal tubes to store the CSF samples. However, we later switched to low protein binding tubes. We tested five randomly-selected patients and found no significant difference in the levels detected in the two different types of tubes (Students' t-test, $P > 0.05$).

2.5. Statistical analysis

In addition to the three original biomarkers, we tested two ratios, t-tau/Aβ42 and p-tau/Aβ42. The normality of the continuous variables was tested using the Shapiro-Wilk test, which showed that the biomarker distributions were not Gaussian in non-AD and control groups. Analyses of the means between any two groups were conducted using non-parametric tests. Receiver operating characteristic (ROC) curves were depicted for every single item, and area under the curve (AUC) was used to describe diagnostic efficacy. As reported in other studies, combining two or more biomarkers can improve diagnostic efficacy (21, 22). Binary logistic regression was used for biomarker combination diagnosis to magnify the accuracy (23). Factor R, constructed from logistic regression, was used for the diagnostic analysis with the other five items. Cutoff values calculated from ROC curves were chosen based on maximum Youden index (YI, sensitivity + specificity-1) (24). Data analyses and figure creation were conducted using SPSS statistics 23.0 (IBM Corporation, Armonk, New York, US) and Graphpad Prism 5.0 (GraphPad Software. Inc, San Diego,

TABLE 1 Demographic data and biomarker characteristics.

	AD group	Non-AD dementia	Control
Number (M)	52 (20)	53 (28)	20 (10)
Subcategory (*n*)	AD possible (26) AD probable (26)	NPH (9) FTLD (14) Leukoencephalopathy (9) VaD (3) CBD (2) 2° to schizophrenia (2) Other unclarified (14)	MS (4) PN (4) Spinal focal lesion (3) Meningitis (2) Autoimmune (2) Depression (1) Other undiagnosed (6)
Age	57.83 [56.04, 59.61]	53.38* [51.09, 55.66]	47.50* [40.53, 54.47]
MMSE	10.91 [8.73, 13.1]	16.9* [14.4, 19.4]	27.75$^{\gamma}$ [25.04, 30.46]
Aβ42 (pg/mL)	474.3 [441.6, 506.9]	619.2* [558.5, 679.9]	624.6* [512.2, 736.9]
T-Tau (pg/mL)	685.3 [558.6, 812.0]	182.2† [139.4, 224.9]	168.1† [88.52, 255.7]
P-Tau (pg/mL)	86.34 [75.22, 97.45]	39.65† [34.40, 44.91]	34.07† [26.42, 41.73]
T-Tau/Aβ42	1.52 [1.19, 1.85]	0.346† [0.245, 0.447]	1.247† [−0.841, 3.335]
P-tau/Aβ42	0.196 [0.165, 0.227]	0.0766† [0.0618, 0.0915]	0.153† [−0.0525, 0.358]

Data are described as "Mean [95% confidence interval]," except individuals' number "Number (males);" MMSE, Mini-Mental State Examination; NPH, normal pressure hydrocephalus; FTLD, frontotemporal lobe dementia; CBD, corticobasal degeneration; MS, multiple sclerosis; PN, peripheral neuropathy.
*$p < 0.01$ or †$p < 0.0001$, respectively, compared with AD group.

California, US). Any difference with $P < 0.05$ was regarded as significant.

3. Results

3.1. Demographic characteristics and CSF biomarker levels

Demographic characteristics and CSF biomarker levels of participants are shown in detail in Table 1. We found a significant decrease in Aβ42, and a significant increase in t-tau, p-tau, t-tau/Aβ42 and p-tau/Aβ42, in the AD group compared with both the non-AD and control groups (*Ps* < 0.01, Table 1). Differences were detected in age and MMSE across the different groups (Students' *t*-test, $P < 0.01$). To exclude the potential connection between age, cognitive function, and biomarker levels, correlation analyses were performed. However, we found no relationship between age and biomarker levels, nor MMSE scores and biomarker levels (*Ps* > 0.05, see Table 1). Thus, all five items were considered as reliable and predictable for early-onset AD diagnosis. These differences are displayed graphically in Figure 2.

As reported in previous studies, we found that Aβ42 levels were reduced in AD patients compared with the other two groups, while the levels of the other biomarkers were greatly elevated. All biomarkers other than Aβ42 could be used to differentiate AD with $P < 0.0001$, which supports the diagnostic efficacy later reported in Section 3.3. To identify any outliers, we graphed the results in box plots with the whiskers representing the 10–90% interval (Figure 2). Of note, there was a patient in the control group diagnosed with peripheral neuropathy who had an Aβ42 level of 11.92 pg/mL (confirmed by retest), far lower than the average concentration of 621.3 pg/mL. Because of this outlier Aβ value, the corresponding t-tau/Aβ42 exceeded 20 and p-tau/Aβ42 reached 2.01, both of which are located beyond the upper limits, and thus are not displayed in Figures 2D, E.

3.2. Biomarker combination analysis

Since CSF protein levels are continuous variables, relying on a single cutoff value based on statistics is usually insufficient to define a physical or pathological change. We wanted to test whether combining all five biomarkers would mitigate this issue and improve diagnostic efficacy and accuracy. Biomarkers were combined using a statistical tool called binary logistic regression to generate a new value, "factor R," which represents the predicting possibility, and was used to avoid the "yes" or "no" issues of single cutoff values. The combination function for differentiating the early-onset subgroup was defined as:

$$R = \frac{e^{logit\,(g)}}{1 + e^{logit\,(g)}}$$

i. For AD/non-AD:
$Logit\,(g) = Logit\,(g1) = 0.1950.01 \times A\beta 42 + 0.017 \times t - tau + 0.058 \times p - tau - 5.498 \times t - tau/A\beta 42$
ii. For AD/control:
$Logit\,(g) = Logit\,(g2) = 20.130.095 \times A\beta 420.037 \times t - tau + 1.287 \times p - tau + 38.52 \times t - tau/A\beta 42411.05 \times p - tau/A\beta 42$

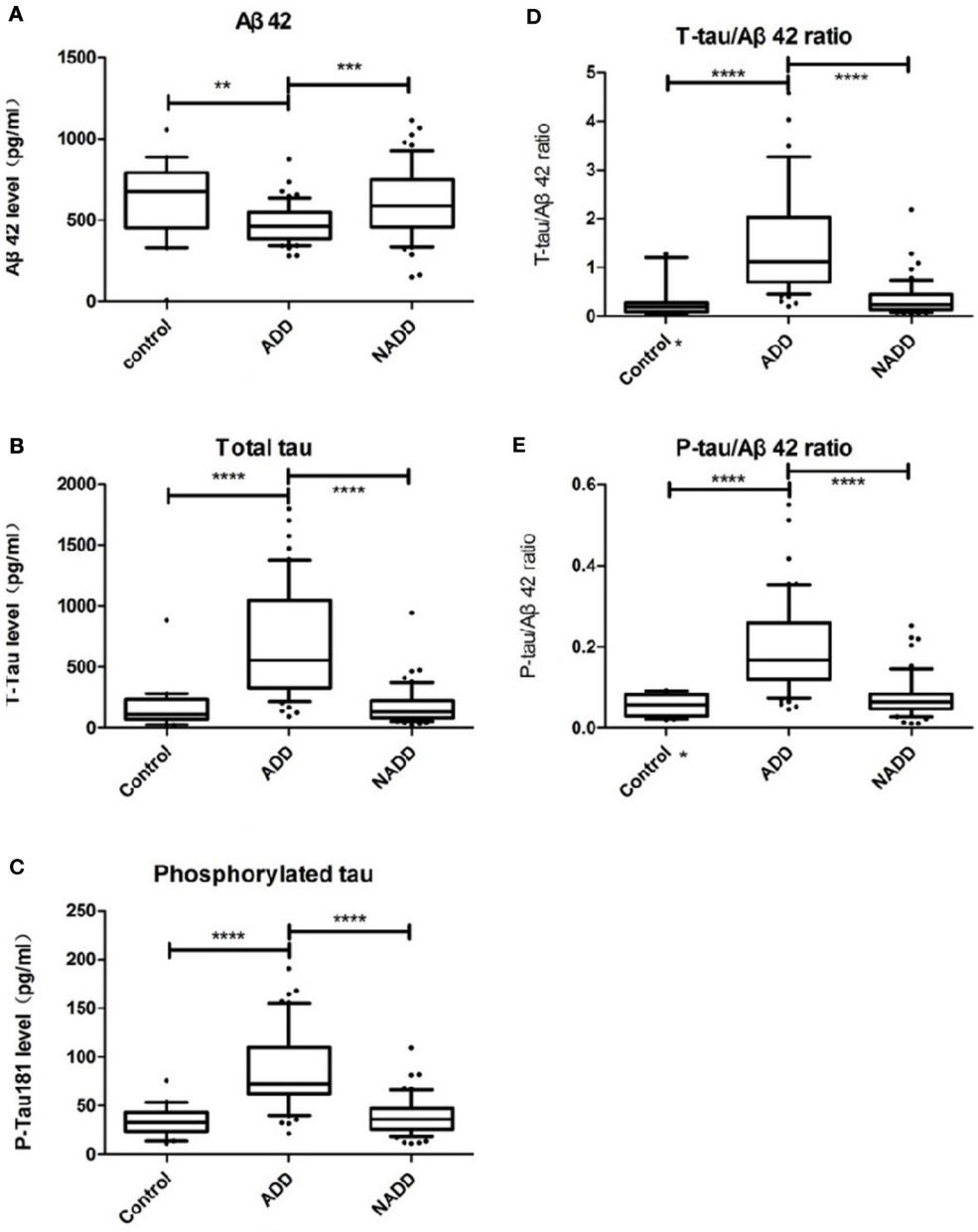

FIGURE 2
Comparison of CSF biomarker levels across groups. **(A–E)** Display Aβ42, t-tau, p-tau, t-tau/Aβ42, p-tau/Aβ42 distributions of the three groups respectively. Box plots present median and interquartile range and whiskers indicate 10–90% interval. In graph **(D, E)** asterisk markers (*) on X axis indicate that there is an outlier value beyond the upper limit. ADD, AD dementia; NADD, non-AD dementia. $^{**}P < 0.01$; $^{***}P < 0.001$; $^{****}P < 0.0001$, between the two groups linked.

R infers predicting value based on logistic regression. Variables include *Aβ42, t-tau, p-tau, t-tau/Aβ42, p-tau/Aβ42*. R was handled as a new biomarker for every individual, and was used, along with the original biomarkers, to estimate the diagnostic accuracy and corresponding cutoff values, in Section 3.3.

3.3. ROC curves and cutoff values

To compare and contrast the results, ROC curves for the five biomarkers and factor R are drawn together in Figure 3. The diagnostic efficacy, estimated as AUC (25), is labeled in the legend in the lower right quadrant. AUCs and

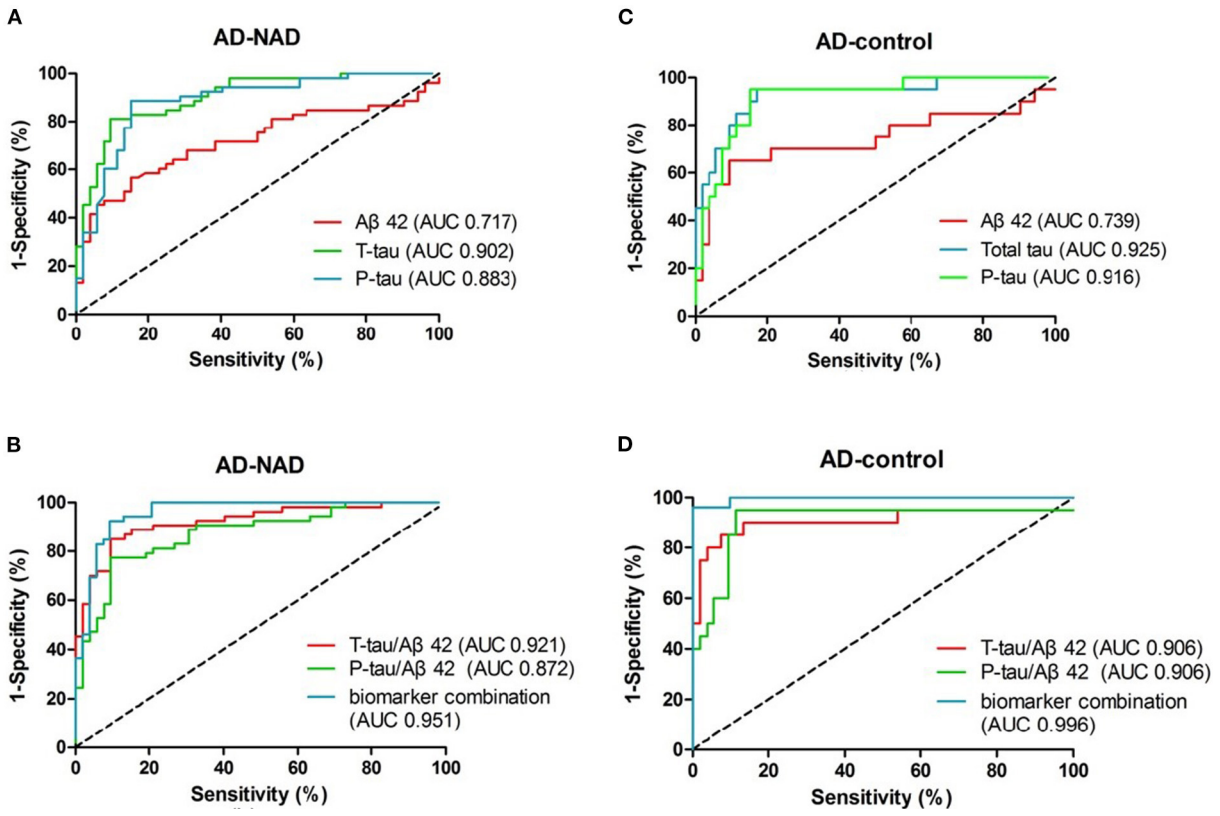

FIGURE 3
ROC curves of CSF biomarkers in the early-onset group. **(A, C)** depict curves of the original biomarkers. **(B, D)** Display the curves of the calculated ratios and the generated predicting factor, respectively. Diagnostic accuracy, the area under the curve (AUC), is labeled in the legend.

their corresponding 95% CIs are described in Table 2. Their corresponding CVs are found in Table 3. To meet the need of optimal clinical use, the CVs reported have highest YI, which means the maximum sensitivity plus specificity. As predicted, we found that the diagnostic efficacy of factor R was higher than the diagnostic efficacies of each of the biomarkers alone [AUC AD vs. non-AD: 0.951, 95% CI (0.911, 0.991); AUC AD vs. control: 0.996, 95% CI (0.988, 1.00)] (Table 2). The second best performer for differentially diagnosing dementia was the t-tau/Aβ42 ratio [AUC AD vs. non-AD: 0.921, 95% CI (0.869, 0.973)], and for distinguishing AD from controls, t-tau [AUC AD vs. control: 0.925, 95% CI (0.852, 0.998)]. According to current guidelines, lumbar puncture and CSF analyses are indicated only for complicated dementia cases; in these cases, based on their maximum YI index, we recommend the following cutoff values for the five measured biomarkers: Aβ42 < 570.9 pg/mL, t-tau > 241.6 pg/mL, p-tau > 56.49 pg/mL, t-tau/Aβ42 ratio > 0.529, and p-tau/Aβ ratio > 0.08465 (Table 3). We found that a cutoff value of 0.4117 for factor R had a higher diagnostic accuracy than each of the five biomarkers alone, with a sensitivity of 86.5 and 100%, and a specificity of 92.4 and 96.2%, for AD vs. non-AD and AD vs. controls, respectively (Table 3).

4. Discussion

Aβ42, both in AD–non-AD differentiation and AD–control differentiation, had relatively low AUC in our study. This low distinguishing power may be due to the wide range of Aβ42 levels (Figure 2) that related to unstability of molecular adhesion. Nevertheless, the other five items were found to have higher diagnostic efficacy than Aβ42 and show promise for use in the clinic. We found that total tau and phosphorylated tau levels distinguished the AD group from the control group best, whereas the best biomarker to distinguish the AD group from the non-AD group was the t-tau/Aβ42 ratio; decreased Aβ42 with increased tau seems specific for AD dementia in degenerative disorders. The predicting factor R, constructed by combining biomarkers, helped to improve the best-individual AUC to 0.951 and 0.996 for AD-non-AD and AD-control groups, respectively. This pattern of data processing may

TABLE 2 AUCs and corresponding 95% CIs.

	AD vs. NAD		AD vs. control	
	AUC	95% CI	AUC	95% CI
Aβ42	0.717	[0.616, 0.818]	0.739	[0.582, 0.896]
T-Tau	0.902	[0.845, 0.960]	0.925	[0.852, 0.998]
^{181}P-Tau	0.883	[0.816, 0.949]	0.916	[0.846, 0.987]
T-tau/Aβ42	0.921	[0.869, 0.973]	0.906	[0.799, 1.013]
^{181}P-tau/Aβ42	0.872	[0.804, 0.940]	0.906	[0.806, 1.006]
R	0.951	[0.911, 0.991]	0.996	[0.988, 1.00]

AD, Alzheimer's disease group; NAD, non-Alzheimer's disease group; R, predicting factor from logistic regression; AUC, area under curve; CI, confidence interval.

TABLE 3 Cutoff values and corresponding sensitivity/specificity.

	AD vs. NAD		AD vs. control	
	CV	SE%, SP%	CV	SE%, SP%
Aβ42 (pg/mL)	<570.9	56.6, 84.6	<620.8	65.0, 90.4
T-Tau (pg/mL)	>241.6	81.1, 90.4	>286.8	82.7, 95.0
^{181}P-Tau (pg/mL)	>56.49	88.7, 84.6	>55.32	84.6, 95.0
T-Tau/Aβ42	>0.5290	84.9, 90.4	>0.4140	92.3, 85.0
^{181}P-tau/ Aβ42	>0.08465	77.4, 90.4	>0.09536	88.5, 95.0
R	>0.4117	86.5, 92.4	>0.2464	100, 96.2

CV, cutoff value; SE%, SP%, sensitivity%, specificity%; AD, Alzheimer's disease group; NAD, non-Alzheimer's disease group; R, predicting factor from logistic regression.

provide a new tool for risk evaluation, with improved prediction capability as more risk factors are revealed.

4.1. Demographic and biomarker differences

Early-onset AD has a different pathological distribution than late-onset AD, which makes it confusing in clinical practice (10, 12). CSF biomarkers were found to reflect Aβ and tau pathophysiology consistently among different clinical subtypes. According to the outcomes of our analyses, CSF biomarkers could help in the differential diagnosis of early-onset types of dementia. We demonstrated that the original CSF biomarker levels of Aβ42, t-tau, and p-tau differed significantly between AD and the other two groups tested. Age and MMSE scores did not contribute to the change in CSF biomarker levels (see Section 3.1), which makes it more likely that changes in biomarker levels are disease-specific rather than aging or cognitive status-related at the time, which differs from previous results (26). In some other studies, t-tau was proposed to reflect the neurodegenerative or cognitive stage, and could be used to predict disease process in AD (1, 2). While still controversial, another study reported a similar conclusion to ours (27). This variation may be due to heterogeneity in how tau protein levels change during disease progression. Our future work will investigate the correlation between biomarker protein levels and individual characteristics, such as age, sex, and cognitive function status, in a larger sample population.

4.2. Diagnostic accuracy of biomarkers and biomarker combination

Aβ42 reduction is regarded as the earliest criteria in CSF diagnostic profiles (2, 4, 24). However, in our study as well as others, Aβ42 was found to have low diagnostic accuracy. Under our defined CV condition, Aβ42 provided a sensitivity of only 0.55–0.65, but a specificity of 0.84–0.91, meaning it can reliably exclude non-AD patients with normal Aβ42 levels, but fails to detect all patients with AD. This phenomenon may be due to multiple cleavage points in the amyloid protein precursor, which produces different beta-amyloid proteins with various biological functions (28). Another potential cause of Aβ42 diversity is systemic or measurement bias. Measurements of CSF biomarker levels are sensitive to changes in the environment. To reduce the influence of internal and external laboratory differences, we complied with a proposed standard (9). Moreover, we retested all samples in this study and demonstrated that there was no significant bias in measurement either due to analytic

performance or long-term storage. Whether the low diagnostic efficacy of Aβ42 is specific to early-onset AD is still unknown.

We found that tau protein, which reflects the destruction of neurons, was more reliable for AD diagnosis, with an AUC around 0.9. We speculate that this may be due to our exclusion of some definite non-AD dementia samples with extremely high t-tau levels, like Creutzfeldt-Jakob disease. For example, some patients with prion disease had t-tau levels over 1,000 pg/mL. Unlike degenerative disorders, these excluded diseases manifest with rapid cognitive decline and can be screened using many other well-developed clinical tests. The tau protein levels in patients with these diseases approaches the average levels seen in AD groups in some other studies (20, 29). This was the reason we revised the exclusion criteria to exclude these diseases. In some basic studies of the etiology and pathology of AD, p-tau correlated well with the neurofibrillary tangles in involved cerebral domains. Hyperphosphorylation of tau protein was once believed to drive tangle formation (30). Very little evidence from our work supports this, as p-tau was not superior in diagnostic accuracy (AUC and YI) compared with t-tau. One explanation is that p-tau in neurofibrillary tangles does not escape into CSF, which means that p-tau in CSF does not reflect the substantial p-tau burden in the brain. New positron-emission tomography/CT tracers for p-tau could be used to test this hypothesis in the future (31).

Biomarker combination, like some other established predicting functions, is often more accurate than using the original biomarkers (21, 22, 32). In our study we found that the t-tau/Aβ42 ratio, with an AUC of 0.92, is excellent at differentially diagnosing dementia. This can be explained using mathematics theory which says that the ratio expands when the numerator increases and the denominator decreases. The difference between the ratios in each group therefore broadens giving a better definition of an optimal cutoff value. However, this ratio was not more useful at screening AD patients from control patients, compared with total tau alone. We speculate that elevated tau plus decreased Aβ42 is somehow specific to AD or other degenerative disorders, rather than non-degenerative neurological diseases. Changes to Aβ42 and tau levels vary differently in those non-degenerative diseases, which makes the ratio less effective in this field. Unexpectedly, we found that combining biomarkers and their ratios further into a logistic regression generated factor R increased the AUCs to a range over 0.95. This higher diagnostic accuracy means that this predicting function can be used as an alternative to the original biomarker CVs and diagnostic decision trees (20). We believe that factor R could help us confidently predict the diagnostic possibility of a patient with borderline biomarker levels.

4.3. Limitations

Our study has several limitations. First, our sample sizes for the non-AD and the non-cognitive disturbance group were small. The non-AD group was composed of various diseases, with limited numbers of each type, as described in Section 2.2. Intrinsic variances of biomarker levels from different dementias distort the biomarker distributions from a normal Gaussian distribution, which introduces bias into the analysis of non-AD dementia. Some extreme conditions, like Creutzfeldt-Jakob disease and brain metastasis, that show greatly elevated t-tau levels (over 1,000 pg/mL), were excluded from the non-AD group of our analysis to reduce this bias. Second, the diagnoses we made were all clinically based, and lacked conclusive postmortem autopsy evidence, which may have introduced diagnostic errors. Third, patients visiting our center are more severely cognitively impaired. Thus, the cognitive decline in our AD group was more severe than the other groups, and even than that in some other studies (20, 29). The main purpose of our study was to detect early-stage AD; thus, patients with relatively mild cognitive impairment will need to be studied next.

5. Conclusion

In conclusion, the biomarkers we investigated, Aβ42, total-tau, p-tau, and the t-tau/Aβ42, p-tau/Aβ42 ratios, can be used to differentiate AD dementia from other types of degenerated dementia patients, in early-onset subgroups. The functions we constructed raised the prediction accuracy of the biomarkers to even higher levels, highlighting the importance of combining biomarkers. Our cutoff values, based on a Chinese population from PUMCH dementia cohort, were similar to previous reports (22, 29, 32). Clinical practice with biomarker cutoff values would improve early diagnosis. As far as we know, we are the first to report on these biomarkers in the exclusive Chinese population. Thus, our work not only expands on a novel tool for clinical AD diagnosis in our center, and it may become part of the reference data standard for CSF biomarker diagnosis of AD worldwide. Our future work will focus on increasing recruitment from our clinics to create a more representative dataset, thereby reducing bias and error.

Data availability statement

The raw data supporting the conclusions of this article will be made available by the authors, without undue reservation.

Ethics statement

The studies involving human participants were reviewed and approved by Institutional Review Board of the Peking Union Medical College Hospital (No. ZS2009). The patients/participants provided their written informed consent to participate in this study.

Author contributions

DL performed the data analyses, samples collection, and wrote the manuscript. CM helped perform the analysis with constructive discussions. LS performed samples storage and ELISA analyses. XH, JL, CL, and LD helped to perform cognitive and systematic assessment. QX possessed the sample storage and basic science laboratory. JG contributing to the conception, construction, and fund of this whole study. All authors contributed to the article and approved the submitted version.

Funding

This work was supported by the National Key Research and Development Program (Grant Nos. 2020YFA0804500 and 2020YFA0804501), CAMS Innovation Fund for Medical Sciences (Grant Nos. 2020-I2M-C&T-B-010 and 2021-I2M-1-020), and the National Natural Science Foundation of China (Grant Nos. 81550021 and 30470618).

Acknowledgments

We thank Mrs. Shanshan Chu and Wei Jin for their great effort in participant recruitment, as well as information collection and recording work.

Conflict of interest

The authors declare that the research was conducted in the absence of any commercial or financial relationships that could be construed as a potential conflict of interest.

Publisher's note

References

1. Ruan Q, D'Onofrio G, Sancarlo D, Greco A, Yu Z. Potential fluid biomarkers for pathological brain changes in Alzheimer's disease: implication for the screening of cognitive frailty. *Mol Med Rep.* (2016) 14:3184–98. doi: 10.3892/mmr.2016.5618

2. Jack CR Jr, Bennett DA, Blennow K, Carrillo MC, Dunn B, Haeberlein SB, et al. NIA-AA research framework: toward a biological definition of Alzheimer's disease. *Alzheimers Dement.* (2018) 14:535–62. doi: 10.1016/j.jalz.2018.02.018

3. McKhann GM, Knopman DS, Chertkow H, Hyman BT, Jack CR Jr, Kawas CH, et al. The diagnosis of dementia due to Alzheimer's disease: recommendations from the national institute on aging-Alzheimer's association workgroups on diagnostic guidelines for Alzheimer's disease. *Alzheimers Dement.* (2011) 7:263–9. doi: 10.1016/j.jalz.2011.03.005

4. Dubois B, Feldman HH, Jacova C, Hampel H, Molinuevo JL, Blennow K, et al. Advancing research diagnostic criteria for Alzheimer's disease: the IWG-2 criteria. *Lancet Neurol.* (2014) 13:614–29. doi: 10.1016/S1474-4422(14)70090-0

5. Dubois B, Feldman HH, Jacova C, DeKosky ST, Barberger-Gateau P, Cummings J, et al. Research criteria for the diagnosis of Alzheimer's disease: revising the NINCDS–ADRDA criteria. *Lancet Neurol.* (2007) 6:734–46. doi: 10.1016/S1474-4422(07)70178-3

6. Maddalena A, Papassotiropoulos A, Müller-Tillmanns B, Jung HH, Hegi T, Nitsch RM, et al. Biochemical diagnosis of Alzheimer disease by measuring the cerebrospinal fluid ratio of phosphorylated tau protein to β-amyloid peptide42. *Arch Neurol.* (2003) 60:1202–6. doi: 10.1001/archneur.60.9.1202

7. Wiltfang J, Esselmann H, Bibl M, Hüll M, Hampel H, Kessler H, et al. Neurochemical diagnosis of Alzheimer's dementia by CSF Aβ42, Aβ42/Aβ40 ratio and total tau. *Neurobiol Aging.* (2004) 25:273–81. doi: 10.1016/S0197-4580(03)00086-1

8. Li G, Sokal I, Quinn JF, Leverenz JB, Brodey M, Schellenberg GD, et al. CSF tau/A 42 ratio for increased risk of mild cognitive impairment: a follow-up study. *Neurology.* (2007) 69:631–9. doi: 10.1212/01.wnl.0000267428.62582.aa

9. Mattsson N, Andreasson U, Persson S, Carrillo MC, Collins S, Chalbot S, et al. CSF biomarker variability in the Alzheimer's association quality control program. *Alzheimers Dement.* (2013) 9:251–61. doi: 10.1016/j.jalz.2013.05.401

10. Mendez MF. Early-Onset Alzheimer disease. *Neurol Clin.* (2017) 35:263–81. doi: 10.1016/j.ncl.2017.01.005

11. Koedam ELGE, Lauffer V, Van Der Vlies AE, Van Der Flier WM, Scheltens P, Pijnenburg YAL. Early-versus late-onset Alzheimer's disease: more than age alone. *J Alzheimers Dis.* (2010) 19:1401–8. doi: 10.3233/JAD-2010-1337

12. Mendez MF. Early-onset Alzheimer's disease: nonamnestic subtypes and type 2 AD. *Arch Med Res.* (2012) 43:677–85. doi: 10.1016/j.arcmed.2012.11.009

13. Snowden JS, Thompson JC, Stopford CL, Richardson AM, Gerhard A, Neary D, et al. The clinical diagnosis of early-onset dementias: diagnostic accuracy and clinicopathological relationships. *Brain.* (2011) 134:2478–92. doi: 10.1093/brain/awr189

14. Hamelin L, Bertoux M, Bottlaender M, Corne H, Lagarde J, Hahn V, et al. Sulcal morphology as a new imaging marker for the diagnosis of early onset Alzheimer's disease. *Neurobiol Aging.* (2015) 36:2932–9. doi: 10.1016/j.neurobiolaging.2015.04.019

15. Chiaravalloti A, Koch G, Toniolo S, Belli L, Di Lorenzo F, Gaudenzi S, et al. Comparison between early-onset and late-onset Alzheimer's disease patients with amnestic presentation: CSF and 18F-FDG PET study. *Dement Geriatr Cogn Dis Extra.* (2016) 6:108–19. doi: 10.1159/000441776

16. Peng G, Wang J, Feng Z, Liu P, Zhang Y, He F, et al. Clinical and neuroimaging differences between posterior cortical atrophy and typical amnestic Alzheimer's disease patients at an early disease stage. *Sci Rep.* (2016) 6:29372. doi: 10.1038/srep29372

17. American Psychiatric Association. *Diagnostic and Statistical Manual of Mental Disorders.* 5th edition. Arlington, VA: American Psychiatric Association (2013). doi: 10.1176/appi.books.9780890425596

18. Mortamais M, Ash JA, Harrison J, Kaye J, Kramer J, Randolph C, et al. Detecting cognitive changes in preclinical Alzheimer's disease: a review of its feasibility. *Alzheimers Dement.* (2017) 13:468–92. doi: 10.1016/j.jalz.2016.06.2365

19. Campo Md, Mollenhauer B, Bertolotto A, Engelborghs S, Hampel H, Simonsen AH, et al. Recommendations to standardize preanalytical confounding factors in Alzheimer's and Parkinson's disease cerebrospinal fluid biomarkers: an update. *Biomark Med.* (2012) 6:419–30. doi: 10.2217/bmm.12.46

20. Mofrad RB, Schoonenboom NS, Tijms BM, Scheltens P, Visser PJ, van der Flier WM, et al. Decision tree supports the interpretation of CSF biomarkers in Alzheimer's disease. *Alzheimers Dement.* (2019) 11:1–9. doi: 10.1016/j.dadm.2018.10.004

21. Schoonenboom NSM, Reesink FE, Verwey NA, Kester MI, Teunissen CE, van de Ven PM, et al. Cerebrospinal fluid markers for differential dementia diagnosis in a large memory clinic cohort. *Neurology*. (2012) 78:47–54. doi: 10.1212/WNL.0b013e31823ed0f0

22. Mattsson N, Zetterberg H, Hansson O, Andreasen N, Parnetti L, Jonsson M, et al. CSF biomarkers and incipient Alzheimer disease in patients with mild cognitive impairment. *JAMA*. (2009) 302:385–93. doi: 10.1001/jama.2009.1064

23. Shi M, Tang L, Toledo JB, Ginghina C, Wang H, Aro P, et al. Cerebrospinal fluid α-synuclein contributes to the differential diagnosis of Alzheimer's disease. *Alzheimers Dement.* (2018) 14:1052–62. doi: 10.1016/j.jalz.2018.02.015

24. Seeburger JL, Holder DJ, Combrinck M, Joachim C, Laterza O, Tanen M, et al. Cerebrospinal fluid biomarkers distinguish postmortem-confirmed Alzheimer's disease from other dementias and healthy controls in the OPTIMA cohort. *J Alzheimers Dis.* (2015) 44:525–39. doi: 10.3233/JAD-141725

25. Eusebi P. Diagnostic accuracy measures. *Cerebrovasc Dis.* (2013) 36:267–72. doi: 10.1159/000353863

26. Shoji M, Kanai M, Matsubara E, Tomidokoro Y, Shizuka M, Ikeda Y, et al. The levels of cerebrospinal fluid Abeta40 and Abeta42(43) are regulated age-dependently. *Neurobiol Aging*. (2001) 22:209–15. doi: 10.1016/S0197-4580(00)00229-3

27. Clark CM, Xie S, Chittams J, Ewbank D, Peskind E, Galasko D, et al. Cerebrospinal fluid tau and β-amyloid: how well do these biomarkers reflect autopsy-confirmed dementia diagnoses? *Arch Neurol.* (2003) 60:1696–702. doi: 10.1001/archneur.60.12.1696

28. Sinha S, Lieberburg I. Cellular mechanisms of beta-amyloid production and secretion. *Proc Natl Acad Sci USA*. (1999) 96:11049–53. doi: 10.1073/pnas.96.20.11049

29. Park SA, Chae WS, Kim HJ, Shin HS, Kim S, Im JY, et al. cerebrospinal fluid biomarkers for the diagnosis of Alzheimer disease in South Korea. *Alzheimer Dis Assoc Disord.* (2017) 31:13–8. doi: 10.1097/WAD.0000000000000184

30. Duyckaerts C, Delatour B, Potier M-C. Classification and basic pathology of Alzheimer disease. *Acta Neuropathol.* (2009) 118:5–36. doi: 10.1007/s00401-009-0532-1

31. Molinuevo JL, Ayton S, Batrla R, Bednar MM, Bittner T, Cummings J, et al. Current state of Alzheimer's fluid biomarkers. *Acta Neuropathol.* (2018) 136:821–53. doi: 10.1007/s00401-018-1932-x

32. Duits FH, Teunissen CE, Bouwman FH, Visser P-J, Mattsson N, Zetterberg H, et al. The cerebrospinal fluid "Alzheimer profile": easily said, but what does it mean? *Alzheimers Dement.* (2014) 10:713–23.e2. doi: 10.1016/j.jalz.2013.12.023

frontiers | Frontiers in Neurology

TYPE Original Research
PUBLISHED 12 January 2023
DOI 10.3389/fneur.2022.1099391

OPEN ACCESS

EDITED BY
Wael M. Y. Mohamed,
International Islamic University Malaysia, Malaysia

REVIEWED BY
Budbazar Enkhjargal,
Boston University, United States
Liang Wen,
Zhejiang University, China

*CORRESPONDENCE
Yaqiang Li
✉ 1227351538@qq.com

†These authors have contributed equally to this work

SPECIALTY SECTION
This article was submitted to Neurological Biomarkers, a section of the journal Frontiers in Neurology

RECEIVED 15 November 2022
ACCEPTED 28 December 2022
PUBLISHED 12 January 2023

CITATION
Sun Z, Li Y, Chang F and Jiang K (2023) Utility of serum amyloid A as a potential prognostic biomarker of aneurysmal subarachnoid hemorrhage.
Front. Neurol. 13:1099391.
doi: 10.3389/fneur.2022.1099391

Utility of serum amyloid A as a potential prognostic biomarker of aneurysmal subarachnoid hemorrhage

Zhongbo Sun[1†], Yaqiang Li[1,2*†], Fu Chang[1] and Ke Jiang[1]

[1]Department of Neurosurgery, First Affiliated Hospital of Anhui University of Science and Technology (First People's Hospital of Huainan), Huainan, China, [2]Department of Neurology, People's Hospital of Lixin County, Bozhou, China

Objectives: Inflammation plays a vital role in the aneurysmal subarachnoid hemorrhage (aSAH), while serum amyloid A (SAA) has been identified as an inflammatory biomarker. The present study aimed to elucidate the relationship between SAA concentrations and prognosis in aSAH.

Methods: From prospective analyses of patients admitted to our department between March 2016 and August 2022, aSAH patients with complete medical records were evaluated. Meanwhile, the healthy control group consisted of the age and sex matched individuals who came to our hospital for healthy examination between March 2018 and August 2022. SAA level was measured by enzyme-linked immunosorbent assay kit (Invitrogen Corp). The Glasgow Outcome Scale (GOS) was used to classify patients into good (GOS score of 4 or 5) and poor (GOS score of 1, 2, or 3) outcome.

Results: 456 patients were enrolled in the study, thereinto, 200 (43.86%) patients had a poor prognosis at the 3-months follow-up. Indeed, the SAA of poor outcome group were significantly increased compared to good outcome group and healthy control group [36.44 (32.23–41.00) vs. 28.99 (14.67–34.12) and 5.64 (3.43–7.45), $P < 0.001$]. In multivariate analyses, SAA served for independently predicting the poor outcome after aICH at 3 months [OR:1.129 (95% CI, 1.081–1.177), $P < 0.001$]. After adjusting the underlying confounding factors, the odds ratio (OR) of depression after aSAH was 2.247 (95% CI: 1.095–4.604, $P = 0.021$) for the highest tertile of SAA relative to the lowest tertile. With an AUC of 0.807 (95% CI, 0.623–0.747), SAA demonstrated an obviously better discriminatory ability relative to CRP, WBC, and IL-6. SAA as an indicator for predicting poor outcome after aSAH had an optimal cut-off value of 30.28, and the sensitivity and specificity were 61.9 and 78.7%, respectively.

Conclusions: Elevated level of SAA was associated with poor outcome at 3 months, suggesting that SAA might be a useful inflammatory markers to predict prognosis after aSAH.

KEYWORDS

inflammation, aneurysmal subarachnoid hemorrhage, aSAH, serum amyloid A, SAA

1. Introduction

Aneurysmal subarachnoid hemorrhage (aSAH) is a serious life-threatening acute cerebrovascular disease that severely damages the patient's central nervous system and has pathophysiological effects on several organs of the body (1, 2). The mortality rate of aSAH patients is reported to be about 33%, and at least 20% of survivors have poor long-term functional outcomes. Additionally, the 3-month mortality rate of aSAH patients is as high as 47–49%, and most of the survivors still have serious sequelae, which seriously affect the quality of survival (3, 4). Clinically, Hunt and Hess (HH) scale and Modified Fisher (MF) score are mostly used to predict the prognosis of aSAH at an early stage, but this approach is highly subjective and there are cases in which the HH and MF score are high at the time of admission, but the prognosis is good. Therefore, relying on only these approaches to estimate the prognosis of patients with aSAH remains limited.

Although the pathophysiological mechanisms of early brain injury after aSAH are complex, inflammation has been shown to develop in early stages sufficient to be involved in early brain injury after aSAH (5–7). Accumulating studies have shown that inflammatory biomarkers have drawn the attention of clinicians and can be used to assess the severity of aSAH and reflect prognosis (3, 8, 9). Serum amyloid A (SAA) is a apolipoprotein that is presented in the high-density lipoprotein (HDL) fraction of serum and is responsible for the chemotactic recruitment of inflammatory cells to sites of inflammation (10). It is also mainly synthesized by hepatocytes and plays a very important role in the diagnosis of acute and chronic inflammation as a widely used non-specific inflammatory marker in clinical practice. Notably, the concentration of SAA was significantly increased in the blood and liver of traumatic brain injury mice in the early stages (11). Elevated SAA concentrations in peripheral blood have been reported in adult patients suffering from traumatic brain injury and severe polytrauma (12). In addition, a recent study revealed that elevated serum SAA concentrations, which were strongly associated with inflammation and hemorrhagic severity, were independently associated with mortality and poor outcomes after intracerebral hemorrhage (ICH) (13). Other studies have found that an increased SAA is significantly correlated with inflammatory conditions, including atherosclerosis, post-stroke cognitive impairment, and myocardial infarction (14–16).

By now, few studies have focused on SAA as a prognostic marker of neurological outcome, and no study has suggested a cutoff SAA for predicting poor outcome in patients with aSAH. Therefore, the study aimed at investigating the relationship between SAA and poor outcome in patients with aSAH, as well as further establishing a cutoff SAA value as a prognostic marker for assessing functional outcome in aSAH patients.

2. Materials and methods

2.1. Subjects

The present analysis was conducted as a component of a larger study that aimed to investigate clinical outcome in aneurysmal subarachnoid hemorrhage (aSAH) using a 3-month naturalistic prospective design. Patients with aSAH were consecutively enrolled from the First Affiliated Hospital of Anhui University of Science and Technology (First People's Hospital of Huainan) from March 2016 to August 2022, within 24 h after the onset of aSAH. Patients diagnosed with aSAH through the following were included: subarachnoid hemorrhage diagnosed by head computed tomography, and an aneurysm confirmed with digital subtraction angiography (DSA) or computed tomography angiography (CTA). Patients were not included if they: (1) had aneurysms caused by trauma, arteriovenous malformations or other causes; (2) had no SAA and CRP data. (3) had a history of cerebrovascular disease and brain tumors. (4) had a combination of infectious diseases, immune dysfunction, hematological diseases, or severe organ function impairment. (5) had refused to undergo surgical treatment. (6) had severe renal or liver diseases. At last, the study included 456 cases with aSAH in total (Figure 1). This study has obtained the approval of the institutional ethics review board of the participating center, and obtained all participants' written informed consent following the Helsinki Declaration of 1975. Meanwhile, the healthy control group consisted of the age and sex matched individuals who came to our hospital for healthy examination between March 2018 and August 2022. Controls (180 healthy individuals) were composed of 90 males and 90 females, as well as their mean value was 66.19 y (range, 35–75 y; SD, 8.43 y) at age.

All patients were treated according to guidelines for the management of aSAH, including prevention and management of rebleeding, vasospasm, and other complications (17). Determining the treatment of aneurysm, in the judgment of an experienced neurosurgeon, should be a comprehensive decision based on the characteristics of the patient and the aneurysm. All patients undergo oral or intravenous pumping of nimodipine to prevent vasospasm. Intracranial hypertension was treated with head elevation, mannitol injection and cerebrospinal fluid drainage, such as extraventricular or lumbar drainage. Antibiotherapy was only initiated when systemic clinical and biological criteria indicate the presence of a bacterial infection, for example, pneumonia, urinary tract infection, or bloodstream infection. Bacteriological sampling was performed at this time point and treatment was adjusted once results were obtained.

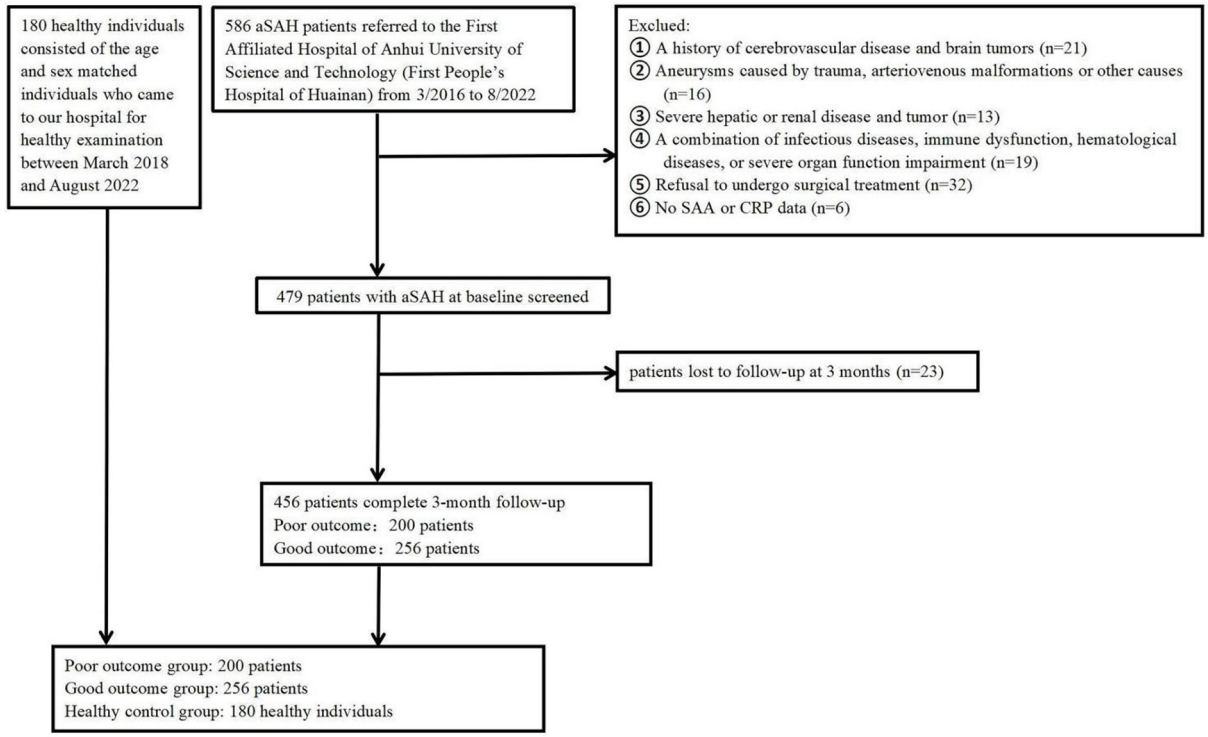

FIGURE 1
Flowchart of participant selection. aSAH, Aneurysmal subarachnoid hemorrhage; SAA, serum amyloid A; CRP, C-reactive protein.

2.2. Data collection and assessment

We collected the sociodemographic and clinical characteristics regarding aSAH patients on admission, such as the age, gender, marital status, vascular risk factor (hypertension, diabetes mellitus, current smoking, alcohol consumption), diameter and location of aneurysm, operation of aneurysm (clip and coil), and adopted a standard case report form. The Hunt and Hess (HH) grade and World Federation of Neurosurgical Societies Scale served for assessing the clinical severity for all aSAH patients at the time of emergency department admission. Non-severe SAH is classified as HH grade I-III, and severe SAH is qualified as HH grade IV or V. The World Federation of Neurosurgical Societies Scale (WFNS 1–5) was used to classify patients into good (WFNS 1–2) and poor (WFNS 3–5) clinical status. The severity of the hemorrhage was determined using the modified fisher score. The primary outcome of interest was prognostic within 3 months following emergency department admission. Patients' clinical outcomes were determined by telephone interviews or clinical visits after 3 months of hemorrhage, using the Glasgow Outcome Scale (GOS). The GOS was used to dichotomize the patients in good (GOS score of 4 or 5) and poor (GOS score of 1, 2, or 3) outcome.

2.3. Blood collection and laboratory test

Blood samples were collected from peripheral veins within 30 min of arrival at the emergency department. The routine laboratory methods were conducted to measure serum glucose (G), hemoglobin (Hb), white blood cell count (WBC), platelet (Plt) count, C-reactive protein (CRP), total cholesterol (TC), triglycerides (TG), high density lipoprotein cholesterol (HDL-C), low density lipoprotein-cholesterol (LDL-C), apolipoprotein A (ApoA), and apolipoprotein B (ApoB). A sandwich enzyme-linked immunosorbent assay kit (BMS213-2, Invitrogen Corp, USA) served for measuring the IL-6. The SAA level was measured by enzyme-linked immunosorbent assay kit (EHSAA1, Invitrogen Corp, USA) and the operation was carried out strictly in accordance with the manufacturer's instructions. For the purpose of minimizing assay variation, professional clinical technicians who did not know the clinical outcomes or neuroimaging findings took charge of analyzing all samples in duplicate on the same day randomly.

2.4. Statistical analysis

SPSS 23.0 statistical software SPSS (Inc., Chicago, IL, USA) served for the statistical analyses. Data for continuous variables

TABLE 1 Clinical and demographic characteristics of the samples under study.

Variables	Total ($n = 456$)	3-month functional outcome		Healthy controls ($n = 180$)	*P*-value
		Poor outcome ($n = 200$)	Good outcome ($n = 256$)		
Demographic characteristics					
Gender, male, *n* (%)	208 (45.61)	86 (43)	122 (47.66)	90 (50)	0.373
Age, years, mean ± SD	65.96 ± 8.26	66.31 ± 7.98	65.53 ± 8.58	66.19 ± 8.43	0.556
Vascular risk factors (%)					
Hypertension	294 (64.47)	134 (67)	160 (62.5)		0.319
Diabetes mellitus	143 (31.36)	61 (30.5)	82 (32.03)		0.727
Current smoking	144 (31.58)	69 (34.5)	75 (29.30)		0.236
Alcohol consumption	135 (29.61)	62 (31)	73 (28.52)		0.564
Laboratory findings (IQR)					
WBC, $\times 10^9$/L, median (IQR)	6.79 (5.68–8.25)	7.15 (5.83–8.64)	6.53 (5.61–7.80)		0.004
CRP, mg/L, median (IQR)	7.56 (5.97–11.77)	10.86 (6.99–15.00)	6.45 (5.63–8.85)		<0.001
IL−6, ng/L, median (IQR)	5.3 (4.60–8.18)	5.3 (4.9–8.2)	5.1 (4.3–7.88)		0.007
Plt, $\times 10^9$/L, median (IQR)	213 (174–247)	206 (173–246)	217 (176–247)		0.271
TG, mmol/L, median (IQR)	1.37 (0.96–1.99)	1.31 (0.92–2.02)	1.38 (0.97–1.93)		0.860
TC, mmol/L, median (IQR)	4.45 (3.76–5.27)	4.46 (3.76–5.05)	4.48 (3.75–5.51)		0.446
Glucose, mmol/L, median (IQR)	5.31 (4.76–6.89)	5.15 (4.70–6.70)	5.40 (4.80–6.90)		0.152
RBC, $\times 10^{12}$/L, median (IQR)	4.76 (4.51–5.22)	4.78 (4.51–5.21)	4.83 (4.52–5.25)		0.530
Hb, g/L, median (IQR)	139 (132–144)	138 (131–144)	140 (134–145)		0.098
HDL–C, mmol/L, median (IQR)	1.03 (0.86–1.24)	1.01 (0.83–1.17)	1.04 (0.86–1.30)		0.061
LDL–C, mmol/L, median (IQR)	2.52 (1.97–3.18)	2.45 (1.87–3.06)	2.56 (1.99–3.22)		0.076
ApoA, g/L, median (IQR)	1.25 (1.11–1.47)	1.26 (1.10–1.45)	1.28 (1.12–1.48)		0.362
ApoB, g/L, median (IQR)	0.87 (0.68–1.04)	0.85 (0.69–1.00)	0.87 (0.70–1.03)		0.425
Serum amyloid A, mg/L, median (IQR)	32.99 (26.53–37.44)	36.44 (32.23–41.00)[a]	28.99 (14.67–34.12)[b]	5.64 (3.43–7.45)	<0.001
Hunt and hess grade, *n* (%)					
I–II	315 (69.08)	151 (75.5)	164 (64.06)		0.009
III–V	141 (30.92)	91 (45.5)	50 (19.53)		<0.001
Modified fisher scale, *n* (%)					
I–II	147 (32.23)	84 (42.20)	73 (28.52)		0.042
III–IV	309 (67.76)	159 (79.5)	150 (58.59)		<0.001
Operation of aneurysm, *n* (%)					0.781
Clip	87 (19.08)	37 (18.5)	50 (19.53)		
Coil	369 (80.92)	163 (81.5)	206 (80.47)		
Aneurysm location, *n* (%)					0.128
Anterior circulation	408 (89.47)	174 (87)	234 (91.41)		
Posterior circulation	48 (10.53)	26 (13)	22 (8.59)		
Size of aneurysm, mm, mean (SD)	4.8 (4.5–5.8)	4.8 (4.5–5.9)	4.8 (4.4–5.5)		0.448

(Continued)

TABLE 1 (Continued)

Variables	Total ($n = 456$)	3-month functional outcome		Healthy controls ($n = 180$)	*P*-value
		Poor outcome ($n = 200$)	Good outcome ($n = 256$)		
WFNS score on admission, median (IQR)	2 (2–3)	2 (2–4)	2 (2–3)		0.002
Systolic arterial pressure, mmHg, mean (SD)	138 (130–149)	141 (130–150)	136 (130–148)		0.194
Diastolic arterial pressure, mmHg, mean (SD)	91 (89–100)	94 (90–101)	90 (89–100)		0.219
Acute hydrocephalus, *n* (%)	30 (6.58)	10 (5)	20 (7.81)		0.229
Intraventricular hemorrhage, *n* (%)	32 (7.02)	14 (7)	18 (7.03)		0.990
Seizure, *n* (%)	45 (9.87)	20 (10)	25 (9.77)		0.934
Infection, *n* (%)	144 (31.58)	76 (38)	68 (26.56)		0.009

[a] $P < 0.001$ compared to good outcome.
[b] $P < 0.001$ compared to healthy control.

were in the form of mean ± standard deviation (SD) or median (interquartile range), which was decided by whether the tested data presented normal or non-normal distribution.The Kolmogorovor Smirnov test or Shapiro-Wilk test was used to investigate the normality of the data distribution. Chi-square assisted in evaluating categorical variables. In the case of conducting abnormal distribution test on the continuous variables, the Kruskal-Wallis test and Mann-Whitney U test served for comparing the difference among three groups and that between two groups, respectively. Student's *t*-test or one-way analysis of variance (ANOVA) served for analyzing the normally distributed continuous variables. We included the variables with $p < 0.5$ confirmed by the univariate analysis into the final multivariable analysis. The relationship between serum SAA concentrations and poor clinical outcome was assessed with a binary logistic regression analysis. Bivariate correlations were analyzed with Pearson or Spearman rank correlation analyses. The admission SAA was taken into account for dividing patients into tertiles (Q1 ≤ 29.23, Q2 29.33–35.44, Q3 ≥ 35.54). We applied three models for the multivariable regression analyses, for recognizing the factors that could predict the poor clinical outcome, with model 1 targeting age and sex; model 2 targeting model 1 as well as vascular risk factors; model 3 targeting variables with $P < 0.05$ confirmed by the univariate analysis (WBC, hunt and hess grade, modified fisher scale, WFNS score on admission, CRP and IL-6). Also, the association was in the form of OR with 95% CI. Besides, a ROC curve analysis assisted in identifying the cutoff point on the SAA levels on admission, which could the most sensitively and specifically serve for predicting the poor clinical outcome at the 3-months follow-up. We calculated the AUC regarding SAA for measuring the test accuracy. $P < 0.05$ reported statistical significance.

3. Results

3.1. Demographics and symptoms

The study included aSAH patients at the participating center from March 2016 to August 2022. We first enrolled 586 participants, followed by excluding 130 participants, including 23 participants who were not followed up at 3 months, six participants who did not provide their SAA or CRP data, and 101 participants who conformed to the exclusion criteria, such as a history of cerebrovascular disease and brain tumors, a combination of infectious diseases, immune dysfunction, hematological diseases, and severe organ function impairment, severe hepatic or renal disease, as well as refusal to undergo surgical treatment etc. Eventually, the study yielded 456 patients (208 males, aged 64.99 ± 8.54 years), that included 200 (43.86%) patients in poor outcome group after aSAH and 256 (78.29%) patients in good outcome group after aSAH. Relative to patients in good outcome group after aSAH, those in poor outcome group presented higher baseline Hunt and Hess grade ($P < 0.001$), higher modified fisher score ($P < 0.001$), higher WFNS score on admission ($P < 0.001$), higher proportions of infection ($P = 0.009$), higher WBC ($P = 0.018$), higher CRP ($P = 0.011$), higher IL-6 ($P < 0.001$), as well as higher SAA ($P < 0.001$). The basic characteristics of the 456 patients were presented in Table 1.

3.2. SAA values of patients and healthy controls

Table 1 compares the baseline characteristics between the patients and healthy controls. The median value (IQR) of

SAA for all aSAH patients was significantly higher than normal subjects (32.99 (26.53–37.44) vs. 5.64 (3.43–7.45), $P < 0.001$). Moreover, a significant inter-group difference in SAA at admission was revealed ($P < 0.001$). Indeed, the results showed that the SAA of poor outcome group were significantly increased compared to good outcome group and healthy control group (36.44 (32.23–41.00) vs. 28.99 (14.67–34.12) and 5.64 (3.43–7.45), $P < 0.001$). The differences were not significant in age and sex percentage among poor outcome group, good outcome group, and healthy controls group ($P > 0.05$). Figure 2 revealed that serum SAA concentrations in patients with poor outcome were significantly higher than those in good outcome group and healthy control group.

3.3. Baseline characteristics exhibited by all participants in SAA tertiles

Tertiles of the SAA level were taken into account for dividing all patients into three subgroups, ensuring that each subgroup had sufficient patient categories from 2.45 to 49.98 (Q1, 152 patients; Q2, 152 patients; Q3, 152 patients). The cut-off values (COV) for stratifying the SAA into tertiles were: (Q1) 2.45–29.23, (Q2) 29.33–35.44, (Q3) 35.54–49.98. Ascending tertiles of SAA reported higher baseline Hunt and Hess grade ($P < 0.001$), higher modified fisher score ($P < 0.001$), higher WFNS score on admission ($P = 0.015$), higher WBC ($P = 0.018$), higher CRP ($P = 0.011$), and higher IL-6 ($P < 0.001$) (Table 2). The poor and good outcome groups presented significant differences in terms of the SAA ($\chi 2 = 110.09$, $P < 0.001$). Actually, for the poor outcome group, the percentage of patients in the lowest tertile (2.45–29.23) and the highest tertile (35.54–49.98) were remarkably lower and higher, respectively. Besides, there were 17 (8.5%), 77 (38.5%), and 106 (53%) poor outcome patients after aSAH in Tertile 1, Tertile 2, and Tertile 3, respectively (Table 3).

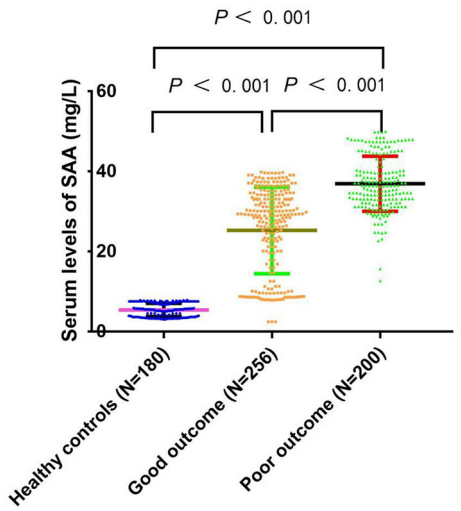

FIGURE 2
Comparison of SAA concentrations among the poor prognosis, good prognosis, and healthy controls. SAA denotes serum amyloid A. SAA concentrations are reported as the medians and interquartile ranges.

3.4. Association between the level of SAA and poor outcome after aSAH

We conducted the multivariate logistic regression analysis by including Hunt and Hess grade (III–IV vs. I–II), modified fisher scale (III–IV vs. I–II), WFNS score on admission, WBC, CRP, and IL-6 as independent variables, confirming that CRP (OR 1.209, 95% CI: 1.117–1.328, $P = 0.012$), SAA (OR 1.129, 95% CI: 1.081–1.177, $P = 0.000$), Hunt and Hess grade (III–IV vs. I–II) (OR 8.667, 95%CI: 7.045–12.996, $P = 0.012$), modified fisher scale (III–IV vs. I–II) (OR 6.743, 95% CI: 6.228–9.217, $P = 0.011$), and WFNS score on admission (OR 1.621, 95%CI: 1.212–2.153, $P = 0.007$) could independently predict the poor outcome at 3 months after aSAH (Table 4). Correlation analyses indicated the positive relationship between SAA and CRP ($r = 0.297$, $P < 0.001$), and the positive relationship between SAA and IL-6 in all patients on admission ($r = 0.206$, $P = 0.024$). Similarly, an obviously weak positive correlation was found between SAA and the modified fisher scores ($r = 0.191$, $P = 0.041$). Moreover, a weak positive correlation also existed between SAA and WFNS score ($r = 0.113$, $P = 0.016$).

In the logistic regression model without making any adjustments and the model with multiple adjustments, we took all participants as a whole, considering the poor outcome and the lowest tertile as the dependent variable and the reference, respectively for investigating SAA (Table 5). In the logistic regression model without making any adjustments, for patients with admission SAA, the highest quartile presented more poor outcome relative to the lowest tertile (non-adjusted: OR 2.780, 95% CI: 1.224–6.313, $P < 0.001$). In the logistic regression model that adjusted for the confounders of age, sex, vascular risk factors (hypertension, diabetes mellitus, current smoking, alcohol consumption), hunt and hess grade (III–V vs. I–II), modified fisher scale (III–IV vs. I–II), and WFNS score on admission, as well as laboratory data (WBC, CRP, and IL-6), the highest tertile of SAA could independently predict poor outcome prevalence (model 1B: OR = 2.362, 95% CI = 1.139–4.896, $P = 0.021$; model 2C: OR = 2.259, 95% CI = 1.070–4.770, $P < 0.001$; model 3D: OR = 2.247, 95% CI =1.095–4.604, $P = 0.021$). As revealed by the ROC curve, the estimated optimal cutoff of SAA that predicted the poor outcome was 30.28, with the sensitivity and specificity reaching 61.9 and 78.7%, respectively and the AUC at 0.807 (95%CI, 0.769–0.846; $P = 0.004$) (Figure 3).

TABLE 2 Baseline characteristics of patients with aSAH according to SAA tertiles.

Variables	SAA			*P*-value
	Q1 (≤29.23, *n* = 152)	Q2 (29.33–35.44, *n* = 152)	Q3 (≥35.54, *n* = 152)	
Demographic characteristics				
Gender, male, *n* (%)	65 (42.76)	70 (46.05)	73 (63.16)	0.648
Age, years, mean ± SD	68 (60–71)	68 (62–71)	68 (61–71)	0.482
Vascular risk factors (%)				
Hypertension	90 (59.21)	100 (65.79)	104 (68.42)	0.225
Diabetes mellitus	40 (26.32)	45 (29.61)	58 (38.16)	0.071
current smoking	42 (27.63)	48 (31.58)	54 (35.53)	0.334
Alcohol consumption	40 (26.32)	50 (32.89)	45 (29.61)	0.454
Laboratory findings (IQR)				
WBC, $\times 10^9$/L, median (IQR)	6.44 (5.63–7.79)	6.7 (5.46–8.38)	7.12 (6.04–8.69)	0.016
CRP, mg/L, median (IQR)	6.63 (5.77–8.95)	8.0 (6.0–12)	8.99 (6.25–14.67)	<0.001
IL−6, ng/L, median (IQR)	4.9 (3.9–6.4)	5.40 (4.83–8.50)	5.30 (4.80–8.50)	<0.001
Plt, $\times 10^9$/L, median (IQR)	216 (161–241)	231 (173–241)	210 (180–257)	0.645
TG, mmol/L, median (IQR)	1.37 (0.99–1.93)	1.32 (0.86–1.78)	1.42 (0.72–2.26)	0.064
TC, mmol/L, median (IQR)	4.55 (3.77–5.64)	4.32 (3.74–5.05)	4.55 (3.71–5.20)	0.434
Glucose, mmol/L, median (IQR)	5.40 (4.8–6.80)	5.20 (4.70–7.20)	5.30 (4.6–6.3)	0.473
RBC, $\times 10^{12}$/L, median (IQR)	4.94 (4.56–5.25)	4.67 (4.51–5.21)	1.01 (0.82–1.17)	0.108
Hb, g/L, median (IQR)	140 (134–145)	138 (134–144)	140.0 (132.0–145.0)	0.697
HDL–C, mmol/L, median (IQR)	1.05 (0.86–1.30)	1.02 (0.86–1.27)	1.01 (0.82–1.17)	0.158
LDL–C, mmol/L, median (IQR)	2.55 (1.96–3.23)	2.46 (1.94–3.14)	2.55 (1.94–3.08)	0.448
ApoA, g/L, median (IQR)	1.29 (1.13–1.50)	1.26 (1.10–1.44)	1.27 (1.09–1.47)	0.368
ApoB, g/L, median (IQR)	0.87 (0.70–1.04)	0.86 (0.68–1.01)	0.85 (0.69–0.99)	0.630
Serum amyloid A, mg/L, median (IQR)	20.11 (8.69–26.69)	32.99 (30.86–34.12)	39.11 (37.44–44.99)	<0.001
Hunt & Hess grade, *n* (%)				
I–II	84 (55.26)	96 (63.16)	135 (88.81)	<0.001
III–V	30 (19.74)	34 (22.37)	105 (69.08)	<0.001
Modified Fisher scale, *n* (%)				
I–II	37 (24.34)	45 (29.61)	65 (42.76)	0.009
III–IV	85 (55.92)	102 (67.11)	122 (80.26)	<0.001
Operation of aneurysm, *n* (%)				
Clip	25 (16.45)	31 (20.39)	31 (20.39)	0.600
Coil	118 (77.63)	120 (78.95)	131 (86.18)	0.124
Aneurysm Location, *n* (%)				
Anterior circulation	130 (85.53)	140 (92.11)	138 (90.79)	0.141
Posterior circulation	15 (9.87)	16 (10.53)	17 (11.18)	0.933
Size of aneurysm, mm, mean (SD)	4.8 (4.5–5.7)	4.8 (4.5–5.8)	4.8 (4.5–5.8)	0.418
WFNS score on admission, median (IQR)	2 (1–3)	2 (2–3)	2 (2–3)	0.015
Systolic arterial pressure, mmHg, mean (SD)	136 (130–147)	137 (132–149)	140 (133–152)	0.058

(Continued)

TABLE 2 (Continued)

Variables	SAA			*P*-value
	Q1 (≤29.23, *n* = 152)	Q2 (29.33–35.44, *n* = 152)	Q3 (≥35.54, *n* = 152)	
Diastolic arterial pressure, mmHg, mean (SD)	90 (89–100)	90 (89–100)	94 (90–102)	0.108
Acute hydrocephalus, *n* (%)	9 (5.92)	10 (6.58)	11 (7.24)	0.898
Intraventricular hemorrhage, *n* (%)	10 (6.58)	11 (7.19)	11 (7.24)	0.967
Seizure, *n* (%)	14 (9.21)	18 (11.84)	13 (8.55)	0.726
Infection, *n* (%)	40 (31.58)	50 (38)	54 (26.56)	0.197

TABLE 3 SAA tertiles of patients.

Variables	Poor outcome (*n* = 200)	Good outcome (*n* = 256)	$\chi 2$	*P*-value
SAA			110.09	<0.001
Tertile 1 (2.45–29.23)	17 (8.5%)	135 (52.73%)	98.86	<0.001
Tertile 2 (29.33–35.44)	77 (38.5%)	75 (29.30%)	4.28	0.039
Tertile 3 (35.44–49.98)	106 (53%)	46 (17.97%)	62.01	<0.001

SAA, serum amyloid A.

4. Discussion

To our best knowledge, the study is the first prospective cohort study exploring the relationship between SAA and poor prognosis at 3 months in aSAH patients. The main findings in the current study were that, (1) serum concentrations of SAA were significantly higher in patients with poor outcome of aSAH than in patients with favorable outcome of aSAH; (2) Serum SAA concentrations in aSAH patients were positively correlated with admission WFNS score, Modified Fisher score, IL-6 concentrations and serum CRP concentrations; (3) serum SAA emerged as an independent predictor for 3-month worse prognosis; (4) compared to CRP and IL-6, serum SAA concentrations were highly discriminatory for clinical outcomes under the ROC curve; (5) high-level SAA at admission exhibited an obvious relation to the poor outcome 3 months after aSAH and documented that after adjusting major confounders, patients in the highest SAA quartile presented a poor outcome risk 2.247-fold higher than those in the lowest SAA quartile, which epidemiologically proved the potential effectiveness of SAA for predicting the poor outcome at 3 months. These findings suggest that increased serum SAA concentrations may be highly correlated with inflammation and closely associated with a worsening prognosis of aSAH. Therefore, SAA may be a useful therapeutic target for the treatment of patients with aSAH. Here, SAA can well serve for treating aSAH patients as an useful therapeutic target.

Inflammation has been well-documented to be implicated in the pathogenesis of brain injury associated with aSAH. The balance between inflammatory and anti-inflammatory factors clearly affects the development of aSAH (5–7). SAA is an acute phase response protein produced by hepatocytes and belongs to a highly heterogeneous class of proteins in the apolipoprotein family. SAA is the main becoming amyloid A protein serum precursor in amyloidosis, which is composed of the same cluster of genes encoding a polymorphic protein that is more common in various inflammatory responses (18). SAA exerts immunomodulatory effects and assists in tissue regeneration by activating collagenases and acts as a chemotactic agent for monocytes, T cells, mast cells and neutrophils (19). SAA concentrations are elevated to varying degrees in various infectious and inflammatory diseases as well as in oncological diseases (18). Recently, accumulating evidence has shown that SAA plays a crucial role in the inflammation of several human diseases, e.g., acute primary basal ganglia hemorrhage, ischemic stroke, inflammatory rheumatic diseases, acute myocardial

TABLE 4 Univariate logistic regression analysis of 3-month poor outcome after aSAH.

Variables	OR	95% CI	*P*-value
Infection	1.106	0.859–1.332	0.286
WBC	1.062	0.912–1.256	0.349
CRP	1.209	1.117–1.328	0.012
IL−6	1.072	0.867–1.131	0.081
SAA	1.129	1.081–1.177	<0.001
Hunt and Hess grade (III–IV vs. I–II)	8.667	7.045–12.996	0.012
Modified Fisher Scale (III–IV vs. I–II)	6.743	6.228–9.217	0.011
WFNS score on admission	1.621	1.212–2.153	0.007

TABLE 5 Unadjusted and adjusted associations between quartile of SAA levels and poor outcome at 90 days.

	Tertile	OR[A]	95% CI	*P*-value
Unadjusted	Middle	2.601	0.757–8.123	0.026
	Highest	2.780	1.224–6.313	<0.001
Model 1B	Middle	2.162	0.636–7.350	0.217
	Highest	2.362	1.139–4.896	0.021
Model 2C	Middle	2.102	0.623–7.496	0.224
	Highest	2.259	1.070–4.770	0.033
Model 3D	Middle	2.144	1.139–3.867	0.124
	Highest	2.247	1.095–4.604	0.021

A Reference OR (1.000) is the lowest tertile of SAA for poor outcome after aneurysmal subarachnoid hemorrhage.
B Model 1: adjusted for age, sex.
C Model 2: adjusted for covariates from Model 1 and further adjusted for Vascular risk factors (Hypertension, diabetes mellitus, current smoking, alcohol consumption).
D Model 3: adjusted for covariates from Model 2 and further adjusted for variables with $p < 0.05$ in univariate analysis (WBC, CRP, IL−6, infection, hunt and hess grade (III–V vs. I–II), modified fisher scale (III–IV vs. I–II), and WFNS score on admission).

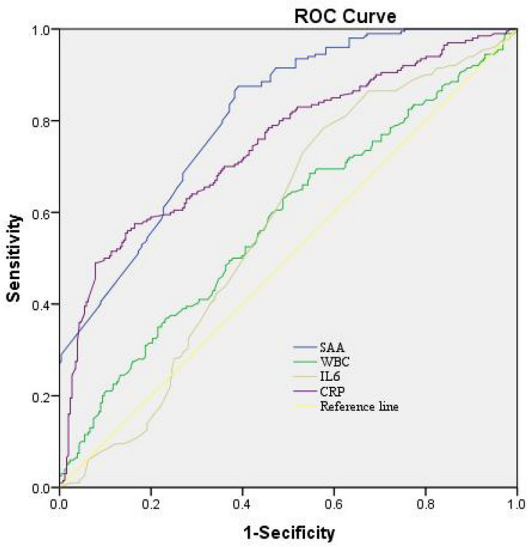

FIGURE 3
The ROC curves for the prediction of poor outcome. Predictive values of SAA, CRP, IL-6, and WBC for depression at 3-month after aSAH. AUC 0.573 (95%CI, 0.521–0.626; $P = 0.004$) for IL-6; 0.748 (95%CI, 0.702–0.794; $P = 0.007$) for CRP; 0.579 (95%CI, 0.526–0.632; $P = 0.004$) for WBC; and 0.807 (95%CI, 0.623–0.747; $P = 0.004$) for SAA. SAA had the COV of 30.28, and the sensitivity and specificity were 61.9 and 78.7%, respectively. ROC, receiver operating characteristic; SAA, serum amyloid A; AUC, area under the curve; CI, confidence interval; CRP, C-reactive protein; IL-6, interleukin-6; WBC, White blood cell; COV, cut-off value.

infarction, acute myocardial infarction, traumatic brain injury, and hypoxic ischemic encephalopathy (13, 20–24). The current study verified a similar result that there was a significant elevation of serum SAA concentrations after aSAH, as compared to normal reference values. In addition, a significantly higher concentration of SAA has been reported in mice with cerebral ischemia, and it has also been found to mediate microglia activation *via* gene knockout techniques (25). Alternatively, a recent animal study on mice with traumatic brain injury revealed that serum SAA may be a novel neuroinflammation-based, and severity-dependent, biomarker for acute traumatic brain injury (26). Recent studies have found that elevated IL-6 levels induce neuroinflammation and may be strongly associated with poor outcomes of aSAH (27). CRP, similar to SAA, is an acute-phase protein whose peripheral blood concentration not only reflects the degree of systemic inflammatory response, but also the degree of inflammatory response in the brain (28–30). The interesting finding in this study was that serum SAA concentrations were in close correlation with systemic inflammation reflected by CRP and IL-6 concentrations. Therefore, it is assumed that serum SAA might at least be involved in the acute systemic inflammation caused by aSAH brain injury.

Up until now, it remains unclear whether circulating SAA is associated with the prognosis of acute brain injury. In the present study of 456 patients with aSAH, we found that serum SAA concentrations were strongly correlated with WFNS scores as well as modified Fisher scores. Consistent with previous studies on acute cerebral hemorrhage (13), on the other hand, we support the hypothesis that serum SAA concentrations can reflect the clinical severity after acute brain injury, including acute cerebral hemorrhage and aSAH. Our study revealed that serum SAA was independently associated with 90-day poor outcome even after correcting for conventional prognostic determinants, such as WFNS scores and modified Fisher scores, which are the two common determinants for prognosis of aSAH (8, 31–33). In addition, under ROC curve, serum SAA concentrations showed significant prognostic accuracy in differentiating patients with poor prognosis from those with good prognosis at 3 months after aSAH. Previous extensive numerous studies had revealed that patients with a poor prognosis after aSAH had a significant increase in inflammatory or inflammatory-related disease markers including IL-33, serum stanniocalcin 1, and red blood cell distribution width (8, 32, 34). Interestingly, we performed some discriminatory ability comparisons of AUC between serum SAA concentrations and three common biochemical variables, namely serum CRP concentrations, serum IL-6 concentrations, and blood leukocyte counts (35–37). It was demonstrated that the prognostic predictive ability of serum SAA concentrations were considerably higher than that of serum CRP concentrations, IL-6 concentrations, and blood leukocyte count. At the same time, the optimal point of serum SAA concentration was selected for the differentiation of those patients with poor prognosis with moderate-high sensitivity and specificity. In other words, serum SAA could be used as a promising prognostic biomarker for the treatment of human aSAH.

5. Conclusions

The current study 456 aSAH patients have demonstrated that increased SAA concentrations in circulating blood have relation to admission WFNS scores and modified Fisher scores in addition to peripheral CRP concentrations, as well as serum SAA concentrations are independently associated with poor outcome at 3 months after aSAH. An intriguing finding of this study was the high discriminatory ability of serum SAA concentrations for poor outcomes after aSAH. In summary, it is demonstrated that that SAA on admission may be an important biomarker of inflammatory disease assessing the prognosis after aSAH.

Data availability statement

The raw data supporting the conclusions of this article will be made available by the authors, without undue reservation.

Ethics statement

The studies involving human participants were reviewed and approved by the First Affiliated Hospital of Anhui University of Science and Technology (First People's Hospital of Huainan). Participants provided informed consent prior to inclusion in this study.

Author contributions

ZS and YL designed the research study and analyzed the data. YL, FC, KJ, and ZS performed the research. YL wrote the manuscript. All authors contributed to editorial changes in the manuscript and read and approved the final manuscript.

Funding

This work was supported by the Huainan Key Scientific Research Project (2018A369) and the Natural Science Foundation of Health Commission of Anhui Province (2016qk1108).

Conflict of interest

The authors declare that the research was conducted in the absence of any commercial or financial relationships that could be construed as a potential conflict of interest.

Publisher's note

References

1. Virani SS, Alonso A, Benjamin EJ, Bittencourt MS, Callaway CW, Carson AP, et al. Heart disease and stroke statistics-2020 update: a report from the american heart association. *Circulation.* (2020) 141:e139–596. doi: 10.1161/CIR.0000000000000757

2. Lai X, Zhang W, Ye M, Liu X, Luo X. Development and validation of a predictive model for the prognosis in aneurysmal subarachnoid hemorrhage. *J Clin Lab Anal.* (2020) 34:e23542. doi: 10.1002/jcla.23542

3. Zhang P, Li Y, Zhang H, Wang X, Dong L, Yan Z, et al. Prognostic value of the systemic inflammation response index in patients with aneurismal subarachnoid hemorrhage and a Nomogram model construction. *Br J Neurosurg.* (2020) 12:1–7. doi: 10.1080/02688697.2020.1831438

4. Shi L, Wang Z, Liu X, Li M, Zhang S, Song X. Bax inhibitor-1 is required for resisting the Early Brain Injury induced by subarachnoid hemorrhage through regulating IRE1-JNK pathway. *Neurol Res.* (2018) 40:189–96. doi: 10.1080/01616412.2018.1424699

5. Provencio JJ, Vora N. Subarachnoid hemorrhage and inflammation: bench to bedside and back. *Semin Neurol.* (2005) 25:435–44. doi: 10.1055/s-2005-923537

6. Frontera JA, Provencio JJ, Sehba FA, McIntyre TM, Nowacki AS, Gordon E, et al. The role of platelet activation and inflammation in early brain injury following subarachnoid hemorrhage. *Neurocrit Care.* (2017) 26:48–57. doi: 10.1007/s12028-016-0292-4

7. Wu A, Liu R, Dai W, Jie Y, Yu G, Fan X, et al. Lycopene attenuates early brain injury and inflammation following subarachnoid hemorrhage in rats. *Int J Clin Exp Med.* (2015) 8:14316–22.

8. Gong J, Zhu Y, Yu J, Jin J, Chen M, Liu W, et al. Increased serum interleukin-33 concentrations predict worse prognosis of aneurysmal subarachnoid hemorrhage. *Clin Chim Acta.* (2018) 486:214–8. doi: 10.1016/j.cca.2018.08.011

9. Zhang Q, Zhang G, Wang L, Zhang W, Hou F, Zheng Z, et al. Clinical value and prognosis of C reactive protein to lymphocyte ratio in severe aneurysmal subarachnoid hemorrhage. *Front Neurol.* (2022) 13:868764. doi: 10.3389/fneur.2022.868764

10. Schweizer J, Bustamante A, Lapierre-Fétaud V, Faura J, Scherrer N, Azurmendi Gil L, et al. SAA (Serum Amyloid A): a novel predictor of stroke-associated infections. *Stroke.* (2020) 51:3523–30. doi: 10.1161/STROKEAHA.120.030064

11. Villapol S, Kryndushkin D, Balarezo MG, Campbell AM, Saavedra JM, Shewmaker FP, et al. Hepatic expression of serum amyloid A1 is induced by traumatic brain injury and modulated by telmisartan. *Am J Pathol.* (2015) 185:2641–52. doi: 10.1016/j.ajpath.2015.06.016

12. Rael LT, Bar-Or R, Salottolo K, Mains CW, Slone DS, Offner PJ, et al. Injury severity and serum amyloid A correlate with plasma oxidation-reduction potential in multi-trauma patients: a retrospective analysis. *Scand J Trauma Resusc Emerg Med.* (2009) 17:57. doi: 10.1186/1757-7241-17-57

13. Huangfu XQ, Wang LG, Le ZD, Tao B. Utility of serum amyloid A as a potential prognostic biomarker of acute primary basal ganglia hemorrhage. *Clin Chim Acta.* (2020) 505:43–8. doi: 10.1016/j.cca.2020.02.022

14. Zhang Y, Feng Y, Zuo J, Shi J, Zhang S, Yang Y, et al. Elevated serum amyloid A is associated with cognitive impairment in ischemic stroke patients. *Front Neurol.* (2021) 12:789204. doi: 10.3389/fneur.2021.789204

15. Katayama T, Nakashima H, Takagi C, Honda Y, Suzuki S, Iwasaki Y, et al. Serum amyloid a protein as a predictor of cardiac rupture in acute myocardial infarction patients following primary coronary angioplasty. *Circ J.* (2006) 70:530–5. doi: 10.1253/circj.70.530

16. Gao A, Gupta S, Shi H, Liu Y, Schroder AL, Witting PK, et al. Pro-inflammatory serum amyloid a stimulates renal dysfunction and enhances atherosclerosis in Apo E-deficient mice. *Int J Mol Sci.* (2021) 22:12582. doi: 10.3390/ijms222212582

17. Connolly ES, Rabinstein AA, Carhuapoma JR, Derdeyn CP, Dion J, Higashida RT, et al. Guidelines for the management of aneurysmal subarachnoid hemorrhage: a guideline for healthcare professionals from the American heart association/American stroke association. *Stroke.* (2012) 43:1711–37. doi: 10.1161/STR.0b013e3182587839

18. Sack GH. Serum amyloid A - a review. *Mol Med.* (2018) 24:46. doi: 10.1186/s10020-018-0047-0

19. Frame NM, Gursky O. Structure of serum amyloid A suggests a mechanism for selective lipoprotein binding and functions: SAA as a hub in macromolecular interaction networks. *Amyloid.* (2017) 24:13–4. doi: 10.1018/13506129.2016.1270930

20. Sorić Hosman I, Kos I, Lamot L. Serum Amyloid A in inflammatory rheumatic diseases: a compendious review of a renowned biomarker. *Front Immunol.* (2021) 11:631299. doi: 10.3389/fimmu.2020.631299

21. Metwalli O, Hashem E, Ajabnoor MA, Alama N, Banjar ZM. Study of some inflammatory mediators in the serum of patients with atherosclerosis and acute myocardial infarction. *Cureus.* (2021) 13:e18450. doi: 10.7759/cureus.18450

22. Yeh SJ, Chen CH, Lin YH, Tsai LK, Lee CW, Tang SC, et al. Serum amyloid A predicts poor functional outcome in patients with ischemic stroke receiving endovascular thrombectomy: a case control study. *J Neurointerv Surg.* (2022) 20:8234. doi: 10.1136/neurintsurg-2021-018234

23. Soriano S, Moffet B, Wicker E, Villapol S. Serum amyloid A is expressed in the brain after traumatic brain injury in a sex-dependent manner. *Cell Mol Neurobiol.* (2020) 40:1199–211. doi: 10.1007/s10571-020-00808-3

24. Aly H, Hamed Z, Mohsen L, Ramy N, Arnaoot H, Lotfy A. Serum amyloid A protein and hypoxic ischemic encephalopathy in the newborn. *J Perinatol.* (2011) 31:263–8. doi: 10.1038/jp.2010.130

25. Yu J, Zhu H, Taheri S, Mondy W, Bonilha L, Magwood GS, et al. Serum amyloid A-mediated inflammasome activation of microglial cells in cerebral ischemia. *J Neurosci.* (2019) 39:9465–9476. doi: 10.1523/JNEUROSCI.0801-19.2019

26. Wicker E, Benton L, George K, Furlow W, Villapol S. Serum amyloid A protein as a potential biomarker for severity and acute outcome in traumatic brain injury. *Biomed Res Int.* (2019) 3:5967816. doi: 10.1155/2019/5967816

27. Yao Y, Fang X, Yuan J, Qin F, Yu T, Xia D, et al. Interleukin-6 in cerebrospinal fluid small extracellular vesicles as a potential biomarker for prognosis of aneurysmal subarachnoid hemorrhage. *Neuropsychiatr Dis Treat.* (2021) 17:1423–31. doi: 10.2147/NDT.S304394

28. Elhechmi YZ, Hassouna M, Chérif MA, Ben Kaddour R, Sedghiani I, Jerbi Z. Prognostic value of serum C-reactive protein in spontaneous intracerebral hemorrhage: when should we take the sample? *J Stroke Cerebrovasc Dis.* (2017) 26:1007–12. doi: 10.1016/j.jstrokecerebrovasdis.2016.11.129

29. Gaastra B, Barron P, Newitt L, Chhugani S, Turner C, Kirkpatrick P, et al. CRP (C-Reactive Protein) in outcome prediction after subarachnoid hemorrhage and the role of machine learning. *Stroke.* (2021) 52:3276–85. doi: 10.1161/STROKEAHA.120.030950

30. Di Napoli M, Godoy DA, Campi V. del Valle M, Piñero G, Mirofsky M, et al. C-reactive protein level measurement improves mortality prediction when added to the spontaneous intracerebral hemorrhage score. *Stroke.* (2011) 42:1230–6. doi: 10.1161/STROKEAHA.110.604983

31. Zan X, Deng H, Zhang Y, Wang P, Chong W, Hai Y, et al. Lactate dehydrogenase predicting mortality in patients with aneurysmal subarachnoid hemorrhage. *Ann Clin Transl Neurol.* (2022) 9:1565–73. doi: 10.1002/acn3.51650

32. Hong DY, Kim SY, Kim JY, Kim JW. Red blood cell distribution width is an independent predictor of mortality in patients with aneurysmal subarachnoid hemorrhage. *Clin Neurol Neurosurg.* (2018) 172:82–6. doi: 10.1016/j.clineuro.2018.06.044

33. Zhou J, Ying X, Zhang J, Chen M, Chen M. Emerging role of serum dickkopf-1 in prognosis of aneurysmal subarachnoid hemorrhage. *Clin Chim Acta.* (2021) 521:116–21. doi: 10.1016/j.cca.2021.07.009

34. Jun Q, Luo W. Early-stage serum Stanniocalcin 1 as a predictor of outcome in patients with aneurysmal subarachnoid hemorrhage. *Medicine.* (2021) 23:100:e28222. doi: 10.1097/MD.0000000000028222

35. Romero FR, Bertolini Ede F, Figueiredo EG, Teixeira MJ. Serum C-reactive protein levels predict neurological outcome after aneurysmal subarachnoid hemorrhage. *Arq Neuropsiquiatr.* (2012) 70:202–5. doi: 10.1590/s0004-282x2012000300009

36. Krzyzewski RM, Kliś KM, Kwinta BM, Stachura K, Guzik TJ, Gasowski J. High leukocyte count and risk of poor outcome after subarachnoid hemorrhage: a meta-analysis. *World Neurosurg.* (2020) 135:e541–7. doi: 10.1016/j.wneu.2019.12.056

37. Simon M, Grote A. Interleukin 6 and aneurysmal subarachnoid hemorrhage. A narrative review. *Int J Mol Sci.* (2021) 22:4133. doi: 10.3390/ijms22084133

frontiers | Frontiers in Neurology

TYPE Original Research
PUBLISHED 24 January 2023
DOI 10.3389/fneur.2022.1023761

OPEN ACCESS

EDITED BY
Wael M. Y. Mohamed,
International Islamic University Malaysia, Malaysia

REVIEWED BY
Weiming Liu,
Beijing Tiantan Hospital, Capital Medical University, China
Rastislav Pjontek,
University Hospital RWTH Aachen, Germany

*CORRESPONDENCE
Shizhong Zhang
✉ zhangshizhong@smu.edu.cn

†These authors have contributed equally to this work

SPECIALTY SECTION
This article was submitted to Neurological Biomarkers, a section of the journal Frontiers in Neurology

RECEIVED 20 August 2022
ACCEPTED 31 December 2022
PUBLISHED 24 January 2023

CITATION
Zhang H, He X, Xie L, Zhang H, Hou X and Zhang S (2023) Correlation between cerebrospinal fluid abnormalities before ventriculoperitoneal shunt and postoperative intracranial infection in adult patients with hydrocephalus: A clinical study. *Front. Neurol.* 13:1023761. doi: 10.3389/fneur.2022.1023761

Correlation between cerebrospinal fluid abnormalities before ventriculoperitoneal shunt and postoperative intracranial infection in adult patients with hydrocephalus: A clinical study

Huan Zhang[1†], Xiaozheng He[2†], Linghai Xie[2], Hongbo Zhang[2], Xusheng Hou[2] and Shizhong Zhang[2*]

[1]Department of Neurosurgery, Affiliated Hospital No. 2 of Nantong University, First People's Hospital of Nantong City, Nantong, China, [2]Guangdong Provincial Key Laboratory on Brain Function Repair and Regeneration, Department of Functional Neurosurgery, Zhujiang Hospital of Southern Medical University, Guangzhou, China

Objective: To identify the relationship between preoperative cerebrospinal fluid (CSF) leukocyte, chloride, glucose, aspartate aminotransferase, lactate dehydrogenase, adenosine deaminase, lactic acid and protein levels and ventriculoperitoneal shunt infection.

Methods: Records of 671 consecutive adult patients who underwent ventriculoperitoneal shunt surgery for the treatment of hydrocephalus at Zhujiang Hospital affiliated with Southern Medical University from January 2011 to March 2022 were reviewed. The patients were divided into infection and non-infection groups based on the presence of postoperative infection. For all patients, we analyzed age; sex; primary disease; preoperative CSF leukocyte, chloride, glucose, aspartate aminotransferase, lactate dehydrogenase, adenosine deaminase, lactic acid and protein levels; postoperative temperature; and postoperative infection.

Results: A total of 397 patients were included, 28 (7.05%) of whom had an infection within 6 months of the operation and the remaining had no infection. There was no significant difference in age, sex, primary disease, leukocyte, chloride ion, aspartate aminotransferase, lactate dehydrogenase, adenosine deaminase and protein levels in CSF between infection group and non-infection group ($p > 0.05$). The postoperative infection rate of patients with CSF glucose <2.8 mmol/L ($x^2 = 11.650$, $p = 0.001$) and CSF lactic acid >2.8 mmol/L ($x^2 = 12.455$, $p < 0.001$) was higher than that of patients with CSF glucose level ≥2.8 mmol/L and CSF lactic acid level in the range of (1–2.8) mmol/L, respectively, with statistical difference. Compared with the non-infection group, the level of CSF glucose ($t = 4.113$, $p < 0.001$) was significantly lower, and the level of CSF lactic acid ($t = 6.651$, $p < 0.001$) was significantly higher in the infection group. Multivariate logistic regression analysis showed that preoperative cerebrospinal fluid glucose <2.8 mmol/L (OR = 3.911, 95% CI: 1.653~9.253, $p = 0.002$) and cerebrospinal fluid lactate >2.8 mmol/L (OR = 4.712, 95% CI: 1.892~11.734, $p = 0.001$) are risk factors for infection after ventriculoperitoneal shunt. ROC analysis revealed that the area under the curve (AUC) for CSF glucose and lactic acid level were 0.602 (95% CI: 0.492–0.713) and 0.818 (95% CI: 0.738–0.898), respectively. The infection group had higher rates of fever and body temperature on postoperative day 3–7 ($p < 0.05$).

Conclusions: For adult hydrocephalus patients without clinical manifestations of intracranial infection but only with simple abnormality of cerebrospinal fluid, when

the content of glucose in cerebrospinal fluid is <2.8 mmol/L, and the content of lactic acid is >2.8 mmol/L, it is recommended to perform ventriculoperitoneal shunt after further improvement of cerebrospinal fluid indicators, otherwise, hasty operation will increase the postoperative infection rate. The postoperative fever rate of ventriculoperitoneal shunt surgery is high and the body temperature drops rapidly. If there is still fever after day 3 after surgery, whether there is intracranial infection should be considered.

KEYWORDS

ventriculoperitoneal shunt, cerebrospinal fluid, hydrocephalus, infection, risk factors

Introduction

Hydrocephalus refers to the imbalance between cerebrospinal fluid (CSF) production and absorption, and/or the obstruction of its pathways, resulting in disturbed CSF dynamics and the abnormal accumulation of excess CSF in either the ventricle or subarachnoid space, which then dilatates these areas (1, 2). Hydrocephalus commonly occurs in neurosurgical patients ranging from newborns to adults. It can be divided into primary and acquired hydrocephalus according to its etiology. Acquired hydrocephalus is known as a common sequelae in patients with post-hemorrhagic conditions, including brain trauma, intracranial hemorrhage, brain tumors, and intracranial infection, among others (3). The development of hydrocephalus is accompanied by a series of pathophysiological changes in periventricular structures and even the whole brain. Without timely and effective intervention, these changes can lead to serious consequences, such as serious neurological dysfunction, cognitive disturbances, and memory deficits. A ventriculoperitoneal shunt is the most common and effective method for the treatment of hydrocephalus (4–6). Early shunt surgery in patients leads to a better prognosis (2, 7, 8), therefore, early treatment is imperative.

Preoperative intracranial infection is an absolute contraindication for a ventriculoperitoneal shunt (9), however, it is difficult to diagnose, especially occult intracranial infections. CSF bacterial culture is the gold standard for diagnosis of intracranial infections in clinical practice, but the low positive rate and time-consuming procedure required for culture limits its use in practice. Clinically, most patients with hydrocephalus require prompt surgical treatment and thus, cannot wait for CSF bacterial culture results. For the vast majority of patients with negative CSF bacterial cultures, intracranial infection is assessed by CSF leukocyte count, chloride, glucose, aspartate aminotransferase, lactate dehydrogenase, adenosine deaminase, lactic acid, and protein levels in combination with clinical symptoms (fever, meningeal irritation sign). The clinical diagnosis of intracranial infection can be challenging due to issues such as the lack of a unified diagnostic standard as well as high false negative/positive rates (10, 11). However, because ventriculoperitoneal shunts are urgently needed for most hydrocephalus patients to improve symptoms, the presence of intracranial infection directly affects the patients' treatment plan and prognosis. Clinically, ventriculoperitoneal shunt operations are often still performed although the CSF leukocyte, chloride, glucose, aspartate aminotransferase, lactate dehydrogenase, adenosine deaminase, lactic acid and protein levels are not within normal range, and often do not result in postoperative intracranial infection. Therefore, the aim of this study was to identify the relationship between preoperative CSF leukocyte count, chloride, glucose, aspartate aminotransferase, lactate dehydrogenase, adenosine deaminase, lactic acid and protein levels and postoperative ventriculoperitoneal shunt infection.

Subjects and methods

Patients

We reviewed 671 consecutive adult patients who underwent ventriculoperitoneal shunt surgery for hydrocephalus treatment at Zhujiang Hospital affiliated with Southern Medical University from January 2011 to March 2022.

Inclusion and exclusion criteria

The inclusion criteria for this study were stable vital signs, absence of fever and neck stiffness, no previous operations, preoperative lumbar puncture results, negative CSF bacterial culture, normal preoperative blood levels of leukocyte, glucose, chloride, aspartate aminotransferase, lactate dehydrogenase, adenosine deaminase, lactic acid and protein, operative time within 2 h, and at least a 6-month follow-up. The exclusion criteria were as follows: no cerebrospinal fluid examination within 48 h before surgery; abnormal preoperative blood levels of leukocytes, glucose, chloride, aspartate aminotransferase, lactate dehydrogenase, adenosine deaminase, lactic acid and protein; clear history of intracranial infection within 3 months before the surgery; positive CSF bacteria culture within 3 months before the surgery; preoperative procalcitonin >0.05; preoperative fever; positive meningeal irritation sign; previous history of a ventriculoperitoneal shunt; operative time over 2 h; follow-up time of <6 months; and a diabetes diagnosis. Ultimately, we enrolled 397 patients who met the inclusion criteria.

Treatment and research methods

All patients were treated with prophylactic antibiotics half an hour before ventriculoperitoneal shunt surgery and symptomatic treatment after surgery. All patients completed lumbar puncture and CSF collection within 48 h before surgery, and the laboratory

TABLE 1 Single factor analysis of the difference between the two groups in gender, primary disease and CSF parameters.

Variable	Non-infection group ($n = 369$) n (%)	Infection group ($n = 28$) n (%)	Infection rate (%)	Chi-square	p-value
Gender				0.001	0.981
Male	210 (56.9)	16 (57.1)	7.1%		
Female	159 (43.1)	12 (42.9)	7.0%		
Primary disease				2.939	0.816
Cerebral hemorrhage	243 (65.9)	17 (60.7)	6.5%		
Brain tumor	67 (18.2)	6 (21.4)	8.2%		
Idiopathic normal pressure hydrocephalus	19 (5.1)	1 (3.6)	5.0%		
Tuberculous meningitis	11 (3.0)	1 (3.6)	8.3%		
Cerebral infarction	13 (3.5)	1 (3.6)	7.1%		
Cerebral cyst	9 (2.4)	2 (7.1)	18.2%		
Others	7 (1.9)	0 (0)	0.0%		
CSF leukocyte level				0.684	0.408
(0–8) $\times 10^6$/L	252 (68.3)	17 (60.7)	6.3%		
>8 $\times 10^6$/L	117 (31.7)	11 (39.3)	8.6%		
CSF chloride level				0.821	0.663
<120 mmol/L	114 (30.9)	8 (28.6)	6.6%		
(120–130) mmol/L	228 (61.8)	19 (67.9)	7.7%		
>130 mmol/L	27 (7.3)	1 (3.6)	3.6%		
CSF glucose level				11.650	0.001
<2.8 mmol/L	62 (16.8)	12 (60.7)	16.2%		
≥2.8 mmol/L	307 (76.4)	16 (39.3)	5.0%		
CSF aspartate aminotransferase level				<0.001	>0.999
(5–20) U/L	304 (82.4)	23 (82.1)	7.0%		
>20 U/L	65 (17.6)	5 (17.9)	7.1%		
CSF lactate dehydrogenase level				1.520	0.218
(3–40) U/L	299 (81.0)	20 (71.4)	6.3%		
>40 U/L	70 (19.0)	8 (28.6)	10.3%		
CSF adenosine deaminase level				<0.001	>0.999
(0–8) U/L	330 (89.4)	25 (89.3)	7.0%		
>8 U/L	39 (10.6)	3 (10.7)	7.1%		
CSF lactic acid level				12.455	<0.001
(1–2.8) mmol/L	329 (89.2)	18 (64.3)	5.2%		
>2.8 mmol/L	40 (10.8)	10 (35.7)	20%		
CSF protein level				2.245	0.325
<450 mg/L	176 (47.7)	12 (42.9)	6.4%		
(450–1,000) mg/L	129 (35.0)	8 (28.6)	5.8%		
>1,000 mg/L	64 (17.3)	8 (28.6)	11.1%		

department of Zhujiang Hospital affiliated with Southern Medical University completed routine and biochemical examination of CSF. Collect and compare the general clinical data, preoperative cerebrospinal fluid test results and postoperative temperature of patients in the infection group and non-infection group, and determine the correlation between preoperative routine and biochemical indicators of cerebrospinal fluid and intracranial infection after ventriculoperitoneal shunt.

Clinical data collection

We retrospectively analyzed the following data: age; sex; protopathy; and preoperative CSF leukocyte, chloride, glucose, and protein levels. The normal ranges for CSF were as follows: white blood cell (WBC) count, (0–8) $\times$ 10^6/L; chloride, (120–130) mmol/L; glucose, (2.8–4.5) mmol/L; aspartate aminotransferase, (5–20) mmol/L; lactate dehydrogenase, (3–40) U/L; adenosine deaminase, (0–8) U/L; lactic acid, (1–2.8) mmol/L and protein, (150–450) mg/L. The highest body temperature was recorded on the day of surgery and 1–7 days after surgery. A temperature higher than 37.3°C was defined as a fever.

Diagnostic criteria of intracranial infection

Current Centers for Disease Control and Prevention/National Healthcare Safety Network criteria for diagnosis of meningitis were used (12). Intracranial infection must meet at least one of the following criteria: (1) Patient has organism (s) identified from brain tissue or dura by a culture or non-culture based microbiologic testing method which is performed for purposes of clinical diagnosis or treatment, for example, not Active Surveillance Culture/Testing (ASC/AST). (2) Patient has an abscess or evidence of intracranial infection on gross anatomic or histopathologic exam. (3) Patient has at least two of the following signs or symptoms: headache, dizziness, fever (>38.0°C), localizing neurologic signs, changing level of consciousness, or confusion. And at least one of the following: (a) organism (s) seen on microscopic examination of brain or abscess tissue obtained by needle aspiration or during an invasive procedure or autopsy. (b) imaging test evidence suggestive of infection (for example, ultrasound, CT scan, MRI, radionuclide brain scan, or arteriogram), which if equivocal is supported by clinical correlation, specifically, physician documentation of antimicrobial treatment for intracranial infection. c. diagnostic single antibody titer (IgM) or 4-fold increase in paired sera (IgG) for organism. Meningitis or ventriculitis must meet at least one of the following criteria: (1) Patient has organism (s) identified from cerebrospinal fluid (CSF) by a culture or non-culture based microbiologic testing method which is performed for purposes of clinical diagnosis or treatment for example, not Active Surveillance Culture/Testing (ASC/AST). (2) Patient has at least two of the following: (i) fever (>38.0°C) or headache (Note: Elements of "*i*" alone may not be used to meet the two required elements), (ii) meningeal sign (s), and (iii) cranial nerve sign (s) And at least one of the following: (a) increased white cells, elevated protein, and decreased glucose in CSF (per reporting laboratory's reference range). (b) organism (s) seen on Gram stain of CSF. (c) organism (s) identified from blood by a culture or non-culture based microbiologic testing method which is performed for purposes of clinical diagnosis or treatment, for example, not Active Surveillance Culture/Testing (ASC/AST). (d) diagnostic single antibody titer (IgM) or 4-fold increase in paired sera (IgG) for organism.

Statistical analysis

SPSS statistical software (Version 25.0. Armonk, NY: IBM Corp) was used for all data analyses. First, single factor analysis was performed on the data. Continuous variables are presented as mean $\pm$ standard deviation and range, and categorical variables are presented as the number of cases. To compare baseline variables, the chi-square and Fisher's exact tests were used for categorical variables, and a Student's *t*-test was used for continuous variables. A p-value < 0.05 was considered statistically significant. A logistic stepwise regression was used to analyze the multiple risk factors for infection after a ventriculoperitoneal shunt. The probability of stepwise entry was 0.05 and the probability of removal was 0.10. The ROC curve was used to analyze how well each factor predicted postoperative infection.

Results

Demographics and patient characteristics

A total of 397 patients were included; 28 (7.05%) developed an infection within 6 months after the operation and the remaining 369 (92.95%) did not develop an infection. A summary of patient demographics and clinical characteristics is shown in Tables 1, 3. Of the 397 patients, 226 were males and 171 females and the average age was 49.80 $\pm$ 0.75 years. There were 260 cases of cerebral hemorrhage, 73 cases of brain tumor, 20 cases of idiopathic normal pressure hydrocephalus, 12 cases of tuberculous meningitis, 14 cases of cerebral infarction, 11 cases of cerebral cyst, and 7 cases of others. Of the 28 infected patients, all infections occurred within 6 months after surgery, including 10 cases (35.7%) 1 week, 2 cases (7.1%) 2 weeks, 10 cases (35.7%) 1 month, 3 cases (10.7%) 2 months, 2 cases (7.1%) 4 months, and 1 case (3.6%) six months after surgery (Table 2).

TABLE 2 Time distribution of postoperative infection.

Infection time after surgery	Case	Proportion (%)
1 week	10	35.7
2 weeks	2	7.1
1 month	10	35.7
2 months	3	10.7
4 months	2	7.1
6 months	1	3.6
Total	28	100

TABLE 3 Single factor analysis of the difference between the two groups in age and CSF parameters.

Variable	Non-infection group (Mean ± SD)	Infection group (Mean ± SD)	*T*-value	*p*-value
Age (years)	49.87 ± 15.18	48.52 ± 10.26	0.634	0.530
CSF leukocyte level ($\times 10^6$/L)	14.14 ± 67.56	19.39 ± 44.17	0.404	0.686
CSF chloride level (mmol/L)	121.84 ± 10.14	123.56 ± 5.94	0.885	0.376
CSF glucose level (mmol/L)	3.40 ± 0.88	2.71 ± 0.49	4.113	<0.001
CSF aspartate aminotransferase level (U/L)	14.07 ± 20.02	13.14 ± 8.94	0.243	0.808
CSF lactate dehydrogenase level (U/L)	29.65 ± 50.98	24.85 ± 14.25	0.496	0.620
CSF adenosine deaminase level (U/L)	2.49 ± 3.41	2.34 ± 2.63	0.231	0.817
CSF lactic acid level (mmol/L)	2.08 ± 0.70	3.00 ± 0.77	6.651	<0.001
CSF protein level (mg/L)	577.36 ± 373.55	693.60 ± 407.23	1.577	0.116

Single factor analysis of infectious factors after ventriculoperitoneal shunt operation

The patients were divided into non-infection and infection groups, based on the presence of infection after ventriculoperitoneal shunt operation. Chi-square and Fisher exact tests were used to analyze and compare the differences in sex; age; protopathy; and preoperative CSF leukocyte, chloride, glucose, aspartate aminotransferase, lactate dehydrogenase, adenosine deaminase, lactic acid and protein levels between the two groups. There were 28 cases of infection after operation, yielding an infection rate of 7.05% (28/397). The postoperative infection rate of patients with CSF glucose level <2.8 mmol/L ($x^2 = 11.650$, $p = 0.001$) and lactic acid level >2.8 mmol/L ($x^2 = 12.455$, $p<0.001$) was higher than that of patients with CSF glucose level ≥2.8 mmol/L and CSF lactic acid level in the range of (1–2.8) mmol/L, respectively, with statistical difference. There was no significant difference in sex, primary disease, CSF leukocyte, chloride, aspartate aminotransferase, lactate dehydrogenase, adenosine deaminase, and protein levels between infected group and non-infected group (all $p > 0.05$; Table 1).

A Student's *t*-test was used to analyze and compare the differences in age and preoperative CSF leukocyte, chloride, glucose, aspartate aminotransferase, lactate dehydrogenase, adenosine deaminase, lactic acid and protein levels between the non-infection and infection groups. Compared with the non-infection group, the level of CSF glucose ($t = 4.113$, $p < 0.001$) was significantly lower, and the level of CSF lactic acid ($t = 6.651$, $p < 0.001$) was significantly higher in the infection group. There was no significant difference in age, CSF leukocyte level, CSF chloride level, CSF aspartate aminotransferase level, CSF lactate dehydrogenase level, CSF adenosine deaminase level and CSF protein level between infected and non-infected patients (all $p > 0.05$; Table 3).

Multivariate analysis of infectious factors after ventriculoperitoneal shunt operation

The results of univariate analysis showed that there were statistically significant differences in preoperative CSF glucose and lactic acid level. Because of the interaction among preoperative leukocyte, chloride, glucose, aspartate aminotransferase, lactate dehydrogenase, adenosine deaminase, lactic acid and protein levels, CSF indicators were all introduced into binary logistic stepwise regression analyses as independent variables. Multivariate logistic regression analysis showed that preoperative CSF glucose <2.8 mmol/L and CSF lactate >2.8 mmol/L are risk factors for infection after ventriculoperitoneal shunt. Compared with patients with preoperative glucose level in cerebrospinal fluid ≥2.8 mmol/L, patients with glucose level <2.8 mmol/L had a 2.911-fold increased probability of intracranial infection after surgery (OR = 3.911, 95% CI: 1.653∼9.253, $p = 0.002$); Compared with patients with preoperative cerebrospinal fluid lactic acid level of 1–2.8 mmol/L, patients with lactic acid level >2.8 mmol/L had a 3.712-fold increased probability of intracranial infection after surgery (OR = 4.712, 95% CI: 1.892∼11.734, $p = 0.001$; Table 4). Using ROC to understand the effect of these two factors, we found that the area under the curve (AUC) for CSF glucose and lactic acid levels were 0.602 (95% CI: 0.492–0.713) and 0.818 (95% CI: 0.738–0.898), respectively (Figure 1).

The relationship between postoperative body temperature and infection

Postoperative fever of the 397 patients who underwent surgery are shown for different times post-operation in Table 5. Most of the patients had no fever on the day of the surgery, with only 10.6% of patients experiencing fever. The proportion of the patients with a fever was highest on the first day after the surgery, with a rate of 54.9%, though this fever typically gradually decreased over time.

There was no statistically significant difference in the fever rate on the day of surgery, the 1st and the 2nd day after surgery between the non-infection and infection groups (all $p > 0.05$). However, compared to the non-infection group, the fever rate of the infection group was significantly higher on postoperative day 3–7 (all $p < 0.05$; Table 6).

Compared to the non-infection group, patients in the infection group had significantly higher body temperatures on postoperative day 3–7 (all $p < 0.05$). However, there was not a significant difference in body temperature between the non-infection and infection groups on the day of surgery, the 1st and the 2nd days after surgery

10.3389/fneur.2022.1023761

TABLE 4 Multifactor analysis of postoperative infection caused by cerebrospinal fluid parameters before ventriculoperitoneal shunt.

CSF parameters	*B*	SE	Wald	OR	95% CI	*p*-value
CSF leukocyte level ($\times 10^6$/L)						
0–8*						
>8	0.152	0.445	0.116	1.164	0.487∼2.781	0.733
CSF chloride level (mmol/L)						
<120*						
120–130	0.364	0.467	0.607	1.439	0.576∼3.594	0.436
>130	−0.495	1.108	0.199	0.610	0.070∼5.349	0.655
CSF glucose level (mmol/L)						
<2.8	1.364	0.439	9.634	3.911	1.653∼9.253	0.002
≥2.8*						
CSF aspartate aminotransferase level (U/L)						
5–20*						
>20	−0.376	0.614	0.376	0.686	0.206∼2.286	0.540
CSF lactate dehydrogenase level (U/L)						
3–40*						
>40	0.371	0.524	0.501	1.449	0.519∼4.048	0.479
CSF adenosine deaminase level (U/L)						
0–8*						
>8	−0.103	0.699	0.022	0.902	0.229∼3.551	0.883
CSF lactic acid level (mmol/L)						
1–2.8*						
>2.8	1.550	0.466	11.088	4.712	1.892∼11.734	0.001
CSF protein level (mg/L)						
<450*						
450–1,000	−0.019	0.500	0.001	0.981	0.368∼2.614	0.970
>1,000	0.082	0.547	0.022	1.085	0.371∼3.171	0.881
Constant	−3.583	0.527	46.207	0.028		0

*Reference group.

(all $p > 0.05$). The body temperature of the patients in the non-infection group peaked on the first day after surgery and then gradually decreased, dropping below 37.3°C on the 4th day. The body temperature of the patients in the infection group also reached the peak on the first day after surgery, but the subsequent drop was not obvious, and it was always above 37.3°C on the 2nd to 7th days after surgery (Table 7).

Discussion

Many patients with hydrocephalus secondary to cerebral hemorrhage after brain trauma, spontaneous cerebral hemorrhage, brain tumors, cerebral infarction and other diseases, often due to the impact of the primary disease or the impact of surgical procedures taken to treat the primary disease, leading to the occurrence of aseptic inflammation in the ventricular system, resulting in long-term abnormality of routine and biochemical parameters of cerebrospinal fluid (10, 11). A few patients with idiopathic hydrocephalus also have this situation. However, patients with such hydrocephalus often need to be checked for improved CSF indicators through repeated lumbar punctures, external lumbar cistern drainage, and external lateral ventricle drainage, among other, thus missing the best time for operation, ultimately delaying or even aggravating the condition (2, 13, 14). Rammos et al. (15) reported that the average time for external ventricular drainage before the conversion to internal drainage was 14.1 days, though this could sometime last as long as 45 days. Bota et al. (16) reported that the infection rate associated with extraventricular drainage was 0–22%, and the infection rate showed a straight increase between days 3 and 9 after operation. In hydrocephalus, if the central nervous system becomes involved in infection, the treatment becomes very difficult. There are few reports on the safe range of routine and biochemical indicators of cerebrospinal fluid in hydrocephalus patients undergoing ventriculoperitoneal shunt, and most clinicians choose the time of ventriculoperitoneal shunt based on experience. Therefore, this study

10.3389/fneur.2022.1023761

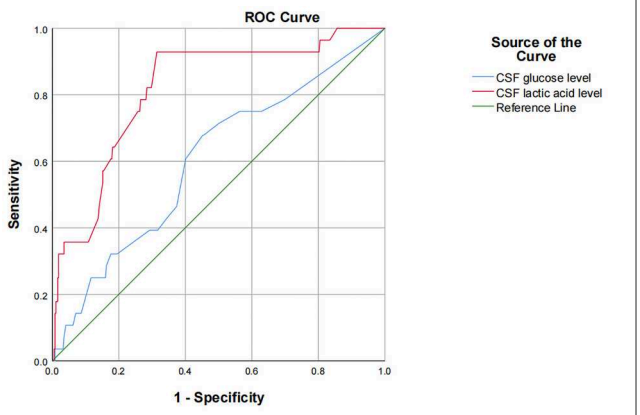

FIGURE 1
Roc curve of cerebrospinal fluid glucose and lactate levels.

retrospectively analyzed the clinical characteristics of 397 patients with hydrocephalus and attempted to summarize the relationship between abnormal preoperative CSF leukocyte, chloride, glucose, aspartate aminotransferase, lactate dehydrogenase, adenosine deaminase, lactic acid and protein levels and postoperative infection after a ventriculoperitoneal shunt to guide appropriate operation time for hydrocephalus patients with abnormal CSF.

The incidence of infection after a ventriculoperitoneal shunt can vary in prevalence, ranging from about 3–12% (16). In our study, 28 of the total 397 patients (7.05%) had postoperative infection, consistent with the reported postoperative infection rate in most international clinical centers. In our study, there was no difference in the CSF leukocyte, chloride, aspartate aminotransferase, lactate dehydrogenase, adenosine deaminase and protein levels between the non-infection and infection groups; however, there were significant differences in CSF glucose and lactic acid levels. Therefore, this study demonstrates that abnormal CSF leukocyte, chloride, aspartate aminotransferase, lactate dehydrogenase, adenosine deaminase and protein levels do not increase the infection rate after ventriculoperitoneal shunt surgery. Due to the presence of aseptic inflammation and the interference of CSF with various indicators, CSF leukocytes, chloride, aspartate aminotransferase, lactate dehydrogenase, adenosine deaminase and proteins could not accurately reflect intracranial infection. Therefore, for hydrocephalus patients with no fever, negative meningeal stimulation, and a negative CSF bacterial culture, if only CSF leucocyte, chloride, aspartate aminotransferase, lactate dehydrogenase, adenosine deaminase and protein levels are abnormal, the ventriculoperitoneal shunt should be performed as early as possible, as avoiding external drainage increases the risk of infection and delays the timing of shunt surgery. The physical properties of normal CSF are similar to that of water. Brydon et al. (17, 18) studied CSF of 126 patients with hydrocephalus of different etiologies and found that its physical properties do not change significantly and are still similar to those of water. Rammos et al. (15) reported that CSF protein levels and RBC counts do not have adverse effects on shunt survival, and therefore, increased protein or RBC counts should not delay the transition of ventriculoperitoneal shunt into ventriculoperitoneal shunt, consistent with the findings of this study.

TABLE 5 Statistical table of postoperative fever.

Group	The day of surgery	The 1st day after surgery	The 2nd day after surgery	The 3rd day after surgery	The 4th day after surgery	The 5th day after surgery	The 6th day after surgery	The 7th day after surgery
Fever	42 (10.6%)	218 (54.9%)	174 (43.8%)	158 (39.8%)	141 (35.5%)	109 (27.5%)	74 (18.6%)	72 (18.1%)
No fever	355 (89.4%)	179 (45.1%)	223 (56.2%)	239 (60.2%)	256 (64.5%)	288 (72.5%)	323 (81.4%)	325 (81.9%)

TABLE 6 Comparison of postoperative fever between the non-infection and infection groups.

Postoperative body temperature	Non-infection group ($n = 247$) n (%)	Infection group ($n = 25$) n (%)	Chi-square	p-value
The day of surgery			0.000	>0.999
No fever	330 (89.4)	25 (89.3)		
Fever	39 (10.6)	2 (10.7)		
The 1st day after surgery			0.410	0.522
No fever	168 (45.5)	11 (39.3)		
Fever	201 (54.5)	17 (60.7)		
The 2nd day after surgery			0.083	0.774
No fever	208 (56.4)	15 (53.6)		
Fever	161 (43.6)	13 (46.4)		
The 3rd day after surgery			7.539	0.006
No fever	229 (62.1)	10 (35.7)		
Fever	140 (37.9)	18 (64.3)		
The 4th day after surgery			8.352	0.004
No fever	245 (66.4)	11 (39.3)		
Fever	124 (33.6)	17 (60.7)		
The 5th day after surgery			7.687	0.006
No fever	274 (74.3)	14 (50.0)		
Fever	95 (25.7)	14 (50.0)		
The 6th day after surgery			24.239	<0.001
No fever	310 (84.0)	13 (46.4)		
Fever	59 (16.0)	15 (53.6)		
The 7th day after surgery			16.242	<0.001
No fever	310 (82.6%)	15 (56%)		
Fever	59 (17.4%)	13 (44%)		

This study showed that CSF glucose below the normal range and CSF lactic acid above the normal range increase the postoperative infection rate. Moreover, multivariate logistic stepwise regression analysis indicates that preoperative CSF glucose <2.8 mmol/L and CSF lactate >2.8 mmol/L are risk factors for infection after ventriculoperitoneal shunt. Compared with patients with preoperative glucose level in cerebrospinal fluid ≥2.8 mmol/L, patients with glucose level <2.8 mmol/L had a 2.911-fold increased probability of intracranial infection after surgery (OR = 3.911, 95% CI: 1.653∼9.253, $p = 0.002$); Compared with patients with preoperative cerebrospinal fluid lactic acid level of 1–2.8 mmol/L, patients with lactic acid level >2.8 mmol/L had a 3.712-fold increased probability of intracranial infection after surgery (OR = 4.712, 95% CI: 1.892∼11.734, $p = 0.001$). Using ROC to understand the effect of these two factors, we found that the area under the curve (AUC) for CSF glucose and lactic acid levels were 0.602 (95% CI: 0.492–0.713) and 0.818 (95% CI: 0.738–0.898), respectively. One possible explanation for this is that it may be difficult to culture pathogenic bacteria from patients with low CSF glucose level or high CSF lactate level due to preoperative empirical, broad-spectrum antibiotic use, even if there is actually an insidious intracranial infection, ultimately leading to a postoperative shunt infection. When hydrocephalus patients with occult intracranial infection are implanted into the ventriculoperitoneal shunt system, the bacteria in the ventricles attach to and proliferate on the ventriculoperitoneal shunt system, and form bacterial biofilms that are difficult to kill by antibiotics (19). Finally, the patients show obvious intracranial infection. CSF glucose content accounts for 1/2∼2/3 of the blood glucose value, mainly because glucose in peripheral serum is transported into cerebrospinal fluid through glucose transporter. In patients with intracranial infection, CSF glucose levels decrease, though the mechanism by which this change occurs in the central nervous system is not fully understood. Intracranial infection increases glycolysis and thus reduces the glucose in CSF. Intracranial infection also affects the function of glucose transporters, thereby reducing the transport of glucose from blood to CSF. The content of lactic acid in cerebrospinal fluid is very low. Most of it is the product of anaerobic fermentation of glucose in cerebrospinal fluid, which is not easily affected by the level of lactic acid in peripheral blood, so lactic acid can accurately reflect the metabolism in the brain (20). The change in CSF glucose and lactic acid content may be more sensitive and specific to the diagnosis of occult intracranial infection. Mrria et al. (21) demonstrated that

TABLE 7 Comparison of postoperative body temperature between the non-infection and infection groups.

Group	Temperature on the day of surgery (°C)	Temperature on the 1st day after surgery (°C)	Temperature on the 2nd day after surgery (°C)	Temperature on the 3rd day after surgery (°C)	Temperature on the 4th day after surgery (°C)	Temperature on the 5th day after surgery (°C)	Temperature on the 6th day after surgery (°C)	Temperature on the 7th day after surgery (°C)
Non-infection group (Mean ± SD)	36.83 ± 0.59	37.64 ± 0.73	37.56 ± 0.60	37.32 ± 0.83	37.27 ± 0.43	37.28 ± 0.64	37.13 ± 0.44	37.13 ± 0.60
Infection group (Mean ± SD)	36.88 ± 0.56	37.98 ± 0.99	37.81 ± 0.70	37.79 ± 0.75	37.79 ± 0.57	37.80 ± 0.87	37.81 ± 0.91	37.81 ± 0.92
T-value	0.439	1.739	1.832	2.872	4.692	3.091	3.946	3.885
p-value	0.661	0.093	0.077	0.004	<0.001	0.004	<0.001	0.001

low glucose content in CSF is of high diagnostic and predictive value for intracranial infections caused by specific bacteria. The change in CSF glucose content is more effective than CSF WBC count for detecting intracranial infection. A prospective study by Pedro Grille et al. (22) showed that CSF glucose and lactic acid had the best diagnostic accuracy for ventriculostomy-related infection, with an AUC of 0.951 and 0.900 ($p = 0.001$), respectively. CSF WBC count and protein level were not able to diagnose ventriculostomy-related infection better than CSF glucose and lactic acid. Tavares et al. (23) conducted a prospective study on 28 neurosurgical patients and found that CSF glucose level is better than leukocyte count and protein index for the diagnosis of intracranial infection. Eduardo et al. (10) found that the sensitivity of 3 mmol/L CSF lactic acid to bacterial meningitis was 95%, the specificity was 94%, and the negative predictive value was 99.3%. A prospective study conducted by Maskin et al. (24) also drew a similar conclusion that the increase of cerebrospinal fluid lactic acid has a better predictive value in the diagnosis of intracranial infection than the increase of the number of cells in cerebrospinal fluid. When the level of CSF lactic acid is ≥4 mmol/L, the sensitivity and specificity of the diagnosis of intracranial infection are 97 and 78% respectively. Two other meta-analyses pointed out that the accuracy of cerebrospinal fluid lactic acid in the diagnosis of intracranial infection was better than other indicators in cerebrospinal fluid (25, 26). Therefore, the content of glucose and lactic acid in cerebrospinal fluid has high diagnostic value for intracranial infection. In this study, when cerebrospinal fluid glucose <2.8 mmol/L, the infection rate was as high as 16.2%, while when cerebrospinal fluid lactic acid >2.8 mmol/L, the infection rate was as high as 20%, both of which were significantly higher than the infection rate of this study of 7.05%. Therefore, it is reasonable to believe that such patients have latent intracranial infection before surgery, leading to infection after ventriculoperitoneal shunt surgery. To sum up, for patients with hydrocephalus without clinical manifestations of intracranial infection such as fever and positive meningeal irritation sign, if their CSF glucose level is <2.8 mmol/L and CSF lactic acid is >2.8 mmol/L, it is recommended to conduct further examination and treatment for the cerebrospinal fluid, and the ventriculoperitoneal shunt should be considered after their CSF glucose and lactic acid content are improved to the normal range.

Many health centers have studied infection risk factors after shunt surgery to better predict the risk of infection and take preventive measures. These risk factors include premature infants, young patients, specific causes of hydrocephalus, postoperative CSF leakage, duration of surgery (9, 27, 28), and previous stream operations, even the largest risk factors (29–31). Therefore, for premature infants, young patients, and patients with previous histories of shunt surgery, more attention should be given to ensure aseptic operating conditions and to reduce the exposure and contact of the shunt system during surgery. Additional measures could include wearing double gloves (28), soaking the shunt tube with antibiotics (32, 33), and limiting the use of perioperative antibiotics (34).

Ventriculoperitoneal shunt surgery is a common neurosurgery and postoperative infection is one of the most serious complications, often leading to failed surgery and sometimes even requiring the removal of the shunt. Early diagnosis and treatment of postoperative infection may prevent the failure of shunt surgery, so it is very important. Fever is one of the main manifestations of infection, but early postoperative fever is also common in neurosurgery (35–37), making infection difficult to distinguish in patients. Understanding

fever trends are important, as the body temperature of non-infected patients tends to decrease over time. In this study, the body temperature of patients without infection after ventriculoperitoneal shunt surgery presented with a single peak in fever the first day after surgery, which then gradually decreased, reaching lower than 37.3°C on the 4th days, and normalizing thereafter. However, the body temperature of infected patients did not decrease significantly over time. Though their temperature also peaked on the first day after surgery, it remained higher than 37.3°C from day 2–7 after surgery. The body temperature of the infected patients was higher than those without infection from day 3–7 after surgery. Unsurprisingly, the fever rate of the infection group from day 3–7 after surgery was significantly higher than that of the non-infection group (64.3 vs. 37.9, 60.7 vs. 33.6, 50.0 vs. 25.7, 53.6 vs. 16.0, 44.0 vs. 17.4%, respectively). The common cause of fever after neurosurgery is usually heat absorption, therefore a physiological fever caused by the liquefaction and necrosis of the tissue and the absorption of this necrotic tissue into the blood, activating neutrophils, eosinophils, and mononuclear macrophage systems to release endogenous pyrogen. Although the trauma of ventriculoperitoneal shunt surgery is small, it changes CSF circulation. Additionally, the shunt system is implanted into the human body, which is actually an indoor surgery. If small amounts of blood or surgical materials are mixed with CSF during the surgery, postoperative fever can occur. As the ventriculoperitoneal shunt drainage accelerates, the CSF circulation increases, meaning that the fever should also subside faster. Thus, fever after ventriculoperitoneal shunt surgery typically subsides faster than other neurosurgeries; the body temperature is generally within normal range by the third day after surgery. If a fever persists after the third day, then the clinician should be notified. When the fever cannot otherwise be explained, a lumbar puncture should be considered so that the CSF can be tested. When combined with other clinical manifestations, such as positive meningeal stimulation, aggravation of consciousness, headache, vomiting, and redness and swelling in the shunt, the prospect of an intracranial infection should be given serious consideration and anti-infection therapies should be utilized.

Post-ventriculoperitoneal shunt infections generally occur within 6 months after surgery (38, 39), with ∼70% diagnosed within a month after surgery and more than 90% diagnosed within 6 months (40). In this study, infections occurred in all 28 infected patients within 6 months after surgery; 10 patients (35.7%) were infected 1 week, 2 patients (7.1%) were infected 2 weeks, 10 patients (35.7%) were infected 1 month, 3 patients (10.7%) were infected 2 months, two patients (7.1%) were infected 4 months, and 1 patient (3.6%) was infected 6 months after surgery, consistent with the infection time reported in the literature. The early onset of infection could be due to the presence of skin or related pathogens during the operation, which could be results from a lack of strict aseptic operating conditions and contamination of the shunt system (41). It could also be due to abnormal CSF before surgery indicating the presence of an occult intracranial infection, leading to the outbreak of an intracranial infection in the early postoperative period. Ventriculoperitoneal shunt infection is the most serious complication of ventriculoperitoneal shunt surgery for hydrocephalus and can prolong the hospital stay, cost more money, and even lead to death. Therefore, once intracranial infection is considered, standardized treatment should be promptly conducted. Of the 25 cases of infection in our study, one case was treated only with antibiotics; 10 cases were treated with antibiotics first and shunts were then removed and ventricular drainage was performed because of poor infection control; and 14 cases were treated by removing the shunts, using extraventricular drainage, and giving systemic antibiotics. The one patient who was only treated with antibiotics died; however, the intracranial infection was resolved in all other cases. During shunt infection, pathogenic bacteria proliferate on the material of the shunt to form a dense "biofilm" that protects the bacteria from being killed by antibodies, leukocytes, and antibiotics (42). Therefore, it is very difficult to treat shunt infection with systemic or intraventricular antibiotics, necessitating the removal of shunt tube (43, 44). Schreffler et al. (45) concluded that the best treatment for intracranial infection is removal of the shunt, external ventricular drainage, and application of antibiotics.

This study is a single-center retrospective study with inherent limitations, meaning that all results need to be verified with multi-center, prospective studies. Ventriculoperitoneal shunt shunts the cerebrospinal fluid in the lateral ventricles, but the cerebrospinal fluid circulation of patients with hydrocephalus is affected, so the cerebrospinal fluid obtained by lumbar puncture may not represent the nature of the cerebrospinal fluid in the lateral ventricles. Therefore, the difference and correlation between cerebrospinal fluid obtained by lumbar puncture and cerebrospinal fluid in lateral ventricle need further prospective study.

Conclusions

For adult hydrocephalus patients without clinical manifestations of intracranial infection but only with simple abnormality of cerebrospinal fluid, when the content of glucose in cerebrospinal fluid is <2.8 mmol/L, and the content of lactic acid is more than 2.8 mmol/L, it is recommended to perform ventriculoperitoneal shunt after further improvement of cerebrospinal fluid indicators, otherwise, hasty operation will increase the postoperative infection rate. The postoperative fever rate of ventriculoperitoneal shunt surgery is high and the body temperature drops rapidly. If there is still fever after day 3 after surgery, whether there is intracranial infection should be considered.

Data availability statement

The raw data supporting the conclusions of this article will be made available by the authors, without undue reservation.

Ethics statement

The studies involving human participants were reviewed and approved by the Ethics Committee of Zhujiang Hospital of Southern Medical University. Written informed consent from the patients/participants or patients/participants' legal guardian/next of kin was not required to participate in this study in accordance with the national legislation and the institutional requirements.

Author contributions

HuZ: conceptualization, methodology, software, validation, formal analysis, investigation, data curation, writing—original

draft, and writing—reviewing and editing. XHe: conceptualization, methodology, formal analysis, and writing—reviewing and editing. LX: investigation and data curation. HoZ and XHo: writing—reviewing and editing. SZ: conceptualization, methodology, resources, writing—reviewing and editing, supervision, and project administration. All authors contributed to the article and approved the submitted version.

Acknowledgments

Sincere appreciation is given to the teachers and colleagues from Zhujiang Hospital of Southern Medical University who participated in this study with great cooperation.

Conflict of interest

The authors declare that the research was conducted in the absence of any commercial or financial relationships that could be construed as a potential conflict of interest.

Publisher's note

References

1. Rekate HL, Aygok GA, Kouzelis K, Klinge PM, Pollay M. Fifth international hydrocephalus workshop, Crete, Greece, May 20–23, 2010: themes and highlights. In: Aygok GA, Rekate HL, editors. *Hydrocephalus. Acta Neurochirurgica Supplementum*. Vienna: Springer Vienna (2012). p. 1–7. doi: 10.1007/978-3-7091-0923-6_1

2. Hochstetler A, Raskin J, Blazer-Yost BL. Hydrocephalus: historical analysis and considerations for treatment. *Eur J Med Res.* (2022) 27:168. doi: 10.1186/s40001-022-00798-6

3. Del Bigio MR. Biological reactions to cerebrospinal fluid shunt devices: a review of the cellular pathology. *Neurosurgery.* (1998) 42:319–26. doi: 10.1097/00006123-199802000-00064

4. Torsnes L, Blåfjelldal V, Poulsen FR. Treatment and clinical outcome in patients with idiopathic normal pressure hydrocephalus: a systematic review. *Dan Med J.* (2014) 61:A4911.

5. Stagno V, Navarrete EA, Mirone G, Esposito F. Management of hydrocephalus around the world. *World Neurosurg.* (2013) 79:S23.e17–20. doi: 10.1016/j.wneu.2012.02.004

6. Sotelo J, Izurieta M, Arriada N. Treatment of hydrocephalus in adults by placement of an open ventricular shunt. *J Neurosurg.* (2001) 94:873–9. doi: 10.3171/jns.2001.94.6.0873

7. Kemaloglu S, Özkan Ü, Bukte Y, Ceviz A, Özates M. Timing of shunt surgery in childhood tuberculous meningitis with hydrocephalus. *Pediatr Neurosurg.* (2002) 37:194–8. doi: 10.1159/000065398

8. Roblot P, Mollier O, Ollivier M, Gallice T, Planchon C, Gimbert E, et al. Communicating chronic hydrocephalus: a review. *Rev Med Interne.* (2021) 42:781–8. doi: 10.1016/j.revmed.2021.05.018

9. McGirt MJ, Zaas A, Fuchs HE, George TM, Kaye K, Sexton DJ. Risk factors for pediatric ventriculoperitoneal shunt infection and predictors of infectious pathogens. *Clin Infect Dis.* (2003) 36:858–62. doi: 10.1086/368191

10. Mekitarian Filho E, Horita SM, Gilio AE, Nigrovic LE. Cerebrospinal fluid lactate level as a diagnostic biomarker for bacterial meningitis in children. *Int J Emerg Med.* (2014) 7:14. doi: 10.1186/1865-1380-7-14

11. Tamune H, Takeya H, Suzuki W, Tagashira Y, Kuki T, Honda H, et al. Cerebrospinal fluid/blood glucose ratio as an indicator for bacterial meningitis. *Am J Emerg Med.* (2014) 32:263–6. doi: 10.1016/j.ajem.2013.11.030

12. Horan TC, Andrus M, Dudeck MA. CDC/NHSN surveillance definition of health care–associated infection and criteria for specific types of infections in the acute care setting. *Am J Infect Control.* (2008) 36:309–32. doi: 10.1016/j.ajic.2008.03.002

13. Yao J, Liu D. Logistic regression analysis of risk factors for intracranial infection after multiple traumatic craniotomy and preventive measures. *J Craniofac Surg.* (2019) 30:1946–8. doi: 10.1097/SCS.0000000000004972

14. López-Amor L, Viña L, Martín L, Calleja C, Rodríguez-García R, Astola I, et al. Infectious complications related to external ventricular shunt. Incidence and risk factors. *Rev Esp Quimioter.* (2017) 30:327–33.

15. Rammos S, Klopfenstein J, Augsburger L, Wang H, Wagenbach A, Poston J, et al. Conversion of external ventricular drains to ventriculoperitoneal shunts after aneurysmal subarachnoid hemorrhage: effects of site and protein/red blood cell counts on shunt infection and malfunction: clinical article. *JNS.* (2008) 109:1001–4. doi: 10.3171/JNS.2008.109.12.1001

16. Bota DP, Lefranc F, Vilallobos HR, Brimioulle S, Vincent J-L. Ventriculostomy-related infections in critically ill patients: a 6-year experience. *J Neurosurg.* (2005) 103:468–72. doi: 10.3171/jns.2005.103.3.0468

17. Brydon HL, Hayward R, Harkness W, Bayston R. Physical properties of cerebrospinal fluid of relevance to shunt function. 1: the effect of protein upon CSF viscosity. *Br J Neurosurg.* (1995) 9:639–44. doi: 10.1080/02688699550040927

18. Brydon HL, Hayward R, Harkness W, Bayston R. Physical properties of cerebrospinal fluid of relevance to shunt function. 2: the effect of protein upon CSF surface tension and contact angle. *Br J Neurosurg.* (1995) 9:645–52. doi: 10.1080/02688699550040936

19. Vl G, Garg K, Tandon V, Borkar SA, Satyarthi GD, Singh M, et al. Effect of topical and intraventricular antibiotics used during ventriculoperitoneal shunt insertion on the rate of shunt infection—a meta-analysis. *Acta Neurochir.* (2022) 164:1793–803. doi: 10.1007/s00701-022-05248-0

20. Begovac J, Baće A, Soldo I, Lehpamer B. Lactate and glucose in cerebrospinal fluid heavily contaminated with blood. *Acta Med Croatica.* (1991) 45:341–5.

21. Karanika M, Vasilopoulou VA, Katsioulis AT, Papastergiou P, Theodoridou MN, Hadjichristodoulou CS. Diagnostic clinical and laboratory findings in response to predetermining bacterial pathogen: data from the meningitis registry. *PLoS ONE.* (2009) 4:e6426. doi: 10.1371/journal.pone.0006426

22. Grille P, Verga F, Biestro A. Diagnosis of ventriculostomy-related infection: is cerebrospinal fluid lactate measurement a useful tool? *J Clin Neurosci.* (2017) 45:243–7. doi: 10.1016/j.jocn.2017.07.031

23. Tavares WM, Machado AG, Matushita H, Plese JPP. CSF markers for diagnosis of bacterial meningitis in neurosurgical postoperative patients. *Arq Neuro-Psiquiatr.* (2006) 64:592–5. doi: 10.1590/S0004-282X2006000400012

24. Maskin LP, Capparelli F, Mora A, Hlavnicka A, Orellana N, Díaz MF, et al. Cerebrospinal fluid lactate in post-neurosurgical bacterial meningitis diagnosis. *Clin Neurol Neurosurg.* (2013) 115:1820–5. doi: 10.1016/j.clineuro.2013.05.034

25. de Almeida SM, Faria FL, de Goes Fontes K, Buczenko GM, Berto DB, Raboni SM, et al. Quantitation of cerebrospinal fluid lactic acid in infectious and non-infectious neurological diseases. *Clin Chem Lab Med.* (2009) 47:755–61. doi: 10.1515/CCLM.2009.160

26. Sakushima K, Hayashino Y, Kawaguchi T, Jackson JL, Fukuhara S. Diagnostic accuracy of cerebrospinal fluid lactate for differentiating bacterial meningitis from aseptic meningitis: a meta-analysis. *J Infect.* (2011) 62:255–62. doi: 10.1016/j.jinf.2011.02.010

27. Simon TD, Butler J, Whitlock KB, Browd SR, Holubkov R, Kestle JRW, et al. Risk factors for first cerebrospinal fluid shunt infection: findings from a multi-center prospective cohort study. *J Pediat.* (2014) 164:1462–8.e2. doi: 10.1016/j.jpeds.2014.02.013

28. Drake JM. Does double gloving prevent cerebrospinal fluid shunt infection? *J Neurosurg Pediat.* (2006) 104:3–4. doi: 10.3171/ped.2006.104.1.3

29. Tuan TJ, Thorell EA, Hamblett NM, Kestle JRW, Rosenfeld M, Simon TD. Treatment and microbiology of repeated cerebrospinal fluid shunt infections in children. *Pediat Infect Dis J.* (2011) 30:731–5. doi: 10.1097/INF.0b013e318218ac0e

30. Simon TD, Hall M, Dean JM, Kestle JRW, Riva-Cambrin J. Reinfection following initial cerebrospinal fluid shunt infection: clinical article. *PED.* (2010) 6:277–85. doi: 10.3171/2010.5.PEDS09457

31. Parker SL, Attenello FJ, Sciubba DM, Garces-Ambrossi GL, Ahn E, Weingart J, et al. Comparison of shunt infection incidence in high-risk subgroups receiving antibiotic-impregnated vs. standard shunts. *Childs Nerv Syst.* (2009) 25:77–83. doi: 10.1007/s00381-008-0743-0

32. Pattavilakom A, Xenos C, Bradfield O, Danks RA. Reduction in shunt infection using antibiotic impregnated CSF shunt catheters: an Australian

prospective study. *J Clin Neurosci.* (2007) 14:526–31. doi: 10.1016/j.jocn.2006.11.003

33. Kuruoglu T, Altun G, Kuruoglu E, Turan DB, Önger ME. Actions of N-acetylcysteine, daptomycin, vancomycin, and linezolid on methicillin-resistant *Staphylococcus aureus* biofilms in the ventriculoperitoneal shunt infections: an experimental study. *Chin Neurosurg J.* (2022) 8:15. doi: 10.1186/s41016-022-00284-2

34. Biyani N, Grisaru-Soen G, Steinbok P, Sgouros S, Constantini S. Prophylactic antibiotics in pediatric shunt surgery. *Childs Nerv Syst.* (2006) 22:1465–71. doi: 10.1007/s00381-006-0120-9

35. Halvorson K, Shah S, Fehnel C, Thompson B, Stevenson Potter N, Levy M, et al. Procalcitonin is a poor predictor of non-infectious fever in the neurocritical care unit. *Neurocrit Care.* (2017) 27:237–41. doi: 10.1007/s12028-016-0337-8

36. Wang Z, Shen M, Qiao M, Zhang H, Tang Z. Clinical factors and incidence of prolonged fever in neurosurgical patients. *J Clin Nurs.* (2017) 26:411–7. doi: 10.1111/jocn.13409

37. de Kunder SL, ter Laak-Poort MP, Nicolai J, Vles JSH, Cornips EMJ. Fever after intraventricular neuroendoscopic procedures in children. *Childs Nerv Syst.* (2016) 32:1049–55. doi: 10.1007/s00381-016-3085-3

38. Jung YT, Lee SP, Cho JI. An improved one-stage operation of cranioplasty and ventriculoperitoneal shunt in patient with hydrocephalus and large cranial defect. *Kor J Neurotrauma.* (2015) 11:93. doi: 10.13004/kjnt.2015.11.2.93

39. Raffa G, Marseglia L, Gitto E, Germanò A. Antibiotic-impregnated catheters reduce ventriculoperitoneal shunt infection rate in high-risk newborns and infants. *Childs Nerv Syst.* (2015) 31:1129–38. doi: 10.1007/s00381-015-2685-7

40. Choux M, Genitori L, Lang D, Lena G. Shunt implantation: reducing the incidence of shunt infection. *J Neurosurg.* (1992) 77:875–80. doi: 10.3171/jns.1992.77.6.0875

41. Bir S, Sapkota S, Maiti T, Konar S, Bollam P, Nanda A. Evaluation of ventriculoperitoneal shunt-related complications in intracranial meningioma with hydrocephalus. *J Neurol Surg B.* (2016) 78:030–6. doi: 10.1055/s-0036-1584309

42. Brydon HL, Bayston R, Hayward R, Harkness W. Reduced bacterial adhesion to hydrocephalus shunt catheters mediated by cerebrospinal fluid proteins. *J Neurol Neurosurg Psychiatry.* (1996) 60:671–5. doi: 10.1136/jnnp.60.6.671

43. Vajramani GV, Jones G, Bayston R, Gray WP. Persistent and intractable ventriculitis due to retained ventricular catheters. *Br J Neurosurg.* (2005) 19:496–501. doi: 10.1080/02688690500495299

44. Tunkel AR, Hartman BJ, Kaplan SL, Kaufman BA, Roos KL, Scheld WM, et al. Practice guidelines for the management of bacterial meningitis. *Clin Infect Dis.* (2004) 39:1267–84. doi: 10.1086/425368

45. Schreffler RT, Schreffler AJ, Wittler RR. Treatment of cerebrospinal fluid shunt infections: a decision analysis. *Pediat Infect Dis J.* (2002) 21:632–6. doi: 10.1097/00006454-200207000-00006

frontiers | Frontiers in Neurology

TYPE Original Research
PUBLISHED 10 March 2023
DOI 10.3389/fneur.2023.1125674

OPEN ACCESS

EDITED BY
Wael M. Y. Mohamed,
International Islamic University Malaysia, Malaysia

REVIEWED BY
Pengfei Wang,
Weihai Municipal Hospital, China
Kyle Walsh,
University of Cincinnati, United States

*CORRESPONDENCE
Suijun Zhu
✉ chaolinaweiminfu@126.com

SPECIALTY SECTION
This article was submitted to Neurological Biomarkers, a section of the journal Frontiers in Neurology

RECEIVED 16 December 2022
ACCEPTED 20 February 2023
PUBLISHED 10 March 2023

CITATION
Li W, Lv X, Ma Y, Cai Y and Zhu S (2023) Prognostic significance of serum NLRC4 in patients with acute supratentorial intracerebral hemorrhage: A prospective longitudinal cohort study. *Front. Neurol.* 14:1125674. doi: 10.3389/fneur.2023.1125674

Prognostic significance of serum NLRC4 in patients with acute supratentorial intracerebral hemorrhage: A prospective longitudinal cohort study

Wei Li[1,2], Xuan Lv[1,2], Yijun Ma[1,2], Yong Cai[1,2] and Suijun Zhu[1,2]*

[1]Department of Neurosurgery, First People's Hospital of Linping District, Hangzhou, China, [2]Department of Neurosurgery, Linping Campus, The Second Affiliated Hospital of Zhejiang University School of Medicine, Hangzhou, China

Objective: Caspase activation and recruitment domain-containing protein 4 (NLRC4) is implicated in neuroinflammation. The aim of the study was to discern the potential ability of serum NLRC4 in assessment of prognosis after intracerebral hemorrhage (ICH).

Methods: In this prospective, observational study, serum NLRC4 levels were quantified in 148 acute supratentorial ICH patients and 148 controls. Severity was evaluated using the National Institutes of Health Stroke Scale (NIHSS) and hematoma volume, and poststroke 6-month functional outcome was estimated according to the modified Rankin Scale (mRS). Early neurologic deterioration (END) and 6-month poor outcome (mRS 3–6) were deemed as the two prognostic parameters. Multivariate models were established for investigating associations, and receiver operating characteristic (ROC) curves were configured to indicate predictive capability.

Results: Patients had substantially higher serum NLRC4 levels than controls (median, 363.2 pg/ml vs. 74.7 pg/ml). Serum NLRC4 levels had independent correlation with NIHSS scores [β, 0.308; 95% confidence interval (CI), 0.088–0.520], hematoma volume (β, 0.527; 95% CI, 0.385–0.675), serum C-reactive protein levels (β, 0.288; 95% CI, 0.109–0.341) and 6-month mRS scores (β, 0.239; 95% CI, 0.100–0.474). Serum NLRC4 levels above 363.2 pg/ml were independently predictive of END (odds ratio, 3.148; 95% CI, 1.278–7.752) and 6-month poor outcome (odds ratio, 2.468; 95% CI, 1.036–5.878). Serum NLRC4 levels significantly distinguished END risk [area under ROC curve (AUC), 0.765; 95% CI, 0.685–0.846] and 6-month poor outcome (AUC, 0.795; 95% CI, 0.721–0.870). In terms of predictive ability for 6-month poor outcome, serum NLRC4 levels combined with NIHSS scores and hematoma volume was superior to NIHSS scores combined with hematoma volume, NIHSS scores and hematoma volume (AUC, 0.913 vs. 0.870, 0.864 and 0.835; all $P < 0.05$). Nomograms were built to reflect prognosis and END risk of combination models, where serum NLRC4, NIHSS scores and hematoma volume were enforced. Calibration curves confirmed stability of combination models.

Conclusions: Markedly raised **s**erum NLRC4 levels following ICH, in close relation to illness severity, are independently associated with poor prognosis. Such results are indicative of the notion that determination of serum NLRC4 may aid in severity assessment and prediction of functional outcome of ICH patients.

KEYWORDS

intracerebral hemorrhage, early neurologic deterioration, outcome, prognosis, severity, biomarkers, NLRC4

1. Introduction

Spontaneous intracerebral hemorrhage (ICH) is one of the commonest lethal stroke subtypes (1). Its pathologic mechanisms mainly include hypertensive arteriopathy and cerebral amyloid angiopathy (2). ICH ranks second in order of stroke incidence, but it leads to a highest percentage of stroke mortality (3). Its poor prognosis is not only correlated with extent of initial hemorrhagic brain injury, but also with occurrence of some in-hospital adverse affairs, such as early neurologic deterioration (END) (4). Thus, it is equally paramount to discriminate patients at risk of either poor prognosis or END in clinical work of ICH (5). During recent decades, some biomarkers have been increasingly noted in neuroscience field with respect to prognostic predictive ability in ICH (6).

ICH-induced secondary brain injury is a harmful factor, thereby worsening neurological function and even resulting in death of patients (7). Neuroinflammation plays an essential role in occurrence and development of secondary brain injury (8). The inflammasome, which is identified as a part of the innate immune system, can cleave pro-caspase-1 to form caspase-1, which subsequently induces pro-interleukin-1beta and pro-interleukin-18 to mature, afterwards transforming into interleukin-1beta and interleukin-18, and finally leading to inflammatory reaction (9). Caspase activation and recruitment domain-containing protein 4 (NLRC4) is expressed in brain tissues and can mediate sterile inflammasome activation in microglia and astrocytes (10). NLRC4 inflammasome contributes to acute brain injury *via* involvement in neuroinflammation and its inhibition could obviously attenuate brain injury, subsequently improving neurological function of rats with ICH or ischemic stroke (11, 12). Hence, it is postulated that NLRC4 may be a biomarker of acute brain injury. In this study, we measured serum NLRC4 levels in a cohort of ICH patients and further strived to explore its prognostic role in human ICH.

TABLE 1 Baseline characteristics between controls and patients with acute supratentorial intracerebral hemorrhage.

Components	Controls	Patients	*P* value
Age (years)	61.2 ± 15.2	60.6 ± 13.0	0.645
Gender (male/female)	78/70	94/54	0.059
BMI (kg/m^2)	24.7 ± 4.1	25.5 ± 3.5	0.077
Cigarette smoking	50 (33.8%)	54 (36.5%)	0.626
Alcohol drinking	47 (31.8%)	61 (41.2%)	0.091

Data were shown as frequency (proportion), mean ± standard deviation or median (percentiles 25th-75th) as appropriate. The Chi-square test, Fisher exact test, Student's *t*-test or Mann-Whitney test was in use for intergroup comparisons. BMI means body mass index.

Abbreviations: END, early neurologic deterioration; ICH, intracerebral hemorrhage; NIHSS, National Institutes of Health Stroke Scale; ROC, receiver operating characteristic; mRS, modified Rankin scale; NLRC4, caspase activation and recruitment domain-containing protein 4.

2. Materials and methods

2.1. Participant enrollment

In this prospective, observational, cohort study, we consecutively enrolled patients with non-traumatic supratentorial ICH, who were initially admitted for treatment to our hospital between January 2018 to April 2021. Criteria for participation in the current study included age equal to or above 18 years, voluntary consent to participate in this study, definite verification of the first-time stroke, conservative treatment of hematoma, and hospital admission within the first 24 h after symptom development. Exclusion criteria were as follows: secondary ICH, primary intraventricular hemorrhage, oncopathologies of extra-cerebral and cerebral location, and some specific or severe diseases

TABLE 2 Factors in relation to serum caspase activation and recruitment domain-containing protein 4 levels following acute intracerebral hemorrhage.

Variables	ρ	*P* value
Age (y)	0.067	0.418
Gender (male/female)	−0.096	0.246
BMI (kg/m^2)	0.050	0.546
Hypertension	−0.014	0.870
DM	0.015	0.856
Hyperlipidemia	−0.027	0.748
Coronary heart disease	−0.011	0.897
Cigarette smoking	0.008	0.927
Alcohol drinking	−0.054	0.513
Prior usage of statins	−0.007	0.932
Prior usage of anticoagulants	0.100	0.229
Prior usage of antiplatelet agents	0.060	0.468
Admission time (h)	−0.006	0.945
Blood-collection time (h)	−0.043	0.600
SAP (mmHg)	−0.030	0.721
DAP (mmHg)	−0.063	0.450
MAP (mmHg)	−0.037	0.658
Lobar hemorrhage	0.028	0.738
IVH	0.165	0.046
SAH	0.114	0.169
NIHSS scores	0.568	<0.001
Hematoma volume (ml)	0.519	<0.001
Serum CRP levels (mg/l)	0.546	<0.001
Blood leucocyte count (×109/l)	0.168	0.041
Blood glucose levels (mmol/l)	0.210	0.010

Via the Spearman's correlation coefficient test, correlations were summarized as ρ values. NIHSS denotes National Institutes of Health Stroke Scale; CRP, C-reactive protein; SAH, subarachnoid hemorrhage; IVH, intraventricular hemorrhage; SAP, systolic arterial pressure; DAP, diastolic arterial pressure; MAP, mean arterial pressure; BMI, body mass index; DM, diabetes mellitus.

in the medical history, such as moderate-severe head trauma, and severe cardiac hepatic pulmonary or renal dysfunction. Between April 2020 and April 2021, a group of physical examinees were recruited as controls at our hospital. The study complied with the tenets of the Declaration of Helsinki and was implemented with the approval of the ethics committee at our hospital. Written informed consent for participation in the study was obtained from patients' proxies or controls themselves.

2.2. Data obtainment

Upon arrival at emergency room, we inquired about patients' demographics, complaints, medical history, and medication history, as well as checked patients' vital signs. All patients underwent neurological examination with a supplementary assessment of the severity of neurological deficit according to the National Institutes of Health Stroke Scale (NIHSS). Immediate head computerized tomography (CT) scans were accomplished and The ICH diagnosis was established based on CT images. Bleeding size was calculated in accordance with $0.5 \times A \times B \times C$ formula, where A, B, C are the main maximum dimensions of the hemorrhagic focus measured in three projections (13). Supratentorial hematomas included cerebral lobar and deep ones. Subarachnoidal or intraventricular hematoma was determined on the initial head CT images. END was deemed as an increase of $\geq$4 in the NIHSS score or death within 24 h after hospitalization (14). Patients were followed up until death or the completion of poststroke 6 months and assessment of 6-month neurological functional status was fulfilled utilizing modified Rankin scale (mRS). In terms of mRS score, scores 3–6 indicated a worse outcome (15).

2.3. Immune analysis

Venous blood samples, which were collected from patients and controls, were immediately put in 5 ml gel-containing biochemistry tubes, and then were centrifuged within half an hour. Obtained serum was placed in Eppendorf tubes and preserved at −80°C until analysis. Frozen serum samples were thawed, and afterwards serum NLRC4 levels were in duplicate determined using an enzyme-linked immunosorbent assay kit according to the manufacturer's instruction manual (SinoGeneclon Biotech, HangZhou, China). Two results were averaged for final statistical analysis.

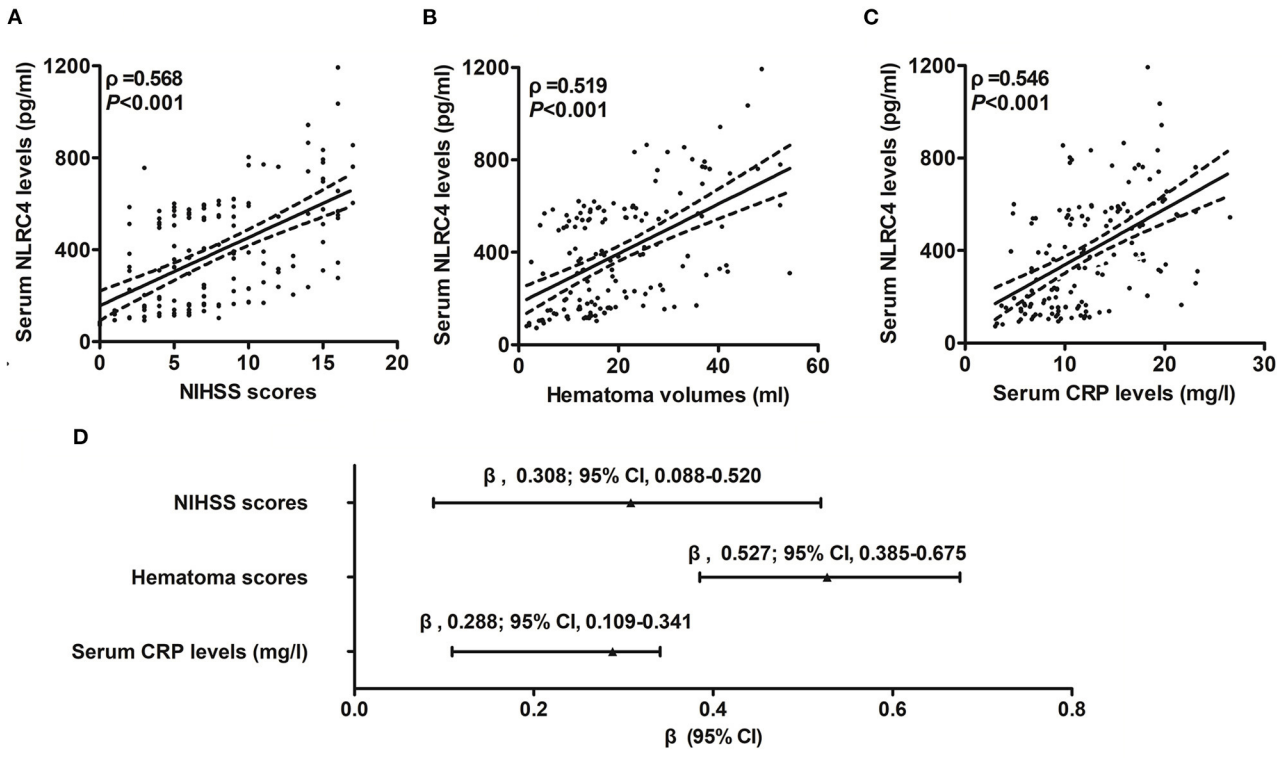

FIGURE 1
Correlation of serum caspase activation and recruitment domain-containing protein 4 levels with hemorrhagic severity and degree of inflammatory response after acute intracerebral hemorrhage. **(A)** Serum caspase activation and recruitment domain-containing protein 4 levels in correlation with National Institutes of Health Stroke Scale score. **(B)** Serum caspase activation and recruitment domain-containing protein 4 levels in correlation with hematoma volume. **(C)** Serum caspase activation and recruitment domain-containing protein 4 levels in correlation with serum C-reactive protein levels. **(D)** Multivariate results correlated with serum caspase activation and recruitment domain-containing protein 4 levels. Serum caspase activation and recruitment domain-containing protein 4 levels were closely correlated with National Institutes of Health Stroke Scale score, hematoma volume and serum C-reactive protein levels (all $P < 0.05$). NLRC4 indicates caspase activation and recruitment domain-containing protein 4; NIHSS, National Institutes of Health Stroke Scale; 95% CI, 95% confidence interval; CRP, C-reactive protein.

2.4. Statistical analysis

The data were statistically analyzed using Statistical Package for the Social Sciences 19.0 (SPSS Inc., Chicago, IL, USA), MedCalc 9.6.4.0 (MedCalc Software, Mariakerke, Belgium) and R software (version 3.5.1; https://www.r-project.org). The Kolmogorov-Smirnov test was done to check normality of distribution of quantitative data. Mean (standard deviation) was given for normally-distributed data, while median (25th and 75th percentiles) was reported for those non-normally-distributed data. To compare the two samples, non-normally distributed continuous variables were assessed by the non-parametric Mann-Whitney U test, normally distributed continuous variables were assessed by the independent-sample *t* test, and categorical variables were assessed by the Chi-square tests or Fisher's exact test where appropriate. To compare the multiple samples, the Kruskal-Wallis test was utilized. The interconnection of the parameters was investigated using the Spearman test and then two multivariate linear regression models were built, where serum NLRC4 levels and mRS scores were regarded as the two independent variables. In addition, two binary logistic regression models were established, where END and 6-month poor prognosis were considered as the two independent variables. To investigate the predictive performance, area under receiver operating characteristic curve (AUC) was employed. A cutoff threshold was selected to yield the maximum Youden index. Nomograms and its calibration curve were plotted for analyzing discriminatory efficiency and stability of models. *P* values <0.05 were designated as statistically significance.

3. Results

3.1. Participant selection and characteristics

Initially, a total of 198 supratentorial ICH patients fitted inclusion criteria, and then 50 patients were excluded because of secondary ICH (12 cases), primary intraventricular hemorrhage (8 cases), oncopathologies of extra-cerebral and cerebral location (10 cases), some specific or severe diseases in the medical history (15 cases), loss to follow-up (2 cases), unavailable blood samples (2 cases) and incomplete clinical data (1 case). Eventually, 148 patients

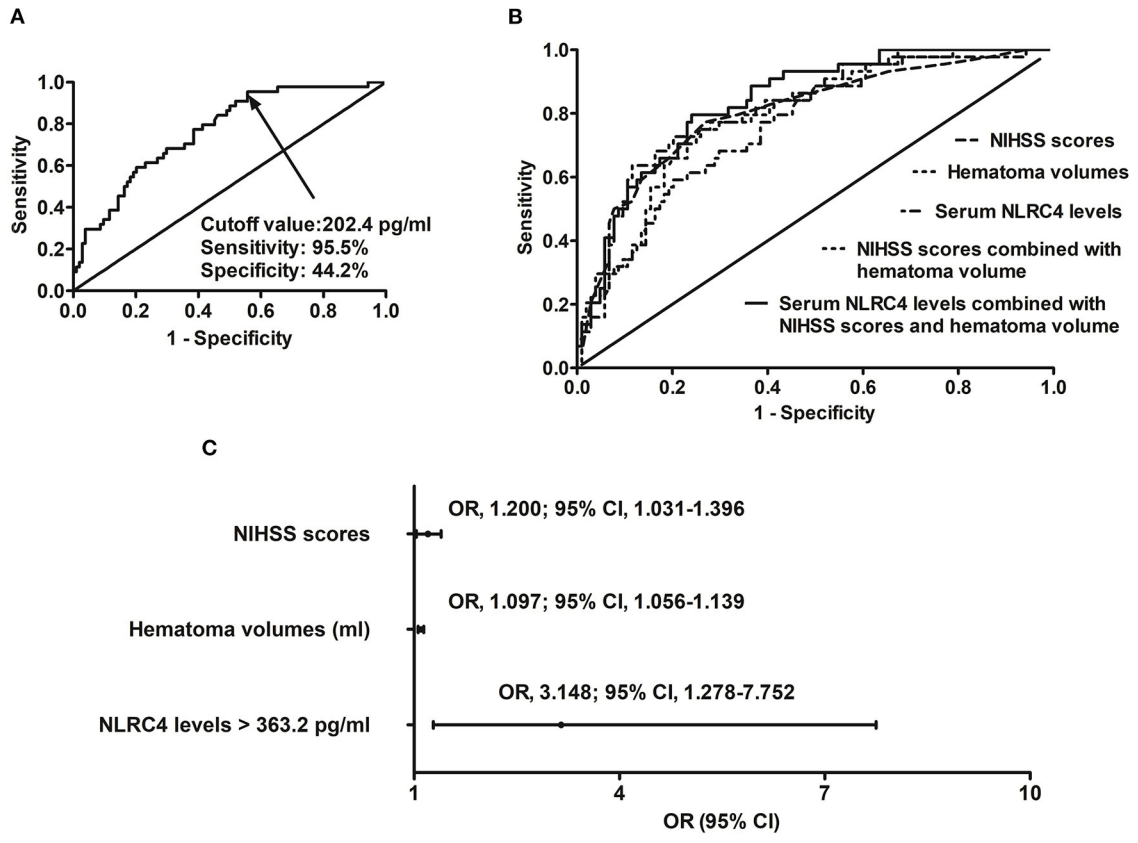

FIGURE 2
Relationship between serum caspase activation and recruitment domain-containing protein 4 levels and risk of early neurologic deterioration after intracerebral hemorrhage. **(A)** Discriminatory ability concerning serum caspase activation and recruitment domain-containing protein 4 levels for early neurologic deterioration. **(B)** Comparison of distinguishable ability of various variables for early neurologic deterioration. **(C)** Multivariate results associated with early neurologic deterioration. Serum caspase activation and recruitment domain-containing protein 4 levels were independently predictive of early neurologic deterioration and were in possession of high predictive performance for early neurologic deterioration (all $P < 0.05$). NLRC4 indicates caspase activation and recruitment domain-containing protein 4; NIHSS, National Institutes of Health Stroke Scale; 95% CI, 95% confidence interval; OR, odds ratio; END, early neurologic deterioration.

were investigated for further analysis. Alternatively, 148 controls were recruited. Table 1 shows that age, gender, body mass index, alcohol drinking and cigarette smoking did not significantly differ between patients and controls (all $P > 0.05$).

Among this cohort of ICH patients, the investigated chronic diseases included hypertension (93 cases), diabetes mellitus (33

TABLE 3 Factors in relation to early neurologic deterioration following acute intracerebral hemorrhage.

Variables	Presence of END	Absence of END	*P* value
Age (y)	59.4 ± 13.7	61.1 ± 12.7	0.491
Gender (male/female)	29/15	65/39	0.694
BMI (kg/m^2)	25.3 ± 3.0	25.5 ± 3.7	0.661
Hypertension	30 (68.2%)	63 (60.6%)	0.382
DM	16 (36.4%)	17 (16.4%)	0.007
Hyperlipidemia	13 (29.6%)	33 (31.7%)	0.793
Coronary heart disease	4 (9.1%)	11 (10.6%)	0.784
Cigarette smoking	18 (40.9%)	36 (34.6%)	0.467
Alcohol drinking	22 (50.0%)	39 (37.5%)	0.158
Prior usage of statins	12 (27.3%)	21 (20.2%)	0.344
Prior usage of anticoagulants	3 (6.8%)	7 (6.7%)	0.985
Prior usage of antiplatelet agents	7 (15.9%)	14 (13.5%)	0.697
Admission time (h)	9.7 (6.3–15.1)	10.9 (7.3–14.7)	0.405
Blood-collection time (h)	11.9 (7.4–16.9)	12.2 (9.0–16.6)	0.554
SAP (mmHg)	141.5 ± 20.9	149.4 ± 25.2	0.070
DAP (mmHg)	83.6 ± 9.4	87.1 ± 11.5	0.074
MAP (mmHg)	102.9 ± 12.6	107.8 ± 15.7	0.064
Lobar hemorrhage	12 (27.3%)	31 (29.8%)	0.756
IVH	14 (31.8%)	27 (26.0%)	0.467
SAH	7 (15.9%)	6 (5.8%)	0.059
NIHSS scores	13 (9–15)	6 (4–9)	<0.001
Hematoma volume (ml)	27 (19–37)	14 (10–20)	<0.001
Serum CRP levels (mg/l)	16.6 (11.9–19.2)	10.1 (7.1–13.3)	<0.001
Blood leucocyte count (×109/l)	8.6 (6.8–11.3)	8.4 (6.2–10.2)	0.243
Blood glucose levels (mmol/l)	14.0 (10.8–18.0)	11.0 (8.6–13.6)	<0.001
NLRC4 levels > 363.2 pg/ml	34 (77.3%)	40 (38.5%)	<0.001

Data were presented as frequency (proportion), mean ± standard deviation or median (upper-lower quartiles). Data were compared using the Chi-square test, Fisher exact test, Student's *t*-test or Mann-Whitney test. NIHSS denotes National Institutes of Health Stroke Scale; CRP, C-reactive protein; NLRC4, caspase activation and recruitment domain-containing protein 4; SAH, subarachnoid hemorrhage; IVH, intraventricular hemorrhage; SAP, systolic arterial pressure; DAP, diastolic arterial pressure; MAP, mean arterial pressure; BMI, body mass index; DM, diabetes mellitus; END, early neurologic deterioration.

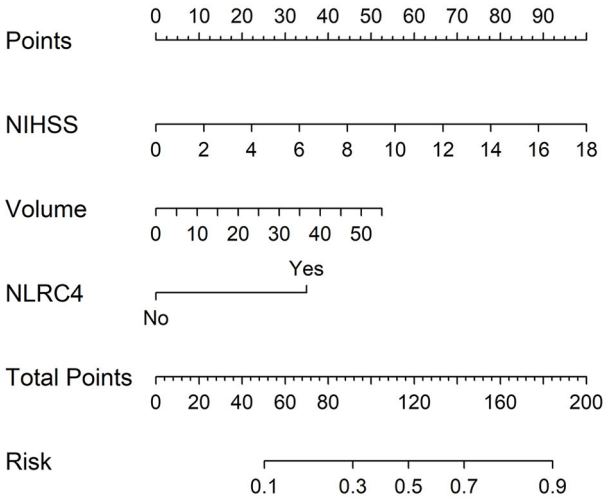

FIGURE 3
Nomogram for predicting early neurologic deterioration after acute intracerebral hemorrhage. Combination model contained serum caspase activation and recruitment domain-containing protein 4 levels, National Institutes of Health Stroke Scale scores and hematoma volume. Nomogram showed predictive risk assessment. NLRC4 indicates serum caspase activation and recruitment domain-containing protein 4 levels >363.2 pg/ml; NIHSS, National Institutes of Health Stroke Scale; END, early neurologic deterioration.

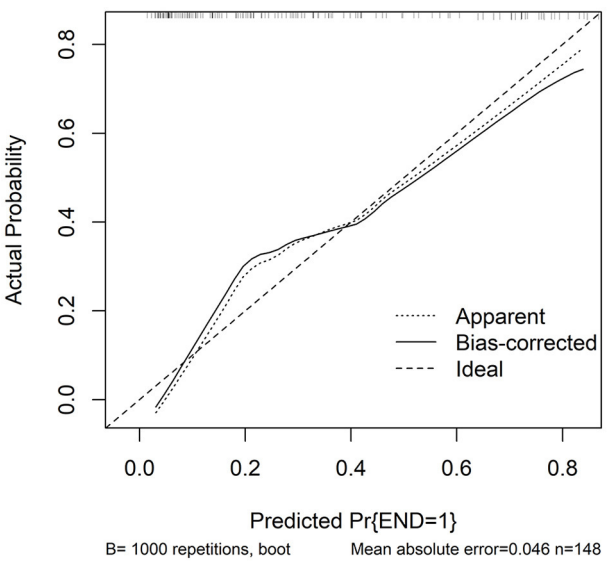

FIGURE 4
Calibration curve in prediction of early neurologic deterioration. Combination model contained serum caspase activation and recruitment domain-containing protein 4 levels, National Institutes of Health Stroke Scale scores and hematoma volume. Calibration curve displayed that such a combination model had stability to medium-high extent. NLRC4 indicates serum caspase activation and recruitment domain-containing protein 4 levels >363.2 pg/ml; NIHSS, National Institutes of Health Stroke Scale; END, early neurologic deterioration.

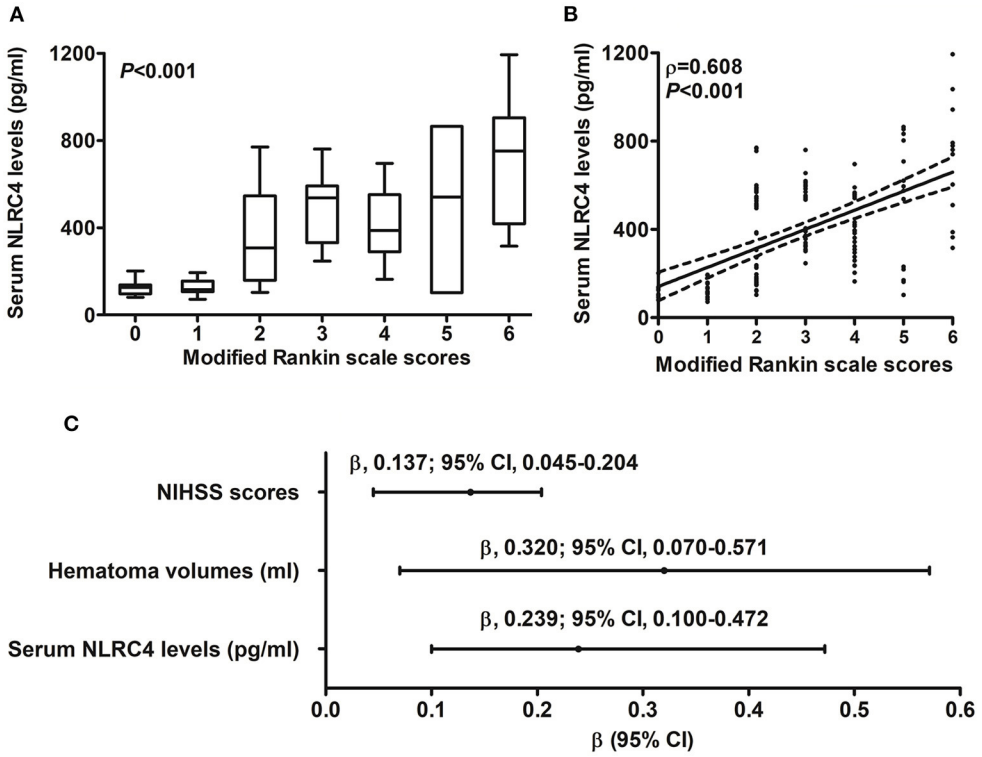

FIGURE 5
Relationship between serum caspase activation and recruitment domain-containing protein 4 levels and 6-month modified Rankin scale scores after intracerebral hemorrhage. **(A)** Serum caspase activation and recruitment domain-containing protein 4 levels among subgroups divided by modified Rankin scale scores. **(B)** Serum caspase activation and recruitment domain-containing protein 4 levels in correlation to modified Rankin scale scores. **(C)** Multivariate analysis correlated with modified Rankin scale scores. Serum caspase activation and recruitment domain-containing protein 4 levels were strongly correlated with modified Rankin scale scores, which was whether identified as the categorical or continuous variable (all $P < 0.05$). NLRC4 indicates caspase activation and recruitment domain-containing protein 4; NIHSS, National Institutes of Health Stroke Scale; 95% CI, 95% confidence interval.

cases), hyperlipidemia (46 cases) and coronary heart disease (15 cases); the collected specific medications included statins (33 cases), anticoagulants (10 cases) and antiplatelet agents (21 cases). As regards radiological characteristics, lobar hematoma accounted for 29.1% (43/148) of all supratentorial hemorrhage, 43 patients had intraventricular hematoma and 13 patients had subarachnoid hematoma. In addition, NIHSS scores ranged from 0 to 17 (median, 6; lower-upper quartiles, 4–11) and hematoma ranged from 3 to 55 ml (median, 17 ml; lower-upper quartiles, 12–27 ml). Admission time since symptom onset varied from 0.5 to 24.0 h (median, 10.6 h; percentiles 25th−75th, 7.0–14.7 h).

3.2. Serum NLRC4 levels and disease severity

Serum NLRC4 levels of ICH patients ranged from 72.0 to 1,193.5 pg/ml (median, 363.2 pg/ml; percentiles 25th−75th, 163.2–568.4 pg/ml) and those of controls ranged from 10.1 to 319.6 pg/ml (median, 74.7 pg/ml; percentiles 25th−75th, 33.5–95.0 pg/ml). By statistical analysis, ICH patients displayed substantially higher serum NLRC4 levels than controls ($P < 0.001$). In Table 2, besides NIHSS scores (Figure 1A), hematoma volume (Figure 1B) and serum C-reactive protein levels (Figure 1C), intraventricular hemorrhage, blood glucose levels and blood leucocyte count were all highly related to serum NLRC4 levels (all $P < 0.05$). The above-mentioned six significantly correlated variables were incorporated into the multivariate linear regression model and subsequently it was revealed that NIHSS scores, hematoma volume and serum C-reactive protein levels retained to be in independently correlation with serum NLRC4 levels (all $P < 0.05$; Figure 1D).

3.3. Serum NLRC4 levels and development of END

A total of 44 ICH patients experienced END. In patients with development of END, serum NLRC4 levels ranged from 102.6 to 1,193.5 pg/ml (median, 561.2 pg/ml; percentiles 25th−75th, 368.2–748.6 pg/ml); in those with no END risk, they ranged from 72.0 to 854.4 pg/ml (median, 260.4 pg/ml; percentiles 25th−75th, 148.8–523.7 pg/ml). By statistical analysis, END patients exhibited profoundly higher admission serum NLRC4 levels than non-END patients ($P < 0.001$). A cutoff value of serum NLRC4 levels, namely 202.4 pg/ml, was chosen, which predicted END

TABLE 4 Factors in relation to modified Rankin scale scores at 6 months following acute intracerebral hemorrhage.

Variables	ρ	*P* value
Age (y)	0.131	0.113
Gender (male/female)	−0.079	0.339
BMI (kg/m^2)	−0.072	0.387
Hypertension	0.067	0.415
DM	0.162	0.049
Hyperlipidemia	0.012	0.883
Coronary heart disease	−0.119	0.150
Cigarette smoking	−0.077	0.351
Alcohol drinking	0.074	0.368
Prior usage of statins	0.092	0.268
Prior usage of anticoagulants	0.049	0.554
Prior usage of antiplatelet agents	0.012	0.887
Admission time (h)	−0.105	0.206
Blood-collection time (h)	−0.080	0.331
SAP (mmHg)	0.027	0.746
DAP (mmHg)	0.042	0.609
MAP (mmHg)	0.035	0.670
Lobar hemorrhage	−0.073	0.378
IVH	0.242	0.003
SAH	0.122	0.141
NIHSS scores	0.714	<0.001
Hematoma volume (ml)	0.657	<0.001
Serum CRP levels (mg/l)	0.422	<0.001
Blood leucocyte count (×109/l)	0.147	0.075
Blood glucose levels (mmol/l)	0.263	0.001
Serum NLRC4 levels (pg/ml)	0.608	<0.001

Bivariate correlations were performed by the Spearman's correlation coefficient test. NIHSS denotes National Institutes of Health Stroke Scale; CRP, C-reactive protein; NLRC4, caspase activation and recruitment domain-containing protein 4; SAH, subarachnoid hemorrhage; IVH, intraventricular hemorrhage; SAP, systolic arterial pressure; DAP, diastolic arterial pressure; MAP, mean arterial pressure; BMI, body mass index; DM, diabetes mellitus.

with maximum Youden index (Figure 2A). Under ROC curve (Figure 2B), serum NLRC4 levels (AUC, 0.765; 95% CI, 0.685–0.846) had insignificantly lower predictive ability than NIHSS scores (AUC, 0.802; 95% CI, 0.722–0.882; $P = 0.464$) and hematoma volume (AUC, 0.791; 95% CI, 0.715–0.866; $P = 0.590$), and serum NLRC4 levels combined with NIHSS scores and hematoma volume (AUC, 0.835; 95% CI, 0.769–0.901) displayed insignificantly higher predictive capability than NIHSS scores ($P = 0.125$), hematoma volume ($P = 0.116$), and NIHSS scores combined with hematoma volume (AUC, 0.810; 95% CI, 0.734–0.885; $P = 0.170$).

In accordance with median value of serum NLRC4 levels (i.e., 363.2 pg/ml), serum NLRC4 levels were considered as the categorical variable. Table 3 displays that, in comparison to patients without development of END, END patients tended to have significantly raised proportions of diabetes mellitus and NLRC4 levels >363.2 pg/ml, and were prone to possess substantially elevated NIHSS scores, hematoma volume, blood glucose levels and serum C-reactive protein levels (all $P < 0.01$). When the preceding significant variables were entered into the binary logistic regression model, NIHSS score, hematoma volume and NLRC4 levels >363.2 pg/ml were the three independent predictors of END (all $P < 0.05$; Figure 2C). In Figure 3, a nomogram, which contained NIHSS scores, hematoma volume and NLRC4 levels >363.2 pg/ml, was established to predict END risk. In Figure 4, its calibration curve showed this model had medium-high stability.

3.4. Serum NLRC4 levels and experience of 6-month poor prognosis

When serum mRS score was regarded as the categorial variable, serum NRLC4 levels were substantially lowest in patients with mRS score 0, followed by patients with mRS scores 1, 2, 3, 4 and 5 in order of ascending serum NRLC4 levels, and were significantly highest in patients with mRS score 6 ($P < 0.001$; Figure 5A). When serum mRS score was deemed as the continuous variable, serum NRLC4 levels had significantly positively correlation with mRS scores ($P < 0.001$; Figure 5B). In Table 4, besides serum NRLC4 levels, other variables highly correlated with mRS scores referred to diabetes mellitus, intraventricular hemorrhage, NIHSS scores, hematoma volume, serum C-reactive protein levels and blood glucose levels (all $P < 0.05$). The multivariate linear regression model, which contained the aforementioned variables, showed that serum NRLC4 levels, NIHSS scores and hematoma volume were remained independently correlated with mRS scores (all $P < 0.05$; Figure 5C).

In patients with possibility of poor prognosis, serum NLRC4 levels ranged from 102.6 to 1,193.5 pg/ml (median, 535.7 pg/ml; percentiles 25th−75th, 324.2–603.8 pg/ml); in those at no risk of poor prognosis, they ranged from 72.0 to 770.8 pg/ml (median, 163.2 pg/ml; percentiles 25th−75th, 124.2–505.6 pg/ml). By statistical analysis, as compared to patients with good prognosis, those with poor prognosis showed substantially enhanced serum NRLC4 levels ($P < 0.001$). Under ROC curve, serum NRLC4 levels >229.8 pg/ml discriminated patients at risk of poor prognosis with maximum Youden index (Figure 6A). In Figure 6B, the prognostic predictive efficiency of serum NRLC4 levels (AUC, 0.795; 95% CI, 0.721–0.870) was equivalent to those of NIHSS scores(AUC, 0.864; 95% CI, 0.808–0.920; $P = 0.096$) and hematoma volume (AUC, 0.835; 95% CI, 0.771–0.900; $P = 0.349$); and serum NRLC4 levels combined with NIHSS scores and hematoma volume (AUC, 0.913; 95% CI, 0.869–0.956) had substantially higher prognostic predictive ability than NIHSS scores ($P = 0.008$), hematoma volume ($P = 0.002$) and combination of NIHSS scores and hematoma volume (AUC, 0.870; 95% CI, 0.816–0.925; $P = 0.018$).

Just as listed in Table 5, patients with poor prognosis, in comparison to other remainders, were likely to show markedly rising percentage of NLRC4 levels >363.2 pg/ml ($P < 0.05$), and were prone to display substantially increased NIHSS scores,

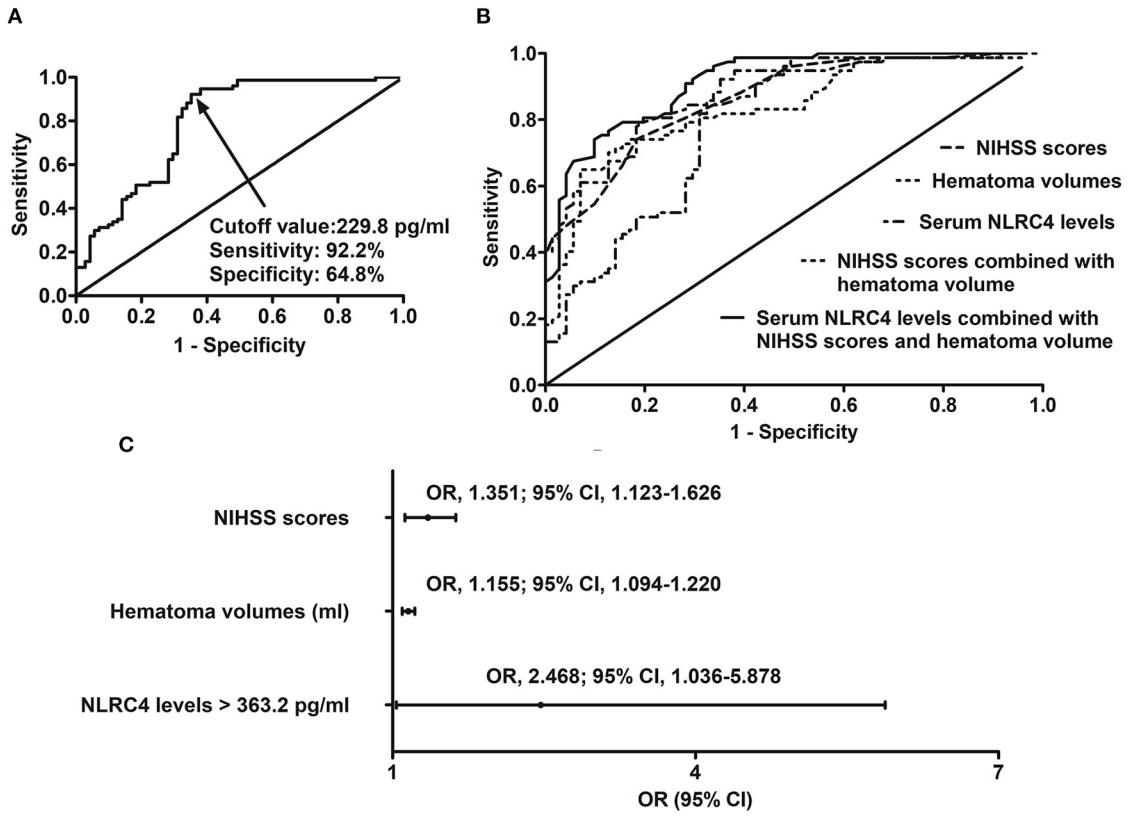

FIGURE 6
Relation of serum caspase activation and recruitment domain-containing protein 4 levels to poor 6-month prognosis after intracerebral hemorrhage. **(A)** Predictive value of serum caspase activation and recruitment domain-containing protein 4 levels for poor prognosis. **(B)** Comparison of predictive ability of various variables for poor prognosis. **(C)** Multivariate results associated with poor prognosis. Serum caspase activation and recruitment domain-containing protein 4 levels were independently predictive of poor prognosis and were in possession of high predictive power for poor prognosis (all $P < 0.05$). NLRC4 indicates caspase activation and recruitment domain-containing protein 4; NIHSS, National Institutes of Health Stroke Scale; 95% CI, 95% confidence interval; OR, odds ratio.

hematoma volume, blood leucocyte count and serum C-reactive protein levels (all $P < 0.05$). The binary logistic regression model, which included the above variables, demonstrated that the factors independently associated with poor prognosis were NIHSS scores, hematoma volume and NLRC4 levels >363.2 pg/ml (all $P < 0.05$; Figure 6C). NIHSS scores, hematoma volume and NLRC4 levels >363.2 pg/ml were combined to differentiate between good prognosis and poor prognosis, whose predictive ability was indicated by a nomogram (Figure 7). In addition, the configured calibration curve confirmed that there is a medium-high stability for such a model (Figure 8).

4. Discussion

To the best of our knowledge, this is a first series for enrolling a medium sample size of supratentorial ICH patients, and further investigating whether there is a significant elevation of serum NLRC4 levels following ICH, and whether serum NLRC4 acts as an inflammatory biomarker, which is in possession of a prognostic significance in ICH. The main findings of the current study were that (1) serum NLRC4 levels were markedly higher in ICH patients than in controls; (2) serum NLRC4 levels had independent correlation with admission serum C-reactive protein levels, NIHSS scores, hematoma volume and END, as well as 6-month mRS scores and poor prognosis following ICH; and (3) in terms of prognostic predictive ability, combination of serum NLRC4 levels with NIHSS scores and hematoma volume had significantly higher AUC than NIHSS scores, hematoma volume and combination of NIHSS scores with hematoma volume. In a word, determination of serum NLRC4 may be of clinical significance to ICH severity assessment and prognostic prediction.

The pathophysiological processes of acute brain injury caused by ICH are very complicated (1). Besides primary brain injury which is directly induced by hematoma, secondary brain injury is complex, referring to oxidation, neuroinflammation, apoptosis and autophagy (7). Compelling data have demonstrated that secondary brain injury is a crucial factor in the aggravation of neurological dysfunction following ICH (16). Neuroinflammation, an essential participant of secondary brain injury, leads to disruption of the blood-brain barrier and massive neuronal cell death, including apoptosis and necrosis, finally impairing neurological function, and even resulting in death of ICH patients (17).

The nucleotide-binding and oligomerization domain-like receptor family, intracellular innate immune sensors, responds to innate immunity by forming inflammasomes (18). NLRC4

TABLE 5 Factors in relation to 6-month worse outcome following acute intracerebral hemorrhage.

Variables	mRS 3–6	mRS 0–2	*P* value
Age (y)	61.7 ± 13.5	59.3 ± 12.4	0.271
Gender (male/female)	45/32	49/22	0.182
BMI (kg/m^2)	25.1 ± 3.3	25.8 ± 3.8	0.225
Hypertension	51 (66.2%)	42 (59.2%)	0.373
DM	21 (22.3%)	12 (16.9%)	0.130
Hyperlipidemia	26 (33.8%)	20 (28.2%)	0.462
Coronary heart disease	7 (9.1%)	8 (11.3%)	0.661
Cigarette smoking	24 (31.2%)	30 (42.3%)	0.162
Alcohol drinking	38 (49.4%)	23 (32.4%)	0.036
Prior usage of statins	19 (24.7%)	14 (19.7%)	0.469
Prior usage of anticoagulants	7 (9.1%)	3 (4.2%)	0.331
Prior usage of antiplatelet agents	12 (15.6%)	9 (12.7%)	0.612
Admission time (h)	9.8 (6.9–13.8)	11.4 (7.5–15.4)	0.159
Blood-collection time (h)	11.9 (9.1–15.8)	12.9 (8.7–17.5)	0.305
SAP (mmHg)	148.0 ± 24.6	146.0 ± 24.0	0.617
DAP (mmHg)	86.7 ± 11.2	85.3 ± 10.8	0.449
MAP (mmHg)	107.1 ± 15.1	105.5 ± 14.8	0.520
Lobar hemorrhage	24 (31.2%)	19 (26.8%)	0.555
IVH	25 (32.5%)	16 (22.5%)	0.177
SAH	8 (10.4%)	5 (7.0%)	0.472
NIHSS scores	10 (7–15)	4 (3–7)	<0.001
Hematoma volume (ml)	24 (17–35)	13 (8–16)	<0.001
Serum CRP levels (mg/l)	13.8 (10.5–18.5)	9.3 (6.7–12.0)	<0.001
Blood leucocyte count (×10^9/l)	9.1 (7.1–11.3)	7.8 (5.9–9.9)	0.015
Blood glucose levels (mmol/l)	12.4 (9.5–15.6)	11.0 (9.3–12.8)	0.115
NLRC4 levels > 363.2 pg/ml	52 (67.5%)	22 (31.0%)	<0.001

Data were presented as frequency (proportion), mean ± standard deviation or median (upper-lower quartiles). Data were compared using the Chi-square test, Fisher exact test, Student's *t*-test or Mann-Whitney test. NIHSS denotes National Institutes of Health Stroke Scale; CRP, C-reactive protein; NLRC4, caspase activation and recruitment domain-containing protein 4; mRS, modified Rankin scale; SAH, subarachnoid hemorrhage; IVH, intraventricular hemorrhage; SAP, systolic arterial pressure; DAP, diastolic arterial pressure; MAP, mean arterial pressure; BMI, body mass index; DM, diabetes mellitus.

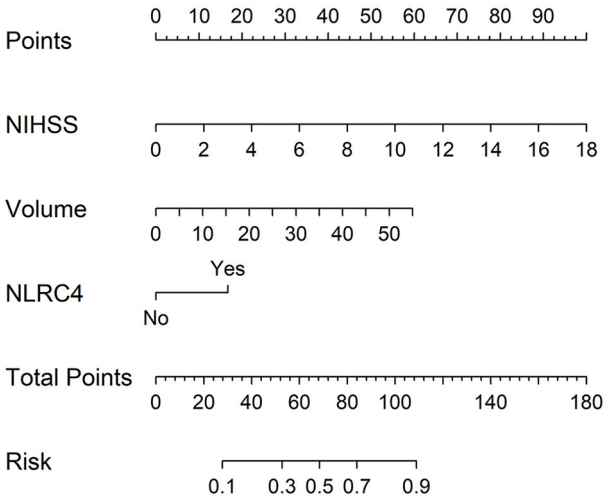

FIGURE 7
Nomogram for predicting poor 6-month prognosis after acute intracerebral hemorrhage. Combination model contained serum caspase activation and recruitment domain-containing protein 4 levels, National Institutes of Health Stroke Scale scores and hematoma volume. Nomogram showed predictive risk assessment. NLRC4 indicates serum caspase activation and recruitment domain-containing protein 4 levels >363.2 pg/ml; NIHSS, National Institutes of Health Stroke Scale.

is a member of them and is responsible to process pro-interleukin-1beta and pro-interleukin-18 into a maturation state to promote inflammation (19). A previous experimental study showed that NLRC4 expressions were enhanced in a time-dependent manner following ICH, and peaked at 24 h following ICH (20). Another animal study demonstrated that there was a substantial upregulation of NLRC4 expressions after cerebral ischemia and NLRC4 was mainly localized in neurons (21). NLRC4 could mediate sterile inflammasome activation in microglia and astrocytes (22). Also, NLRC4 substantially enhanced the release of interleukin-1beta and interleukin-18, increased accumulation of microglia, led to neuronal death, damaged blood–brain barrier permeability, and aggravated brain edema of rats with ICH (12). Our study found serum NLRC4 levels were markedly higher in ICH patients than in controls, and moreover elevated NLRC4 levels were independently correlated with serum C-reactive protein levels after ICH. Such findings were supportive of the notion that at least a portion of NLRC4 in peripheral blood of ICH patients may stem from ICH-injured brain tissues, and NLRC4 may be involved in neuroinflammation after ICH. In addition, increased peripheral inflammation, which may be induced *via* neuroimmune interaction, is implicated in pathophysiological processes after ICH and may be highly related to poor prognosis after ICH (23, 24). NLRC4 is responsible to process pro-interleukin-1beta and pro-interleukin-18 into a maturation state to promote inflammation (19). Besides production from cells in central nervous system (21, 22), NLRC4 may be derived from peripheral cells (25, 26). Thus, NLRC4 may participate in inflammatory response after ICH *via* central and peripheral pathways. Moreover, NLRC4 has potential to be a therapeutic target of ICH.

Up to date, it has remained unclear that whether serum NLRC4 levels are correlated with hemorrhagic severity and prognosis after ICH. Using the four multivariate regression models, we revealed the close relationship between serum NLRC4 levels and NIHSS scores, hematoma volume, 6-month mRS scores, END in addition to 6-month poor prognosis after human ICH. More intriguingly, serum NLRC4 levels combined with NIHSS scores and hematoma volume had significantly higher prognostic predictive ability, but not substantially higher END predictive ability, than

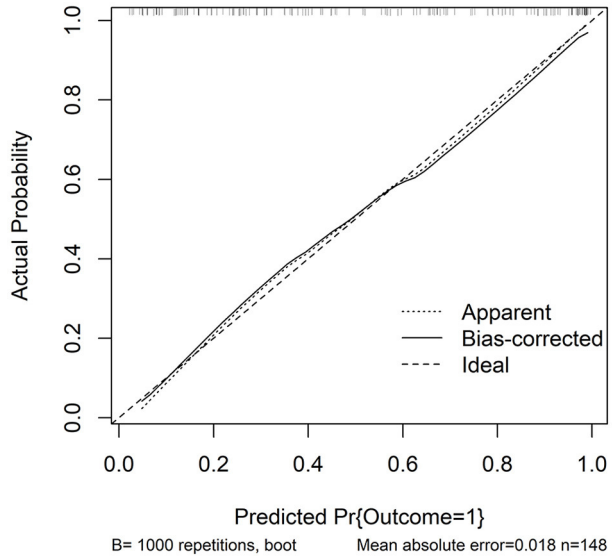

FIGURE 8
Calibration curve for predicting poor 6-month prognosis after acute intracerebral hemorrhage. Combination model contained serum caspase activation and recruitment domain-containing protein 4 levels, National Institutes of Health Stroke Scale scores and hematoma volume. Calibration curve displayed that such a combination model had stability to medium-high extent. NLRC4 indicates serum caspase activation and recruitment domain-containing protein 4 levels >363.2 pg/ml; NIHSS, National Institutes of Health Stroke Scale.

NIHSS scores, hematoma volume, and combination of NIHSS scores with hematoma volume. Furthermore, the nomogram using combination model was configured to aid in predicting the risk of 6-month poor prognosis and further the built calibration curve showed the stable predictive capability for 6-month poor prognosis after ICH. In consideration of the intimate relation of serum NLRC4 levels to illness severity and long-term poor prognosis, serum NLRC4 may be a promising biochemical marker, which can have the potential to be predictive of worse clinical outcome following acute ICH.

Strengths of our study are that (1) relationships between serum NLRC4 levels and severity plus clinical outcome after ICH were all verified by multivariate analysis; and (2) we only enrolled patients with supratentorial ICH and therefore there is a high homogeneity of data, thereby leading to more scientific and reliable conclusions. Weaknesses of the current study are that (1) a single-center study was undertaken and hence a larger cohort study was warranted to validate the conclusions; (2) although a prospective study was performed to investigate association of serum NLRC4 levels with prognosis, its correlation with serum C-reactive protein levels was determined using only a cross-sectional study; and its effect-cause relationship is still unclear and needs to be further verified; (3) clearly, other proteins related to NLRP1, NLRP3, NLRC4 and AIM2 may be involved in inflammatory role of ICH. This study was designed to investigate prognostic role of serum NLRC4 in ICH. Admittedly, a further study is warranted for determining prognostic roles of other serum proteins in ICH; (4) the aim of this study was to ascertain role of serum NLRC4 as a prognostic biomarker in ICH. Mechanisms pertaining to poor outcome and END may involve its participation in inflammatory reaction. Because some patients would die after admitted into hospital, only admission serum NLRC4 levels can predict risk of poor prognosis and END of all patients. Possibly, to investigating dynamic change of serum NLRC levels would provide some new information; (5) we have made us of calibration curve to validate the stability of such a model. If a separate independent validation is done, it is more perfect.

5. Conclusions

To the best of our knowledge, our study, for the first time, found that (1) serum NLRC4 levels, which are statistically significantly elevated after ICH, are correlated independently positively with the intensity of neurological symptoms, hemorrhagic focus volume and extent of peripheral inflammation in ICH patients; (2) serum NLRC4 is an independent predictor of END and 6-month poor prognosis; and (3) when combined with NIHSS scores and hematoma volume, serum NLRC4 is in possession of high prognostic predictive ability. Such data indicate that determination of serum NLRC4, which is identified as an inflammatory biomarker, may be in clinical use for objectification of ICH patients' state and, along with NIHSS scores and hematoma volume, may be allowed to efficiently predict functional outcome after ICH onset.

Data availability statement

The raw data supporting the conclusions of this article will be made available by the authors, without undue reservation.

Ethics statement

The studies involving human participants were reviewed and approved by First People's Hospital of Linping District. The patients/participants provided their written informed consent to participate in this study.

Author contributions

All authors listed have made a substantial, direct, and intellectual contribution to the work and approved it for publication.

Acknowledgments

We thank all study participants, their relatives, and the staffs at the recruitment centers for their invaluable contributions.

Conflict of interest

The authors declare that the research was conducted in the absence of any commercial or financial relationships that could be construed as a potential conflict of interest.

Publisher's note

References

1. Qureshi AI, Tuhrim S, Broderick JP, Batjer HH, Hondo H, Hanley DF. Spontaneous intracerebral hemorrhage. *N Engl J Med.* (2001) 344:1450–60. doi: 10.1056/NEJM200105103441907

2. Sheth KN. Spontaneous intracerebral hemorrhage. *N Engl J Med.* (2022) 387:1589–96. doi: 10.1056/NEJMra2201449

3. Sansing LH. Intracerebral hemorrhage. *Semin Neurol.* (2016) 36:223–4. doi: 10.1055/s-0036-1583296

4. You S, Zheng D, Delcourt C, Sato S, Cao Y, Zhang S, et al. Determinants of early versus delayed neurological deterioration in intracerebral hemorrhage. *Stroke.* (2019) 50:1409–14. doi: 10.1161/STROKEAHA.118.024403

5. Law ZK, Dineen R, England TJ, Cala L, Mistri AK, Appleton JP, et al. Predictors and outcomes of neurological deterioration in intracerebral hemorrhage: results from the TICH-2 randomized controlled trial. *Transl Stroke Res.* (2021) 12:275–83. doi: 10.1007/s12975-020-00845-6

6. Müller M, Tapia-Perez JH, Yildiz C, Rashidi A, Luchtmann M. Alterations in inflammatory markers and clinical outcome after spontaneous intracerebral hemorrhage—preliminary results. *J Stroke Cerebrovasc Dis.* (2020) 29:104861. doi: 10.1016/j.jstrokecerebrovasdis.2020.104861

7. Zhu H, Wang Z, Yu J, Yang X, He F, Liu Z, et al. Role and mechanisms of cytokines in the secondary brain injury after intracerebral hemorrhage. *Prog Neurobiol.* (2019) 178:101610. doi: 10.1016/j.pneurobio.2019.03.003

8. Aronowski J, Zhao X. Molecular pathophysiology of cerebral hemorrhage: secondary brain injury. *Stroke.* (2011) 42:1781–6. doi: 10.1161/STROKEAHA.110.596718

9. Pandey A, Shen C, Feng S, Man SM. Cell biology of inflammasome activation. *Trends Cell Biol.* (2021) 31:924–39. doi: 10.1016/j.tcb.2021.06.010

10. Duncan JA, Canna SW. The NLRC4 inflammasome. *Immunol Rev.* (2018) 281:115–23. doi: 10.1111/imr.12607

11. Poh L, Kang SW, Baik SH, Ng GYQ, She DT, Balaganapathy P, et al. Evidence that NLRC4 inflammasome mediates apoptotic and pyroptotic microglial death following ischemic stroke. *Brain Behav Immun.* (2019) 75:34–47. doi: 10.1016/j.bbi.2018.09.001

12. Gan H, Zhang L, Chen H, Xiao H, Wang L, Zhai X, et al. The pivotal role of the NLRC4 inflammasome in neuroinflammation after intracerebral hemorrhage in rats. *Exp Mol Med.* (2021) 53:1807–18. doi: 10.1038/s12276-021-00702-y

13. Kothari RU, Brott T, Broderick JP, Barsan WG, Sauerbeck LR, Zuccarello M, et al. The ABCs of measuring intracerebral hemorrhage volumes. *Stroke.* (1996) 27:1304–5. doi: 10.1161/01.str.27.8.1304

14. Specogna AV, Turin TC, Patten SB, Hill MD. Factors associated with early deterioration after spontaneous intracerebral hemorrhage: a systematic review and meta-analysis. *PLoS ONE.* (2014) 9:e96743. doi: 10.1371/journal.pone.0096743

15. Sreekrishnan A, Dearborn JL, Greer DM, Shi FD, Hwang DY, Leasure AC, et al. Intracerebral hemorrhage location and functional outcomes of patients: a systematic literature review and meta-analysis. *Neurocrit Care.* (2016) 25:384–91. doi: 10.1007/s12028-016-0276-4

16. Nobleza COS. Intracerebral hemorrhage. *Continuum (Minneap Minn).* (2021) 27:1246–77. doi: 10.1212/CON.0000000000001018

17. Kashif H, Shah D, Sukumari-Ramesh S. Dysregulation of microRNA and intracerebral hemorrhage: roles in neuroinflammation. *Int J Mol Sci.* (2021) 22:8115. doi: 10.3390/ijms22158115

18. Leissinger M, Kulkarni R, Zemans RL, Downey GP, Jeyaseelan S. Investigating the role of nucleotide-binding oligomerization domain-like receptors in bacterial lung infection. *Am J Respir Crit Care Med.* (2014) 189:1461–8. doi: 10.1164/rccm.201311-2103PP

19. Sundaram B, Kanneganti TD. Advances in understanding activation and function of the NLRC4 inflammasome. *Int J Mol Sci.* (2021) 22:1048. doi: 10.3390/ijms22031048

20. Jin P, Qi D, Cui Y, Lenahan C, Zhang JH, Tao X, et al. Aprepitant attenuates NLRC4-dependent neuronal pyroptosis via NK1R/PKCδ pathway in a mouse model of intracerebral hemorrhage. *J Neuroinflammation.* (2022) 19:198. doi: 10.1186/s12974-022-02558-z

21. Habib P, Harms J, Zendedel A, Beyer C, Slowik A. Gonadal hormones E2 and P mitigate cerebral ischemia-induced upregulation of the AIM2 and NLRC4 inflammasomes in rats. *Int J Mol Sci.* (2020) 21:4795. doi: 10.3390/ijms21134795

22. Freeman L, Guo H, David CN, Brickey WJ, Jha S, Ting JP, et al. members NLRC4 and NLRP3 mediate sterile inflammasome activation in microglia and astrocytes. *J Exp Med.* (2017) 214:1351–70. doi: 10.1084/jem.20150237

23. Jiang C, Wang Y, Hu Q, Shou J, Zhu L, Tian N, et al. Immune changes in peripheral blood and hematoma of patients with intracerebral hemorrhage. *FASEB J.* (2020) 34:2774–91. doi: 10.1096/fj.201902478R

24. Walsh KB, Zhang X, Zhu X, Wohleb E, Woo D, Lu L, et al. Intracerebral hemorrhage induces inflammatory gene expression in peripheral blood: global transcriptional profiling in intracerebral hemorrhage patients. *DNA Cell Biol.* (2019) 38:660–9. doi: 10.1089/dna.2018.4550

25. Souza COS, Ketelut-Carneiro N, Milanezi CM, Faccioli LH, Gardinassi LG, Silva JS. NLRC4 inhibits NLRP3 inflammasome and abrogates effective antifungal CD8+ T cell responses. *iScience.* (2021) 24:102548. doi: 10.1016/j.isci.2021.102548

26. Fusco WG, Duncan JA. Novel aspects of the assembly and activation of inflammasomes with focus on the NLRC4 inflammasome. *Int Immunol.* (2018) 30:183–93. doi: 10.1093/intimm/dxy009

frontiers | Frontiers in Neurology

TYPE Original Research
PUBLISHED 05 April 2023
DOI 10.3389/fneur.2023.1139598

OPEN ACCESS

EDITED BY
Wael M. Y. Mohamed,
International Islamic University Malaysia, Malaysia

REVIEWED BY
Dorota Zyśko,
Wroclaw Medical University, Poland
Alessandro Orlando,
Trauma Research LLC, United States

*CORRESPONDENCE
Wang Maofeng
✉ wzmcwmf@163.com

†These authors have contributed equally to this work

SPECIALTY SECTION
This article was submitted to Neurological Biomarkers, a section of the journal Frontiers in Neurology

RECEIVED 07 January 2023
ACCEPTED 06 March 2023
PUBLISHED 05 April 2023

CITATION
Jianling Q, Lulu J, Liuyi Q, Lanfang F, Xu M, Wenchen L and Maofeng W (2023) A nomogram for predicting the risk of pulmonary embolism in neurology department suspected PE patients: A 10-year retrospective analysis. *Front. Neurol.* 14:1139598. doi: 10.3389/fneur.2023.1139598

A nomogram for predicting the risk of pulmonary embolism in neurology department suspected PE patients: A 10-year retrospective analysis

Qiang Jianling[1†], Jin Lulu[1†], Qiu Liuyi[2], Feng Lanfang[3], Ma Xu[4], Li Wenchen[5] and Wang Maofeng[1*]

[1]Department of Biomedical Sciences Laboratory, Affiliated Dongyang Hospital of Wenzhou Medical University, Dongyang, Zhejiang, China, [2]Department of Pathology, Affiliated Dongyang Hospital of Wenzhou Medical University, Dongyang, Zhejiang, China, [3]Department of Respiratory, Affiliated Dongyang Hospital of Wenzhou Medical University, Dongyang, Zhejiang, China, [4]Department of Vascular Surgery, Affiliated Dongyang Hospital of Wenzhou Medical University, Dongyang, Zhejiang, China, [5]Department of Neurology, Affiliated Dongyang Hospital of Wenzhou Medical University, Dongyang, Zhejiang, China

Objective: The purpose of this retrospective study was to establish a numerical model for predicting the risk of pulmonary embolism (PE) in neurology department patients.

Methods: A total of 1,578 subjects with suspected PE at the neurology department from January 2012 to December 2021 were considered for enrollment in our retrospective study. The patients were randomly divided into the training cohort and the validation cohort in the ratio of 7:3. The least absolute shrinkage and selection operator regression were used to select the optimal predictive features. Multivariate logistic regression was used to establish the numerical model, and this model was visualized by a nomogram. The model performance was assessed and validated by discrimination, calibration, and clinical utility.

Results: Our predictive model indicated that eight variables, namely, age, pulse, systolic pressure, hemoglobin, neutrophil count, low-density lipoprotein, D-dimer, and partial pressure of oxygen, were associated with PE. The area under the receiver operating characteristic curve of the model was 0.750 [95% confidence interval (CI): 0.721–0.783] in the training cohort and 0.742 (95% CI: 0.689–0.787) in the validation cohort, indicating that the model showed a good differential performance. A good consistency between the prediction and the real observation was presented in the training and validation cohorts. The decision curve analysis in the training and validation cohorts showed that the numerical model had a good net clinical benefit.

Conclusion: We established a novel numerical model to predict the risk factors for PE in neurology department suspected PE patients. Our findings may help doctors to develop individualized treatment plans and PE prevention strategies.

KEYWORDS

pulmonary embolism, neurology department, retrospective analysis, risk assessment models, nomogram

Introduction

Pulmonary embolism (PE) is a fatal cardiovascular disorder that remains a challenge to doctors during clinical diagnosis and treatment. Approximately 300,000 people die from PE every year in the United States of America, which ranks PE high among the causes of cardio-cerebrovascular mortality (1). This is especially true in elderly patients as it is hard to distinguish their symptoms of PE from other mild illnesses (2). The proportion of elderly patients in neurology departments cannot be neglected; the characteristics of these neurology department patients include aging, being bedridden for a long term, and presenting many concomitant diseases. These elderly patients are prone to lower extremity deep vein thrombosis and to develop PE (3). The presence of PE is a risk factor for stroke, cerebral infraction, and transient ischemic attack (4–6). Furthermore, PE-related death accounts for 20–25% of early deaths in stroke patients (7). Therefore, timely and accurate diagnosis of PE is crucial for the prognosis of neurology department patients.

Computed tomography pulmonary angiography (CTPA) is recommended for the diagnosis and risk-level assessment of PE (8–10). However, CTPA is time-consuming and expensive and can even cause serious side effects in patients. Therefore, it would be convenient to have a simple and fast risk prediction model to predict the probability of PE occurrence. Many researchers had created a variety of risk assessment models (RAMs) to predict PE, and their usability has been continuously validated. Robert-Ebadi et al. verified the feasibility of the simplified Geneva score in the clinic in 2017 (11). Freund et al. explored the safety of the PE rule-out criteria with a randomized clinical trial in 2018 (12). In addition, in 2019, van der Pol et al. assessed whether a pregnancy-adapted algorithm could help pregnant women avoid the imaging diagnosis for safety reasons (13). Furthermore, Kirsch et al. (14) demonstrated the ability of the Wells score to predict PE, which indicated that a Wells score above 4 was associated with PE; however, the performance of the Wells score was unreliable.

There have been many debates regarding the use of these RAMs; however, there are no consensual methods to diagnose PE. Currently, a RAM specifically for use with neurology department patients has not been developed. In recent years, we published a number of articles related to PE (15–17), and on this basis, we wanted to develop a numerical model that could rapidly determine the risk of PE in neurology department patients.

The numerical model (18, 19) is a graphical description of data, which presents the regression model in an accessible way, thus simplifying the risk assessment, providing a user-friendly interface for medical practitioners to map the probability of events to a single patient, and enhancing the clinical decision-making of doctors and patients. Therefore, the purpose of this study was to develop and validate a numerical model for the prediction of the risk of PE in neurology department suspected PE patients.

Materials and methods

Study population

Neurology department patients with suspected PE who were admitted at the Affiliated Dongyang Hospital of the Wenzhou Medical University from January 2012 to December 2021 were considered for enrollment in our study. The patients who had undergone CTPA examination were suspected PE. The subjects' data were retrospectively collected from our clinical research data platform. After baseline data clearance and extraction, the medical records of 1,578 subjects were included in the statistical analysis. Subjects were randomly divided into the training cohort and the validation cohort at a ratio of 7:3.

Ethical approval for this retrospective study was obtained from the Medical Ethics Committee of the Affiliated Dongyang Hospital of the Wenzhou Medical University (No.: 2022-YX-160), and the requirement for informed consent was waived as the medical information of all patients was anonymized and de-identified prior to conducting the analysis. Our study was conducted in accordance with the Declaration of Helsinki.

Study outcomes and data collection

Pulmonary embolism (PE) was defined in accordance with the criteria of the European Society of Cardiology Guidelines (20). The diagnosis of PE was based on a filling defect of the pulmonary artery system (including the subsegment pulmonary artery) in computed tomography pulmonary angiography (CTPA). The past medical history, complications, individual clinical features, and clinical biomarker data were collected. The indicators we chose, for example, blood oxygen saturation, systolic blood pressure, and diastolic pressure, were strictly defined from admission to CTPA, and the lowest result was selected; for other indicators, the highest result was selected. Our research flowchart is shown in Figure 1.

Statistical analysis

Data were statistically analyzed by RStudio software for Windows. Categorical variables were expressed as frequency with percentages and were compared using the chi-square (χ^2) test or Fisher's exact test. Continuous variables were expressed as the mean with standard deviation (SD) or median and interquartile range (IQR), and were compared using the Student's *t*-test or the Mann–Whitney *U*-test. All subjects contained 58 variables. To guarantee the reliability of the data, five indicators with missing values >20% were deleted. The "mice" package in R software for multiple imputation techniques was used (21) to impute the remaining missing predictor values. The "glmnet" package for the least absolute shrinkage and selection operator regression (LASSO) analysis was used to select the optimal predictive features, and

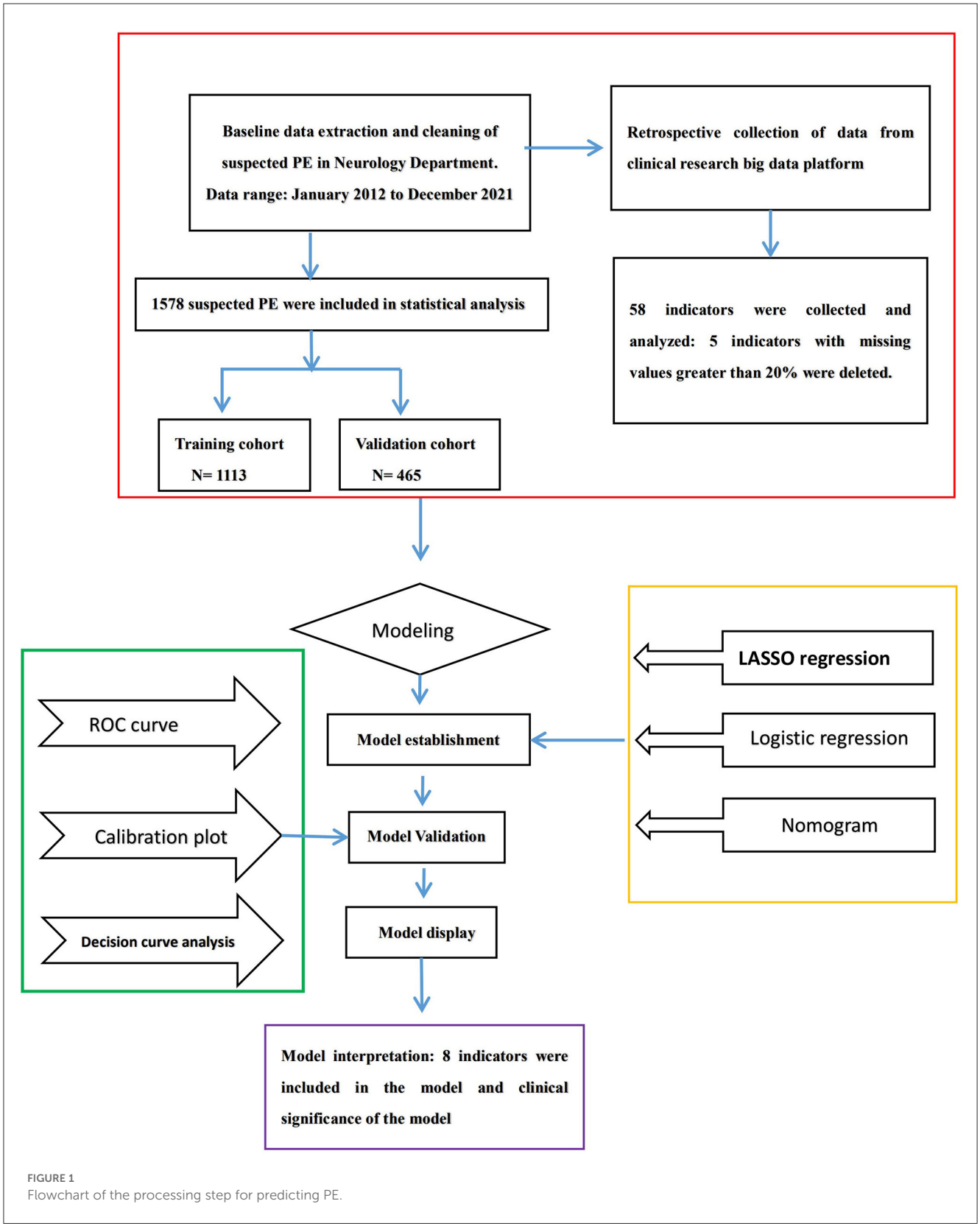

FIGURE 1
Flowchart of the processing step for predicting PE.

an "rms" package for multivariate logistic regression analysis was used to establish the numerical model (22–24). The "regplot" package in R software was used for the nomogram. The features were presented as the odds ratio (OR) and 95% confidence interval (CI). A two-sided p-value of <0.05 was considered to statistically significant.

TABLE 1 Baseline characteristics of subjects.

Variables	Total (n = 1,578)	No PE (n = 1,194)	PE (n = 384)	p
Gender, *n* (%)				0.114
Women	822 (52.1)	608 (50.9)	214 (55.7)	
Men	756 (47.9)	586 (49.1)	170 (44.3)	
Age (years), median (Q1, Q3)	75 (65, 81)	73 (63, 81)	78 (71, 83)	<0.001
Breathing (/min), median (Q1, Q3)	22 (20, 25)	22 (20, 24)	23 (20, 28)	<0.001
Pulse (/min), median (Q1, Q3)	98 (88, 111)	96 (86, 108)	103.5 (96, 118.25)	<0.001
Systolic pressure (mmHg), median (Q1, Q3)	99 (92, 107)	100 (92, 109)	96 (91, 104)	<0.001
Diastolic pressure (mmHg), median (Q1, Q3)	52 (46, 58)	52 (47, 59)	50 (45, 54)	<0.001
Headache, *n* (%)				0.914
No	1,471 (93.2)	1,114 (93.3)	357 (93)	
Yes	107 (6.8)	80 (6.7)	27 (7)	
Dizzy, *n* (%)				0.069
No	1,400 (88.7)	1,049 (87.9)	351 (91.4)	
Yes	178 (11.3)	145 (12.1)	33 (8.6)	
Chest tightness, *n* (%)				0.502
No	1,354 (85.8)	1,029 (86.2)	325 (84.6)	
Yes	224 (14.2)	165 (13.8)	59 (15.4)	
Anhelation, *n* (%)				0.086
No	1,467 (93)	1,118 (93.6)	349 (90.9)	
Yes	111 (7)	76 (6.4)	35 (9.1)	
Hemoptysis, *n* (%)				0.159
No	1,572 (99.6)	1,191 (99.7)	381 (99.2)	
Yes	6 (0.4)	3 (0.3)	3 (0.8)	
Chest pain, *n* (%)				1
No	1,558 (98.7)	1,179 (98.7)	379 (98.7)	
Yes	20 (1.3)	15 (1.3)	5 (1.3)	
Syncope, *n* (%)				<0.001
No	1,359 (86.1)	995 (83.3)	364 (94.8)	
Yes	219 (13.9)	199 (16.7)	20 (5.2)	
Cough, *n* (%)				0.114
No	1,321 (83.7)	1,010 (84.6)	311 (81)	
Yes	257 (16.3)	184 (15.4)	73 (19)	
Fever, *n* (%)				0.62
No	1,542 (97.7)	1,165 (97.6)	377 (98.2)	
Yes	36 (2.3)	29 (2.4)	7 (1.8)	
Lower limb edema, *n* (%)				0.932
No	1,548 (98.1)	1,172 (98.2)	376 (97.9)	
Yes	30 (1.9)	22 (1.8)	8 (2.1)	
COPD, *n* (%)				0.022
No	1,349 (85.5)	1,035 (86.7)	314 (81.8)	
Yes	229 (14.5)	159 (13.3)	70 (18.2)	
Hypertension, *n* (%)				0.111
No	561 (35.6)	438 (36.7)	123 (32)	
Yes	1,017 (64.4)	756 (63.3)	261 (68)	
Diabetes, *n* (%)				0.173
No	1,297 (82.2)	972 (81.4)	325 (84.6)	
Yes	281 (17.8)	222 (18.6)	59 (15.4)	
Coronary heart disease, *n* (%)				0.133
No	1,241 (78.6)	950 (79.6)	291 (75.8)	
Yes	337 (21.4)	244 (20.4)	93 (24.2)	

(Continued)

TABLE 1 (Continued)

Variables	Total (n = 1,578)	No PE (n = 1,194)	PE (n = 384)	p
Hyperlipidemia, *n* (%)				1
No	1,525 (96.6)	1,154 (96.6)	371 (96.6)	
Yes	53 (3.4)	40 (3.4)	13 (3.4)	
Atrial fibrillation, *n* (%)				<0.001
No	1,435 (90.9)	1,110 (93)	325 (84.6)	
Yes	143 (9.1)	84 (7)	59 (15.4)	
Operation, *n* (%)				0.149
No	1,567 (99.3)	1,188 (99.5)	379 (98.7)	
Yes	11 (0.7)	6 (0.5)	5 (1.3)	
Tumor, *n* (%)				0.484
No	1,477 (93.6)	1,121 (93.9)	356 (92.7)	
Yes	101 (6.4)	73 (6.1)	28 (7.3)	
Smoke, *n* (%)				0.179
No	1,152 (73)	861 (72.1)	291 (75.8)	
Yes	426 (27)	333 (27.9)	93 (24.2)	
Drink, *n* (%)				0.144
No	1,051 (66.6)	783 (65.6)	268 (69.8)	
Yes	527 (33.4)	411 (34.4)	116 (30.2)	
WBC (10^9/L), median (Q1, Q3)	7.35 (5.65, 9.77)	7.1 (5.52, 9.49)	8.14 (6.42, 10.68)	<0.001
Lactate (mmol/L), median (Q1, Q3)	1.5 (1.2, 2.07)	1.5 (1.2, 2)	1.55 (1.2, 2.1)	0.523
RBC (10^{12}/L), median (Q1, Q3)	4.32 (4, 4.68)	4.33 (4, 4.68)	4.32 (4.01, 4.65)	0.918
Mg (mmol/L), median (Q1, Q3)	0.9 (0.84, 0.96)	0.9 (0.85, 0.96)	0.89 (0.84, 0.95)	0.011
HGB (g/L), median (Q1, Q3)	133 (122, 143)	132 (121.25, 143)	134 (123, 143)	0.212
Hct, median (Q1, Q3)	0.4 (0.37, 0.43)	0.4 (0.37, 0.43)	0.41 (0.38, 0.43)	0.131
Neutrophil percent, median (Q1, Q3)	0.73 (0.64, 0.83)	0.71 (0.62, 0.82)	0.78 (0.69, 0.86)	<0.001
Neutrophil count(10^9/L), median (Q1, Q3)	5.11 (3.63, 7.72)	4.84 (3.47, 7.38)	6.18 (4.38, 8.55)	<0.001
Lymphocyte percent, median (Q1, Q3)	0.27 (0.2, 0.34)	0.27 (0.2, 0.34)	0.25 (0.19, 0.32)	<0.001
Lymphocyte count (10^9/L), median (Q1, Q3)	1.58 (1.25, 2.03)	1.6 (1.27, 2.05)	1.53 (1.21, 2)	0.109
PLT (10^9/L), median (Q1, Q3)	211 (174, 254.75)	211 (175, 252.75)	211.5 (170, 260.25)	0.642
ALB (g/L), median (Q1, Q3)	37.7 (35.2, 40.2)	37.9 (35.62, 40.4)	37 (34.7, 39.4)	<0.001
PDW (%), median (Q1, Q3)	16 (13.8, 16.4)	15.9 (13.4, 16.3)	16.1 (15.6, 16.4)	<0.001
RDW (%), median (Q1, Q3)	0.13 (0.12, 0.14)	0.13 (0.12, 0.14)	0.13 (0.13, 0.14)	0.46
HDL (mmol/L), median (Q1, Q3)	1.08 (0.91, 1.3)	1.07 (0.9, 1.29)	1.11 (0.96, 1.32)	0.009
LDL (mmol/L), median (Q1, Q3)	2.45 (1.92, 3.03)	2.4 (1.9, 2.97)	2.6 (2, 3.17)	0.001
Apolipoprotein A1 (g/L), median (Q1, Q3)	1.11 (0.93, 1.34)	1.1 (0.93, 1.33)	1.11 (0.94, 1.38)	0.235
Apolipoprotein B(g/L), median (Q1, Q3)	0.85 (0.69, 1.02)	0.84 (0.69, 1.01)	0.88 (0.71, 1.05)	0.061
TG(mmol/L), median (Q1, Q3)	1.28 (0.98, 1.76)	1.29 (1, 1.8)	1.21 (0.93, 1.56)	0.002
TC (mmol/L), median (Q1, Q3)	4.22 (3.62, 4.93)	4.2 (3.6, 4.86)	4.37 (3.7, 5.04)	0.033
Fibrinogen (g/L), median (Q1, Q3)	3.64 (2.99, 4.54)	3.58 (2.97, 4.48)	3.83 (3.07, 4.67)	0.024
D-Dimer (mg/L), median (Q1, Q3)	1.62 (0.78, 4.99)	1.19 (0.69, 3.59)	4.3 (2.07, 8.27)	<0.001
PT(s), median (Q1, Q3)	13.6 (13, 14.3)	13.5 (13, 14.2)	13.9 (13.3, 14.5)	<0.001
APTT(s), median (Q1, Q3)	37.2 (34.6, 40.3)	37 (34.5, 40.1)	37.65 (35, 40.82)	0.038
TT(s), median (Q1, Q3)	16.5 (15.9, 17.1)	16.5 (15.9, 17)	16.5 (15.9, 17.1)	0.853
PO_2 (mmHg), median (Q1, Q3)	73.3 (64.4, 86)	74.7 (65.22, 89.7)	69.6 (62.7, 78.43)	<0.001
FIO_2 (%), median (Q1, Q3)	29 (21, 33)	21 (21, 33)	29 (21, 33)	0.131

WBC, white blood cell count; RBC, red blood cell count; Mg, magnesium; HGB, hemoglobin; Hct, hematocrit; PLT, platelet count; ALB, albumin; PDW, platelet distribution width; RDW, red blood cell distribution width; HDL, high-density lipoprotein; LDL, low-density lipoprotein; TG, triglyceride; TC, total cholesterol; PT, prothrombin time; APTT, activated partial prothrombin time; TT, thrombin time; PO_2, arterial partial pressure of oxygen; and FIO_2, oxygen concentration fraction in the inhaled gas.

10.3389/fneur.2023.1139598

TABLE 2 The baseline characteristics of the enrolled patients in the training and validation cohorts.

Variables	Total ($n = 1,578$)	Training ($n = 1,113$)	Validation ($n = 465$)	p
PE, *n* (%)				0.576
No	1,194 (75.7)	847 (76.1)	347 (74.6)	
Yes	384 (24.3)	266 (23.9)	118 (25.4)	
Gender, *n* (%)				1
Women	822 (52.1)	580 (52.1)	242 (52)	
Men	756 (47.9)	533 (47.9)	223 (48)	
Age (years), median (Q1, Q3)	75 (65, 81)	74 (65, 81)	76 (66, 82)	0.156
Breathing (/min), median (Q1, Q3)	22 (20, 25)	22 (20, 25)	22 (20, 25)	0.954
Pulse (/min), median (Q1, Q3)	98 (88, 111)	98 (88, 112)	98 (88, 110)	0.899
Systolic pressure (mmHg), median (Q1, Q3)	99 (92, 107)	99 (92, 108)	98 (92, 106)	0.208
Diastolic pressure (mmHg), median (Q1, Q3)	52 (46, 58)	52 (47, 58)	51 (46, 58)	0.219
Headache, *n* (%)				0.506
No	1,471 (93.2)	1,034 (92.9)	437 (94)	
Yes	107 (6.8)	79 (7.1)	28 (6)	
Dizzy, *n* (%)				0.721
No	1,400 (88.7)	990 (88.9)	410 (88.2)	
Yes	178 (11.3)	123 (11.1)	55 (11.8)	
Chest tightness, *n* (%)				0.813
No	1,354 (85.8)	957 (86)	397 (85.4)	
Yes	224 (14.2)	156 (14)	68 (14.6)	
Anhelation, *n* (%)				0.413
No	1,467 (93)	1,039 (93.4)	428 (92)	
Yes	111 (7)	74 (6.6)	37 (8)	
Hemoptysis, *n* (%)				1
No	1,572 (99.6)	1,109 (99.6)	463 (99.6)	
Yes	6 (0.4)	4 (0.4)	2 (0.4)	
Chest pain, *n* (%)				0.492
No	1,558 (98.7)	1,097 (98.6)	461 (99.1)	
Yes	20 (1.3)	16 (1.4)	4 (0.9)	
Syncope, *n* (%)				0.745
No	1,359 (86.1)	956 (85.9)	403 (86.7)	
Yes	219 (13.9)	157 (14.1)	62 (13.3)	
Cough, *n* (%)				0.573
No	1,321 (83.7)	936 (84.1)	385 (82.8)	
Yes	257 (16.3)	177 (15.9)	80 (17.2)	
Fever, *n* (%)				0.682
No	1,542 (97.7)	1,086 (97.6)	456 (98.1)	
Yes	36 (2.3)	27 (2.4)	9 (1.9)	
Lower limb edema, *n* (%)				0.344
No	1,548 (98.1)	1,089 (97.8)	459 (98.7)	
Yes	30 (1.9)	24 (2.2)	6 (1.3)	
COPD, *n* (%)				0.533
No	1,349 (85.5)	947 (85.1)	402 (86.5)	
Yes	229 (14.5)	166 (14.9)	63 (13.5)	
Hypertension, *n* (%)				0.983
No	561 (35.6)	395 (35.5)	166 (35.7)	
Yes	1,017 (64.4)	718 (64.5)	299 (64.3)	
Diabetes, *n* (%)				0.739
No	1,297 (82.2)	912 (81.9)	385 (82.8)	
Yes	281 (17.8)	201 (18.1)	80 (17.2)	

(Continued)

TABLE 2 (Continued)

Variables	Total ($n = 1,578$)	Training ($n = 1,113$)	Validation ($n = 465$)	p
Coronary heart disease, *n* (%)				0.608
No	1,241 (78.6)	871 (78.3)	370 (79.6)	
Yes	337 (21.4)	242 (21.7)	95 (20.4)	
Hyperlipidemia, *n* (%)				0.135
No	1,525 (96.6)	1,081 (97.1)	444 (95.5)	
Yes	53 (3.4)	32 (2.9)	21 (4.5)	
Atrial fibrillation, *n* (%)				0.278
No	1,435 (90.9)	1,006 (90.4)	429 (92.3)	
Yes	143 (9.1)	107 (9.6)	36 (7.7)	
Operation, *n* (%)				1
No	1,567 (99.3)	1,105 (99.3)	462 (99.4)	
Yes	11 (0.7)	8 (0.7)	3 (0.6)	
Tumor, *n* (%)				0.776
No	1,477 (93.6)	1,040 (93.4)	437 (94)	
Yes	101 (6.4)	73 (6.6)	28 (6)	
Smoke, *n* (%)				0.453
No	1,152 (73)	806 (72.4)	346 (74.4)	
Yes	426 (27)	307 (27.6)	119 (25.6)	
Drink, *n* (%)				0.707
No	1,051 (66.6)	745 (66.9)	306 (65.8)	
Yes	527 (33.4)	368 (33.1)	159 (34.2)	
WBC (10^9/L), median (Q1, Q3)	7.35 (5.65, 9.77)	7.35 (5.66, 9.78)	7.3 (5.6, 9.69)	0.754
Lactate (mmol/), median (Q1, Q3)	1.5 (1.2, 2.07)	1.5 (1.2, 2)	1.5 (1.1, 2.1)	0.606
RBC (10^{12}/L), median (Q1, Q3)	4.32 (4, 4.68)	4.33 (4, 4.67)	4.3 (4, 4.69)	0.906
Mg (mmol/L), median (Q1, Q3)	0.9 (0.84, 0.96)	0.9 (0.85, 0.96)	0.9 (0.84, 0.96)	0.809
HGB (g/L), median (Q1, Q3)	133 (122, 143)	133 (122, 143)	132 (122, 143)	0.758
Hct, median (Q1, Q3)	0.4 (0.37, 0.43)	0.4 (0.37, 0.43)	0.4 (0.37, 0.43)	0.892
Neutrophil percent, median (Q1, Q3)	0.73 (0.64, 0.83)	0.73 (0.64, 0.82)	0.74 (0.64, 0.84)	0.212
Neutrophil count (10^9/L), median (Q1, Q3)	5.11 (3.63, 7.72)	5.11 (3.65, 7.66)	5.06 (3.55, 7.83)	0.92
Lymphocyte percent, median (Q1, Q3)	0.27 (0.2, 0.34)	0.27 (0.2, 0.34)	0.27 (0.2, 0.34)	0.78
Lymphocyte count (10^9/L), median (Q1, Q3)	1.58 (1.25, 2.03)	1.58 (1.25, 2.05)	1.57 (1.25, 2.01)	0.427
PLT (10^9/L), median (Q1, Q3)	211 (174, 254.75)	212 (175, 255)	208 (169, 253)	0.097
ALB (g/L), median (Q1, Q3)	37.7 (35.2, 40.2)	37.7 (35.3, 40.3)	37.8 (35.1, 40.1)	0.396
PDW (%), median (Q1, Q3)	16 (13.8, 16.4)	15.9 (13.8, 16.4)	16 (13.7, 16.3)	0.93
RDW (%), median (Q1, Q3)	0.13 (0.12, 0.14)	0.13 (0.12, 0.14)	0.13 (0.13, 0.14)	0.842
HDL (mmol/L), median (Q1, Q3)	1.08 (0.91, 1.3)	1.09 (0.91, 1.31)	1.06 (0.9, 1.28)	0.155
LDL (mmol/L), median (Q1, Q3)	2.45 (1.92, 3.03)	2.46 (1.94, 3.02)	2.39 (1.81, 3.04)	0.166
Apolipoprotein A1 (g/L), median (Q1, Q3)	1.11 (0.93, 1.34)	1.11 (0.93, 1.35)	1.09 (0.92, 1.31)	0.098
Apolipoprotein B(g/L), median (Q1, Q3)	0.85 (0.69, 1.02)	0.85 (0.69, 1.02)	0.85 (0.69, 1.01)	0.51
TG (mmol/L), median (Q1, Q3)	1.28 (0.98, 1.76)	1.28 (0.99, 1.76)	1.25 (0.95, 1.74)	0.382
TC (mmol/L), median (Q1, Q3)	4.22 (3.62, 4.93)	4.25 (3.65, 4.93)	4.2 (3.58, 4.91)	0.29
Fibrinogen (g/L), median (Q1, Q3)	3.64 (2.99, 4.54)	3.63 (3.01, 4.5)	3.65 (2.96, 4.72)	0.507
D-Dimer (mg/L), median (Q1, Q3)	1.62 (0.78, 4.99)	1.5 (0.76, 4.65)	1.94 (0.83, 5.4)	0.081
PT(s), median (Q1, Q3)	13.6 (13, 14.3)	13.6 (13, 14.3)	13.7 (13.1, 14.3)	0.027
APTT(s), median (Q1, Q3)	37.2 (34.6, 40.3)	37.1 (34.6, 40.2)	37.6 (34.8, 40.6)	0.177
TT(s), median (Q1, Q3)	16.5 (15.9, 17.1)	16.5 (15.9, 17.1)	16.4 (15.9, 17)	0.159
PO_2 (mmHg), median (Q1, Q3)	73.3 (64.4, 86)	72.9 (64.3, 85.5)	73.6 (64.6, 88.3)	0.482
FIO_2 (%), median (Q1, Q3)	29 (21, 33)	29 (21, 33)	21 (21, 33)	0.541

WBC, white blood cell count; RBC, red blood cell count; Mg, magnesium; HGB, hemoglobin; Hct, hematocrit; PLT, platelet count; ALB, albumin; PDW, platelet distribution width; RDW, red blood cell distribution width; HDL, high-density lipoprotein; LDL, low-density lipoprotein; TG, triglyceride; TC, total cholesterol; PT, prothrombin time; APTT, activated partial prothrombin time; TT, thrombin time; PO_2, arterial partial pressure of oxygen; and FIO_2, oxygen concentration fraction in the inhaled gas.

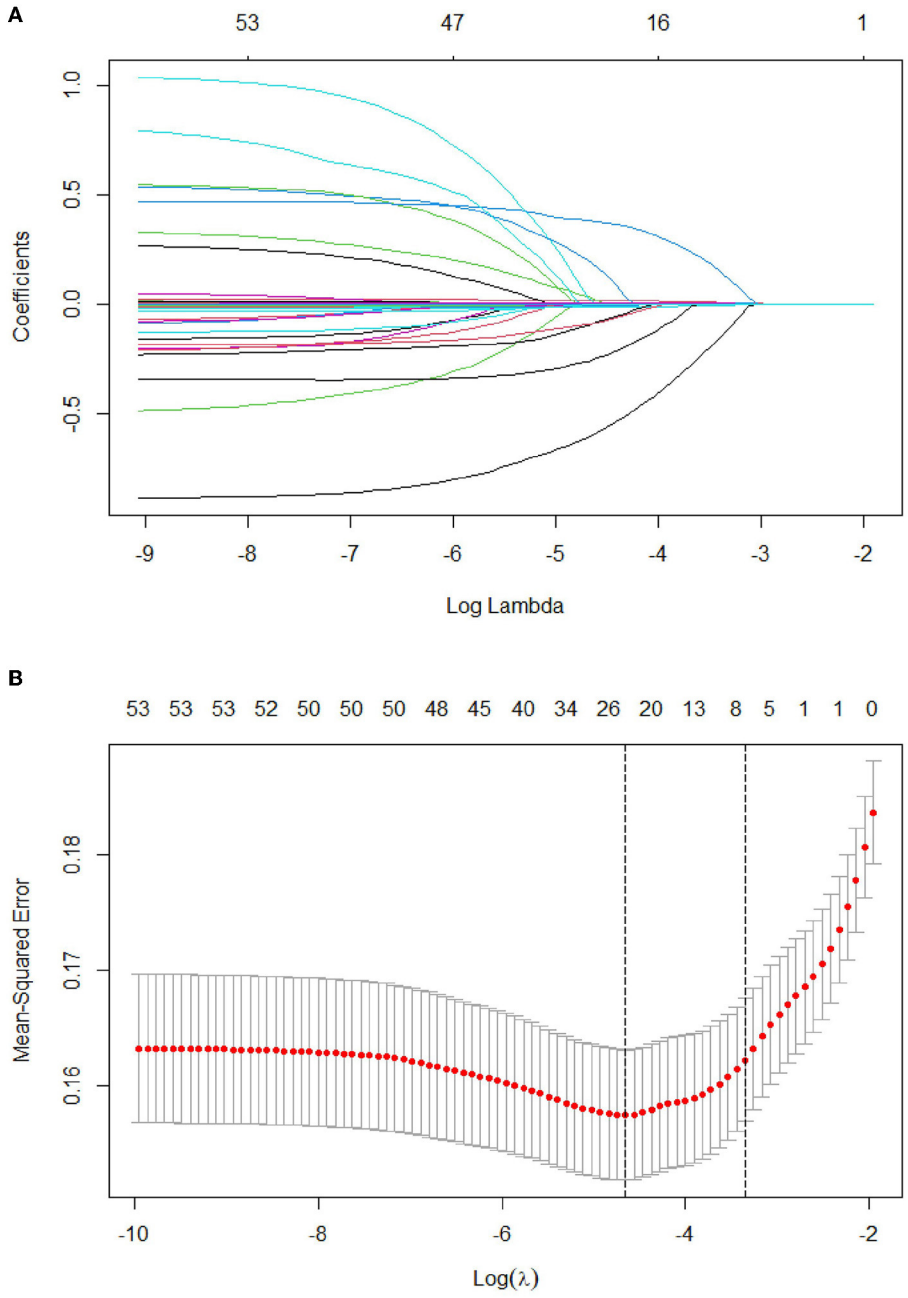

FIGURE 2
Tuning parameter selection using the LASSO regression in the training cohort. **(A)** LASSO coefficient profiles of the clinical features. **(B)** The optimal penalization coefficient lambda was generated in the LASSO *via* 10-fold cross-validation. The lambda value of the 1-fold mean square error for the training cohort was given.

Model development, validation, and evaluation

The least absolute shrinkage and selection operator regression analysis was used to select the optimal predictive features, and a multivariable logistic regression analysis was used to establish a numerical model to predict PE in the training cohort. The model performance was assessed and validated for discrimination, calibration, and clinical utility in both cohorts (25). The differentiation in the model was evaluated using the "pROC" package for the area under the receiver operating characteristic (ROC) curve (AUC), the "calibrate" package for calibration curve analysis to evaluate the calibration of the model, and the "rmda" package for decision curve analysis (DCA), which were used to quantify the net benefit under different threshold probabilities to determine the clinical utility of the model.

Results

Characteristics of the study population

After excluding five variables with missing information in more than 20% of patients, we involved 53 variables with missing data in <20% of patients involved in this study (shown in Supplementary Figure 1). The missing data for the 53 variables ranged from 0.00 to 18.69%; thus, the multiple imputation technique was used to impute the missing data. A total of 1,578 subjects with suspected PE were enrolled in this study. The incidence of PE in our study was 24.33%. The baseline characteristics of neurology department patients with suspected PE are displayed in Table 1. We divided the patients into the training cohort (1,113 patients) and the validation cohort (465 patients). Basic characteristics of the patients in the training and validation cohorts are presented in Table 2.

TABLE 3 Final model coefficients.

Variables	β	SE	OR	95% CI	*P*
Age	0.039	0.008	1.04	1.02–1.06	<0.001
Pulse	0.006	0.004	1.01	1–1.01	0.135
Systolic_pressure	−0.019	0.006	0.98	0.97–0.99	0.002
HGB	0.009	0.005	1.01	1–1.02	0.05
Neutrophil count	0.016	0.022	1.02	0.97–1.06	0.462
LDL	0.219	0.092	1.24	1.04–1.49	0.018
D-Dimer	0.093	0.015	1.1	1.07–1.13	<0.001
PO_2	−0.004	0.003	1	0.99-1	0.175

HGB, hemoglobin; LDL, low-density lipoprotein; and PO_2, arterial partial pressure of oxygen.

Selected predictors

Of the 53 variables, eight potential predictive features were finally selected based on the LASSO regression analysis (Figures 2A, B). The optimal predictors included age, pulse, systolic pressure, hemoglobin (HGB), neutrophil count (N), low-density lipoprotein (LDL), D-dimer (DD), and partial pressure of oxygen (PO_2). The eight potential predictive features screened from the LASSO regression analysis were used to create the final model based on the multivariable logistic regression analysis in the training cohort (Table 3). The prevalence of PE is 23.9% in the training and 25.4% in the validation cohorts (Table 2). The sensitivity of our model is 94.17%, the specificity is 17.56%, the positive predictive

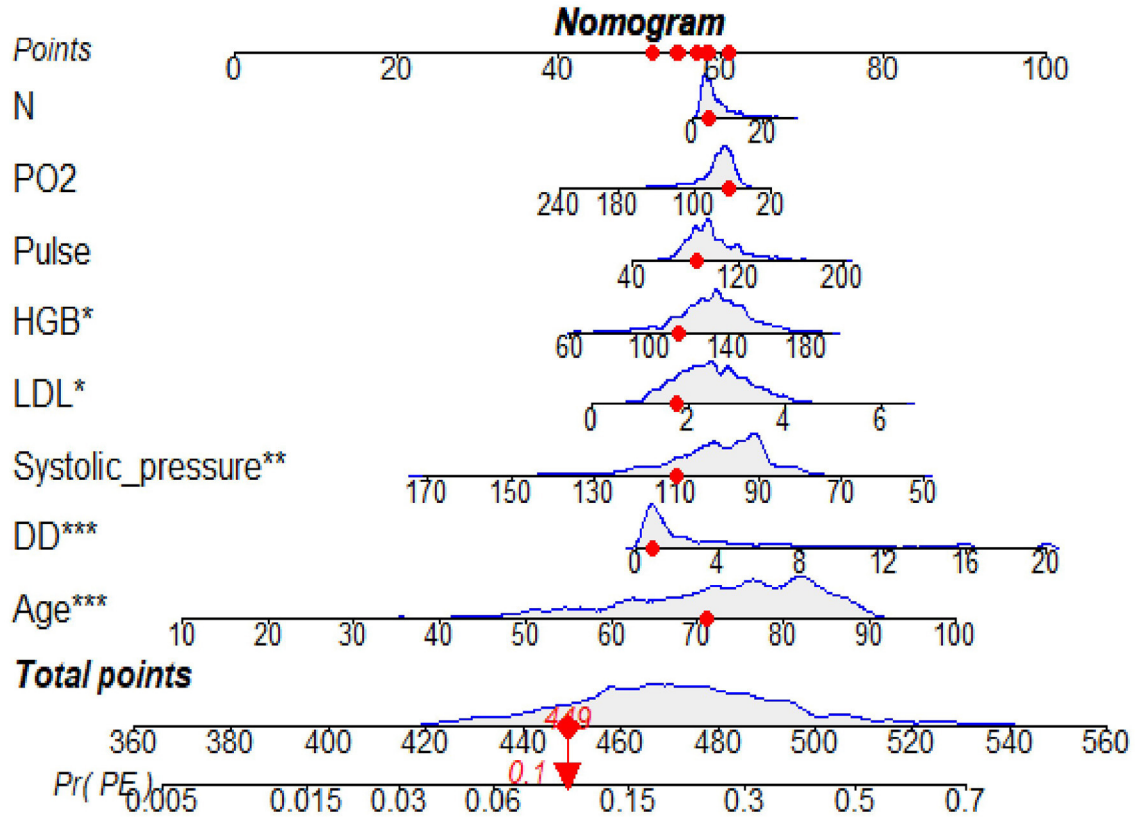

FIGURE 3
A nomogram based on the combination of eight indicators was developed using logistic regression analysis. If the neurology department patient had a total score of 449 points, this corresponded to an ~10% risk of PE and then the probability of the PE was 0.1 (red numbers). HGB, hemoglobin; *N*, neutrophil count; LDL, low-density lipoprotein; DD, D-dimer; PO2, oxygen partial pressure (PO_2). *$p < 0.05$, **$p < 0.01$, ***$p < 0.001$.

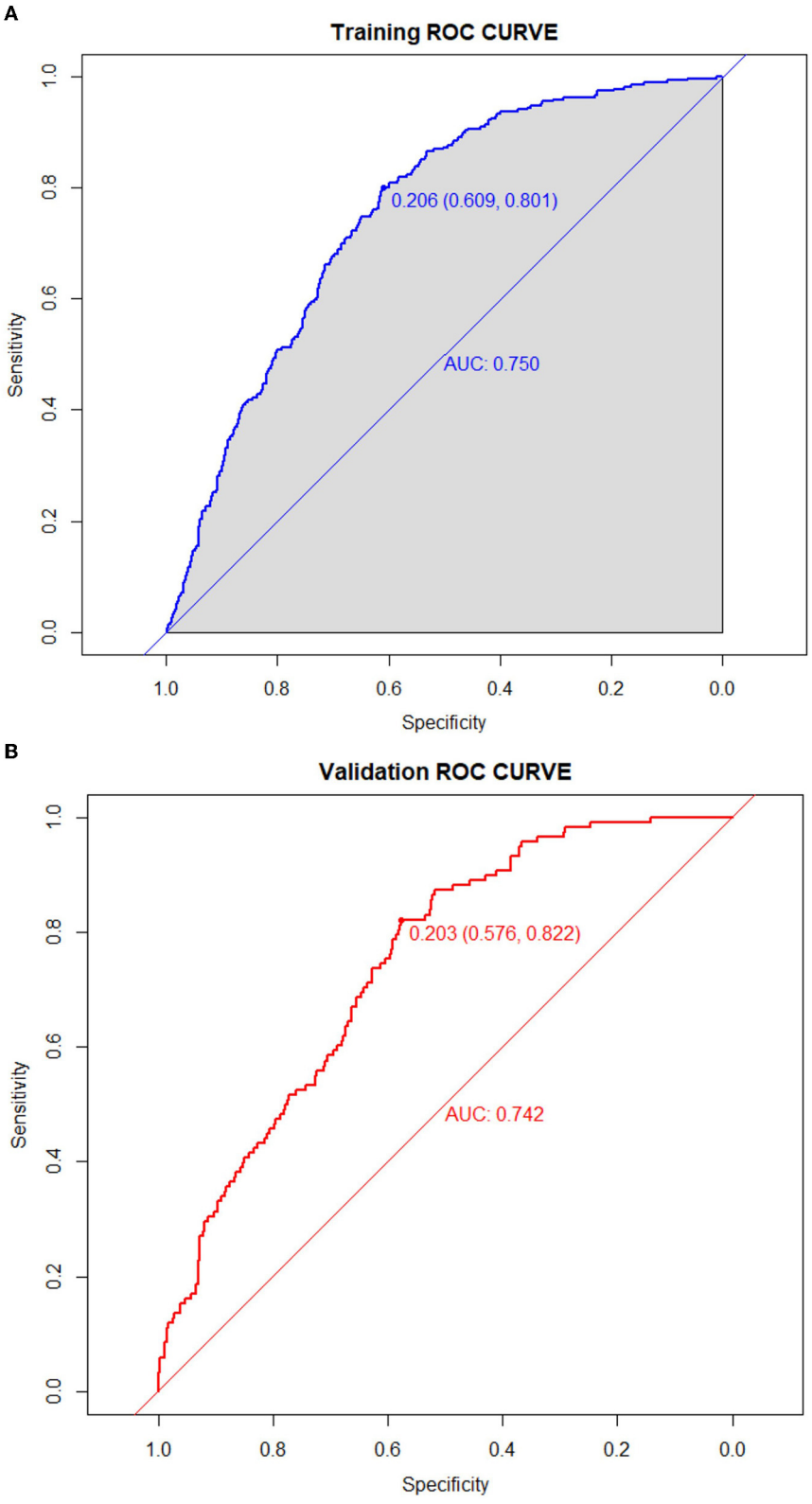

FIGURE 4
Receiver operating characteristic curves of the model distinguishing PE from non-PE in the training **(A)** and validation **(B)** cohorts.

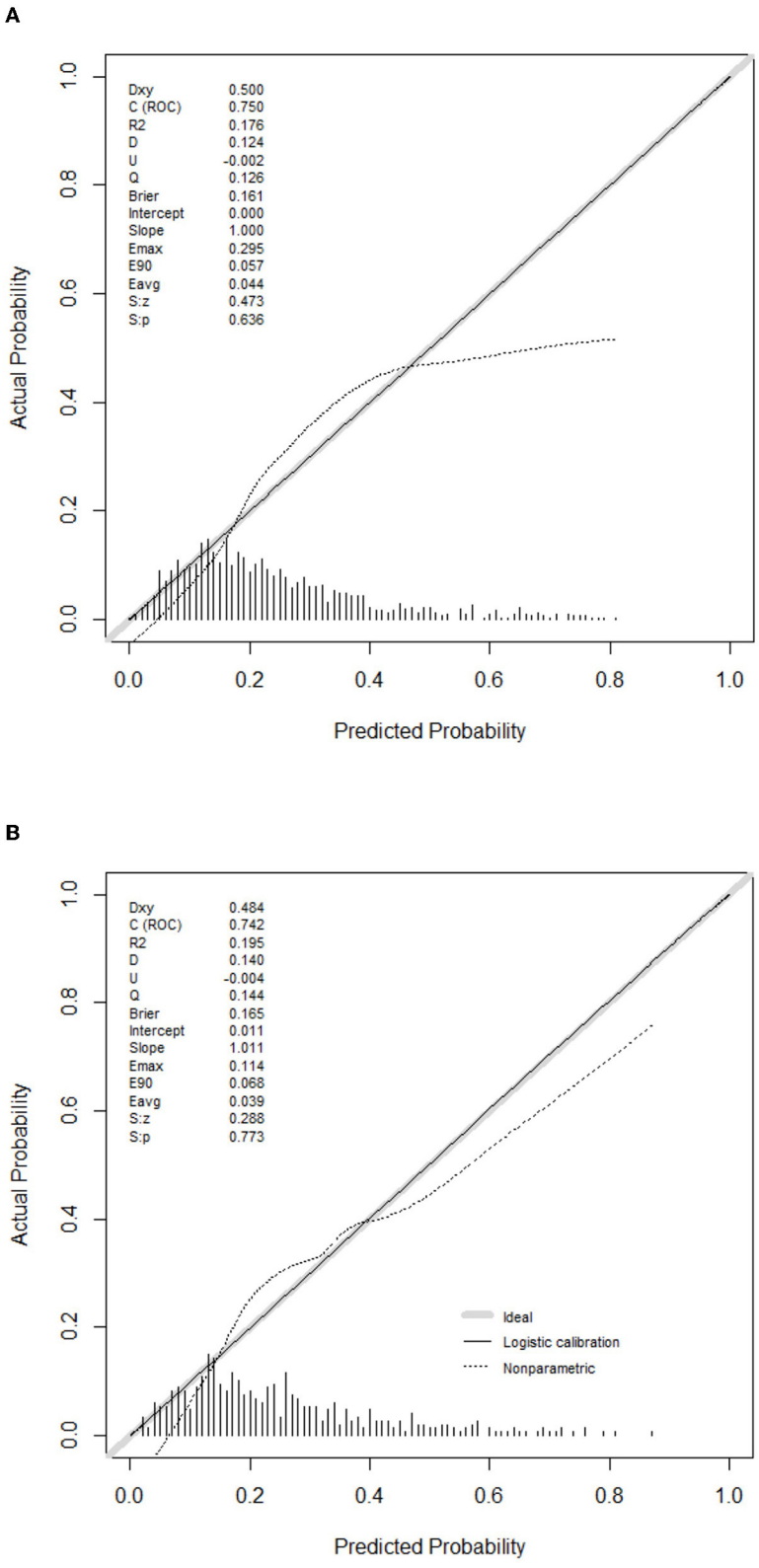

FIGURE 5
Calibration curves of the model in the training **(A)** and validation **(B)** cohorts.

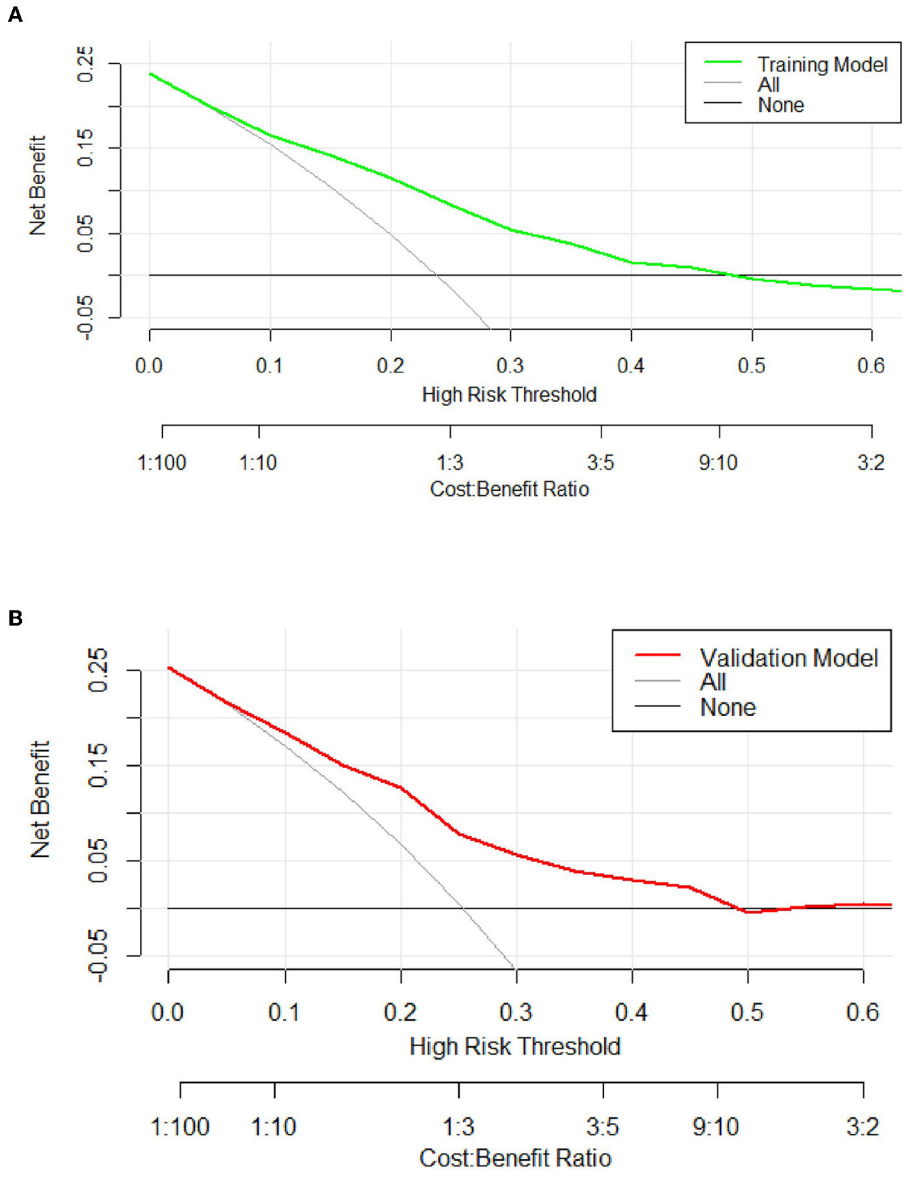

FIGURE 6
The decision curve of the model in the training **(A)** and validation **(B)** cohort. If the risk threshold is <50%, the nomogram model will obtain more benefit than all treatments (assuming that all neurology department patients were PE) or no treatment (assuming all neurology department patients were non-PE).

value is 77.47%, and the negative predictive value is 50% in the training cohort.

Construction and validation of the model

The predictive model for PE was visualized by a nomogram in the training cohort, which is shown in Figure 3. Model discrimination, as quantified by the AUC, was 0.750 (95% CI: 0.721–0.783) in the training cohort and 0.742 (95% CI: 0.689–0.787) in the validation cohort, indicating that this numerical model can successfully distinguish PE from non-PE (Figures 4A, B). The calibration plots in the training and validation cohorts are shown in Figures 5A, B, which demonstrate a good consistency between the prediction and the real observation. The DCA in the training and validation cohorts indicated that the numerical model had a good net clinical benefit (Figures 6A, B).

Discussion

In this study, we developed and validated a simple model to determine the possible risk factors for PE based on a 10-year retrospective study in a comprehensive hospital in China. Our novel numerical model incorporated eight parameters, namely, age, pulse, systolic pressure, HGB, N, LDL, DD, and PO_2. All parameters are readily available clinical features and biomarkers in routine health examinations. Notably, the ROC

analysis showed that the AUC was 0.750 (95% CI: 0.721–0.783), indicating that our model displayed good discrimination and calibration. Furthermore, the DCA in the training and validation cohorts indicated that our model had a good net clinical benefit.

Our research found that DD (OR: 1.10; 95% CI: 1.07–1.13) is an independent predictive factor for the increased risk of PE. This result is in accordance with other observations (26, 27), which found that a high DD level was attributable to the possibility of developing PE. In terms of biomarkers, DD is the only biomarker currently used in routine practice for predicting PE; however, it is unlikely to have adequate specificity in neurology department patients for positivity. A large sample study from 2000 to 2015 showed increased hospitalization rates and the highest inpatient mortality due to PE in elderly patients (28). In addition, a retrospective study demonstrated an association between age and the severity of submassive PE stadium (29). Our model also showed that age (OR: 1.04; 95% CI: 1.02–1.06) is a high-risk factor for PE, which is similar to previous studies. In our model, most of the factors were positively associated with the risk of PE, whereas systolic blood pressure and PO_2 were negatively associated. A previous study showed that low systolic pressure was connected with an increased risk of PE-related mortality (30, 31). In hemodynamically stable patients, a lower PO_2 (<8 kPa) was still associated with an elevated risk of mortality (32). These conclusions were consistent with those of our study. Our data also revealed that two clinical symptoms, including pulse and systolic pressure, were incorporated into the model to predict PE. Consistent with our result, a previous study (33) showed that pulse and systolic pressure were good predictors in a model for the prognosis of PE. Relevant studies (34–37) have also shown that inflammation and dyslipidemia are factors affecting PE, which is similar to the presence of inflammation and blood lipid indicators in our model. However, there are still some differences between the indicators included in our model and those included in the previous models (38). Three possible explanations for the discrepant results are as follows: (1) there are no such indicators in our clinical research data platform; (2) indicators with missing values >20% were deleted; and (3) indicators were not included in the model after the analysis.

This retrospective study suggested that a nomogram developed with clinical features and biomarkers to generate a personalized evaluation of PE risk in neurology department patients may distinguish patients at high risk of PE. For example, if the neurology department patient had a total score of 449 points, this corresponded to an ∼10% risk of PE, and the probability of the PE was 0.1. Clinicians can use this simple numerical model to categorize the neurology department patients as PE-likely or PE-unlikely, thus reducing unnecessary CTPA examinations. This model may also be helpful to identify high-risk patients early, evaluate thrombosis, and implement active and individualized anticoagulation therapy.

This study is subject to certain limitations. In this retrospective study, five indicators (blood oxygen saturation, BMI, ejection fraction, troponin T, and brain natriuretic peptide precursor) with missing values > 20% were deleted. Moreover, the additional disadvantages of this study were the limited sample of participants and a lack of information on sufficient variables. Additionally, the data were collected as a single-center retrospective study.

In conclusion, we developed a novel numerical model for selecting the risk factors for PE in suspected-PE patients in a neurology department. Our findings may help decision-makers weigh the risk of PE and appropriately select PE prevention strategies. In the future, a large-scale prospective multicenter cohort study would help to form an improved and updated clinical decision-making system.

Data availability statement

The raw data supporting the conclusions of this article will be made available by the authors, without undue reservation.

Ethics statement

The studies involving human participants were reviewed and approved by the Medical Ethics Committee of Affiliated Dongyang Hospital of Wenzhou Medical University. Written informed consent for participation was not required for this study in accordance with the national legislation and the institutional requirements.

Author contributions

WM conceived and designed the research strategy. QJ, JL, and WM wrote the manuscript text. QL, FL, MX, and LW collected the clinical data and participated in the writing of the manuscript. WM, MX, and LW contributed to the analysis and interpretation of the data. All authors contributed to this manuscript and approved the submitted version of the manuscript.

Funding

This study received funding from the Zhejiang Provincial Natural Science and Public Welfare Foundation of China (Grant No. LTGY23H200002) and the Jinhua Science and Technology Foundation, Zhejiang Province, China (Grant No. 2022-3-012).

Conflict of interest

The authors declare that the research was conducted in the absence of any commercial or financial relationships that could be construed as a potential conflict of interest.

Publisher's note

All claims expressed in this article are solely those of the authors and do not necessarily represent those of

their affiliated organizations, or those of the publisher, the editors and the reviewers. Any product that may be evaluated in this article, or claim that may be made by its manufacturer, is not guaranteed or endorsed by the publisher.

Supplementary material

The Supplementary Material for this article can be found online at: https://www.frontiersin.org/articles/10.3389/fneur.2023.1139598/full#supplementary-material

References

1. Wendelboe AM, Raskob GE. Global burden of thrombosis: epidemiologic aspects. *Circ Res.* (2016) 118:1340–7. doi: 10.1161/CIRCRESAHA.115.306841

2. Toplis E, Mortimore G. The diagnosis and management of pulmonary embolism. *Br J Nurs.* (2020) 29:22–6. doi: 10.12968/bjon.2020.29.1.22

3. Kim KA, Choi SY, Kim R. Endovascular treatment for lower extremity deep vein thrombosis: an overview. *Korean J Radiol.* (2021) 22:931–43. doi: 10.3348/kjr.2020.0675

4. Cherng SC, Wang YF, Fan YM, Yang SP, Huang WS. Iliofemoral vein thrombosis and pulmonary embolism associated with a transient ischemic attack in a patient with antiphospholipid syndrome. *Clin Nucl Med.* (2001) 26:84–5. doi: 10.1097/00003072-200101000-00029

5. Tassi R, Guideri F, Acampa M, Domenichelli C, Martini G. Acute ischemic stroke and concomitant massive pulmonary embolism: a challenge. *Neurol Sci.* (2021) 42:4777–80. doi: 10.1007/s10072-021-05494-7

6. Vindis D, Hutyra M, Sanak D, Kral M, Cechakova E, Littnerova S, et al. Patent foramen ovale and the risk of cerebral infarcts in acute pulmonary embolism-a prospective observational study. *J Stroke Cerebrovasc Dis.* (2018) 27:357–64. doi: 10.1016/j.jstrokecerebrovasdis.2017.09.004

7. Sherman DG, Albers GW, Bladin C, Fieschi C, Gabbai AA, Kase CS, et al. The efficacy and safety of enoxaparin versus unfractionated heparin for the prevention of venous thromboembolism after acute ischaemic stroke (prevail study): an open-label randomised comparison. *Lancet.* (2007) 369:1347–55. doi: 10.1016/S0140-6736(07)60633-3

8. Konstantinides SV, Meyer G. The 2019 Esc guidelines on the diagnosis and management of acute pulmonary embolism. *Eur Heart J.* (2019) 40:3453–5. doi: 10.1093/eurheartj/ehz726

9. Pang W, Zhang Z, Wang Z, Zhen K, Zhang M, Zhang Y, et al. Higher incidence of chronic thromboembolic pulmonary hypertension after acute pulmonary embolism in Asians than in Europeans: a meta-analysis. *Front Med.* (2021) 8:721294. doi: 10.3389/fmed.2021.721294

10. Wang X, Zhao H, Cui N. The role of electrical impedance tomography for management of high-risk pulmonary embolism in a postoperative patient. *Front Med.* (2021) 8:773471. doi: 10.3389/fmed.2021.773471

11. Robert-Ebadi H, Mostaguir K, Hovens MM, Kare M, Verschuren F, Girard P, et al. Assessing clinical probability of pulmonary embolism: prospective validation of the simplified geneva score. *J Thromb Haemost.* (2017) 15:1764–9. doi: 10.1111/jth.13770

12. Freund Y, Cachanado M, Aubry A, Orsini C, Raynal PA, Feral-Pierssens AL, et al. Effect of the pulmonary embolism rule-out criteria on subsequent thromboembolic events among low-risk emergency department patients: the proper randomized clinical trial. *JAMA.* (2018) 319:559–66. doi: 10.1001/jama.2017.21904

13. van der Pol LM, Tromeur C, Bistervels IM, Ni Ainle F, van Bemmel T, Bertoletti L, et al. Pregnancy-adapted years algorithm for diagnosis of suspected pulmonary embolism. *N Engl J Med.* (2019) 380:1139–49. doi: 10.1056/NEJMoa1813865

14. Kirsch B, Aziz M, Kumar S, Burke M, Webster T, Immadi A, et al. Wells score to predict pulmonary embolism in patients with coronavirus disease 2019. *Am J Med.* (2021) 134:688–90. doi: 10.1016/j.amjmed.2020.10.044

15. Wang MF, Li FX, Feng LF, Zhu CN, Fang SY, Su CM, et al. Development and validation of a novel risk assessment model to estimate the probability of pulmonary embolism in postoperative patients. *Sci Rep.* (2021) 11:18087. doi: 10.1038/s41598-021-97638-0

16. Ji QY, Wang MF, Su CM, Yang QF, Feng LF, Zhao LY, et al. Clinical symptoms and related risk factors in pulmonary embolism patients and cluster analysis based on these symptoms. *Sci Rep.* (2017) 7:14887. doi: 10.1038/s41598-017-14888-7

17. Wang M, Zhang J, Ji Q, Yang Q, Zhao F, Li W, et al. Evaluation of platelet distribution width in chronic obstructive pulmonary disease patients with pulmonary embolism. *Biomark Med.* (2016) 10:587–96. doi: 10.2217/bmm.15.112

18. Grimes DA. The nomogram epidemic: resurgence of a medical relic. *Ann Intern Med.* (2008) 149:273–5. doi: 10.7326/0003-4819-149-4-200808190-00010

19. Levy DA Li H, Sterba KR, Hughes-Halbert C, Warren GW, Nussenbaum B, et al. Development and validation of nomograms for predicting delayed postoperative radiotherapy initiation in head and neck squamous cell carcinoma. *JAMA Otolaryngol Head Neck Surg.* (2020) 146:455–64. doi: 10.1001/jamaoto.2020.0222

20. Nolan MT, Creati L, Koczwara B, Kritharides L, Lynam J, Lyon AR, et al. First European Society of Cardiology Cardio-Oncology Guidelines: a big leap forward for an emerging specialty. *Heart Lung Circ.* (2022) 31:1563–7. doi: 10.1016/j.hlc.2022.11.003

21. Peyre H, Leplege A, Coste J. Missing data methods for dealing with missing items in quality of life questionnaires. a comparison by simulation of personal mean score, full information maximum likelihood, multiple imputation, and hot deck techniques applied to the Sf-36 in the French 2003 Decennial Health Survey. *Qual Life Res.* (2011) 20:287–300. doi: 10.1007/s11136-010-9740-3

22. Hu X, Shen F, Zhao Z, Qu X, Ye J. An individualized gait pattern prediction model based on the least absolute shrinkage and selection operator regression. *J Biomech.* (2020) 112:110052. doi: 10.1016/j.jbiomech.2020.110052

23. Narala S, Li SQ, Klimas NK, Patel AB. Application of least absolute shrinkage and selection operator logistic regression for the histopathological comparison of chondrodermatitis nodularis helicis and hyperplastic actinic keratosis. *J Cutan Pathol.* (2021) 48:739–44. doi: 10.1111/cup.13931

24. Yang S, Wu H. A novel Pm25 concentrations probability density prediction model combines the least absolute shrinkage and selection operator with quantile regression. *Environ Sci Pollut Res Int.* (2022) 29:78265–91. doi: 10.1007/s11356-022-21318-3

25. Wu J, Zhang H, Li L, Hu M, Chen L, Xu B, et al. A nomogram for predicting overall survival in patients with low-grade endometrial stromal sarcoma: a population-based analysis. *Cancer Commun.* (2020) 40:301–12. doi: 10.1002/cac2.12067

26. Damodaram M, Kaladindi M, Luckit J, Yoong W. D-dimers as a screening test for venous thromboembolism in pregnancy: is it of any use? *J Obstet Gynaecol.* (2009) 29:101–3. doi: 10.1080/01443610802649045

27. Hassanin IM, Shahin AY, Badawy MS, Karam K. D-dimer testing versus multislice computed tomography in the diagnosis of postpartum pulmonary embolism in symptomatic high-risk women. *Int J Gynaecol Obstet.* (2011) 115:200–1. doi: 10.1016/j.ijgo.2011.05.024

28. Pauley E, Orgel R, Rossi JS, Strassle PD. Age-stratified national trends in pulmonary embolism admissions. *Chest.* (2019) 156:733–42. doi: 10.1016/j.chest.2019.05.021

29. Keller K, Beule J, Coldewey M, Dippold W, Balzer JO. Impact of advanced age on the severity of normotensive pulmonary embolism. *Heart Vessels.* (2015) 30:647–56. doi: 10.1007/s00380-014-0533-4

30. Keller K, Beule J, Balzer JO, Dippold W. Blood pressure for outcome prediction and risk stratification in acute pulmonary embolism. *Am J Emerg Med.* (2015) 33:1617–21. doi: 10.1016/j.ajem.2015.07.009

31. Quezada A, Jimenez D, Bikdeli B, Moores L, Porres-Aguilar M, Aramberri M, et al. Systolic blood pressure and mortality in acute symptomatic pulmonary embolism. *Int J Cardiol.* (2020) 302:157–63. doi: 10.1016/j.ijcard.2019.11.102

32. Ye W, Chen X, Li X, Guo X, Gu W. Arterial partial pressure of oxygen and diffusion function as prognostic biomarkers for acute pulmonary embolism. *Respir Med.* (2022) 195:106794. doi: 10.1016/j.rmed.2022.106794

33. Lei M, Liu C, Luo Z, Xu Z, Jiang Y, Lin J, et al. Diagnostic management of inpatients with a positive D-dimer test: developing a new clinical decision-making rule for pulmonary embolism. *Pulm Circ.* (2021) 11:2045894020943378. doi: 10.1177/2045894020943378

34. Goldhaber SZ, Bounameaux H. Pulmonary embolism and deep vein thrombosis. *Lancet.* (2012) 379:1835–46. doi: 10.1016/S0140-6736(11)61904-1

35. Shao C, Wang J, Tian J, Tang YD. Coronary artery disease: from mechanism to clinical practice. *Adv Exp Med Biol.* (2020) 1177:1–36. doi: 10.1007/978-981-15-2517-9_1

36. Jara-Palomares L, Otero-Candelera R, Elias-Hernandez T, Cayuela-Dominguez A, Ferrer-Galvan M, Alfaro MJ, et al. dyslipidemia as a long-term marker for survival in pulmonary embolism. *Rev Port Pneumol.* (2011) 17:205–10. doi: 10.1016/j.rppneu.2011.03.006

37. Rodríguez-Núñez N, Ruano-Raviña A, Lama A, Ferreiro L, Ricoy J, Álvarez-Dobaño JM, et al. Impact of cardiovascular risk factors on the clinical presentation and survival of pulmonary embolism without identifiable risk factor. *J Thorac Dis.* (2020) 12:5411–9. doi: 10.21037/jtd-20-1634

38. Zhou Q, Xiong XY, Liang ZA. Developing a nomogram-based scoring tool to estimate the risk of pulmonary embolism. *Int J Gen Med.* (2022) 15:3687–97. doi: 10.2147/IJGM.S359291

frontiers | Frontiers in Neurology

TYPE Review
PUBLISHED 05 May 2023
DOI 10.3389/fneur.2023.1094709

OPEN ACCESS

EDITED BY
Wael MY Mohamed,
International Islamic University Malaysia, Malaysia

REVIEWED BY
Jian-Hong Shi,
Affiliated Hospital of Hebei University, China
Yiye Shao,
Fudan University, China

*CORRESPONDENCE
Weijun Zhang
✉ susan7888@163.com
Feng Zhu
✉ zhuf@zucc.edu.cn

RECEIVED 10 November 2022
ACCEPTED 03 April 2023
PUBLISHED 05 May 2023

CITATION
Mao S, Wu J, Yan J, Zhang W and Zhu F (2023) Dysregulation of miR-146a: a causative factor in epilepsy pathogenesis, diagnosis, and prognosis. *Front. Neurol.* 14:1094709. doi: 10.3389/fneur.2023.1094709

Dysregulation of miR-146a: a causative factor in epilepsy pathogenesis, diagnosis, and prognosis

Shiqi Mao[1], Jinhan Wu[1], Jingkai Yan[1], Weijun Zhang[2]* and Feng Zhu[1,3]*

[1]Department of Clinical Medicine, School of Medicine, Zhejiang University City College, Hangzhou, China, [2]Department of Neurology, Zhejiang Provincial Hospital of Traditional Chinese Medicine, Hangzhou, China, [3]Key Laboratory of Novel Targets and Drug Study for Neural Repair of Zhejiang Province, School of Medicine, Zhejiang University City College, Hangzhou, China

miR-146a is an NF-κB-dependent miRNA that acts as an anti-inflammatory miRNA *via* the Toll-like receptor (TLR) pathway. miR-146a targets multiple genes and has been identified to directly or indirectly regulate processes other than inflammation, including intracellular Ca changes, apoptosis, oxidative stress, and neurodegeneration. miR-146a is an important regulator of gene expression in epilepsy development and progression. Furthermore, miR-146a-related single nucleotide polymorphisms (SNPs) and single nucleotide variants (SNVs) contribute to the genetic susceptibility to drug resistance and seizure severity in epilepsy patients. This study summarizes the abnormal expression patterns of miR-146a in different types and stages of epilepsy and its potential molecular regulation mechanism, indicating that miR-146a can be used as a novel biomarker for epilepsy diagnosis, prognosis, and treatment.

KEYWORDS

miR-146a, epilepsy, NF-κB, inflammation, diagnosis, prognosis

1. Introduction

Epilepsy is one of the most prevalent neurological disorders associated with multiple genetic and environmental factors. One-third of epilepsy patients suffer from relapsing drug-resistant epilepsy (DRE) (1). Recurrent seizures and unsynchronized neuronal firing in epilepsy majorly impact daily functioning and physical and mental health (2). Although inflammation, changes in synaptic strength, neuronal death, gliosis, and ion channel dysfunction have been reported as the underlying pathological processes in epilepsy, their pathogenesis remains incompletely understood. In addition, current clinical treatments cannot meet the needs of the patients (3). Current antiepileptic drugs (AEDs) provide only symptomatic epilepsy treatment, and there is no evidence that they have disease-modifying properties (4). Therefore, new epilepsy biomarkers and therapeutic targets are crucial for developing new diagnostic methods and personalized treatments.

miRNAs are a class of small non-coding RNAs—19–25 nucleotides in length (5). They bind to the 3'-untranslated regions of target mRNAs and inhibit the translation or degradation of target genes, thereby fine-tuning their function (6). As high-throughput sequencing technologies develop, emerging evidence suggests that dysregulation of miRNAs can affect epilepsy through both direct and indirect mechanisms (7). miRNAs have been implicated in synaptic structure and function, neurogenesis, neuronal migration,

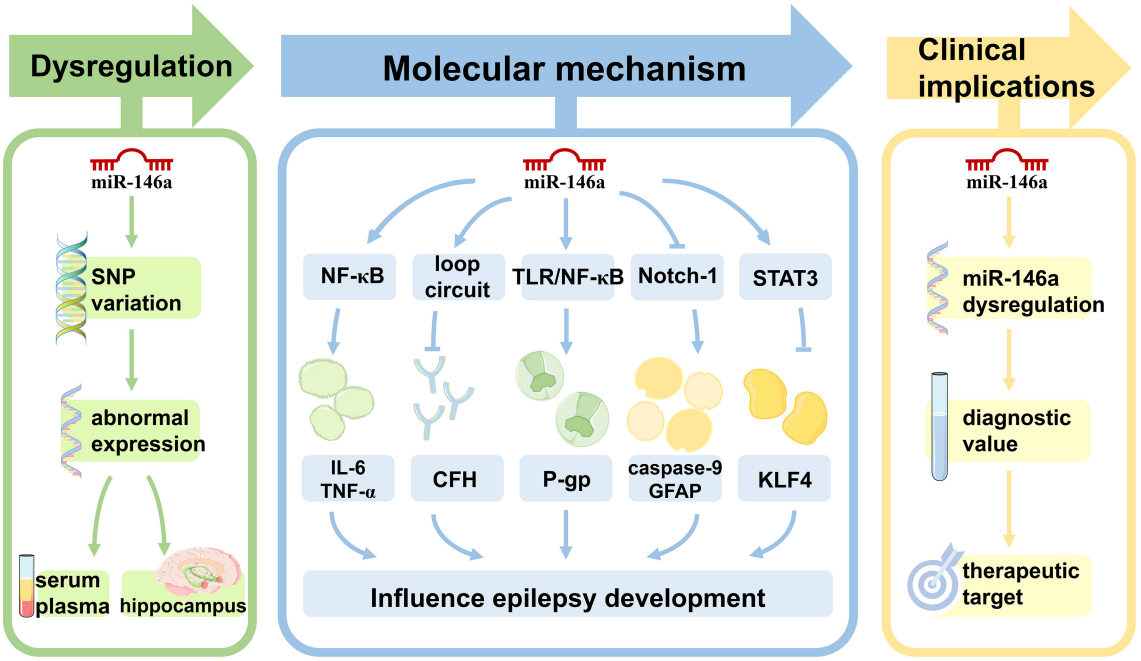

FIGURE 1
The role of miR-146a in epilepsy. Single nucleotide polymorphisms within miR-146a are significantly associated with the risk of epilepsy. In both animal models of epilepsy and human subjects, the expression pattern of miR-146a is aberrant in peripheral blood and/or brain. miR-146a is an NF-κB-dependent miRNA that acts as an anti-inflammatory miRNA *via* the Toll-like receptor pathway, targeting multiple genes to directly or indirectly regulate processes other than inflammation, including intracellular Ca changes, apoptosis, oxidative stress, and neurodegeneration in epilepsy development and progression. miR-146a may be used as a novel biomarker for epilepsy diagnosis, prognosis, and treatment.

inflammation, transcription, and cell death in epilepsy pathophysiology (8). Basic and clinical studies have revealed that changes in miRNA expression at the brain level and changes in circulating miRNA levels in plasma are important diagnostic biomarkers of epilepsy (9). Acceptable sensitivity and specificity have validated high levels of miRNAs as biomarkers of epilepsy (10). Brain-enriched miR-146a is one of the most widely studied miRNAs in epilepsy. In this review, we focus on the role of miR-146a as an essential regulator of epilepsy development and progression and highlight its potential use as a therapeutic target and novel biomarker for epilepsy (Figure 1).

The human miR-146 family consists of two genes: miR-146a and miR-146b. miR-146a is in the long non-coding RNA host gene MIR3142HG on chromosome 5q33.3. miR-146a is highly conserved across species. Sequencing data collected from the miRBase database provided evidence that the miR-146a-5p strand is the biologically active "guide strand" (11). The primary transcript (pri-miR-146a) is under the control of a unique distinct promoter region enriched with CpG islands. It is a transcriptional regulatory sequence of more than 16kb upstream of the miR-146a locus (12). Several putative transcription factor binding sites have been identified, including at least one for CCAAT/enhancer-binding protein-β (C/EBP-β), one for interferon regulatory factor 3/7 (IRF3/7), and two for nuclear factor kappa-light-chain-enhancer of activated B cells (NF-κB) (13). Despite redundant target sequences among miR-146 family members, differences in their promoter regulatory sequences allow for the cell-specific regulation of miR-146a expression (14). miR-146 is expressed in neurons, astrocytes, and microglia (15). In addition, the long non-coding RNA nucleolar protein interacting with the FHA domain of pKi-67 (NIFK) and small nucleolar RNA host gene 16 (SNHG16) regulates miR-146a activity by base pairing and sequestering miRNAs away from their targets (16, 17).

miR-146a is central to neuroinflammation by modulating the NF-κB signaling pathway activity. It substantially impacts the homeostasis of immune and brain cells, neuronal identities, identity acquisition, and immune response regulation in the nervous system (18). Abnormal expression of miR-146a can cause the uncontrolled generation of neurotoxic inflammatory factors, such as IL-1, TNF-α, nitric oxide (NO), and hydrogen peroxide (H_2O_2), eventually leading to neuronal death and neurodegeneration (19, 20). Elevated expression of miR-146a in neural stem cells can lead to increased differentiation into neuronlike cells, higher neurite outgrowth, and branching (21). The two most important single nucleotide polymorphisms (SNPs) in miR-146a, rs2910164 and rs57095329, can affect the level of mature miR-146a, which is related to susceptibility to nervous system diseases (22).

2. miR-146a-associated variations and epilepsy

SNPs can affect the function or expression of a gene. Based on their location, miRNA-associated SNPs are

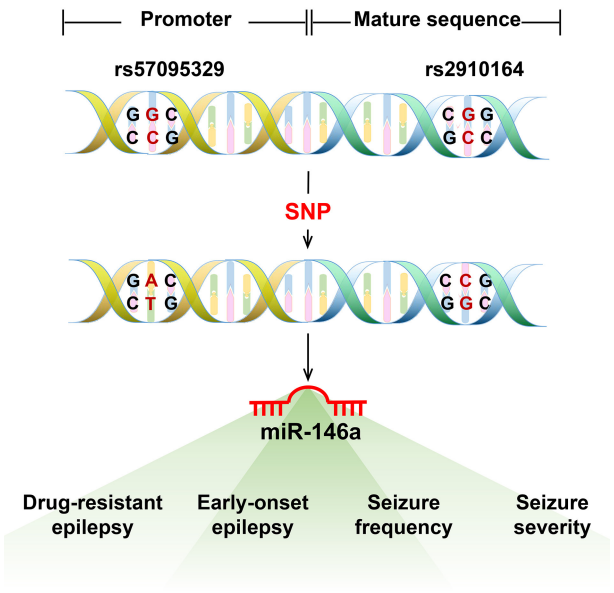

FIGURE 2
The most evaluated single nucleotide polymorphism (SNP) in miR-146a associated with epilepsy. The most evaluated SNPs associated with epilepsy susceptibility were n.60G > C (rs2910164) and n.-411A > G (rs57095329), located in the mature sequence and promoter region of miR-146a. The GC and CC genotypes of SNV rs2910164 in miR-146a are genetic susceptibility markers for DRE or early-onset epilepsy. The SNP rs57095329 in the miR-146a gene is associated with susceptibility to DRE and seizure frequency and also contributes to genetic susceptibility to DRE and seizure severity in children with epilepsy.

classified into SNP sites on miRNA genes and their target genes (23).

Single nucleotide polymorphisms in the sequences of miRNAs or their 3′-UTR target genes may affect the risk of epilepsy and expression of their target genes, thereby increasing disease susceptibility (23). The most evaluated SNPs associated with epilepsy susceptibility were n.60G > C (rs2910164) and n.-411A > G (rs57095329), which are located in the mature sequence and promoter region of miR-146a, respectively (8) (Figure 2). Boschiero et al. demonstrated that the GC genotype of SNV rs2910164 was associated with reduced miR-146a expression compared with the wild-type homozygous (GG) genotype and appeared to be associated with susceptibility to drug-resistant epilepsy (24). GC and CC genotypes of SNV rs2910164 in miR-146a are genetic susceptibility markers for DRE and early-onset epilepsy (8). Another study demonstrated that although a G-to-C substitution in SNP rs2910164 in miR-146a could influence miR-146a expression, it did not play a major role in TLE pathogenesis or some important clinical variables of TLE (25). Recent studies have found that SNP rs57095329 in the miR-146a gene is associated with susceptibility to DRE and seizure frequency (26) and contributes to genetic susceptibility to DRE and seizure severity in children with epilepsy (27).

3. Abnormal expression of miR-146a in epilepsy

In 2010, Aronica et al. first documented the altered expression pattern of miR-146a in epileptic rats and patients with temporal lobe epilepsy (28). They found that miR-146a expression levels were upregulated in astrocytes from temporal lobe epilepsy (TLE) patients with hippocampal sclerosis (HS), particularly in areas of neuronal destruction and gliosis. Since then, increasing evidence has depicted that miR-146a is abnormally expressed in human epilepsy patients and animal models (Tables 1, 2).

As illustrated in Table 1, the expression level of miR-146a was upregulated in the serum of patients with focal and generalized epilepsy (30, 31). Similar findings were observed in the frontal cortex of a pilocarpine-induced status epilepticus (SE) model (40). Furthermore, studies have shown displayed differences in the expression levels of miR-146a between various time points after seizures and in the control group (Table 2). Omran et al. found that in the hippocampus of a rat model of medial temporal lobe epilepsy (MTLE), miR-146a expression was the highest in the latent phase and lowest in the acute phase (36). Another study reported that miR-146a expression was significantly increased in the hippocampal granulosa cell layer (GCL) of TLE rats during the first spontaneous seizure, latency, and chronic phases after SE (29).

However, Song et al. demonstrated that miR-146a is downregulated in the hippocampus of rats with lithium-pilocarpine-induced chronic TLE (43). miR-146a downregulation has been reported in blood samples from children with epileptic encephalopathy (37). In addition, some studies have revealed that miRNA expression profiles in the brain and plasma are inconsistent. For example, in a study of epileptic rats, miR-146a expression was found to be upregulated in the brain 1 week after the onset of the disease. However, enhanced plasma expression was not observed until 3–4 months after chronic seizures (39).

4. The biological relevance of miR-146a in epilepsy

In addition to IRAK1/2 and TRAF6, the first reported targets of miR-146a, many other miR-146a targets that directly or indirectly regulate biological processes beyond inflammation, including intracellular Ca^{2+} changes, apoptosis, oxidative stress, and neurodegeneration, have been identified (Figures 3, 4) (44). miR-146a has been identified as a neuroimmune system mediator with major effects on immune and brain cell homeostasis, acquisition of neuronal identity, and modulation of immune responses in the nervous system (18).

Based on the properties of its target genes, miR-146a has various biological implications in the pathophysiology and progression of epilepsy. According to these findings, abnormal expression patterns and inefficient function of miR-146a are associated with epilepsy.

TABLE 1 Abnormal expression of miR-146a in epileptic patients.

Seizure types	Control group	Level	miR-146a	Reference
Specimen in adult				
PR-TLE with HS	Non-HS cases	Hippocampus	Upregulation	(28)
Epileptic patients	Non-epileptic patients	Hippocampus	Upregulation	(29)
FE and GE	Healthy controls	Serum	Upregulation	(30)
GS and PS	Healthy controls	Serum	Upregulation	(31)
TLE	Healthy controls	Serum	Upregulation	(32)
GGE	Healthy controls	Serum	Upregulation	(33)
Epileptic patients	Healthy controls	Plasma	Upregulation	(34)
FIAS	Favorable response to AEDs patients	Serum	Upregulation	(35)
Specimen in children				
DR-MTLE	No brain disease patients	Hippocampus	Upregulation	(36)
EEs	Healthy controls	Serum	Downregulation	(37)
IE	Healthy controls	Plasma	Upregulation	(38)

TLE, temporal lobe epilepsy; HS, hippocampal sclerosis; FE, focal epilepsy; GE, generalized epilepsy; GS, generalized seizures; PS, partial seizures; GGE, genetic generalized epilepsies; MTLE, mesial temporal lobe epilepsy; FIAS, focal impaired awareness seizures; EEs, epileptic encephalopathies; IE, idiopathic epilepsy; AED, antiepileptic Drugs; PR, pharmacologically refractory; DR, drug-resistant.

4.1. NF-κB and miR-146a in epilepsy

NF-κB is an essential regulator of inflammation and plays an important role in the occurrence and development of epilepsy (45). It is well known that miR-146a plays a crucial role in epileptogenesis as a negative feedback regulator of pro-inflammatory signaling pathways. Furthermore, seizure activity promotes downstream events activated by NF-κB, including inflammation and oxidative stress. This pathway also regulates neuronal excitability and seizure susceptibility (Figures 2, 3). Consequently, it appears that the role of miR-146a in epilepsy extends beyond that of neuroinflammation.

Most studies have revealed that miR-146a is significantly upregulated in epilepsy patients and experimental animal models. miR-146a silencing significantly reduced IL-1, IL-6, and IL-18 levels in the hippocampus of TLE rats and reduced neuronal damage in the CA1 and CA3 regions of the hippocampus (41). However, Wang et al. found opposite results by examining the effects of intracerebroventricular injection of miR-146a antagomir/agomir in an immature rat model of lithium/pilocarpine-induced status epilepticus (46). In the miR-146a antagomir injection group, the latency to generalized convulsions was shorter, the duration and degree of seizures were more severe, the expression level of miR-146a was clearly decreased, and IL-1β, TNF-α, TLR4, and NF-κB were significantly upregulated. The opposite was true for rats treated with miR-146a agomir.

4.2. Complement factor H (CFH) and miR-146a in epilepsy

Complement factor H is an essential and potent inhibitor of alternative complement activation (47). Researchers have confirmed that the persistence of complement activation contributes to a sustained inflammatory response and destabilizes neuronal networks in a TLE rat model (48). As displayed in Figure 3, in chronic TLE rats, enhanced miR-146a can boost IL-1β by downregulating the expression of CFH. Increased IL-1β further upregulated miR-146a expression, forming a miR-146a–CFH–IL-1β loop circuit that initiates an inflammatory cascade and perpetuates inflammation in TLE (Figures 3, 4) (49). However, another study, downregulating miR-146a by intracerebroventricular injection of antagomir-146a enhanced hippocampal expression of CFH and decreased seizure susceptibility in a TLE model (50).

4.3. P-glycoprotein and miR-146a in epilepsy

Activation of the TLR/NF-κB signaling pathway has recently been demonstrated to increase P-glycoprotein (P-gp) levels in the brains of rats with kainic acid-kindled epilepsy (Figure 3) (51). To the best of our knowledge, P-gp overexpression in epileptic patients and animal models is closely associated with antiepileptic drug resistance. Deng et al. found that miR-146a may decrease the level of P-gp expressed in the cerebral vessels of SE rats by downregulating the NF-κB signaling pathway (42). However, Zhang et al. reported that miR-146a gene silencing attenuates pathological changes and improves drug resistance in refractory epilepsy (52). According to this study, silencing of miR-146a downregulated P-gp expression and alleviated inflammation by regulating the high-mobility group box 1 protein (HMGB1)/TLR4/NF-κB signaling pathway.

10.3389/fneur.2023.1094709

TABLE 2 Abnormal expression of miR-146a in animal models of epilepsy.

Experimental epilepsy models	Control group	Time points after seizures	Level	miR-146a	Reference
ES induced SE in rats	Implant but not stimulate	Latent phase	Hippocampus	Upregulation	(28)
		Chronic phase			
		Latent phase	Hippocampus	Upregulation	(39)
		Chronic phase			
		Chronic phase	Plasma		
Li–Pc induced SE in rats	NS	Chronic phase	The frontal cortex	Upregulation	(40)
		Latent phase	GCL; plasma	Upregulation	(29)
		Chronic phase			
		Acute phase	Hippocampus	Upregulation	(41)
		Chronic phase	Para-hippocampal cortex hippocampus	Upregulation	(42)
		Chronic phase	Hippocampus	Downregulation	(43)
Li–Pc induced SE in immature rats	No seizures	Latent phase	Hippocampus	Upregulation	(36)
		Chronic phase			

TLE, temporal lobe epilepsy; HS, hippocampal sclerosis; MTLE, mesial temporal lobe epilepsy; SE, status epilepticus; GCL, granule cell layer; KA, kainic acid; ES, electrical stimulation; Li, lithium; Pc, pilocarpine; NS, normal saline.

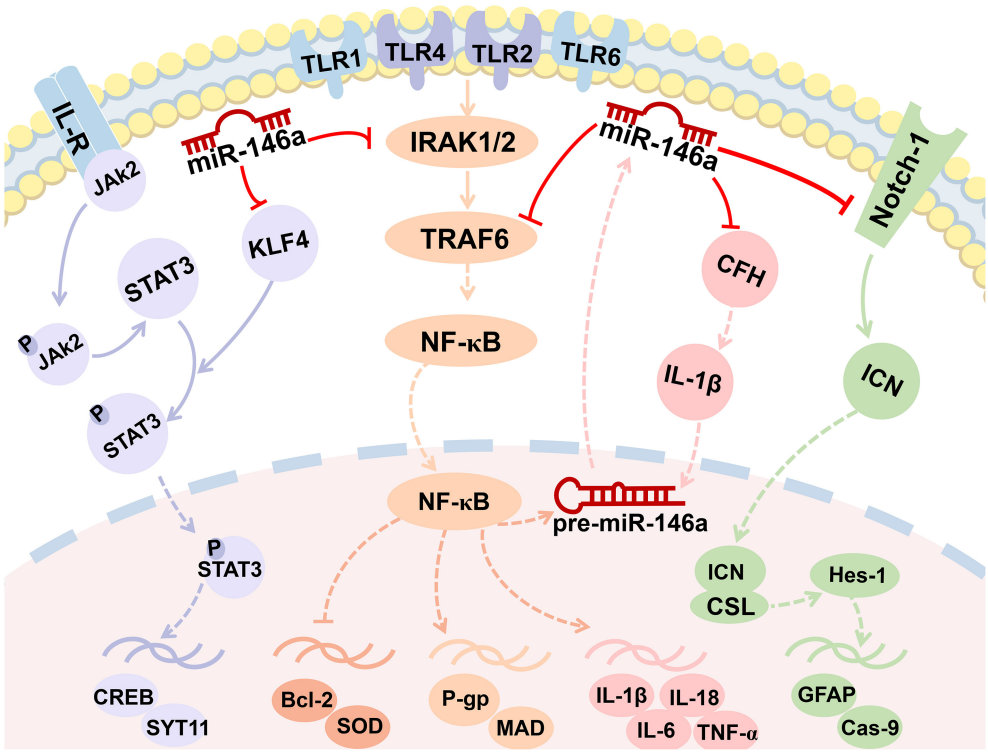

FIGURE 3
MiR-146a is involved in the regulation of multiple signaling pathways. miR-146a plays a crucial role in epileptogenesis as a negative feedback regulator of NF-κB signaling pathways. Enhanced miR-146a can boost IL-1β by downregulating the expression of CFH and forming a miR-146a-CFH-IL-1β loop circuit. The Notch-1 signaling pathway and JAK2/STAT3 signaling pathway were both the targets of miR-146a.

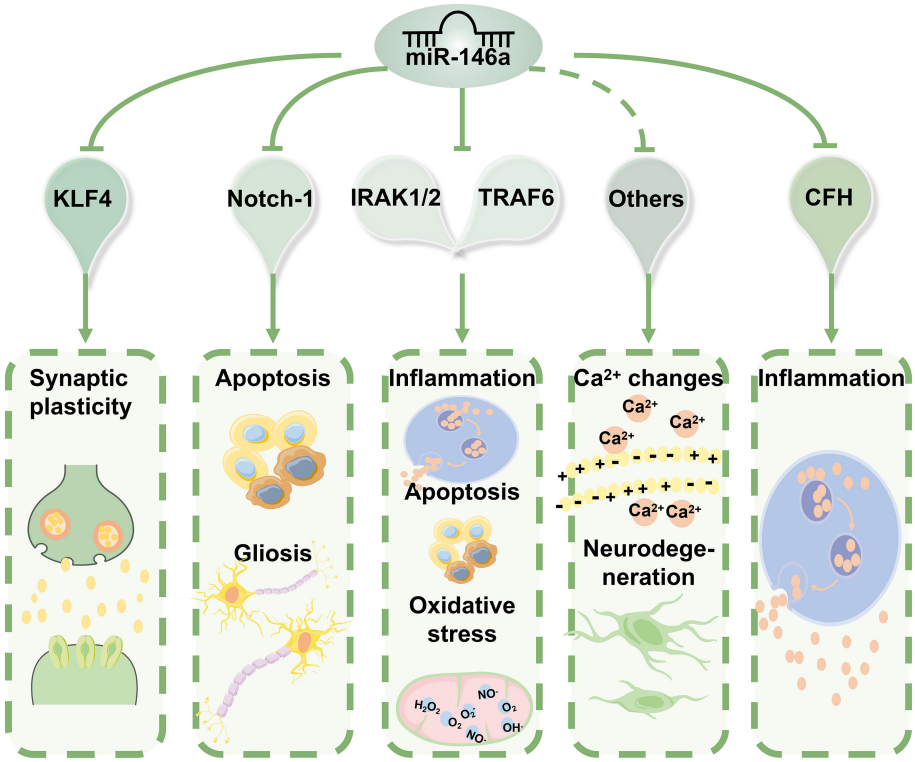

FIGURE 4
The molecular mechanisms of miR-146a in epilepsy. miR-146a acts as an anti-inflammatory miRNA can directly or indirectly regulate biological processes beyond inflammation, including intracellular Ca^{2+} changes, apoptosis, oxidative stress, and neurodegeneration. Based on the properties of its targets, miR-146a can have various biological implications in the pathophysiology and progression of epilepsy.

4.4. Notch-1 and miR-146a in epilepsy

Notch signaling is well known for its requirement in the maintenance of neural stem/progenitor cells and the specification of glial cells (53, 54). Notch-1 has been identified as a target of miR-146a (Figures 3, 4) (55). The inhibitory role of miR-146a downregulation in neural damage in TLE is related to the inhibition of Notch signaling (41). It was found that miR-146a silencing inhibited apoptosis and gliosis in the hippocampus of TLE rats by downregulating the expression levels of caspase-9 and glial fibrillary acidic protein (GFAP) through Notch-1 signaling.

4.5. Signal transducer and activator of transcription 3 (STAT3) and miR-146a in epilepsy

Recent studies have highlighted the importance of miR-146a in epileptic synaptic plasticity. It was confirmed that miR-146a directly binds and downregulates the transcription factor Krüppel-like factor 4 (KLF4) to activate STAT3 and mediate epilepsy seizures by affecting synaptic plasticity in the pentylenetetrazole-kindling mouse model of epilepsy (Figures 3, 4) (56).

4.6. Other signaling pathways and miR-146a in epilepsy

Further molecular mechanisms underlying the role of miR-146a downregulation in cell apoptosis may be attributed to the mitigation of oxidative stress and inflammation (Figures 3, 4). miR-146a siRNA injection significantly decreased the levels of malondialdehyde (MDA), IL-1β, IL-6, and IL-18 but increased the level of superoxide dismutase (SOD) (41). Additionally, apoptosis is regulated by several signaling pathways, with the Bcl-2 protein family playing an important role (55). Zhang et al. revealed that treatment with a miR-146a inhibitor protected neurons from lithium/pilocarpine-induced toxicity and reversed lithium-pilocarpine-induced neuronal injury, partially by inhibiting the Bcl-2/Bax apoptotic pathway (57).

5. Molecular mechanism of miRNA-146a regulating target gene related to epilepsy

MicroRNAs regulate gene expression by targeting the 3′-UTR of mRNA, resulting in translational repression, mRNA degradation, or both. miR-146a was the first miRNA identified as NF-κB-dependent (58). Typically, miR-146a acts as an anti-inflammatory miRNA through the Toll-like receptor (TLR) pathway, regulating

the expression of its target mRNAs, including interleukin 1 (IL-1) receptor-associated kinase-1/2 (IRAK1/2), tumor necrosis factor (TNF) receptor-associated factor 6 (TRAF6), and typical inflammatory modulators (NF-κB, TNF-α, IL-1β, and IL-6) (14). In response, the NF-κB interaction site on the miR-146a promoter allows interaction between NF-κB and AP1 to induce transcription at this site. It operates in a negative feedback loop by inhibiting two upstream NF-κB signaling components, IRAK1 and TRAF6 (Figure 3) (59).

Bioinformatics analysis indicated that miR-146a had overlapping target recognition sites within the CFH mRNA 3′-untranslated region (3′-UTR; 5′-TTTAGTATTAA-3′) (60). By binding to the putative sequence on the 3′-UTR of *cfh* mRNA and inhibiting both mRNA and protein expression of CFH, miR-146a may affect seizure susceptibility (50).

Online target gene prediction software (TargetScan) was used to identify a binding site for miRNA-146a in the 3′-UTR of Notch-1. Notch-1 was confirmed to be a target gene of miR-146a using a luciferase reporter assay (55). Notch signaling is required for epileptogenesis and neurogenesis (54). Once this pathway is blocked, neurogenesis is enhanced during the acute phase of epilepsy and neurogenesis during epileptogenesis is reduced (61).

A previous study identified pronounced effects of KLF4 knockout on promoting axon growth in developing neurons and facilitating regenerative axon growth after CNS injury (62). Ying et al. synthesized a mutated sequence of the binding site between miR-146a and KLF4 according to the prediction of the binding sites using the online software TargetScan and indicated that miR-146a targeted and inhibited KLF4 affecting epileptic seizures (56). Intriguingly, the circular RNA ANKS1B can act as a miRNA sequester for miR-146a to mediate post-transcriptional regulation of KLF4 expression (63).

6. Clinical implications of miR-146a in epilepsy

One of the potential clinical applications of miR-146a is the use of biofluid profiles for molecular diagnostics (64). Epilepsy diagnosis is primarily clinical, and evidence of the utility of circulating nucleic acids in epilepsy is underdeveloped relative to other diseases (65). Analyses performed on patient sera revealed that miR-146a is a suitable candidate as a circulating diagnostic molecule for several models of epilepsy (Table 3), distinguishing between epileptic patients and healthy subjects and even assessing disease risk and treatment responses.

6.1. The diagnostic value of miR-146a in epilepsy

A pilot study found that miR-146a is a possible circulating diagnostic molecule (32). The miR-146a average expression in serum was 0.15 ± 0.11 in TLE patients compared to 0.07 ± 0.04 in healthy controls (t-test, p-value < 0.05). Moreover, there was a significant correlation between serum miR-146a levels and sex in the drug-resistant subjects (p-value < 0.05).

TABLE 3 The diagnostic value of miR-146a in epilepsy.

Number of samples	Seizure type	Healthy controls	Level	Diagnostic results	Diagnostic performance			Reference
					AUC	Sensitivity	Specificity	
180	GS:57	90	Serum	Predict epilepsy	0.786	–	–	(30)
	PS: 33				0.887*	–	–	
289	GS:78	112	Serum	Improve the current diagnosis	0.784	81.9%	65.2%	(31)
	PS:39							
162	DR:76	–	Serum	Discriminate AED-resistant	0.64	–	–	(35)
	DRE:86							
146	GGE:79	67	Serum	Discriminate GGE patients	0.85#	80%#	73%#	(33)
50	IE:30	20	Plasma	Predict epilepsy in children	0.763	73.7%	60%	(38)
150	EP:80	70	Plasma	Complicate with cognitive dysfunction	0.808	87.8%	68.2%	(34)

AUC, Area under the receiver operating characteristic curve; TLE, temporal lobe epilepsy; GS, generalized seizures; PS, partial seizures; GGE, genetic generalized epilepsies; IE, idiopathic epilepsy; EP, epileptic patients; AED, antiepileptic drugs; DR, drug-sensitive; DRE, drug-resistant epilepsy; *, Combined with miR-106b; #, Combined with miR-155 and mir-132.

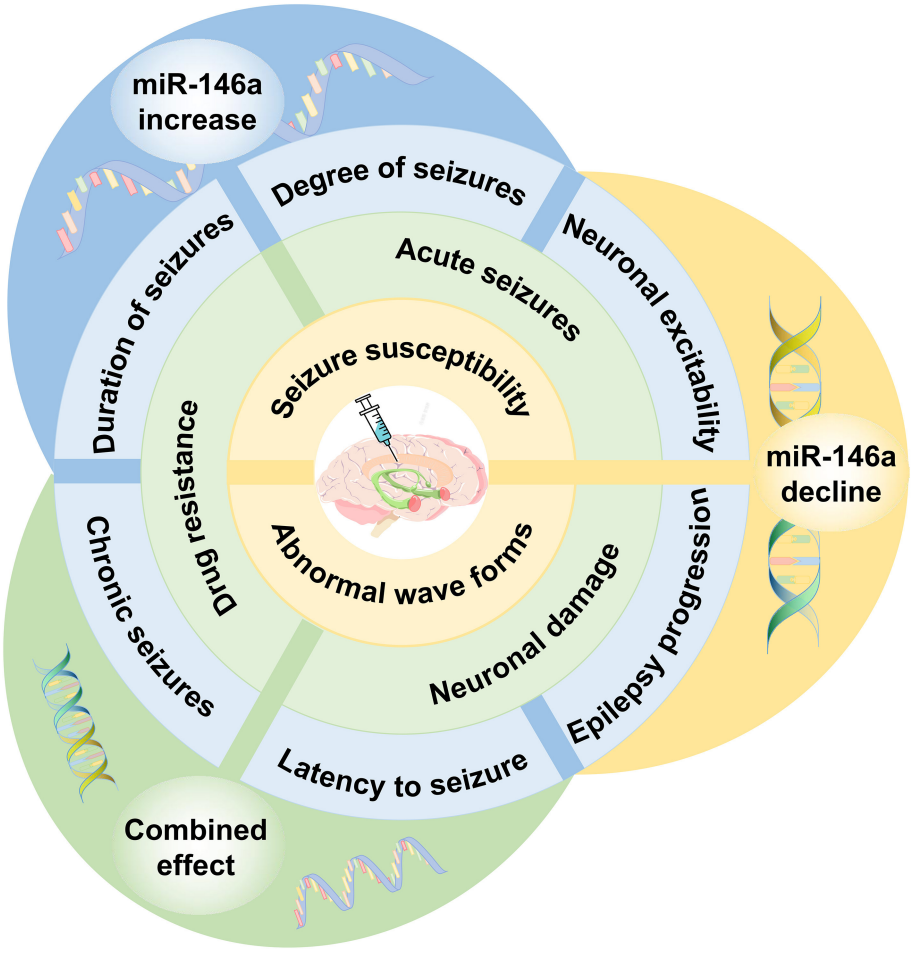

FIGURE 5
The effect of miR-146a as a therapeutic target in epilepsy. Regulating the expression of miR-146a to the optimal level can delay seizure onset, decrease seizure susceptibility, and improve drug resistance. miR-146a bears considerable potential for potential epilepsy therapeutic strategies.

Other studies' receiver-operating characteristic (ROC) curve and logistic regression analysis demonstrated that patients with elevated circulating miR-146a levels had a significantly increased risk of developing DRE (Table 3). Its effect was independent of temporal lobe sclerosis, epilepsy duration, family history, age at first seizure, body mass index (BMI), smoking, and gender. Decision curve analysis highlighted that evaluation of circulating miR-146a leads to superior clinical benefits for DRE prognosis and patient risk stratification (35). Elnady et al. evaluated circulating miR-146a as a diagnostic and prognostic biomarker in pediatric epilepsy patients and found that miR-146a expression levels were 14.65-fold higher in epileptic patients than in healthy controls (38). The ROC curve of serum miR-146a demonstrated a significant area under the curve (AUC) value of 0.763 for predicting epilepsy.

Recently, miR-146a was proposed as a diagnostic marker for genetically generalized epilepsy (GGE) in a panel of circulating miRNAs. The combined serum levels of miR-146a, miR-155, and miR-132 performed well as diagnostic biomarkers, discriminating GGE patients from controls with an AUC of 0.85, 80% specificity, and 73% sensitivity (33). Some researchers have found that miR-146a is strongly associated with cognitive dysfunction, anxiety, and depression in patients with epilepsy and reflects the severity of complications, indicating that it may serve as a potential biomarker for epilepsy (34).

6.2. The role of miR-146a as a therapeutic target in epilepsy

Several researchers have focused on the therapeutic role of miR-146a. Some studies have attempted to regulate the expression of miR-146a and bring it to the optimal level by silencing or mimicking it with a synthetic antagomir or oligonucleotide mimic (Figure 5).

Iori et al. presented the first proof-of-concept data on disease modification using a transiently applied intervention after the onset of epilepsy (66). The results suggested that injection of miR-146a mimics reduced the number of seizures and the progression of the disease, including the postponement of disseminated seizures, improvement of structural hippocampal damage, and reduction in apoptosis of regional cells. Similarly, another study found that

intracerebroventricular injection of miR-146a agomir inhibited NF-κB activity, alleviated neuroinflammation, and relieved seizures in SE rats (46). Intranasal administration of miR-146a mimics delayed seizure onset in a model of lithium-pilocarpine-induced status epilepticus (67). Meanwhile, studies have demonstrated that the injection of miR-146a mimics into the hippocampus of status epilepticus rats downregulated P-gp expression and improved drug resistance in refractory epilepsy (42).

However, other studies have reported contradictory results. Li et al. depicted that administration of miR-146a agomir in the hippocampal region upregulated the expression of miR-146a and increased abnormal waveforms in chronic TLE rat models (49). Downregulating miR-146a by intracerebroventricular injection of antagomir-146a enhanced hippocampal expression of CFH in the TLE model and decreased seizure susceptibility (50). Stereotactic injection of miR-146a antagomir reduced seizure scores in epileptic mice (56). Silencing of miR-146a downregulates P-gp expression and alleviates inflammation, which attenuates pathological changes and improves drug resistance in refractory epilepsy (52). According to a recent study, using miR-146a inhibitors to block pathogenic activation of NF-κB pathway in SE brain may have a neuroprotective function (57).

Overall, dynamic variations in miR-146a expression have been reported throughout distinct phases of epileptogenesis. These studies may promote miR-146a application as a biomarker and a novel therapeutic approach for epilepsy. The mechanism by which miR-146a functions as a biomarker in different stages of epilepsy remains unknown, and other variables that must be considered, such as age, comorbidities, and the nature of the induced injury, may affect the level of miR-146a expression. Some studies have revealed that miR-146a and other miRNA assays may have better sensitivity and specificity for predicting epilepsy. However, the altered biofluid profiles require further investigation. Furthermore, the levels of miR-146a expression must be measured separately in drug-resistant and drug-responsive patients because functions, targets, and processes of miR-146a in the development and pathogenesis of refractory epilepsy remain unclear, and it is not a predictor of drug response. Currently, miR-146a application as a biomarker of epilepsy is limited. Additional validation in large-scale studies is beneficial.

Previous studies have indicated that treatment with either anti-miR-146a or a miR-146a mimic ameliorates the latency, frequency, and duration of induced seizures in animal models of epilepsy, emphasizing the causality and reversibility of the effects of miR-146a in epilepsy. However, the rationale for the discrepancies between these studies remains unclear (21). A better understanding of the signaling pathways/feedback loops that can modulate the expression and action of miR-146a can help further therapeutic development. Extensive studies should be conducted in different epilepsy models, and other examples of the preclinical uses of miR-146a for treatment require further study.

7. Conclusion and prospects

In this review, we project a large summary of the role of miR-146a in brain functions, its expression in various models of epilepsy, and mechanistic links between their dysregulation in epileptic brain tissue and targeting for seizure control or disease modification. In the same line, we summarized the findings to date on circulating miRNA-146a levels as potential biomarker tools for diagnosing epilepsy and emphasized the application prospects of miR-146a in epilepsy therapy. It has been demonstrated that miR-146a, a crucial inflammation-related regulator, has advantages in therapeutic and diagnostic applications because of its ability to regulate message feedback circuits multi-directionally. Despite its potential, further exploration and verification are required to evaluate the different interfering factors in various types and stages of epilepsy.

Much work should be carried out before miR-146a can be used as a safe and effective therapeutic target for epilepsy, especially concerning its delivery methods and capacity for target specificity. There remains a major challenge in formulating medications that can regulate miR-146a expression, bring it to the optimal level, and improve drug development for targeted therapy. miRNA-targeting therapeutics must generally be administered *via* a route that circumvents the BBB or modifications that facilitate uptake *via* a systemic route (68). Intrathecal administration *via* lumbar puncture is invasive and inconvenient. Intranasal delivery may be a less invasive solution. Other safety-related risks arising from the difficulty in predicting the off-target effects of miRNA inhibition should be considered. As exosomes can cross the blood–brain barrier, exosomes originating in epileptogenic tissue may provide a means for non-invasive monitoring of seizure susceptibility and response to treatment (69). Because of the robust association between miR-146a and autoimmunity, miR-146a has a promising future for treating epilepsy based on intestinal microecosystems (70).

In conclusion, miR-146a, with the mentioned acts and potential, may be an ideal diagnostic marker and target/agent for epilepsy. Detailed information on the mechanisms and functional roles of miR-146a in epilepsy, which will be needed to develop novel candidate drugs for disease treatment, will require further investigation, and some of the unanswered questions and future directions should be considered.

Author contributions

SM, JW, and JY: collected and analyzed the literature, drafted the figures, and wrote the manuscript. WZ and FZ: conceived and gave the final approval of the submitted version. All authors have read and agreed to the published version of the manuscript.

Funding

This study was supported by the Zhejiang Basic Public Welfare Research Project (LGD22H090003), the Medical and Health Science and Technology Program of Zhejiang Province (No. 2020RC088), and the Hangzhou Agricultural and Social Development Research Project (20201203B152).

Conflict of interest

The authors declare that the research was conducted in the absence of any commercial or financial relationships that could be construed as a potential conflict of interest.

Publisher's note

References

1. Sills GJ, Rogawski MA. Mechanisms of action of currently used antiseizure drugs. *Neuropharmacology*. (2020) 168:107966. doi: 10.1016/j.neuropharm.2020.107966

2. Villa C, Lavitrano M, Combi R. Long non-coding RNAS and related molecular pathways in the pathogenesis of epilepsy. *Int J Mol Sci.* (2019) 20:4898. doi: 10.3390/ijms20194898

3. Guerrini R, Balestrini S, Wirrell EC, Walker MC. Monogenic epilepsies: disease mechanisms, clinical phenotypes, and targeted therapies. *Neurology*. (2021) 97:817–31. doi: 10.1212/WNL.0000000000012744

4. Magheru C, Magheru S, Coltau M, Hoza A, Moldovan C, Sachelarie L, et al. Antiepileptic drugs and their dual mechanism of action on carbonic anhydrase. *J Clin Med*. (2022) 11:2614. doi: 10.3390/jcm11092614

5. Zhang Q, Zhong C, Yan Q, Zeng LH, Gao W, Duan S. miR-874: an important regulator in human diseases. *Front Cell Dev Biol.* (2022) 10:784968. doi: 10.3389/fcell.2022.784968

6. Alkan AH, Akgül B. Endogenous miRNA sponges. *Methods Mol Biol.* (2022) 2257:91–104. doi: 10.1007/978-1-0716-1170-8_5

7. Juzwik CA, Drake S, Zhang Y, Paradis-Isler N, Sylvester A, Amar-Zifkin A, et al. microRNA dysregulation in neurodegenerative diseases: a systematic review. *Prog Neurobiol.* (2019) 182:101664. doi: 10.1016/j.pneurobio.2019.101664

8. Buainain RP, Boschiero MN, Camporeze B, de Aguiar PHP, Marson FAL, Ortega MM. Single-nucleotide variants in microRNAs sequences or in their target genes might influence the risk of epilepsy: a review. *Cell Mol Neurobiol.* (2022) 42:1645–58. doi: 10.1007/s10571-021-01058-7

9. Bauer S, Schütz V, Strzelczyk A, Rosenow F. Is there a role for microRNAs in epilepsy diagnostics? *Expert Rev Mol Diagn.* (2020) 20:693–701. doi: 10.1080/14737159.2020.1745065

10. Yakovleva KD, Dmitrenko DV, Panina IS, Usoltseva AA, Gazenkampf KA, Konovalenko OV, et al. Expression profile of miRs in mesial temporal lobe epilepsy: systematic review. *Int J Mol Sci.* (2022) 23:951. doi: 10.3390/ijms23020951

11. Paterson MR, Kriegel AJ. MiR-146a/b: a family with shared seeds and different roots. *Physiol Genom.* (2017) 49:243–52. doi: 10.1152/physiolgenomics.00133.2016

12. Iacona JR, Lutz CS. miR-146a-5p: expression, regulation, and functions in cancer. *Wiley Interdiscip Rev RNA*. (2019) 10:e1533. doi: 10.1002/wrna.1533

13. Taganov KD, Boldin MP, Chang KJ, Baltimore D. NF-kappaB-dependent induction of microRNA miR-146, an inhibitor targeted to signaling proteins of innate immune responses. *Proc Natl Acad Sci USA*. (2006) 103:12481–6. doi: 10.1073/pnas.0605298103

14. Rusca N, Monticelli S. MiR-146a in immunity and disease. *Mol Biol Int.* (2011) 2011:437301. doi: 10.4061/2011/437301

15. Li YY, Cui JG, Dua P, Pogue AI, Bhattacharjee S, Lukiw WJ. Differential expression of miRNA-146a-regulated inflammatory genes in human primary neural, astroglial and microglial cells. *Neurosci Lett.* (2011) 499:109–13. doi: 10.1016/j.neulet.2011.05.044

16. Zhou YX, Zhao W, Mao LW, Wang YL, Xia LQ, Cao M, et al. Long non-coding RNA NIFK-AS1 inhibits M2 polarization of macrophages in endometrial cancer through targeting miR-146a. *Int J Biochem Cell Biol.* (2018) 104:25–33. doi: 10.1016/j.biocel.2018.08.017

17. Han W, Du X, Liu M, Wang J, Sun L, Li Y. Increased expression of long non-coding RNA SNHG16 correlates with tumor progression and poor prognosis in non-small cell lung cancer. *Int J Biol Macromol.* (2019) 121:270–8. doi: 10.1016/j.ijbiomac.2018.10.004

18. Aslani M, Mortazavi-Jahromi SS, Mirshafiey A. Efficient roles of miR-146a in cellular and molecular mechanisms of neuroinflammatory disorders: an effectual review in neuroimmunology. *Immunol Lett.* (2021) 238:1–20. doi: 10.1016/j.imlet.2021.07.004

19. Moradi Z, Rabiei Z, Anjomshoa M, Amini-Farsani Z, Massahzadeh V, Asgharzade S. Neuroprotective effect of wild lowbush blueberry (Vaccinium angustifolium) on global cerebral ischemia/reperfusion injury in rats: downregulation of iNOS/TNF-α and upregulation of miR-146a/miR-21 expression. *Phytother Res.* (2021) 35:6428–40. doi: 10.1002/ptr.7296

20. Jiao G, Pan B, Zhou Z, Zhou L, Li Z, Zhang Z. MicroRNA-21 regulates cell proliferation and apoptosis in H_2O_2-stimulated rat spinal cord neurons. *Mol Med Rep.* (2015) 12:7011–6. doi: 10.3892/mmr.2015.4265

21. Nguyen LS, Fregeac J, Bole-Feysot C, Cagnard N, Iyer A, Anink J, et al. Role of miR-146a in neural stem cell differentiation and neural lineage determination: relevance for neurodevelopmental disorders. *Mol Autism.* (2018) 9:38. doi: 10.1186/s13229-018-0219-3

22. Ahmed Ali M, Gamil Shaker O, Mohamed Eid H, Elsayed Mahmoud E, Mahmoud Ezzat E, Nady Gaber S. Relationship between miR-155 and miR-146a polymorphisms and susceptibility to multiple sclerosis in an Egyptian cohort. *Biomed Rep.* (2020) 12:276–84. doi: 10.3892/br.2020.1286

23. Xiao W, Wu Y, Wang J, Luo Z, Long L, Deng N, et al. Network and pathway-based analysis of single-nucleotide polymorphism of miRNA in temporal lobe epilepsy. *Mol Neurobiol.* (2019) 56:7022–31. doi: 10.1007/s12035-019-1584-4

24. Boschiero MN, Camporeze B, Santos JSD, Costa LBD, Bonafé GA, Queiroz LS. et al. The single nucleotide variant n60G>C in the microRNA-146a associated with susceptibility to drug-resistant epilepsy. *Epilepsy Res.* (2020) 162:106305. doi: 10.1016/j.eplepsyres.2020.106305

25. Manna I, Labate A, Mumoli L, Pantusa M, Ferlazzo E, Aguglia U, et al. Relationship between genetic variant in pre-microRNA-146a and genetic predisposition to temporal lobe epilepsy: a case-control study. *Gene.* (2013) 516:181–3. doi: 10.1016/j.gene.2012.09.137

26. Cui L, Tao H, Wang Y, Liu Z, Xu Z, Zhou H, et al. A functional polymorphism of the microRNA-146a gene is associated with susceptibility to drug-resistant epilepsy and seizures frequency. *Seizure.* (2015) 27:60–5. doi: 10.1016/j.seizure.2015.02.032

27. Li Y, Wang J, Jiang C, Zheng G, Lu X, Guo H. Association of the genetic polymorphisms in pre-microRNAs with risk of childhood epilepsy in a Chinese population. *Seizure.* (2016) 40:21–6. doi: 10.1016/j.seizure.2016.04.011

28. Aronica E, Fluiter K, Iyer A, Zurolo E, Vreijling J, van Vliet EA, et al. Expression pattern of miR-146a, an inflammation-associated microRNA, in experimental and human temporal lobe epilepsy. *Eur J Neurosci.* (2010) 31:1100–7. doi: 10.1111/j.1460-9568.2010.07122.x

29. Roncon P, Soukupovà M, Binaschi A, Falcicchia C, Zucchini S, Ferracin M, et al. MicroRNA profiles in hippocampal granule cells and plasma of rats with pilocarpine-induced epilepsy—comparison with human epileptic samples. *Sci Rep.* (2015) 5:14143. doi: 10.1038/srep14143

30. An N, Zhao W, Liu Y, Yang X, Chen P. Elevated serum miR-106b and miR-146a in patients with focal and generalized epilepsy. *Epilepsy Res.* (2016) 127:311–6. doi: 10.1016/j.eplepsyres.2016.09.019

31. Wang J, Yu JT, Tan L, Tian Y, Ma J, Tan CC, et al. Genome-wide circulating microRNA expression profiling indicates biomarkers for epilepsy. *Sci Rep.* (2015) 5:9522. doi: 10.1038/srep09522

32. De Benedittis S, Fortunato F, Cava C, Gallivanone F, Iaccino E, Caligiuri ME, et al. Circulating microRNA: the potential novel diagnostic biomarkers to predict drug resistance in temporal lobe epilepsy, a pilot study. *Int J Mol Sci.* (2021) 22:702. doi: 10.3390/ijms22020702

33. Martins-Ferreira R, Chaves J, Carvalho C, Bettencourt A, Chorão R, Freitas J, et al. Circulating microRNAs as potential biomarkers for genetic generalized epilepsies: a three microRNA panel. *Eur J Neurol.* (2020) 27:660–6. doi: 10.1111/ene.14129

34. Huang H, Cui G, Tang H, Kong L, Wang X, Cui C, et al. Relationships between plasma expression levels of microRNA-146a and microRNA-132 in epileptic patients and their cognitive, mental and psychological disorders. *Bioengineered.* (2022) 13:941–9. doi: 10.1080/21655979.2021.2015528

35. Leontariti M, Avgeris M, Katsarou MS, Drakoulis N, Siatouni A, Verentzioti A, et al. Circulating miR-146a and miR-134 in predicting drug-resistant epilepsy in patients with focal impaired awareness seizures. *Epilepsia.* (2020) 61:959–70. doi: 10.1111/epi.16502

36. Omran A, Peng J, Zhang C, Xiang QL, Xue J, Gan N, et al. Interleukin-1β and microRNA-146a in an immature rat model and children with mesial temporal lobe epilepsy. *Epilepsia.* (2012) 53:1215–24. doi: 10.1111/j.1528-1167.2012.03540.x

37. Ünalp A, Coskunpinar E, Gunduz K, Pekuz S, Baysal BT, Edizer S, et al. Detection of deregulated miRNAs in childhood epileptic encephalopathies. *J Mol Neurosci.* (2022) 72:1234–42. doi: 10.1007/s12031-022-02001-1

38. Elnady HG, Abdelmoneam N, Eissa E, Hamid ERA, Zeid DA, Abo-Shanab AM, et al. MicroRNAs as potential biomarkers for childhood epilepsy open access. *Maced J Med Sci.* (2019) 7:3965–9. doi: 10.3889/oamjms.2019.634

39. Gorter JA, Iyer A, White I, Colzi A, van Vliet EA, Sisodiya S, et al. Hippocampal subregion-specific microRNA expression during epileptogenesis in experimental temporal lobe epilepsy. *Neurobiol Dis.* (2014) 62:508–20. doi: 10.1016/j.nbd.2013.10.026

40. Matos G, Scorza FA, Mazzotti DR, Guindalini C, Cavalheiro EA, Tufik S, et al. The effects of sleep deprivation on microRNA expression in rats submitted to pilocarpine-induced status epilepticus. *Prog Neuropsychopharmacol Biol Psychiatry.* (2014) 51:159–65. doi: 10.1016/j.pnpbp.2014.02.001

41. Huang H, Cui G, Tang H, Kong L, Wang X, Cui C, et al. Silencing of microRNA-146a alleviates the neural damage in temporal lobe epilepsy by down-regulating Notch-1. *Mol Brain.* (2019) 12:102. doi: 10.1186/s13041-019-0523-7

42. Deng X, Shao Y, Xie Y, Feng Y, Wu M, Wang M, et al. MicroRNA-146a-5p Downregulates the expression of P-glycoprotein in rats with lithium-pilocarpine-induced status epilepticus. *Biol Pharm Bull.* (2019) 42:744–50. doi: 10.1248/bpb.b18-00937

43. Song YJ, Tian XB, Zhang S, Zhang YX, Li X, Li D, et al. Temporal lobe epilepsy induces differential expression of hippocampal miRNAs including let-7e and miR-23a/b. *Brain Res.* (2011) 1387:134–40. doi: 10.1016/j.brainres.2011.02.073

44. Ammal Kaidery N, Ahuja M, Sharma SM, Thomas B. An emerging role of miRNAs in neurodegenerative diseases: mechanisms and perspectives on miR146a. *Antioxid Redox Signal.* (2021) 35:580–94. doi: 10.1089/ars.2020.8256

45. Cai M, Lin W. The Function of NF-Kappa B during epilepsy, a potential therapeutic target. *Front Neurosci.* (2022) 16:851394. doi: 10.3389/fnins.2022.851394

46. Wang X, Yin F, Li L, Kong H, You B, Zhang W, et al. Intracerebroventricular injection of miR-146a relieves seizures in an immature rat model of lithium-pilocarpine induced status epilepticus. *Epilepsy Res.* (2018) 139:14–9. doi: 10.1016/j.eplepsyres.2017.10.006

47. Kiss MG, Ozsvár-Kozma M, Porsch F, Göderle L, Papac-Miličević N, Bartolini-Gritti B, et al. Complement factor H modulates splenic B cell development and limits autoantibody production. *Front Immunol.* (2019) 10:1607. doi: 10.3389/fimmu.2019.01607

48. Aronica E, Boer K, van Vliet EA, Redeker S, Baayen JC, Spliet WG, et al. Complement activation in experimental and human temporal lobe epilepsy. *Neurobiol Dis.* (2007) 26:497–511. doi: 10.1016/j.nbd.2007.01.015

49. Li TR, Jia YJ, Ma C, Qiu WY, Wang Q, Shao XQ, et al. The role of the microRNA-146a/complement factor H/interleukin-1β-mediated inflammatory loop circuit in the perpetuate inflammation of chronic temporal lobe epilepsy. *Dis Model Mech.* (2018) 11:dmm031708. doi: 10.1242/dmm.031708

50. He F, Liu B, Meng Q, Sun Y, Wang W, Wang C. Modulation of miR-146a/complement factor H-mediated inflammatory responses in a rat model of temporal lobe epilepsy. *Biosci Rep.* (2016) 36:6. doi: 10.1042/BSR20160290

51. Shao Y, Wang C, Hong Z, Chen Y. Inhibition of p38 mitogen-activated protein kinase signaling reduces multidrug transporter activity and anti-epileptic drug resistance in refractory epileptic rats. *J Neurochem.* (2016) 136:1096–105. doi: 10.1111/jnc.13498

52. Zhang H L, Lin Y H, Qu Y, Chen Q. The effect of miR-146a gene silencing on drug-resistance and expression of protein of P-gp and MRP1 in epilepsy. *Eur Rev Med Pharmacol Sci.* (2018) 22:2372–9.

53. Tang H, Lai Y, Zheng J, Chen K, Jiang H, Xu G. MiR-146a Promotes tolerogenic properties of dendritic cells and through targeting notch1 signaling. *Immunol Invest.* (2020) 49:555–70. doi: 10.1080/08820139.2019.1708385

54. Yuan P, Han W, Xie L, Cheng L, Chen H, Chen J, et al. The implications of hippocampal neurogenesis in adolescent rats after status epilepticus: a novel role of notch signaling pathway in regulating epileptogenesis. *Cell Tissue Res.* (2020) 380:425–33. doi: 10.1007/s00441-019-03146-z

55. Ghafouri-Fard S, Glassy MC, Abak A, Hussen BM, Niazi V, Taheri M. The interaction between miRNAs/lncRNAs and Notch pathway in human disorders. *Biomed Pharmacother.* (2021) 138:111496. doi: 10.1016/j.biopha.2021.111496

56. Chen J, Chen Y, Li Y. miR-146a/KLF4 axis in epileptic mice: A novel regulator of synaptic plasticity involving STAT3 signaling. *Brain Res.* (2022) 1790:147988. doi: 10.1016/j.brainres.2022.147988

57. Chen Y, Zhang H, Qu Y, Wang A. Antagonist targeting microRNA-146a protects against lithium-pilocarpine-induced status epilepticus in rats by nuclear factor-κB pathway. *Mol Med Rep.* (2018) 17: 5356-5361. doi: 10.3892/mmr.2018.8465

58. Olivieri F, Prattichizzo F, Giuliani A, Matacchione G, Rippo MR, Sabbatinelli J, et al. miR-21 and miR-146a: the microRNAs of inflammaging and age-related diseases. *Ageing Res Rev.* (2021) 70:101374. doi: 10.1016/j.arr.2021.101374

59. Su W, Aloi MS, Garden GA. MicroRNAs mediating CNS inflammation: Small regulators with powerful potential. *Brain Behav Immun.* (2016) 52:1–8. doi: 10.1016/j.bbi.2015.07.003

60. Lukiw WJ, Alexandrov PN, Zhao Y, Hill JM. Bhattacharjee S. Spreading of Alzheimer's disease inflammatory signaling through soluble micro-RNA. *Neuroreport.* (2012) 23:621–6. doi: 10.1097/00001756-201207110-00009

61. Li Y, Wu L, Yu M, Yang F, Wu B, Lu S, et al. HIF-1α is Critical for the activation of notch signaling in neurogenesis during acute epilepsy. *Neuroscience.* (2018) 394:206–19. doi: 10.1016/j.neuroscience.2018.10.037

62. van Battum EY, Verhagen MG, Vangoor VR, Fujita Y, Derijck AAHA, O'Duibhir E, et al. An image-based miRNA screen identifies miRNA-135s as regulators of CNS axon growth and regeneration by targeting kruppel-like factor 4. *J Neurosci.* (2018) 38:613–30. doi: 10.1523/JNEUROSCI.0662-17.2017

63. Fan C, Li Y, Lan T, Wang W, Long Y, Yu SY. Microglia secrete miR-146a-5p-containing exosomes to regulate neurogenesis in depression. *Mol Ther.* (2022) 30:1300–14. doi: 10.1016/j.ymthe.2021.11.006

64. Pitkänen A, Ekolle Ndode-Ekane X, Lapinlampi N, Puhakka N. Epilepsy biomarkers - Toward etiology and pathology specificity. *Neurobiol Dis.* (2019) 123:42–58. doi: 10.1016/j.nbd.2018.05.007

65. Whitlock JH, Soelter TM, Williams AS, Hardigan AA, Lasseigne BN. Liquid biopsies in epilepsy: biomarkers for etiology, diagnosis, prognosis, and therapeutics. *Hum Cell.* (2022) 35:15–22. doi: 10.1007/s13577-021-00624-x

66. Iori V, Iyer A M, Ravizza T, Beltrame L, Paracchini L, Marchini S, et al. Blockade of the IL-1R1/TLR4 pathway mediates disease-modification therapeutic effects in a model of acquired epilepsy. *Neurobiol Dis.* (2017) 99:12–23. doi: 10.1016/j.nbd.2016.12.007

67. Tao H, Zhao J, Liu T, Cai Y, Zhou X, Xing H, et al. Intranasal delivery of mir-146a mimics delayed seizure onset in the lithium-pilocarpine mouse model. *Mediators Inflamm.* (2017) 2017:6512620. doi: 10.1155/2017/6512620

68. Morris G, O'Brien D, Henshall DC. Opportunities and challenges for microRNA-targeting therapeutics for epilepsy. *Trends Pharmacol Sci.* (2021) 42:605–16. doi: 10.1016/j.tips.2021.04.007

69. Cukovic D, Bagla S, Ukasik D, Stemmer PM, Jena BP, Naik AR, et al. Exosomes in epilepsy of tuberous sclerosis complex: carriers of pro-inflammatory MicroRNAs. *Noncoding RNA.* (2021) 7:40. doi: 10.3390/ncrna7030040

70. Anzola A, González R, Gámez-Belmonte R, Ocón B, Aranda CJ, Martínez-Moya P, et al. miR-146a regulates the crosstalk between intestinal epithelial cells, microbial components and inflammatory stimuli. *Sci Rep.* (2018) 8:17350. doi: 10.1038/s41598-018-35338-y

frontiers | Frontiers in Neurology

TYPE Review
PUBLISHED 12 May 2023
DOI 10.3389/fneur.2023.1123407

OPEN ACCESS

EDITED BY
Stefania Mondello,
University of Messina, Italy

REVIEWED BY
Olli Tenovuo,
University of Turku, Finland
Sergio Bagnato,
Giuseppe Giglio Foundation, Italy
Yizhen Tang,
Harvard Medical School, United States

*CORRESPONDENCE
Shazia Malik
✉ maliks15@mcmaster.ca
Michel Rathbone
✉ mrathbon@mcmaster.ca

RECEIVED 14 December 2022
ACCEPTED 26 April 2023
PUBLISHED 12 May 2023

CITATION
Malik S, Alnaji O, Malik M, Gambale T, Farrokhyar F and Rathbone MP (2023) Inflammatory cytokines associated with mild traumatic brain injury and clinical outcomes: a systematic review and meta-analysis. *Front. Neurol.* 14:1123407. doi: 10.3389/fneur.2023.1123407

Inflammatory cytokines associated with mild traumatic brain injury and clinical outcomes: a systematic review and meta-analysis

Shazia Malik[1]*, Omar Alnaji[2], Mahnoor Malik[3], Teresa Gambale[4], Forough Farrokhyar[5] and Michel P. Rathbone[4]*

[1]Neurosciences Graduate Program, McMaster University, Hamilton, ON, Canada, [2]Faculty of Life Sciences, McMaster University, Hamilton, ON, Canada, [3]Bachelor of Health Sciences Program, McMaster University, Hamilton, ON, Canada, [4]Division of Neurology, Department of Medicine, McMaster University, Hamilton, ON, Canada, [5]Department of Surgery and Department of Health Research Methods, Evidence, and Impact, McMaster University, Hamilton, ON, Canada

Mild traumatic brain injuries (mTBIs) trigger a neuroinflammatory response, which leads to perturbations in the levels of inflammatory cytokines, resulting in a distinctive profile. A systematic review and meta-analysis were conducted to synthesize data related to levels of inflammatory cytokines in patients with mTBI. The electronic databases EMBASE, MEDLINE, and PUBMED were searched from January 2014 to December 12, 2021. A total of 5,138 articles were screened using a systematic approach based on the PRISMA and R-AMSTAR guidelines. Of these articles, 174 were selected for full-text review and 26 were included in the final analysis. The results of this study demonstrate that within 24hours, patients with mTBI have significantly higher levels of Interleukin-6 (IL-6), Interleukin-1 Receptor Antagonist (IL-1RA), and Interferon-γ (IFN-γ) in blood, compared to healthy controls in majority of the included studies. Similarly one week following the injury, patients with mTBI have higher circulatory levels of Monocyte Chemoattractant Protein-1/C-C Motif Chemokine Ligand 2 (MCP-1/CCL2), compared to healthy controls in majority of the included studies. The results of the meta-analysis also confirmed these findings by demonstrating significantly elevated blood levels of IL-6, MCP-1/CCL2, and Interleukin-1 beta (IL-1β) in the mTBI population compared to healthy controls ($p<0.0001$), particularly in the acute stages (<7days). Furthermore, it was found that IL-6, Tumor Necrosis Factor-alpha (TNF-α), IL-1RA, IL-10, and MCP-1/CCL2 were associated with poor clinical outcomes following the mTBI. Finally, this research highlights the lack of consensus in the methodology of mTBI studies that measure inflammatory cytokines in the blood, and also provides direction for future mTBI research.

KEYWORDS

concussion, neuroinflammation, mTBI, cytokines, traumatic brain injury

1. Introduction

Most traumatic brain injuries are classified as mild traumatic brain injuries (mTBI) or concussions. mTBI induces a variety of symptoms including headaches and other physical, cognitive, and emotional symptoms, commonly referred to as post-concussion symptoms. These symptoms often resolve spontaneously within a few days to months. However, up to 56% of

individuals with mTBI either develop prolonged symptoms or do not recover (1–4). Persistent post-concussive symptoms are usually associated with increased healthcare costs, disability, and reduced quality of life (5–9).

Interestingly, post-concussion like symptoms appear to be nonspecific to mTBIs, as they are also seen in individuals who have sustained other bodily injuries (10–14). Following a head injury, a cascade of acute neurochemical, metabolic, and cellular changes are triggered within the brain (15). Neuroinflammation is a secondary consequence of mTBI that appears to be one of many factors associated with post-concussion symptoms (16, 17). It is observed that post-concussion like symptoms are associated with inflammatory cytokines independent of head injuries (18). For example, headache, one of the most common post-concussion symptoms, is associated with elevated levels of Tumor Necrosis Factor-alpha (TNF-α), Interleukin-1 beta (IL-1β) and Interleukin-10 (IL-10) (19, 20). Similarly, depression is associated with elevated C-Reactive Protein (CRP) and Interleukin-6 (IL-6) levels, while anxiety is associated with an increase in CRP, TNF-α, and Interferon-γ (IFN-γ) levels (21–23). The same holds true for chronic subjective dizziness which is associated with elevated TNF-α and IFN-γ levels (24). Furthermore, IL-1β is associated with benign paroxysmal positional vertigo (BPPV) (25). This indicates that inflammation is associated with various post-concussion like symptoms, irrespective of the triggering cause.

To establish an association between the inflammatory cytokines and mTBI-related symptoms, the best approach one can take is to measure cytokine levels intracranially. Since mTBI is a minor injury with no signs of obvious trauma on routine imaging, it is not feasible to undertake a lumbar puncture to measure intracranial cytokine levels. To overcome this issue, many studies attempting to study inflammation in mTBI measure cytokine levels peripherally in blood. However, as mentioned earlier, inflammation is not exclusive to mTBI, so while measuring cytokine levels peripherally is convenient, it can present issues in differentiating the source of inflammation. Hence, it is important to characterize the inflammatory cytokine profile that is unique to patients with mTBI, both in blood and CSF.

A systematic review and meta-analysis were conducted to examine and analyze the evidence presented from clinical studies linking mTBI with various inflammatory cytokines, both in blood and CSF. Our primary aim is to compare the inflammatory cytokine levels between populations with mTBI and healthy control (HC) groups. The secondary aim is to compare the inflammatory cytokine levels between the population with mTBI and trauma control (TC) groups. Finally, the last aim is to explore the associations between the post-mTBI inflammatory cytokine levels and clinical outcomes and prognosis. This research would help us identify the inflammatory cytokine profile exclusive to mTBI, that sets it apart from healthy controls as well as trauma controls. In addition, this research would help us identify the inflammatory cytokines that have the most potential to be used as prognostic mTBI biomarkers.

2. Methodology

2.1. Search strategy

A systematic screening approach in fulfillment of the Preferred Reporting Items for Systematic Reviews and Meta-analyses (PRISMA) and the Revised Assessment of Multiple Systematic Reviews (R-AMSTAR) guidelines was implemented (26). Potentially eligible studies were identified by systematically searching the databases PUBMED, EMBASE and MEDLINE. The searches were limited to literature published from January 2014 to December 12, 2021. Studies published prior to January 2014 were discussed in our previous study (18). The search strategy was developed using combinations of the following MeSH terms: ("mild traumatic brain injur*" OR "concussion") AND ("neuroinflammat*" OR "cytokine*"). A secondary manual search, using Google Scholar, was also conducted to ensure that all relevant articles were captured.

2.2. Study screening

Citations were uploaded into Covidence for title, abstract, and full-text screening as well as duplicate removal. Two independent reviewers conducted the study screening in duplicate, from title to full-text screening stages (SM and OA). Disagreements regarding article inclusion were settled by mutual consensus after discussing the disputed articles together. Any further discrepancies were discussed with other team members and eventually resolved by the principal investigator (TG and MR).

2.3. Selection criteria

Only studies providing information on inflammatory cytokines in the CSF, blood, plasma, or serum of the patients with mTBI were considered for review. The research question and inclusion/exclusion criteria were established *a priori*. Inclusion criteria were defined as: (1) concussions or mild traumatic brain injuries, (2) neuroinflammation, (3) inflammatory cytokines, and (4) articles published in English. Exclusion criteria were defined as: (1) complicated mild and more severe forms of traumatic brain injuries with Glasgow Coma Scale (GCS) < 13, (2) no blood or CSF cytokines, (3) no comparison healthy or trauma controls or baseline (pre-mTBI) groups, (4) review articles, abstracts or letter to editors, (5) cadaver/non-human studies, and (6) articles that included TBIs but did not make distinctions between the various types of TBIs. The reference lists of related studies were also searched for additional reports.

2.4. Data extraction

Two independent reviewers (SM and MM) abstracted the relevant data from the included articles on an Excel sheet. The characteristics extracted from each study included the author, publication year, study design, sample size, mTBI setting, mTBI diagnostic criteria, control type, and patient demographics (e.g., age, sex, etc.). Details about the number of previous mTBIs, time since last mTBI, and GCS data were also recorded. Furthermore, data regarding methods of cytokine measurement, type of biospecimen analyzed, the time interval between injury and cytokine measurement, cytokine levels (both mTBI and control groups), along with any relevant *p*-values, were recorded. In addition, any acute or chronic functional outcomes associated with a particular cytokine were noted. This included the presence of persistent symptoms, reduced or lack of return to normal

activities (work, school, and sports), abnormal neurocognitive function, and Glasgow Outcome Scores (GOSE).

To conduct the meta-analysis, the mean cytokine concentrations, and their standard deviations (SD) for case and control groups were extracted at each follow-up visit. The timing of cytokine concentration measurement varied from <24 h to >1 month. Other descriptive statistics such as medians and measures of variance (e.g., 95% confidence intervals [CI] and range) were also extracted. Efforts were made to contact the authors of studies that presented their data as either medians, or in a log-transformed format only, to ensure that all possible mean values were available to conduct a thorough meta-analysis. Data from studies that had overlapping populations was extracted but a distinction was made in the analysis.

2.5. Reporting quality

Risk of bias and study quality were evaluated using the Newcastle-Ottawa Quality Assessment Scale (NOS) (27). A score of 0 or 1 was given for each category/criterion on the NOS scale, where the maximum possible score of 8/8 could be achieved (maximum score of 1 for each category). The total scores were categorized according to the methodological quality of each study. Potential confounding factors (including type of biospecimen, assay type, time since mTBI, type of mTBI population and control for confounding inflammatory variables etc.) were also considered for a more detailed bias and quality analysis of studies.

2.6. Data analysis

Review Manager (RevMan) Version 5.4 (The Cochrane Collaboration, 2020) was used for the meta-analysis. Meta-analyses were conducted whenever the mean values of an inflammatory cytokine were available in at least three or more studies, with a minimum of 30 participants in each study. For the studies that did not report SD, it was calculated from SEM (Standard error of mean) and CI 95% (Confidence Interval 95%) using the following formulas:

$$\text{SEM} = \frac{\text{Upper limit of CI 95\%} - \text{Lower limit of CI 95\%}}{3.92}$$

$$\text{SD} = \text{SEM} \times \sqrt{n}\ \left(\text{number of participants}\right)$$

Due to a limited number of studies that qualified for the meta-analysis, only four analyses were conducted comparing mean TNF-α, IL-6, IL-1β, and MCP-1/CCL2 levels in serum/plasma/blood between patients with mTBI and healthy control groups. A high level of heterogeneity was expected due to the utilization of different assay methods (i.e., Multiplex and ELISA), time of cytokine measurement, control for inflammatory variables, and different blood fractions and dilutions used. To account for this heterogeneity, a random effects model and inverse variance approach were utilized to estimate the pooled standardized (Std.) mean differences, their corresponding 95% confidence interval, and *p*-values. The Std. mean difference is used when the included studies measure the same outcome in different ways. It standardizes the differences in the measurement of the same outcome before pooling the means. It does not however remove the heterogeneity among the study population. Random effects models are preferable if significant heterogeneity is expected as this model accounts for both within-study variability and between-study variability. Heterogeneity was tested using Cochrane's Q test with the *p*-value set at 0.1 for significance and quantified using the I^2 statistic ($I^2 > 40\%$ as low, 40–60% as moderate, and > 60% as substantial heterogeneity). The sources of heterogeneity were evaluated and the risk of bias across studies, publication bias, and selective reporting were assessed. Sensitivity analyses were conducted by excluding the studies in which mean and standard deviation were estimated (from reported standard deviations and range values) to assess the consistency of the estimated mean differences. If multiple studies conducted by the same group had overlapping populations, only the most recent study with the largest mTBI population size was included in the meta-analysis. If cytokines were measured at different time points, the time-point with the largest population size was used for the total cytokine analysis. For acute and chronic cytokine analysis, the most time-appropriate data consistent with the timings of the other studies was used.

3. Results

3.1. Study characteristics

A total of 5,138 studies were yielded across the three databases Embase, 139 from Medline, 662 articles from PubMed, and 7 from other sources. After removing duplicates, a systematic screening process was conducted as shown in Figure 1, yielding a total of 26 articles that met the selection criteria (Figure 1). Out of the 26 studies, 25 compared blood cytokine levels between patients with mTBI and healthy controls and 3 studies compared the levels between patients with mTBI and trauma controls (some studies had both control types). Only one study compared cytokine level differences in the CSF. This CSF data was not included in the qualitative or quantitative analysis, but the results are available in Table 1. The characteristics of the 26 included studies are described in Table 1.

A total of 3,248 participants were included across all studies, where 1,746 of these patients had at least one mTBI. There were 1,502 controls, 1,431 of which were healthy controls, and 71 were trauma controls. The mean sample size of patients with at least one mTBI was 67.15 ± 50.11 whereas, the mean sample size for controls was 57.24 ± 39.02. The mean age of patients with at least one mTBI was 27.37 years, and the mean age of control patients was 27.14 years. 74.5% of mTBI patients were male. Sport-related injuries were the most common source of mTBI in the majority of included studies (42%), followed by general trauma (31%), and military-related injuries (27%). The diagnostic criteria used for mTBI diagnosis was heterogenous.

3.2. Study quality

Most studies in this review have a level of evidence of IV ($N = 14$; 53.8%). There was substantial agreement between the two reviewers at the title/abstract screening stage ($\kappa = 0.80$ [95%CI, 0.70–0.90]) and the full-text screening stage ($\kappa = 0.79$ [95%CI, 0.60–0.90]). The mean

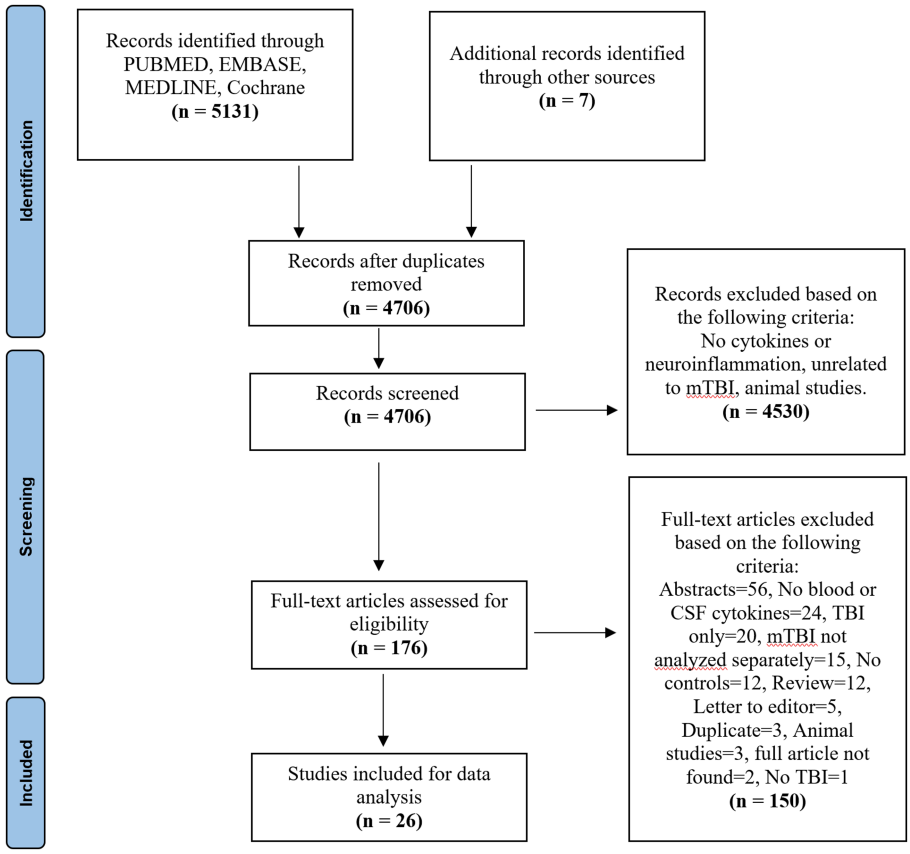

FIGURE 1
PRISMA flow chart.

NOS score for the included studies was 6.38 ± 1.19, which indicates a fair quality of evidence for non-randomized studies. The areas of best performance based on the NOS checklist were the case definition ($N = 25$; 96%) and the definition of controls ($N = 25$; 96%). The area of worst performance was the non-response rate (the number of patients that were lost to follow-up), which was not provided in any of the included studies.

3.3. mTBI vs. healthy controls: qualitative review of blood inflammatory cytokines

The most common blood inflammatory cytokines assessed in the included studies were IL-6, TNF-α, IL-10, IL-1β, Interleukin-8 (IL-8), IFN-γ, Interleukin-1 Receptor Antagonist (IL-1RA), Interleukin 4 (IL-4), and MCP-1/CCL2 (Figure 2). It should be noted that MCP-1 is also referred to as CCL-2 and both these terms are used interchangeably. Most of the included studies extracted peripheral inflammatory cytokine specimens from plasma (46%, $n = 12$). The remaining studies extracted inflammatory cytokines from either serum (38%, $n = 10$) or whole blood (15%, $n = 4$). About 42% of the studies ($n = 11$), assessed cytokine levels within 24 hrs of injury. However, most studies (53.8%, $n = 14$) assessed cytokine levels 30 days or later following a mTBI. The systematic review found elevated levels of IL-6 (time points: <24 h, 1–7 days and ≥ 30 days), TNF-α (≥30 days), IL-1β (1–7 days), IL-8 (time points: <24 h and ≥ 30 days), IFN-γ (<24 h), IL-1RA (<24 h), and MCP-1/CCL2 (time points: 1–7 days and ≥ 30 days) in patients with mTBI, compared with healthy controls, where any significant findings were replicated in at least two studies. The evidence was particularly strong for IL-6, IFN-γ, IL-1RA levels (at <24 h), and MCP-1/CCL2 (between 1 and 7 days), where ≥60% of the studies found significant elevated levels in patients with mTBI compared to healthy controls at these time points.

There are four groups of research articles that had subject overlap, where the participant pools were utilized multiple times by researchers in the same group. These groups are labeled as Groups A, B, C, and D. Group A published four of the included studies (28–31), Group B published two studies (32, 33), Group C published four studies (34–37), and finally Group D published three articles (38–40). For this review, clear distinctions were made if two or more studies had overlapping populations at a certain time point. This is to avoid any potential impact on the statistical analysis and the results of this review, caused by falsely giving undue weight to a certain study population.

3.3.1. IL-6

Blood IL-6 levels were assessed in 65% of the included studies ($n = 17/26$) (28–37, 40–46) (Supplementary Figure S1). Out of these, most studies (65%, $n = 11/17$) showed significantly elevated IL-6 levels in patients with mTBI at a minimum of one time-point

TABLE 1 Study characteristics.

Author year	Population	Biomarkers tested	Biomarker assessment	Specimen used	Sig. data	Time (acute/ chronic)	mTBI Dx/ setting	Variable control	Prognosis/outcome
Shan et al. (47)	mTBI = 55 TC = 17 HC = 44	TNF-α, IL-1β, CXCL1, CXCL8, and CCL2	ELISA (R&D Systems, United States)	Plasma	None of the biomarkers selected have a sig. difference between the groups.	Acute mTBI (1–8) hours mTBI (9–24) hours OI < 24 h	Zurich 2012/general trauma	Yes	NR
Meier et al. (28)	mTBI = 106 HC = 134	IL-6, IL-1RA, and CRP	Multiplex (Meso Scale Diagnostics, United States)	Serum	IL-6, IL-1RA, and CRP are sig. elevated at <6 h in mTBI groups compared to healthy ($p = 0.001$) IL-1RA is sig. elevated at 24–48 h in mTBI groups compared to healthy ($p < 0.05$).	Acute Pre-injury baseline Within 6 h 24–48 h	CDC/SRC	Partial	Elevated IL-1RA ($p = 0.03$) and IL-6 ($p = 0.08$) ass. with symptom duration.
Nitta et al. (29)	mTBI = 40 HC = 43	IL-6, IL-1β, IL-1RA, IL-10, TNF-α, CRP, and IFN-γ	Multiplex (Meso Scale Diagnostics, United States)	Serum	IL-1RA and IL-6 levels at 6 h visit are sig. higher in athletes with mTBI ($p < 0.001$).	Acute Baseline (6 h) 24–48 h Days 8, 15, and 45	CDC/SRC	Partial	IL-6 levels at 6 h ass. with the duration of symptoms ($p = 0.031$).
Feng et al. (48)	mTBI = 16 HC = 11	TNF-α	ELISA (Biotech Co., China)	Plasma CSF	Plasma TNF-α is sig. higher in mTBI compared to controls ($p = 0.009$) Day 3 plasma TNF-α is sig. higher than day 1, 5, and 7 ($p < 0.05$) CSF TNF-α levels higher (non-sig) in mTBI patients at Day 3	Acute Days 1, 3, 5, and 7	GCS/general trauma	Yes	NR
Goetzl et al. (45)	mTBI = 32 HC = 21	IL-6	ELISA (R&D Systems, United States)	Plasma NDE levels	IL-6 sig. Increased in both acute ($p < 0.0001$) and chronic ($p < 0.1$) mTBI compared to controls.	Acute: 7 days Chronic: 3–12 months	NCAA/SRC	No	NR
Battista et al. (40)	mTBI = 41 HC = 55	IL-6	Ella™ (Protein Simple, Biotechne, United States).	Plasma	No sig. results (differences).	Acute <7 days	Berlin 2016/SRC	No	No sig. correlation between IL-6 and either symptom burden or days to medical clearance ($p > 0.05$).
Tylicka et al. (51)	mTBI = 29 HC = 13	IL-8, IL-11	ELISA (R&D Systems, United Kingdom).	Plasma	IL-8 sig. higher in mTBI ($p = 0.033$)	Acute 2–6 h	GCS/general trauma	Yes	NR
Rusiecki et al. (41)	mTBI = 90 HC = 50	IL-1α, IL1β, IL4, IL-6, IL8, IL-10, TNFα, MCP-1, IL-13, IL-17, TNF-β	Multiplex (Ray Biotech, United States)	Serum	Controls' cytokine levels are greater than cases' for IL-6 ($p = 0.02$), IL-8 ($p = 0.01$) and IL-1β ($p = 0.05$)	Chronic 281.8 days (mean)	DoD-VA criteria/ military	Partial	Decreased IL-8 levels ass. with PTSD ($p = 0.01$)
Begum et al. (52)	mTBI = 23 HC = 12	92 cytokines	Multiplex (Olink Biosciences, Sweden)	Serum	IL-7 levels sig. Increased in mTBI ($p < 0.05$) MCP-1 was sig. reduced in mTBI at >1 week ($p = 0.03$) CXCL1 was sig. increased in mTBI at <1 week ($p = 0.02$)	Acute: 2–5 days Chronic: 15–75 days	ACRM/SRC	Partial	Reduced MCP-1 levels relate to an increase in the number ($r = 0.455$, $p = 0.013$) and severity of symptoms ($r = -0.378$, $p = 0.043$).
Vedantam et al. (53)	mTBI = 53 TC = 12	IL-1β, IL-2, IL-4, IL-6, IL-10, IL12p70, IL-17a, IFNγ, TNFα	Luminex Magpix (Luminex, United States)	Plasma	Sig. elevated IL-2 ($p = 0.014$) and IL-6 ($p = 0.01$) levels in mTBI within 24 h post-injury. Sig. elevation in IL-6 ($p = 0.044$) at 6 months post-injury in mTBI.	Acute: < 24 h Chronic: 6 months	ACRM/general trauma	No	At 24 h, elevated IL-2 ($p = 0.001$) and lower IL-6 ($p = 0.035$) and IL-17a levels ($p = 0.007$) ass. with severe PCS at 1 week ($p = 0.001$). At 6 months, elevated IL-10 ass. with depression ($p = 0.004$) and PTSD ($p = 0.001$).

(Continued)

10.3389/fneur.2023.1123407

TABLE 1 (Continued)

Author year	Population	Biomarkers tested	Biomarker assessment	Specimen used	Sig. data	Time (acute/ chronic)	mTBI Dx/ setting	Variable control	Prognosis/outcome
O'Brien et al. (50)	mTBI = 58 HC = 47	IL-1β and IL-18	Simoa (Quanterix, MA)	Serum	No sig. results (differences).	Acute: Baseline, 2, 6, and 13 days	NR/SRC	Partial	NR
Sun et al. (33)	mTBI = 95 HC = 54	CCL2, IL-1β, IL-4, IL-6, IL-8, IL-10, IL-12, IFN-γ, TNF-α	Multiplex (Luminex, United States)	Serum	CCL2, IL-1β, and IL-6 levels (acute) higher in mTBI at all time points compared to HC ($p < 0.001$), except IL-1β at 3 months time-point.	Acute and Chronic Cohort 1: within 7 days post injury, 1 month, 3 months Cohort 2: within 7 days post injury	WHO/general trauma	Yes	Elevated CCL2 level ass. with more severe PCS ($p < 0.001$) and predicted information processing speed at 3 months ($p = 0.009$). IL-1β is negatively ass. with working memory in acute phase ($p < 0.001$) and positively in chronic phase ($p = 0.015$).
Battista et al. (39)	mTBI = 42 TC =30 HC = 102	IFN-γ, IL-8, TNF-α, MCP-1, MCP-4, MCP-1β, MIP-1α.	Multiplex (Meso Scale Diagnostics, United States)	Plasma supernatant	Patients with mTBI have higher levels of MCP-4 ($p < 0.001$) and MIP-1β ($p = 0.001$) compared to HC.	Acute 2–7 days	Berlin 2016/SRC	No	MCP-1 ($p = 0.007$) and MCP-4 ($p < 0.001$) positively correlate with days to recovery in mTBI patients.
Guedes et al. (35)	mTBI = 150 HC = 45	TNF-α, IL-6, IL-10,	Simoa (Quanterix, Lexington, MA)	Plasma	No sig. differences in the plasma or exosomal concentrations of any biomarker.	Chronic 6.83–9.53 years (median)	DoD–VA/military	No	PCS severity correlate with plasma TNF-α ($r = -0.2328$, $p = 0.02$). PTSD correlated weakly with plasma TNF-α ($r = -0.2267$, $p = 0.0255$). A marginally sig. correlation between PTSD and exosomal IL-6 ($r = 0.1893$, $p = 0.08$).
Gill et al. (34)	mTBI = 42 HC = 22	TNFα, IL-6, IL-10	Simoa (Quanterix, Lexington, MA)	NDEs from blood	mTBI has elevated concentrations of IL-10 ($p < 0.05$).	Chronic >3 months	WARCAT/military	Yes	Exosomal IL-10 levels are related to PTSD symptoms ($B = 0.8$, $t = 2.60$, $p < 0.01$). IL-10 regression model ($p < 0.01$) shows PTSD sig. related ($p < 0.01$) and depression ($p = 0.063$) and PCS severity do not relate to exosomal IL-10 ($p = 0.26$).
Thompson et al. (42)	mTBI = 171 HC = 122	IL-1β, IL-2, IL-4, IL-5, IL-6, IL-7, IL-8, IL-10, IL-12, IFN-γ and TNF-α	Multiplex (Bio-Rad, United States)	Plasma	Within 24 h of injury, concentrations of IL-1β, IL-2, IL-4, IL-5, IL-6, IL-7, IL-8, IL-10, IL-12, IFN-γ, and TNF-α were sig. elevated in mTBI. At 1 month, TNF-α, Il-7 and IL-8 levels were sig. elevated in mTBI. At 6 months, TNF-α, IL-7, IL-8 and IL-12 were sig. elevated in mTBI. These comparisons are for ages 21–54.	Acute: <24 h Chronic: 1 and 6 months.	CDC/general trauma	Yes	NR
Edwards et al. (37)	mTBI = 45 HC = 49	IL-6, IL-10, and TNF-α	Simoa (Quanterix, Lexington, MA)	Serum	At <8 h IL-6 levels in mTBI are greater than HC ($p < 0.001$). No sig. differences at the second time point.	Acute < 8 h and 24 h later	DoD–VA/military	Yes	NR
Kanefsky et al. (36)	mTBI = 61 HC = 82	TNF-α, IL-6 and IL-10	Simoa (Quanterix, Lexington, MA)	Plasma	IL-6 elevated in the mTBI w LOC group compared to both the mTBI w/out LOC and control groups ($p < 0.001$ for both comparisons).	NR	WARCAT/military	Yes	Increased TNF-α in mTBI ass. with severe PTSD ($r = 0.36$, $p = 0.005$). mTBIs with LOC are ass. with elevated IL-6 levels and pain, compared to mTBI without LOC and HC.

(Continued)

10.3389/fneur.2023.1123407

TABLE 1 (Continued)

Author year	Population	Biomarkers tested	Biomarker assessment	Specimen used	Sig. data	Time (acute/ chronic)	mTBI Dx/ setting	Variable control	Prognosis/outcome
Brahmajothi and Abou-Donia (46)	mTBI = 5 HC = 5	TNF-α, IL-6,	ELISA (R&D Systems, United States)	Plasma	TNF-α and IL6 sig. elevated in chronic stages, but not acute ($p < 0.0001$).	Acute: baseline Chronic: 1–2 yrs.	NR/military	No	NR
Powell et al. (43)	mTBI = 55 HC = 49	IL-6	ELISA (ALPCO Diagnostics, United States)	Venous blood	No sig. results (differences).	Chronic 1+ yrs.	Self reported/ military	No	NR
Bai et al. (32)	mTBI = 112 HC = 72	IL-6, CCL2, IL-1B	Multiplex (Luminex, United States)	Serum	IL-1β, IL-6, and CCL2 acutely elevated in mTBI relative to HC (all for $p < 0.001$).	Acute <7 days	WHO/general trauma	Partial	NR
Brett et al. (30)	mTBI = 73 HC = 128	IL-6, IL-1RA, and CRP	Multiplex (Meso Scale Diagnostics, United States)	Serum	No sig. results (differences).	NR	DoD-VA/SRC	Partial	Sig. interaction between prior mTBI and IL-1RA levels on the ImPACT memory composite, $p = 0.044$. At low levels of IL-1RA, athletes with multiple mTBI had worse memory performance than those without prior mTBI ($p = 0.014$). Higher IL-1RA levels sig. ass. with more symptoms (elevated BSI-GSI scores, $p = 0.046$) and worse memory ($p = 0.017$).
Chaban et al. (49)	mTBI = 207 HC = 207	IFN-γ, IL-8, IL-9, TNF-α, IL-1RA, MCP-1	Multi-plex (Bio-Rad, Unitd States)	Plasma	IFN-γ, IL-8, IL-17A, IL-9, MCP-1 and TNF-α were sig. higher in mTBI than HC at all time points.	Acute: <72 h and 2 weeks. Chronic: 3 and 12 months.	WHO/general trauma	Yes	NR
Battista et al. (38)	mTBI = 16 HC = 27	MCP-1, MCP-4	Multiplex (Meso Scale Diagnostics, United States)	Venous blood	MCP-1 and MCP-4 were elevated in acute mTBI.	Acute <7 days	NR/SRC	Partial	NR
Ryan et al. (44)	mTBI = 104 HC = 98	IL-2, IL-4, IL-6, IL-8, IL-10, IL-17A, IFN-γ TNF-α	Multiplex (Meso Scale Diagnostics, United States)	Peripheral blood plasma	IL-6 and IL-1RA sig. elevated in mTBI ($p < 0.005$). IL-8, IL-10, IL-17A, TNF-α sig. reduced (p-value <0.0001) in mTBI.	Acute: Less than 24 h	GCS 14–15/SRC	Yes	NR
Meier et al. (31)	mTBI = 23 HC = 47	IL-6, IL-10, IL-1β, IL-1RA and TNF-α	Multiplex (Meso Scale Diagnostics, United States)	Serum	Serum IL-6 and IL-1RA levels sig. elevated in mTBI relative to baseline levels ($p < 0.05$).	Acute Pre-injury baseline Within 6 h	CDC/SRC	Partial	IL-6 levels at 6 h are sig. positively ass. with symptom duration ($p = 0.042$) but not Il-1RA levels ($p = 0.12$).

10.3389/fneur.2023.1123407

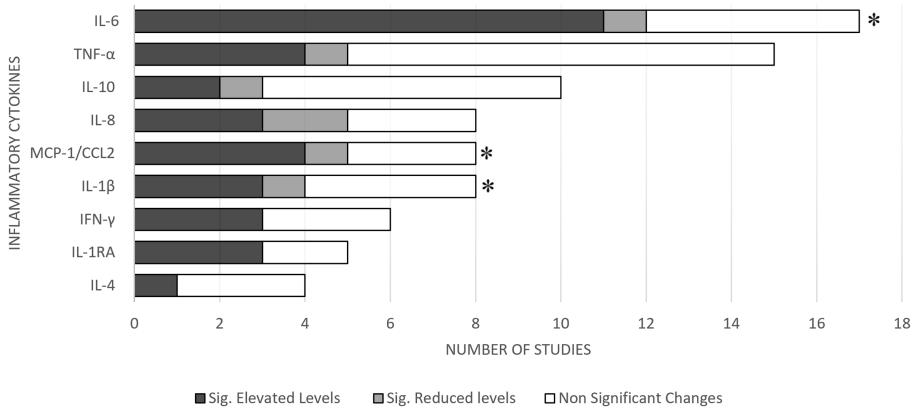

FIGURE 2
Summary of results for mTBI vs. healthy controls. * Meta-analysis demonstrated acutely elevated levels of the respective cytokines in patients with mTBI.

compared to healthy controls (28, 29, 31–33, 36, 37, 42, 44–46). On the other hand, one study showed significantly reduced IL-6 levels in the mTBI population compared to healthy controls (5.8%, $n = 1/17$) (41). The remaining studies showed no significant differences between the two populations at any time point (29.4%, $n = 5/17$) (30, 34, 35, 40, 43). It should be noted that there was a subject overlap to some extent between the four studies conducted by Group A (28–31), two by Group B (32, 33) and three by Group C (34–36).

Within 24 h, six out of seven studies measuring IL-6 showed elevated levels in the mTBI population (28, 29, 31, 37, 42, 44). Out of these six studies, three studies were conducted by group A (28, 29, 31). The one study that did not find any significant differences between the two populations at this time point, had a very small sample size ($n = 5$) for each group (46).

Out of the 16 studies comparing IL-6 levels, only 35.2% of the studies completely and 35.2% of the studies partially controlled for the confounding inflammatory variables. The remaining studies (29.6%) did not control for any confounding inflammatory variables. Confounding inflammatory variables include factors such as infections, auto-immune diseases, anti-inflammatory drug intake and other conditions that affect cytokine levels.

3.3.2. TNF-α

Our review identified 15 studies comparing circulating TNF-α levels between patients with mTBI and healthy controls (29, 31, 33–37, 39, 41, 42, 44, 46–49) (Supplementary Figure S2). Out of these, four studies (25.6%; $n = 4/15$) showed significantly elevated TNF-α levels, and one found significantly reduced levels in patients with mTBI at a minimum of one time-point, compared to healthy controls (42, 44, 46, 48, 49). Although all of these studies looked at blood cytokines, one looked at CSF and found elevated TNF-alpha associated with mTBI (48).The remaining 10 studies showed no significant differences in the TNF-α levels between cases and controls (29, 31, 33–35, 37, 39, 41, 42, 47).

From the studies comparing TNF-α levels, 60% ($n = 9$) of the studies completely and 20% ($n = 3$) partially controlled for confounding inflammatory variables. The remaining studies did not control for any confounding inflammatory variable. There was a subject overlap to some extent between the two studies conducted by Group A (29, 31) and three studies by Group C (34–36).

3.3.3. IL-10

Ten studies assessed IL-10 levels in the blood following an mTBI (29, 31, 33–37, 41, 42, 44) (Supplementary Figure S3). This review identified that two out of these ten studies (34, 42) found significantly elevated levels; whereas one study found significantly reduced levels (44) in mTBI patients at a minimum of one time-point, compared to healthy controls. The remaining studies found no significant differences between the two populations.

Out of all studies comparing IL-10 levels, 60% ($n = 6/10$) of the studies completely and 30% ($n = 3/10$) partially controlled for confounding inflammatory variables. The one remaining study did not control for any confounding inflammatory variables. There was a subject overlap to some extent between the two studies conducted by Group A (29, 31) and three by Group C (34–36).

3.3.4. IL-1β

A total of eight studies compared IL-1β levels in blood between mTBI patients and healthy controls (29, 31–33, 41, 42, 47, 50) (Supplementary Figure S4). Three out of eight studies showed significantly elevated IL-1β levels in patients with mTBI compared to healthy controls at a minimum of one time point (31–33, 42, 50). On the other hand, one study showed significantly reduced IL-1β levels in patients with mTBI compared to healthy controls (41). The remaining four studies, however, found no significant IL-1β level differences in blood between the cases and controls (29, 47).

Out of the eight studies comparing IL-1β levels, 37.5% ($n = 3$) of the studies completely and 62.5% ($n = 5$) partially controlled for the confounding inflammatory conditions. There was a subject overlap to some extent between the two studies conducted by Group A (29, 31) and the two by Group B (32, 33).

3.3.5. IL-8

Eight of the included studies assessed IL-8 levels in blood following an mTBI (33, 39, 41, 42, 44, 49–51) (Supplementary Figure S5). Three of the included studies showed

significantly elevated IL-8 levels in patients with mTBI, compared to healthy controls (42, 49, 51). Furthermore, two studies showed a significant reduction in IL-8 levels in the mTBI population when compared to healthy controls (41, 44). The remaining studies showed no significant differences in IL-8 levels between the cases and controls.

Out of the eight studies measuring IL-8 levels in blood, 62.5% ($n = 5$) completely and 37.5% ($n = 3$) partially controlled for the confounding inflammatory conditions.

3.3.6. IFN-γ

Six of the included studies assessed IFN-γ levels in blood following an mTBI (29, 33, 39, 42, 44, 49) (Supplementary Figure S6). Out of these, three studies showed significantly elevated IFN-γ levels in patients with mTBI, when compared to healthy controls at a minimum of one time point (42, 44, 49); whereas the remaining three studies showed no significant differences between the two populations (29, 33, 39).

Within 24 hrs, two out of three studies measuring blood IFN-γ levels showed elevated levels in mTBI population, but one study did not find any significant differences between the two populations during this period (29, 42, 44).

Out of the six studies comparing IFN-γ levels, 67% ($n = 4$) of the studies completely and 33% ($n = 2$) partially controlled for the confounding inflammatory variables.

3.3.7. IL-1RA

Blood IL-1RA levels were assessed in five of the included studies (28–31, 49) (Supplementary Figure S7). Out of these, three studies showed significantly elevated IL-1RA levels in patients with mTBI when compared to healthy controls at less than 24 hrs (28, 29, 31). The two remaining studies showed no such differences at any time point (30, 49).

Of the five studies assessing IL-1RA levels, 20% ($n = 1$) of the studies completely controlled for the confounding inflammatory variables whereas 80% ($n = 4$) partially controlled for them. It should be noted that there was a subject overlap to some extent between the four studies conducted by Group A (28–31).

3.3.8. IL-4

Circulating IL-4 levels were assessed in four of the identified studies (33, 41, 42, 44) (Supplementary Figure S8). Out of these, one study showed significantly elevated IL-4 levels in patients with mTBI, compared to healthy controls at a minimum of one time point (42). The remaining three studies, however, did not report any significant differences (33, 41, 44).

Out of the four studies comparing IL-4 levels, 75% ($n = 3$) of the studies completely and 25% ($n = 1$) of them partially controlled for the confounding inflammatory conditions.

3.3.9. MCP-1/CCL2

Circulating MCP-1/CCL2 levels were assessed in eight of the identified studies (32, 33, 38, 39, 41, 47, 49, 52) (Supplementary Figure S9). Out of these, four studies reported significantly elevated MCP-1/CCL2 levels in the mTBI population when compared to healthy controls (32, 33, 38, 49); whereas one study reported a significant reduction in MCP-1/CCL2 levels in the mTBI population (52). The remaining studies showed no significant differences in MCP-1/CCL2 levels between the two populations.

Within 1 week, four out of six studies measuring MCP-1/CCL2 showed elevated levels in the mTBI population (32, 33, 38, 49) but the remaining two studies found no significant differences between the two populations at this time point (39, 52).

Out of the eight studies comparing MCP-1/CCL2 levels, 37.5% ($n = 3$) completely and 50% ($n = 4$) partially controlled for the confounding inflammatory conditions. The remaining studies did not control for any confounding inflammatory variables. There was a subject overlap to some extent between the two studies conducted by Group D (38, 39) and the two by Group B (32, 33).

3.4. mTBI vs. healthy controls: meta-analysis of blood inflammatory cytokines

Eleven studies (12 cohorts) involving 987 participants with mTBI were utilized to conduct the meta-analyses for IL-6, TNF-α, IL-1β, and MCP-1/CCL2 levels in the blood. The results show significantly higher circulating levels of IL-6, IL-1β, and MCP-1/CCL2 in the mTBI population in the acute stages (within 1 week), compared to healthy controls. No differences were observed for any inflammatory cytokine in the chronic stages.

3.4.1. IL-6

Six studies (seven cohorts) were included in the IL-6 analysis, involving 586 participants with mTBI and 348 healthy controls (Figure 3). The analysis shows no significant differences in the levels of IL-6 in blood between the two populations (SMD: 0.2 [95% CI: −0.11, 0.51] pg/mL, $p = 0.20$, $I^2 = 80\%$) (Figure 3A). The large heterogeneity is partly due to inconsistent results from the included studies due to differences in the timings of assessment, the fraction of blood specimen analyzed, techniques of biomarker assessment, and inflammatory confounding variables.

Further sub-analysis based on timing, i.e., acute and chronic stages showed significantly elevated circulating IL-6 levels in mTBI population compared to healthy population in the acute stages (less than 7 days) (SMD: 0.49 [0.21, 0.77] pg/mL, $p = 0.0007$, $I^2 = 55\%$) (Figure 3B). However, no significant differences were observed between the two populations (SMD: −0.17 [95% CI: −0.37 to 0.04] pg./mL, $p = 0.11$) in the chronic stages (more than 6 months) (Figure 3C).

3.4.2. TNF-α

Seven studies were included in the TNF-α meta-analysis, involving 648 participants with mTBI and 352 healthy controls (Figure 4). The analysis shows no significant differences in the levels of TNF-α in the blood between the cases and controls (SMD: −0.02 [95% CI: −0.45, 0.42] pg/mL, $p = 0.95$, $I^2 = 90\%$) (Figure 4A).

Further sub-analyses also showed no differences between the two populations at both acute and chronic stages (Figures 4B,C), and heterogeneity remained high.

3.4.3. IL-1β

Four studies (five cohorts) were included in the IL-1β analysis, involving 263 participants with mTBI and 176 healthy controls

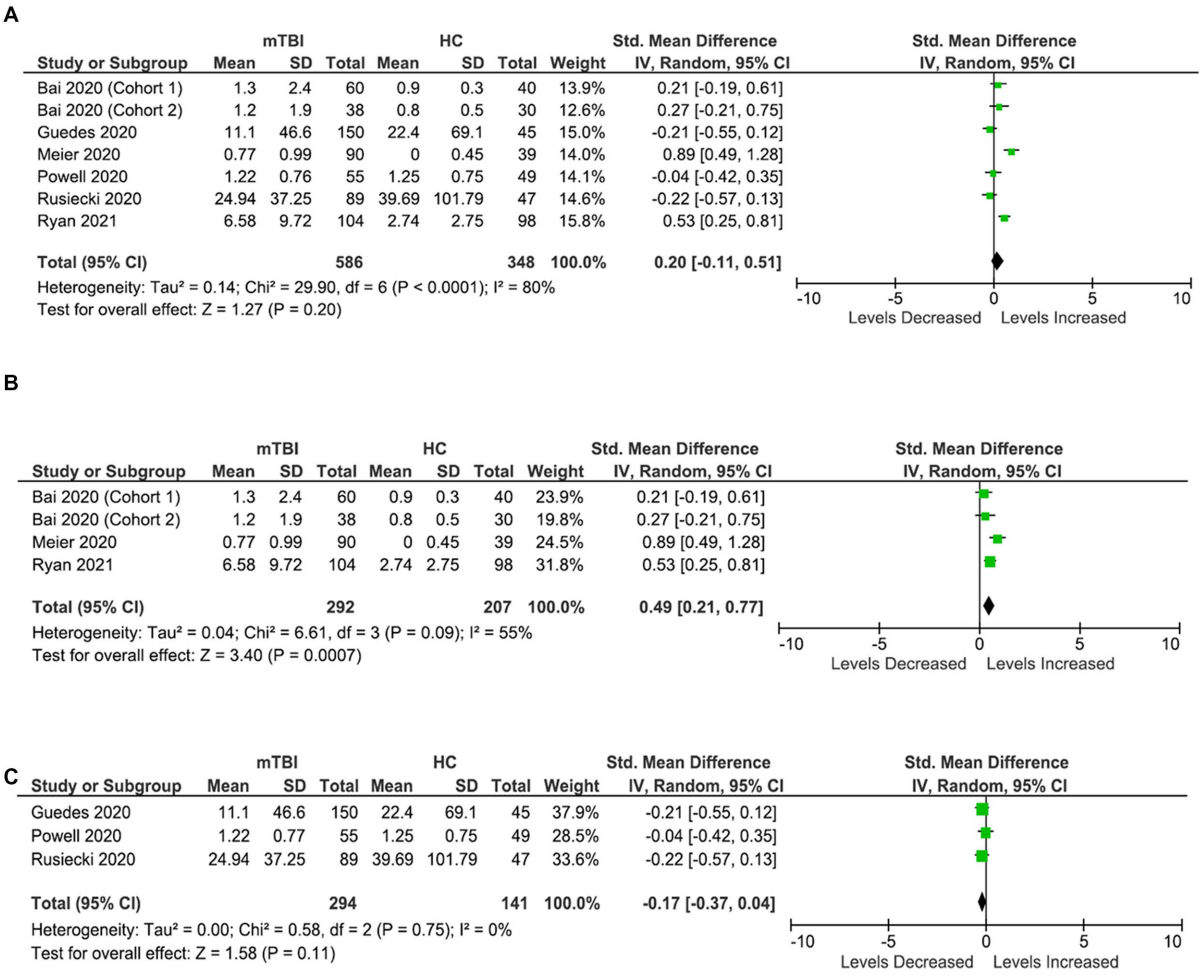

FIGURE 3
IL-6 meta-analysis. **(A)** All studies. **(B)** Acute IL-6 meta-analysis. **(C)** Chronic IL-6 meta-analysis.

(Figure 5). The analysis showed no significant difference in the levels of IL-1β in the blood between the cases and controls (SMD: 0.16 [95% CI: −0.22, 0.54] pg/mL) ($p = 0.40$, $I^2 = 72\%$) (Figure 5A).

Further sub-analyses showed significantly elevated blood IL-1β levels in the mTBI population in the acute stages (< 7 days) and brought down the heterogeneity (SMD: 0.42 [95% CI: 0.10, 0.74] pg/mL) ($p = 0.01$, $I^2 = 40\%$) (Figure 5B). A meta-analysis on chronic levels could not be conducted due to an insufficient number of studies.

3.4.4. MCP-1/CCL2

Four studies (five cohorts) were included in MCP-1/CCL2 analysis, involving 441 patients with mTBI and 227 healthy control subjects (Figure 6). Patients with mTBI had significantly elevated concentrations of MCP-1/CCL2 (SMD: 0.38 [95% CI: 0.21, 0.54] pg/mL) ($p = 0.00001$, $I^2 = 0\%$) (Figure 6A) in the blood compared to healthy controls.

Further sub-analysis based on timings demonstrated that blood MCP-1/CCL2 levels are particularly elevated in the acute stages in patients with mTBI compared to healthy controls (within 7 days) (SMD: 0.40 [95% CI: 0.22, 0.59] pg/mL) ($p = 0.0001$, $I^2 = 0\%$) (Figure 6B). Sub-meta-analysis on chronic levels was not possible due to insufficient data.

3.5. mTBI vs. trauma controls

Only three studies compared inflammatory cytokine levels in the blood between the patients with mTBI and trauma controls (38, 47, 53).

Shan et al. found no significant differences in the TNF-α, IL-1β, and the chemokines (CXCL1, CXCL8, and MCP-1/CCL2) levels in acute stages (<24 h) between the two groups (47). Vedantam et al. observed significantly elevated IL-2 and IL-6 levels in patients with mTBI in the acute stages (<24 h); however, in the chronic stages only IL-6 levels remained elevated (53). Battista et al. found that athletes with sport-related concussion had higher levels of the chemokines' monocyte chemoattractant protein-4 (MCP-4) ($p < 0.001$) and macrophage inflammatory protein-1β (MIP-1β) ($p = 0.001$) compared to healthy athletes (within 1 week of injury). At medical clearance, there were no significant biomarker contributions towards the class separation between athletes with SRC vs. healthy athletes (39).

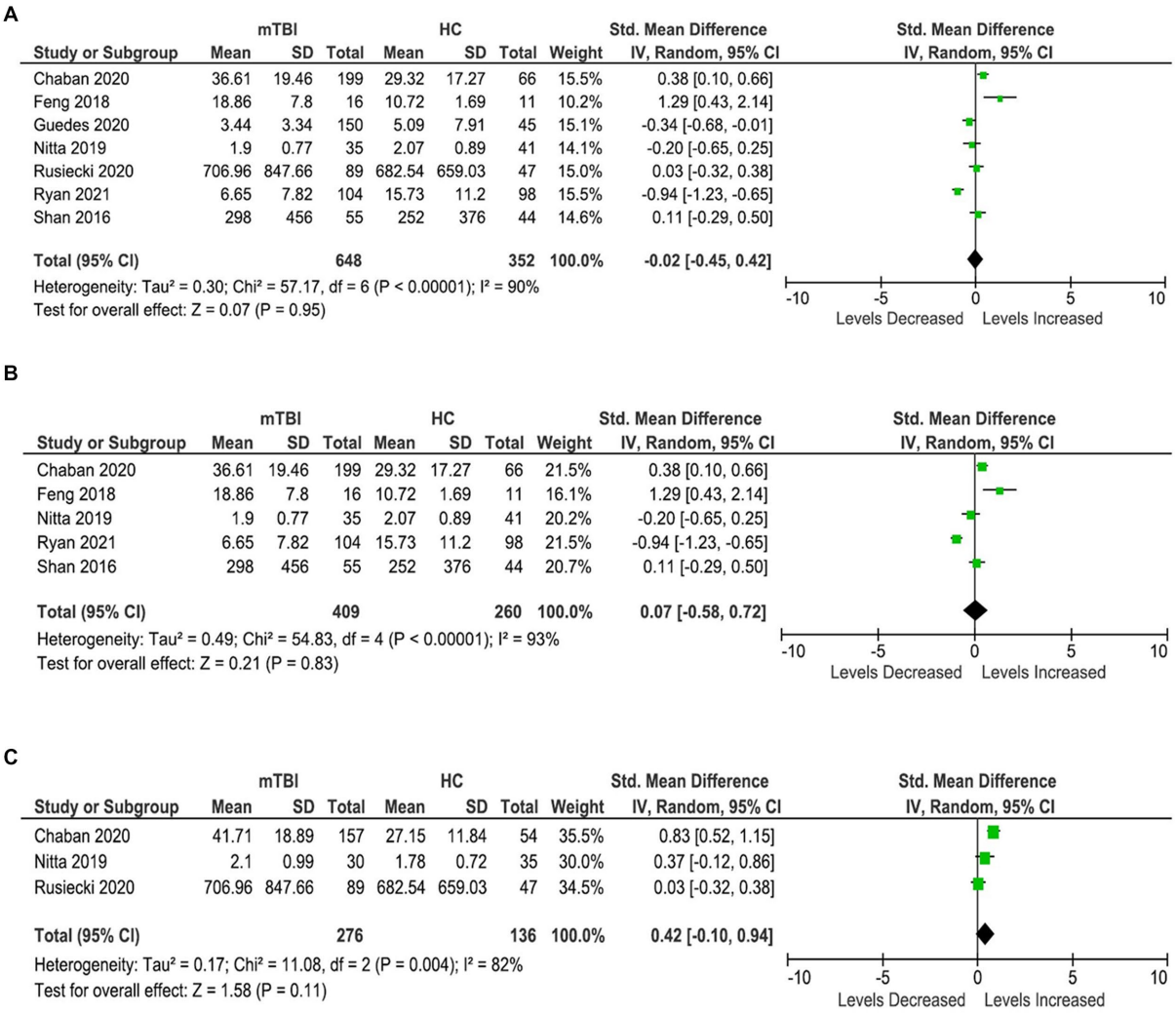

FIGURE 4
TNF-α meta-analysis. **(A)** All studies. **(B)** Acute TNF-α meta-analysis. **(C)** Chronic TNF-α meta-analysis.

3.6. Prognosis

The relationship between inflammatory cytokines in the blood and mTBI prognosis was analyzed in 13 studies (Table 1).

For this analysis, the population was considered to have poor functional outcomes if they had any of the following conditions:

- Persistent symptoms (including emotional/psychological)
- Reduced or lack of return to normal activities (work, school, and sports)
- Abnormal neurocognitive tests/functioning
- Low GOSE scores (<8).

3.6.1. IL-6

Some studies showed that elevated IL-6 levels in the blood at 6 h post-mTBI are significantly associated with the duration of symptoms ($p = 0.031$) (28, 29, 31). On the contrary, Battista et al. showed that there is no significant correlation between IL-6 levels and either symptom burden or days to medical clearance (40).

Guedes et al. found a mild correlation between elevated IL-6 levels in the blood and PTSD in the chronic stages (35).

3.6.2. MCP-1/CCL2

Acutely elevated MCP-1/CCL2 levels in the blood are associated with greater PCS severity and are positively associated with information processing speed at three months post-injury (33). Similarly, acutely elevated MCP-1/CCL2 levels in the blood (within 1 week) are positively correlated with days to recovery in athletes with sport-related mTBI (39). On the other hand, Begum et al. reports that reduced serum MCP-1/CCL2 levels in blood are associated with an increase in the number ($r = 0.455$, $p = 0.013$) and severity of symptoms ($r = -0.378$, $p = 0.043$) (52).

3.6.3. TNF-α

Plasma TNF-α levels correlate with persistent PCS and PTSD symptoms (35, 36). Within the mTBI groups, increased circulating TNF-α concentrations is associated with greater PTSD symptoms ($r = 0.36$, $p = 0.005$) (36).

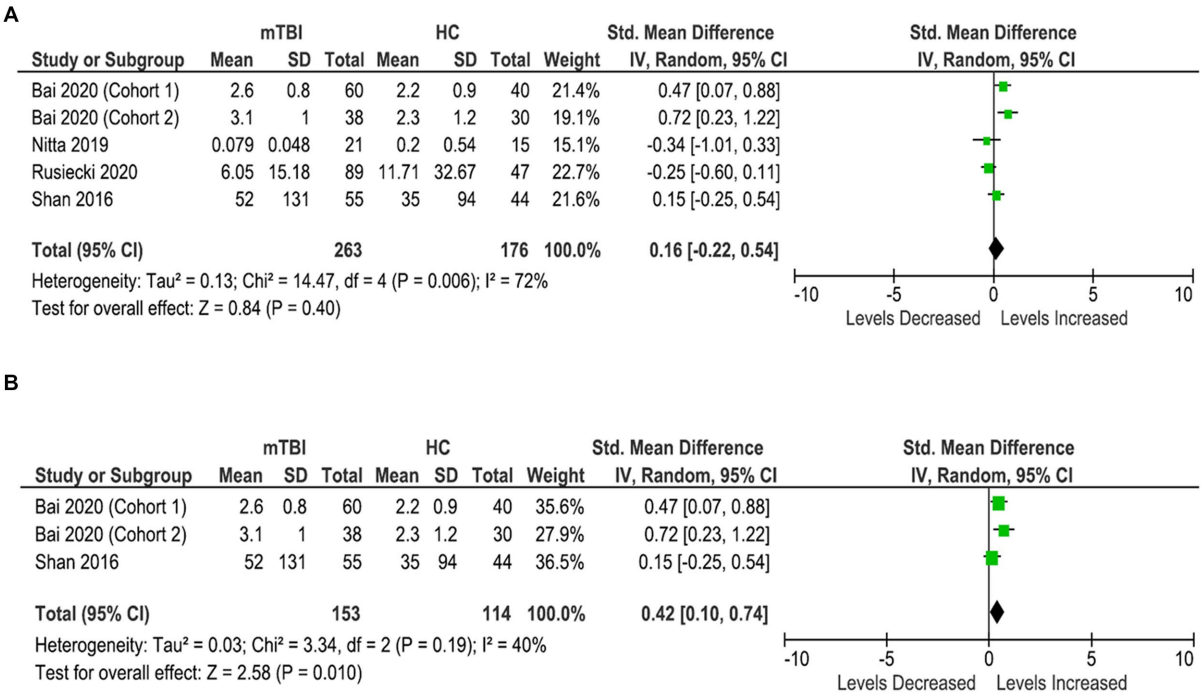

FIGURE 5
IL-1β meta-analysis. **(A)** All studies. **(B)** Acute IL-1β meta-analysis.

3.6.4. IL-1RA

Acutely elevated circulating IL-1RA levels (within 6 h of mTBI) appear to be significantly associated with greater symptom duration ($p = 0.03$) (28). In addition, there is a significant interaction between prior concussions and levels of IL-1RA on the ImPACT Memory Composite scores ($p = 0.044$) (30). At low levels, athletes with multiple mTBIs show worse memory performance than those without prior mTBIs ($p = 0.014$). Overall, elevated levels are associated with greater symptoms (higher BSI-GSI scores, $\chi 2(1) = 3.98$, $p = 0.046$) and worse memory (ImPACT Speed Composite scores, $\chi 2(1) = 5.67$, $p = 0.017$) (30).

3.6.5. IL-10

At three months post-mTBI, elevated circulating IL-10 levels are found to be related to PTSD symptoms ($B = 0.8$, $t = 2.60$, $p < 0.01$) (34). At the six month mark, elevated plasma IL-10 levels are associated with greater depression scores ($p = 0.004$) and more severe PTSD symptoms ($p = 0.001$) (53).

4. Discussion

This study reports significantly higher blood concentrations of IL-6, CCL-2/MCP1, and IL-1β in subjects with mTBI, compared to healthy controls, particularly in the acute stages. While both positive and negative results have been reported for the individual studies, this report strengthens the evidence that mTBI is accompanied by a peripheral inflammatory response (15, 17, 18, 54–56).

Despite extensive knowledge about the protracted recovery and long-term consequences of mTBI, challenges associated with its diagnosis, prognosis, and management remain unresolved. This could be partly attributed to a lack of understanding of mTBI pathophysiology. mTBI appears to be a multifaceted problem, with various biological and non-biological factors at play that determine the clinical outcome (57–59). Neuroinflammation constitutes one of the many secondary pathologies associated with mTBI and represents only a single piece of an intricate puzzle (60). Understanding this neuroinflammation would unravel one of many unknowns of mTBI. To achieve this objective, we have conducted a systematic review and meta-analysis to consolidate and analyze the data on the inflammatory cytokines associated with mTBI. As a result, we are able to identify a few circulating inflammatory cytokines associated with mTBI. The results of the systematic review show significantly elevated levels of IL-6, IFN-γ, IL-1RA (within 24 h), and MCP-1/CCL2 (between 1–7 days) in blood in patients with mTBI, compared to healthy controls. These results are further supported by the results of the meta-analysis which demonstrate significantly elevated blood levels of IL-6, IL-1β, and MCP-1/CCL2 levels in mTBI during the acute stages (within a week). Taken together, these results show a strong association between elevated IL-6, IL-1β, and MCP-1/CCL-2 levels in blood and mTBI during the acute stages. However, due to inherent heterogeneity associated with cytokine-related data, these findings should be interpreted with caution.

IL-6 is a non-specific indicator of inflammation. It is one of the most frequently measured cytokines in mTBI studies. Our review shows that circulating IL-6 levels are consistently higher in patients with mTBI, compared to healthy controls, in the majority of the

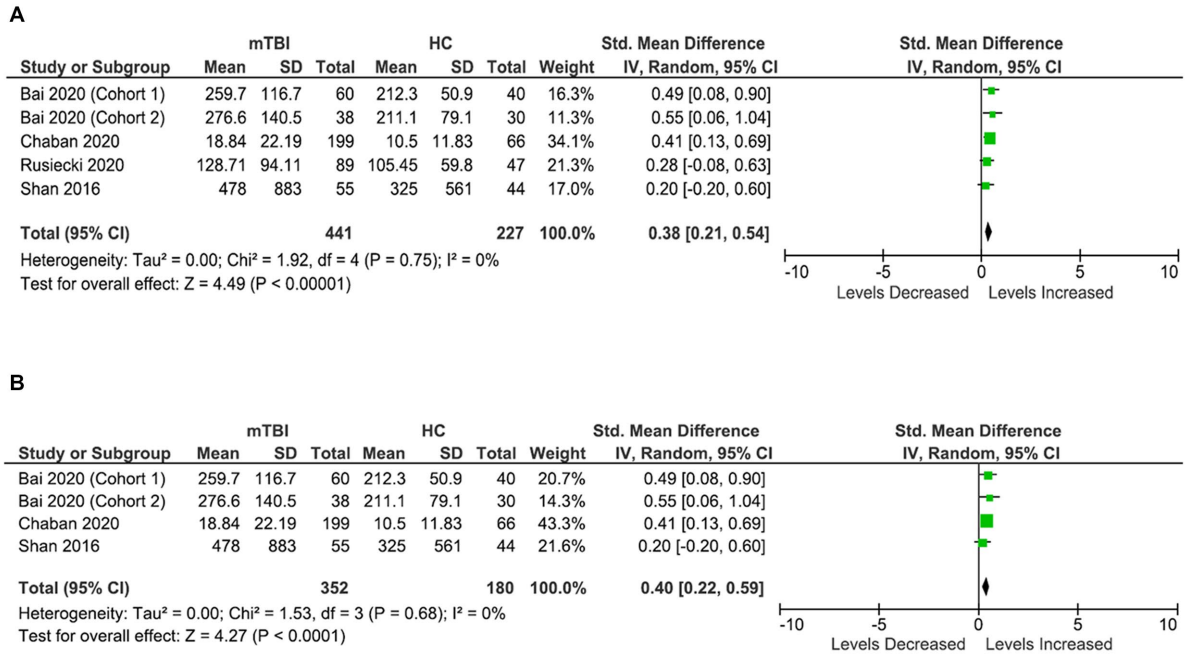

FIGURE 6
MCP-1/CCL2 meta-analysis. **(A)** All studies. **(B)** Acute MCP-1/CCL2 meta-analysis.

studies (65%, $n = 11/17$), especially during the acute stages. Interestingly, blood IL-6 levels also seem to be elevated in individuals with mTBI, when compared to those with trauma controls, particularly during the acute phase (53). Apart from IL-6, the peripheral inflammatory cytokine profile associated with mTBI appears to be quite different than the one associated with bodily trauma controls (39). However, due to limited availability of data, no meaningful inferences can be drawn on the circulating inflammatory cytokine level differences between the patients with mTBI and trauma controls without further research. This review also shows that acutely elevated IL-6 levels in blood are consistently associated with poor prognosis, particularly in terms of duration of symptoms (28, 29, 31). However, one study found no significant correlation between IL-6 levels in blood and either symptom burden or days to medical clearance (40). This discrepancy can be attributed to differences in the timings of cytokine level measurements, as Battista et al. (40) measured IL-6 levels in the late acute stages compared to others. Chronically, IL-6 appears to be associated with PTSD (35). Overall, these findings indicate that circulating IL-6, while not highly specific, is a strong indicator of mTBI in early acute stages and could be used to predict clinical outcomes.

MCP-1/CCL2, belongs to the chemokine family of cytokines and is also a non-specific marker of inflammation. This review uncovers a strong association between elevated blood MCP-1/CCL2 levels and mTBI. This association is particularly strong within the first week following an mTBI, as 66% of the studies measuring blood MCP-1/CCL-2 show elevated levels in patients with mTBI, compared to healthy controls. This finding is further supported by the results of the meta-analysis. Beyond 1 week, MCP-1/CCL2 levels remain elevated, extending into the chronic stages; however, the evidence is more robust within 1 week of the mTBI. With regards to prognosis, the evidence is quite conflicting as some studies indicate associations between elevated levels of MCP-1/CCL-2 levels and greater symptom severity, days to recovery, and information processing speed (33, 39). On the other hand, Begum et al. reports that reduced serum MCP-1/CCL2 levels are associated with an increase in the number ($r = 0.455$, $p = 0.013$) and severity of symptoms ($r = -0.378$, $p = 0.043$) (52). In addition, due to limited data available, no meaningful inferences can be drawn on MCP-1/CCL-2 level differences between the patients with mTBI and trauma controls without further research. Overall, we can infer that MCP-1/CCL2, just like IL-6, is also a strong indicator of acute mTBI and could be used to predict clinical outcomes.

This meta-analysis also shows significantly elevated IL-1β levels in the acute stages (within a week), compared to healthy controls. TNF-α is the second most common cytokine explored in mTBI studies. This review, however, is unable to detect any significant differences in TNF-α levels between the patients with mTBI and healthy controls. In addition, despite the evidence of elevated IL-1RA, IL-8, and IFN-γ levels in patients with mTBI, particularly within 24 h, we were not able to conduct a meta-analysis due to a limited number of studies.

While this review suggests that TNF-α (35, 36, 61), IL-1RA (28, 30) and IL-10 (34, 53), in addition to IL-6 (29, 31, 35, 36) and MCP-1/CCL2 (33, 39) have the potential to predict the outcome of mTBI, this data is too limited to draw concrete conclusions about these associations.

Neuroinflammation plays both a protective and detrimental role in mTBI (15, 17, 62). While it usually offers neuroprotection early on after an mTBI, persistent neuroinflammation appears to be associated with poorer outcomes (62). As a result, further research is necessary

to study the levels of inflammatory cytokines in the chronic stages and their association with persistent symptoms and recovery. Identifying these chronic cytokines may not only be beneficial in monitoring the prognosis of mTBI but may also aid in developing and monitoring targeted treatment strategies for persistent post-concussive symptoms. Although it appears promising, the inherent non-specific nature of these cytokines makes them an unsuitable candidate for the suggested use when employed alone. Recently, many specific markers of neuronal injury, such as UCHL1, GFAP, and S100B have gained much popularity as specific markers of brain injury. Future research may consider utilizing these cytokines in combination with neuronal injury markers to assess prognosis and monitor treatment efficacy, as suggested by others (63). Additionally, future studies may benefit from measuring cytokines and conducting clinical assessment longitudinally at multiple time points to fully understand the relationship between the biomarker recovery trajectory and mTBI recovery trajectory (64).

This study highlights the significant heterogeneity in blood-based inflammatory cytokine data related to mTBI. We acknowledge this limitation and recommend that future studies adopt standardized cytokine analysis methods to minimize data heterogeneity and associated outliers that can result in a 100-fold change across studies. This heterogeneity not only jeopardizes data reliability, accuracy, and reproducibility but also hinders progress in the field. MacDonald et al. recognized and elaborated on these limitations and proposed potential solutions to mitigate them. Incorporating these strategies in future research will help address this issue (63).

4.1. Limitations

Our findings must be interpreted with caution.

First, this review shows that there is considerable heterogeneity in the data, leading to difficulties in pooling and analyzing the data to formulate a meaningful conclusion. Heterogeneity was caused by many reasons, some of which include differences in the time elapsed between the initial mTBI and blood sample collection, cytokine analysis technique, blood fraction used for analysis, confounding variable control, mTBI diagnostic criteria, data reporting and functional outcomes measured. Hence, there is a need for a standardized approach in acquiring and reporting data to allow for comparisons.

Secondly, the results of this review show that about 76% of mTBI patients were male. This is because most studies are conducted in the military (27%) and sports populations (42%), which happen to be male-dominant settings. Since females are more at-risk for poor recovery and develop persistent symptoms more frequently compared to males (65–67), we could not assess prognosis accurately based on this data. Future studies, especially those assessing prognosis in mTBI patients, may want to incorporate more female participants in their studies.

Thirdly, the cytokine alterations observed in the mTBI population do not necessarily reflect a pathophysiology associated with head injury alone. There are other variables that should be considered while measuring cytokine levels as they are known to cause considerable fluctuations. These include time of blood collection, sex differences, other injuries (orthopedic, whiplash, muscle strains, etc.) at the time of mTBI, acute and chronic illnesses, co-existing psychiatric conditions, and medication intake amongst others. While we attempted to take some of these limitations into account, the results should still be interpreted with caution due to the factors mentioned above.

Lastly, most studies reported their results using medians or log-transformed means. Although this way of reporting leads to more consistent results, a thorough meta-analysis cannot be conducted using medians as we have found in this review. Future studies should follow a more standardized methodology so that the data reported using means and SD is not as heterogeneous and is more consistent to allow for a more thorough analysis.

4.2. Strengths

This systematic review and meta-analysis has several strengths. An exhaustive effort was made to capture the data by searching a variety of databases and acquiring the missing data by directly contacting the authors, extracting data from graphs and tables, or using standardized estimation methods for calculating the mean (SD). Although the latter two strategies may not be accurate, they provide estimates that are closer to the real value and are frequently employed in meta-analyses.

A systematic review with a similar aim was recently published (68). However, our study stands out because it included 15 additional studies. Hence, due to the availability of more data, we were able to conduct a meta-analysis that has not been accomplished before. Visser et al., just like our study, was able to identify IL-6 as a promising biomarker for brain injury (68). It was, however, unable to establish an association between other cytokines (such as MCP-1/CCL2 and IL-1β) and mTBI as we did.

4.3. Conclusion

Overall, we found substantial evidence of increased inflammatory cytokine levels in patients with mTBI. The evidence was particularly strong for IL-6, IL-1β, and MCP-1/CCL2. The results of this study were however limited by low study numbers as well as methodological heterogeneity between the studies.

Author contributions

SM and MR defined the research of interest and were involved in topic selection. SM and OA carried out the literature search and developed Table 1. SM, MM, and OA collected the data. FF, SM, and OA performed the meta-analysis. SM wrote the first draft of the manuscript and prepared all the figures. MM, OA, TG, FF, and MR reviewed the manuscript and made contributions for improvement. All authors helped to revise the paper. All authors contributed to the article and approved the submitted version.

Funding

This research was supported by McMaster University, Canada.

Conflict of interest

The authors declare that the research was conducted in the absence of any commercial or financial relationships that could be construed as a potential conflict of interest.

Publisher's note

All claims expressed in this article are solely those of the authors and do not necessarily represent those of their affiliated organizations, or those of the publisher, the editors and the reviewers. Any product that may be evaluated in this article, or claim that may be made by its manufacturer, is not guaranteed or endorsed by the publisher.

Supplementary material

The Supplementary material for this article can be found online at: https://www.frontiersin.org/articles/10.3389/fneur.2023.1123407/full#supplementary-material

References

1. Hiploylee C, Dufort PA, Davis HS, Wennberg RA, Tartaglia MC, Mikulis D, et al. Longitudinal study of postconcussion syndrome: not everyone recovers. *J Neurotraum*. (2017) 34:1511–23. doi: 10.1089/neu.2016.4677

2. Maas AIR, Menon DK, Adelson PD, Andelic N, Bell MJ, et al. Traumatic brain injury: integrated approaches to improve prevention, clinical care, and research. *Lancet Neurol*. (2017) 16:987–1048. doi: 10.1016/s1474-4422(17)30371-x

3. Iverson GL. Outcome from mild traumatic brain injury. *Curr Opin Psychiatry*. (2005) 18:301–17. doi: 10.1097/01.yco.0000165601.29047.ae

4. Madhok DY, Yue JK, Sun X, Suen CG, Coss NA, Jain S, et al. Clinical predictors of 3- and 6-month outcome for mild traumatic brain injury patients with a negative head CT scan in the emergency department: a TRACK-TBI pilot study. *Brain Sci*. (2020) 10:269. doi: 10.3390/brainsci10050269

5. Ewing-Cobbs L, Cox CS, Clark AE, Holubkov R, Keenan HT. Persistent postconcussion symptoms after injury. *Pediatrics*. (2018) 142:e20180939. doi: 10.1542/peds.2018-0939

6. Pavlov V, Thompson-Leduc P, Zimmer L, Wen J, Shea J, Beyhaghi H, et al. Mild traumatic brain injury in the United States: demographics, brain imaging procedures, health-care utilization and costs. *Brain Inj*. (2019) 33:1151–7. doi: 10.1080/02699052.2019.1629022

7. Ganesalingam K, Yeates KO, Ginn MS, Taylor HG, Dietrich A, Nuss K, et al. Family burden and parental distress following mild traumatic brain injury in children and its relationship to post-concussive symptoms. *J Pediatr Psychol*. (2008) 33:621–9. doi: 10.1093/jpepsy/jsm133

8. Graff HJ, Siersma V, Møller A, Kragstrup J, Andersen LL, Egerod I, et al. Labour market attachment after mild traumatic brain injury: nationwide cohort study with 5-year register follow-up in Denmark. *BMJ Open*. (2019) 9:e026104. doi: 10.1136/bmjopen-2018-026104

9. Fallesen P, Campos B. Effect of concussion on salary and employment: a population-based event time study using a quasi-experimental design. *BMJ Open*. (2020) 10:e038161. doi: 10.1136/bmjopen-2020-038161

10. Voormolen DC, Cnossen MC, Polinder S, Gravesteijn BY, Steinbuechel NV, Real RGL, et al. Prevalence of post-concussion-like symptoms in the general population in Italy, The Netherlands and the United Kingdom. *Brain Inj*. (2019) 33:1078–86. doi: 10.1080/02699052.2019.1607557

11. Iverson GL, McCracken LM. 'Postconcussive' symptoms in persons with chronic pain. *Brain Inj*. (2009) 11:783–90. doi: 10.1080/026990597122990

12. Lees-Haley PR, Fox DD, Courtney JC. A comparison of complaints by mild brain injury claimants and other claimants describing subjective experiences immediately following their injury. *Arch Clin Neuropsychol*. (2001) 16:689–95. doi: 10.1093/arclin/16.7.689

13. Meares S, Shores EA, Taylor AJ, Batchelor J, Bryant RA, Baguley IJ, et al. Mild traumatic brain injury does not predict acute postconcussion syndrome. *J Neurol Neurosurg Psychiatry*. (2008) 79:300–6. doi: 10.1136/jnnp.2007.126565

14. Meares S, Shores EA, Taylor AJ, Batchelor J, Bryant RA, Baguley IJ, et al. The prospective course of postconcussion syndrome: the role of mild traumatic brain injury. *Neuropsychology*. (2011) 25:454–65. doi: 10.1037/a0022580

15. Kumar A, Loane DJ. Neuroinflammation after traumatic brain injury: opportunities for therapeutic intervention. *Brain Behav Immun*. (2012) 26:1191–201. doi: 10.1016/j.bbi.2012.06.008

16. Verboon LN, Patel HC, Greenhalgh AD. The immune system's role in the consequences of mild traumatic brain injury (concussion). *Front Immunol*. (2021) 12:620698. doi: 10.3389/fimmu.2021.620698

17. Patterson ZR, Holahan MR. Understanding the neuroinflammatory response following concussion to develop treatment strategies. *Front Cell Neurosci*. (2012) 6:58. doi: 10.3389/fncel.2012.00058

18. Rathbone ATL, Tharmaradinam S, Jiang S, Rathbone MP, Kumbhare DA. A review of the neuro- and systemic inflammatory responses in post concussion symptoms: introduction of the "post-inflammatory brain syndrome" PIBS. *Brain Behav Immun*. (2015) 46:1–16. doi: 10.1016/j.bbi.2015.02.009

19. Perini F, D'Andrea G, Galloni E, Pignatelli F, Billo G, Alba S, et al. Plasma cytokine levels in migraineurs and controls. *Headache J Head Face Pain*. (2005) 45:926–31. doi: 10.1111/j.1526-4610.2005.05135.x

20. Conti P, D'Ovidio C, Conti C, Gallenga CE, Lauritano D, Caraffa A, et al. Progression in migraine: role of mast cells and pro-inflammatory and anti-inflammatory cytokines. *Eur J Pharmacol*. (2018) 844:87–94. doi: 10.1016/j.ejphar.2018.12.004

21. Colasanto M, Madigan S, Korczak DJ. Depression and inflammation among children and adolescents: a meta-analysis. *J Affect Disorders*. (2020) 277:940–8. doi: 10.1016/j.jad.2020.09.025

22. Ng A, Tam WW, Zhang MW, Ho CS, Husain SF, McIntyre RS, et al. IL-1β, IL-6, TNF-α and CRP in elderly patients with depression or Alzheimer's disease: systematic review and meta-analysis. *Sci Rep-uk*. (2018) 8:12050. doi: 10.1038/s41598-018-30487-6

23. Costello H, Gould RL, Abrol E, Howard R. Systematic review and meta-analysis of the association between peripheral inflammatory cytokines and generalised anxiety disorder. *BMJ Open*. (2019) 9:e027925. doi: 10.1136/bmjopen-2018-027925

24. Fang Z, Huang K, Gil C-H, Jeong J-W, Yoo H-R, Kim H-G. Biomarkers of oxidative stress and endogenous antioxidants for patients with chronic subjective dizziness. *Sci Rep-uk*. (2020) 10:1478. doi: 10.1038/s41598-020-58218-w

25. Gucluturk MT, Unal ZN, Ismi O, Cimen MBY, Unal M. The role of oxidative stress and inflammatory mediators in benign paroxysmal positional vertigo. *J Int Adv Otology*. (2016) 12:101–5. doi: 10.5152/iao.2015.1412

26. Group P-PMoher D, Shamseer L, Clarke M, Ghersi D, Liberati A, et al. Preferred reporting items for systematic review and meta-analysis protocols (PRISMA-P) 2015 statement. *Syst Rev*. (2015) 4:1. doi: 10.1186/2046-4053-4-1

27. Wells G, Shea B, O'Connell D, Robertson J, Peterson J, Welch V, et al. (2000). The Newcastle-Ottawa Scale (NOS) for assessing the quality of nonrandomized studies in meta-analysis.

28. Meier TB, Huber DL, Bohorquez-Montoya L, Nitta ME, Savitz J, Teague TK, et al. A prospective study of acute blood-based biomarkers for sport-related concussion. *Ann Neurol*. (2020) 87:907–20. doi: 10.1002/ana.25725

29. Nitta ME, Savitz J, Nelson LD, Teague TK, Hoelzle JB, McCrea MA, et al. Acute elevation of serum inflammatory markers predicts symptom recovery after concussion. *Neurology*. (2019) 93:e497–507. doi: 10.1212/wnl.0000000000007864

30. Brett BL, Savitz J, Nitta M, España L, Teague TK, Nelson LD, et al. Systemic inflammation moderates the association of prior concussion with hippocampal volume and episodic memory in high school and collegiate athletes. *Brain Behav Immun*. (2020) 89:380–8. doi: 10.1016/j.bbi.2020.07.024

31. Meier T, Guedes VA, Smith EG, Sass D, Mithani S, Vorn R, et al. Extracellular vesicle-associated cytokines in sport-related concussion. *Brain Behav Immun*. (2021) 100:83–7. doi: 10.1016/j.bbi.2021.11.015

32. Bai L, Bai G, Wang S, Yang X, Gan S, Jia X, et al. Strategic white matter injury associated with long-term information processing speed deficits in mild traumatic brain injury. *Hum Brain Mapp*. (2020) 41:4431–41. doi: 10.1002/hbm.25135

33. Sun Y, Bai L, Niu X, Wang Z, Yin B, Bai G, et al. Elevated serum levels of inflammation-related cytokines in mild traumatic brain injury are associated with cognitive performance. *Front Neurol*. (2019) 10:1120. doi: 10.3389/fneur.2019.01120

34. Gill J, Mustapic M, Diaz-Arrastia R, Lange R, Gulyani S, Diehl T, et al. Higher exosomal tau, amyloid-beta 42 and IL-10 are associated with mild TBIs and chronic symptoms in military personnel. *Brain Inj*. (2018) 32:1359–66. doi: 10.1080/02699052.2018.1471738

35. Guedes VA, Kenney K, Shahim P, Qu B-X, Lai C, Devoto C, et al. Exosomal neurofilament light: a prognostic biomarker for remote symptoms after mild traumatic brain injury? *Neurology*. (2020) 94:e2412–23. doi: 10.1212/wnl.0000000000009577

36. Kanefsky R, Motamedi V, Mithani S, Mysliwiec V, Gill JM, Pattinson CL. Mild traumatic brain injuries with loss of consciousness are associated with increased

inflammation and pain in military personnel. *Psychiatry Res*. (2019) 279:34–9. doi: 10.1016/j.psychres.2019.07.001

37. Edwards KA, Gill JM, Pattinson CL, Lai C, Brière M, Rogers NJ, et al. Interleukin-6 is associated with acute concussion in military combat personnel. *BMC Neurol*. (2020) 20:209. doi: 10.1186/s12883-020-01760-x

38. Battista APD, Churchill N, Schweizer TA, Rhind SG, Richards D, Baker AJ, et al. Blood biomarkers are associated with brain function and blood flow following sport concussion. *J Neuroimmunol*. (2018) 319:1–8. doi: 10.1016/j.jneuroim.2018.03.002

39. Battista APD, Churchill N, Rhind SG, Richards D, Hutchison MG. Evidence of a distinct peripheral inflammatory profile in sport-related concussion. *J Neuroinflamm*. (2019) 16:17. doi: 10.1186/s12974-019-1402-y

40. Battista APD, Rhind SG, Richards D, Hutchison MG. An investigation of plasma interleukin-6 in sport-related concussion. *PLoS One*. (2020) 15:e0232053. doi: 10.1371/journal.pone.0232053

41. Rusiecki J, Levin LI, Wang L, Byrne C, Krishnamurthy J, Chen L, et al. Blast traumatic brain injury and serum inflammatory cytokines: a repeated measures case-control study among U.S. military service members. *J Neuroinflamm*. (2020) 17:20. doi: 10.1186/s12974-019-1624-z

42. Thompson HJ, Martha SR, Wang J, Becker KJ. Impact of age on plasma inflammatory biomarkers in the 6 months following mild traumatic brain injury. *J Head Trauma Rehab*. (2020) 35:324–31. doi: 10.1097/htr.0000000000000606

43. Powell JR, Boltz AJ, DeCicco JP, Chandran A, DeLellis SM, Healy ML, et al. Neuroinflammatory biomarkers associated with mild traumatic brain injury history in special operations forces combat soldiers. *J Head Trauma Rehab*. (2020) 35:300–7. doi: 10.1097/htr.0000000000000598

44. Ryan E, Kelly L, Stacey C, Huggard D, Duff E, McCollum D, et al. Mild-to-severe traumatic brain injury in children: altered cytokines reflect severity. *J Neuroinflamm*. (2022) 19:36. doi: 10.1186/s12974-022-02390-5

45. Goetzl EJ, Elahi FM, Mustapic M, Kapogiannis D, Pryhoda M, Gilmore A, et al. Altered levels of plasma neuron-derived exosomes and their cargo proteins characterize acute and chronic mild traumatic brain injury. *FASEB J*. (2019) 33:5082–8. doi: 10.1096/fj.201802319r

46. Brahmajothi MV, Abou-Donia MB. Monitoring from battlefield to bedside: serum repositories help identify biomarkers, perspectives on mild traumatic brain injury. *Mil Med*. (2020) 185:197–204. doi: 10.1093/milmed/usz301

47. Shan R, Szmydynger-Chodobska J, Warren OU, Mohammad F, Zink BJ, Chodobski A. A new panel of blood biomarkers for the diagnosis of mild traumatic brain injury/concussion in adults. *J Neurotraum*. (2016) 33:49–57. doi: 10.1089/neu.2014.3811

48. Feng G, Feng J, Zhang S, Tong Y, Zhang Q, Yang X, et al. Altered levels of α-melanocyte stimulating hormone in cerebrospinal fluid and plasma of patients with traumatic brain injury. *Brain Res*. (2018) 1696:22–30. doi: 10.1016/j.brainres.2018.05.044

49. Chaban V, Clarke GJB, Skandsen T, Islam R, Einarsen CE, Vik A, et al. Systemic inflammation persists the first year after mild traumatic brain injury: results from the prospective trondheim mild traumatic brain injury study. *J Neurotraum*. (2020) 37:2120–30. doi: 10.1089/neu.2019.6963

50. O'Brien WT, Symons GF, Bain J, Major BP, Costello DM, Sun M, et al. Elevated serum interleukin-1β levels in male, but not female, collision sport athletes with a concussion history. *J Neurotraum*. (2021) 38:1350–7. doi: 10.1089/neu.2020.7479

51. Tylicka M, Matuszczak E, Hermanowicz A, Dębek W, Karpińska M, Kamińska J, et al. BDNF and IL-8, but not UCHL-1 and IL-11, are markers of brain injury in children caused by mild head trauma. *Brain Sci*. (2020) 10:665. doi: 10.3390/brainsci10100665

52. Begum G, Reddy R, Yakoub KM, Belli A, Davies DJ, Pietro VD. Differential expression of circulating inflammatory proteins following sport-related traumatic brain injury. *Int J Mol Sci*. (2020) 21:1216. doi: 10.3390/ijms21041216

53. Vedantam A, Brennan J, Levin HS, McCarthy JJ, Dash PK, Redell JB, et al. Early versus late profiles of inflammatory cytokines after mild traumatic brain injury and their association with neuropsychological outcomes. *J Neurotraum*. (2021) 38:53–62. doi: 10.1089/neu.2019.6979

54. Woodcock T, Morganti-Kossmann MC. The role of markers of inflammation in traumatic brain injury. *Front Neurol*. (2013) 4:18. doi: 10.3389/fneur.2013.00018

55. Simon DW, McGeachy MJ, Bayır H, Clark RSB, Loane DJ, Kochanek PM. The far-reaching scope of neuroinflammation after traumatic brain injury. *Nat Rev Neurol*. (2017) 13:171–91. doi: 10.1038/nrneurol.2017.13

56. Morganti-Kossmann MC, Semple BD, Hellewell SC, Bye N, Ziebell JM. The complexity of neuroinflammation consequent to traumatic brain injury: from research evidence to potential treatments. *Acta Neuropathol*. (2019) 137:731–55. doi: 10.1007/s00401-018-1944-6

57. Wäljas M, Iverson GL, Lange RT, Hakulinen U, Dastidar P, Huhtala H, et al. A prospective biopsychosocial study of the persistent post-concussion symptoms following mild traumatic brain injury. *J Neurotraum*. (2015) 32:534–47. doi: 10.1089/neu.2014.3339

58. Kenzie ES, Parks EL, Bigler ED, Lim MM, Chesnutt JC, Wakeland W. Concussion as a multi-scale complex system: an interdisciplinary synthesis of current knowledge. *Front Neurol*. (2017) 8:513. doi: 10.3389/fneur.2017.00513

59. Kenzie ES, Parks EL, Bigler ED, Wright DW, Lim MM, Chesnutt JC, et al. The dynamics of concussion: mapping pathophysiology, persistence, and recovery with causal-loop diagramming. *Front Neurol*. (2018) 9:203. doi: 10.3389/fneur.2018.00203

60. Giza CC, Hovda DA. The new neurometabolic cascade of concussion. *Neurosurgery*. (2014) 75:S24–33. doi: 10.1227/neu.0000000000000505

61. Parkin GM, Clarke C, Takagi M, Hearps S, Babl FE, Davis GA, et al. Plasma tumor necrosis factor alpha is a predictor of persisting symptoms post-concussion in children. *J Neurotraum*. (2019) 36:1768–75. doi: 10.1089/neu.2018.6042

62. Loane DJ, Kumar A. Microglia in the TBI brain: the good, the bad, and the dysregulated. *Exp Neurol*. (2016) 275:316–27. doi: 10.1016/j.expneurol.2015.08.018

63. McDonald SJ, Shultz SR, Agoston DV. The known unknowns: an overview of the state of blood-based protein biomarkers of mild traumatic brain injury. *J Neurotraum*. (2021) 38:2652–66. doi: 10.1089/neu.2021.0011

64. Bui LA, Yeboah D, Steinmeister L, Azizi S, Hier DB, Wunsch DC, et al. Heterogeneity in blood biomarker trajectories after mild TBI revealed by unsupervised learning. *Ieee Acm Transactions Comput Biology Bioinform*. (2022) 19:1365–78. doi: 10.1109/tcbb.2021.3091972

65. Iverson GL, Gardner AJ, Terry DP, Ponsford JL, Sills AK, Broshek DK, et al. Predictors of clinical recovery from concussion: a systematic review. *Brit J Sport Med*. (2017) 51:941–8. doi: 10.1136/bjsports-2017-097729

66. Fehr SD, Nelson LD, Scharer KR, Traudt EA, Veenstra JM, Tarima SS, et al. Risk factors for prolonged symptoms of mild traumatic brain injury. *Clin J Sport Med*. (2019) 29:11–7. doi: 10.1097/jsm.0000000000000494

67. Booker J, Sinha S, Choudhari K, Dawson J, Singh R. Description of the predictors of persistent post-concussion symptoms and disability after mild traumatic brain injury: the SHEFBIT cohort. *Brit J Neurosurg*. (2019) 33:367–75. doi: 10.1080/02688697.2019.1598542

68. Visser K, Koggel M, Blaauw J, van der Horn HJ, Jacobs B, van der Naalt J. Blood-based biomarkers of inflammation in mild traumatic brain injury: a systematic review. *Neurosci Biobehav Rev*. (2021) 132:154–68. doi: 10.1016/j.neubiorev.2021.11.036

frontiers | Frontiers in Neurology

TYPE Original Research
PUBLISHED 25 May 2023
DOI 10.3389/fneur.2023.1189898

OPEN ACCESS

EDITED BY
Wael M. Y. Mohamed,
International Islamic University Malaysia, Malaysia

REVIEWED BY
Hipólito Nzwalo,
University of Algarve, Portugal
Michal Bar,
University Hospital Ostrava, Czechia

*CORRESPONDENCE
Yang Hong
hongyangcmu@126.com

†These authors have contributed equally to this work and share first authorship

RECEIVED 20 March 2023
ACCEPTED 03 May 2023
PUBLISHED 25 May 2023

CITATION
Zhang J, Liu C, Hu Y, Yang A, Zhang Y and Hong Y (2023) The trend of neutrophil-to-lymphocyte ratio and platelet-to-lymphocyte ratio in spontaneous intracerebral hemorrhage and the predictive value of short-term postoperative prognosis in patients. *Front. Neurol.* 14:1189898. doi: 10.3389/fneur.2023.1189898

The trend of neutrophil-to-lymphocyte ratio and platelet-to-lymphocyte ratio in spontaneous intracerebral hemorrhage and the predictive value of short-term postoperative prognosis in patients

Jian Zhang[1,2†], Chunlong Liu[3†], Yaofeng Hu[1], Aoran Yang[1], Yonghui Zhang[2] and Yang Hong[1*]

[1]Department of Neurosurgery, Shengjing Hospital of China Medical University, Shenyang, China, [2]Department of Neurosurgery, The Seventh Clinical College of China Medical University, Fushun, China, [3]Department of Hepatobiliary and Pancreatic Surgery, Fuyang People's Hospital, Anhui Medical University, Fuyang, China

Background: Neutrophil-to-lymphocyte ratio (NLR) and platelet-to-lymphocyte ratio (PLR) play an important role in the inflammatory response in various diseases, but the role in the course of spontaneous intracerebral hemorrhage (ICH) is unclear.

Methods: This study retrospectively collected baseline characteristics and laboratory findings, including NLR and PLR at different time points, from spontaneous ICH patients undergoing surgery between January 2016 and June 2021. Patients were scored using the modified Rankin Scale (mRS) to evaluate their functional status at 30 days post-operation. Patients with mRS score ≥3 were defined as poor functional status, and mRS score <3 was defined as good functional status. The NLR and PLR were calculated at admission, 48 h after surgery and 3–7 days after surgery, respectively, and their trends were observed by connecting the NLR and PLR at different time points. Multivariate logistic regression analysis was used to identify independent risk factors affecting the prognosis of ICH patients at 30 days after surgery.

Results: A total of 101 patients were included in this study, and 59 patients had a poor outcome at 30 days after surgery. NLR and PLR gradually increased and then decreased, peaking at 48 h after surgery. Univariate analysis demonstrated that admission Glasgow Coma Scale (GCS) score, interval from onset to admission, hematoma location, NLR within 48 h after surgery and PLR within 48 h after surgery were associated with poor 30-day prognosis. In multivariate logistic regression analysis, NLR within 48 h after surgery (OR, 1.147; 95% CI, 1.005, 1.308; P, 0.042) was an independent risk factor for 30-day after surgery prognosis in spontaneous ICH patients.

Conclusion: In the course of spontaneous intracerebral hemorrhage, NLR and PLR initially increased and subsequently decreased, reaching their peak values at 48 h after surgery. High NLR within 48 h after surgery was an independent risk factor for poor prognosis 30 days after surgery in spontaneous ICH patients.

KEYWORDS

spontaneous intracerebral hemorrhage, neutrophil-to-lymphocyte ratio, platelet-to-lymphocyte ratio, surgery, prognosis, marker

1. Introduction

Cerebrovascular disease (CVD) is a significant cause of death and disability worldwide, including acute ischemic stroke (AIS) and intracerebral hemorrhage (ICH), mostly caused by acute arterial occlusion and rupture (1, 2). ICH occurs in 10–15% of all stroke types and places a huge economic burden on society and families (3). Spontaneous ICH is a non-traumatic hemorrhagic disease that develops in 10–30 per 100,000 people globally, affecting approximately 2 million people worldwide, and has a high mortality and disability rate (4). In selected patients surgery can be life saving. However, identifying the early prognosis in ICH patients after surgery is more difficult. At present, the indicators for prognostic evaluation in ICH patients after surgery focus on the general condition of the patient at admission, such as GCS score, pupil size, pupil reactivity, hematoma location, hematoma volume, and whether the hematoma extends into the ventricle. However, these prognostic indicators have different drawbacks (5).

Neutrophil-to-lymphocyte ratio (NLR) and platelet-to-lymphocyte ratio (PLR) are indicators of inflammatory response and coagulation status, which play an important role in the prognosis prediction of stroke. A larger cohort study revealed that pre-thrombolytic levels of NLR and PLR were significantly associated with early neurological deterioration following thrombolysis in patients with acute ischemic stroke (6). Furthermore, a recent retrospective study demonstrated the predictive value of elevated levels of NLR in both the development of stroke-associated pneumonia in ICH patients and the early identification of pneumonia severity (7). The study indicated that the neuroinflammatory response was associated with secondary brain injury after spontaneous ICH, thus the inflammatory markers NLR and PLR might be markers of prognosis in ICH patients. In the early stages of ICH, microglia activate and release chemokines to recruit peripheral inflammatory cells are the main cause of secondary brain injury (8). Over time, leukocyte infiltration increase in the injury site, releasing large amounts of inflammatory mediators, which may exacerbate secondary brain injury. In addition, activated platelets begin to promote the recruitment of leukocytes at the site of injury, further aggravating the injury (9). There is increasing evidence that NLR and PLR are more accurate compared to other markers. NLR and PLR can effectively assess early neurological deterioration and long-term survival of stroke patients (8, 10). Regarding the relationship between inflammatory indicators and ICH, current studies focused on a point of time or a period of time (11), ignoring the trend of inflammatory indicators over the course of the disease. Surgery is an important part of the therapy for spontaneous ICH, intervening in the disease process by effectively reducing intracranial pressure, relieving the hematoma-occupying effect and preventing the massive release of inflammatory mediators (12). Different surgical methods vary in the degree of hematoma removal, but equally differ in the degree of brain tissue damage. In Addition, it is controversial whether different surgical methods can improve the prognosis of spontaneous ICH patients (13, 14).

2. Methods

2.1. Study design

This study retrospectively collected clinical data from 101 spontaneous ICH patients undergoing craniotomy and minimally invasive puncture and drainage (MIPD) between January 2016 and June 2021. The Medical Ethics Review Committee of Liaoning Health Industry Group Fukuang General Hospital approved this study, which was conducted under the guidelines of the World Medical Association Helsinki Declaration in 1975. Informed written consent was obtained from all patients or their relatives.

Inclusion criteria: (1) age > 18 years old and first presentation; (2) spontaneous ICH confirmed by computed tomography (CT); (3) craniotomy or MIPD for hematoma drainage within 24 h of onset.

Exclusion criteria: (1) age < 18 years; (2) secondary ICH due to trauma, aneurysm, arteriovenous malformation, cavernous angioma, smoldering disease, tumor stroke, or coagulation disorders; (3) infectious diseases, cancer, chronic heart disease, liver or kidney disease, rheumatic immune system disease, hematologic diseases, and other diseases affecting peripheral blood cells; (4) patients without CT or angiography at 24 h after admission; (5) admission GCS score < 5, patients were paralyzed or in a vegetative state before the onset of the disease; (6) incomplete follow-up data.

2.2. Preoperative patient management

All patients included in this study were managed and treated according to the American Heart Association/American Stroke Management Guidelines (15). Upon admission, patients were monitored for vital signs, assessed for consciousness with GCS scores, and immediately underwent CT to assess the hemorrhage location, hematoma volume, and whether there was a combined ventricular hemorrhage and subarachnoid hemorrhage, while peripheral blood was collected. Two experienced neurosurgeons developed the surgical procedure based on the clinical situation of each ICH patient, including access location and bone window size.

2.3. Clinical parameter evaluation

We retrospectively collected demographic characteristics, general clinical characteristics, imaging findings, and laboratory findings of all ICH patients enrolled in this study, including age, sex, hypertension history, diabetes history, admission systolic blood pressure, admission diastolic blood pressure, admission GCS score, interval from onset to admission, hematoma location (supratentorial and infratentorial), hematoma volume (calculated using ABC/2 software) (16), ventricular hemorrhage, subarachnoid hemorrhage, and surgery methods (craniotomy and MIPD).

Laboratory test results including serum potassium ion, serum glucose, fibrinogen (FIB), prothrombin time (PT), activated partial thromboplastin time (APTT), thrombin time (TT), and D-dimer were collected from patients on admission. On admission, 48 h after surgery and 3–7 days after surgery white blood cell (WBC), absolute neutrophil (NE) count, absolute lymphocyte (L) count, and platelet (PLT) count were measured. NLR was defined as neutrophil count to lymphocyte count ratio and PLR was defined as platelet count to lymphocyte count ratio. NLR and PLR were assessed at admission, 48 h post-surgery, and 3–7 days post-surgery. NLR values were labeled as NLR1, NLR2, and NLR3, while PLR values were labeled as PLR1, PLR2, and PLR3, respectively. Both NLR and PLR values were considered continuous variables and were compared between the good and poor prognosis groups using Student's t-test to identify potential differences across various time points. A statistically significant difference was established if $p < 0.05$.NLR and PLR were presented as mean ± standard deviation values. Line segments were used to connect NLR and PLR data points from different time points to analyze the trends of inflammatory indicators in all patients, craniotomy group patients, and MIPD group patients separately.

2.4. Surgery method

The craniotomy group routinely performed hematoma removal according to the preoperatively designed surgical approach and bone window size, aspirating the hematoma as cleanly as possible, and whether the bone flap was preserved or not depended on the intraoperative situation. The MIPD group punctured the hematoma according to the pre-designed direction, location and depth after installing and commissioning the stereotactic instrument, and slowly drained the blood using a 5 mL syringe.

2.5. Postoperative patient management

Standardized management of postoperative patients according to the American Heart Association/American Stroke Management Guidelines. In the MIPD group, we gave 5 mL of saline mixed with 20–30,000 units of urokinase every 4–6 h postoperatively in order to liquefy the hematoma. Regular cranial CT examinations were performed to assess the effect of hematoma removal, and the drainage tube was removed when the hematoma disappeared or the remaining hematoma volume was less than 10 mL and the patient's vital signs were stable. Peripheral blood specimens were collected daily at 7:00 am after surgery. Patient prognosis was assessed using the mRS to acquire patients' survival functional status and outcomes at 30 days after surgery with outpatient or telephone follow-up visits (17). Patients with mRs ≥3 defined as poor prognosis and mRs <3 as good prognosis at 30 days postoperatively.

2.6. Statistical analysis

Statistical analysis of the data was performed using SPSS 25.0 (IBM Corporation, Almonk, NY, USA). Graphs were plotted using GraphPad Prism 9.0 (GraphPad Software, San Diego, CA, USA). All continuous variables were expressed as mean ± standard deviation or median (interquartile range, IQR) and analyzed using Student's *t*-test or Mann–Whitney test. All categorical variables were expressed as frequencies (percentages) and analyzed using chi-square tests. Variables included in the univariate analysis that were significant ($p < 0.10$) were entered into multivariate logistic regression and defined as independent risk factors for poor outcome. The receiver operating characteristic analysis (ROC) were used to assess different variables. $p < 0.05$ was considered to be statistically significant.

3. Results

3.1. ICH patients' general information

In this study, a total of 101 spontaneous ICH patients (69 males and 32 females) with a median age of 59 years (IQR: 53.5–66 years) were included, 42 in the favorable prognosis group and 59 in the poor prognosis group (Table 1). The median time from patient onset to admission was 3 h (IQR: 2–5 h). 70% patients had hypertension history. The GCS score on admission was 9 (IQR: 8–12). Among all patients, 86 (84.2%) had hematoma locations supratentorial and 16 (15.8%) were infratentorial. Of all patients with supratentorial hematomas, 50 (49.5%) were located in the basal ganglia and 35 (34.7%) in the cerebral lobes. The hematoma volume was 40.0 mL (IQR: 28.3–60.6 mL). 24 patients (23.8%) had combined subarachnoid hemorrhage. All patients underwent surgical treatment, 77 (76.2%) underwent craniotomy and 24 (23.8%) underwent MIPD. Of all the ICH patients who underwent craniotomy, 8 had preserved bone flaps, 3 had basal ganglia hemorrhage, and 5 had lobar hemorrhage. Among the 3 patients with basal ganglia hemorrhage, 2 displayed poor functional status at 30 days post-operation, while 1 showed good functional status. Regarding the 5 patients with lobar hemorrhage, all of them had a good functional outcome at 30 days post-operation.

3.2. Univariate and multifactor analysis

In univariate analysis, admission GCS score, interval from onset to admission, hematoma location, NLR and PLR within 48 h after surgery were risk factors for 30-day postoperative prognosis in spontaneous ICH patients ($p < 0.05$). In addition, univariate analysis showed that age, sex, medical history, hematoma volume, combined ventricular hemorrhage, combined subarachnoid hemorrhage, surgical method, coagulation, serum potassium, serum glucose and other time points of NLR and PLR were not associated with prognosis ($p > 0.05$) (Tables 1, 2). In multivariate logistic analysis, NLR within 48 h after surgery was an independent risk factor for 30-day postoperative prognosis in spontaneous ICH patients ($p < 0.05$) (Table 3).

3.3. Trend of NLR, PLR, and ROC curve

Figures 1, 2 described the changing patterns of NLR and PLR during the course of ICH disease, respectively. Figures 1A,2A showed that NLR and PLR exhibited a trend of increasing and then decreasing, and reached a peak within 48 h after surgery. The same trend was observed for the different surgical modalities (Figures 1B,C, 2B,C).

TABLE 1 Baseline characteristics of ICH patients.

Characteristic	Total (n = 101)	Favorable Outcome (n = 42)	Poor Outcome (n = 59)	p value
Male, n (%)	69 (68.3%)	25 (59.2%)	44 (74.6%)	0.109
Age, IQR, Y	59.0 (53.5–66.0)	59.0 (54.8–67.0)	60.0 (53.0–66.0)	0.641
Admission systolic blood pressure, IQR, mmHg	177.0 (160.5–200.0)	175.5 (160.0–190.8)	177.0 (163.0–205.0)	0.200
Admission diastolic blood pressure, IQR, mmHg	102.0 (93.0–112.5)	103.0 (90.0–114.3)	102.0 (95.0–112.0)	0.354
Hypertension, n (%)	70 (69.3%)	29 (69.0%)	41 (69.5%)	0.962
Diabetes, n (%)	13 (12.9%)	3 (7.1%)	10 (16.9%)	0.147
Admission GCS score, IQR	9.0 (8.0–12.0)	10.0 (8.0–12.0)	8.0 (7.0–10.0)	0.031*
Interval from onset to admission, IQR, h	3.0 (2.0–5.0)	3.3 (2.0–6.3)	2.5 (1.5–4.0)	0.039*
Hematoma volume, IQR, mL	40.0 (28.3–60.6)	38.9 (18.8–55.1)	40.9 (30.5–62.0)	0.410
Hematoma location				0.042*
Basal ganglia, n (%)	50 (49.5%)	15 (35.7%)	35 (59.3%)	
Cerebral lobe, n (%)	35 (34.7%)	17 (40.5%)	18 (30.5%)	
Cerebellum, n (%)	16 (15.8%)	10 (23.8%)	6 (10.2%)	
Intraventricular hemorrhage, n (%)	55 (54.5%)	19 (45.2%)	36 (61.0%)	0.117
Subarachnoid hemorrhage, n (%)	24 (23.8%)	13 (31.0%)	11 (18.6%)	0.152
Surgical approach				0.338
Craniotomy, n (%)	77 (76.2%)	30 (71.4%)	47 (79.7%)	
MIPD, n (%)	24 (23.8%)	12 (28.6%)	12 (2%)	

GCS, Glasgow coma scale; MIPD, minimally invasive puncture and drainage; IQR, Interquartile range; *$p < 0.05$.

The differences in NLR and PLR between the two surgical modalities (Figure 3) at admission, 48 h after surgery and 3–7 days after surgery were not significant ($p > 0.05$). The ROC curve results showed the area under the curve (AUC) was 0.593 for NLR2, 0.577 for PLR2, 0.690 for admission GCS score combined with NLR2, and 0.663 for admission GCS combined with PLR2 (Figure 4).

4. Discussion

In this study, NLR and PLR showed an increase followed by a decrease during spontaneous ICH and peaked within 48 h postoperatively. The two surgeries showed the same trend of change. This study found that measuring elevated levels of NLR and PLR within 48 h following surgery in spontaneous ICH patients is associated with a higher likelihood of poor prognosis. These results highlight the potential clinical importance of utilizing NLR and PLR as early biomarkers for prognosis in ICH patients following surgery. However, further research is needed to fully assess the reliability and efficacy of these biomarkers in predicting treatment outcomes.

The immune inflammatory response is closely associated with secondary brain injury after the occurrence of ICH. After hematoma formation, the blood–brain barrier (BBB) is disrupted, and the extravasated blood activates microglia, causing them to release large amounts of inflammatory factors and chemokines, which promote leukocyte infiltration in the surrounding brain tissue (18, 19). Neutrophils are the first immune cells to migrate through the damaged BBB to the hematoma (20). Neutrophils further damage the BBB by releasing myeloperoxidase, elastase and other inflammatory mediators, aggravating microvascular and brain tissue damage (20, 21). In a population-based study of ICH, neutrophil infiltration around brain tissue occurred as early as 8 h after hemorrhage, whereas in animals it occurred as early as 4 h after hemorrhage and peaked 2–3 days after onset (22, 23). In the acute phase of ICH, lymphopenia is considered to be the main marker of brain injury. The decrease in lymphocytes includes apoptosis and inactivation, mainly due to catecholamines and steroids produced by sympathetic and hypothalamic–pituitary–adrenal axis activation (24). Brain injury occurs after the infiltration of brain tissue around a large number of neutrophils and lymphocytes, the over-recruitment of immune cells make the body in a state of immunosuppression (25). After ICH occurs, platelets activate and accumulate around the vascular endothelial cells, prompting fibrinogen precipitation and collecting more platelets around the damaged brain tissue to make the blood in a hypercoagulable state, the aggregated platelets release numerous inflammatory factors to enhance the inflammatory response (26). The immune inflammatory response plays an important role in the process of spontaneous ICH, NLR and PLR are indicators of the overall and local inflammation and stress status of the organism. NLR and PLR have greater potential to become biological markers for estimating the severity of secondary brain injury and disease progression after ICH.

In this study, we found that NLR and PLR in spontaneous ICH patients showed a trend of increasing and then decreasing, peaking within 48 h after surgery. Previous studies had shown that peripheral neutrophils were significantly higher in ischemic and hemorrhagic stroke patients on admission, while lymphocytes usually remained unchanged or decreased. Thus, local and systemic inflammatory changes in patients with brain injury can be manifested through

TABLE 2 Laboratory tests of ICH patients.

Hematological variables	Favorable outcome (n = 42)		Poor outcome (n = 59)		p value
	Mean ± SD	Med (IQR 25–75 %)	Mean ± SD	Med (IQR 25–75 %)	
Admission					
WBC (10^9/L)	12.5 ± 3.3	11.8 (10.6–14.7)	12.4 ± 6.2	11.3 (8.6–14.6)	0.928
Neutrophils (10^9/L)	10.6 ± 3.0	10.4 (8.2–12.8)	9.9 ± 4.8	9.3 (6.3–12.8)	0.370
Lymphocytes (10^9/L)	1.3 ± 0.7	1.2 (0.8–1.6)	1.7 ± 1.4	1.2 (0.9–1.7)	0.165
Platelets (10^9/L)	226.0 ± 66.6	220.5 (171.3–270.3)	216.0 ± 76.0	211.0 (163.0–246.0)	0.496
NLR1	9.9 ± 4.7	8.7 (6.5–12.6)	8.7 ± 5.9	7.8 (4.0–11.6)	0.276
PLR1	202.9 ± 79.2	206.3 (143.6–271.8)	174.3 ± 86.8	153.35 (105.7–222.2)	0.094
Glucose (mmol/L)	8.3 ± 3.1	7.2 (6.2–10.0)	9.3 ± 3.2	8.4 (6.7–11.4)	0.117
K^+(mmol/L)	3.7 ± 0.6	3.8 (3.4–4.0)	3.7 ± 0.5	3.7 (3.4–4.1)	0.994
FIB(g/L)	3.2 ± 0.8	3.1 (2.7–3.7)	3.4 ± 1.4	3.1 (2.5–3.7)	0.410
PT(s)	12.8 ± 1.4	12.7 (12.0–13.2)	12.8 ± 0.9	12.7 (12.1–13.4)	0.767
APTT(s)	31.8 ± 5.5	30.1 (28.3–34.2)	31.6 ± 4.9	31.4 (27.5–34.5)	0.853
TT(s)	17.0 ± 1.6	17.3 (15.9–18.0)	17.0 ± 2.3	16.8 (15.9–18.0)	0.989
D-dimer(mg/l)	1.3 ± 2.7	0.6 (0.4–1.1)	1.2 ± 1.6	0.5 (0.3–1.1)	0.674
48 h after surgery					
WBC (10^9/L)	13.1 ± 3.4	10.7 (10.4–15.1)	13.1 ± 3.2	13.2 (10.7–15.4)	0.963
Neutrophils (10^9/L)	10.8 ± 2.9	10.8 (8.4–13.1)	11.2 ± 3.2	10.7 (8.6–14.0)	0.572
Lymphocytes (10^9/L)	1.3 ± 0.6	1.1 (0.9–1.6)	1.1 ± 0.5	1.1 (0.7–1.5)	0.044*
Platelets (10^9/L)	212.9 ± 58.2	207.0 (175.3–258.0)	206.2 ± 63.5	200.0 (163.0–246.0)	0.589
NLR2	9.3 ± 3.6	9.1 (6.6–11.8)	13.7 ± 10.4	10.5 (6.2–17.0)	0.004*
PLR2	183.9 ± 76.2	181.4 (111.7–245.4)	234.8 ± 139.3	184.0 (127.5–307.5)	0.021*
3-7d after surgery					
WBC (10^9/L)	10.1 ± 2.7	9.9 (8.8–11.6)	11.2 ± 3.2	10.6 (9.1–13.7)	0.085
Neutrophils (10^9/L)	7.7 ± 2.4	7.5 (5.8–9.4)	8.7 ± 2.9	7.9 (6.8–11.3)	0.072
Lymphocytes (10^9/L)	1.4 ± 0.7	1.4 (1.1–2.0)	1.4 ± 0.7	1.3 (0.9–2.0)	0.828
Platelets (10^9/L)	255.6 ± 82.2	267.5 (191.0–327.5)	232.4 ± 89.0	213.0 (162.0–279.5)	0.187
NLR3	6.5 ± 3.3	5.1 (3.5–8.1)	7.5 ± 4.8	6.6 (4.6–9.1)	0.236
PLR3	209.8 ± 107.4	165.8 (143.2–239.5)	195.2 ± 103.4	163.6 (127.0–234.8)	0.495

WBC, White blood cell; FIB, Fibrinogen; PT, Prothrombin time; APTT, Activated partial thromboplastin time; TT, Thrombin time; NLR1, admission neutrophil to lymphocyte ratio; PLR1, admission Platelet to lymphocyte ratio; NLR2, Neutrophil to lymphocyte ratio at 48 h after surgery; PLR2, Platelet to lymphocyte ratio at 48 h after surgery; NLR3, Neutrophil to lymphocyte ratio within 3–7 d after surgery; PLR3, Platelet to lymphocyte ratio within 3–7 d after surgery; Med, median; IQR, Interquartile range; SD, standard deviation; *$p < 0.05$.

NLR. However, this similar trend is not reflected in stroke patients who receive non-surgical treatment. Most previous studies have focused on whether NLR can be a predictor of prognosis in certain diseases (6, 27–29), neglecting its trend in disease, especially in the surgical treatment of ICH. The reasons affecting this trend are unclear. We speculate that this may be related to the evolution of the hematoma. In the early stage, as the hematoma progresses, the inflammatory response gradually becomes stronger and the NLR increases, and as the disease improves, the inflammatory response gradually subsides and the NLR begins to decrease (30). In addition, the early surgical intervention relieves the mechanical compression of the brain tissue by the hematoma as well as prevents the massive release of inflammatory products (31, 32), which may also be influential factors in producing this change. There is a close relationship between the inflammatory response of the organism and the hypercoagulable state. The inflammatory response can contribute to a hypercoagulable state and thrombosis in the organism (33). The thrombosis can trigger inflammatory reactions in turn (34, 35). PLR is a platelet count to lymphocyte count ratio that reflects the interrelationship between inflammation and hypercoagulable state of the body (36), and plays an important role in the assessment of inflammatory response in many diseases (37, 38). Considering the effect of different surgical methods in inflammatory response, in this study we studied the trend of inflammatory indicators in craniotomy and MIPD separately. We found that NLR and PLR were more valuable in predicting the prognosis of spontaneous ICH patients within 48 h after surgery compared to other time points.

In this study, we performed a univariate analysis of NLR2 and PLR2, and we found that NLR2 and PLR2 were risk factors for prognosis in ICH patients (OR, 1.093, 95% CI 1.016 ~ 1.17.6; OR, 1.004, 95% CI 1.000 ~ 1.0008), whereas admission GCS score was a

TABLE 3 Univariate and multifactorial analysis of factors associated with poor postoperative prognosis in ICH patients.

	Univariate analysis		Multivariate analysis	
	OR (95 CI %)	*p* value	OR (95 CI %)	*p* value
Sex	0.051 (0.214–1.173)	0.111	0.475 (0.173–1.304)	0.149
Age	0.991 (0.956–1.028)	0.637	1.009 (0.966–1.055)	0.694
Admission GCS score	0.825 (0.690–0.985)	0.034	0.815 (0.663–1.055)	0.052
Interval from onset to admission	0.912 (0.834–0.998)	0.045	0.904 (0.817–1.001)	0.052
Basal ganglia hemorrhage	0.381 (0.168–0.863)	0.021	0.415 (0.164–1.054)	0.064
NLR2	1.093 (1.016–1.176)	0.017	1.147 (1.005–1.308)	0.042
PLR2	1.004 (1.000–1.008)	0.041	0.997 (0.990–1.005)	0.500

GCS, Glasgow coma scale; NLR2, Neutrophil to lymphocyte ratio at 48 h after surgery; PLR2, Platelet to lymphocyte ratio at 48 h after surgery; OR, Odds ratios; CI, Confidence interval.

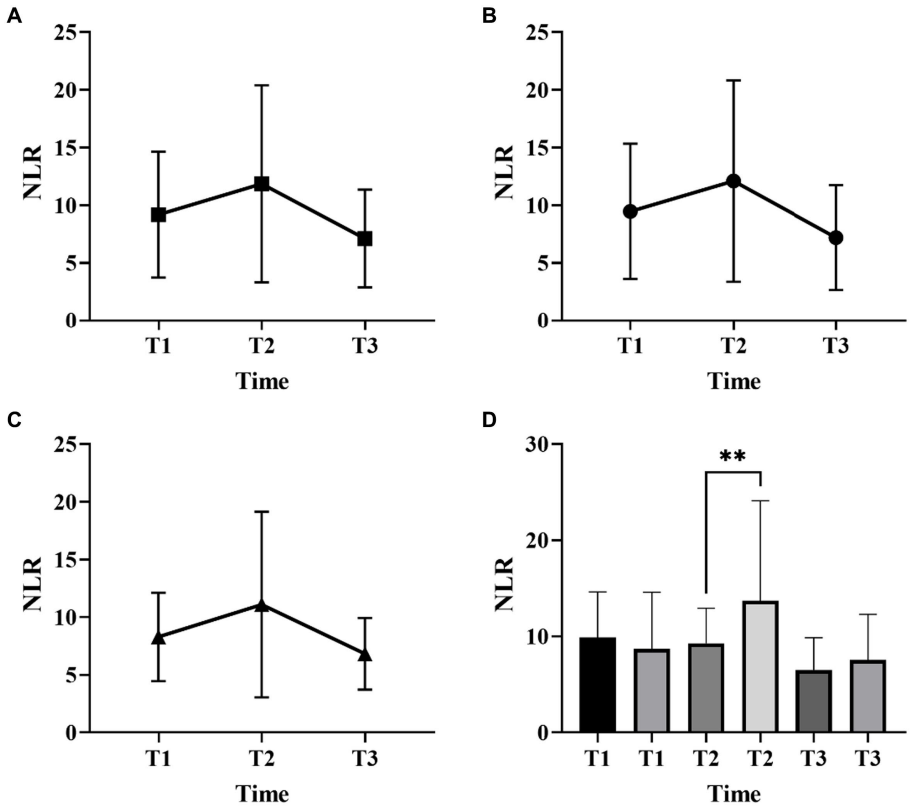

FIGURE 1
Neutrophil-to-lymphocyte ratio (NLR) changes over time in patients with ICH with two surgical methods (**A**, all patients; **B**, craniotomy; **C**, MIPD; **D**, comparison of NLR at different time points in ICH patients with favorable and poor prognosis; T1, at admission; T2, at 48 h after surgery; T3, within 3-7 days after surgery; $^{**}p < 0.05$).

factor for patient prognosis (OR 0.825, 95% CI, 0.690 ~ 0.985).NLR and PLR play an important role in the prognosis of stroke and can be used as complementary indicators of prognosis (6, 7). NLR and PLR are simpler and easier to obtain than the high cost of CT exams. In addition, NLR and PLR can be dynamically observed during the course of the disease and the presence of peaks can help in early intervention and timely adjustment of the treatment plan, especially 48 h after surgery. In this study, we analyzed trends in NLR and PLR over the course of the disease from three groups: all patients, the craniotomy group, and the MIPD group, respectively. NLR and PLR in all three groups showed an increase followed by a decrease and reached a peak within 48 h after surgery. A retrospective study on surgical treatment of spontaneous ICH showed that patients treated with craniotomy had higher postoperative NLR than those treated with minimally invasive surgery, possibly because craniotomy damaged more brain tissue damage (31). However, in this study, we compared NLR levels between the craniotomy and MIPD groups at different time points, and we found no significant difference in NLR levels. We also compared the PLR levels of the two groups at different time points and found that the PLR in the MIPD group was slightly higher than that in the craniotomy group at 48 h after surgery, but there was no

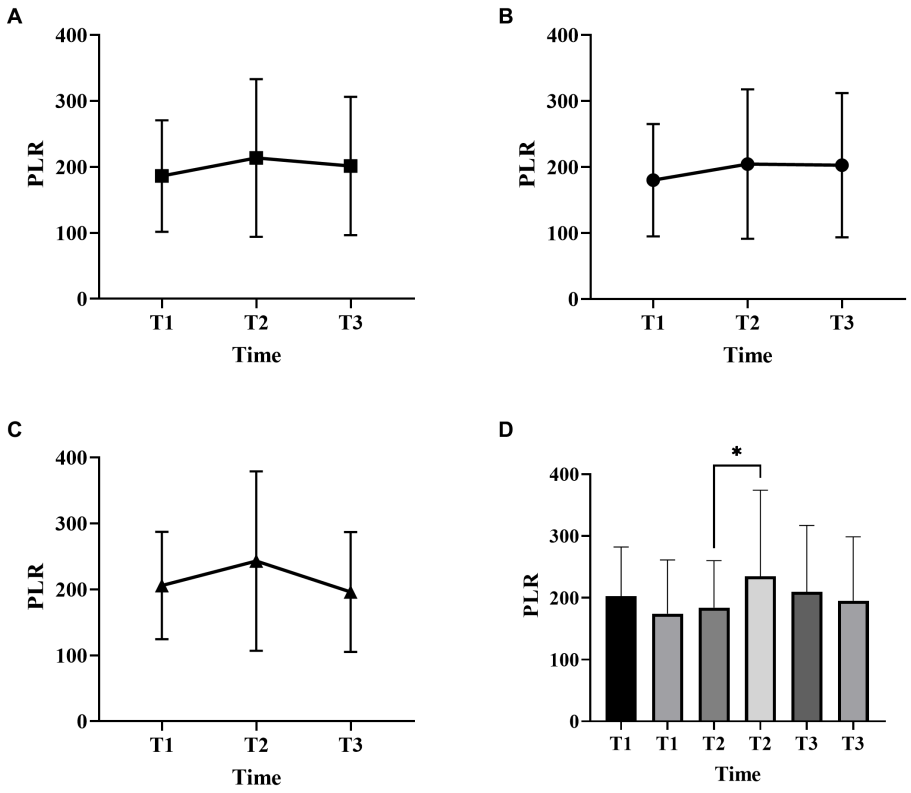

FIGURE 2
Platelet-to-lymphocyte ratio (PLR) changes over time in patients with ICH with two surgical methods (**A**, all patients; **B**, craniotomy; **C**, MIPD; **D**, comparison of PLR at different time points in ICH patients with favorable and poor prognosis; T1, at admission; T2, at 48 h after surgery; T3, within 3-7 days after surgery, *$p < 0.05$).

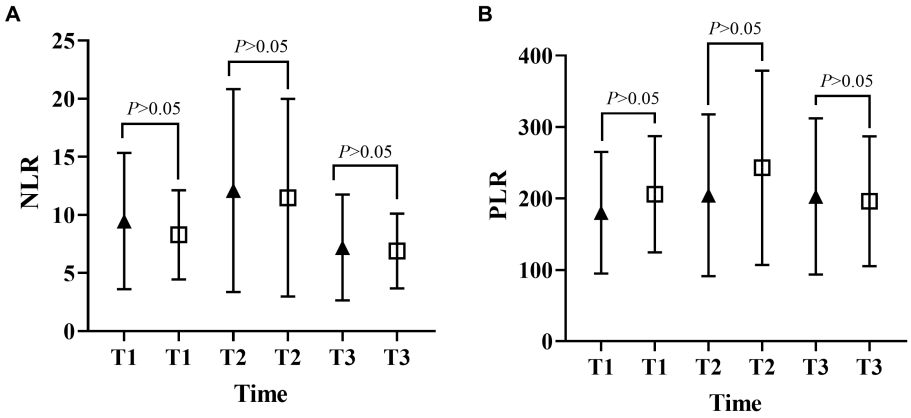

FIGURE 3
Differences in NLR and PLR between the open and MIPD groups in various time points (**A**, neutrophil-to-lymphocyte ratio; **B**, platelet-to-lymphocyte ratio; T1, at admission; T2, at 48 h after surgery; T3, within 3–7 days after surgery).

significant difference between the groups, which we believe may be related to the higher blood loss during the craniotomy. In addition, we found peak NLR ≥ 14.34 and 13.93,peak PLR ≥ 300.85 and 304.93 in the craniotomy and MIPD groups, suggesting a poorer prognosis. The threshold values in our study were similar to previous studies, which reported NLRs in the range of 12.97–14.46 (31, 39). There was considerable debate as to whether different surgical approaches could improve the early prognosis of ICH patients. In a prospective non-randomized comparative study investigating 198 spontaneous ICH patients, including 114 patients treated with craniotomy and 84 patients treated with MIPD, researchers found no difference in mortality between the two groups at 30 days and 1 year postoperatively, however neurological functional outcomes at 1 year were significantly higher in the MIPD

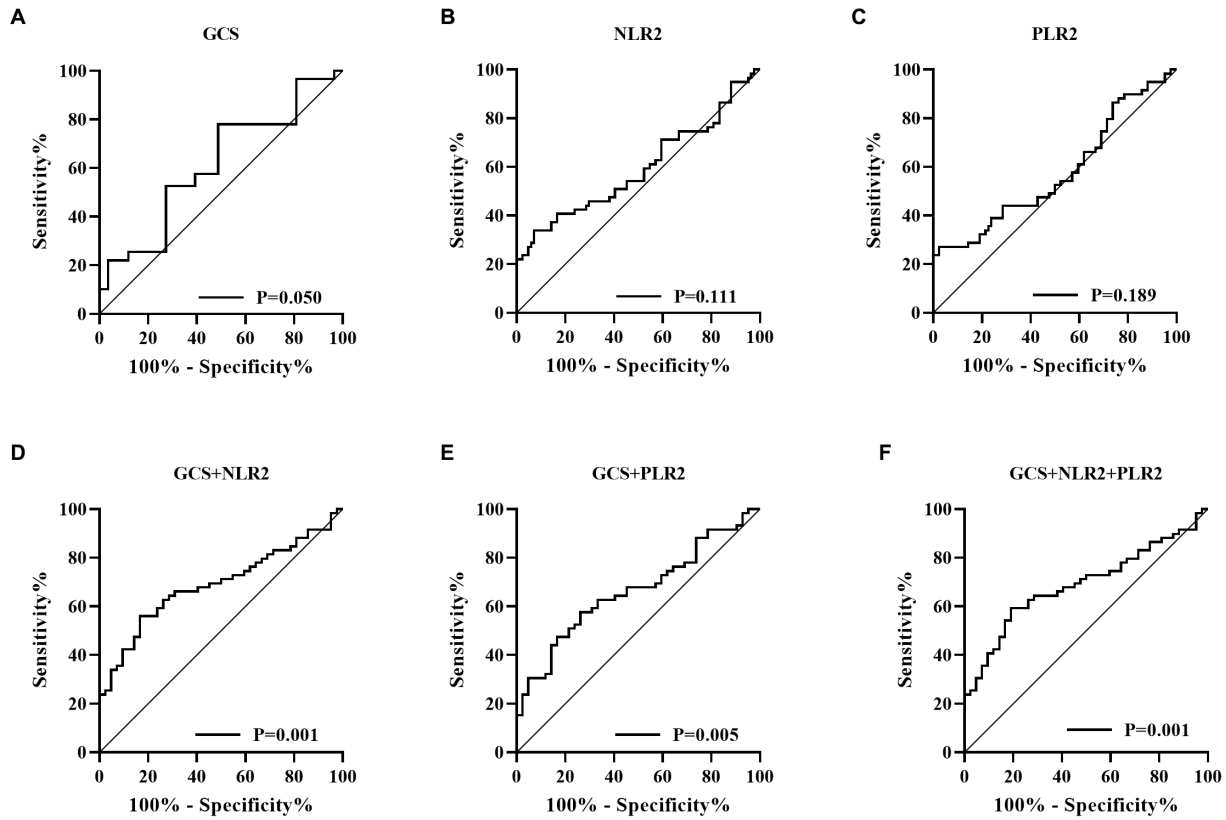

FIGURE 4
Receiver operating characteristic (ROC) curve (**A**, Glasgow coma scale; **B**, Neutrophil to lymphocyte ratio; **C**, Platelet to lymphocyte ratio; **D**, GCS combined with NLR2; **E**, GCS combined with PLR2; **F**, GCS combined with NLR2 and PLR2).

group than in the craniotomy group (40). In addition, a large, high-quality meta-analysis showed that the timing of surgery was an important factor in patient survival outcomes, and that the differences in early mortality and improved long-term functional outcomes in ICH patients between different surgical approaches, including open and minimally invasive surgery, were not statistically significant (41). Our study also found no difference between craniotomy and MIPD in improving the early prognosis of ICH patients, but further follow-up and studies are needed for the long-term functional outcome of patients. The ROC curve results showed an AUC of 0.593 for NLR2 and 0.577 for PLR2, which were not particularly satisfactory. However, we combined the admission GCS scores separately and found an AUC of 0.690 and 0.663. In clinical work, it is important to obtain information on the inflammatory response of ICH patients during the disease process, which is easily achieved by detecting dynamic changes in NLR and PLR compared to serial CT examinations. The temporal trend of NLR and PLR allows neurosurgeons to better comprehend the disease course. Additionally, the emergence of peak NLR and PLR values is a reflection of the inflammatory and coagulation response of the body, which occurs independently of infection and therefore obviates the need for unnecessary antibiotic treatment. Moreover, NLR and PLR are essential prognostic indicators that aid neurosurgeons in evaluating ICH patient outcomes. Currently constructed prognostic models for ICH patients rely mainly on clinical information, such as admission GCS score and hematoma volume, ignoring the role of inflammatory indicators in predicting prognosis. We describe the pattern and value of NLR and PLR changes in spontaneous ICH patients after surgery, providing a new idea to explore the prognostic biological indicators of spontaneous ICH.

This study has some limitations. First, it was a small retrospective study with a limited sample size, and a large, multicenter retrospective study should be conducted in the future. Second, we failed to perform a specific stratified analysis of the bleeding site, which may have some limitations, and we will further investigate the specific site of bleeding in future work. Finally, due to the complexity of spontaneous ICH, future studies should focus more on leukocyte subunit immune function.

5. Conclusion

The NLR and PLR in spontaneous ICH patients showed a trend of increasing and then decreasing, reaching a peak within 48 h after surgery. Peak NLR and PLR were risk factors affecting the prognosis of spontaneous ICH patients 30 days after surgery, with peak NLR being an independent risk factor affecting prognosis.

Data availability statement

The original contributions presented in the study are included in the article/supplementary material, further inquiries can be directed to the corresponding author.

Ethics statement

The studies involving human participants were reviewed and approved by the Medical Ethics Review Committee of the Fukuang General Hospital of Liaoning Health Group. The patients/participants provided their written informed consent to participate in this study.

Author contributions

JZ, CL, and YHo conceived and designed the study. JZ, CL, YHu, AY, YZ, and YHo collected and cleaned the data. JZ performed the data analysis and drafted the manuscript. YZ, YHo, YHu, and AY helped revise the manuscript. All authors read and approved the final manuscript.

Funding

This study was funded by the Natural Science Foundation of Liaoning Province (No. 20180530024).

Conflict of interest

The authors declare that the research was conducted in the absence of any commercial or financial relationships that could be construed as a potential conflict of interest.

Publisher's note

References

1. Dias RA, Dias L, Azevedo E, Castro P. Acute inflammation in cerebrovascular disease: a critical reappraisal with focus on human studies. *Life (Basel)*. (2021) 11:1103. doi: 10.3390/life11101103

2. Krishnamurthi RV, Ikeda T, Feigin VL. Global, regional and country-specific burden of Ischaemic stroke, intracerebral Haemorrhage and subarachnoid Haemorrhage: a systematic analysis of the global burden of disease study 2017. *Neuroepidemiology*. (2020) 54:171–9. doi: 10.1159/000506396

3. Lan X, Han X, Li Q, Yang QW, Wang J. Modulators of microglial activation and polarization after intracerebral haemorrhage. *Nat Rev Neurol*. (2017) 13:420–33. doi: 10.1038/nrneurol.2017.69

4. Masomi-Bornwasser J, Kurz E, Frenz C, Schmitt J, Wesp DMA, König J, et al. The influence of oxidative stress on neurological outcomes in spontaneous intracerebral hemorrhage. *Biomol Ther*. (2021) 11:1615. doi: 10.3390/biom11111615

5. Reith FCM, Van den Brande R, Synnot A, Gruen R, Maas AIR. The reliability of the Glasgow coma scale: a systematic review. *Intensive Care Med*. (2016) 42:3–15. doi: 10.1007/s00134-015-4124-3

6. Gong P, Liu Y, Gong Y, Chen G, Zhang X, Wang S, et al. The association of neutrophil to lymphocyte ratio, platelet to lymphocyte ratio, and lymphocyte to monocyte ratio with post-thrombolysis early neurological outcomes in patients with acute ischemic stroke. *J Neuroinflammation*. (2021) 18:51. doi: 10.1186/s12974-021-02090-6

7. Wang R-H, Wen W-X, Jiang Z-P, Du Z-P, Ma Z-H, Lu A-L, et al. The clinical value of neutrophil-to-lymphocyte ratio (NLR), systemic immune-inflammation index (SII), platelet-to-lymphocyte ratio (PLR) and systemic inflammation response index (SIRI) for predicting the occurrence and severity of pneumonia in patients with intracerebral hemorrhage. *Front Immunol*. (2023) 14:1115031. doi: 10.3389/fimmu.2023.1115031

8. Sulhan S, Lyon KA, Shapiro LA, Huang JH. Neuroinflammation and blood-brain barrier disruption following traumatic brain injury: pathophysiology and potential therapeutic targets. *J Neurosci Res*. (2020) 98:19–28. doi: 10.1002/jnr.24331

9. Chen Y, Tian J, Chi B, Zhang S, Wei L, Wang S. Factors associated with the development of coagulopathy after open traumatic brain injury. *J Clin Med*. (2021) 11:185. doi: 10.3390/jcm11010185

10. Lattanzi S, Cagnetti C, Provinciali L, Silvestrini M. Neutrophil-to-lymphocyte ratio predicts the outcome of acute intracerebral hemorrhage. *Stroke*. (2016) 47:1654–7. doi: 10.1161/STROKEAHA.116.013627

11. Shi M, Li XF, Zhang TB, Tang QW, Peng M, Zhao WY. Prognostic role of the neutrophil-to-lymphocyte ratio in intracerebral hemorrhage: a systematic review and Meta-analysis. *Front Neurosci*. (2022) 16:825859. doi: 10.3389/fnins.2022.825859

12. Cordonnier C, Demchuk A, Ziai W, Anderson CS. Intracerebral haemorrhage: current approaches to acute management. *Lancet*. (2018) 392:1257–68. doi: 10.1016/S0140-6736(18)31878-6

13. Magid-Bernstein J, Girard R, Polster S, Srinath A, Romanos S, Awad IA, et al. Cerebral hemorrhage: pathophysiology, treatment, and future directions. *Circ Res*. (2022) 130:1204–29. doi: 10.1161/CIRCRESAHA.121.319949

14. Fu C, Wang N, Chen B, Wang P, Chen H, Liu W, et al. Surgical management of moderate basal Ganglia intracerebral hemorrhage: comparison of safety and efficacy of endoscopic surgery, minimally invasive puncture and drainage, and craniotomy. *World Neurosurg*. (2019) 122:e995–e1001. doi: 10.1016/j.wneu.2018.10.192

15. Powers WJ, Rabinstein AA, Ackerson T, Adeoye OM, Bambakidis NC, Becker K, et al. 2018 guidelines for the early management of patients with acute Ischemic stroke: a guideline for healthcare professionals from the American Heart Association/American Stroke Association. *Stroke*. (2018) 49:e46–e110. doi: 10.1161/STR.0000000000000158

16. Kothari RU, Brott T, Broderick JP, Barsan WG, Sauerbeck LR, Zuccarello M, et al. The ABCs of measuring intracerebral hemorrhage volumes. *Stroke*. (1996) 27:1304–5. doi: 10.1161/01.str.27.8.1304

17. Banks JL, Marotta CA. Outcomes validity and reliability of the modified Rankin scale: implications for stroke clinical trials: a literature review and synthesis. *Stroke*. (2007) 38:1091–6. doi: 10.1161/01.STR.0000258355.23810.c6

18. Zhou Y, Wang Y, Wang J, Anne Stetler R, Yang QW. Inflammation in intracerebral hemorrhage: from mechanisms to clinical translation. *Prog Neurobiol*. (2014) 115:25–44. doi: 10.1016/j.pneurobio.2013.11.003

19. Xu S, Lu J, Shao A, Zhang JH, Zhang J. Glial cells: role of the immune response in ischemic stroke. *Front Immunol*. (2020) 11:294. doi: 10.3389/fimmu.2020.00294

20. Hermann DM, Kleinschnitz C, Gunzer M. Implications of polymorphonuclear neutrophils for ischemic stroke and intracerebral hemorrhage: predictive value, pathophysiological consequences and utility as therapeutic target. *J Neuroimmunol*. (2018) 321:138–43. doi: 10.1016/j.jneuroim.2018.04.015

21. Liesz A, Dalpke A, Mracsko E, Antoine DJ, Roth S, Zhou W, et al. DAMP signaling is a key pathway inducing immune modulation after brain injury. *J Neurosci*. (2015) 35:583–98. doi: 10.1523/JNEUROSCI.2439-14.2015

22. Gong C, Hoff JT, Keep RF. Acute inflammatory reaction following experimental intracerebral hemorrhage in rat. *Brain Res*. (2000) 871:57–65. doi: 10.1016/s0006-8993(00)02427-6

23. Mackenzie JM, Clayton JA. Early cellular events in the penumbra of human spontaneous intracerebral hemorrhage. *J Stroke Cerebrovasc Dis*. (1999) 8:1–8. doi: 10.1016/s1052-3057(99)80032-9

24. Meisel C, Schwab JM, Prass K, Meisel A, Dirnagl U. Central nervous system injury-induced immune deficiency syndrome. *Nat Rev Neurosci*. (2005) 6:775–86. doi: 10.1038/nrn1765

25. Römer C, Engel O, Winek K, Hochmeister S, Zhang T, Royl G, et al. Blocking stroke-induced immunodeficiency increases CNS antigen-specific autoreactivity but does not worsen functional outcome after experimental stroke. *J Neurosci*. (2015) 35:7777–94. doi: 10.1523/JNEUROSCI.1532-14.2015

26. Riojas CM, Ekaney ML, Ross SW, Cunningham KW, Furay EJ, Brown CVR, et al. Platelet dysfunction after traumatic brain injury: a review. *J Neurotrauma*. (2021) 38:819–29. doi: 10.1089/neu.2020.7301

27. Turak O, Özcan F, Işleyen A, Başar FN, Gül M, Yilmaz S, et al. Usefulness of neutrophil-to-lymphocyte ratio to predict in-hospital outcomes in infective endocarditis. *Can J Cardiol*. (2013) 29:1672–8. doi: 10.1016/j.cjca.2013.05.005

28. Fusar-Poli L, Natale A, Amerio A, Cimpoesu P, Grimaldi Filioli P, Aguglia E, et al. Neutrophil-to-lymphocyte, platelet-to-lymphocyte and monocyte-to-lymphocyte ratio in bipolar disorder. *Brain Sci*. (2021) 11:58. doi: 10.3390/brainsci11010058

29. Du Y, Wang A, Zhang J, Zhang X, Li N, Liu X, et al. Association between the neutrophil-to-lymphocyte ratio and adverse clinical prognosis in patients with spontaneous intracerebral hemorrhage. *Neuropsychiatr Dis Treat*. (2022) 18:985–93. doi: 10.2147/NDT.S358078

30. Wang F, Xu F, Quan Y, Wang L, Xia JJ, Jiang TT, et al. Early increase of neutrophil-to-lymphocyte ratio predicts 30-day mortality in patients with spontaneous intracerebral hemorrhage. *CNS Neurosci Ther*. (2019) 25:30–5. doi: 10.1111/cns.12977

31. Zhao Y, Xie Y, Li S, Hu M. The predictive value of neutrophil to lymphocyte ratio on 30-day outcomes in spontaneous intracerebral hemorrhage patients after surgical treatment: a retrospective analysis of 128 patients. *Front Neurol*. (2022) 13:963397. doi: 10.3389/fneur.2022.963397

32. Zhang F, Tao C, Hu X, Qian J, Li X, You C, et al. Association of Neutrophil to lymphocyte ratio on 90-day functional outcome in patients with intracerebral hemorrhage undergoing surgical treatment. *World Neurosurg*. (2018) 119:e956–61. doi: 10.1016/j.wneu.2018.08.010

33. Favas TT, Dev P, Chaurasia RN, Chakravarty K, Mishra R, Joshi D, et al. Neurological manifestations of COVID-19: a systematic review and meta-analysis of proportions. *Neurol Sci*. (2020) 41:3437–70. doi: 10.1007/s10072-020-04801-y

34. Aksu K, Donmez A, Keser G. Inflammation-induced thrombosis: mechanisms, disease associations and management. *Curr Pharm Des*. (2012) 18:1478–93. doi: 10.2174/138161212799504731

35. Branchford BR, Carpenter SL. The role of inflammation in venous thromboembolism. *Front Pediatr*. (2018) 6:142. doi: 10.3389/fped.2018.00142

36. Koupenova M, Clancy L, Corkrey HA, Freedman JE. Circulating platelets as mediators of immunity, inflammation, and thrombosis. *Circ Res*. (2018) 122:337–51. doi: 10.1161/CIRCRESAHA.117.310795

37. Qin B, Ma N, Tang Q, Wei T, Yang M, Fu H, et al. Neutrophil to lymphocyte ratio (NLR) and platelet to lymphocyte ratio (PLR) were useful markers in assessment of inflammatory response and disease activity in SLE patients. *Mod Rheumatol*. (2016) 26:372–6. doi: 10.3109/14397595.2015.1091136

38. Luo S, Yang WS, Shen YQ, Chen P, Zhang SQ, Jia Z, et al. The clinical value of neutrophil-to-lymphocyte ratio, platelet-to-lymphocyte ratio, and D-dimer-to-fibrinogen ratio for predicting pneumonia and poor outcomes in patients with acute intracerebral hemorrhage. *Front Immunol*. (2022) 13:13. doi: 10.3389/fimmu.2022.1037255

39. Chen W, Wang X, Liu F, Tian Y, Chen J, Li G, et al. The predictive role of postoperative neutrophil to lymphocyte ratio for 30-day mortality after intracerebral hematoma evacuation. *World Neurosurg*. (2020) 134:e631–5. doi: 10.1016/j.wneu.2019.10.154

40. Wang G-Q, Li S-Q, Huang Y-H, Zhang W-W, Ruan W-W, Qin J-Z, et al. Can minimally invasive puncture and drainage for hypertensive spontaneous basal ganglia intracerebral hemorrhage improve patient outcome: a prospective non-randomized comparative study. *Mil Med Res*. (2014) 1:1. doi: 10.1186/2054-9369-1-10

41. Sondag L, Schreuder FHBM, Boogaarts HD, Rovers MM, Vandertop WP, Dammers R, et al. Neurosurgical intervention for Supratentorial intracerebral hemorrhage. *Ann Neurol*. (2020) 88:239–50. doi: 10.1002/ana.25732

frontiers | Frontiers in Neurology

TYPE Systematic Review
PUBLISHED 02 June 2023
DOI 10.3389/fneur.2023.1153690

OPEN ACCESS

EDITED BY
Stefania Mondello,
University of Messina, Italy

REVIEWED BY
Vitalie Lisnic,
Nicolae Testemitanu State University of Medicine and Pharmacy, Moldova
José Antonio Monge-Argilés,
Hospital General Universitario Dr. Balmis, ISABIAL, Spain

*CORRESPONDENCE
Carlos Alva-Diaz
✉ alvacarl@crece.uss.edu.pe

RECEIVED 29 January 2023
ACCEPTED 03 May 2023
PUBLISHED 02 June 2023

CITATION
Cabanillas-Lazo M, Quispe-Vicuña C, Cruzalegui-Bazán C, Pascual-Guevara M, Mori-Quispe N and Alva-Diaz C (2023) The neutrophil-to-lymphocyte ratio as a prognostic biomarker in Guillain-Barre syndrome: a systematic review with meta-analysis. *Front. Neurol.* 14:1153690. doi: 10.3389/fneur.2023.1153690

The neutrophil-to-lymphocyte ratio as a prognostic biomarker in Guillain-Barre syndrome: a systematic review with meta-analysis

Miguel Cabanillas-Lazo[1,2,3], Carlos Quispe-Vicuña[1,2,3], Claudia Cruzalegui-Bazán[1,2,3], Milagros Pascual-Guevara[1,2,3], Nicanor Mori-Quispe[4] and Carlos Alva-Diaz[1,4,5]*

[1]Red de Eficacia Clínica y Sanitaria (REDECS), Lima, Peru, [2]Sociedad Científica de San Fernando, Lima, Peru, [3]Facultad de Medicina, Universidad Nacional Mayor de San Marcos, Lima, Peru, [4]Servicio de Neurología, Departament de Medicina y Oficina de Apoyo a la Docencia e Investigación (OADI), Hospital Daniel Alcides Carrión, Callao, Peru, [5]Universidad Señor de Sipán, Chiclayo, Peru

Background and objectives: Guillain-Barre syndrome (GBS) is an immune-mediated neuropathy. This has raised the possibility that the neutrophil-lymphocyte ratio (NLR) may be a biomarker of its activity. We conducted a systematic review and meta-analysis to summarize the evidence of NLR as a potential biomarker for GBS.

Methods: We systematically searched databases (PubMed, Ovid-Medline, Embase, Scopus, Web of Science, SciELO Citation Index, LILACS, and Google Scholar) until October 2021 for studies evaluating pre-treatment NLR values in GBS patients. A meta-analysis using a random-effects model to estimate pooled effects was realized for each outcome and a narrative synthesis when this was not possible. Subgroup and sensitivity analysis were realized. GRADE criteria were used to identify the certainty of evidence for each result.

Results: Ten studies from 745 originally included were selected. Regarding GBS patients versus healthy controls, a meta-analysis of six studies (968 patients) demonstrated a significant increase in NLR values in GBS patients (MD: 1.76; 95% CI: 1.29, 2.24; I2 = 86%) with moderate certainty due to heterogeneity of GBS diagnosis criteria used. Regarding GBS prognosis, assessed by Hughes Score $\geq$ 3, NLR had a sensitivity between 67.3 and 81.5 and a specificity between 67.3 and 87.5 with low certainty due to imprecision, and heterogeneity. In relation to respiratory failure, NLR had a sensitivity of 86.5 and specificity of 68.2 with high and moderate certainty, respectively.

Discussion: With moderate certainty, mean NLR is higher in GBS patients compared to healthy controls. Furthermore, we found that NLR could be a prognostic factor for disability and respiratory failure with low and moderate certainty, respectively. These results may prove useful for NLR in GBS patients; however, further research is needed.

Systematic review registration: https://www.crd.york.ac.uk/PROSPERO/, identifier: CRD42021285212.

KEYWORDS

Guillain-Barre syndrome, NLR, neutrophil to lymphocyte ratio, diagnosis, prognosis

1. Introduction

Guillain-Barre syndrome (GBS), an immune-mediated peripheral neuropathy, is the most common cause of acute flaccid paralysis and is characterized by rapidly progressive weakness or sensory loss usually followed by slow clinical recovery (1). The annual global incidence rate is 1–2 cases per 100,000 people per year (2). The global prevalence of GBS has shown an increase of 6.4% from 1990 to 2019, reporting in the latter year, more than 150,000 cases and more than 44 000 years lived with disability (YLD) (3). Also, Asia and Central and South America are the regions with the highest frequency (30–65%) of the axonal subtype of GBS which is the most severe subtype of the disease (4). In addition, death or severe disability results in almost 20% of patients despite adequate treatment (5).

The most frequent risk factor of GBS is gastrointestinal and respiratory infection (6), which generates a cellular and humoral response by T and B cells. The latter induces an antiganglioside antibody response that crosses the blood-nerve barrier and activate the complement. Likewise, T-cell activation leads to cytokine release, Schwann cell damage and myelin destruction (7). This mechanism results in axonal degeneration of motor and sensory fibers of cranial and peripheral nerves (1). This is known as "molecular mimicry autoimmunity."

Despite that the role of the neutrophil in GBS pathophysiology is not well understood, several investigations suggest the neutrophil-to-lymphocyte ratio (NLR) as a possible index of immune function, since the systemic inflammation generated by the disease usually results in neutrophilia and lymphocytopenia (1, 6–8).

Although the diagnosis of GBS is mainly based on a combination of clinical criteria, cerebrospinal fluid (CSF) analysis and nerve conduction studies (Brighton criteria); some criteria are not present in early stages of the disease, such as cytological albumin dissolution (after the first week) or alterations in neuroconduction studies (after the second week) (9). This has led to the search for biomarkers to establish a rapid and accurate diagnosis, using serum, peripheral nervous tissue and CSF as the main sources.

Despite all this, there is a lack of accessible and reliable biomarkers of systemic inflammation in neurology, which could provide information to differentiate or predict GBS activity (10–12). The neutrophil-to-lymphocyte ratio (NLR) is calculated from the white blood cell count and is a new biomarker used in neurological diseases such as autoimmume encephalitis and multiple sclerosis (8, 13). Even now, it's part of routine blood tests and is therefore available for research as possible alternatives. So, the importance of NLR lies of its performance, its low cost, its availability in routine examinations and its easy acceptance by physicians and patients.

NLR is more reflective of systemic inflammation compared to other leukocyte subtypes, is easier to obtain by blood test, and is stable and reliable (14). Given that the prognosis of GBS is not fully elucidated, NLR could be an accessible prognostic factor of GBS activity and severity. For those reasons, this systematic review summarizes current knowledge about the potential of NLR as a biomarker in GBS.

2. Methods

This systematic review was reported according to the Preferred Reporting Items for Systematic Reviews and Meta-Analyses (PRISMA) (15). The study protocol was registered in PROSPERO with the code CRD42021285212.

2.1. Data sources

We searched in PubMed, Ovid-Medline, Embase, Scopus, Web of Science, SciELO Citation Index, LILACS and Google Scholar until October 2021. The search strategy is detailed in Supplementary Table 1. There were no restrictions on language or publication date. We completed the search by reviewing the bibliographic references of the included studies and selecting the articles that met the requirements.

2.2. Eligibility criteria

Studies were included if they met the following criteria: (1) Analytical observational studies (cross-sectional, case-control and cohort studies); (2) Studies included adult participants (aged > 18 years old) and (3) NLR values assessed at pre-treatment period in GBS patients. We excluded narrative and systematic reviews, studies in non-humans, case reports, conference abstracts and letters.

2.3. Study selection

Results from electronic searches were exported to Endnote X9 and duplicate documents were removed. After, two reviewers (CCB and MPG) performed a peer review process using Rayyan QCRI (https://rayyan.qcri.org/) for the selection of articles according to the inclusion criteria and then reading the full text. Any discrepancies were resolved by consensus or a third author (CAD). The complete list of excluded articles is provided in Supplementary Table 2.

2.4. Outcomes

Our outcomes were (1) Assessment of NLR comparing GBS patients with healthy control subjects (NLR is the biochemical parameter calculated by dividing the absolute neutrophil count by the absolute lymphocyte count); and (2) Assessment of NLR comparing GBS mild and severe, which was assessed with at least one of the following from discharge: (a) Hughes's score (16) using a scale from 0 to 6 ranging from no symptoms to death, (b) Medical Research Council (MRC) scale (17) using a scale from 0 to 5 ranging from no visible contraction to active movement against full resistance, or (c) respiratory failure.

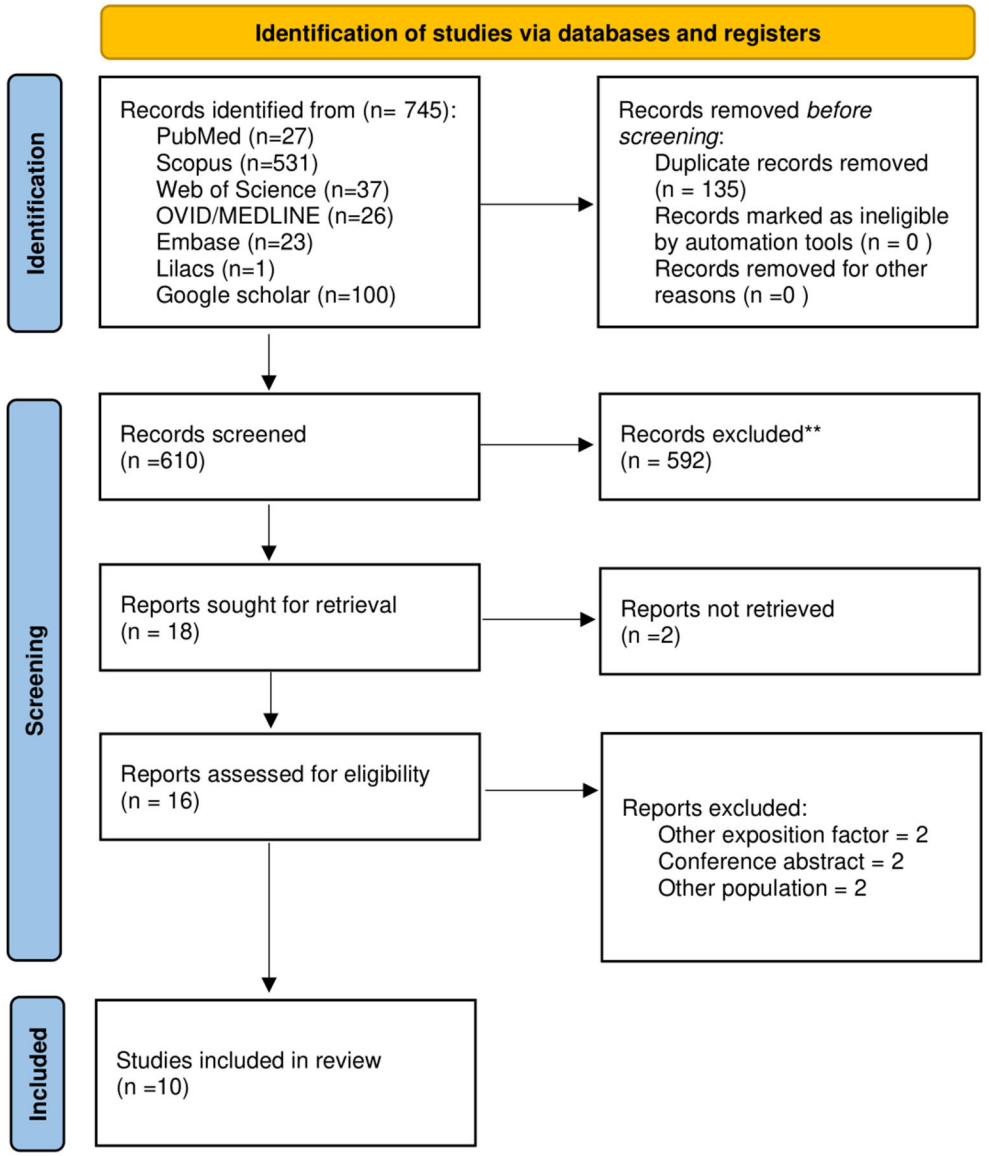

FIGURE 1
PRISMA flowchart of included studies.

2.5. Data extraction

Two authors (CCB and MPG) independently carried out information using a data extraction form and any disagreements were resolved by consensus and ultimately a third author (CAD). We extracted the following information: title of the study, first author, year of publication, study design, country where the study was performed, number of participants, sex, age, sample time, criteria for diagnosis of GBS, mean or median NLR according to sample stratification, follow-up crude and adjusted association measures, type of outcome and its definition. We contacted the corresponding author through email if additional data was needed.

2.6. Risk of bias assessment

The quality of the studies was assessed with the Newcastle Ottawa Scale (18) by two authors (MCL and CQV) and any discrepancies were resolved by consensus. This tool evaluates the quality of published observational studies and is based on three items: selection, comparability, and outcome/exposure. Each item has sub-items, on which a star-based score was assigned. Studies with scores ≥ 6 were considered as having a low risk of bias (high quality), scores of 4–5 as having a moderate risk of bias, and scores < 4 as having a high risk of bias (19). If the studies had a double design (cases and controls, cohorts), the design was considered according to the main objective of the study.

TABLE 1 Characteristics of included studies evaluating the clinical significance of neutrophil-to-lymphocyte ratio (NLR) in Guillain-Barré syndrome (GBS) ($n = 10$).

Study-ID	Country	Study design	GBS diagnostic criteria	N GBS	N Controls	Match GBS-control	Characteristics of the GBS population: age (years) mean	Blood sample time	Follow-up
Bedel et al. (20)	Turkey	Case-control	Asbury (1990)	98	101	NR	Male (%): 63.3 Age: 55.02 (17.4)*	Admission	NR
Ethemoglu and Calik (21)	Turkey	Retrospective cohort and Case-control	NR	68	63	Age	Male (%): NR Age: 48.5 (19.0)*	Day post admission	3 months
Geyik et al. (22)	Turkey	Retrospective cohort and Case-control	Asbury (1990)	94	101	Age Gender	Male (%): 66 Age: 48.7 (20.6)*	Admission	1 month
Hashim et al. (23)	Egypt	Prospective Cohort and Case-control	Asbury (1990)	35	40	Age Gender	Male (%): 42.9 Age: 32.29 (13.4)*	Admission	1 month
Huang et al. (24)	China	Retrospective cohort and Case-control	Dutch Neuromuscular Research Support consensus (2001)	117	217	Age Gender	Male (%): 62.4 Age: 49.36 (16.9)*	Day post admission	2 months
Gümüşyayla and Vural (25)	Turkey	Retrospective cohort and Case-control	NR	50	49	NR	Male (%): NR Age: 52.8 (17.0)*	Day post admission	3 months
Sahin et al. (26)	Turkey	Retrospective cohort	Asbury (1990)	24	NR	NR	Male (%): NR Age: 41 (16.0)*	Admission	6 months
Tunç (27)	Turkey	Retrospective cohort	Asbury (1990)	81	NR	NR	Male (%): 54.3 Age: 52.3 (18.4)*	Day post admission	1 month
Ning et al. (28)	China	Retrospective cohort	Asbury (1990)	426	NR	NR	Male (%): 59.6 Age: 49.5 (4.7)*	Admission	NR
Ozdemir (6)	Turkey	Retrospective cohort	Brighton (2011)	62	NR	NR	Male (%): 58.1 Age: 48.0 (19.9)*	Admission	Discharge

*Mean (standard deviation). NR, not reported.

10.3389/fneur.2023.1153690

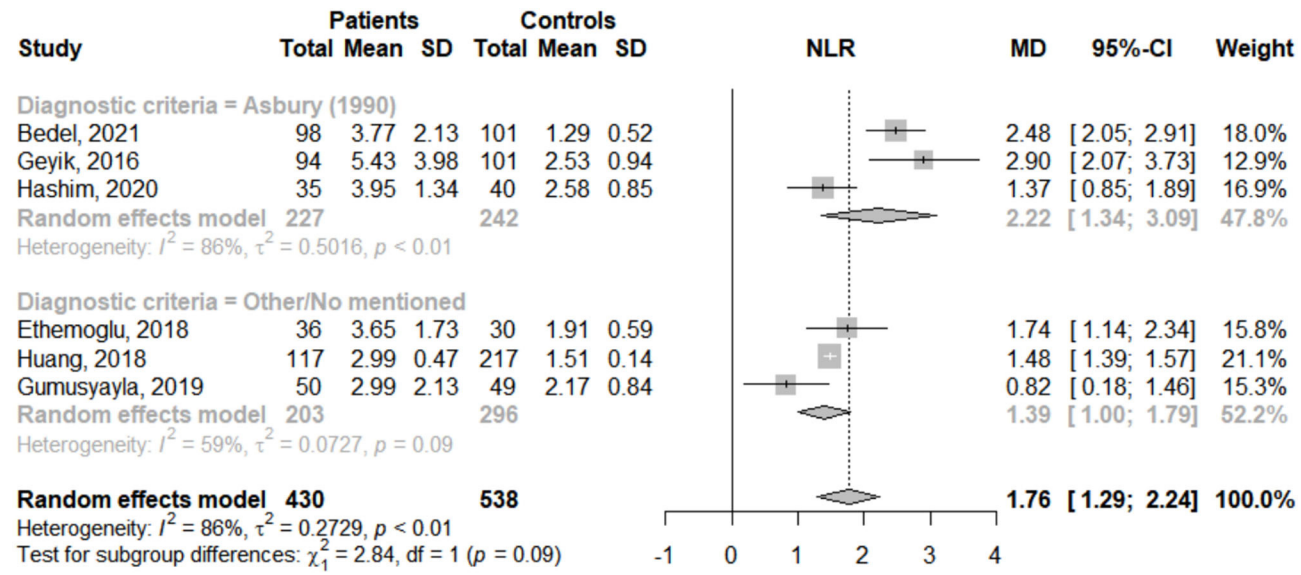

FIGURE 2
Mean difference of neutrophil-to-lymphocyte ratio (NLR) between GBS patients and healthy controls according to reported diagnostic criteria.

2.7. Statistical analysis

A meta-analysis was planned for each outcome; however, when this was not possible due to unavailable data, narrative synthesis was performed. Meta-analyses were performed using the inverse variance method and the randomized effects model. The variance between studies ($\tau 2$) was estimated using the DerSimonian-Laird method. Mean differences (MD) with their 95% confidence intervals (CI 95%) were pooled if the studies had a confounder control. Heterogeneity between studies was assessed using the I^2 statistic. Heterogeneity was defined as low if I^2 < 30%, moderate if I^2 = 30–60%, and high if I^2 > 60%. The metacont function of the meta-package in R 4.1.0 was used (www.r-project.org).

We performed subgroup analyses by reported diagnostic criteria. Finally, we performed a leave-one-out sensitivity analysis, and other only including studies with case-control matches.

2.8. Evidence certainty assessment

Two authors (CQV and CCB) assessed the certainty of our pooled results and narrative synthesis applying the Grading of Recommendation, Assessment, Development, and Evaluation (GRADE) on continuous outcomes (29) and narrative synthesis (30), respectively. This assessment is based on five domains: study limitations (risk of bias of the studies included), imprecision (sample size and confidence interval), indirectness (generalizability), inconsistency (heterogeneity), and publication bias as stated in the GRADE handbook (31) and prognostic factor (32). We adapted the assessment to our results. The certainty of the evidence was characterized as high, moderate, low, or very low.

2.9. Ethical considerations

This systematic review included published and open information in which no human subjects participated. Thus, no ethics committee approval was required.

3. Results

3.1. Study selection

We identified 745 studies through our systematic search. We removed duplicated and screened 610. Finally, 10 articles (6, 20–28) were included (Figure 1).

3.2. Characteristics of studies

Five studies (21–25) included both cohort and case-control designs, four (6, 26–28) included only retrospective cohorts and one (20) was a case-control study. The total number of participants was 1,626 (1,055 GBS patients and 571 healthy controls). The average age range of GBS patients was between 32.3 and 55.0. The studies characteristics are summarized in Table 1.

3.3. GBS patients and healthy controls

Among the ten studies that met our inclusion criteria, six (20–25) were pooled. A total of 968 participants were selected, of which 430 were assigned to the GBS group and 538 to the control group. In the pooled analysis, a significant increase in NLR was observed in GBS vs. control groups but with high heterogeneity (MD: 1.76; 95% CI: 1.29; 2.24; I^2 = 86%) (Figure 2).

TABLE 2 Characteristics of included studies evaluating the use of neutrophil-to-lymphocyte ratio (NLR) as a prognosis factor of Guillain-Barré syndrome (GBS) patients ($n = 9$).

Study-ID	Number of analized patients	Outcome	NLR mean (SD) in poor outcome	NLR mean (SD) in good outcome	Correlation NLR-Hughes	NLR cutoff	Sensitivity (%)	Specificity (%)	Area under the curve (AUC)	Follow-up
Geyik et al. (22)	94	Response to plasmapheresis†	9.10 (3.89)	4.67 (3.57)	0.36*	NR	NR	NR	NR	1 month after discharge
Hashim et al. (23)	35	Hughes score ≥ 3	5.11 (1.78)	3.60 (1.18)	0.55*	4.40	81.5	87.5	0.85	1 month after admission
Huang et al. (24)	117	Hughes score ≥ 3	3.37 (0.83)	2.34 (0.45)	NR	3.05	67.3	67.3	0.72	2 months after admission
Ethemoglu and Calik (21)	36	Hughes score ≥3	2.92 (1.69)	4.38 (1.49)	NR	NR	NR	NR	NR	At discharge
Gümüşyayla and Vural (25)	50	Hughes score	NR	NR	0.36**	NR	NR	NR	NR	3 months after admission
Tunç (27)	81	Hughes score	NR	NR	0.23*	NR	NR	NR	NR	1 month after admission
Ning et al. (28)	426	Respiratory failure	6.69 (1.19)	2.70 (0.43)	NR	3.5	86.5	68.2	0.79	NR
Sahin et al. (26)	24	MRC sum score	NR	NR	0.007¥**	NR	NR	NR	NR	6 months after admission
Ozdemir (6)	62	Hughes score	NR	NR	NR††	NR	NR	NR	NR	At discharge

SD, Standard deviation; NR, Not reported; MRC, Medical Research Council. *Pearson r, **Spearman rho. †Outcome not specified; ††Correlation r no specified but described as not significant; ¥Correlation between NLR and MRC2st score.

10.3389/fneur.2023.1153690

TABLE 3 Summary of findings.

Outcome	No. of participants (studies)	Certainty of the evidence (GRADE)	Anticipated absolute effects	95% CI
			Mean difference (MD)	
Mean difference between GBS patients and healthy participants	968 (6 observational studies)	⨁⨁⨁◯ Moderate[a]	1.76	1.29–2.24
Sensitivity for prognosis Hughes's score ≥ 3	152 (2 observational studies)	⨁⨁◯◯ Low[b,c]	The studies showed a sensitivity of 67.3 to 81.5 for prognosis in GBS patients.	
Specificity for prognosis Hughes's score ≥ 3	152 (2 observational studies)	⨁⨁◯◯ Low[b,c]	The studies showed a specificity of 67.3 to 87.5 for prognosis in GBS patients	
Sensitivity for prognosis Respiratory failure	426 (1 observational study)	⨁⨁⨁⨁ High	The study showed a sensitivity of 86.5 of the NLR for predicting respiratory failure in GBS patients.	
Specificity for prognosis Respiratory failure	426 (1 observational study)	⨁⨁⨁◯ Moderate[c]	The study showed a specificity of 68.2 of the NLR for predicting respiratory failure in GBS patients.	

CI, confidence interval; MD, mean difference. GRADE Working Group grades of evidence: High certainty, we are very confident that the true effect lies close to that of the estimate of the effect. Moderate certainty, we are moderately confident in the effect estimate: the true effect is likely to be close to the estimate of the effect, but there is a possibility that it is substantially different. Low certainty, our confidence in the effect estimate is limited: the true effect may be substantially different from the estimate of the effect. Very low certainty, we have very little confidence in the effect estimate: the true effect is likely to be substantially different from the estimate of effect. [a]High inconsistency was detected in meta-analyses. The calculated I^2 was >60%. [b]Inconsistency: values of studies are heterogeneous among themselves. [c]Imprecision due to confidence interval <70% in one study.

To identify potential sources of heterogeneity, subgroup analysis was performed according to reported diagnostic criteria. NLR was significantly higher in GBS patients compared to healthy controls regardless of whether GBS was diagnosed with Asbury criteria (MD: 2.22; 95% CI: 1.34; 3.09; $I^2 = 86\%$) or other/no mentioned (MD: 1.39; 95% CI: 1.00; 1.79; $I^2 = 59\%$) (Figure 2). In addition, heterogeneity was high among studies that used the Asbury criteria and moderate in those that used other/no mentioned.

Regarding sensitive analysis, when single studies were sequentially removed, no significant effect on the pooled MD was observed, with an effect size ranging from 1.59 to 1.94 and I^2 ranged from 76 to 89 (Supplementary Table 3). Additionally, when studies without case-control match were excluded, no significant effect was described (MD: 1.75; 95% CI: 1.29; 2.21; $I^2 = 75\%$). These suggest that the results estimated by meta-analysis were stable (Supplementary Table 4).

3.4. GBS mild and severe

Nine studies (6, 21–28) (925 GBS patients) assessed NLR as a poor prognostic factor. Only three reported sensitivity and specificity. Regarding prognosis of disability (Hughes ≥ 3), Hashim et al. (23) included 35 patients whose cut-off point was 4.4 with a sensitivity of 81.5% and specificity of 87.5%, Huang et al. (24) included 117 participants whose cut-off point was 3.05 with a sensitivity of 67.3% and specificity of 67.3% (Table 2).

3.5. Respiratory failure

For the respiratory failure outcome, only one large-size study reported this. Ning et al. (28) included 426 patients whose cut-off point was 3.5 with a sensitivity of 86.5% and a specificity of 68.2% (Table 2).

3.6. Risk-of-bias assessment

We performed the risk of bias of the ten included studies. Eight articles had "low risk of bias." Among the cohort studies, Gümüşyayla et al. (25) scored the lowest for deficiencies in the comparability domain, while Ning et al. (28), Huang et al. (24), and Ethemoglu et al. (21) scored the highest. The only case-control design considered for risk of bias assessment (20) scored 6/9 for deficiencies in information response rate and the selection of controls (Supplementary Table 5).

3.7. Evidence certainty

Regarding GBS patients and healthy controls, we judged the certainty of the included evidence as moderate. We started the evaluation from high certainty because we included observational studies (comparative observational design). We downgraded according to the high heterogeneity between the studies ($I^2 = 86\%$) (Table 3). About the severity and respiratory failure outcome, we started the assessment from high certainty because all included studies were observational studies (cohort design). For severity, Hughes's score ≥ 3 had a low certainty for sensitivity and specificity, downgraded according to inconsistency due to high heterogeneity (studies showed a sensitivity of 67.3 to 81.5 and specificity of 67.3 to 87.5) and imprecision (sensitivity and specificity crossed through the imprecision point of 70%). For respiratory failure, was assessed as moderate and high certainty to specificity and sensitivity, respectively, downgraded according to imprecision (specificity crossed through the imprecision point of 70%).

4. Discussion

4.1. Summary of main results

Our results revealed a higher mean NLR in GBS patients compared to healthy controls. Furthermore, we found that NLR could be a prognostic factor for disability and respiratory failure.

4.2. NLR in GBS patients vs. healthy controls

Our pooled analysis showed that mean NLR was significantly higher in GBS patients than in healthy patients. These results were not altered by any study or by studies reporting case-control matching as our sensitivity analysis demonstrates. This agrees with previous reviews that evaluated the NLR in other autoimmune diseases. Olsson et al. (8) evaluated 4 case-control studies and found that the NLR was higher in patients with MS than in healthy controls. Similarly, Paliogiannis et al. (33) reported that a meta-analysis of 12 studies showed a higher values NLR (SMD = 0.69, 95% CI 0.53–1.85, $p < 0.001$) in patients with psoriasis than in healthy patients. In turn, Erre et al. (34) and Ma et al. (35) reported similar results for rheumatoid arthritis (SMD = 0.79, 95% CI 0.55–1.03; $p < 0.001$) and systemic lupus erythematosus (SMD = 1.004, 95% CI = 0.781–1.227, $P < 0.001$), respectively. This would show that high NLR values could differentiate between autoimmune diseases and healthy persons. The biological mechanism that would explain these relationship between NLR and GBS, is the increase of immune cells such as neutrophils, macrophages, dendritic cells and T cells in response to peripheral nerve injury (36).

4.3. NLR as prognostic factor in GBS patients

Despite its importance and novelty, the presence of systematic reviews about NLR and its prognosis in neurological diseases, specifically autoimmune diseases, is limited. Olsson et al. (8) reported five studies that evaluated NLR as a prognostic factor in multiple sclerosis. Among these, one reported that high NLR (>3.9) was an independent predictor of disability progression ($p = 0.001$). Also, Guzel et al. (37) reported that a cut-off point of 4.52 (sensitivity: 96.1%; specificity: 57.1%) in multiple sclerosis patients have a discriminatory capacity for disability [Expanded Disability Status Scale (EDSS) $\geq$ 5]. These results were similar to our results in patients with GBS where the cut-off points were 4.40 (sensitivity: 81.5%; specificity: 87.5%) and 3.05 (sensitivity: 67.3%; specificity: 67.3%) for disability (Hughes $\geq$ 3). This is also supported by an observational study in which 34 patients with autoimmune encephalitis presented a cut-off value of 4.82 (sensitivity: 78%; specificity: 88%) to predict severity defined as Modified Rankin Scale (mRS) score > 3 (13). This can be explained by the presence of serum low-density neutrophils (LDN), which are immature and degranulated cells with immunomodulatory capacity that are prematurely mobilized from the bone marrow (38, 39). These LDNs secrete higher levels of proinflammatory cytokines, including interleukin 10 and interferon 21 (40). Levels of this cell type have been correlated with poor prognosis in patients with GBS (41). However, despite the findings, the pathological levels of NLR for different diseases have not yet been standardized, with a possible range of normality being between 0.78 and 3.53 (42).

Otherwise, one of our included studies also evaluated the ability of NLR to predict respiratory failure in patients with GBS with a cut-off point of 3.5 (sensitivity: 86.5%; specificity: 68.2%). According to Moisa et.al. (43), NLR with a cut-off point > 2 was found to predict the need for mechanical ventilation and >11 for mortality at 48 h after admission to ICU in patients with severe or critical pneumonia due to COVID-19. Nair et al. (44) also reported a cut-off point of 4.6 (sensitivity: 79.2%; specificity: 62.3%) for ventilatory assistance 24 h after admission to ICU, which is supported by an SR where the NLR cut-off points ranged from 3.3 to 5.9 predicted a severe COVID-19 condition defined as present respiratory failure (45). As mentioned above, the correlation between NLR and a worse prognosis in GBS could be because neutrophils are one of the first lines of response to peripheral nerve injury so it proliferates within the first hours of trauma (46). This would make the NLR more susceptible to any poor prognosis with respect to other biomarkers.

4.4. Recommendations for future research

According to GRADE approach, the certainty of evidence from the NLR was moderate in GBS patients vs. healthy controls due to high heterogeneity between studies. In our subgroup analysis by GBS diagnostic criteria, it was possible to observe differences in effect size and heterogeneity. This aspects should be expanded in future studies, in addition to taking into account the Brighton criteria (47), since only one study reported using them (6). Finally, we recommend conducting studies that use the NLR for the differential diagnosis of other polyneuropathies (chronic inflammatory demyelinating polyradiculoneuropathy, metabolic diseases, toxicity, others).

Certainty for sensitivity and specificity for poor prognosis (Hughes $\geq$ 3) was low due to heterogeneity and imprecision. Therefore, prospective studies with long-term follow-up are needed to determine optimal cut-off point taking into account the different prognosis of axonal and demyelinating GBS (48, 49). In addition, since majority of included studies was realized in one country (Turkey), it is recommended to analyze the NLR in different GBS populations due there are variations in clinical patterns and severity between Europe/America and Asia (50). On the other hand, the modified Erasmus GBS Outcome Score (mEGOS) is a validated tool that predicts short- and long-term disability with clinical variables that are easy to obtain at admission (51), so the NLR could be added to that tool for better prognostic accuracy. Regarding the prognosis of respiratory failure, the evidence was moderate based on a single large size cohort; however, there are no data about the time in which this failure will be established so more studies are recommended to evaluate the NLR as a prognostic of early requirement of mechanic ventilation. Like mEGOS, there is a validated tool that predicts respiratory failure (EGRIS) based on three simple variables (52, 53), so NLR could also be a biomarker to take into account due to its similar characteristics.

4.5. Clinical applicability

NLR is not only an indicator of systemic inflammation but can also serve as an early warning of a pathological state or process (54). For neurological diseases, it has demonstrated clinical utility in assessing the activity or prognosis of diseases such as multiple sclerosis (8). Our results show that the NLR was significantly higher in GBS patients with respect to healthy patients and that, in turn, it was also a poor prognostic factor. The early identification of GBS patients with poor prognosis could benefit them since they can be treated with different doses, although this is not yet conclusive (55, 56). In addition, determine who will have respiratory failure may allow early intubation and reduce the risk of early-onset pneumonia (57). Several biomarkers associated with GBS such as cerebrospinal lipids (58) or IL-8 have been reported to differentiate GBS from chronic inflammatory demyelinating polyneuropathy (CIDP) (59).However, the clinical importance of NLR lies in the simplicity of its performance, its low cost, its availability in routine examinations and its easy acceptance by physicians and patients. Therefore, if its role is confirmed with more and better studies, it should be recommended for its diagnostic and prognostic application.

4.6. Limitations and strengths

There are some limitations to this systematic review. First, most of the studies were retrospective in nature, so their results could be prone to confounding. In addition, most on the included studies were realized in only one country (Turkey) so it's necessary to analyze the NLR values of other GBS patients from different parts of the world, to seek for variations in clinical patterns and severity. Also, there was significant heterogeneity among the included articles in our meta-analysis. However, our results were strengthened by sensitivity analyzes performed. Our study also has strengths. This is the first systematic review that evaluates the clinical significance of NLR in the diagnosis and prognosis of GBS. Second, we conducted a comprehensive systematic search without language or time restrictions. Finally, we performed an assessment of the certainty of our results using the GRADE criteria.

4.7. Conclusions

Based on the evidence available, with moderate certainty, mean NLR is higher in GBS patients compared to healthy controls. Furthermore, with low and moderate certainty, we found that NLR could be a prognostic factor for disability and respiratory failure, respectively. Future prospective studies in different regions with long-term follow-up are required to determine optimal cut-off values considering the possibility of including NLR in validated prognostic tools.

Data availability statement

The original contributions presented in the study are included in the article/Supplementary material, further inquiries can be directed to the corresponding author.

Author contributions

MC-L: drafting/revision of the manuscript for content, including medical writing for content, study concept or design, and analysis or interpretation of data. CQ-V and CA-D: drafting/revision of the manuscript for content, including medical writing for content, major role in the acquisition of data, and study concept or design. CC-B, MP-G, and NM-Q: drafting/revision of the manuscript for content, including medical writing for content, and major role in the acquisition of data. All authors contributed to the article and approved the submitted version.

Conflict of interest

The authors declare that the research was conducted in the absence of any commercial or financial relationships that could be construed as a potential conflict of interest.

Publisher's note

Supplementary material

The Supplementary Material for this article can be found online at: https://www.frontiersin.org/articles/10.3389/fneur.2023.1153690/full#supplementary-material

References

1. van den Berg B, Walgaard C, Drenthen J, Fokke C, Jacobs BC, van Doorn PA. Guillain-Barré syndrome: pathogenesis, diagnosis, treatment and prognosis. *Nat Rev Neurol.* (2014) 10:469–82. doi: 10.1038/nrneurol.2014.121

2. Sejvar JJ, Baughman AL, Wise M, Morgan OW. Population incidence of Guillain-Barré syndrome: a systematic review and meta-analysis. *Neuroepidemiology.* (2011) 36:123–33. doi: 10.1159/000324710

3. Bragazzi NL, Kolahi AA, Nejadghaderi SA, Lochner P, Brigo F, Naldi A, et al. Global, regional, and national burden of Guillain-Barré syndrome and its underlying causes from 1990 to 2019. *J Neuroinflammation.* (2021) 18:264. doi: 10.1186/s12974-021-02319-4

4. Kuwabara S, Yuki N. Axonal guillain-barré syndrome: concepts and controversies. *Lancet Neurol.* (2013) 12:1180–8. doi: 10.1016/S1474-4422(13)70215-1

5. Jasti AK, Selmi C, Sarmiento-Monroy JC, Vega DA, Anaya JM, Gershwin ME. Guillain-Barré syndrome: causes, immunopathogenic mechanisms and treatment. *Expert Rev Clin Immunol.* (2016) 12:1175–89. doi: 10.1080/1744666X.2016.1193006

6. Ozdemir HH. Analysis of the albumin level, neutrophil-lymphocyte ratio, and platelet-lymphocyte ratio in Guillain-Barré syndrome. *Arq Neuropsiquiatr.* (2016) 74:718–22. doi: 10.1590/0004-282X20160132

7. Rodríguez Y, Rojas M, Pacheco Y, Acosta-Ampudia Y, Ramírez-Santana C, Monsalve DM, et al. Guillain-barré syndrome, transverse myelitis and infectious diseases. *Cell Mol Immunol.* (2018) 15:547–62. doi: 10.1038/cmi.2017.142

8. Olsson A, Gustavsen S, Gisselø Lauridsen K, Chenoufi Hasselbalch I, Sellebjerg F, Bach Søndergaard H, et al. Neutrophil-to-lymphocyte ratio and CRP as biomarkers in multiple sclerosis: a systematic review. *Acta Neurol Scand.* (2021) 143:577–86. doi: 10.1111/ane.13401

9. Leonhard SE, Mandarakas MR, Gondim FAA, Bateman K, Ferreira MLB, Cornblath DR, et al. Diagnosis and management of guillain-barré syndrome in ten steps. *Nat Rev Neurol.* (2019) 15:671–83. doi: 10.1038/s41582-019-0250-9

10. Mayeux R. Biomarkers: potential uses and limitations. *NeuroRx.* (2004) 1:182–8. doi: 10.1602/neurorx.1.2.182

11. Mondello S, Salama MM, Mohamed WMY, Kobeissy FH. Editorial: biomarkers in Neurology. *Front Neurol.* (2020) 11:190. doi: 10.3389/fneur.2020.00190

12. Ballman KV. Biomarker: predictive or prognostic? *J Clin Oncol.* (2015) 33:3968–71. doi: 10.1200/JCO.2015.63.3651

13. Zeng Z, Wang C, Wang B, Wang N, Yang Y, Guo S, et al. Prediction of neutrophil-to-lymphocyte ratio in the diagnosis and progression of autoimmune encephalitis. *Neurosci Lett.* (2019) 694:129–35. doi: 10.1016/j.neulet.2018.12.003

14. Ji Z, Liu G, Guo J, Zhang R, Su Y, Carvalho A, et al. The neutrophil-to-lymphocyte ratio is an important indicator predicting in-hospital death in AMI patients. *Front Cardiovasc Med.* (2021) 8:706852. doi: 10.3389/fcvm.2021.706852

15. Page MJ, McKenzie JE, Bossuyt PM, Boutron I, Hoffmann TC, Mulrow CD, et al. The PRISMA 2020 statement: an updated guideline for reporting systematic reviews. *BMJ.* (2021) 372:n71. doi: 10.1136/bmj.n71

16. Hughes RA, Newsom-Davis JM, Perkin GD, Pierce JM. Controlled trial prednisolone in acute polyneuropathy. *Lancet.* (1978) 2:750–3. doi: 10.1016/S0140-6736(78)92644-2

17. van Koningsveld R, Steyerberg EW, Hughes RA, Swan AV, van Doorn PA, Jacobs BC, et al. clinical prognostic scoring system for Guillain-Barré syndrome. *Lancet Neurol.* (2007) 6:589–94. doi: 10.1016/S1474-4422(07)70130-8

18. Mendoza-Chuctaya G, Montesinos-Segura R, Agramonte-Vilca M, Aguirre-Tenorio L. Características y prevalencia de partos domiciliarios en un distrito rural de la sierra del perú, 2015-2016. *Rev Chil Obstet Ginecol.* (2018) 83:377–85. doi: 10.4067/s0717-75262018000400377

19. Ulloque-Badaracco JR, Ivan Salas-Tello W, Al-Kassab-Córdova A, Alarcón-Braga EA, Benites-Zapata VA, Maguiña JL, et al. Prognostic value of neutrophil-to-lymphocyte ratio in COVID-19 patients: a systematic review and meta-analysis. *Int J Clin Pract.* (2021) 75:e14596. doi: 10.1111/ijcp.14596

20. Bedel C, Korkut M, Hospital R. The clinical significance of neutrophil lymphocyte ratio, monocyte lymphocyte ratio and platelet lymphocyte ratio in patients with guillain-barré syndrome. *Haydarpaşa Numune Med J.* (2021) 61:341–5. doi: 10.14744/hnhj.2019.38233

21. Ethemoglu O, Calik M. Effect of serum inflammatory markers on the prognosis of adult and pediatric patients with Guillain-Barré syndrome. *Neuropsychiatr Dis Treat.* (2018) 14:1255–60. doi: 10.2147/NDT.S162896

22. Geyik S, Bozkurt H, Neyal M, Yigiter R, Kuzudisli S, Kul S, et al. The clinical significance of the neutrophil-to-lymphocyte ratio in patients with Guillain-Barré syndrome independent of infection. *Med Sci Discov.* (2016) 3:305–11. doi: 10.17546/msd.90383

23. Hashim NA, Mohamed WS, Emad EM. Neutrophil–lymphocyte ratio and response to plasmapheresis in Guillain–Barré syndrome: a prospective observational study. *Egypt J Neurol Psychiatry Neurosurg.* (2020) 56:17. doi: 10.1186/s41983-020-0154-z

24. Huang Y, Ying Z, Quan W, Xiang W, Xie D, Weng Y, et al. The clinical significance of neutrophil-to-lymphocyte ratio and monocyte-to-lymphocyte ratio in Guillain-Barré syndrome. *Int J Neurosci.* (2018) 128:729–35. doi: 10.1080/00207454.2017.1418342

25. Gümüşyayla S, Vural G. The predictive value of neutrophil-lymphocyte ratio in disability of gullain-barr? syndrome. *Bakirköy Tip Dergisi.* (2019) 15:187. doi: 10.4274/BTDMJB.galenos.2019.20171214071335

26. Sahin S, Cinar N, Karsidag S. Are cerebrospinal fluid protein levels and plasma neutrophil/lymphocyte ratio associated with prognosis of guillain barré syndrome? *Neurol Int.* (2017) 9:7032. doi: 10.4081/ni.2017.7032

27. Tunç A. Early predictors of functional disability in Guillain-Barré Syndrome. *Acta Neurol Belg.* (2019) 119:555–9. doi: 10.1007/s13760-019-01133-3

28. Ning P, Yang B, Yang X, Huang H, Shen Q, Zhao Q, et al. Lymphocyte-based ratios for predicting respiratory failure in Guillain-Barré syndrome. *J Neuroimmunol.* (2021) 353:577504. doi: 10.1016/j.jneuroim.2021.577504

29. Guyatt GH, Thorlund K, Oxman AD, Walter SD, Patrick D, Furukawa TA, et al. GRADE guidelines: 13. preparing summary of findings tables and evidence profiles-continuous outcomes. *J Clin Epidemiol.* (2013) 66:173–83. doi: 10.1016/j.jclinepi.2012.08.001

30. Murad MH, Mustafa RA, Schünemann HJ, Sultan S, Santesso N. Rating the certainty in evidence in the absence of a single estimate of effect. *Evid Based Med.* (2017) 22:85–7. doi: 10.1136/ebmed-2017-110668

31. Schünemann H, Brozek J, Guyatt G, Oxman A. *GRADE Handbook for Grading Quality of Evidence and Strength of Recommendation 2008.* Available online at: https://gdt.gradepro.org/app/handbook/handbook.html

32. Huguet A, Hayden JA, Stinson J, McGrath PJ, Chambers CT, Tougas ME, et al. Judging the quality of evidence in reviews of prognostic factor research: adapting the GRADE framework. *Syst Rev.* (2013) 2:71. doi: 10.1186/2046-4053-2-71

33. Paliogiannis P, Satta R, Deligia G, Farina G, Bassu S, Mangoni AA, et al. Associations between the neutrophil-to-lymphocyte and the platelet-to-lymphocyte ratios and the presence and severity of psoriasis: a systematic review and meta-analysis. *Clin Exp Med.* (2019) 19:37–45. doi: 10.1007/s10238-018-0538-x

34. Erre GL, Paliogiannis P, Castagna F, Mangoni AA, Carru C, Passiu G, et al. Meta-analysis of neutrophil-to-lymphocyte and platelet-to-lymphocyte ratio in rheumatoid arthritis. *Eur J Clin Invest.* (2019) 49:e13037. doi: 10.1111/eci.13037

35. Ma L, Zeng A, Chen B, Chen Y, Zhou R. Neutrophil to lymphocyte ratio and platelet to lymphocyte ratio in patients with systemic lupus erythematosus and their correlation with activity: a meta-analysis. *Int Immunopharmacol.* (2019) 76:105949. doi: 10.1016/j.intimp.2019.105949

36. Hagen KM, Ousman SS. The neuroimmunology of Guillain-Barré Syndrome and the potential role of an aging immune system. *Front Aging Neurosci.* (2021) 12:613628. doi: 10.3389/fnagi.2020.613628

37. Guzel I, Mungan S, Oztekin ZN, Ak F. Is there an association between the Expanded Disability Status Scale and inflammatory markers in multiple sclerosis? *J Chin Med Assoc.* (2016) 79:54–7. doi: 10.1016/j.jcma.2015.08.010

38. Morisaki T, Goya T, Ishimitsu T, Torisu M. The increase of low density subpopulations and CD10 (CALLA) negative neutrophils in severely infected patients. *Surg Today.* (1992) 22:322–7. doi: 10.1007/BF00308740

39. Ng LG, Ostuni R, Hidalgo A. Heterogeneity of neutrophils. *Nat Rev Immunol.* (2019) 19:255–65. doi: 10.1038/s41577-019-0141-8

40. Rahman S, Sagar D, Hanna RN, Lightfoot YL, Mistry P, Smith CK, et al. Low-density granulocytes activate T cells and demonstrate a non-suppressive role in systemic lupus erythematosus. *Ann Rheum Dis.* (2019) 78:957–66. doi: 10.1136/annrheumdis-2018-214620

41. Ren K, Yang A, Lu J, Zhao D, Bai M, Ding J, et al. Association between serum low-density neutrophils and acute-onset and recurrent Guillain-Barré syndrome. *Brain Behav.* (2022) 12:e2456. doi: 10.1002/brb3.2456

42. Forget P, Khalifa C, Defour JP, Latinne D, Van Pel MC, De Kock M. What is the normal value of the neutrophil-to-lymphocyte ratio? *BMC Res Notes.* (2017) 10:12. doi: 10.1186/s13104-016-2335-5

43. Moisa E, Corneci D, Negoita S, Filimon CR, Serbu A, Negutu MI, et al. Dynamic changes of the neutrophil-to-lymphocyte ratio, systemic inflammation index, and derived neutrophil-to-lymphocyte ratio independently predict invasive mechanical ventilation need and death in critically Ill COVID-19 patients. *Biomedicines.* (2021) 9:1656. doi: 10.3390/biomedicines9111656

44. Nair PR, Maitra S, Ray BR, Anand RK, Baidya DK, Subramaniam R. Neutrophil-to-lymphocyte ratio and platelet-to-lymphocyte ratio as predictors of the early requirement of mechanical ventilation in COVID-19 patients. *Indian J Crit Care Med.* (2020) 24:1143–4. doi: 10.5005/jp-journals-10071-23663

45. Yang AP, Liu JP, Tao WQ, Li HM. The diagnostic and predictive role of NLR, d-NLR and PLR in COVID-19 patients. *Int Immunopharmacol.* (2020) 84:106504. doi: 10.1016/j.intimp.2020.106504

46. Liu JA, Yu J, Cheung CW. Immune actions on the peripheral nervous system in pain. *Int J Mol Sci.* (2021) 22:1448. doi: 10.3390/ijms22031448

47. Fokke C, van den Berg B, Drenthen J, Walgaard C, van Doorn PA, Jacobs BC. Diagnosis of Guillain-Barré syndrome and validation of Brighton criteria. *Brain.* (2014) 137:33–43. doi: 10.1093/brain/awt285

48. Arami MA, Yazdchi M, Khandaghi R. Epidemiology and characteristics of Guillain-Barré syndrome in the northwest of Iran. *Ann Saudi Med.* (2006) 26:22–7. doi: 10.5144/0256-4947.2006.22

49. Tian J, Cao C, Li T, Zhang K, Li P, Liu Y, et al. Electrophysiological subtypes and prognostic factors of Guillain-Barre Syndrome in Northern China. *Front Neurol.* (2019) 10:714. doi: 10.3389/fneur.2019.00714

50. Doets AY, Verboon C, van den Berg B, Harbo T, Cornblath DR, Willison HJ, et al. Regional variation of Guillain-Barré syndrome. *Brain.* (2018) 141:2866–77. doi: 10.1093/brain/awy232

51. Doets AY, Lingsma HF, Walgaard C, Islam B, Papri N, Davidson A, et al. Predicting outcome in Guillain-Barré Syndrome: international validation of the modified erasmus GBS outcome score. *Neurology.* (2022) 98:e518–32. doi: 10.1212/WNL.0000000000013139

52. Doets AY, Walgaard C, Lingsma HF, Islam B, Papri N, Yamagishi Y, et al. International validation of the erasmus Guillain-Barré Syndrome respiratory insufficiency score. *Ann Neurol.* (2022) 91:521–31. doi: 10.1002/ana.26312

53. Malaga M, Rodriguez-Calienes A, Marquez-Nakamatsu A, Recuay K, Merzthal L, Bustamante-Paytan D, et al. Predicting mechanical ventilation using the egris in Guillain-Barré Syndrome in a Latin American country. *Neurocrit Care.* (2021) 35:775–82. doi: 10.1007/s12028-021-01218-z

54. Zahorec R. Neutrophil-to-lymphocyte ratio, past, present and future perspectives. *Bratisl Lek Listy.* (2021) 122:474–88. doi: 10.4149/BLL_2021_078

55. van Koningsveld R, Schmitz PI, Meché FG, Visser LH, Meulstee J, van Doorn PA. Effect of methylprednisolone when added to standard treatment with intravenous immunoglobulin for Guillain-Barré syndrome: randomised trial. *Lancet.* (2004) 363:192–6. doi: 10.1016/S0140-6736(03)15324-X

56. Walgaard C, Jacobs BC, Lingsma HF, Steyerberg EW, van den Berg B, Doets AY, et al. Second intravenous immunoglobulin dose in patients with Guillain-Barré syndrome with poor prognosis (SID-GBS): a double-blind, randomised, placebo-controlled trial. *Lancet Neurol.* (2021) 20:275–83. doi: 10.1016/S1474-4422(20)30494-4

57. Orlikowski D, Sharshar T, Porcher R, Annane D, Raphael JC, Clair B. Prognosis and risk factors of early onset pneumonia in ventilated patients with Guillain-Barré syndrome. *Intensive Care Med.* (2006) 32:1962–9. doi: 10.1007/s00134-006-0332-1

58. Péter M, Török W, Petrovics-Balog A, Vígh L, Vécsei L, Balogh G. Cerebrospinal fluid lipidomic biomarker signatures of demyelination for multiple sclerosis and Guillain-Barré syndrome. *Sci Rep.* (2020) 10:18380. doi: 10.1038/s41598-020-75502-x

59. Breville G, Lascano AM, Roux-Lombard P, Lalive PH. IL-8 as a potential biomarker in Guillain-Barre Syndrome. *Eur Cytokine Netw.* (2019) 30:130–4. doi: 10.1684/ecn.2019.0436

frontiers | Frontiers in Neurology

TYPE Original Research
PUBLISHED 14 July 2023
DOI 10.3389/fneur.2023.1177479

OPEN ACCESS

EDITED BY
Wael M. Y. Mohamed,
International Islamic University Malaysia, Malaysia

REVIEWED BY
Honghao Wang,
Guangzhou First People's Hospital, China
Haiqiang Qin,
Capital Medical University, China

*CORRESPONDENCE
Yu-sheng Li
✉ fccliyusheng@zzu.edu.cn
Yuan Gao
✉ fccgaoy1@zzu.edu.cn

†These authors have contributed equally to this work

RECEIVED 01 March 2023
ACCEPTED 16 June 2023
PUBLISHED 14 July 2023

CITATION
Yang Y-h, Li S-s, Wang Y-c, Yu L-l, Zhu H-h, Wu J-h, Yu W-k, An L, Yuan W-x, Ji Y, Xu Y-m, Gao Y and Li Y-s (2023) Correlation between neutrophil gelatinase phase lipocalin and cerebral small vessel disease.
Front. Neurol. 14:1177479.
doi: 10.3389/fneur.2023.1177479

Correlation between neutrophil gelatinase phase lipocalin and cerebral small vessel disease

Ying-hao Yang†, Shan-shan Li†, Yun-chao Wang, Lu-lu Yu, Hang-hang Zhu, Jing-hao Wu, Wen-kai Yu, Lu An, Wen-xin Yuan, Yan Ji, Yu-ming Xu, Yuan Gao* and Yu-sheng Li*

Department of Neurology, The First Affiliated Hospital of Zhengzhou University, Zhengzhou, Henan, China

Background: Cerebral small vessel disease (CSVD) is common in the elderly population. Neutrophil gelatinase-associated lipocalin (NGAL) is closely related to cardiovascular and cerebrovascular diseases. NGAL causes pathological changes, such as damage to the vascular endothelium, by causing inflammation, which results in other related diseases. The purpose of this study was to investigate whether serum NGAL levels could predict disease severity in patients with CSVD.

Methods: The patients with CSVD who visited the Department of Neurology at the First Affiliated Hospital of Zhengzhou University between January 2018 and June 2022 were prospectively included. The total CSVD burden score was calculated using whole-brain magnetic resonance imaging (MRI), and the patients were divided into a mild group (total CSVD burden score < 2 points) and a severe group (total CSVD burden score ≥ 2 points). Age, sex, height, smoking and alcohol consumption history, medical history, and serological results of patients were collected to perform the univariate analysis. Multivariate logistic regression was used to analyze the risk factors that affect CSVD severity. The multiple linear regression method was used to analyze which individual CSVD markers (periventricular white matter hyperintensities, deep white matter hyperintensities, lacune, and cerebral microbleed) play a role in the association between total CSVD burden score and NGAL.

Results: A total of 427 patients with CSVD (140 in the mild group and 287 in the severe group) were included in the study. A multivariate logistic regression analysis showed that the following factors were significantly associated with CSVD severity: male sex [odds ratio(OR), 1.912; 95% confidence interval (CI), 1.150–3.179], age (OR, 1.046; 95% CI, 1.022–1.070), history of cerebrovascular disease (OR, 3.050; 95% CI, 1.764–5.274), serum NGAL level (OR, 1.005; 95% CI, 1.002–1.008), and diabetes (OR, 2.593; 95% CI, 1.424–4.722). A multivariate linear regression shows that periventricular white matter hyperintensities and cerebral microbleed are associated with serum NGAL concentrations ($P < 0.05$).

Conclusion: Serum NGAL level is closely related to CSVD severity and is a risk factor for the burden of CSVD brain damage. Serum NGAL has high specificity in reflecting the severity of CSVD.

KEYWORDS

cerebral small vessel disease, inflammation, neuroimaging, total CSVD burden score, risk factors

1. Introduction

CSVD refers to a group of clinical, cognitive, imaging, and pathological manifestations caused by structural and functional changes in small vessels, including cerebral small arteries and their distal branches, arterioles, capillaries, small venules, and venules (1, 2). CSVD can cause many types of vascular injury, which should be treated as a whole-brain disease (1, 2). The main imaging features of CSVD include recent small subcortical infarcts, presumed vascular-origin lacunae, presumed vascular-origin white matter hyperintensity (WMH), enlarged perivascular spaces (EPVSs), cerebral microbleed (CMB), and brain atrophy (3).

Although studies on the pathogenesis, etiology, and clinical manifestations of CSVD have made progress in recent years, clear diagnostic criteria and mechanisms of pathogenesis are lacking (4). Currently, CSVD is diagnosed mainly based on clinical and comprehensive imaging findings. The total CSVD burden score, which is a composite assessment for CSVD based on the four imaging features (WMH, CMB, EPVSs, and lacunar infarcts) of CSVD, may be more suitable for evaluating the overall brain damage based on imaging characteristics in CSVD (5). The pathogenesis of CSVD is believed to be a diffuse endothelial injury, which leads to increased vascular permeability, damage to the vessel wall, impaired autoregulation, and lumen narrowing and occlusion in the late stage, thus triggering discrete focal parenchymal ischemia and infarction (6). Studies have found that neutrophil gelatinase-associated lipocalin (NGAL) and NGAL/matrix metalloproteinase (MMP)-9 complexes act as pro-inflammatory factors in cardiovascular diseases. They play a role in the inflammatory response, the integrity of the endothelium, vascular remodeling, and plaque vulnerability (7–9). Cardiovascular and cerebrovascular diseases have certain similarities, which are reflected in common risk factors and mechanisms of occurrence (10). We performed this study to explore the relationship between NGAL and CSVD. By collecting the clinical and imaging data of patients, we calculated the total CSVD burden score to evaluate the correlation between serum NGAL level and CSVD severity.

2. Materials and methods

2.1. Patient selection

(i) According to the inclusion and exclusion criteria, 427 patients who were diagnosed with CSVD and had clinical manifestations such as dizziness, headache, paresthesias, fatigue, memory loss, and ataxia in the Department of Neurology, The First Affiliated Hospital of Zhengzhou University, Henan, China from January 2018 to June 2022 were included. Two neurology physicians collected the patient demographics, clinical characteristics, and imaging data and assessed the total CSVD burden score in each patient.

(ii) Inclusion criteria: (a) age $\geq$ 18 years; (b) CSVD lesions on magnetic resonance imaging (MRI) of the head with any of the following: WMH, and Fazekas score $\geq$ 2; Fazekas score = 1 and at least two vascular risk factors (e.g., hypertension, hyperlipidemia, diabetes, obesity, current smoking, and previous vascular events other than stroke); or Fazekas score = 1 with lacunar lesions; (c) independence in daily life, modified Rankin Scale (mRS) $\leq$ 2; and (d) provided signed informed consent.

(iii) Exclusion criteria: (a) in acute cerebral infarction, hyperintense lesions on diffusion-weighted imaging and >20 mm in diameter; (b) acute intracerebral hemorrhage; (c) acute subarachnoid hemorrhage, history of cerebrovascular malformation or aneurysmal subarachnoid hemorrhage, or discovery of untreated aneurysm (>3 mm in diameter); (d) diagnosed neurodegenerative diseases, such as Alzheimer's disease (11) and Parkinson's disease (12); (e) clear white matter lesions of non-vascular origin, such as multiple sclerosis, white matter dysplasia in adults, and metabolic encephalopathy; (f) psychiatric illness, such as depression, bipolar disorder, and acute anxiety disorder, diagnosed according to the Diagnostic and Statistical Manual of Mental Disorders (DSM-5); (g) contraindications to MRI (such as claustrophobia); (h) severe organic diseases, such as malignancy, severe chronic heart failure, and severe chronic renal failure, with an expected survival time of <5 years; (i) being unable to complete the follow-up due to geographical or other reasons; and (j) concurrent participation in other clinical trials.

This study was approved by the Ethics Committee of the First Affiliated Hospital of Zhengzhou University.

2.2. Brain MRI

The total CSVD burden score was calculated using whole-brain MRI. (i) lacunar infarcts (LIs) $\geq$ 1 (1 point); (ii) WMH: according to the Fazekas scale (13), if there are irregular paraventricular hyperintensities extending to the deep white matter with a Fazekas score of 3 and/or the deep white matter lesions have begun to fuse or have high fusion in a large area with a Fazekas score of 2 or 3. WMH was scored as 1; (iii) cerebral microbleed (CMB): microbleeds are defined as small (5 mm) round lesions on low-intensity gradient echo images in the cerebellum, brainstem, basal ganglia, white matter, or cortical-subcortical junction; 1 point is awarded for $\geq$1 cerebral microbleed (3); (iv) EPVSs: EPVSs in the basal ganglia (EPVS-BS) are associated with CSVD and can be

Abbreviations: CSVD, cerebral small vessel disease; NGAL, neutrophil gelatinase-associated lipocalin; MRI, magnetic resonance imaging; WMH, white matter hyperintensity; EPVSs, enlarged perivascular spaces; CMB, cerebral microbleed; MMP, matrix metalloproteinase; mRS, modified Rankin Scale; Lis, lacunar infarcts; TC, total cholesterol; LDL-C, low-density lipoprotein; HDL-C, high-density lipoprotein; TG, triglyceride; NVU, neurovascular unit; MCP, monocyte chemoattractant protein; ZMP, zinc metalloprotease; TIMP, tissue inhibitor of matrix metalloproteinase; NO, nitric oxide; EPVS-BS, EPVSs in the basal ganglia; AUC, area under the curve; HbA1, glycosylated hemoglobin; HCY, homocysteine; IL, interleukin; NGAL/MMP-9, NGAL/MMP-9 complex; BBB, blood–brain barrier.

classified according to the number of EPVSs: mild EPVSs, ≤10; moderate EPVSs, 11–25; and extensive EPVSs, >25. Moderate or severe (>10) EPVS-BS was scored as 1 (14, 15).

The total CSVD score was calculated according to these criteria, and the patients were divided into mild and severe groups based on a total CSVD score of <2 points and ≥2 points (total score of four points), respectively.

2.3. Data collection

Age, sex, height, smoking and alcohol consumption history, medical history, and serological results of patients were collected. Median cubital venous blood was collected after fasting for 8 h to determine the plasma NGAL levels. On the day of blood sample collection, the serum was prepared by centrifugation of whole blood at 3,000 r·min^{-1} and a radius of 10 cm for 10 min, and the supernatant was aspirated to avoid hemolysis and stored in a refrigerator at −80°C. A Human NGAL ELISA kit was obtained from Wuhan Huamei Biological Engineering Co., Ltd. in China (CSB-E09408h), and all samples were run in a single batch. According to the manufacturer's instructions, plasma NGAL levels were detected using an enzyme-linked immunosorbent assay, and the samples were prevented from repeated freezing and thawing. One replicate well was set for each sample for repeated measurements, and the average value was used for statistical analysis to reduce experimental errors.

2.4. Statistical methods

SPSS statistical software (26.0) was used for data analysis, and the count data were expressed as frequencies. If the data were distributed normally, the independent sample *t*-test was used, otherwise, the Mann–Whitney *U*-test was used; when theoretical frequency (T) was ≥5, Pearson's chi-square test was used; when T was <5 and T was ≥1, the continuity-adjusted chi-squared test was used; and when $T < 1$, Fisher's exact test was used. Risk factors that were significantly ($p < 0.05$) associated with CSVD severity in the univariate analysis were entered into multivariable analyses. Multivariate logistic regression analysis by the Forward LR method was performed with CSVD patients with the CSVD load score level as the dependent variable. Differences were considered statistically significant at a *P*-value of <0.05. The area under the receiver-operating characteristic curve (AUC) was used to evaluate the predictive value of serum NGAL for the severity of CSVD. Youden index (the sum of sensitivity and specificity minus 1, Youden index = sensitivity + specificity − 1) indicates the total ability of the test method to find real patients and non-patients. After calculating the Youden index, we sorted it and picked the largest Youden index, which is the best cutoff point, and then, we obtained its corresponding threshold values of AUC.

We further grouped individual CSVD markers separately: the mild group (which does not affect the total load score) and the severe group (which affects the total load score), for example, periventricular white matter hyperintensities (PWMH) in the mild group (Fazekas score < 3) and the PWMH severe group (Fazekas score = 3). Multiple linear regression was used to analyze the effect of individual CSVD markers (periventricular white matter hyperintensity, deep white matter hyperintensity, perivascular space enlargement, lacunes, and cerebral microbleed) on the relationship between total CSVD burden score and the NGAL level.

3. Results

3.1. Baseline characteristics

A total of 427 patients with CSVD were included in the study (140 in the mild group and 287 in the severe group).

3.2. Univariate analysis

The univariate analysis included the following parameters: there were significant differences in age, sex, hypertension, diabetes, cerebrovascular history, blood glucose, serum NGAL levels, serum total cholesterol (TC) levels, serum low-density lipoprotein (LDL-C) levels, glomerular filtration rate, HbA1 (%) levels, and absolute neutrophil count (ANC) among the groups ($P < 0.05$). There were no significant differences in cardiovascular history, smoking, alcohol consumption, serum triglyceride (TG) levels, serum high-density lipoprotein (HDL-C) levels, and homocysteine between the groups (Table 1).

3.3. Multivariate analysis

We performed a multivariate logistic regression analysis on the statistically significant risk factors after preliminary screening. The results revealed that the following were significant risk factors for the total CSVD burden score ($P < 0.05$): male sex [odds ratio (OR), 1.912; 95% confidence interval (CI), 1.150–3.179], age (OR, 1.046; 95% CI, 1.022–1.070), history of cerebrovascular disease (OR, 3.050; 95% CI, 1.764–5.274), serum NGAL level (OR, 1.005; 95% CI, 1.002–1.008), and diabetes (OR, 2.593; 95% CI, 1.424–4.722) (Table 2).

3.4. Receiver-operating characteristic curve

The receiver-operating characteristic curve analysis revealed the following cutoffs: age of 70.5 years (sensitivity, 30.5%; specificity, 90.5%; AUC, 0.652), serum NGAL of 146.9 ng/ml (sensitivity, 55%; specificity, 75.9%; AUC, 0.674), history of cerebrovascular disease (sensitivity, 46.1%; specificity, 79.6%; AUC, 0.628), male sex (sensitivity, 67.7%; specificity, 48.9%; AUC, 0.583), and diabetes (sensitivity, 34.8%; specificity, 83.9%; AUC, 0.593). Serum NGAL has a higher area under the curve than traditional factors such as age and sex (Table 3). The receiver-operating characteristic curve is shown in Figure 1.

TABLE 1 Study population characteristics and their correlation with total CSVD burden.

Variable	Severe group ($n = 140$)	Mild group ($n = 287$)	*P*-value
Age	64.05 ± 10.96	57.67 ± 11.14	<0.001*
Sex/male	193 (67.2%)	72 (51.4%)	0.002*
Cerebrovascular disease	130 (45.9%)	28 (20.1%)	<0.001*
Cardiovascular history	32 (11.2%)	13 (9.4%)	0.564
Hypertension	202 (70.4%)	81 (58.3%)	0.013*
Diabetes	102 (35.5%)	22 (15.8%)	<0.001*
Smoking	70 (24.4%)	25 (18.0%)	0.137
Alcohol consumption history	38 (13.4%)	15 (10.8%)	0.442
NGAL	149.58 (103.77–220.78)	111.76 (81.41–140.39)	<0.001*
Blood glucose	5.43 (4.77–6.90)	5.04 (4.70–5.69)	0.001*
TC	3.78 (3.00–4.48)	4.09 (3.48–4.92)	0.011*
TG	1.14 (0.85–1.62)	1.29 (0.97–1.70)	0.079
H-LDL	1.07 (0.87–1.30)	1.14 (0.91–1.34)	0.331
L-LDL	2.18 (1.67–2.86)	2.44 (1.89–3.25)	0.011*
GFR	91.76 (81.66–100.12)	96.43 (89.52–103.80)	<0.001*
HCY	13.16 (10.81–16.83)	12.29 (10.46–16.43)	0.082
HbA1 (%)	6.04 (5.60–7.08)	5.8 (5.55–6.20)	0.001*
ANC	4.08 (3.22–5.35)	3.36 (2.62–4.22)	<0.001*

NGAL, neutrophil gelatinase-associated lipocalin; TC, total cholesterol; TG, triglyceride; HDL, high-density lipoprotein cholesterol; LDL, low-density lipoprotein cholesterol; GFR, glomerular filtration rate; HCY, homocysteine; HbA1, glycosylated hemoglobin; ANC, absolute neutrophil count; ※$P < 0.05$.

TABLE 2 Multiple regression analysis of clinical characteristics affecting the total CSVD burden score.

Variable	Group	*P*	OR	OR (95% CI)
Sex	Women*			
	Men	0.012	1.912	1.150–3.179
Age		<0.001	1.046	1.022–1.070
Cerebrovascular disease	No*			
	Yes	<0.001	3.050	1.764–5.274
NGAL		0.001	1.005	1.002–1.008
Diabetes	No*			
	Yes	0.002	2.593	1.424–4.722

NGAL, neutrophil gelatinase-associated lipocalin. *Control.

3.5. Multiple linear regression

We analyzed the effect of individual SVD markers on the total CSVD burden score (Table 4).

TABLE 3 ROC curve analysis.

Index	Threshold	Sensitivity (%)	Specificity (%)	Area under the curve
Age	≥70.5	30.5	90.5	0.652
NGAL	≥146.9	55.0	75.9	0.674
Cerebrovascular disease	Yes	46.1	79.6	0.628
Sex	Male	67.7	48.9	0.583
Diabetes	Yes	34.8	83.9	0.593

NGAL, neutrophil gelatinase-associated lipocalin.

4. Discussion

In this study, we analyzed 427 patients with CSVD, including 140 in the mild group and 287 in the severe group, and found that the serum NGAL level was a risk factor for CSVD severity. Furthermore, serum NGAL level has different effects on individual SVD markers, especially between PWMH and DWMH.

CSVD is a dynamic disorder of the whole brain, and abnormal neurovascular unit (NVU) function plays an important role in its pathogenesis (16). The NVU is composed of neurons, astrocytes, vascular endothelial cells (EC), pericytes, and vascular smooth muscle cells that interact to regulate the fluid and nutrient entry into the interstitium, regulate cerebral blood flow, maintain and repair myelin sheaths, and scavenge metabolites for normal cellular function (1, 17, 18). Changes in the structure or function of the NVU can lead to CSVD. Common mechanisms for the destruction of the NVU include chronic cerebral ischemia and hypoperfusion (19), endothelial dysfunction (20), blood–brain barrier (BBB) disruption (21), interstitial fluid reflux disorders, inflammatory responses (22), and genetic factors (23).

4.1. Inflammatory responses and NGAL

Growing evidence suggests that inflammatory cytokines are associated with an increased risk of stroke, cardiovascular disease, and dementia (24–26). Additionally, the study by Gu et al. (27) and other studies reported that inflammatory biomarkers may play an active role in cerebrovascular injury.

NGAL is also known as ferritin or lipocalin 2 (28). The levels of NGAL in the brain originate not only from the brain but also from the blood (29). NGAL has been found to promote pro-inflammatory activation of glial cells and might enhance the infiltration of neutrophils and macrophages into the brain in certain conditions (30). NGAL can also promote the production of cytokines [such as interleukin (IL)-6, IL-8, and monocyte chemoattractant protein (MCP)-1] (7). The pro-inflammatory effect of NGAL plays an important role in the development of CSVD (31).

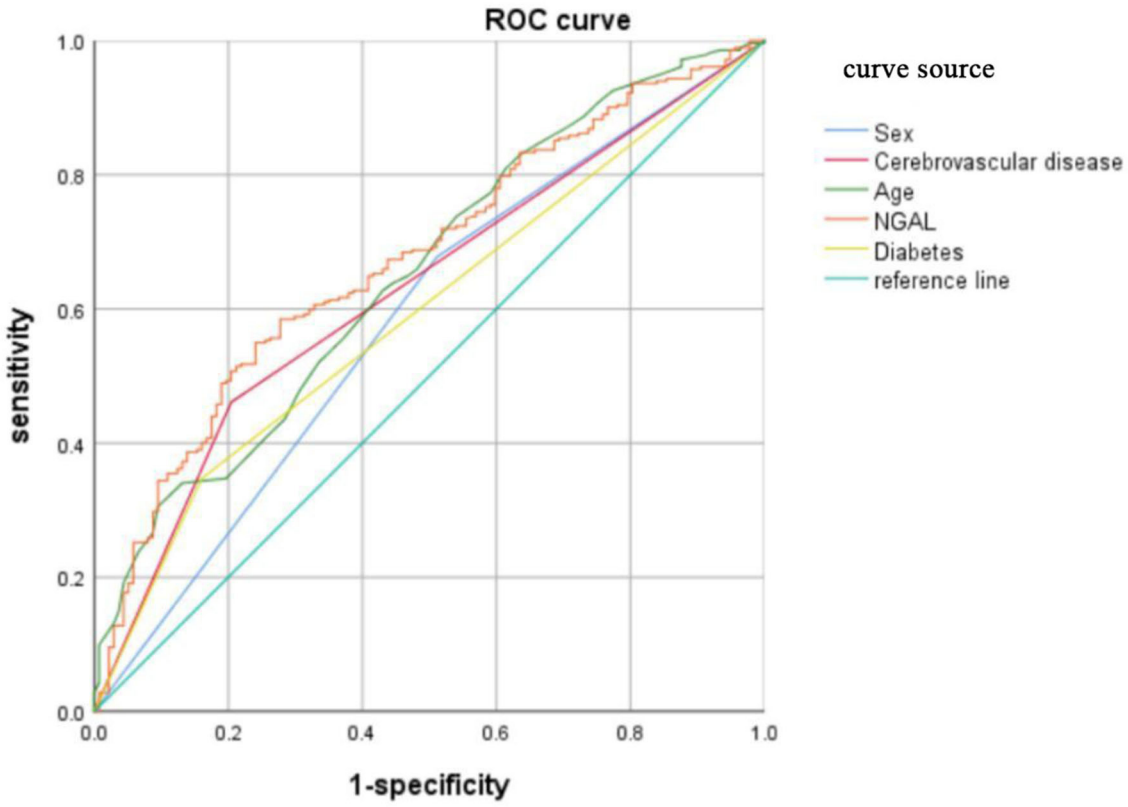

FIGURE 1
The receiver-operating characteristic curve.

TABLE 4 Multiple linear regression results.

Marker	Beta	*P*
PWMH	0.137	0.019
DWMH	0.044	0.455
CMB	0.126	0.029
Lacune	0.011	0.845

PWMH, periventricular white matter hyperintensities; DWMH, deep white matter hyperintensities; CMB, cerebral microbleed.

4.2. Blood-brain barrier disruption and NGAL

MMP-9 is a member of the zinc metalloprotease (ZMP) family. MMP-9 can destroy the BBB to allow macromolecules, such as fibrin, to enter the brain tissue, causing cerebral edema and structural damage (32). NGAL can form a heterodimer with the metalloprotease MMP-9 (NGAL/MMP-9) with stable biological activity (33). NGAL/MMP-9 prevents MMP-9 degradation and prolongs its activity by resisting the inhibitory effects of the tissue inhibitor of matrix metalloproteinase (TIMP) on MMP-9 (8).

A study found that NGAL can reduce the levels of the tight junction proteins claudin-5 and zonula occludens-1 in cultured brain endothelial cells (34). NGAL increases the BBB permeability, which can subsequently increase the leakage from blood vessels and macromolecules such as albumin and enter the brain parenchyma, thus aggravating CSVD (35).

4.3. Chronic cerebral ischemia, hypoperfusion, and NGAL

It is generally believed that NGAL, NGAL/MMP-9 complex, and cardiovascular disease, especially coronary heart disease and heart failure, are closely related (36, 37). The NGAL/MMP-9 complex allows leukocytes and cytokines to invade the intima and promotes the development of atherosclerosis (38). NGAL can also promote fibroblast hyperproliferation after myocardial infarction, thus resulting in interstitial myocardial fibrosis, increased left ventricular remodeling, and consequent heart failure (39). To our knowledge, cerebrovascular and cardiovascular diseases are similar in pathogenesis to some extent. We raised the hypothesis that NGAL may cause CSVD via the thickening of the vessel wall and narrowing of the lumen, leading to long-term chronic hypoperfusion of the cerebral. However, we still need more experiments to verify.

4.4. Endothelial dysfunction and NGAL

Endothelial dysfunction is commonly defined as a reduction in the bioavailability of nitric oxide (NO) in an EC (40). NGAL

may disrupt the nitric oxide (NO) signaling pathway to reduce NO production (41). Dysregulation of NO leads to excessive vasoconstriction that affects cerebral blood flow (hypoperfusion), and long-term chronic cerebral ischemia increases the burden of CSVD (42, 43).

From the above analysis, it appears that the mechanism of NGAL causing the progression of CSVD is not independent but rather the overlapping of various mechanisms. These results also imply that we should pay more attention to NGAL.

A previous study reported that age is an important risk factor for CSVD (44), and the incidence of CSVD is highly age-related and does not vary by sex, ethnicity, or geography (45). Recent research showed that estrogen can promote cerebral blood flow, which is beneficial to nerve repair. Low serum estrogen levels can reduce cerebral blood flow and weaken neural repair mechanisms, which increases the risk of CSVD (46). A recent Mendelian randomization study strongly suggests a causal relationship between diabetes and CSVD, in particular with lacunar stroke and WMH (47). This is consistent with our conclusions.

In both ischemic and hemorrhagic stroke conditions, the most important etiopathogenesis is vascular damage. Occluded or ruptured cerebral blood vessels can cause inflammation, which in turn can be involved in stroke progression (48, 49). Stroke and CSVD have similar characteristics in cerebrovascular injury. A series of changes in the inflammation caused by stroke may lead to CSVD or accelerate the progression of CSVD.

However, several potential limitations should be acknowledged in the present study. First, it is a single-center study, and the sample size included in this study is relatively small. Second, according to the study results, the effect size of the NGAL level is low (OR, 1.005; 95% CI, 1.002–1.008). We did not include EPVS in the multiple linear regressions because of the low proportion of EPVS in our sample. Therefore, we need more experiments and large samples of data to verify. In our study, although the serum NGAL level is a non-traditional risk factor, indicating the degree of whole-brain small vessel damage in CSVD, sensitivity is not very high, which means that patients with cerebral small vessel disease who belonged to the severe group may be missed and diagnosed as a mild group by only using NGAL. However, we generally do not judge a certain disease based on only one biomarker in clinical trials. The combination of imaging and biomarkers is more beneficial to the diagnosis of CSVD.

CSVD is diagnosed mainly based on clinical and comprehensive imaging findings. However, the high cost, equipment requirements, and subjective judgment report are also limitations of imaging. The serum NGAL reflects the disease status of CSVD, which can give hints to clinicians and is more convenient and economical. Moreover, the combination of clinical, imaging, and NGAL may be more beneficial to the diagnosis of CSVD and the prediction of severity of CSVD. Our study is also conducive to the exploration and understanding of the mechanism of CSVD.

5. Conclusion

NGAL was originally used to evaluate renal damage. Recently, much attention has been paid to its role in cardiovascular diseases. However, there are few clinical studies on its role in cerebrovascular diseases, especially CSVD. This study fills this gap in the literature. We found that age, sex, history of stroke, diabetes, and serum NGAL level were closely related to the severity of CSVD and were risk factors for the overall brain damage burden in CSVD. We need to pay attention to NGAL and further explore the role of NGAL in CSVD in the future.

Data availability statement

The original contributions presented in the study are included in the article/supplementary material, further inquiries can be directed to the corresponding authors.

Ethics statement

The studies involving human participants were reviewed and approved by the Ethics Committee of the First Affiliated Hospital of Zhengzhou University (2021-KY-1059-002). The patients/participants provided their written informed consent to participate in this study.

Author contributions

Y-mX and Y-sL: conception, design, and administrative support. Y-hY and Y-cW: provision of study materials or patients. S-sL, L-lY, and H-hZ: collection and assembly of data. J-hW, W-kY, LA, W-xY, YG, and YJ: data analysis and interpretation. All authors: manuscript writing and final approval of the manuscript.

Funding

A major project co-constructed by the Ministry of Medical Science and Technology in Henan Province (SBGJ202101016).

Acknowledgments

We thank all participants and investigators for this study.

Conflict of interest

The authors declare that the research was conducted in the absence of any commercial or financial relationships that could be construed as a potential conflict of interest.

Publisher's note

All claims expressed in this article are solely those of the authors and do not necessarily represent those of their affiliated organizations, or those of the publisher, the editors and the reviewers. Any product that may be evaluated in this article, or claim that may be made by its manufacturer, is not guaranteed or endorsed by the publisher.

References

1. Pantoni L. Cerebral small vessel disease: from pathogenesis and clinical characteristics to therapeutic challenges. *Lancet Neurol.* (2010) 9:689–701. doi: 10.1016/S1474-4422(10)70104-6

2. Shi Y, Wardlaw J. Update on cerebral small vessel disease: a dynamic whole-brain disease. *Stroke Vasc Neurol.* (2016) 1:83–92. doi: 10.1136/svn-2016-000035

3. Wardlaw J, Smith E, Biessels G, Cordonnier C, Fazekas F, Frayne R, et al. Neuroimaging standards for research into small vessel disease and its contribution to ageing and neurodegeneration. *Lancet Neurol.* (2013) 12:822–38. doi: 10.1016/S1474-4422(13)70124-8

4. Ren B, Tan L, Song Y, Li D, Xue B, Lai X, et al. Cerebral small vessel disease: neuroimaging features, biochemical markers, influencing factors, pathological mechanism and treatment. *Front Neurol.* (2022) 13:843953. doi: 10.3389/fneur.2022.843953

5. Zhu H, Li Z, Lv J, Zhao R. Effects of cerebral small vessel disease on the outcome of patients with ischemic stroke caused by large artery atherosclerosis. *Neurol Res.* (2018) 40:381–90. doi: 10.1080/01616412.2018.1446283

6. Wardlaw J, Smith C, Dichgans M. Mechanisms of sporadic cerebral small vessel disease: insights from neuroimaging. *Lancet Neurol.* (2013) 12:483–97. doi: 10.1016/S1474-4422(13)70060-7

7. Eilenberg W, Stojkovic S, Piechota-Polanczyk A, Kaun C, Rauscher S, Gröger M, et al. Neutrophil gelatinase-associated lipocalin (NGAL) is associated with symptomatic carotid atherosclerosis and drives pro-inflammatory state *in vitro*. *J Vasc Surg.* (2016) 63:1664. doi: 10.1016/j.jvs.2016.03.434

8. Hemdahl A, Gabrielsen A, Zhu C, Eriksson P, Hedin U, Kastrup J, et al. Expression of neutrophil gelatinase-associated lipocalin in atherosclerosis and myocardial infarction. *Arterioscler Thromb Vasc Biol.* (2006) 26:136–42. doi: 10.1161/01.ATV.0000193567.88685.f4

9. Power C, Henry S, Del Bigio M, Larsen P, Corbett D, Imai Y, et al. Intracerebral hemorrhage induces macrophage activation and matrix metalloproteinases. *Ann Neurol.* (2003) 53:731–42. doi: 10.1002/ana.10553

10. Liu R, Shao J. Research progress on risk factors related to intracranial artery, carotid artery, and coronary artery stenosis. *Front Cardiovasc Med.* (2022) 9:970476. doi: 10.3389/fcvm.2022.970476

11. McKhann G, Knopman D, Chertkow H, Hyman B, Jack C, Kawas C, et al. The diagnosis of dementia due to Alzheimer's disease: recommendations from the National Institute on Aging-Alzheimer's Association workgroups on diagnostic guidelines for Alzheimer's disease. *Alzheimers Dement.* (2011) 7:263–9. doi: 10.1016/j.jalz.2011.03.005

12. Emre M, Aarsland D, Brown R, Burn D, Duyckaerts C, Mizuno Y, et al. Clinical diagnostic criteria for dementia associated with Parkinson's disease. *Mov. Disord.* (2007) 22:1689–707; quiz 1837. doi: 10.1002/mds.21507

13. Fazekas F, Chawluk J, Alavi A, Hurtig H, Zimmerman R. MR signal abnormalities at 15 T in Alzheimer's dementia and normal aging. *Am J Roentgenol.* (1987) 149:351–6. doi: 10.2214/ajr.149.2.351

14. Doubal F, MacLullich A, Ferguson K, Dennis M, Wardlaw J. Enlarged perivascular spaces on MRI are a feature of cerebral small vessel disease. *Stroke.* (2010) 41:450–4. doi: 10.1161/STROKEAHA.109.564914

15. Staals J, Makin S, Doubal F, Dennis M, Wardlaw J. Stroke subtype, vascular risk factors, and total MRI brain small-vessel disease burden. *Neurology.* (2014) 83:1228–34. doi: 10.1212/WNL.0000000000000837

16. Iadecola C. The neurovascular unit coming of age: a journey through neurovascular coupling in health and disease. *Neuron.* (2017) 96:17–42. doi: 10.1016/j.neuron.2017.07.030

17. Stanimirovic D, Friedman A. Pathophysiology of the neurovascular unit: disease cause or consequence? *J Cereb Blood Flow Metab.* (2012) 32:1207–21. doi: 10.1038/jcbfm.2012.25

18. Zhang C, Wong S, van de Haar H, Staals J, Jansen J, Jeukens C, et al. Blood-brain barrier leakage is more widespread in patients with cerebral small vessel disease. *Neurology.* (2017) 88:426–32. doi: 10.1212/WNL.0000000000003556

19. Wong S, Jansen J, Zhang C, Hoff E, Staals J, van Oostenbrugge R, et al. Blood-brain barrier impairment and hypoperfusion are linked in cerebral small vessel disease. *Neurology.* (2019) 92:e1669–77. doi: 10.1212/WNL.0000000000007263

20. Armulik A, Abramsson A, Betsholtz C. Endothelial/pericyte interactions. *Circ Res.* (2005) 97:512–23. doi: 10.1161/01.RES.0000182903.16652.d7

21. Farrall A, Wardlaw J. Blood-brain barrier: ageing and microvascular disease–systematic review and meta-analysis. *Neurobiol Aging.* (2009) 30:337–52. doi: 10.1016/j.neurobiolaging.2007.07.015

22. Low A, Mak E, Rowe J, Markus H, O'Brien J. Inflammation and cerebral small vessel disease: a systematic review. *Ageing Res Rev.* (2019) 53:100916. doi: 10.1016/j.arr.2019.100916

23. Gould D, Phalan F, van Mil S, Sundberg J, Vahedi K, Massin P, et al. Role of COL4A1 in small-vessel disease and hemorrhagic stroke. *N Engl J Med.* (2006) 354:1489–96. doi: 10.1056/NEJMoa053727

24. Li Y, Lu J, Wang J, Deng P, Meng C, Tang H. Inflammatory cytokines and risk of ischemic stroke: a Mendelian randomization study. *Front Pharmacol.* (2021) 12:779899. doi: 10.3389/fphar.2021.779899

25. Reckelhoff J. Cardiovascular disease, estrogen deficiency, and inflammatory cytokines. *Hypertension*. (2006) 48:372–3. doi: 10.1161/01.HYP.0000235866.97871.9d

26. Romero-Sevilla R, López-Espuela F, Fuentes J, de San Juan B, Portilla-Cuenca J, Hijon C, et al. Role of inflammatory cytokines in the conversion of mild cognitive impairment to dementia: a prospective study. *Curr Alzheimer Res.* (2022) 19:68–75. doi: 10.2174/1567205019666220127102640

27. Gu Y, Gutierrez J, Meier I, Guzman V, Manly J, Schupf N, et al. Circulating inflammatory biomarkers are related to cerebrovascular disease in older adults. *Neurol Neuroimmunol Neuroinflamm.* (2019) 6:e521. doi: 10.1212/NXI.0000000000000521

28. Kjeldsen L, Johnsen AH, Sengeløv, H, Borregaard N. Isolation and primary structure of NGAL, a novel protein associated with human neutrophil gelatinase. *J Biol Chem.* (1993) 268:10425–32. doi: 10.1016/S0021-9258(18)82217-7

29. Ferreira A, Santos T, Sampaio-Marques B, Novais A, Mesquita S, Ludovico P, et al. Lipocalin-2 regulates adult neurogenesis and contextual discriminative behaviours. *Mol Psychiatry.* (2018) 23:1031–9. doi: 10.1038/mp.2017.95

30. Behrens V, Voelz C, Müller N, Zhao W, Gasterich N, Clarner T, et al. Lipocalin 2 as a putative modulator of local inflammatory processes in the spinal cord and component of organ cross talk after spinal cord injury. *Mol Neurobiol.* (2021) 58:5907–19. doi: 10.1007/s12035-021-02530-7

31. Wan S, Dandu C, Han G, Guo Y, Ding Y, Song H, et al. Plasma inflammatory biomarkers in cerebral small vessel disease: A review. *CNS Neurosci Ther.* (2023) 29:498–515. doi: 10.1111/cns.14047

32. Gurney K, Estrada E, Rosenberg G. Blood-brain barrier disruption by stromelysin-1 facilitates neutrophil infiltration in neuroinflammation. *Neurobiol Dis.* (2006) 23:87–96. doi: 10.1016/j.nbd.2006.02.006

33. Coles M, Diercks T, Muehlenweg B, Bartsch S, Zölzer V, Tschesche H, et al. The solution structure and dynamics of human neutrophil gelatinase-associated lipocalin. *J Mol Biol.* (1999) 289:139–57. doi: 10.1006/jmbi.1999.2755

34. Mondal A, Bose D, Saha P, Sarkar S, Seth R, Kimono D, et al. Lipocalin 2 induces neuroinflammation and blood-brain barrier dysfunction through liver-brain axis in murine model of nonalcoholic steatohepatitis. *J Neuroinflammation.* (2020) 17:201. doi: 10.1186/s12974-020-01876-4

35. Wardlaw J, Sandercock P, Dennis M, Starr J. Is breakdown of the blood-brain barrier responsible for lacunar stroke, leukoaraiosis, and dementia? *Stroke.* (2003) 34:806–12. doi: 10.1161/01.STR.0000058480.77236.B3

36. Siasos G, Tousoulis D, Michalea S, Oikonomou E, Vavuranakis M, Athanasiou D, et al. Novel biomarkers assessing renal function in heart failure: relation to inflammatory status and cardiac remodelling. *Curr Med Chem.* (2014) 21:3976–83. doi: 10.2174/0929867321666140826114656

37. Soylu K, Aksan G, Nar G, Özdemir M, Gülel O, Inci S, et al. Serum neutrophil gelatinase-associated lipocalin levels are correlated with the complexity and the severity of atherosclerosis in acute coronary syndrome. *Anat J Cardiol.* (2015) 15:450–5. doi: 10.5152/akd.2014.5513

38. Malek F. The importance of NGAL and cystatin C biomarkers in cardiovascular diseases-editorial. *Vnitr Lek.* (2012) 58:261–2.

39. Martínez-Martínez E, Buonafine M, Boukhalfa I, Ibarrola J, Fernández-Celis A, Kolkhof P, et al. Aldosterone target NGAL (neutrophil gelatinase-associated lipocalin) is involved in cardiac remodeling after myocardial infarction through NFκB pathway. *Hypertension.* (2017) 70:1148–56. doi: 10.1161/HYPERTENSIONAHA.117.09791

40. Harrison D. Cellular and molecular mechanisms of endothelial cell dysfunction. *J Clin Invest.* (1997) 100:2153–7. doi: 10.1172/JCI119751

41. Gu Y, Sun W, Xu Z, Wang J, Hu X, Lu Z, et al. Neutrophil gelatinase-associated lipocalin 2 accelerates hypoxia-induced endothelial cell injury via eNOS/NRF2 signalling. *Cell J.* (2021) 23:435–44. doi: 10.22074/cellj.2021.7167

42. Deplanque D, Lavallee P, Labreuche J, Gongora-Rivera F, Jaramillo A, Brenner D, et al. Cerebral and extracerebral vasoreactivity in symptomatic lacunar stroke patients: a case-control study. *Int J Stroke.* (2013) 8:413–21. doi: 10.1111/j.1747-4949.2011.00755.x

43. Gunarathne A, Patel J, Kausar S, Gammon B, Hughes E, Lip G. Glycemic status underlies increased arterial stiffness and impaired endothelial function in migrant South Asian stroke survivors compared to European Caucasians: pathophysiological insights from the West Birmingham Stroke Project. *Stroke.* (2009) 40:2298–306. doi: 10.1161/STROKEAHA.109.548388

44. Li T, Huang Y, Cai W, Chen X, Men X, Lu T, et al. Age-related cerebral small vessel disease and inflammaging. *Cell Death Dis.* (2020) 11:932. doi: 10.1038/s41419-020-03137-x

45. Hilal S, Mok V, Youn Y, Wong A, Ikram M, Chen C. Prevalence, risk factors and consequences of cerebral small vessel diseases: data from three Asian countries. *J Neurol Neurosurg Psychiatry.* (2017) 88:669–74. doi: 10.1136/jnnp-2016-315324

46. Sijens PE, Oudkerk M, de Leeuw FE, de Groot JC, Achten E, Heijboer R, et al. 1H chemical shift imaging of the human brain at age 60-90 years reveals metabolic differences between women and men. *Magn Reson Med.* (1999) 42:24–31. doi: 10.1002/(SICI)1522-2594(199907)42:1<24::AID-MRM5>3.0.CO;2-3

47. Liu J, Rutten-Jacobs L, Liu M, Markus H, Traylor M. Causal impact of type 2 diabetes mellitus on cerebral small vessel disease: a Mendelian randomization analysis. *Stroke.* (2018) 49:1325–31. doi: 10.1161/STROKEAHA.117.020536

48. Pawluk H, Kołodziejska R, Grześk G, Kozakiewicz M, Wozniak A, Pawluk M, et al. Selected mediators of inflammation in patients with acute ischemic stroke. *Int J Mol Sci.* (2022) 23:10614. doi: 10.3390/ijms231810614

49. Yang Z, Liu Q, Shi H, Jiang X, Wang S, Lu Y, et al. Interleukin 17A exacerbates ER-stress-mediated inflammation of macrophages following ICH. *Mol Immunol.* (2018) 101:38–45. doi: 10.1016/j.molimm.2018.05.020

Frontiers in Neurology

Explores neurological illness to improve patient care

The third most-cited clinical neurology journal explores the diagnosis, causes, treatment, and public health aspects of neurological illnesses. Its ultimate aim is to inform improvements in patient care.

Discover the latest Research Topics

See more →

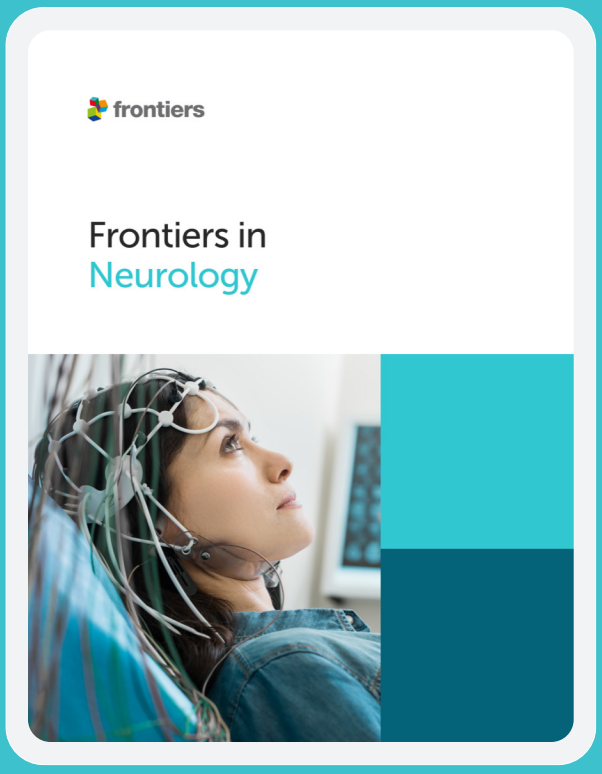

Frontiers

Avenue du Tribunal-Fédéral 34
1005 Lausanne, Switzerland
frontiersin.org

Contact us

+41 (0)21 510 17 00
frontiersin.org/about/contact